ISSN 0021-9673

VOL. 639 NO. 2 JUNE 11, 1993

THIS ISSUE COMPLETES VOL. 639

JOURNAL OF CHROMATOGRAPHY

INCLUDING ELECTROPHORESIS AND OTHER SEPARATION METHODS

ELSEVIER

JOURNAL OF CHROMATOGRAPHY

INCLUDING ELECTROPHORESIS AND OTHER SEPARATION METHODS

Scope. The *Journal of Chromatography* publishes papers on all aspects of **chromatography, electrophoresis** and related methods. Contributions consist mainly of research papers dealing with chromatographic theory, instrumental developments and their applications. The section *Biomedical Applications*, which is under separate editorship, deals with the following aspects: developments in and applications of chromatographic and electrophoretic techniques related to clinical diagnosis or alterations during medical treatment; screening and profiling of body fluids or tissues related to the analysis of active substances and to metabolic disorders; drug level monitoring and pharmacokinetic studies; clinical toxicology; forensic medicine; veterinary medicine; occupational medicine; results from basic medical research with direct consequences in clinical practice. In *Symposium volumes*, which are under separate editorship, proceedings of symposia on chromatography, electrophoresis and related methods are published.

Submission of Papers. The preferred medium of submission is on disk with accompanying manuscript (see *Electronic manuscripts* in the Instructions to Authors, which can be obtained from the publisher, Elsevier Science Publishers B.V., P.O. Box 330, 1000 AH Amsterdam, Netherlands). Manuscripts (in English; *four* copies are required) should be submitted to: Editorial Office of *Journal of Chromatography*, P.O. Box 681, 1000 AR Amsterdam, Netherlands, Telefax (+31-20) 5862 304, or to: The Editor of *Journal of Chromatography, Biomedical Applications*, P.O. Box 681, 1000 AR Amsterdam, Netherlands. Review articles are invited or proposed in writing to the Editors who welcome suggestions for subjects. An outline of the proposed review should first be forwarded to the Editors for preliminary discussion prior to preparation. Submission of an article is understood to imply that the article is original and unpublished and is not being considered for publication elsewhere. For copyright regulations, see below.

Publication. The *Journal of Chromatography* (incl. *Biomedical Applications*) has 40 volumes in 1993. The subscription prices for 1993 are:

J. Chromatogr. (incl. *Cum. Indexes, Vols. 601–650*) + *Biomed. Appl.* (Vols. 612–651):
Dfl. 8520.00 plus Dfl. 1320.00 (p.p.h.) (total *ca.* US$ 5466.75)

J. Chromatogr. (incl. *Cum Indexes, Vols. 601–650*) only (Vols. 623–651):
Dfl. 7047.00 plus Dfl. 957.00 (p.p.h.) (total *ca.* US$ 4446.75)

Biomed. Appl. only (Vols. 612–622):
Dfl. 2783.00 plus Dfl. 363.00 (p.p.h.) (total *ca.* US$ 1747.75).

Subscription Orders. The Dutch guilder price is definitive. The US$ price is subject to exchange-rate fluctuations and is given as a guide. Subscriptions are accepted on a prepaid basis only, unless different terms have been previously agreed upon. Subscriptions orders can be entered only by calender year (Jan.–Dec.) and should be sent to Elsevier Science Publishers, Journal Department, P.O. Box 211, 1000 AE Amsterdam, Netherlands, Tel. (+31-20) 5803 642, Telefax (+31-20) 5803 598, or to your usual subscription agent. Postage and handling charges include surface delivery except to the following countries where air delivery via SAL (Surface Air Lift) mail is ensured: Argentina, Australia, Brazil, Canada, China, Hong Kong, India, Israel, Japan*, Malaysia, Mexico, New Zealand, Pakistan, Singapore, South Africa, South Korea, Taiwan, Thailand, USA. *For Japan air delivery (SAL) requires 25% additional charge of the normal postage and handling charge. For all other countries airmail rates are available upon request. Claims for missing issues must be made within six months of our publication (mailing) date, otherwise such claims cannot be honoured free of charge. Back volumes of the *Journal of Chromatography* (Vols. 1–611) are available at Dfl. 230.00 (plus postage). Customers in the USA and Canada wishing information on this and other Elsevier journals, please contact Journal Information Center, Elsevier Science Publishing Co. Inc., 655 Avenue of the Americas, New York, NY 10010, USA, Tel. (+1-212) 633 3750, Telefax (+1-212) 633 3764.

Abstracts/Contents Lists published in Analytical Abstracts, Biochemical Abstracts, Biological Abstracts, Chemical Abstracts, Chemical Titles, Chromatography Abstracts, Current Awareness in Biological Sciences (CABS), Current Contents/Life Sciences, Current Contents/Physical, Chemical & Earth Sciences, Deep-Sea Research/Part B: Oceanographic Literature Review, Excerpta Medica, Index Medicus, Mass Spectrometry Bulletin, PASCAL-CNRS, Referativnyi Zhurnal, Research Alert and Science Citation Index.

US Mailing Notice. *Journal of Chromatography* (ISSN 0021-9673) is published weekly (total 52 issues) by Elsevier Science Publishers (Sara Burgerhartstraat 25, P.O. Box 211, 1000 AE Amsterdam, Netherlands). Annual subscription price in the USA US$ 4446.75 (subject to change), including air speed delivery. Second class postage paid at Jamaica, NY 11431. **USA POSTMASTERS**: Send address changes to *Journal of Chromatography*, Publications Expediting, Inc., 200 Meacham Avenue, Elmont, NY 11003. Airfreight and mailing in the USA by Publications Expediting.

See inside back cover for Publication Schedule, Information for Authors and information on Advertisements.

0021-9673/93/$06.00

Printed in the Netherlands

CONTENTS

(Abstracts/Contents Lists published in Analytical Abstracts, Biochemical Abstracts, Biological Abstracts, Chemical Abstracts, Chemical Titles, Chromatography Abstracts, Current Awareness in Biological Sciences (CABS), Current Contents/Life Sciences, Current Contents/Physical, Chemical & Earth Sciences, Deep-Sea Research/Part B: Oceanographic Literature Review, Excerpta Medica, Index Medicus, Mass Spectrometry Bulletin, PASCAL-CNRS, Referativnyi Zhurnal, Research Alert and Science Citation Index)

REGULAR PAPERS

Column liquid chromatography

Gas chromatography

(Continued overleaf)

SHORT COMMUNICATIONS

Column liquid chromatography

(Continued overleaf)

Journal of Chromatography, 639 (1993) 87–96
Elsevier Science Publishers B.V., Amsterdam

CHROM. 24 988

Modelling of the retention behaviour of solutes in micellar liquid chromatography with organic modifiers

J.R. Torres-Lapasió, R.M. Villanueva-Camañas, J.M. Sanchis-Mallols, M.J. Medina-Hernández and M.C. García-Alvarez-Coque*

Departamento de Química Analítica, Facultad de Química, Universitat de Valencia, 46100 Burjassot (Valencia) (Spain)

(First received November 16th, 1992; revised manuscript received February 2nd, 1993)

ABSTRACT

Most of the reported procedures for the determination of compounds by micellar liquid chromatography make use of micellar mobile phases containing an alcohol. The retention of a solute in a purely micellar eluent has been adequately described by the linear equation $1/k'$ *vs.* micelle concentration. This equation seems also to be valid for mobile phases with the same alcohol concentration and varying micelle concentrations. A model to describe the retention behaviour of solutes in any mobile phase of surfactant and alcohol is proposed, which makes use of the elution data in five mobile phases of surfactant with different amounts of alcohol. A function of the type $1/k' = A\mu + B\varphi + C\mu\varphi + D$, where μ and φ are surfactant and alcohol concentration, respectively, proved to be satisfactory for different solutes (catecholamines, amino acids, phenols and other aromatic compounds).

INTRODUCTION

Armstrong and Henry [1] indicated in 1980 the feasibility of using mobile phases containing a surfactant solution above the critical micelle concentration (cmc) in reversed-phase liquid chromatography (RPLC). The technique was called micellar liquid chromatography (MLC). The complexity of MLC is much greater than that of conventional RPLC with aqueous–organic solvents, owing to the large number of possible solute–micellar mobile phase–stationary phase interactions, which affect the retention of the solutes. Other factors to be considered are micelle concentration, pH and ionic strength. Almost any compound can be determined by MLC [2].

The retention of a solute usually decreases with increasing micelle concentration in the mobile phase, the retention change depending greatly on the nature of the solute. Three models have been proposed to describe the retention of solutes at various micelle concentrations: the three-phase model of Armstrong and Nome [3], the equilibrium approach of Arunyanart and Cline Love [4] and the model of Foley [5], which considers the interactions with the micelles as a secondary equilibrium. These models lead to similar equations, which can be written as

$$\frac{1}{k'} = \frac{K_{AM}}{(V_S/V_M)P_{SW}} \cdot [M] + \frac{1}{(V_S/V_M)P_{SW}} \qquad (1)$$

where k' is the capacity factor, [M] is the total concentration of surfactant in the mobile phase minus the cmc, V_S the volume of the stationary phase, V_M the volume of the mobile phase in the column, P_{SW} the partition coefficient of the solute between the stationary phase and water and K_{AM} the solute–micelle binding constant. This equation has been verified experimentally for a large number of solutes [6–9].

* Corresponding author.

The most serious problems with MLC are, on the one hand, the weak solvent strength of purely micellar eluents and, on the other, the poor efficiency of the chromatographic peaks compared with aqueous–organic mobile phases, which has been related to a restricted mass transfer of the solute towards the stationary phase [10]. Dorsey *et al.* [11] recommended the addition of an organic solvent, such as a short-chain alcohol, to the micellar eluent, to enhance the chromatographic efficiency. The addition of alcohols also causes an increase in solvent strength, the effect being larger with more hydrophobic solutes. Ternary surfactant–water–organic modifier eluents have been called hybrid micellar eluents [12]. It has been indicated that eqn. 1 is also valid for these eluents [12,13].

When hybrid micellar eluents were first used, they were severely criticized. However, most of the papers published in the last 5 years on MLC reported procedures with these eluents. Our own experience with the determination of different drugs (diuretics, narcotics, stimulants, anabolic steroids and β-blockers) has shown that in most instances, the retention of the solutes with purely micellar eluents is excessive, which forces one to add a modifier to achieve adequate retention times [9,14]. To predict the retention behaviour of a solute in hybrid micellar eluents, it is necessary to find an equation to describe the change in capacity factor with varying concentrations of surfactant and modifier.

Schoenmakers *et al.* [15] proposed in conventional RPLC the following relationship between capacity factor and volume fraction of organic modifier, φ:

$$\log k' = A\varphi^2 + B\varphi + C \quad (2)$$

where A, B and C are constants which depend on the solute. However, in the usual $1 < k' < 10$ range and a small range of concentrations of modifier, this equation may be approximated to

$$\log k' = -S\varphi + \log k'_0 \quad (3)$$

where S is the solvent strength parameter. The intercept $\log k'_0$ does not coincide with the logarithm of the capacity factor of the solute in a purely aqueous mobile phase, being much smaller [16].

Khaledi *et al.* [17] reported that in hybrid MLC and at a constant micelle concentration, the linear relationship between $\log k'$ and φ is valid. According to them, $\log k'_0$ in eqn. 3 is the logarithm of the capacity factor at a given micelle concentration. However, in the same paper, the plots of retention ($\log k'$) of several amino acids and alkylbenzenes in mobile phases of sodium dodecyl sulphate (SDS) and hexadecyltrimethylammonium bromide (CTAB), respectively, against volume fraction of propanol were not linear, and especially the experimental point for the absence of modifier deviated from linearity. We observed for other solutes that linear $\log k'$ *vs.* φ relationships were only obtained with methanol as modifier [9,18].

Recently, Strasters *et al.* [19] proposed a procedure to describe the change in capacity factor of a solute in hybrid eluents, using the retention data of only five mobile phases. In this approach, linear relationships for $\log k'$ *vs.* total concentration of surfactant, μ, and volume fraction of organic modifier, φ, were assumed. The retention in other mobile phases was calculated by means of a simple linear interpolation. The authors indicated that the agreement between experimental and calculated data for several amino acids and phenols was excellent. However, we found important errors in the prediction of the retention of other solutes when this procedure was applied.

In this paper, a more suitable model is proposed for the description of the retention behaviour in micellar eluents containing an alcohol. In this study, the elution data for five catecholamines in mobile phases of SDS and propanol were used.

EXPERIMENTAL

Reagents

Sodium dodecyl sulphate (99%) was obtained from Merck (Darmstadt, Germany) and propanol (analytical-reagent grade) from Panreac (Barcelona, Spain). The mobile phases were vacuum-filtered through 0.47-μm nylon mem-

branes from Micron-Scharlau (Barcelona, Spain).

Stock standard solutions of the following catecholamines at a $2 \cdot 10^{-3}$ M concentration were prepared in 0.1 M acetic acid from Probus (Barcelona, Spain): L-adrenaline (biochemical), DL-noradrenaline (pure), dopamine hydrochloride (very pure) and adrenalone hydrochloride (pure) from Fluka (Buchs, Switzerland) and isoprenaline, kindly donated by Boehringer-Ingelheim (Barcelona, Spain). Nanopure deionized water (Barnstead Sybron, Boston, MA, USA) was used throughout.

Apparatus

A Hewlett-Packard (Palo Alto, CA, USA) HP 1050 chromatograph with a UV–visible detector (absorbance was measured at 280 nm) and an HP 3396A integrator were used. Data were acquired by means of a PC and Peak–96 software from Hewlett-Packard (Avondale, PA, USA). The sample was injected through a Rheodyne (Cotati, CA, USA) valve with a 20-μl loop. A Spherisorb octadecylsilane ODS-2 (5 μm), analytical column (12 cm × 4.6 mm I.D.) and a precolumn, placed before the injector, of identical characteristics (3.5 cm × 4.6 mm I.D.) from Scharlau were used. The mobile phase flow-rate was 1 ml min^{-1}. The dead volume was determined by injecting water.

RESULTS AND DISCUSSION

The retention of aminochromes [18] and diuretics [9] in SDS mobile phases containing methanol followed eqn. 3, apparently owing to its weak eluent strength. However, deviations from linearity were observed with other alcohols as modifiers (see Fig. 1). With the data plotted in this figure, excluded the point for $\varphi = 0$, the value of k'_0 was calculated from the intercept of the fitted straight-line according to eqn. 3. This value is compared in Table I with the experimental k' value for mobile phases without modifier. The difference between the experimental and calculated k'_0 values is larger with an alcohol of longer alkyl chain length. Curiously, a linear relationship was found between this difference

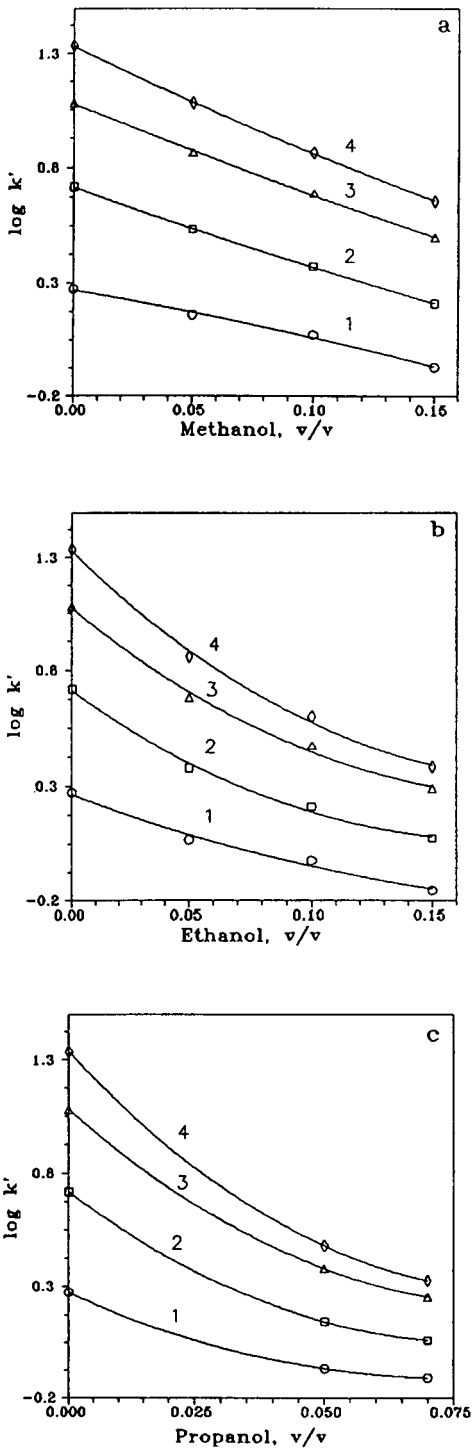

Fig. 1. Log k' *vs.* φ plot for aminochromes: 1 = noradrenochrome; 2 = adrenochrome; 3 = dopaminechrome; 4 = isopropylnoradrenochrome. The mobile phase contained 0.05 M SDS.

TABLE I

THEORETICAL AND EXPERIMENTAL k'_0 VALUES FOR 0.05 *M* SDS

Aminochrome	$k'_{0,exp}$	$k'_{0,calc}$		
		Methanol	Ethanol	Propanol
Noradrenochrome	1.87	1.92	1.54	1.10
Adrenochrome	5.21	4.95	3.33	2.29
Dopaminochrome	12.01	11.21	7.42	5.00
Isopropylnoradrenochrome	21.64	19.49	12.33	7.31

and the number of carbon atoms in the alcohol [18].

The search for an equation that will permit the prediction of the capacity factor of a solute in any micellar eluent containing a given concentration of surfactant and of modifier is not easy. The dependence of the capacity factor on the concentration of micelles seems to be different from the dependence of the capacity factor on the concentration of modifier. Eqn. 1 shows a hyperbolic relationship between k' and [M], and in conventional RPLC a quadratic relationship between log k' and φ has been reported [15].

According to Khaledi *et al.* [12], LC with hybrid micellar eluents is similar to that in purely micellar eluents, based on the similar retention characteristics of homologous series. In contrast, Tomasella *et al.* [13], in a study on the role of the

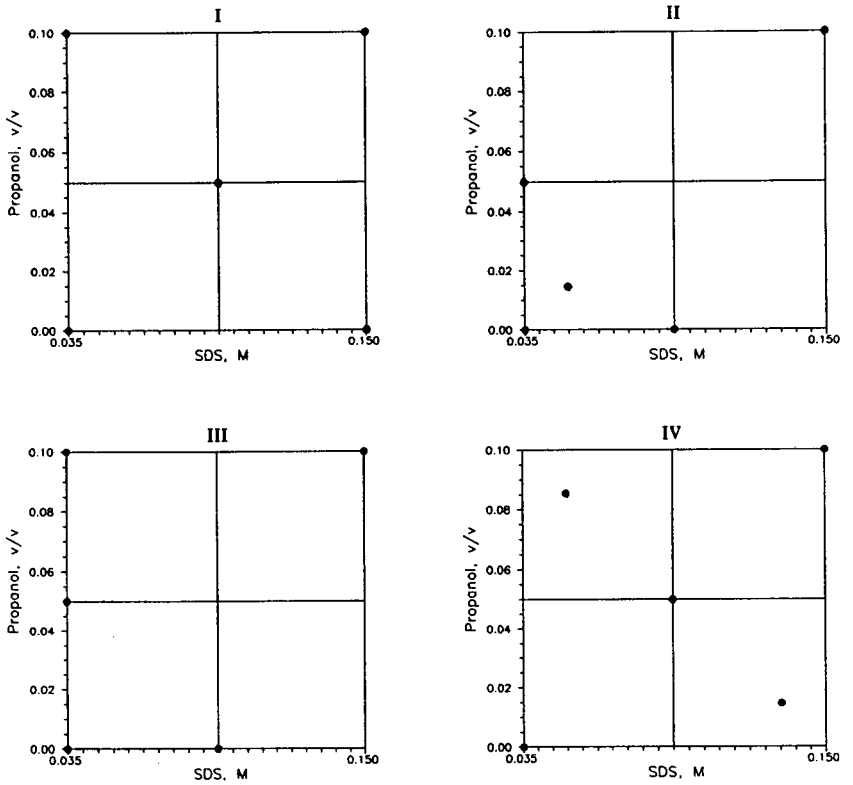

Fig. 2. Experimental designs used to check the retention equations in Table III.

organic modifier in MLC through the use of the free-phase equilibrium model and in correlation with the thermodynamic properties, concluded that, in the presence of a modifier, the retention mechanism is not the same as the mechanism governing aqueous MLC.

The addition of an organic modifier would change certain micellar properties, such as the cmc and the aggregation number of the surfactant, which may influence the retention behaviour of ionic compounds [17]. Also, the equilibrium of the solute is displaced away from the micelle towards the bulk aqueous phase, which becomes more non-polar [13]. On the other hand, the alcohol in the micellar mobile phase solvates the hydrocarbonaceous bonded phase and reduces the amount of sorbed surfactant on the stationary phase. This effect is larger with increasing concentration and hydrophobicity of the modifier [12,17,20]. With hybrid eluents, solute binding constants to micelles and their partitioning into the stationary phase both decrease as a result of the addition of the modifier. However, the K_{AM}/P_{SW} ratio increases and, therefore, the elution power of the mobile phase increases [13].

In the procedure of Strasters *et al.* [19] for predicting retention in hybrid micellar eluents, the retention is determined at five mobile phase compositions (μ,φ), four measurements at the corners of the selected two-dimensional parameter space and one measurement in the centre (see Fig. 2, design I). The extreme values of the parameters are dictated by the practical limitation of the chromatographic system: the lower surfactant concentration must be well above the cmc and must be strong enough to cause elution of all components. The upper surfactant concentration is determined by a combination of the solubility of the surfactant, the viscosity of the resulting mobile phase and the degradation of the efficiency at higher concentrations. The organic modifier concentration is limited to a maximum to ensure the integrity of the micelles. The square parameter space consists of four triangle subspaces. A separate linear model is determined for each of the four subspaces defined by three of the five measurements, *i.e.*, two corner points and the central point. Although it is not explicitly indicated, a different equation of the type

$$\log k' = A\mu + B\varphi + C \quad (4)$$

is fitted in each subspace. The calculation of the k' values is made by interpolation in the subspace where the coordinates belong. The scheme of interpolation followed is not very simple from a practical point of view.

The capacity factors of five catecholamines in thirteen micellar mobile phases, containing SDS and propanol at pH 6.8, are given in Table II. The concentration ranges studied were μ = 0.035–0.15 *M* and φ = 0–0.10 (v/v). The high k' values in mobile phases without propanol were due to the strong electrostatic attraction between the positively charged amine group and the negatively charged surface of the stationary phase. For the catecholamines, the same as with aminochromes and diuretics, when the experimental data were fitted according to eqn. 3 the value of the intercept $\log k'_0$ was smaller than the experimental value in the absence of propanol.

With the procedure of Strasters *et al.* [19], where five mobile phases are used for the calculation of k', large errors were obtained for catecholamines in the prediction of the k' values for the other eight mobile phases assayed. The errors were in the range 7–31% for noradrenaline, 11–37% for adrenaline, 0.4–39% for adrenalone, 9.8–38% for dopamine and 7.6–44% for isoprenaline.

Table III shows some possible models (equations) to describe the retention of the solutes. In these models the reciprocal of the capacity factor (eqns. a–e) and the logarithm of capacity factor (eqns. f–j) are related to the total concentration of surfactant and the volume fraction of modifier through linear and quadratic expressions. In some of them there is a term that includes both variables. The retention of catecholamines was used to evaluate the quality of the models. Five mobile phases were taken according to different experimental designs. Four of these designs are represented in Fig. 2, as an example of those examined. The data were fitted to each model and the errors in the prediction of k' for the

TABLE II

CAPACITY FACTORS OF CATECHOLAMINES IN SEVERAL MOBILE PHASES OF SDS (μ) AND PROPANOL (φ) AT pH = 6.8

Catecholamine	Mobile phase composition					
	Component	Concentration				
	SDS (M)	0.035	0.035	0.035	0.052	0.052
	Propanol (v/v)	0	0.05	0.10	0.015	0.085
		k'				
Noradrenaline		20.26	11.66	8.50	10.47	6.18
Adrenaline		26.54	11.85	8.24	11.63	6.16
Adrenalone		40.63	22.51	13.00	18.56	10.01
Dopamine		51.38	20.62	12.53	20.86	9.66
Isoprenaline		53.05	18.95	11.42	20.22	8.84
	SDS (M)	0.092	0.092	0.092	0.133	
	Propanol (v/v)	0	0.05	0.10	0.015	
		k'				
Noradrenaline		6.87	4.25	3.12	3.78	
Adrenaline		8.40	4.34	3.14	4.13	
Adrenalone		12.68	7.36	5.86	6.42	
Dopamine		15.86	7.07	4.82	7.14	
Isoprenaline		16.56	6.75	4.40	6.97	
	SDS (M)	0.133	0.150	0.150	0.150	
	Propanol (v/v)	0.085	0	0.05	0.10	
		k'				
Noradrenaline		2.23	3.98	2.56	1.88	
Adrenaline		2.20	5.01	2.55	1.92	
Adrenalone		3.99	7.68	3.91	3.08	
Dopamine		3.41	9.33	4.08	2.92	
Isoprenaline		3.23	9.82	3.75	2.64	

thirteen mobile phases were calculated, comparing the experimental and calculated k' values. The global mean relative errors for the five catecholamines and thirteen mobile phases are indicated in Table III.

The smallest errors were achieved with eqns. b and d with the experimental designs in Fig. 2 and with a large number of other experimental designs checked (more than 100). These equations are similar and contain a term including μ and φ. Equivalent coefficients (A–E) in both equations had almost the same value, and the coefficient of the φ^2 term in eqn. d was negligible compared with respect to the $\mu\varphi$ term. In addition, individual relative mean errors for each catecholamine were in most instances lower with eqn. b. Previously, a linear relationship between the reciprocal of k' and the concentration of modifier at a fixed surfactant concentration was suggested [21].

Fig. 3 shows the response surface k' *vs.* (μ,φ) according to eqn. b for noradrenaline. This surface is a slightly asymmetric hyperbolic section, the maximum of the function being located

TABLE III

DESCRIPTION OF THE RETENTION BEHAVIOUR AND GLOBAL MEAN ERRORS OBTAINED WITH THE FIVE CATECHOLAMINES AND THIRTEEN MOBILE PHASES

Relationship	Equation	Relative error (%) ($n = 65$)[a]			
		I	II	III	IV
$1/k' = f(\mu,\varphi)$	(a) $A\mu + B\varphi + C$	50.6	65.3	56.2	74.3
	(b) $A\mu + B\varphi + C\mu\varphi + D$	3.7	4.1	3.7	4.2
	(c) $A\mu + B\varphi^2 + C\varphi + D$	52.2	25.7	55.2	34.2
	(d) $A\mu + B\varphi^2 + C\varphi + D\mu\varphi + E$	3.1	8.1	3.2	4.3
	(e) $A\mu^2 + B\mu + C\varphi^2 + D\varphi + E$	1362	51.6	27.8	131.2
$\log k' = f(\mu,\varphi)$	(f) $A\mu + B\varphi + C$	17.3	16.8	17.5	13.1
	(g) $A\mu + B\varphi + C\mu\varphi + D$	17.3	14.2	15.3	13.0
	(h) $A\mu + B\varphi^2 + C\varphi + D$	12.6	39.7	14.1	13.9
	(i) $A\mu + B\varphi^2 + C\varphi + D\mu\varphi + E$	10.6	101.5	13.2	10.2
	(j) $A\mu^2 + B\mu + C\varphi^2 + D\varphi + E$	70.1	–[b]	8.6	–[b]

[a] Roman numbers correspond to the experimental designs in Figure 2.
[b] No results could be obtained.

at the lower surfactant and propanol concentrations.

Fig. 4 shows plots of the reciprocal of the capacity factor of noradrenaline *vs.* (a) SDS concentration for a constant propanol concentration and (b) propanol concentration for a constant SDS concentration. In Fig. 4, the lines correspond to the calculated data (eqn. b) and the points are experimental data. Good agreement between experimental and calculated data was observed. The capacity factor of noradrenaline decreased at increasing propanol volume fraction for each SDS concentration studied

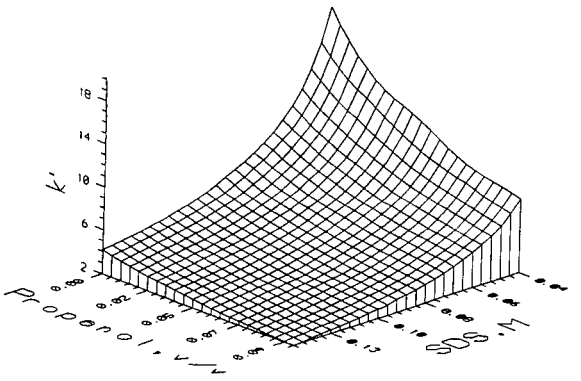

Fig. 3. Response surface k' *vs.* (μ,φ) for noradrenaline (according to equation b in Table III).

(Fig. 4b). However, this effect was attenuated as the surfactant concentration was increased, that is, the eluent strength of propanol decreased at increasing surfactant concentration. A similar observation was made previously for 2-ethylanthraquinone in SDS and several alcohols [21]. The same behaviour was observed with the surfactant (Fig. 4a), *i.e.*, the eluent strength of the surfactant decreased at increasing modifier concentration.

For the five catecholamines, the addition of 10% propanol to a 0.035 *M* SDS mobile phase led to relative diminution of the capacity factors by 58–78%. On the other hand, for purely micellar mobile phases, an increase in SDS concentration from 0.035 to 0.15 *M* led to a relative diminution of 81% for the five catecholamines studied. Consequently, it seems that in contrast to the usual behaviour described in the literature [13], for these compounds the eluent strength of the surfactant is the same as or even larger than that of the alcohol. This was due to the high affinity of the positively charged solute towards the negatively charged micelles at the working pH.

Fig. 5 represents the k' *vs.* (μ,φ) contour map for noradrenaline, following the procedure of Strasters *et al.* [19] and the proposed eqn. b.

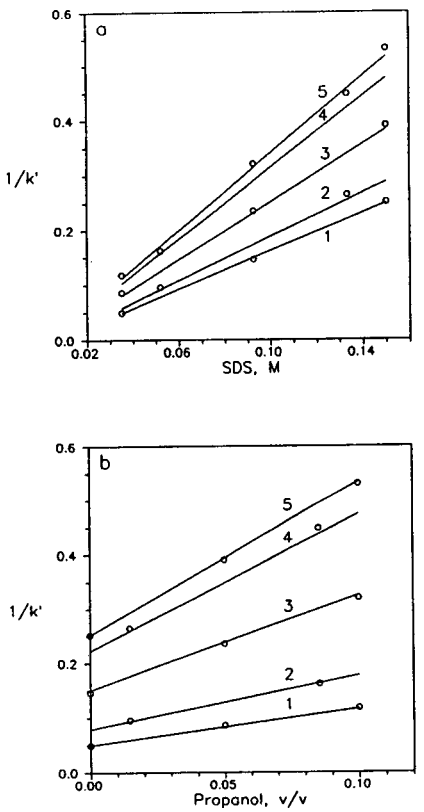

Fig. 4. Retention behaviour for noradrenaline: (a) $1/k'$ *vs.* μ plot for (1) 0, (2) 0.015, (3) 0.05, (4) 0.085 and (5) 0.10 (v/v) propanol; (b) $1/k'$ *vs.* φ plot for (1) 0.035, (2) 0.052, (3) 0.092, (4) 0.133 and (5) 0.150 *M* SDS. Solid lines represent theoretical curves obtained from eqn. b; circles correspond to experimental k' values.

Obvious differences between the contour lines for both models are observed for each k' value.

The calculated k' values according to eqn. b and design I (Fig. 2) are plotted in Fig. 6 against the experimental values for (a) the five catecholamines and thirteen mobile phases, (b) fifteen phenols and five mobile phases [19], (c) thirteen amino acids and five mobile phases [19], and (d) six aromatic compounds and fifteen mobile phases [13]. The equations of the fitted straight lines (linear least squares) were $k'_{calc} = 0.22 + 0.98\ k'_{exp}$ ($r = 0.998$) for catecholamines, $k'_{calc} = 0.05 + 1.00\ k'_{exp}$ ($r = 0.998$) for phenols, $k'_{calc} = -0.41 + 1.05\ k'_{exp}$ ($r = 0.9996$) for amino acids and $k'_{calc} = 0.24 + 0.99\ k'_{exp}$ ($r = 0.996$) for the diverse aromatic compounds. The proximity of the slope to unity and the low intercept revealed the absence of systematic errors. The z value test

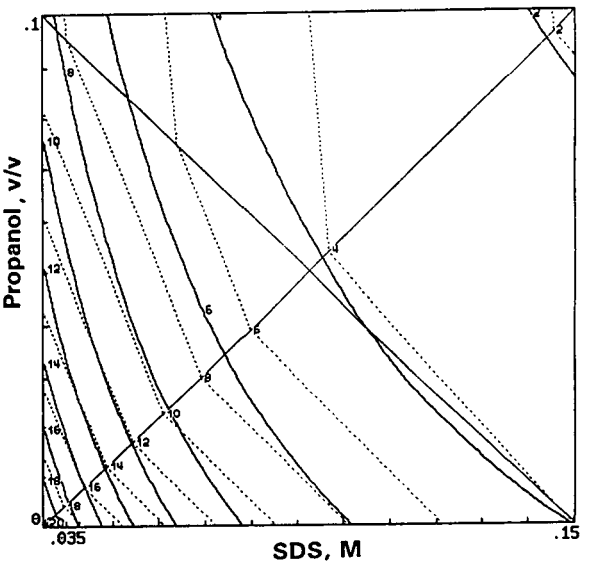

Fig. 5. Contour map k' *vs.* (μ,φ) for noradrenaline, (solid lines) according to eqn. b and (dashed lines) according to Strasters *et al.* [19]. The k' values are indicated on the lines.

for comparing individual differences was also applied [22]. No significant differences existed between the calculated and experimental values.

CONCLUSIONS

The procedure developed by Strasters *et al.* [19] for predicting retention in hybrid micellar eluents requires four different eqns., one for each established subspace. The retention behaviour of a solute in any micellar mobile phase (at any concentration of surfactant and modifier) should preferably be described by a single equation.

The studies performed with the elution data for catecholamines, obtained by us and the elution data for several aromatic compounds, obtained by Tomasella *et al.* [13], indicated that at least for these compounds the retention behaviour in a micellar mobile phase containing an alcohol did not follow a linear log k' *vs.* (μ,φ) model. It was not possible to check this behaviour with phenols and amino acids, as only the elution data in five mobile phases were available.

Several equations and different experimental designs showed that the best results were obtained with an equation of the type $1/k' = A\mu +$

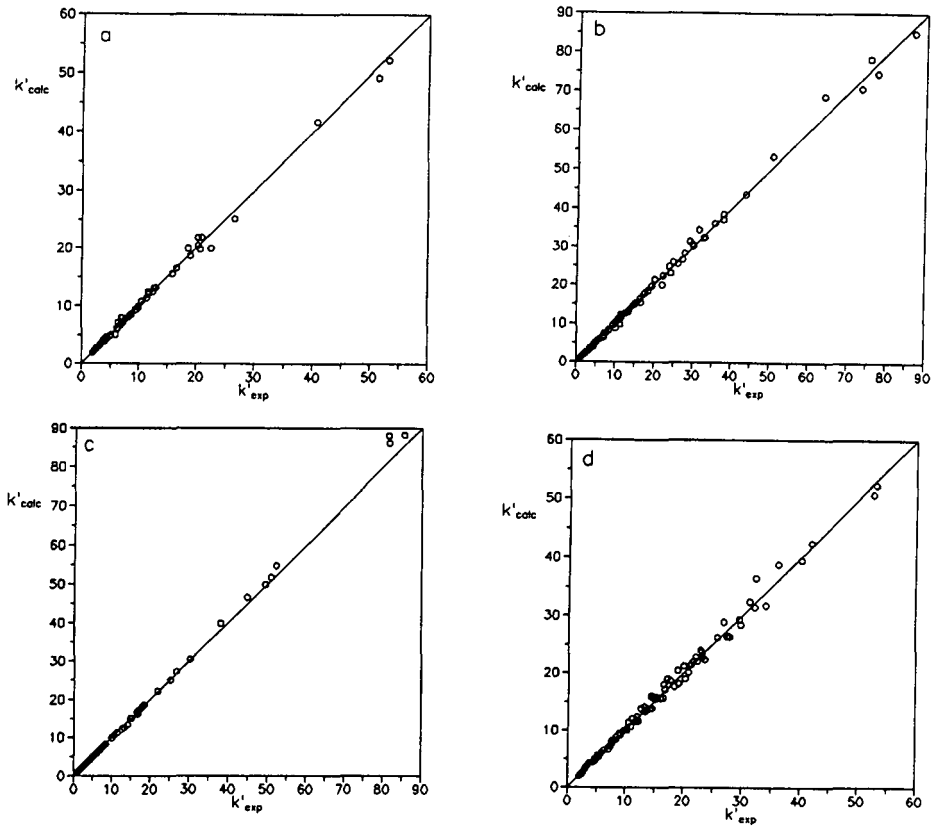

Fig. 6. Calculated k' *vs.* experimental k' values according to eqn. b and design I (Fig. 2) for (a) five catecholamines and thirteen mobile phases, (b) fifteen phenols and five mobile phases [19] (c) thirteen amino acids and five mobile phases [19] and (d) six aromatic compounds and fifteen mobile phases [13].

$B\varphi + C\mu\varphi + D$. This equation was valid for different solutes (catecholamines, amino acids, phenols and other aromatic compounds). The modelling of the retention behaviour is useful for the optimization of resolution in the separation of several compounds, using the elution data for a reduced number of mobile phases. However, more work is necessary on the optimum experimental design.

ACKNOWLEDGEMENT

This work was supported by the DGICYT, Project PB91/629.

REFERENCES

1 D.W. Armstrong and S.J. Henry, *J. Liq. Chromatogr.*, 3 (1980) 657.
2 M.J. Medina Hernández and M.C. García Alvarez-Coque, *Analyst*, 117 (1992) 831.
3 D.W. Armstrong and F. Nome, *Anal. Chem.*, 53 (1981) 1662.
4 M. Arunyanart and L.J. Cline Love, *Anal. Chem.*, 56 (1984) 1557.
5 J.P. Foley, *Anal. Chim. Acta*, 231 (1990) 237.
6 F.G.P. Mullins and G.F. Kirkbright, *Analyst*, 109 (1984) 1217.
7 Y.-N. Kim and P.R. Brown, *J. Chromatogr.*, 384 (1987) 209.
8 F. Palmisano, A. Guerrieri, P.G. Zambonin and T.R.I. Cataldi, *Anal. Chem.*, 61 (1989) 946.
9 E. Bonet Domingo, M.J. Medina Hernández, G. Ramis Ramos and M.C. García Alvarez-Coque, *Analyst*, 117 (1992) 843.
10 P. Yarmchuck, R. Weinberger, R.F. Hirsch and L.J. Cline Love, *J. Chromatogr.*, 283 (1984) 47.
11 J.G. Dorsey, M.T. DeEchegaray and J.S. Landy, *Anal. Chem.*, 55 (1983) 924.
12 M.G. Khaledi, E. Peuler and J. Ngeh-Ngwainbi, *Anal. Chem.*, 59 (1987) 2738.
13 F.P. Tomasella, J. Fett and L.J. Cline Love, *Anal. Chem.*, 63 (1991) 474.

14 J. Sabater Montesinos, M.C. García Alvarez-Coque, G. Ramis Ramos and J.J. Laserna Vázquez, *Quím. Anal.*, in press.
15 P.J. Schoenmakers, H.A.H. Billiet and L. de Galan, *J. Chromatogr.*, 205 (1981) 13.
16 P.R. Haddad and S. Sekulic, *J. Chromatogr.*, 392 (1987) 65.
17 M.G. Khaledi, J.K. Strasters, A.H. Rodgers and E.D. Breyer, *Anal. Chem.*, 62 (1990) 130.
18 R.M. Villanueva Camañas, J.M. Sanchis Mallols and G. Ramis Ramos, unpublished results.
19 J.K. Strasters, E.D. Breyer, A.H. Rodgers and M.G. Khaledi, *J. Chromatogr.*, 511 (1990) 17.
20 M.F. Borgerding, W.L. Hinze, L.D. Stafford, G.W. Fulp, Jr. and W.C. Hamlin, Jr., *Anal. Chem.*, 61 (1989) 1353.
21 M.F. Borgerding, R.L. Williams, W.L. Hinze and F.H. Quina, *J. Liq. Chromatogr.*, 12 (1989) 1367.
22 D.L. Massart, B.G.M. Vandeginste, S.N. Deming, Y. Michotte and L. Kaufman, *Chemometrics: a Textbook*", Elsevier, Amsterdam, 1988, Ch. 3.

Journal of Chromatography, 639 (1993) 97–115
Elsevier Science Publishers B.V., Amsterdam

CHROM. 24 994

Implementation and use of gradient predictions for optimization of reversed-phase liquid chromatography of peptides

Practical considerations

Niklas Lundell*

Institute of Chemistry, Department of Analytical Chemistry, Uppsala University, P.O. Box 531, 751 21 Uppsala (Sweden)

(First received May 22nd, 1992; revised manuscript received February 11th, 1993)

ABSTRACT

The options in the implementation of gradient theory for optimization work are critically reviewed and evaluated for the case of the reversed-phase liquid chromatography of peptides. Various models are covered together with methods for the determination of model parameters. Approaches for calculating retention times and band widths from experimental data are discussed. Different kinds of extrapolation are compared with interpolation. This study was aimed at finding the best compromise between number of experiments, accuracy of predictions and simplicity of calculations. Implementation and the use of gradient predictions can be simple, and practical recommendations are given.

INTRODUCTION

The retention of peptides in reversed-phase liquid chromatography is extremely sensitive to the concentration of organic modifier in the mobile phase [1–5]. It is unusual that a peptide sample can be separated with a reasonable range of retention by isocratic elution. Separation of peptides by reversed-phase liquid chromatography is performed almost exclusively by gradient elution.

The theory of gradient elution is well established [6–8]. From the theory it is clear that the selectivity may vary with gradient slope. This is also commonly the case for peptides and proteins [4,9,10], and the general rule of thumb, that the resolution between all peaks will increase with increased gradient time, is not valid. Retention predictions based on gradient theory therefore emerges as a powerful tool for optimization in the reversed-phase chromatography of peptides, requiring few experiments.

Predictions based on gradient theory are generally highly accurate. In this work the relevant options that exist in the implementation and application of gradient theory are reviewed and evaluated. Four aspects are considered: the accuracy of predictions, the complexity of calculations, the necessary knowledge of the sample and the chromatographic system and the amount of experimental work necessary for making predictions. Gradient theory is regarded here as a tool for optimization of the gradient profile, hence only the accuracy of the predictions is studied and not that of the model parameters themselves.

* Present address: PSQD, Bau 64/140, Hofmann-La Roche AG, CH-4002 Basle, Switzerland.

0021-9673/93/$06.00

The various formulations of gradient theory that have been published are critically examined. Practical recommendations for the implementation of gradient predictions for "real samples" are presented and discussed. The implementation and use of these predictions can be simple and this work will hopefully encourage more peptide chromatographers to use gradient theory.

THEORY

A complete presentation of gradient theory can be found in publications by Jandera and Churáček [8] and Snyder and Stadalius [6,7]. Only the final expressions and the underlying assumptions will be presented in this paper. The notation of Jandera and Churáček has mainly been followed and the symbols are listed at the end of the paper.

Retention volume

Most expressions of retention volume in gradient elution in reversed-phase liquid chromatography are based on a linear relationship between k' and concentration of organic modifier for isocratic elution:

$$\log k' = a - m\varphi \tag{1}$$

From theory based on various models of physical chemistry of chromatography it has been argued that a quadratic model is a more correct description [11,12], and non-linear relationships have also been observed [12–15]. Thorough discussions have resulted in the general opinion that the function is non-linear but can be approximated by a linear function in k' range where most of the migration occurs ($1 < k' < 10$) [13,15–18]. Several workers have also found that they can obtain accurate predictions of retention for peptides and amino acids using expressions based on this assumption [2,19–23]. From a practical point of view, a linear function is advantageous as calculations based on a non-linear model are complex and require more experiments [15,24–26].

Several attempts have been made to relate the parameters a and m to solute properties such as molecular mass and hydrophobicity, but with only limited success [2–4,7,27–29]. In addition, most samples contain solutes for which these properties are unknown, making this approach restricted in application. A correlation between a and m has been sought, again with mixed results [15,30]. In practice, a and m have to be determined experimentally for all solutes in a sample.

Several ways to describe a linear gradient have been given in the literature. The different terms "slope", denoted B, used by Jandera and Churáček, "steepness", b, used by Snyder's group, and "rate", s, can be confusing; see Table I for an explanation. This disparity has been pointed out and discussed by Jandera and Churáček [8,17]. These parameters are related to one another as follows:

$$b = V_m mB = V_m m(s/F) \tag{2}$$

In this paper, the parameter B will mainly be used and all gradients will be considered as linear:

$$\varphi = \varphi_0 + BV \tag{3}$$

On the basis of eqns. 1 and 3, the following expression for the retention volume can be derived [6,8]:

$$V_g = \frac{1}{mB} \cdot \log (2.3 V_m mB k_0' + 1) + V_m \tag{4}$$

where k_0' is k' at the starting concentration of organic modifier;

$$k_0' = 10^{a - m\varphi_0} \tag{5}$$

The gradient is inevitably preceded by an isocratic step, because it takes some time for the gradient to reach the column. The following expression includes migration during the passage of the dwell volume [8,31]:

$$V_g = \frac{1}{mB} \cdot \log (2.3 V_{mg} mB k_0' + 1) + V_m + V_d \tag{6}$$

where V_{mg} is the part of the dead volume where gradient elution occurs. V_{mg} is given by

$$V_{mg} = V_m - \frac{V_d}{k_0'} \tag{7}$$

The only assumption for k_0' in eqn. 6 is that it should be larger than V_d/V_m, otherwise the solute

TABLE I

SIMILAR TERMS DESCRIBING LINEAR GRADIENT

Name	Symbol	Unit	Meaning/advantage/disadvantage
Rate	s	%/min	Change in concentration of organic modifier per unit time. Constant rate means constant gradient time if the starting and final concentration are fixed. Most chromatographers find this measure most natural. Selectivity, retention time and volume will change if the flow is altered, even if the rate is constant
Slope	B	%/ml	Change in concentration of organic modifier per unit volume. Constant slope gives constant selectivity and retention volume (but not retention time). A specified slope says nothing about gradient time
Steepness	b	–	Apparent slope, the "acceleration" of a solute as it migrates through the column. Band width and other separation characteristics are directly related to this, more fundamental, parameter. The steepness is solute dependent; it will not be the same for all solutes eluted with the same gradient. This parameter is also conceptually difficult

will reach the detector before the gradient. If the product $2.3V_{mg}mBk_0'$ is large, the following approximation can be made [2,7,9]

$$V_g = \frac{1}{mB} \cdot \log (2.3V_{mg}mBk_0') + V_m + V_d \quad (8)$$

The latter expression has the benefit of simplifying the parameter fitting (see later description). Note that migration during the dwell volume is still acknowledged.

Band width

In isocratic elution, the band width is dependent on plate number, capacity factor and dead volume, leading to the following expression:

$$W_b = \frac{4V_m}{\sqrt{N}} \cdot (k' + 1) \quad (9)$$

In gradient elution it is generally assumed [6,32] that the band width is dependent on the capacity factor when the compound leaves the column, k_f', apart from plate number and dead volume. This gives

$$W_{bg} = \frac{4V_m}{\sqrt{N}} \cdot (k_f' + 1) \quad (10)$$

where W_{bg} is the band broadening arising from the gradient elution. k_f' is given by [6]

$$k_f' = 1/[2.3V_m mB + 1/(k_0')] \quad (11)$$

As the migration of the tail of the peak is faster than that of the centre, and *vice versa* for the front, bands will be compressed. A peak compression factor, G, has been introduced [33], giving rise to a slightly different expression for W_{bg}, namely

$$W_{bg} = \frac{4V_m}{\sqrt{N}} \cdot (k_f' + 1)G \quad (12)$$

An explicit expression for this peak compression has been derived [34]:

$$G^2 = \frac{1 + p + \frac{p^3}{3}}{(1+p)^3} \quad (13)$$

where the parameter p is given by

$$p = 2.3V_m mB \cdot \frac{k_0'}{k_0' + 1} \quad (14)$$

In some papers, an expression based on the capacity factor when the solute has migrated half way through the column, $\bar{k}$, is used [1,35], leading to a different form of eqn. 10:

$$W_{bg} = \frac{4V_m}{\sqrt{N}} \cdot (\bar{k}/2 + 1) \quad (15)$$

Usually it is stated that [6,10,36]

$$\bar{k} = 1/1.15V_m mB \quad (16)$$

which is based on the assumption that $1/k_0'$ is much smaller than $1.15V_m mB$. The full expression is [7,37]

$$\bar{k} = 1/[1.15V_m mB + 1/(k_0')] \quad (17)$$

Hence eqns. 10 and 15 are equivalent when $1/k_0'$ is much smaller than $1.15V_m mB$, k_f' then becomes equal to $\bar{k}/2$ [36]. When this assumption is not valid, eqn. 10 should be used [7].

When $V_m mB$ is <1, eqn. 13 can be simplified [7]:

$$G = (1 + \bar{k})/(2 + \bar{k}) \quad (18)$$

In some papers, an expression for W_{bg} is made from eqns. 15 and 18, which lead to a simple form [1,35]:

$$W_{bg} = \frac{2V_m}{\sqrt{N}} \cdot (\bar{k} + 1) \quad (19)$$

Note that eqns. 15–19 are all various approximations of the more general expressions seen in eqns. 12–14.

It has been observed that the model for band width gives an underestimate at high values of $V_m mB$ [6,35,38]. Possible causes for this have been thoroughly discussed, without any satisfactory explanation [22]. To compensate for this deviation, an empirical correction factor, J, has been introduced [35]:

$$W_{bg} = J \cdot \frac{4V_m}{\sqrt{N}} \cdot (k_f' + 1)G \quad (20)$$

J has been presented as an empirical polynomial based on experimental data [35]:

$$J = 0.99 + 1.70(V_m mB) - 1.35(V_m mB)^2 + 0.48(V_m mB)^3 - 0.062(V_m mB)^4 \quad (21)$$

In later work by Dolan *et al.* [39], the following correction was used:

$$JG = 1.1 \quad (22)$$

Analogously to the retention volume, one can include the band broadening that takes place during the dwell volume. This leads to [8]

$$W_b = \sqrt{\frac{V_{mi}}{V_m} \cdot W_{bi}^2 + \frac{V_{mg}}{V_m} \cdot W_{bg}^2} \quad (23)$$

where V_m is replaced by V_{mg} in eqns. 11, 14, 20 and 21. W_{bi}, the isocratic band broadening in the starting mobile phase, is given by

$$W_{bi} = \frac{4V_{mi}}{\sqrt{N}} \cdot (k_0' + 1) \quad (24)$$

where V_{mi} is the part of the dead volume where migration occurs isocratically and is given by

$$V_{mi} = V_m - V_{mg} \quad (25)$$

The benefit of approximations

Long mathematical expressions are not practical as they obscure the basic relationships and are tedious to calculate manually. Approximations make long expressions short, hence their popularity. Today calculations are made by computers, and the need for approximations is smaller. Approximations are, however, still meaningful if they can speed up numerical methods, or even better, allow the calculations to be made by a non-iterative procedure. With the assumption of a linear relationship between log k' and φ (eqn. 1), the calculations of retention and band broadening from the parameters of the model are simple. The full expressions (eqns. 6 and 23) should therefore be used. The determination of a and m from gradient runs is more difficult, but with the assumption that $2.3V_{mg}mBk_0'$ is large it is simple (see later discussion). In contrast, there is no benefit in making an approximation for band width, as the plate number can be determined using eqn. 23, as will be shown below.

PARAMETER ESTIMATION

Dead volume, V_m

In the literature, there are various opinions on what exactly the dead volume is and how it should be determined experimentally [40–42]. A recent survey by Maliek and Jinno [43] revealed both controversy and confusion. Several comprehensive reviews have also been published (*e.g.*, ref. 44). In the gradient optimization, the method for determining V_m should be simple and rapid and result in accurate predictions, and does not necessarily have to give the "true" dead volume. It has also been shown that gradient

predictions are not very sensitive to errors in the dead volume [24]. The most common methods are (1) to measure the elution volume for a non-retained solute, "markers" (*e.g.*, refs. 45 and 46), (2) to measure the elution volume for a deuterated mobile phase component, typically D_2O (*e.g.*, refs. 42, 46 and 47) or (3) to measure the retention volume for a set of homologues and then do the determination by a parameter fit based on a thermodynamic model (*e.g.*, refs. 46–49). For practical reasons the first method is preferred, as a detector measuring refractive index is needed in the second method and the third method is too time consuming. The choice of non-retained solute is not obvious, and both inorganic salts and organic compounds have been suggested. Anions have the disadvantage of being excluded from parts of the mobile phase by negatively charged silanol groups, whereas cations are retained [45]. Neutral polar organic solutes seem more promising and in this work the often recommended uracil [44–46] was used.

It is also possible to determine the dead volume by data fitting, as a parameter in the model for retention volume. If the parameters a and m are unknown, which is the usual case, this means that at least three gradients have to be run. As the dead volume can be determined in a matter of minutes this is not a practical alternative, and it is better to use extra gradients for estimation of the dwell volume, as will be described below.

It has been indicated that the accessible volume is reduced if the size of the peptide is close to or larger than the pore size [2,37]. On the other hand, in the work by Larmann *et al.* [50], no difference in retention for large molecules was seen when columns with various pore sizes were used. This indicates that large molecules can reach all parts of the mobile phase in the column. By using columns with large pores (>100 Å) the potential difference is minimized [2,10]. In addition, large pores also promote high plate numbers [51–54] and recoveries of peptides [51,55]. It would also be difficult to determine individual dead volumes, so in practice the dead volumes must be assumed to be equal.

The dead volume, V_m, is dependent on the concentration of organic modifier [42,47,56]. In this work, V_m was determined at two concentrations of organic modifier for comparison. It has also been shown that the elution volume for the non-retained solutes is affected by flow-rate, temperature and amount of solute [45,46]. The determination of V_m should therefore be done at the same temperature and flow-rate as the calibration gradients. The influence of the amount of solute on the elution volume is not very pronounced for uracil [45], which is one reason for its popularity. To check this, the elution volume of uracil was determined with two different amounts of uracil, differing by a factor of 100.

A rough estimate of V_m can be made by assuming that V_m is a fixed proportion of the column volume [57]. This option was not evaluated as a meaningful test would have to involve several columns and also the gain in time is small, as V_m can be estimated within a few minutes.

Dwell volume, V_d

An incorrect estimate of the dwell volume is a common source of error in gradient predictions [21,25,57,58]. There are two experimental methods for estimation that can be regarded as reliable. One approach is to run a slow gradient of a UV-absorbing solution, without a column [27,58]. The dwell volume is then calculated as

$$V_d = V_{1/2} - \frac{1}{2}V_G \quad (26)$$

where $V_{1/2}$ is the volume when the absorbance has reached half its maximum value and V_G is the gradient volume. The other approach is to use more than two calibration gradients, with different slopes. The dwell volume is determined, together with the parameters a and m, by a fitting routine [22,23,58]. In this work the two methods are compared regarding the accuracy of absolute retention and difference in retention between two solutes.

Model parameters, a and m

The model parameters a and m can be determined from calibration gradients by some kind of parameter fitting. The key question is whether $\log (2.3V_m mBk_0' + 1)$ can be approxi-

mated by log $(2.3V_m mBk_0')$, *i.e.*, if eqn. 8 can be used. The two cases lead to different parameter fitting routines, as described in a later section. In this work the parameter fitting was made for both cases, at different values of $2.3V_{mg}mBk_0'$ to establish when the approximation is valid.

Plate number, N

The plate number is usually determined for a small organic molecule, *e.g.*, naphthalene, eluted isocratically with $k' > 3$ with a high concentration of an organic modifier of low viscosity. The plate number that the manufacturer sends with a new column is typically determined in this way as the method gives a high estimate of the plate number. This method of estimating plate numbers will below be referred to as "the conventional isocratic method".

It is important to realise that the plate number is not a given constant for a specific column. It depends on several variables, of which the following are of interest in this context: diffusion rate of the individual components; viscosity of the mobile phase; capacity factor; and flow-rate.

It has been pointed out that the plate number generally is lower when working with peptides, at conventional flow-rates, than when working with small organic molecules [1,4]. The reason for this is the slow diffusion of macromolecules such as peptides [1,36]. The diffusion rate is related to the molecular mass and as peptides can have a broad range of molecular masses, the plate number will vary among peptides [4]. The diffusion rate is also dependent on the solvent. In the reversed-phase liquid chromatography of peptides, acetonitrile is the organic modifier most commonly used. The most popular alternative, 2-propanol [59–61], has a much higher viscosity, giving a lower plate number. The plate number is also related to k' [1,62], which is dependent on gradient slope and solute. In addition, the plate number is also a function of flow-rate, described by, for example, the Knox equation [63]:

$$h = A\nu^{1/3} + B\nu + C\nu \quad (27)$$

As peptides have low diffusion rates, the mass transport term, the C term, in the Knox equation will be large and the highest plate number will be obtained at an unusually low flow-rate [1,4] (the choice of flow-rate will be discussed later).

Despite the differences in plate number, band widths are usually comparable for solutes eluted with the same gradient slope, because band width is related both to the plate number and the parameter m, the latter generally increase with increasing molecular mass. This leads to the impression that the variation in plate number is smaller than it actually is. The prediction of band width relies on the estimate of the plate number, and it is therefore essential to consider as many factors as possible in order to maximize the accuracy of predictions.

Based on extensive approximations, expressions have been derived that relate the parameters B and C in the Knox equation to molecular mass and the structural state of the peptide (native/denatured), particle and pore size of the packing material and viscosity of the mobile phase [64]. This approach to the estimation of plate number has the advantages that the variation of plate number with flow-rate can be predicted and that non-ideal band broadening can be detected. Further, this model can aid in the design and evaluation of column materials. However, this model has limited applicability for optimization of separation involving samples of unknown composition as the solute characteristics and Knox parameter A have to be known.

The plate number can instead be determined experimentally from the same gradient runs that are used for estimating a and m. In comparison with the conventional isocratic method for plate number estimation, this method is superior as the determination is made for the organic modifier that its actually used and individual plate numbers can be assigned to the solutes that are separated. In addition, no information is required about the solute or column characteristics and some degree of non-ideal band broadening can be included, making this approach more useful for optimization than the mechanistic model discussed above. However, variations in flow-rate and k' are not accounted for by this approach. It must also be noted that this method

requires that the band width can be measured for all solutes in the sample (see next section).

It is possible that the overestimate of the number of plates made by the conventional isocratic method can be compensated for by a certain correction factor for band width (see Theory). This is a weak argument for the conventional isocratic method, as the difference between the two methods can vary over a wide range, and a correction factor can both over- and under-compensate for an incorrect estimate of plate number.

For comparison, the plate number was determined in this work both by the conventional isocratic method and individually from calibration gradients. For one peptide the plate number was determined with two organic modifiers for a further comparison.

Retention volume, V_g, and band width, W_b

Accurate measurements of the retention volumes for the peaks in the calibration gradients are important in gradient modelling. To determine plate number from calibration gradients, as presented above, the band widths also have to be measured. Determinations of retention volumes and band widths are the initial and most crucial steps in gradient predictions. This can be a difficult problem [65] as evaluation by commercial integrators is often far from perfect [66,67]. Neither do all integrators measure band widths. The problem is not so severe as long as the peaks do not overlap. It is unusual, however, for all solutes to be well separated in the calibration gradients. The overlap of peaks will affect both the determination of retention time (the peak maxima are not equivalent to the retention times), and band width. Incorrect measurements of retention times are a source of significant errors in gradient predictions [39,57].

The problem can be solved, however, by deconvolution of the peaks. Deconvolution means that the overlapping peaks are separated into individual peaks by mathematical methods. Deconvolution can be done without any assumption of peak shape if a diode-array detector is used and the spectra of the non-resolved solutes are different [68–70]. Diode-array detectors are not available in all laboratories and the very advanced deconvolution software is even more scarce. The alternative is to fit a mathematical model to the peaks. Fitting routines for gaussian models are available in many computer-based evaluation programs or can easily be implemented, which was done in this work. Tailing, non-gaussian peaks are sometimes observed owing to secondary interactions [71,72], although gradient elution promotes symmetrical peaks [6]. If tailing peaks are present, the first action should be to alter the chromatographic conditions to prevent tailing, *e.g.*, by increasing the ionic strength [5,73–76] or by adding amines that can block silanol groups [35,77–79] or by altering the pH [5,61,74]. Unfortunately, the tailing can persist. This situation is difficult to handle as their is no simple model for the peak shape and gradient theory does not include tailing. The "brute force" method is to use a gaussian model giving an overestimated band width. The solute will then be predicted to give wide gaussian peaks instead of tailing peaks. This is an incorrect prediction, but still better than if a plate number based on the conventional isocratic method was used.

Choice of calibration gradients

From a small number of gradient runs the parameters a and m can be estimated and results predicted. If V_m and V_d are known, two calibration gradients are sufficient [2,7,37]. To be able to perform calibration it is crucial that the peaks of each solute in the different calibration gradients are matched, so-called peak tracking. The use of three calibration gradients makes this task easier [10,80,81]. Apart from giving more information in general, the use of three calibration gradients also makes it possible to test whether a peak match hypothesis is correct. This is done by determining the parameters a and m from two gradients, and then predicting the third gradient. An incorrect peak match will show up as a large error in the predicted chromatogram. Peak matching is critical in calibration, as mismatched peaks can lead to gross errors in the predictions.

It has been recommended that the slopes of the calibration gradients used should differ by a factor of three or four in order to obtain good

accuracy in the determination [57]. In peptide separations the selectivity often changes with the gradient slope. This makes it difficult to match peaks as the retention order may be very different in the calibration gradients [10]. In optimization work it is practical to restrict oneself to a narrower span of gradient slopes. The consequence is that extrapolation is often unavoidable in predictions for optimization purposes. The influence of extrapolation on the accuracy of predictions was studied in this work.

The calibration gradients must have different slopes, B, or s/F, and the question then arises of whether one should vary the gradient rate [19,20,39] or the flow-rate [10].

The purpose of using gradient theory for optimization is to save experiments and time. It has been shown that for a given gradient slope (%/ml) the peak capacity is at its maximum at a fairly low flow-rate [13,36,82], corresponding to the maximum plate column. This might lead to the conclusion that one should operate at a low flow-rate. However, for a fixed gradient time the maximum peak capacity is obtained at a high flow-rate, as this will result in a gradient with a smaller slope, *i.e.*, resolving more peaks [4,29,83]. The decrease in the plate number is then counteracted by the decreased slope. In other words, when time is important one should work at a high flow-rate and vary the gradient rate for the calibration gradients. The upper limit of flow-rate is usually set by pressure limitations, and many chromatographers find it inconvenient to work at flow-rates higher than 1.0 ml/min for a column of I.D. 4–5 mm. A constant flow-rate in the calibration gradients also means that one source of variation in the plate number is eliminated. It has further been reported that short gradient times and high flow-rates result in high recoveries [13,84,85]. Predictions based on calibration gradients where the gradient rate is varied lead to more accurate results as opposed to variations in flow-rate [22]. The conclusion is, in contradiction to some earlier statements [2,7,10], that the flow-rate should be kept high and constant and that the slope should be varied by alterations in the gradient rate.

METHODS FOR PARAMETER FITTING

Retention volume: the simple method

If V_m and V_d are known and $2.3V_{mg}mBk'_0$ is large, the parameters a and m can be determined from two calibration gradients [2,37] without having to employ numerical methods (if φ_0 is constant):

$$m = \frac{\log(B_1/B_2)}{V_{g1}B_1 - V_{g2}B_2 + (V_m + V_d)(B_2 - B_1)} \quad (28)$$

$$a = \log\,(10^{mB_i(V_{gi}-V_d-V_m)} + 2.3mB_iV_d) + m\varphi_0 - \log\,(2.3V_mmB_I) \quad (29)$$

Note that $2.3V_{mg}mBk'_0$ does not have to be large for the gradients that are to be predicted; eqn. 6 can then be used. The most effective way of keeping $2.3V_{mg}mBk'_0$ large is to start the calibration gradients at a very low content of organic modifier. It is advisable to verify that the assumption is valid after a and m have been estimated. (Obviously the value of $2.3V_{mg}mBk'_0$ is dependent on the estimation of a and m, but a rough estimate of $2.3V_{mg}mBk'_0$ can be made as long it is larger than about 5).

A third gradient, preferably with an intermediate slope, can be used to verify the peak matching. It is possible to improve a rough estimate of V_d by repeating the determination of a and m with different dwell volumes and look for the best fit of the predicted and actual chromatograms for the third gradient [58]. However, the more general and "automatic" method described below is more practical if one wants to use the third gradient for V_d determination.

Retention volume: the advanced method

A more advanced method for parameter fitting is necessary when $2.3V_{mg}mBk'_0$ is small or if one wants to determine V_d by fitting and/or use all three gradients to determine a and m. This calls for a non-linear fitting method. Several methods are well established and are published with program codes [86]. The fitting is best done in two steps, starting by estimating a, m and V_d for every solute. V_d is then taken as an average of all estimates, as it is not solute dependent, and a

new estimate is made of a and m, now keeping V_d fixed. A non-linear fitting routine can, of course, be used even if $2.3V_{mg}mBk'_0$ is large, making this method more general.

Calculating plate number from calibration gradients

Individual plate number for each solute can easily be determined from eqn. (23) if band widths have been measured. From eqn. 23, N can be expressed as

$$N = \frac{16}{W_b^2} \cdot \left\{ \frac{V_{mi}}{V_m} \cdot [V_{mi}(k'_0 + 1)]^2 + \frac{V_{mg}}{V_m} \cdot [V_{mg}(k'_f + 1)JG]^2 \right\} \quad (30)$$

Note that all necessary parameters on the right-hand side can be calculated from the parameters given in the model of the retention volume.

EXPERIMENTAL

Column

A 10-cm × 4 mm I.D. Sephasil C_{18} column (Pharmacia–LKB Biotechnology, Uppsala, Sweden) was used. The column matrix consisted of 5-μm silica with a pore size of 125 Å.

Instrumentation

A system consisting of a Model 2249 low-pressure mixing gradient pump, a Model 2141 dual-wavelength detector (Pharmacia LKB Biotechnology) and a CMA Model 200 autoinjector (CMA Microdialysis, Stockholm, Sweden) was used. The instrumentation was interfaced with an IBM AT3 personal computer for gradient control and data acquisition.

Software

Evaluation of chromatograms, gradient modeling and prediction were all made with in-house software written in the programming environment ASYST (Asyst Software Technologies, Rochester, NY, USA). A modified Gauss–Newton algorithm was used for fitting gaussian models to the chromatograms. The data fitting was done with a simplex algorithm.

Chemicals

Acetonitrile and 2-propanol were of HPLC gradient grade (Merck). Distilled waster was purified using a Milli-Q system (Millipore, Bedford, MA, USA) fitted with an Organex-Q cartridge. Phosphoric acid and ammonia were of analytical-reagent grade (Merck).

Peptides

The synthetic peptides used were kindly donated by Anders Winter at Pharmacia–LKB Biotechnology and are listed in Table II. All peptides were injected individually.

Gradients

Four gradient slopes, 0.5, 1.0, 2.0 and 4.0%/ml, were used. The buffer consisted of 50 mmol/l phosphoric acid adjusted to pH 2.8 with

TABLE II

PEPTIDES USED IN THIS WORK

No.	M_r	pI	Sequence
1	589	3.1	Met–Val–Asn–Pro–Glu
2	571	3.1	Tyr–Glu–Leu–Phe
3	626	8.4	Pro–Leu–Ile–His–Phe
4	1071	6.5	Thr–Pro–Ile–Pro–Arg–Tyr–Pro–Leu–Asp
5	1858	3.9	His–Thr–Asp–Arg–Glu–His–Thr–Ile–Glu–Thr–Asp–Glu–Met–Glu–Asp
6	1729	9.5	Lys–Tyr–Gly–Asn–Leu–Ser–His–Glu–Lys–Gln–His–Gln–Leu–Phe
7	1689	3.1	Gly–Asn–Gly–Gln–Asp–Val–Met–Ala–Leu–Ala–Thr–Ile–Leu–Ser–Trp–Leu
8	1722	9.6	Gln–Leu–Ser–Leu–Ala–Ile–Phe–His–Ser–Thr–Tyr–Trp–Lys–Ala–Gly

ammonia. Acetonitrile was used as organic modifier for all peptides. Peptide 3 was also eluted with 2-propanol gradients. The acetonitrile gradients started at 2 or 4% and the 2-propanol gradient at 1% of organic solvent.

RESULTS AND DISCUSSION

The retention data and estimates of a and m are given in Table III.

Measures of error

The prediction error for retention volume and difference in retention volume is expressed as a percentage of the gradient volume (not the retention volume!). The gradient volume refers to an imagined gradient going from 0 to 50% organic modifier, a common case in peptide separations, with the relevant slope. This measure is rationalized by the fact that in gradient elution the band width does not increase with increase in retention volume. Consequently, an error of for example 0.1 ml in the prediction of retention volume is of equal concern for solutes with small or large retention volumes. Absolute retention volume is also inappropriate as a measure of error as an error of, for example, 0.1 ml is more serious in a high slope gradient, where peaks are narrow. For band widths the relative error is used. The band width is roughly the same for all peaks and decreases with increasing slope, making a relative measure appropriate. In this paper the error is presented as the median and the 90% percentile. The 90% percentile indicates an upper level of the error.

Determination of dead volume, V_m, and dwell volume, V_d

The dead volume was determined by elution of uracil with two mobile phases containing 50% and 30% of acetonitrile. The amounts injected were 0.03 and 3.0 μg. From the results, given in Table IV, it is clear that the elution volume of uracil is lower with 50% of acetonitrile. This is observed for most dead volume markers [42,47,56]. Thus, the increase in elution volume for uracil on going from 50% to 30% of acetonitrile is probably not due to retention but to an actual change in dead volume. The effect of the amount of uracil on the elution volume is very small, although it is statistically significant ($P = 0.05$).

The determination of the dwell volume by parameter fitting was compared with determination employing a gradient of a UV-absorbing solution. The dwell volume was estimated to be

TABLE III

RETENTION DATA

Gradients with acetonitrile. The model parameters a and m are given with the standard deviation in parentheses based on the combination of calibration described under Results and Discussion.

Peptide	Retention volume (ml)								a	m ($\%^{-1}$)
	Starting concentration 2%				Starting concentration 4%					
	Gradient slope (%/ml)				Gradient slope (%/ml)					
	0.5	1.0	2.0	4.0	0.5	1.0	2.0	4.0		
1	11.55	8.70	6.69	5.29	7.72	6.56	5.52	4.65	1.98(0.14)	0.211(0.022)
2	37.12	22.46	14.07	9.23	33.20	20.47	13.07	8.75	3.38(0.05)	0.130(0.003)
3	35.72	21.36	13.31	8.78	31.71	19.39	12.33	8.25	3.71(0.08)	0.158(0.004)
4	36.75	22.28	13.98	9.20	32.81	20.30	13.00	8.73	3.34(0.05)	0.130(0.003)
5	38.17	21.92	13.25	8.58	33.97	19.87	12.27	8.06	5.39(0.21)	0.244(0.010)
6	24.56	15.15	9.89	6.90	20.54	13.19	8.90	6.37	3.65(0.14)	0.237(0.010)
7	74.15	40.57	22.89	13.59	70.07	38.58	21.90	13.09	6.79(0.13)	0.159(0.003)
8	46.87	26.23	15.36	9.58	42.64	24.12	14.35	9.09	6.78(0.32)	0.259(0.013)

TABLE IV

DETERMINATION OF DEAD VOLUME

The mobile phase consisted of acetonitrile mixed with 50 mmol/l phosphate buffer (pH 2.8). Each determination of V_m was repeated four times. The pooled standard deviation of V_m was 1.8 μl.

Concentration of acetonitrile (%)	Amount of uracil (μg)	V_m (μl)
30	0.03	808
30	3	809
50	0.03	750
50	3	754

2.10 ml from the gradient of a UV-absorbing solution. To find the dwell volume by fitting retention data to the model, more than two calibration gradients have to be made. The overall aim is to keep the number of experiments small, hence the use of three calibration gradients is of most interest. In this work, four different slopes were used, to allow predictions to be made for a gradient not used for calibration. To obtain a realistic situation a combination of three out of four gradients was first selected. For this combination V_d was first determined together with a and m. As one estimate is obtained for each solute, V_d was taken as the average for all solutes. The determination of a and m was then repeated using this V_d as fixed. This procedure was carried out for all combinations of calibration gradients. The average of all V_d estimates based on fitting was 2.47 ml, with V_m set at 0.809 ml.

To evaluate the effect on accuracy, V_g was predicted for the peaks in the gradient not used for calibration. This was repeated for all possible combinations of calibration gradients. It has been concluded by other workers that an error in the estimation of V_m has very little effect on the accuracy of the predictions of retention [24,25,57] and it can be seen in Table V that the variations in the V_m estimates indeed has only a small influence on the prediction error. The best result is obtained using the V_m determined with a mobile phase containing 30% of acetonitrile. This isocratic mobile phase is closer to the average mobile phase during gradient elution in the relevant range and a better estimate of V_m is therefore to be expected.

TABLE V

ERROR IN PREDICTION OF V_g FOR DIFFERENT ESTIMATES OF V_m AND V_d

Eqn. 6 was used for parameter fitting and prediction. The dwell volume was determined, together with the model parameters a and m, by parameter fitting. All combinations of three calibration gradients and starting concentration were considered. The measure of error is explained in the text.

V_m (μl)	Median error/90% percentile (% of V_G)	
	V_d by fit	V_d from UV-absorbing eluent gradient
808	0.40/0.84	0.82/1.51
809	0.40/0.84	0.82/1.51
750	0.40/0.84	0.91/1.69
754	0.40/0.84	0.90/1.68

It is clear that a V_d estimate based on fitting will improve the accuracy, a result that has also been obtained by others [22,23]. When estimating V_d by parameter fitting, the predictions also become less sensitive to small variations in the V_m estimate, as these variations are taken up by V_d. It should be emphasized that the determination of V_d by parameter fitting is sensitive to errors in retention volumes in the calibration gradients. However, as one estimate of V_d is obtained for each solute, the accuracy can be improved by evaluating as many solutes as possible.

Resolution is a more interesting parameter than absolute retention. The error in prediction of resolution is a function of the relative errors in band widths and difference in retention. Sources of prediction error that affect the retention of all solutes in the same direction will therefore have a minor effect on the predictions of resolution. For example, an error in V_d affects the predicted retentions in roughly the same way and the influence on resolution should be small in comparison with the influence on absolute retention.

To evaluate the effect of V_d on resolution, the differences in retention of four peak pairs were predicted and compared with actual values. The results are summarized in Table VI. One can

TABLE VI

ERROR IN PREDICTION OF DIFFERENCES IN V_g BETWEEN PEAK PAIRS FOR THE TWO METHODS FOR ESTIMATION OF V_d

Eqn. 6 was used for parameter fitting and prediction. The dead volume was set at 809 μl. All combinations of three calibration gradients and two starting concentration were considered, as described in the text. The eight peptides were divided into four pairs, *i.e.*, each combination of gradients resulted in four estimates of retention difference. The measure of error is explained in the text.

Method for determination of dwell volume	Median error/90% percentile (% of V_G)
Parameter fitting	0.31/0.68
UV-absorbing eluent gradient	0.36/1.22

conclude that the method for the determination of the dwell volume does not have a large effect on the accuracy for prediction of resolution, which is in agreement with statements made in earlier work [22,25]. The median error is almost the same for both methods but the 90% percentile is higher for the estimation of V_d by the use of a gradient of a UV-absorbing solution. These large errors corresponds to peak pairs that elute early and gradients where φ_0 is large. Under these conditions, the migration during the dwell volume, which is solute dependent, will be more pronounced.

Limit of the $2.3V_{mg}mBk'_0$ approximation

The simple data fit method is based on the assumption that $2.3V_{mg}mBk'_0$ is "large". To establish the limit for this approximation, a and m were determined, with and without this approximation. Predictions where made with eqn. 6, as the approximation is only meaningful in the parameter fitting. The difference between predictions based on fittings with the different models are treated as the error, and the results are presented in Table VII. Note that $2.3V_{mg}mBk'_0$ differs between different calibration gradients, and that only the smallest value is given in Table VII.

In this study, the error is roughly 0.4% of the gradient volume, which is about the same as reported previously [20,22,24,57] (although the error was then expressed as relative retention). In that perspective, one can tolerate a 2.3

TABLE VII

ERRORS IN PREDICTIONS OF V_g DUE TO THE $2.3V_{mg}MBk'_0 \gg 1$ APPROXIMATION IN THE PARAMETER FITTING

The dwell and dead volumes were set at 809 μl and 2.47 ml, respectively. The model parameters a and m were determined by parameter fitting. All combinations of calibration gradients and starting concentration were considered. The error is taken as the difference between predictions based on calibration with and without the approximation. The measure of error is explained in the text.

Peptide	Starting concentration			
	2%		4%	
	$2.3V_{mg}mBk'_0$	Median error/90% percentile (% of V_G)	$2.3V_{mg}mBk'_0$	Median error/90% percentile (% of V_G)
1	6	0.20/0.60	2	0.62/1.15
2	154	0.01/0.06	86	0.02/0.11
3	342	0.00/0.02	164	0.01/0.05
4	143	0.01/0.06	76	0.03/0.12
5	15 900	0.00/0.00	3 650	0.00/0.00
6	304	0.00/0.02	97	0.01/0.05
7	388 000	0.00/0.00	159 000	0.00/0.00
8	403 000	0.00/0.00	75 300	0.00/0.00

$V_{mg}mBk'_0$ value down to *ca.* 50, when using eqn. 8 for parameter fitting. Note that the error decreases with increasing value of m, the guideline given here is only valid for peptides and other solutes with large values of m.

Interpolation versus extrapolation and number of calibration gradients

When optimizing the gradient, it is likely that one wants to predict the result for gradients that are faster or slower than those used for calibration. The question is how far it is acceptable to extrapolate, and whether there is any difference in the accuracy for extrapolation to faster or slower gradients. Extrapolation is compared with interpolation for two and three calibration gradients in Table VIII.

Inherently, extrapolation gives rise to a larger error than interpolation. This has also been observed experimentally [25,39], but from Table VIII it can be seen that extrapolation to faster gradients yields a smaller error than extrapolation to slower gradients. Three calibration gradients give rise to a minor improvement and are also less sensitive to an error in a single retention volume. The practical consequence is that the extrapolation from the calibration gradients is acceptable if the calibration slopes are less than the slopes of the gradients one expects to predict. Low gradient slopes for calibration also simplify peak matching. However, it must be noted that an increase in the experimental error would have a much greater effect on extrapolation than interpolation.

TABLE VIII

ERROR IN PREDICTION OF V_g FOR INTERPOLATION AND EXTRAPOLATION WITH TWO AND THREE CALIBRATION GRADIENTS

The dead and dwell volumes were set at 809 μl and 2.47 ml, respectively. The model parameters a and m were determined by parameter fitting. Combinations of calibration and prediction gradients with the same starting concentration were considered. Gradients are indicated with slope.

Calibration gradient (%/ml)	Predicted gradient	Median error/90% percentile (% of V_G)
Small extrapolation to slower gradients		
1.0, 2.0	0.5	0.45/0.59
1.0, 4.0	0.5	0.27/0.44
2.0, 4.0	1.0	0.58/0.89
1.0, 2.0, 4.0	0.5	0.32/0.45
Large extrapolation to slower gradients		
2.0, 4.0	0.5	0.97/1.45
Small extrapolation to faster gradients		
1.0, 2.0	4.0	0.29/0.47
0.5, 2.0	4.0	0.24/0.39
0.5, 1.0	2.0	0.34/0.45
0.5, 1.0, 2.0	4.0	0.20/0.35
Large extrapolation to faster gradients		
0.5, 1.0	4.0	0.27/0.49
Interpolation		
0.5, 2.0	1.0	0.22/0.30
0.5, 4.0	1.0	0.18/0.32
0.5, 4.0	2.0	0.24/0.37
1.0, 4.0	2.0	0.22/0.35
0.5, 2.0, 4.0	1.0	0.21/0.27
0.5, 1.0, 4.0	2.0	0.26/0.35

Correction factors for band width

The error in band width prediction is related to the model and the plate number error. One would also expect the influence of extrapolation on the error to be different for different correction models.

Three different expressions for band width were evaluated: (i) no correction factor; (ii) J correction according to eqn. 21; and (iii) J correction according to eqn. 22. The cases of extrapolation and interpolation described above were also evaluated. The results are summarized in Table IX.

It is clear that a correction according to eqn. 22 gives the best accuracy. (Eqn. 21 will also fail if the extrapolation is extended even further than in this work, as the polynomial correction contains terms of the fourth order.) However, as the cause of unexpectedly large band broadening at high gradient slopes is uncertain, this observation might be dependent on the instrumentation as one potential reason for this effect is extra-column band broadening.

Determination of plate number

The plate number was first determined by the conventional isocratic method using naphthalene as a test solute and an eluent of acetonitrile–

TABLE IX

ERROR IN PREDICTION OF W_b FOR DIFFERENT BAND WIDTH MODELS AND EXTRAPOLATION WITH TWO AND THREE CALIBRATION GRADIENTS

The dead and dwell volumes were set at 809 μl and 2.47 ml, respectively. The plate number was determined from gradient runs. The model parameters a and m were determined by parameter fitting. All combinations of calibration and prediction gradients with the same starting concentration were considered.

Calibration gradients	Predicted gradient	Median/90% percentile of relative errors (%)		
		Correction method		
		None	Eqn. 21	Eqn. 22
Small extrapolation to slower gradients				
1.0, 2.0	0.5	29/41	16/27	10/19
1.0, 4.0	0.5	38/48	21/28	12/19
2.0, 4.0	1.0	35/39	17/19	8/11
1.0, 2.0, 4.0	0.5	42/56	22/34	13/22
Large extrapolation to slower gradients				
2.0, 4.0	0.5	53/63	26/36	14/24
Small extrapolation to faster gradients				
1.0, 2.0	4.0	37/40	17/21	7/11
0.5, 2.0	4.0	47/52	22/26	10.15
0.5, 1.0	2.0	33/43	17.24	10.15
0.5, 1.0, 2.0	4.0	47/51	21/26	8/13
Large extrapolation to faster gradients				
0.5, 1.0	4.0	56/62	27/31	12/17
Interpolation				
0.5, 2.0	1.0	2/8	2/7	3/7
0.5, 4.0	1.0	9/16	5/12	3/10
0.5, 4.0	2.0	15/27	8/16	5/11
1.0, 4.0	2.0	5/12	4/9	3/8
0.5, 2.0, 4.0	1.0	24/32	13/18	7/11
0.5, 1.0, 4.0	2.0	24/32	12/18	7/11
Overall		32/52	15/27	8/16

water (60:40, v/v), $k' = 4.5$, resulting in a plate number of 8610.

The use of calibration gradients for determinations of plate number (eqn. 30) allows individual plate numbers to be estimated for the organic modifier actually used. Every calibration gradient results in estimates of the individual plate numbers. A median of $\sqrt{N}$ from the calibration is calculated for each solute. $\sqrt{N}$ is chosen for the median, instead of N, because $\sqrt{N}$ is inversely proportional to the estimate of W_b, from which a large part of the error arises. The median is selected instead of the average as there is a risk of gross error in the band width at extremely low resolutions or signal-to-noise ratios. The results are given in Table X. The disparity between the isocratic and gradient method is large and will be even greater for larger peptides.

The effect on the prediction of W_b from plate number estimates by the conventional method and by parameter fitting is shown in Table XI. As expected, the accuracy of the predictions is greatly improved by using plate numbers determined from the calibration gradients. The gain will be larger for larger peptides.

TABLE X

PLATE NUMBERS FOR NINE PEPTIDES DETERMINED BY PARAMETER FITTING FROM FOUR GRADIENTS FOR TWO DIFFERENT ORGANIC MODIFIERS

Band width correction was made according to eqn. 22. The dead and dwell volumes were set at 809 μl and 2.47 ml, respectively. The model parameters a and m were determined by parameter fitting. Only the lower starting concentration for each organic modifier was considered. The plate number estimated by the conventional isocratic methods was 8610.

Peptide	Plate number	
	Acetonitrile	2-Propanol
1	3230	
2	5780	3520
3	4500	
4	5690	
5	2100	
6	1640	
7	3100	
8	1880	

TABLE XI

ERROR IN PREDICTION OF W_b BASED ON DIFFERENT ESTIMATES OF PLATE NUMBER

Band width correction was made according to eqn. 22. The dead and dwell volume were set at 809 μl and 2.47 ml, respectively. The model parameters a and m were determined by parameter fitting. All combinations of three calibration gradients and one prediction gradient with the same starting concentration were considered.

Method for determination of plate number	Median error/90% percentile (%)
Conventional, isocratic	43/72
Parameter fitting, individual	8/17

The error in the prediction of band width is related to the choice of correction factor. This evaluation of the method for determination of plate number was done with correction according to eqn. 22.

In the case of overlapping peaks, the band widths and retention volumes have to be determined after a deconvolution, as described under Theory. Deconvolution is not an easy task, and low signal-to-noise ratios, extremely low resolutions or large area ratios can make the task almost impossible. In addition, the necessary software may not be available to all chromatographers. For non-deconvoluted peaks, the plate number can be taken as the average of the plate number for the solutes in the sample that are well separated. The inaccuracy in retention prediction can be reduced by using more than two calibration gradients.

Test peptides

The purpose of the eight peptides used in this work was to represent possible variations that one can find in peptides. These peptides are still limited: none contains cysteine or methionine and they are not longer than sixteen amino acids. The consequence is that they do not exhibit any higher structure and have fairly high diffusion coefficients. They are chemically well behaved, with no denaturation, rearrangement or oxidation.

It is known that some peptides are not well behaved; typically they undergo permanent

TABLE XII

ERROR SOURCES

Source	Comment
Incorrect gradient formation	Should be checked by running a UV-absorbing gradient without column. Generally small with modern equipment [57,58]
Gradient rounding due to mixing volume	The mixer should have a volume that is less than 20% of the total volume of the gradient. This is rarely a problem with ordinary instrumentation, but can be serious with micro columns. In addition it can pose a difficulty when multi-segmented gradients are used [58]
Incomplete column equilibration	It has been found that 15 column volumes of initial solvent are needed to wash the column completely between the gradients [24]. Incomplete column equilibration will only affect early-eluting solutes
Solvent demixing	Small [20,24,57], and can be further minimized by not starting the gradient with pure buffer, *i.e.*, by having $\varphi_0 > 0\%$

structural changes, their retention parameters change or they undergo slow inverconversions between two or more conformations [3,7,87–90]. This leads to excess band broadening or multiple peaks and can cause deviations between predicted and actual values. These cases can, however, usually be recognized in the calibration gradients. Very few cases of large deviations have been reported [7].

Other sources of error

There are general sources of error that are not related to the choice of the chromatographic models and methods of determining the parameters. They are listed in Table XII together with a judgement of their importance. It was not the aim of this work to explore these issues, and papers have already been published that treat this topic [20,24,25,31,37,57,58].

In the reversed-phase liquid chromatography of peptides, mobile phases containing trifluoroacetic acid (TFA) are popular. It has been shown that these mobile phases degrade the column [91]. If TFA is used as a mobile phase additive it is therefore important that the time between the calibration and prediction gradient is small [20,57].

CONCLUSIONS

It has been confirmed that highly accurate predictions of retention volumes, band widths and resolutions can be made from a small number of calibration gradients if the right precautions are taken. There are various versions of the expressions for retention volume and band width in the literature, most of them being different approximations based on the same fundamental theory. From a practical point of view, considering the tools for calculation that are available today, there is only one approximation that is meaningful. By choosing the right conditions for the calibration gradients, *i.e.*, low starting concentration of organic modifier, one can ensure that this approximation is valid. The determination of the model parameters then becomes simple.

Determination of the dead volume as the elution volume for uracil is simple and was found to be adequate. The dwell volume can be estimated from a gradient run, without a column, with UV-absorbing eluents. The alternative approach is to estimate the dwell volume from parameter fittings of retention data based on three or more calibration gradients, if non-linear fitting routines are available. In agreement with earlier work, it has been shown that determination of the dwell volume by fitting results in more accurate predictions of absolute retention times. The improvement in the accuracy of prediction of differences in retention between peak pairs is, however, minor.

The accuracy of band width prediction can be greatly improved by assigning an individual plate

number to each solute. This is especially important in peptide work, as the plate number is generally much smaller than for small organic compounds, and also varies between peptides. Plate numbers can either be derived from approximating mechanistic models or be determined experimentally. The latter approach is more appropriate for optimization purposes, as it requires no knowledge about the solute or column and can tolerate some non-ideal band broadening. Deviations from the fundamental band width model have been observed by other workers. This was confirmed in this work and the different empirical correction methods suggested in the literature have been evaluated. The simplest approach gave the highest accuracy in this study.

The initial step in making predictions is to evaluate the calibration gradients. A correct match of peaks between runs is crucial, and this task is much simplified if three calibration gradients are run. Determinations of retention volumes and band widths (the latter is needed if individual plate numbers are to be estimated) is difficult in the case of overlapping peaks. Here a simple deconvolution based on a gaussian model is suggested. It is recommended that the calibration gradients are run at a constant and high flow-rate. This will not correspond to the maximum plate number but to the highest peak capacity per unit time. Predictions based on calibration gradients with constant flow-rate are also more accurate.

Gradient prediction is mainly a tool for optimization of the gradient slope. Extrapolation is then often inevitable. It is shown here that extrapolations to faster gradients are associated with smaller errors than extrapolations to slower gradients, suggesting that slow calibration gradients should be preferred.

In summary, gradient prediction is accurate and useful in peptide chromatography and, following the guide-lines presented in this work, its implementation is made simpler.

ACKNOWLEDGEMENTS

The author thanks Pharmacia–LKB Biotechnology for supplying the HPLC instrumentation. Useful discussions with Professor Åke Olin are most appreciated. The author also thanks Dr. Rolf Danielsson for providing the simplex program.

SYMBOLS

φ	Concentration of organic modifier (%)
φ_0	Starting concentration of organic modifier (%)
ν	Reduced velocity
a	Model parameter
B	Gradient slope (%/ml)
b	Gradient steepness
F	Flow-rate (ml/min)
G	Peak compression factor
k'_0	k' at the starting concentration of organic modifier
k'_f	k' when the solute leaves the column
m	Model parameter ($\%^{-1}$)
N	Plate number
s	Gradient rate (%/min)
t	Time (min)
V	Pumped volume (ml)
V_g	Retention volume, gradient elution (ml)
V_G	Gradient volume (ml)
V_d	Dwell volume (ml)
V_m	Dead volume (ml)
W_b	Peak width at base (ml)

REFERENCES

1 L.R. Snyder, M.A. Stadalius and M.A. Quarry, *Anal. Chem.*, 55 (1983) 1412A.
2 M.A. Stadelius, H.S. Gold and L.R. Snyder, *J. Chromatogr.*, 296 (1984) 31.
3 M.-I. Aguilar, A.N. Hodder and M.T.W. Hearn, *J. Chromatogr.*, 327 (1985) 115.
4 J.L. Meek and Z.L. Rossetti, *J. Chromatogr.*, 211 (1981) 15.
5 M.J. O'Hare and E.C. Nice, *J. Chromatogr.*, 171 (1979) 209.
6 L.R. Snyder, in Cs. Horváth (Editor), *High Performance Liquid Chromatography: Advances and Perspectives*, Vol. 1, Academic Press, New York, 1980, p. 207.
7 L.R. Snyder and M.A. Stadalius, in Cs. Horváth (Editor), *High Performance Liquid Chromatography: Advances and Perspectives*, Vol. 4, Academic Press, New York, 1986, p. 195.
8 P. Jandera and J. Churáček, *Gradient Elution in Column Liquid Chromatography, Theory and Practice*, Elsevier, Amsterdam, 1985.

9 B.F.D. Ghrist and L.R.Snyder, *J. Chromatogr.*, 459 (1988) 25.
10 J.L. Glajch, M.A. Quarry, J.F. Vasta and L.R. Snyder, *Anal. Chem.*, 58 (1986) 280.
11 P. Jandera and J. Churáček, *J. Chromatogr.*, 91 (1974) 207.
12 P.J. Schoenmakers, H.A.H. Billiet, R. Tijssen and L. de Galan, *J. Chromatogr.*, 149 (1978) 519.
13 M.T.W. Hearn and B. Grego, *J. Chromatogr.*, 255 (1983) 125.
14 M.T.W. Hearn and B. Grego, *J. Chromatogr.*, 266 (1983) 75.
15 P.J. Schoenmakers, H.A.H. Billiet and L. de Galan, *J. Chromatogr.*, 185 (1979) 179.
16 J.W. Dolan, J.R. Gant and L.R. Snyder, *J. Chromatogr.*, 165 (1979) 31.
17 P. Jandera and J. Churáček, *J. Chromatogr.*, 192 (1980) 1.
18 R.A. Harwick, C.M. Grill and P.R. Brown, *Anal. Chem.*, 51 (1979) 34.
19 B.F.D. Ghrist and L.R. Snyder, *J. Chromatogr.*, 459 (1988) 43.
20 J.W. Dolan, D.C. Lommen and L.R. Snyder, *J. Chromatogr.*, 485 (1989) 91.
21 J. Schmidt, *J. Chromatogr.*, 485 (1989) 421.
22 J.D. Stuart, D.D. Lisi and L.R. Snyder, *J. Chromatogr.*, 485 (1989) 657.
23 S. Heinisch, J.-L. Rocca and M. Kolosky, *Chromatographia*, 29 (1990) 482.
24 M.A. Quarry, R.L. Grob and L.R. Snyder, *J. Chromatogr.*, 285 (1984) 19.
25 L.R. Snyder and M.A. Quarry, *J. Liq. Chromatogr.*, 10 (1987) 1789.
26 S.A. Tomellini, R.A. Harwick and H.B. Woodruff, *Anal. Chem.*, 57 (1985) 811.
27 Y. Sakamoto, N. Kawakami and T. Sasagawa, *J. Chromatogr.*, 442 (1988) 69.
28 M. Kunitani, D. Johnson and L.R. Snyder, *J. Chromatogr.*, 371 (1986) 313.
29 M.T.W. Hearn and M.I. Aguilar, *J. Chromatogr.*, 359 (1986) 31.
30 L.R. Snyder, M.A. Quarry and J.L. Glajch, *Chromatographia*, 24 (1987) 33.
31 M.A. Quarry, R.L. Grob and L.R. Snyder, *J. Chromatogr.*, 285 (1985) 1.
32 P. Jandera and J. Churáček, *J. Chromatogr.*, 91 (1974) 223.
33 L.R. Snyder and D.L. Saunders, *J. Chromatogr. Sci.*, 7 (1969) 195.
34 H. Poppe and J. Panakker, *J. Chromatogr.*, 204 (1981) 77.
35 M.A. Stadelius, H.S. Gold and L.R. Snyder, *J. Chromatogr.*, 327 (1985) 27.
36 M.A. Stadelius, M.A. Quarry and L.R. Snyder, *J. Chromatogr.*, 327 (1985) 93.
37 M.A. Quarry, R.L. Grob and L.R. Snyder, *Anal. Chem.*, 58 (1986) 907.
38 M.T.W. Hearn and M.I. Aguilar, *J. Chromatogr.*, 352 (1986) 35.
39 J.W. Dolan, L.R. Snyder and M.A. Quarry, *Chromatographia*, 24 (1987) 261.
40 A. Alhedai, D.E. Martire and R.P.W. Scott, *Analyst*, 114 (1989) 869.
41 J.H. Knox and R. Kaliszan, *J. Chromatogr.*, 349 (1985) 211.
42 H. Engelhardt, H. Müller and B. Dreyer, *Chromatographia*, 19 (1984) 240.
43 A. Malik and K. Jinno, *Chromatographia*, 30 (1990) 135.
44 R.J. Smith, C.S. Nieass and M.S. Wainwright, *J. Liq. Chromatogr.*, 9 (1986) 1387.
45 P.C. Sadek, P.W. Carr and L.D. Bowers, *LC Mag.*, 3 (1985) 590.
46 B.A. Bidlingmeyer, F.V. Warren, A. Weston and C. Nugent, *J. Chromatogr. Sci.*, 29 (1991) 275.
47 A.M. Krstulovic, H. Colin and G. Guiochon, *Anal. Chem.*, 54 (1982) 2438.
48 H. Wätzig and S. Ebel, *Chromatographia*, 31 (1991) 544.
49 R.J. Laub and S.J. Madden, *J. Liq. Chromatogr.*, 8 (1985) 173.
50 J.P. Larmann, J.J. Destefano, A.P. Goldberg, R.W. Stout, L.R. Snyder and M.A. Stadalius, *J. Chromatogr.*, 255 (1983) 163.
51 N. Tanaka, K. Kimata, Y. Mikawa, K. Hosoya, T. Araki, Y. Ohtsu, Y. Shiojima, R. Tsuboi and H. Tsuchiya, *J. Chromatogr.*, 535 (1990) 13.
52 R.V. Lewis, A. Fallon, S. Stein, K.D. Gibson and S. Udenfriend, *Anal. Biochem.*, 104 (1980) 153.
53 R.R. Walters, *J. Chromatogr.*, 249 (1982) 19.
54 R.V. Lewis and D. Dewald, *J. Liq. Chromatogr.*, 5 (1982) 1367.
55 J.D. Pearson, W.C. Mahoney, M.A. Hermodson and F.E. Regnier, *J. Chromatogr.*, 207 (1981) 325.
56 R.M. McCormick and B.L. Karger, *Anal. Chem.*, 52 (1980) 2249.
57 B.F.D. Ghrist, B.S. Cooperman and L.R. Snyder, *J. Chromatogr.*, 459 (1988) 1.
58 L.R. Snyder and J.W. Dolan, *LC · GC Int.*, 3(10) (1990) 28.
59 K.D. Nugent, W.G. Burton, T.K. Slattery, B.F. Johnson and L.R. Snyder, *J. Chromatogr.*, 443 (1988) 381.
60 A.K. Taneja, S.Y.M. Lau and R.S. Hodges, *J. Chromatogr.*, 317 (1984) 1.
61 C.T. Mant and R.S. Hodges, *J. Liq. Chromatogr.*, 12 (1989) 139.
62 R.W. Stout, J.J. DeStefano and L.R. Snyder, *J. Chromatogr.*, 282 (1983) 263.
63 J.H. Knox, *J. Chromatogr., Sci.*, 15 (1977) 353.
64 M.A. Stadalius, B.F.D. Ghrist and L.R. Snyder, *J. Chromatogr.*, 387 (1987) 21.
65 A.N. Papas, *CRC Crit. Rev. Anal. Chem.*, 20 (1989) 359.
66 A.N. Papas and M.F. Delaney, *Anal. Chem.*, 59 (1987) 54A.
67 A.N. Papa and T.P. Tougas, *Anal. Chem.*, 62 (1990) 234.
68 B.G.M. Vandeginste, G. Kateman, J.K. Strasters, H.A.H. Billiet and L. de Galan, *Chromatographia*, 24 (1987) 127.
69 G.G.R. Seaton and A.F. Fell, *Chromatographia*, 24 (1987) 208.

70 M. Maeder, *Anal. Chem.*, 59 (1987) 527.
71 C.T. Wehr, R.P. Lundgard and K.D. Nugent, *LC · GC Int.*, 2(3) (1989) 24.
72 W.G. Burton, K.D. Nugent, T.K. Slattery, B.R. Summers and L.R. Snyder, *J. Chromatogr.*, 443 (1988) 363.
73 H. Engelhardt, G. Appelt and E. Schweinheim, *J. Chromatogr.*, 499 (1990) 165.
74 C.T. Mant and R.S. Hodges, *Chromatographia*, 24 (1987) 805.
75 W.S. Hancock and J.T. Sparrow, *J. Chromatogr.*, 206 (1981) 71.
76 H. Engelhardt and D. Mathes, *Chromatographia*, 14 (1981) 325.
77 C.D. Leach, M.A. Stadalius, J. Berus and L.R. Snyder, *LC · GC Int.*, 1(5) (1988) 22.
78 A. Sokolowski and K.-G. Wahlund, *J. Chromatogr.*, 189 (1980) 299.
79 K.A. Cohen, J. Chazaud and G. Calley, *J. Chromatogr.*, 282 (1983) 423.
80 J.W. Dolan, *LC · GC Int.*, 3(7) (1990) 17.
81 I. Molnar, R. Boysen and P. Jekow, *J. Chromatogr.*, 485 (1989) 569.
82 G. Jilge, R. Janzen, H. Giesche, K.K. Unger, J.N. Kinkel and M.T.W. Hearn, *J. Chromatogr.*, 397 (1987) 71.
83 N.H.C. Cooke, B.G. Archer, M.J. O'Hare, E.C. Nice and M. Capp, *J. Chromatogr.*, 255 (1983) 115.
84 M.J. O'Hare, M.W. Capp, E.C. Nice, N.H.C. Cooke and B.G. Archer, *Anal. Biochem.*, 126 (1982) 17.
85 P.C. Sadek, P.W. Carr, L.D. Bowers and L.C. Haddad, *Anal. Biochem.*, 153 (1986) 359.
86 W.H. Press, B.P. Flannery, S.A. Teukolsky, W.T. Vetterling, *Numerical Recipies in C*, Cambridge University Press, Cambridge, 1988.
87 L.R. Snyder, in K.M. Gooding and F.E. Regnier (Editors), *HPLC of Biological Macromolecules: Methods and Applications*, Marcel Dekker, New York, 1990, p. 231.
88 S.A. Cohen, K.P. Benedek, S. Dong, Y. Tapuhi and B.L. Karger, *Anal. Chem.*, 56 (1984) 217.
89 M.T.W. Hearn and B. Grego, *J. Chromatogr.*, 296 (1984) 61.
90 M.A. Stadalius, M.A. Quarry, T.H. Mourey and L.R. Snyder, *J. Chromatogr.*, 358 (1986) 17.
91 J.L. Glajch, Kirkland and J. Köhler, *J. Chromatogr.*, 384 (1987) 81.

Journal of Chromatography, 639 (1993) 117–127
Elsevier Science Publishers B.V., Amsterdam

CHROM. 24 993

Optimization strategy for reversed-phase liquid chromatography of peptides

Niklas Lundell* and Karin Markides

Institute of Chemistry, Department of Analytical Chemistry, Uppsala University, P.O. Box 531, 751 21 Uppsala (Sweden)

(First received May 22nd, 1992; revised manuscript received February 11th, 1993)

ABSTRACT

An optimization strategy for the separation of peptides from a complex matrix by reversed-phase liquid chromatography is presented and illustrated with an example. The aim is to find the mobile phase system, *i.e.* buffer and organic modifier used for gradient formation, that admits the steepest gradient with sufficient resolution. The result is a rapid separation where the detection limits are low and the loading capacity is high. This strategy is a hybrid between experimental design used for optimizing the selection of the mobile phase system and gradient theory used for gradient predictions.

INTRODUCTION

Reversed-phase liquid chromatography, which was introduced in the mid-1970s, soon became the most popular technique in liquid chromatography. The first attempts to use this separation mode for peptides were not very successful, as low efficiencies and bad peak shapes were observed [1,2]. These initial problems where later solved by improved column technology and reversed-phase liquid chromatography is now a standard separation technique for peptides and small proteins.

Reversed-phase separations of peptides and proteins are still not trivial, however, and the life sciences continue to present extremely demanding applications for chromatography. Problems such as denaturation [3–5], low recoveries [4,6–9], ghost peaks [6,8], low column stability [10,11] and highly complex samples [12,13] are common problems for the bio-chromatographer. Consequently, method development tends to be highly elaborate.

To aid in method development, several optimization strategies for liquid chromatography have been presented; for an overview, see refs. 14–17. These strategies generally fall into two categories, as follows.

Methods based on retention models. In this category of strategies, the retention of all solutes in the sample is modelled. This is attractive as chromatograms can be simulated and the methods do not require that chromatograms are directly graded by some response function (see below). The models that are made can be either empirical, simple polynomial, or have theoretical foundations. The optimum is located either according to some criteria, applied after the modelling, or the user chooses conditions after visual inspection of simulated chromatograms. The disadvantage is that these strategies demand that the variations in retention times for the components in the sample can be followed as the separation conditions are altered. This so-called peak tracking, illustrated in Fig. 1, can be anything from trivial to impossible [18–25]. A number of factors determine the extent to which

* Corresponding author. Present address: PSQD, Bau 64/140, Hoffmann-La Roche, CH-4002 Basle, Switzerland.

0021-9673/93/$06.00

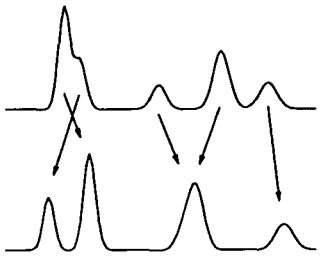

Fig. 1. Peak tracking. The peaks in chromatograms obtained under different conditions are matched.

peak tracking can be applied *i.e.*, the complexity of the sample, which variables are altered and what detection method is selected.

Methods not based on retention models. These methods are straightforward to use, but usually require more experiments than the previous category. No peak tracking is needed and any quantitative variable can be optimized. A response can be seen as a grade or a quality measure for specific separation conditions. This measure is determined from the chromatogram by some response function, *e.g.*, the sum of all resolutions. This response can then be optimized with a search method such as the simplex method [26,27] or by making an empirical model of the response, a so-called response surface. Unfortunately, both methods have significant drawbacks. The simplex method will find an optimum, but it might only be a local optimum. An empirical model of the response can be extremely difficult to make from response values alone, as the response surfaces are often unsmooth [28–31]. A third possibility is to determine the response at various conditions according to an experimental design and then simply take the conditions that result in the highest response as the optimum, without making any model [32]. This last strategy is sometimes referred to as grid searching. It must also be emphasized that it can be difficult to formulate an adequate response function or optimization criteria [33,34]. This will be more of a problem in this category of optimization methods as they rely heavily on a response function.

The large number of optimization strategies proposed in the literature may seem confusing but they are complementary as they aim for different situations. The chromatographer must identify the separation problem and choose optimization methods accordingly. A key question is whether peak tracking is possible or not. The most powerful instrumental tool for peak tracking is multi-channel detection, usually diode-array detection, preferably combined with software that mathematically can resolve peaks [35–37], so-called deconvolution. The outcome is a pure spectrum for every peak, which can support peak tracking. Optimization strategies based on peak tracking with diode-array detection have therefore received considerable attention [38–41]. Unfortunately these strategies are only guaranteed to work if the solutes have different spectra and some degree of resolution. It is also known that a UV spectrum is affected by pH and solvent.

The optimization strategy presented in this work mainly aims at a situation where a small number of peptides are to be separated from an unknown, complex matrix. Typically this means analytical or preparative separation of peptides in biological material such as body fluids, tissue, food or beverages. The mobile phase system, *i.e.*, buffer and organic modifier, and the gradient slope are optimized. The aim is to find separation conditions that allow the separation to be made with a fast gradient. A fast gradient means fast separation, low detection limits and high load capacity.

Peak tracking is difficult in these applications, owing to the complexity of the sample and the fact that spectra of peptides are often identical in the short-wavelength UV range and the differences in the 240–280-nm range are difficult to detect as the absorbance is low. Diode-array detectors are thus of limited use. In addition, they are generally less sensitive than the conventional UV detectors and the deconvolution software is not yet widely available.

The optimization strategies that have been developed so far have either been made for simple matrices with small molecules separated with isocratic elution or have been dedicated to gradient optimization. In this paper, a strategy for peptide separation that optimizes both the mobile phase system and the gradient slope is proposed. Peak tracking is applied to a limited

extent and complex matrices can therefore be handled.

In the proposed optimization strategy, the retention is modelled as a function of gradient slope and response optimization is used for the mobile phase systems. Retention models for gradient elution that are based on chromatographic theory have been found to be highly accurate [42–47]. The input data that are needed can easily be obtained from two or three experiments. On the other hand, variables such as pH, concentration of ion-pairing reagent and composition of organic modifier affect the chromatography in such a way that modelling and peak tracking become more difficult. In addition, there are also experimental limitations on how much these variables can be altered. A strategy based on experimental design and the use of only response values is necessary when these mobile phase variables are used in complex peptide separations. In this work, a mobile phase system that allows variations of pH, concentration of ion-pairing reagent and composition of organic modifier is used.

EXPERIMENTAL

Column

A 10 cm × 4 mm I.D. Sephasil C_{18} column (Pharmacia–LKB Biotechnology, Uppsala, Sweden) was used. The column matrix consisted of 5-μm silica particles with a pore size of 125 Å. The dead volume was determined to be 809 μl by injection of 3 μg of uracil. The column was operated at a flow-rate of 1 ml/min in all experiments.

Mobile phases

All buffers consisted of 50 mmol/l phosphoric acid. The pH was adjusted with ammonia. When trifluoroacetic acid (TFA) was used, it was added before the pH adjustment. The TFA concentration refers to the total volume, including the organic solvent. Consequently, the amount of TFA added to the buffer to be mixed with organic solvent (eluent B or C) was larger than the amount added to eluent A (pure buffer). Gradients were made by mixing three eluents, A, B and C, using the low-pressure mixing facility of the gradient pump. Eluent A was neat buffer and solutions B and C consisted of 50 vol.% of organic solvent in the buffer. The organic solvent was pure acetonitrile for eluent C and a 50:50 mixture of acetonitrile and 2-propanol for eluent B.

Instrumentation

A system consisting of a Model 2249 low-pressure mixing gradient pump, a Model 2141 dual-wavelength detector (Pharmacia–LKB Biotechnology) and a CMA autoinjector (CMA Microdialysis, Stockholm, Sweden) was used. The instrumentation was interfaced with an IBM AT3 personal computer for gradient control and data acquisition.

Software

Evaluation of chromatograms, determination of the parameters in the gradient model and predictions were all made with in-house written software using the programming environment ASYST (Asyst Software Technologies, Rochester, NY, USA) running on an IBM PS/2 Model 55SX computer. A modified Gauss–Newton algorithm was used for the deconvolution of overlapping peaks.

Chemicals

Acetonitrile and 2-propanol were of HPLC gradient grade (Merck). Distilled water was purified using a Milli-Q system (Millipore, Bedford, MA, USA) fitted with an Organex-Q cartridge. Phosphoric acid and ammonia were of analytical-reagent grade (Merck). Trifluoroacetic acid was of spectroscopic grade (Uvasol; Merck) and was distilled before use.

Sample preparation

A 50-mg amount of myoglobin from horse heart (M-1882; Sigma, St. Louis, MO, USA) was dissolved in 5 ml of a 0.1 mol/l solution of ammonium hydrogencarbonate. A 50-mg amount of Trypsin (TPCK treated; Sigma, St. Louis, MO, USA) was dissolved in 2.5 ml of 0.1 mol/l hydrochloric acid and 125 μl of this trypsin solution was added to the myoglobin solution. Digestion was carried out at 37°C for 3 h and was stopped by addition of 1 ml of 30% (v/v) acetic

acid. The digest was spiked with a solution of angiotensin II resulting in a final concentration of 0.14 mg/ml.

RESULT AND DISCUSSION

Gradient predictions

Using gradient theory, it is possible to predict accurately, from two or more gradients, the retention volume and band width at various gradient slopes. The number of experiments for optimization can then be greatly reduced. In this work, gradient prediction was used to determine an adequate gradient steepness for a given mobile phase system, as will be described in the next section.

The fundamental theory of gradient elution in reversed-phase liquid chromatography is well established; a complete presentation of the methodology can be found in publications by Snyder and Stadalius [48,49] and Jandera and Churáček [50]. Most implementations of gradient theory, including this work, rely on a linear relationship between the logarithm of the capacity factor of (k') and the percentage of organic modifier, φ:

$$\log k' = a - m\varphi$$

The band width is assumed to be related to k'_f, the instantaneous value of k' as the solute leaves the column [48,51];

$$W_{bg} = 1.1 \frac{4V_m}{\sqrt{N}} \cdot (k'_f + 1)$$

where k'_f is given by

$$k'_f = 1/[2.30b + 1/(k'_0)]$$

k'_0 is k' in the starting eluent, given by

$$k'_0 = 10^{a - m\varphi_0}$$

The parameter b (gradient steepness) is a function of both the gradient slope and the solute-dependent parameter m, and can be regarded as the apparent slope or the acceleration of a solute as it is exposed to the gradient. This measure is conceptually more difficult (see the discussion by Lundell [47]) than the slope (%/ml) or rate (%/min), but both k'_f and band width are more closely related to this parameter than the ordinary measures. The gradient steepness b is related to the slope, B, and rate, s, as

$$b = V_m mB = V_m m(s/F)$$

The options in the implementation and application of gradient theory have already been presented and evaluated for the case of peptides [47]. The recommendations made were followed here, including the use of individual plate numbers for each solute. Band widths for these calculations were calculated by fitting gaussian functions to the peaks. This method allows band widths to be determined even if the peaks are overlapping.

Aim of optimization

The choice of a quality measure, a so-called response function, is crucial in optimization. There is no universal response function as there are different demands on different separations. The strategy presented in this work is for an optimization of the mobile phase system and the gradient slope, where the gradient is linear and non-segmented. These simple gradients are adequate for the separation of a few peptides from a complex sample. In this work, one peptide is considered but extension to several peptides can be discussed in a similar fashion.

With the proposed optimization strategy, a minimum resolution is chosen. The resolution for the peptide of interest is calculated as

$$R_s = 2 \cdot \frac{V_{g,2} - V_{g,1}}{W_{b,2} + W_{b,1}}$$

and refers to its neighbouring peaks.

For a specific mobile phase system, it is calculated, using gradient theory, how fast a gradient can be run while still obtaining the desired resolution. This limiting gradient steepness is the response. The aim of the optimization is to find the mobile phase system that allows the fastest gradient. A fast gradient means fast separation, symmetrical peaks, low detection limit and high loading capacity, and thus the choice of response. In addition, it has been observed that the recovery increases with decreasing gradient time [52–54].

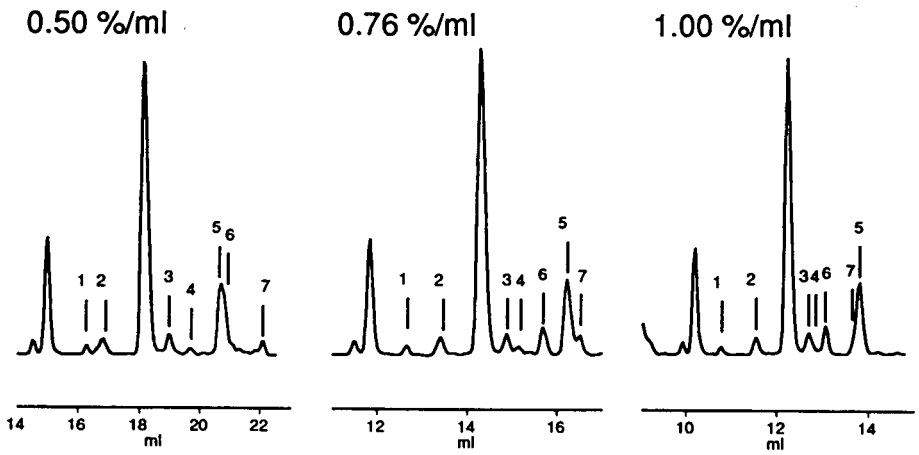

Fig. 2. Chromatogram obtained at 215 nm of an angiotensin II-spiked sample with various gradient slopes. Angiotensin II is the largest peak. The peaks are labelled with numbers. 50 mmol/l phosphate (pH 2.8) was used as buffer and acetonitrile as organic modifier.

The following example illustrates the method. A sample containing angiotensin II as the peptide of interest was eluted using three gradients with different slopes. The angiotensin II peak is shown in Fig. 2 with several interferences at similar retention volumes. Peaks are then matched and the parameters a, m and plate number are determined by data fitting. The resolutions between angiotensin II and the potential interferences are then calculated as a function of gradient slope (Fig. 3). The maximum gradient steepness, b, that gives the desired resolution can then be determined. For example, with a desired resolution of 1.5 the actual maximum gradient slope would be 1.8 ml/min, corresponding to a steepness of 0.26. This steepness is the response for this particular mobile phase system. The choice of response is a central part of this strategy and it is important to understand that the responses that are presented are predicted gradient steepnesses that give the desired resolution, and not gradients that actually have been used.

The size of the smallest interfering peaks that should be taken into account, the limit of concern, is an important issue. In this work, this limit of concern was set to 2% of the analyte peak area at 215 nm. The reasons for this limit are that smaller peaks are difficult to detect and to track in complex samples. It is possible, of course, to optimize the gradient slope by a method not based on gradient predictions, making tracking unnecessary. Unfortunately, it would then be extremely difficult to discover co-elution of very small peaks, making this kind of strategy both time consuming and unreliable.

Several alternative measures of resolution, apart from the traditional one used in this work, have been proposed. The alternative measures,

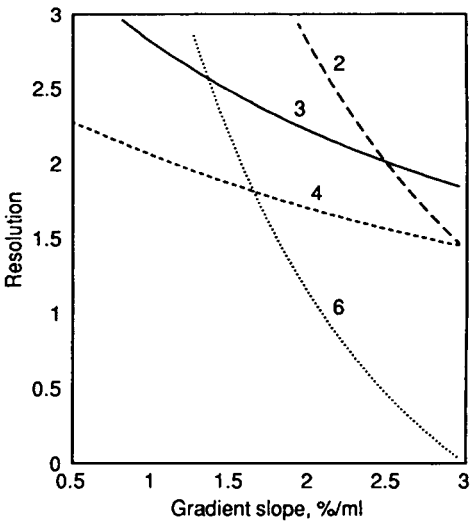

Fig. 3. Resolution between angiotensin II and interferents, numbered according to Fig. 2, as a function of gradient slope, B. Note that gradient steepness, b, is given by $V_m mB$. The parameter m was estimated to be 0.190 for angiotensin II. The resolution of angiotensin II and interferents 1, 5 and 7 is >3.0 in the presented range of gradient slope.

e.g., peak-to-valley ratio, P_v, account for overlap which is dependent on relative areas [33]. R_s was chosen as the measure in this work as it does not vary with the relative amount of the matrix and it is easy to calculate from the gradient predictions.

Selection of mobile phase systems for peptide chromatography

In peptide chromatography, the demands on the mobile phase are high. The mobile phase should allow detection in the 210–230-nm range where the peptide bond absorbs and be highly pure as gradient elution is sensitive towards impurities. It is also essential that the mobile phase minimizes secondary interactions, which lead to bad peak shapes, low efficiency, adsorption, memory effects, low recoveries and bad reproducibility [55–59]. In addition, it is desirable that the mobile phase is not aggressive towards the column to prevent leakage of stationary phase and a shortened column lifetime. Finally, in preparative applications it is convenient if the mobile phase is easy to desalt.

The first attempts at peptide separations by reversed-phase liquid chromatography were not successful owing to a lack of ionic strength in the mobile phase. Addition of acid improved the situation as the ionic strength increased and the pH was lowered, which also reduced silanol interactions [60,61]. Phosphoric acid soon became a popular additive and in 1978 Rivier [62] introduced phosphoric acid with the pH adjusted with triethylamine as buffer. By adding triethylamine, the silanol groups were effectively blocked, which further reduced the silanol interaction.

In 1980, Bennett *et al.* [63] described the use of trifluoroacetic acid (TFA) as a mobile phase additive. TFA is volatile and can be desalted by freeze-drying, therefore making it extremely convenient for preparative separations. TFA also works as an ion-pairing reagent, giving increased retention [64,65]. TFA soon became the standard additive for peptide separations. In the late 1980s several papers appeared that reported some disadvantages with TFA, such as low column stability [10,11,66], significant stationary phase leakage from the column [10], bad peak shapes [6,56,67,68] and low recoveries [6,69]. More recently, formic acid has been suggested as an alternative additive despite its relatively high UV absorbance [70].

The choice of mobile phase is also related to column properties. The interaction with silanol groups, which has been the cause of many problems, is commonly reduced by end-capping and deactivation of the packing material [71–73]. Improvements have also been made in the stability of these silica-based reversed-phase columns [74,75] and, in addition, polymer-based reversed-phase columns with good chromatographic performance are being introduced [11,76–78]. Despite column advances, problems still exist and it is clear that there is no general and perfect mobile phase for the reversed-phase chromatography of peptides.

In this work, phosphoric acid was used as a buffer with TFA added as ion-pairing reagent. This buffer results in high column stability [66], excellent reproducibility and low silanol interactions and, in addition, gives the possibility of manipulating the selectivity by altering both the pH and the TFA concentration. Desalting can also be made with a solid-phase extraction column. This choice of buffer is determined by the practical restrictions put on mobile phase and it spans most of the variations that are possible within these restrictions. In addition, selectivity changes have been observed with the proposed variations in organic modifier [4,79,80], TFA concentration [4,64,81,82] and pH [83,84]. Note that in this work pH is limited to two discrete values, namely 2.8 and 6.5. This is due to the low column stability outside this range and the low buffer capacity in the intermediate range. Clearly, these limitations are not absolute, as both column stability and buffer capacity change gradually with pH. However, considering the necessity for reproducibility, the consequence of column leakage and the large sample loads commonly utilized, only very small deviations from these pH values can be recommended.

It should be stated that the buffer suggested in this work is a compromise. The main disadvantage with this buffer is that it is more complicated to desalt than the more common mobile phase systems with only TFA. The demands are

different for different situations, and the mobile phase selection should always be determined by the application. For example, in separations prior to radioimmunological assay, formic acid could well be used as buffer. UV detection is then only used for the determination of the retention volume for standards, making baseline drift a minor problem.

The low UV absorbance and viscosity of acetonitrile make it the most commonly used organic modifier for peptide separations. By using other organic modifiers different selectivity can be obtained, although the selection is strongly limited by the detection wavelength. The most popular alternative for acetonitrile is propanol, owing to its low UV absorbance, high elution strength and a different selectivity compared with acetonitrile [6,9,81,85,86]. In this work, an acetonitrile–2-propanol mixture was used as the alternative to acetonitrile. This mixture was chosen as a compromise between selectivity and efficiency, as pure 2-propanol has a high viscosity, giving low chromatographic efficiency [4].

The hybrid strategy

The strategy proposed in this work can be described as a hybrid strategy, which means that retention modelling is combined with direct response optimization. An experimental design is made for the mobile phase systems that are considered. The experimental design is illustrated in Fig. 4 and the set values are listed in Table I. The design is a full factorial design, where all combinations of variable settings are considered. By adopting this design, possible synergistic effects can be acknowledged. For each mobile phase system, represented by the corners of the cube in Fig. 4, three gradients with different slopes are run. As explained above, the three gradients are then used to calculate how fast a gradient can be run, with the specific mobile phase system, so that the desired resolution is still obtained. The maximum steepness is called the response for this mobile phase system.

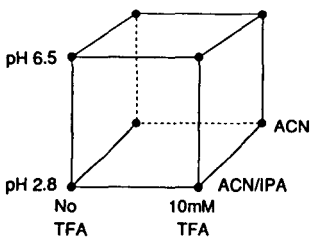

Fig. 4. Experimental design of the mobile phase system. Each corner represents a combination of the set values of the mobile phase variables in Table I. ACN = acetonitrile; IPA = 2-propanol.

TABLE I

MOBILE PHASE VARIABLES USED IN OPTIMIZATION

Variable	Lower value	Upper value
pH	2.8	6.5
TFA concentration (m*M*)	0	10
Organic modifier	Acetonitrile	Acetonitrile–2-propanol (60:40)

The optimum mobile phase system is taken as the one that allows the highest gradient slope. It is important to note that no model is made of either response or retention as a function of the mobile phase variables. The optimization of the mobile phase system is a primitive grid search, based on reasons discussed in a later section.

An example

The strategy described above was applied to the separation of angiotensin II, which was added to a tryptic digest of myoglobin, serving as the matrix. It is important to note that the matrix was considered as unknown. The mobile phase variables presented earlier, and illustrated in Fig. 4, were used. The range of slopes for the three gradient runs was 0.50–1.00%/ml, based on scouting experiments. The gradient slopes were kept low to ensure a high peak capacity which simplifies peak tracking. It has also been shown that extrapolation to faster gradients is more accurate than the opposite [47]. Calibration gradients can therefore be made with slopes lower than the expected optimum. The narrow range of gradient slopes also aids peak tracking as no large selectivity change can be expected over a small range. Extrapolation is, however, inherently more sensitive to experimental error

than interpolation, and care should be taken to minimize those errors [47]. Detection was made with a dual-wavelength detector, which combines high sensitivity with the possibility of using wavelength ratios for peak tracking.

For this application, the resolution required was set to 1.5. The responses, gradient slopes in %/min, are presented in Fig. 5, where the layout of mobile phase systems is the same as in Fig. 4. It is clear that large variations in response are obtained, hence an optimization can result in a major improvement in separation. It can also be seen that the variables are synergistic, *e.g.*, the result at low pH is highly dependent on the setting of the other variables. Using an experimental design is necessary; varying one variable at a time can be misleading.

As can be seen from Fig. 5, the fastest gradient, $b = 0.37$, will be obtained at pH 6.5 with 10 mmol/l TFA and pure acetonitrile as organic modifier. This steepness corresponds to a slope of 2.4%/ml. This is surprisingly fast considering the complexity of the sample. With one of the mobile phases systems, all interferences could not be tracked between the various gradients. The response is then based on the interferences that actually could be tracked. This is not a problem as long as all peaks have been tracked for the mobile phase system that yielded the highest response. In addition, in cases where peak tracking is difficult, there are usually a large number of interferences, making it unlikely that a high response can be obtained. An enlargement of the predicted and actual chromatograms with this mobile phase system (Fig. 6) shows the angiotensin II peak and its potential interferences. The chromatograms match well, despite a large degree of extrapolation of gradient slope. In Fig. 7 a larger portion of the actual chromatogram is shown. The resolution is slightly lower than the predicted value owing to some tailing and interfering peaks smaller than the 2% of the angiotensin II peak. It would, of course, be desirable to have the peptides of interest separated from all interfering peaks. This is almost impossible as for any biological sample there will be hundreds of small interfering peaks. The number of interfering peaks typically increases exponentially as the limit of concern is lowered. The lowest possible limit of concern is set by instrumental noise, but in practice the limit has to be higher. The consequence is that totally pure peaks will never be

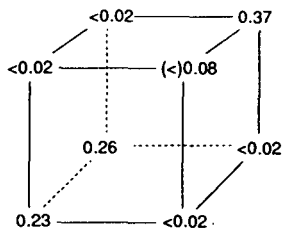

Fig. 5. Responses or the fastest gradient steepness giving the desired solution. The symbol < means that the required resolution is obtained at a gradient steepness lower than that shown. The symbol (<) indicates that not all peaks were tracked but with the peaks that were tracked the desired resolution was obtained at the specified steepness.

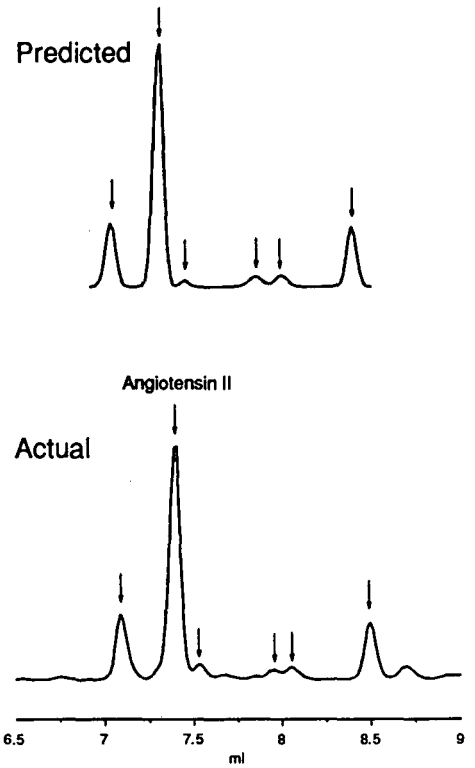

Fig. 6. Predicted and actual chromatograms with the fastest gradient giving the desired resolution with the optimum mobile phase system, *i.e.*, pH 6.5, acetonitrile as organic modifier and TFA added. Peaks that were considered are marked with arrows.

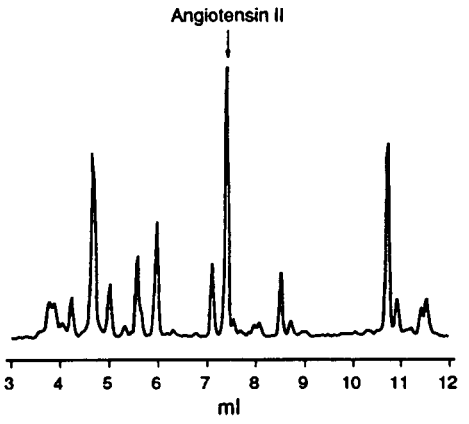

Fig. 7. Actual chromatogram obtained with a gradient starting at 10% of organic modifier.

obtained in separations of complex matrices. In the optimization of a separation it is also meaningless to seek separation from extremely small interferences as there is a natural variation over samples and the contents of these small interferences are likely to vary.

Number of experiments

The number of experiments needed in this strategy is dependent on how many mobile phase variables are considered. In the application presented, three variables were used and 25 experiments were made (three gradient for each mobile phase system and one run under the optimum conditions). It was pointed out earlier that the choice of mobile phase systems is related to the specific application. The number of experiments will be a function of the mobile phase system that is relevant and how many variables one can, and wants to, use. A large number of experiments might be discouraging, but working with a structured strategy the experimental work can usually be made very efficient. It is also our experience that with automated instrumentation the most time-consuming part is the evaluation of the chromatograms and not the experimental work.

Separation of several peptides

The proposed strategy is illustrated here with the separation of one peptide from a complex background. This can easily be extended to several peptides and the aim will then be to obtain a minimum resolution for all peptides of interest with the fastest possible gradient. The limitation of this strategy is that only non-segmented gradients are used.

Extensive use of models

It is tempting to extend the use of retention models, or to use response models, for the prediction of the fastest gradient for an intermediate mobile phase system. There are, however, several reasons for not following this approach. As been pointed out earlier, the pH range is highly restricted. This exclusion of significant variations in pH, which is the most powerful variable, leaves concentration of TFA and composition of organic modifier as quantitative variables. It is possible to make response models for these variables, but models of response are often unsmooth, creating a need for higher order terms and many experiments. The other alternative, *i.e.*, retention models, generally needs quadratic terms, which will increase the number of experiments. Peak tracking can also be difficult when alterations are made to the mobile phase. Finally, it is our experience that with a set pH, the concentration of ion-pairing reagent and the type of organic modifier have no dramatic effect on selectivity, hence fine tuning is rarely meaningful.

CONCLUSIONS

The proposed strategy for optimization of the separation of one peptide from a complex, unknown matrix has been proved to work with a real example. The combination of the predictive capability of gradient theory with experimental design is shown to be extremely powerful. Peak tracking, the weak point in many optimization strategies, is performed to an extent that is realistic for real samples. The selection of mobile phase variables, the initial step in optimization, is crucial in peptide separations by reversed-phase liquid chromatography. This selection is always a compromise, which is dependent on the application. The compromise used in this work

gave acceptable results in terms of peak shape, reproducibility and column stability.

The strategy presented in this work is applicable to a wide range of complex peptide samples. It will hopefully make method development more efficient and eliminate the common trial-and-error approach.

SYMBOLS

φ	Concentration of organic modifier (%)
φ_0	Starting concentration of organic modifier (%)
a	Model parameter
B	Gradient slope (%/ml)
b	Gradient steepness
F	Flow-rate (ml/min)
k'_0	k' at starting concentration of organic modifier
k'_f	k' when the solute leaves the column
m	Model parameter ($\%^{-1}$)
N	Plate number
R_s	Resolution
s	Gradient rate (%/min)
V_g	Retention volume (ml)
V_m	Dead volume (ml)
W_{bg}	Peak width at base (ml)

ACKNOWLEDGEMENTS

The authors tank Pharmacia LKB Biotechnology for providing the HPLC instrumentation. The practical advice and personal support of Margareta Tennander at Pharmacia–LKB Biotechnology are most appreciated.

REFERENCES

1 W.S. Hancock, C.A. Bishop and M.T.W. Hearn, *Science*, 200 (1978) 1168.
2 W.S. Hancock, C.A. Bishop and M.T.W. Hearn, *FEBS Lett.*, 72 (1976) 139.
3 K. Benedek, S. Dong and B.L. Karger, *J. Chromatogr.*, 317 (1984) 227.
4 K.D. Nugent, W.G. Burton, T.K. Slattery, B.F. Johnson and L.R. Snyder, *J. Chromatogr.*, 443 (1988) 381.
5 G. Thévenon and F.E. Regnier, *J. Chromatogr.*, 476 (1989) 499.
6 C.T. Wehr, R.P. Lundgard and K.D. Nugent, *LC·GC Int.*, 2(3) (1989) 24.
7 J.D. Pearson and F.E. Regnier, *J. Liq. Chromatogr.*, 6 (1983) 497.
8 W.G. Burton, K.D. Nugent, T.K. Slattery, B.R. Summers and L.R. Snyder, *J. Chromatogr.*, 443 (1988) 363.
9 K.A. Cohen, K. Schellenberg, K. Benedek, B.L. Karger, B. Grego and M.T.W. Hearn, *Anal. Biochem.*, 140 (1984) 223.
10 J.L. Glajch, J.J. Kirkland and J. Köhler, *J. Chromatogr.*, 384 (1987) 81.
11 N. Tanaka, K. Kimata, Y. Mikawa, K. Hosoya, T. Araki, Y. Ohtsu, Y. Shiojima, R. Tsuboi and H. Tsuchiya, *J. Chromatogr.*, 535 (1990) 13.
12 D.S. Stegehuis, U.R. Tjaden, C.M.B. van den Beld and J. van der Greef, *J. Chromatogr.*, 549 (1991) 185.
13 R. Newcomb, *LC·GC Int.*, 2(9) (1989) 28.
14 C.E. Goewie, *J. Liq. Chromatogr.*, 9 (1986) 1431.
15 A. Drouen, J.W. Dolan, L.R. Snyder, A. Poile and P.J. Schoenmakers, *LC·GC Int.*, 5(2) (1992) 28.
16 P.J. Schoenmakers, *Optimization of Chromatographic Selectivity*, Elsevier, Amsterdam, 1986.
17 J.C. Berridge, *Techniques for the Automated Optimization of HPLC Separation*, Wiley, Chichester, 1985.
18 I. Molnar, R. Boysen and P. Jekow, *J. Chromatogr.*, 485 (1989) 569.
19 J.W. Dolan, *LC·GC Int.*, 3(7) (1990) 17.
20 J.L. Glajch, M.A. Quarry, J.F. Vasta and L.R. Snyder, *Anal. Chem.*, 58 (1986) 280.
21 H.J. Issaq and K.L. McNitt, *J. Liq. Chromatogr.*, 5 (1982) 1771.
22 J.K. Strasters, H.A.H. Billiet, L. de Galan and B.G.M. Vandeginste, *J. Chromatogr.*, 499 (1990) 499.
23 E.P. Lankmayr, W. Wegscheider, J. Daniel-Ivad, I. Kolossváry, G. Csonka and M. Otto, *J. Chromatogr.*, 485 (1989) 557.
24 H.A.H. Billiet and L. de Galan, *J. Chromatogr.*, 485 (1989) 27.
25 J.L. Glajch and J.J. Kirkland, *J. Chromatogr.*, 485 (1989) 51.
26 J.C. Berridge, *J. Chromatogr.*, 244 (1982) 1.
27 A.F. Fell, T.A.G. Noctor, J.E. Mama and B.J. Clark, *J. Chromatogr.*, 434 (1988) 377.
28 P.J. Schoenmakers and T. Blaffert, *J. Chromatogr.*, 384 (1987) 117.
29 P.M.J. Coenegracht, A.K. Smilde and A. Knevelman, *J. Liq. Chromatogr.*, 12 (1989) 77.
30 J.M. Juárez, A. Bermejo, J.L. Bernal, M.J. del Nozal and G.A. García, *Chromatographia*, 29 (1990) 338.
31 Y. Hu and D.L. Massart, *J. Chromatogr.*, 485 (1989) 311.
32 E.P. Lankmayr, W. Wegscheider, J.C. Gfeller, N.M. Djordjevic and B. Schreiber, *J. Chromatogr.*, 485 (1989) 183.
33 H.J.G. Debets, B.L. Bajema and D.A. Doornbos, *Anal. Chim. Acta*, 151 (183) 131.
34 A. Peeters, L. Buydens, D.L. Massart and P.J. Schoenmakers, *Chromatographia*, 26 (1988) 101.
35 B.G.M. Vandeginste, G. Kateman, J.K. Strasters, H.A.H. Billiet and L. de Galan, *Chromatographia*, 24 (1987) 127.

36 G.G.R. Seaton and A.F. Fell, *Chromatographia*, 24 (1987) 208.
37 M. Maeder, *Anal. Chem.*, 59 (1987) 527.
38 A.G. Wright, A.F. Fell and J.C. Berridge, *J. Chromatogr.*, 458 (1988) 335.
39 J.K. Strasters, F. Coolsaet, A. Bartha, H.A.H. Billiet and L. de Galan, *J. Chromatogr.*, 499 (1990) 523.
40 T.P. Bridge, M.H. Williams and A.F. Fell, *J. Liq. Chromatogr.*, 12 (1989) 23.
41 R.J. Lynn, S.D. Patterson and R.E.A. Escott, *LC·GC Int.*, 3(9) (1990) 54.
42 M.A. Stadelius, H.S. Gold and L.R. Snyder, *J. Chromatogr.*, 296 (1984) 31.
43 B.F.D. Ghrist and L.R. Snyder, *J. Chromatogr.*, 459 (1988) 43.
44 J.W. Dolan, D.C. Lommen and L.R. Snyder, *J. Chromatogr.*, 485 (1989) 91.
45 J. Schmidt, *J. Chromatogr.*, 485 (1989) 421.
46 S. Heinisch, J.-L. Rocca and M. Kolosky, *Chromatographia*, 29 (1990) 482.
47 N. Lundell, *J. Chromatogr.*, 639 (1993) 97.
48 L.R. Snyder, in Cs. Horváth (Editor), *High Performance Liquid Chromatography: Advances and Perspectives*, Vol. 1, Academic Press, New York, 1980, p. 207.
49 L.R. Snyder and M.A. Stadalius, in Cs. Horváth (Editor), *High Performance Liquid Chromatography: Advancaes and Perspectives*, Vol. 4, Academic Press, New York, 1986, p. 195.
50 P. Jandera and J. Churáček, *Gradient Elution in Column Liquid Chromatography, Theory and Practice*, Elsevier, Amsterdam, 1985.
51 P. Jandera and J. Churáček, *J. Chromatogr.*, 91 (1974) 223.
52 M.T.W. Hearn and B. Grego, *J. Chromatogr.*, 255 (1983) 125.
53 M.J. O'Hare, M.W. Capp, E.C. Nice, N.H.C. Cooke and B.G. Archer, *Anal. Biochem.*, 126 (1982) 17.
54 P.S. Sadek, P.W. Carr, L.D. Bowers and L.C. Haddad, *Anal. Biochem.*, 153 (1986) 359.
55 K.E. Bij, C. Horváth, W.R. Melander and A. Nahum, *J. Chromatogr.*, 203 (1981) 65.
56 S. Linde and B. Welinder, *J. Chromatogr.*, 536 (1991) 43.
57 J.E. Rivier, *J. Chromatogr.*, 202 (1980) 211.
58 W.S. Hancock and J.T. Sparrow, *J. Chromatogr.*, 206 (1981) 71.
59 C.T. Mant and R.S. Hodges, *Chromatographia*, 24 (1987) 805.
60 W.S. Hancock, C.A. Bishop, R.L. Prestidge, D.R.K. Harding and M.T.W. Hearn, *J. Chromatogr.*, 153 (1978) 391.
61 W.S. Hancock, C.A. Bishop, R.L. Prestidge and M.T.W. Hearn, *Anal. Biochem.*, 89 (1978) 203.
62 J.E. Rivier, *J. Liq. Chromatogr.*, 1 (1978) 343.
63 H.P.J. Bennett, C.A. Browne and S. Solomon, *J. Liq. Chromatogr.*, 3 (1980) 1353.
64 D. Guo, C.T. Mant and R.S. Hodges, *J. Chromatogr.*, 386 (1987) 205.
65 A.N. Starratt and M.E. Stevens, *J. Chromatogr.*, 194 (1980) 421.
66 Data available on request.
67 M.T.W. Hearn, in Cs. Horváth (Editor), *High Peformance Liquid Chromatography: Advances and Perspectives*, Vol. 3, Academic Press, New York, 1983, p. 87.
68 J.A. Smith and M.J. O'Hare, *J. Chromatogr.*, 299 (1984) 13.
69 S. Linde and B.S. Welinder, *J. Chromatogr.*, 548 (1991) 195.
70 D.J. Poll and D.R.K. Harding, *J. Chromatogr.*, 469 (1989) 231.
71 B. Fransson, *J. Chromatogr.*, 361 (1986) 161.
72 C. Dewaele, P. Mussche and M. Verzele, *J. High Resolut. Chromatogr. Chromatogr. Commun.*, 5 (1982) 616.
73 L.A. Witting, D.J. Gisch, R. Ludwig and R. Eksteen, *J. Chromatogr.*, 296 (1984) 97.
74 J.J. Kirkland, J.L. Glajch and R.D. Farlee, *Anal. Chem.*, 61 (1989) 2.
75 K. Larsson, W. Hermann, P. Möller and D. Sanchez, *J. Chromatogr.*, 450 (1988) 71.
76 O. Mikes and J. Coupek, in K.M. Gooding and F. Regnier (Editors), *HPLC of Biological Macromolecules: Methods and Applications*, Marcel Dekker, New York, 1990, p. 25.
77 T. Ohtani, Y. Tamura, M. Kasai, T. Uchida, Y. Yangihara and K. Noguchi, *J. Chromatogr.*, 515 (1990) 175.
78 K.A. Tweeten and T.N. Tweeten, *J. Chromatogr.*, 359 (1986) 111.
79 S.D. Power, M.A. Lochrie and R.O. Poyton, *J. Chromatogr.*, 266 (1983) 585.
80 C.T. Mant and R.S. Hodges, *J. Liq. Chromatogr.*, 12(1 & 2) (1989) 139.
81 H. Linder and W. Helliger, *Chromatographia*, 30 (1990) 518.
82 L.R. Gurley, D.A. Prentice, J.G. Vadez and W.D. Spall, *Anal. Biochem.*, 131 (1983) 465.
83 M. Andre, *J. Chromatogr.*, 351 (1986) 341.
84 W.H. Vensel, V.S. Fujita, G.E. Tarr, E. Margoliash and H. Kayser, *J. Chromatogr.*, 266 (1983) 491.
85 M. Rubinstein, *Anal. Biochem.*, 98 (1979) 1.
86 A.K. Taneja, S.Y.M. Lau and R.S. Hodges, *J. Chromatogr.*, 317 (1984) 1.

Journal of Chromatography, 639 (1993) 129–140
Elsevier Science Publishers B.V., Amsterdam

CHROM. 24 967

Evaluation of stationary phases for the separation of buckminsterfullerenes by high-performance liquid chromatography

Moustapha Diack

Department of Chemistry, University of Tennessee, Knoxville, TN 37996-1501 (USA) and Division of Analytical Chemistry, Oak Ridge National Laboratory, Oak Ridge, TN 37831-6120 (USA)

R.N. Compton

Department of Chemistry, University of Tennessee, Knoxville, TN 37996-1501 (USA) and Chemical Physics Section, Oak Ridge National Laboratory, Oak Ridge, TN 37831-6125 (USA)

Georges Guiochon*

Department of Chemistry, University of Tennessee, Knoxville, TN 37996-1501 (USA) and Division of Analytical Chemistry, Oak Ridge National Labortory, Oak Ridge, TN 37831-6120 (USA)

(First received November 26th, 1992; revised manuscript received February 9th, 1993)

ABSTRACT

The high-performance liquid chromatographic separation of the buckminsterfullerenes C_{60} and C_{70} was studied using different chromatographic systems. Normal-phase (silica), non-aqueous reversed-phase (C_{18}-bonded silica and graphitized carbon black) and charge-transfer complexation with dinitrobenzoylphenylglycine (DNBPG) and 2-(2,4,5,7-tetranitro-9-fluorenylideneamino-oxy)propionic acid (TAPA) were considered as retention mechanisms. Mobile phases of different compositions, but all based on hydrocarbons (toluene, hexane, heptane) as the main solvent, were used. Although it was found that the adsorption of the fullerenes on all the other phase systems is exothermic, their interactions with the charge-transfer phases exhibit an unusual endothermic behavior. The retention times of C_{60} and C_{70} on these phases increase with increasing temperature. The adsorption enthalpy and entropy derived from the Van 't Hoff plots confirm this rare temperature dependence. The adsorption enthalpy is positive whereas the adsorption entropy is strongly positive.

INTRODUCTION

The separation and purification of the buckminsterfullerenes by preparative high-performance liquid chromatography (HPLC) remain a challenging proposition, although their analytical separation is easy and straightforward. A large number of chromatographic separation methods have been described previously. These methods involve the use of gravity, HPLC or Soxhlet extraction liquid chromatographic techniques and the use as stationary phases of silica [1], alumina [2,3], reversed phases on C_{18}-bonded silica [4] or graphite [5], multi-legged phenyl-bonded phases [6] and separation on gel permeation phases [7].

The applicability of these different approaches

* Corresponding author. Address for correspondence: Department of Chemistry, University of Tennessee, Knoxville, TN 37996-1501, USA.

0021-9673/93/$06.00

for preparative purposes is limited, however, by the low throughput generally observed. An efficient separation on a conventional analytical column can be maintained only with sub-milligram amounts. The transposition of the optimized techniques to the semi-preparative (*ca.* 10-mg injection) or preparative level on a wide column (*ca.* 100–1000-mg injection on a *ca.* 5 cm I.D. column) is rendered difficult by some serious limitations due to the complexity of the matrix and the poor solubility of its components in the usual solvents.

The two common techniques available for the generation of fullerenes, laser vaporization and electric discharge, produce a complex soot containing C_{60} and C_{70} in a ratio of approximately 9:1, and varying but small amounts of higher mass fullerenes [4,8]. This is an unfavorable concentration ratio for purification by preparative chromatography. In overloaded elution chromatography, the two components of a binary mixture compete for access to the finite number of adsorption sites on the surface of the stationary phase during their migration along the column. The ease of the separation of the components of the mixture, their production rates and their recoveries depend strongly on their concentration ratio in the original mixture or feed.

As shown theoretically [9] and later proven experimentally [10], the purification of a 1:9 mixture is easier than that of a 9:1 mixture because the displacement effect of the lesser retained by the more retained component sharpens the boundary between the two component bands, improves their resolution and thus increases the recovery. At the same time, the presence of a high concentration of the lesser retained component decreases the adsorption of the more strongly retained one by crowding its molecules out of the surface. This is the "tag-along" effect [9]. The intensity of the displacement and tag-along effects depends on the concentration ratio of the two components and on the column efficiency [9]. The former is greater with a 1:9 mixture and the latter with a 9:1 mixture. Therefore, if one is interested in producing both components in a single step, the purification of a 9:1 mixture is much more difficult than that of a 1:9 mixture, because the displacement effect is weak, and the intense tag-along effect leads to a poor recovery [9]. With a 9:1 mixture, touching band separation is preferable to more strongly overloaded conditions, as it avoids recycling with only a small loss of production [4,10,11]. Finally, it does not seem possible to find a chromatographic system with which the heavier and more polarizable C_{70} would be eluted before C_{60}.

The different members of the fullerene series are insoluble in the most common solvents used in liquid chromatography. They are only slightly soluble in benzene (1.4 mg/ml C_{60}) and toluene (2.2 mg/ml C_{60}). For safety reasons, the latter is the most common solvent used to dissolve them. Some higher boiling solvents, such as mesitylene or pyridine, have been suggested [12] for the extraction of fullerenes from soot, but they are inconvenient for use in routine analytical or preparative chromatography because of their viscosity or odor, and because of increased difficulties in recovering the purified fractions. As already proven [4], however, the use of benzene or toluene as eluent results in very low or nearly negligible retention factors on most phases.

To overcome this limitation, a weaker solvent (linear alkanes, dichloromethane, ethyl acetate, acetonitrile or alcohols) is mixed with toluene to insure an adequate retention, while the sample solvent used is pure toluene or benzene in order to permit the injection of narrow bands of concentrated solutions, and insure an adequate throughput. However, it has been demonstrated both theoretically and practically [13,14] that chromatographic abnormalities (*e.g.*, band deformations, band splitting) can result from the use of a sample solvent having a higher elution strength than the mobile phase. The effect is especially important under overloaded conditions and when the sample solvent is the essential component of the feed. There is often no noticeable effect under analytical conditions because the sample solvent is quickly diluted in the eluent. In contrast, in preparative applications this hinders the purification process and decreases the recovery [13].

A remedy to the first limitation, that origina-

ting from the composition of the feed, should be found in a better understanding of the parameters involved in the process of generation of the fullerenes. The solution to the second is in the development of new types of stationary phases, more selective and more strongly retentive of the fullerenes, thus allowing the use of a stronger eluent compatible with the natural sample solvent. Considerable progress has been made along this line. Charge-transfer chromatography [15] offers a logical and promising approach to the separation of fullerenes.

It has been known for more than a century that certain pairs of organic compounds can form stable molecular complexes [16] by electron transfer from a high electronic density center (*i.e.*, planar polyaromatic compounds) to an electron-deficient center. Chromatographic methods based on the formation of such complexes between an immobilized selectant acceptor and a solute donor or *vice versa* have been termed electron donor–acceptor (EDA) or charge-transfer chromatography [15]. Aromatic or heterocyclic compounds with strongly electron-attracting groups (*i.e.*, NO_2, Cl, Br) are good π-electron acceptors, whereas electron-releasing groups (*i.e.*, CH_3, CH_3O, NH_2) enhance the electron donor properties of the cycle.

For a given electron acceptor, the stability of the EDA complex, and thus the retention time in a given chromatographic system, depend on the intensity of the electron-releasing property of the donor. Consequently, the retention factors of the two components and their separation factor for a given mobile phase concentration should depend on the difference in their respective electron-donor abilities. Based on the evidence that the magnetic susceptibility of C_{70} is twice that of C_{60} [17] and that their second ionization potentials are different [18], it is to be expected that these two molecules should exhibit markedly different electron-donor abilities and can be separated on a suitable stationary phase. The only possible limitation could be that charge-transfer adsorbents are known for their high degree of planar recognition. Thus, strong retention cannot be expected.

Cox *et al.* [19] were the first to separate C_{60} and C_{70} by charge-transfer chromatography using dinitroanilinopropyl-bonded silica as selectant, and a linear gradient of hexane–dichloromethane. They showed that C_{60} (which has twenty aromatic rings, but is not planar) behaves as triphenylene, a planar five-membered aromatic compound, whereas C_{70} elutes somewhere between benzopyrene and coronene. This illustrates the effect of the non-planarity of the analyte on the retention mechanism. Other selectants have also been proposed [20]. Recently a new family of charge-transfer stationary phases, termed "Buckyclutcher", were synthesized [21]. These phases use tripodal dinitro derivatives as selectants. They are reported to exhibit good retention and a high selectivity for the C_{60} and C_{70} fullerenes, even when a 50:50 hexane–toluene solution or pure toluene is used as the mobile phase.

In this paper we describe the chromatographic behavior of the C_{60} and C_{70} fullerenes on (*R*)-(−)-2-(2,4,5,7-tetranitro-9-fluorenylideneaminooxy)propionic acid (TAPA), a chiral stationary phase used earlier for the separation of carbohelicenes [22], and synthesized in our laboratory; we discuss the retention mechanism on this selectant and the optimization of the separation of C_{60} and C_{70} in terms of mobile phase composition and temperature, and finally we compare the behavior of the same compounds on dinitrobenzoylphenylglycine (DNBPG), silica, ODS and graphitized carbon black (GCB).

THEORY

The Gibbs free energy, ΔG, for the equilibrium of a solute in a chromatographic system is related to the retention factor through the partition coefficient, K, by the following equations:

$$\Delta G = -RT \ln K \quad (1)$$

$$k' = FK \quad (2)$$

where R is the universal gas constant, T is the absolute temperature, F is the phase ratio and k' is the retention or column capacity factor.

The dependence of the retention factor on the column temperature can be derived from the following fundamental equations of thermodynamics and the previous relationships:

$$\Delta G = \Delta H - T\,\Delta S \quad (3)$$

$$\ln k' = -\frac{\Delta H}{RT} + \frac{\Delta S}{R} + \ln F \quad (4)$$

where ΔH and ΔS are the molar enthalpy of transfer from the selectant to the eluent and the associated change of the molar standard entropy, respectively.

Because the phase ratio is close to 1 in these phase systems [$F = (1 - \epsilon_T)/\epsilon_T$, with the total porosity of the column, ϵ_T, being approximately 0.5), $\ln F$ can be neglected in eqn. 4, and

$$\ln k' = -\frac{\Delta H}{RT} + \frac{\Delta S}{R} \quad (5)$$

Therefore, if the retention mechanism remains the same over the temperature range considered and the enthalpy is constant (*i.e.*, if we neglect the difference in molar heat capacity of the fullerenes at infinite dilution in the two phases), the enthalpy and entropy of transfer can be derived from the slope and the intercept of a semi-logarithmic plot of the experimental capacity factors *versus* the ratio $1/RT$, commonly referred to as the Van 't Hoff plot.

EXPERIMENTAL

Instrumentation

An HP1090 liquid chromatograph (Hewlett-Packard, Palo Alto, CA, USA) equipped with a multi-solvent-delivery system, an automatic sample-injection system, a photodiode-array detector, a temperature control system, and a data station was used.

Preparative separations were conducted on a Prochrom (Nancy, France) LD-50 axial compression column, with a *ca.* 20 cm × 5 cm I.D. column, fitted to a Biotage (Charlotteville, VA, USA) pumping system.

Columns

A 250 × 4.6 mm I.D. and a 100 × 4.6 mm I.D. column were laboratory-packed with 17.8-μm IMPAQ RG2010 C_{18} silica (PQ, Conshohoken, PA, USA) and with LiChrosorb Si60 silica (EM Separations, Gibbstown, NJ, USA), respectively. In both instances, we used the same standard slurry packing method, with methanol at 6000 p.s.i. (1 p.s.i. = 6894.76 Pa). The efficiencies of these columns were 1900 and 2200 theoretical plates, respectively.

A 250 × 4.6 mm I.D. DNBPG column and a 100 × 4.6 mm I.D. GCB column were obtained from J.T. Baker (Phillipsburg, NJ, USA) and Shandon Scientific (Runcorn, UK), respectively. The efficiency of the DNBPG column was 8000 plates and that of the GCB column 1000 plates.

The synthetic route for the preparation of the chiral TAPA stationary phase is illustrated in Fig. 1. This material was prepared in our laboratory by means of the two-step synthesis reported previously [22]. A 100 × 4.6 mm I.D. column

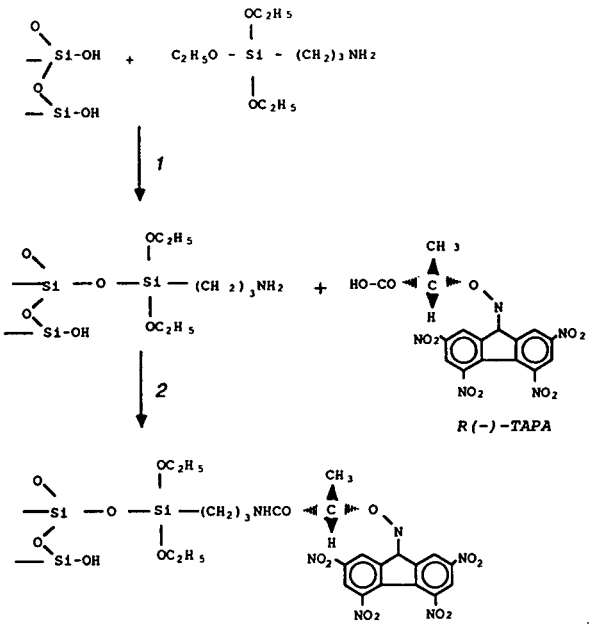

Fig. 1. Synthetic route for the preparation of the chiral (*R*)-(−)-2-(2,4,5,7-tetranitro-9-fluorenylideneaminooxy)-propionic acid (TAPA) adsorbent. Step 1: 1 g of activated (4 h at 120°C) LiChrosorb Si60 was first coupled to 1.3 m*M* of 3-aminopropyltriethoxysilane. The reaction was conducted in toluene, using a refluxing system at 120°C with stirring for 16 h. The aminated silica gel was washed with toluene, methanol and acetone and then dried under vacuum (2 h at 120°C). Step 2: the asymmetric moiety, TAPA, was linked to the aminated silica using dicyclohexylcarbodiimide (DCC) as coupling agent [23]. The reaction was conducted in dry chloroform for 8 h at room temperature. The resulting silica-bonded phase was washed with chloroform, acetone and methanol and dried (1 h at 110°C). The microanalysis of the material gave a carbon content of 12.6%. A 100 × 4.6 mm column was packed using the balanced-slurry technique.

was packed with this phase. The column efficiency was 1600 plates.

Eluent and samples

The different solvents used were all of HPLC grade and were used without further purification.

The samples of fullerenes were obtained from the extraction of a laboratory-made soot using boiling toluene [4]. The purified standard compounds were obtained by preparative chromatography, using a dual silica–alumina column system in the gravity mode, with hexane–toluene (95:5, v/v) as the mobile phase.

Chromatographic measurements

The eluent flow-rate was maintained at 1 ml/min in all experiments. The column efficiencies were measured at room temperature, using standard solutions of C_{60}. The columns void times (t_0) were determined by injecting a small plug of pure toluene and recording the perturbation signal. Under these conditions only very minor variations of t_0 were observed in the temperature range studied.

Determination of Van 't Hoff plots

The Van 't Hoff plots were determined by measuring the capacity factors of the fullerenes over the temperature range 25–95°C when toluene, heptane or their mixtures were used as the mobile phase and 25–70°C when methanol was used. Two different standard solutions (10 g/l) of C_{60} and C_{70} were injected in duplicate for each temperature point. When experiments were completed at a given temperature, the column was allowed to reach equilibrium at the next temperature by flushing it with a constant stream of mobile phase for 35 min prior to making an injection.

RESULTS AND DISCUSSION

Because the retention and separation factors and the column efficiency depend on the eluent composition and the column temperature, we need to optimize them both in order to obtain the best resolution or the maximum production rate. Accordingly, different mobile phase compositions were studied, depending on the type of interaction involved (*e.g.*, adsorption, charge transfer). In all instances, one of our principal goals was the achievement of a high selectivity and a sufficient retention factor at the highest possible toluene concentration in the mobile phase. Heptane was preferred to hexane as the weak solvent, because of the possibility of conducting experiments in a wider temperature range.

Normal- and reversed-phase adsorption chromatography

The use of silica in either the gravity or the HPLC mode has been advocated in the literature for the purification of the fullerenes. With the various stationary phases investigated in this study, however, all the mobile phases used, whatever their composition, resulted in very low retention factors and a poor selectivity for C_{60} and C_{70}. Hence it seems that while silica can purify fullerenes from the polycyclic aromatic hydrocarbons present in the soot, it cannot separate the fullerenes.

Conversely, nearly irreversible adsorption of the fullerenes was observed on the GCB column, even with pure toluene or chloroform as the mobile phase. Heavier, more polarizable solvents such as tetralin and xylene were not considered because of the potential difficulties in eliminating them from the mobile phase after the separation has been achieved.

Fig. 2 shows a plot of the logarithm of the retention factors of C_{60} and C_{70} *versus* the volume fraction of toluene in methanol, on the C_{18} column. Attempts to use heptane–toluene solutions as the mobile phase resulted in a poor selectivity and a low retention. As can be seen in Fig. 2, the retention factors and the separation factor of the two fullerenes decrease rapidly with increasing toluene content of the mobile phase. While the physico-chemical phenomena responsible for retention on chemically bonded C_{18} are not fully understood, this observation can be explained by the solvophobic theory [24], or on the basis of the solubility of fullerenes in the mobile phase [25]. As far as analytical separations are concerned, the C_{60} and C_{70} fullerenes are easily resolved, with a separation factor up to 2.4, using binary mixtures of methanol and

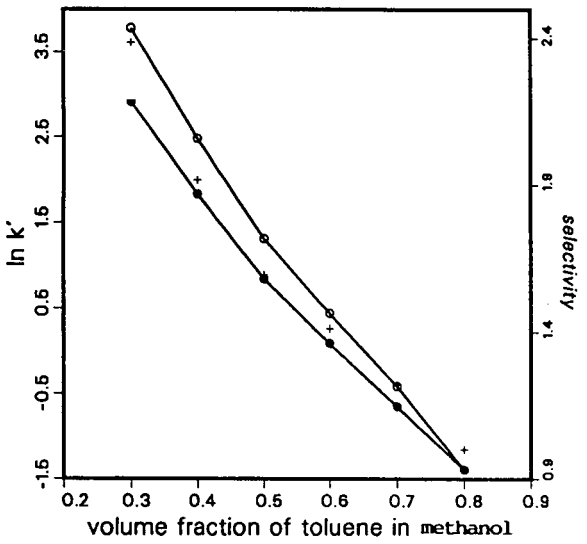

Fig. 2. Plots of the logarithmic retention factors of (●) C_{60} and (○) C_{70} fullerenes against the volume fraction of toluene in methanol. + = Corresponding selectivity. Experimental conditions: column, C_{18} (25 × 0.46 cm I.D.); temperature, 25°C; flow-rate, 1 ml/min; detection, UV at 384 nm; amount injected, 20 μl (10 mg/ml solution in toluene).

toluene as the eluent and toluene as the sample solvent. However, as will be shown later, complications quickly arise when one increases the amount injected.

Charge-transfer chromatography

In Figs. 3 and 4, we show the plots of the logarithm of the retention and separation factors of C_{60} and C_{70} on the DNPBG and the TAPA columns, *versus* the volume fraction of toluene in heptane. As often reported in the literature, quasi-linear plots were obtained in both instances. For a given eluent composition (*e.g.*, 50:50), the retention factors of C_{60} (k'_1) and C_{70} (k'_2), and their selectivity, α, are larger with the TAPA column ($k'_1 = 1.71$, $k'_2 = 3.43$, $\alpha = 2$) than with the DNBPG column ($k'_1 = 0.26$, $k'_2 = 0.35$, $\alpha = 1.35$). TAPA is a stronger electron acceptor than DNBPG.

The chromatograms in Fig. 5 illustrate well the retention behavior of C_{60} and C_{70} on the TAPA column and the decrease in their resolution with increasing toluene concentration in the mobile phase.

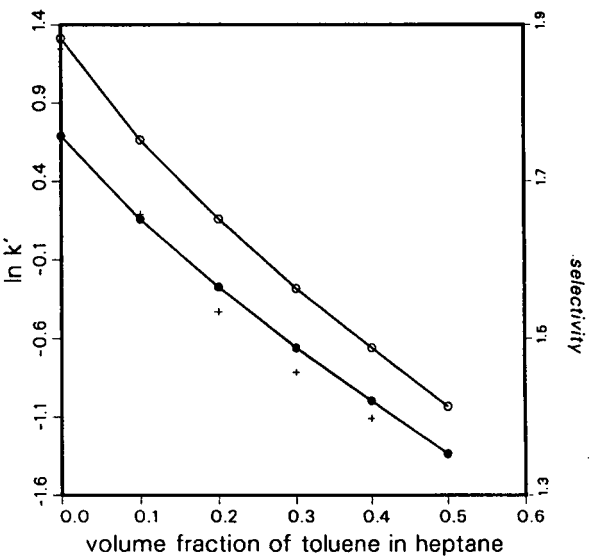

Fig. 3. Plots of the logarithmic retention factors of (●) C_{60} and (○) C_{70} fullerenes against the volume fraction of toluene in heptane. + = Corresponding selectivity. Column, DNBPG (25 × 0.46 cm I.D.); other conditions as Fig. 2.

Influence of temperature on the separation

Our main interest in studying preparative separations of the fullerenes by charge-transfer chromatography lies in the existence of a second

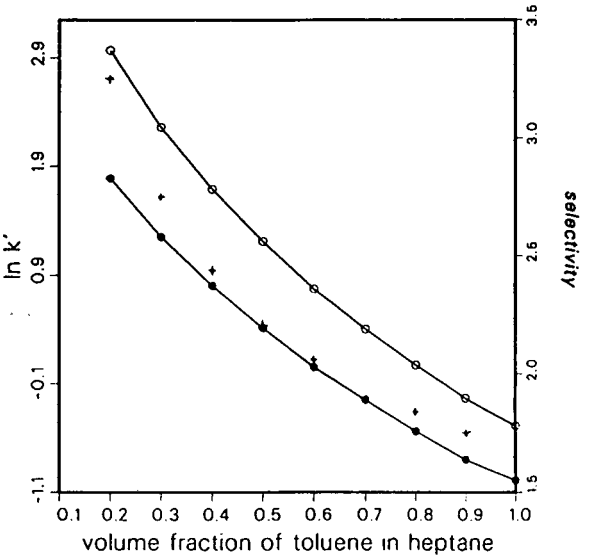

Fig. 4. Plots of the logarithmic retention factors of (●) C_{60} and (○) C_{70} fullerenes against the volume fraction of toluene in heptane. + = Corresponding selectivity. Column, TAPA (10 × 0.46 cm I.D.); other conditions as in Fig. 2.

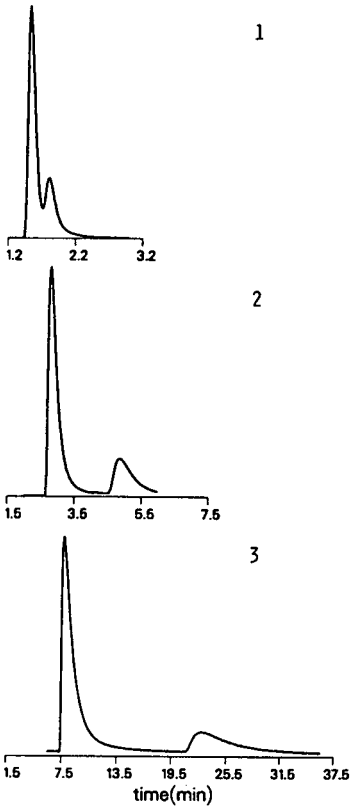

Fig. 5. Chromatogram illustrating the variation in retention time and the selectivity between C_{60} and C_{70} with the mobile phase composition. 1 = Pure toluene; 2 = toluene–heptane (50:50); 3 = toluene–heptane (20:80). Conditions as in Fig. 4.

degree of freedom of the separation related to their peculiar behavior when the column temperature is changed. Figs. 6–8 show the Van 't Hoff plots obtained for C_{60} and C_{70} on the ODS column with methanol–toluene (50:50) (Fig. 6), the DNBPG column with heptane–toluene (90:10) (Fig. 7), and the TAPA column with heptane–toluene (50:50) (Fig. 8). Because of the temperature limitations encountered in the use of the different solutions, and owing to the different boiling points of the solvents used, the temperature range investigated was 25–75°C for Fig. 6 and 25–95°C for Figs. 7 and 8.

The Van 't Hoff plots are all linear in the temperature range studied. The correlation coefficients for a linear fit of the experimental data to the Van 't Hoff plots (eqn. 5) were ≥ 0.989. The same trends were observed for the different

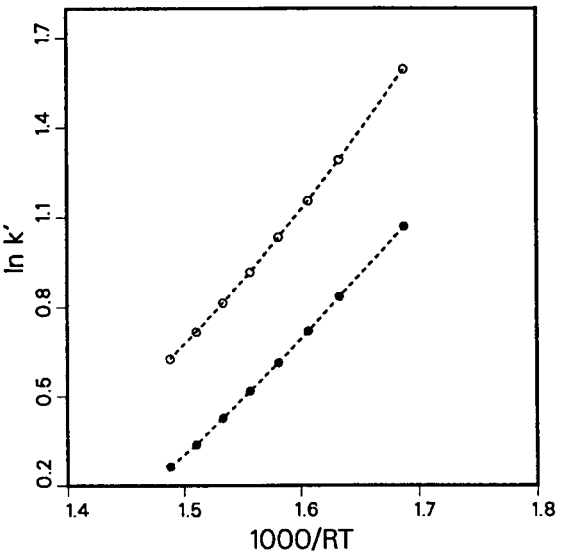

Fig. 6. Van 't Hoff plots of the retention factors for C_{60} and C_{70} [$1000/RT$ in cal^{-1} mol (1 cal = 4.184 J)]. The retention data were measured on a 16.7-μm C_{18} column (25 × 0.46 cm I.D.) at an eluent [toluene–methanol (50:50)] flow-rate of 1 ml/min. The detector setting was 360 nm for C_{60} and 384 nm for C_{70}.

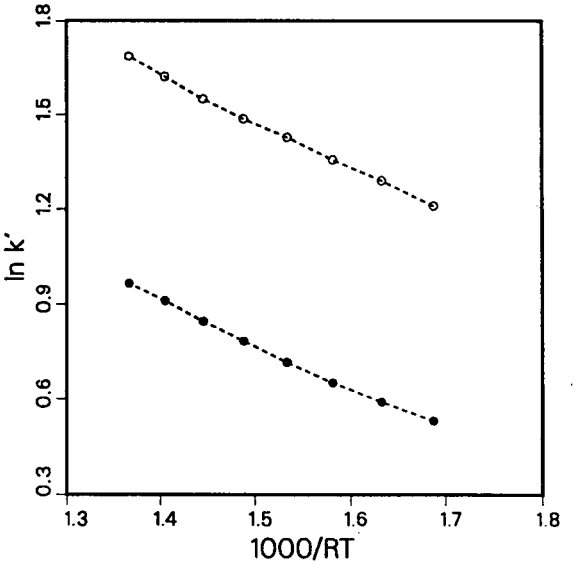

Fig. 7. Van 't Hoff plots of the retention factors for C_{60} and C_{70} ($1000/RT$ in cal^{-1} mol). The retention data were measured on a commercial analytical DNBPG column (25 × 0.46 cm I.D.) at an eluent [toluene–heptane (10:90)] flow-rate of 1 ml/min. The detector setting was 360 nm for C_{60} and 384 nm for C_{70}.

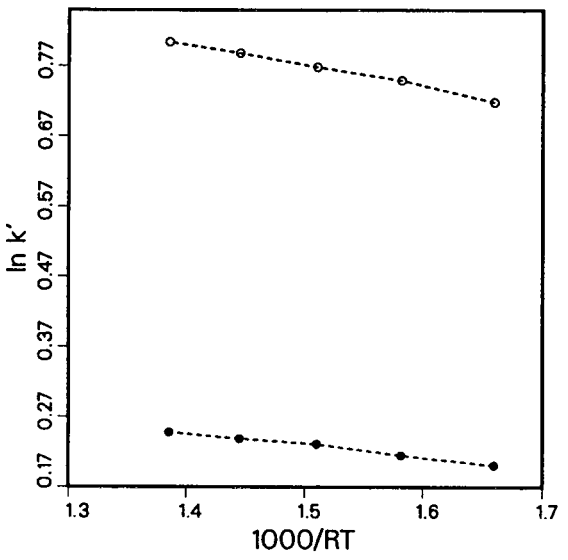

Fig. 8. Van 't Hoff plots of the retention factors for C_{60} and C_{70} ($1000/RT$ in cal^{-1} mol). The retention data were measured on the laboratory-made TAPA column (25 × 0.46 cm I.D.) at an eluent [toluene–heptane (50:50)] flow-rate of 1 ml/min. The detector setting was 360 nm for C_{60} and 384 nm for C_{70}.

solvents, using pure or binary mixtures of various compositions. This suggests that there is a single, or at least a strongly predominant, retention mechanism [26] that does not depend on the solvent composition for the series of solvents studied. This conclusion is consistent with the fact that C_{60} and C_{70} have a single conformation, but it has been shown that they exhibit different phase transitions at low temperatures [27] and one could have expected a non-linear Van 't Hoff plot due to solute–solvent association [28].

As usual in chromatography, the Van 't Hoff plot for the system of ODS with methanol–toluene (50:50) exhibits a positive slope (Fig. 6). Both the adsorption enthalpy and entropy are negative. The adsorption process is exothermic and, as a consequence, the retention times of both solutes decrease with increasing temperature. In contrast, a negative slope is observed for the Van 't Hoff plots obtained with the two charge-transfer systems investigated, DNBPG (Fig. 7) and TAPA (Fig. 8). Therefore, in these two instances the complexation enthalpy and the associated entropy are positive and the heat of complexation is negative. The retention times of C_{60} and C_{70} on the two charge-transfer stationary phases increase with increasing column temperature.

These results substantiate some earlier work done on DNBPG with dichloromethane–hexane (10:90) as the eluent [29]. This unusual temperature dependence was interpreted by assuming that the analytes associate in solution. The oligomers would dissociate when the column temperature increases, allowing more interactions between the selectant and the fullerene members [30]. Indeed, C_{70} seems to undergo some reorganization in an hexagonal close-packed crystal conformation, but a similar behavior has not yet been proven in the liquid phase [27].

It is important to ascertain whether this peculiar behavior is an intrinsic property of the fullerenes, possibly related to their rigid three-dimensional structure and their unique aromatic character. In this connection, we measured the temperature dependence of the retention factors of different planar, non-planar and helicoidal polycyclic aromatic compounds, including *cis*- and *trans*-stilbene, anthracene, phenanthrene, benzo[*e*]- and benzo[*a*]pyrene and hexacarbohelicenes, on the TAPA column. All their retention times decrease rapidly with increasing temperature, suggesting that all these electron-donor compounds undergo an exothermic complexation process on TAPA, whereas the interaction of TAPA with the fullerenes is endothermic. This result suggests that, owing to their non-planar structure and weak aromaticity, the fullerenes are much weaker electron donors than polycyclic aromatic hydrocarbons.

Another interesting feature of Figs. 7 and 8 is that the separation factor of the fullerenes remains virtually independent of the column temperature. A temperature increase does not modify the degree of non-planarity recognition of the selectants. However, noticeable improvements in the experimental band shapes were observed. This can be explained by faster mass-transfer kinetics at higher temperatures.

A negative heat of transfer or a non-linear Van 't Hoff plot is generally related to the effects of solvent or solvent additive [31], to the existence of two different conformers or to a dual reten-

tion mechanism [28,32] for a solute. The two fullerenes C_{60} and C_{70} have a unique conformation, and can behave as both electron acceptor and electron donors. The electron affinity of C_{60} is known to be 2.6 eV. It is improbable that, with the high concentration of toluene in the mobile phases used, a change in column temperature can greatly affect its equilibrium concentration in the stationary phase. Thus, the negative slope of the Van 't Hoff plot can probably be attributed to a high solvation of the solutes at low temperatures.

Practical applications

To illustrate the above discussion, Fig. 9 shows an analytical separation obtained with the injection of 20 μl of a binary mixture of C_{60} and C_{70} (20 mg/ml in toluene) (top) and the chromatogram obtained with an overloaded injection (200 μl of the same solution), in the same ODS column, with methanol–toluene (50:50) as the mobile phase (bottom). A temperature increase of 50°C results in a decrease of *ca.* 5 min in the retention time (dashed line). The profile obtained at 25°C (solid line) is characterized by a pronounced shoulder and a steep rear profile, probably owing to the effect of the sample solvent, as discussed previously [13].

Figs. 10 and 11 illustrate the effect of the column temperature on the separation of the two fullerenes, using DNBPG [injection volume 100 μl; solution 10 mg/ml; mobile phase heptane–toluene (90:10)], and TAPA [same conditions, except mobile phase composition heptane–toluene (50:50)]. Increasing the temperature from 25°C (solid line) to 95°C (dashed line) results in an increase in the retention time. The magnitude of the effect is more pronounced with the TAPA column because of the higher donor ability of the selectant and the higher retention factors. With the DNBPG column, splitting of

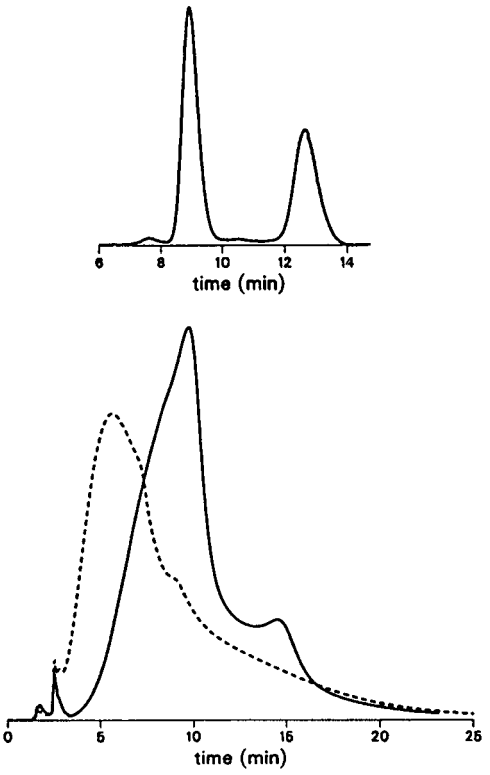

Fig. 9. Separation of C_{60} and C_{70} on a C_{18} bonded silica stationary phase. (top) Analytical injection of a mixture (*ca.* 9:1) of C_{60} and C_{70} at ambient temperature. (bottom) Effect of temperature on the overloaded chromatogram (200 μl of a 20 mg/ml solution) of the same mixture. The temperatures were 25°C (solid line) and 75°C (dashed line) and the experimental conditions as in Fig. 6.

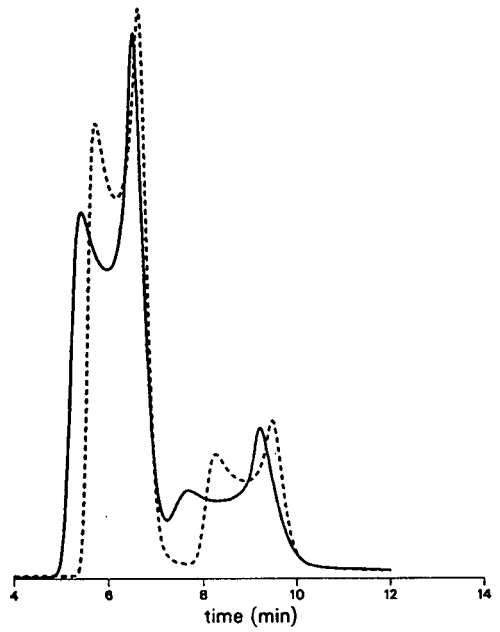

Fig. 10. Effect of temperature on the experimental elution profiles of a mixture (*ca.* 9:1 ratio) of C_{60} and C_{70}. Volume injected, 100 μl (10 mg/ml solution). Column and conditions as in Fig. 7, except for the temperature: solid line at 25°C and dashed line at 95°C. Both C_{60} and C_{70} are eluted as bimodal peaks.

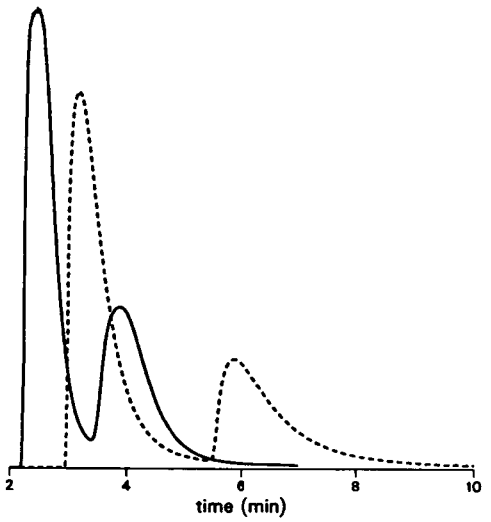

Fig. 11. Effect of temperature on the experimental elution profiles of a mixture (*ca.* 9:1 ratio) of C_{60} and C_{70}. Volume injected, 100 μl (10 mg/ml solution). Column and conditions as in Fig. 8, except for the temperature: solid line at 25°C and dashed line at 95°C.

the C_{60} and C_{70} peaks was observed. This can be attributed to the incompatibility of the sample solvent and the eluent and to the high efficiency of the column [13]. This effect cannot be explained by a chemical reaction.

The enthalpy and entropy of the retention mechanism derived from the Van 't Hoff plots are given in Table I. Our results are comparable to those reported previously [29]. Both the heat of complexation and the related entropy increase with increasing retention factor. The interaction energy measured with TAPA is far greater than that observed for DNBPG, despite the fact that the former was used with a stronger solvent. This confirms again the stronger electron-acceptor ability of TAPA. The data show also that the energy involved in the retention mechanism on the ODS column (hydrophobic interaction) is greater than that measured for the retention mechanism involving a charge-transfer process, although one should bear in mind that the solvent used in the former instance is weaker.

Finally, an attempt was made to produce gram amounts of the purified fullerenes by preparative chromatography, using the conditions optimized for their maximum resolution on the ODS analytical column. Fig. 12 shows the chromatograms obtained with a 4-mg injection (top), on the analytical column (250 × 4.5 mm I.D.) and a 100-mg injection (bottom) on the preparative column. The cut-times for fraction collection with the preparative column are also shown. The two traces are very similar, and are both characterized by a pronounced shoulder. The first fraction contains C_{60} *ca.* 94% pure and the third fraction contains C_{70} *ca.* 90% pure. The intermediate or second fraction contains both fullerenes. This result suggests that an important tag-along effect takes place while the self-displacement effect is nearly absent [9]. The pro-

TABLE I

ADSORPTION THERMODYNAMIC DATA

Stationary phase	Mobile phase composition[a]	Compound	ΔH (cal/mol)	ΔS (cal/mol)
Silica	A, B, C	C_{60}	–	–
		C_{70}		
TAPA	A	C_{60}	1374.0	2.830
		C_{70}	1385.0	3.559
DNBPG	B	C_{60}	182.2	0.503
		C_{70}	219.0	1.203
C_{18}	C	C_{60}	−4060.0	−5.790
		C_{70}	−4830.0	−6.590
GCB	A, B, C, D	C_{60}	–[b]	–[b]
		C_{70}		

[a] A = toluene–heptane (50:50); B = toluene–heptane (10:90); C = toluene–methanol (50:50); D = chloroform.
[b] Nearly irreversible adsorption.

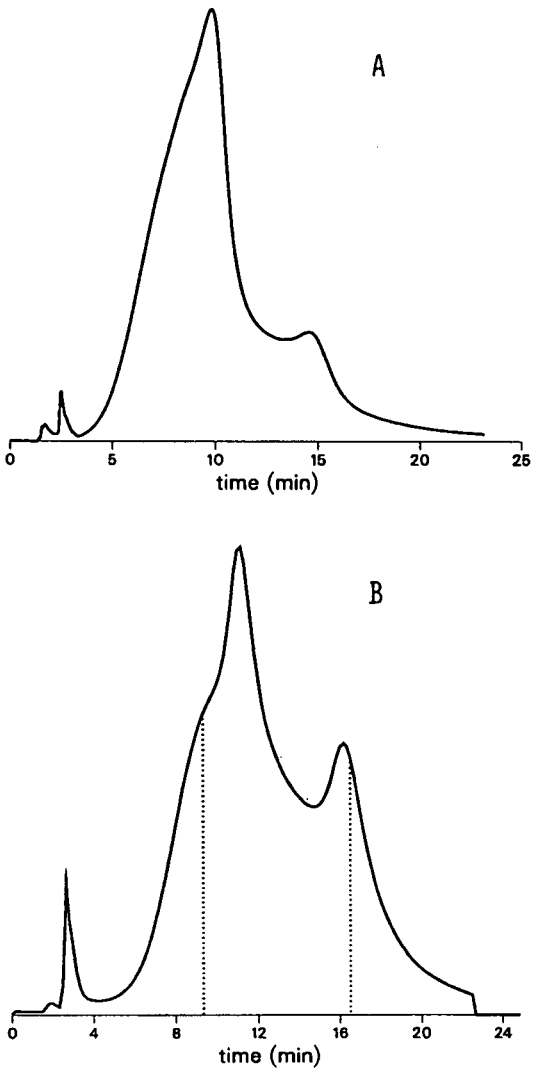

Fig. 12. Comparative band profiles in overloaded mode using the same conditions as in Fig. 6 except for detection at 384 nm. (A) Analytical column (25 × 0.46 cm I.D.) with a flow-rate of 1 ml/min and an injected amount of 4 mg. (B) preparative column (Prochrom LC50, 50 × 5 cm I.D.) with a flow-rate of 90 ml/min and an injected amount of 100 mg. The dotted lines correspond to the fraction collected.

duction rate achieved under such conditions is very low for this poor degree of purification.

During the conclusion of this work, a new method for the purification of C_{60} was described, using activated charcoal and toluene as the mobile phase, in the flash chromatographic mode [33]. This method seems to permit the rapid purification of gram amounts of C_{60}, although the fate of C_{70} and the higher fullerenes is unknown. The large-scale production of the buckminsterfullerenes on this type of stationary phase and on related adsorbents in the HPLC mode is under active investigation in our laboratory.

CONCLUSIONS

The retention of C_{60}, and to a greater extent C_{70}, using most solvents available is quasi-irreversible on GCB. Poor retention of these compounds and very low selectivity is observed on silica. On the other hand, analytical separations of the fullerenes on C_{18}-bonded silica columns, using methanol–toluene mobile phases, are straightforward.

TAPA, a chiral stationary phase, gives a stronger retention, a higher resolution and a better production rate than DNBPG, another charge-transfer adsorbent, for the purification of the C_{60} and C_{70} fullerenes, with toluene–heptane mobile phases. Because of the peculiar behavior observed when the column temperature is increased, the retention time of the fullerenes increasing with increasing temperature while the band shape improves, the application of this type of stationary phase at high temperature for purification purposes seems preferable.

Two major problems are encountered in the preparative separation of fullerenes by HPLC: their poor solubility in common solvents (*e.g.*, alcohols, ethyl acetate, *n*-alkanes) and even in toluene, which is the best solvent, and the poor retention provided by the different stationary phases available for their separation when toluene is used as the mobile phase.

The combination of these two sources of difficulties is what makes the purification of fullerenes by preparative chromatography a most inefficient process. For example, the solubility of C_{60} in *n*-hexane, which is the best mobile phase to use with the different adsorbents suggested (with regard to the retention factor and the selectivity) is *ca.* 40 μg/ml. The injection of a net amount of 1 mg of this cluster (*i.e.*, the same amount as used to obtain the chromatogram shown in Fig. 10) would require the huge volume of 25 ml of the saturated solution. To overcome

this limitation, the poor experimental approach consisting in the use of a stronger sample solvent (*e.g.*, pure toluene or benzene) to insure the injection of a narrow band of concentrated solution and an adequate throughput has been adopted by different workers (*e.g.*, [29]). As explained above (*cf.*, Fig. 10), the resulting chromatogram exhibits severe abnormalities. The complex band interaction pattern observed at high loading [13] does not permit the achievement of an adequate throughput. It is clear that, in order to improve this situation, we need to find more retentive stationary phases and better solvents than toluene.

ACKNOWLEDGEMENTS

This work was supported in part by the cooperative agreement between the University of Tennessee and the Oak Ridge National Laboratory. Support was also provided by the Oak Ridge National Laboratory Director's Research and Development Program.

REFERENCES

1 F. Diederich, R. Ettl, Y. Rubin, R.L. Whetten, R. Beck, M. Alvarez Sanz, D. Sensharma, F. Wudl, K.C. Khemani and A. Koch, *Science*, 252 (1991) 548.
2 J.P. Hare, H.W. Kroto and R. Taylor, *Chem. Phys. Lett.*, 177 (1991) 394.
3 K. Chatterjee, D.H. Parker, P. Wurz, K.R. Lykke, D.M. Gruen and L.M. Stock, *J. Org. Chem.*, 57 (1992) 3253.
4 M. Diack, R.L. Hettich, R.N. Compton and G. Guiochon, *Anal. Chem.*, 64 (1992) 2143.
5 A.M. Vassalo, A.J. Palmisano, L.S.K. Pang and M.A. Wilson, *J. Chem. Soc., Chem. Commun.*, (1992) 60.
6 K. Jinno, K. Yamamato, T. Ueda, H. Nagashima and K. Itoh, *J. Chromatogr.*, 594 (1992) 105.
7 M.S. Meier and J.P. Selegue, *J. Org. Chem.*, 57 (1992) 1924.
8 H. Ajie, M.M. Alvarez, S.J. Anz, R.D. Beck, F. Diederich, K. Fostiropoulos, D.R. Huffman, W. Kratschmer, Y. Rubin, K.E. Schriver, D. Sensharma and R.L. Whettwen, *J. Phys. Chem.*, 94 (1990) 8630.
9 S. Ghodbane and G. Guiochon, *J. Phys. Chem.*, 92 (1988) 3682.
10 A. Katti and G. Guiochon, *J. Am. Chem. Soc.*, 61 (1989) 982.
11 S. Golshan-Shirazi and G. Guiochon, *J. Chromatogr.*, 517 (1990) 229.
12 H. Shinohara, H. Sato, Y. Saito, M. Takayama, A. Izuoka and T. Sugawara, *J. Phys. Chem.*, 95 (1991) 8449.
13 P. Jandera and G. Guiochon, *J. Chromatogr.*, 588 (1991) 1.
14 C.E. Evans and V.L. McGuffin, *J. Am. Chem. Soc.*, 63, (1991) 1393.
15 J. Porath, *J. Chromatogr.*, 159 (1978) 13.
16 M. Godlewicz, *Nature*, 164 (1949) 1132.
17 R.C. Haddon, L.F. Schenmeyer, L.J. Waszczak, S.H. Glarum, R. Tycko, G. Dabbagh, A.R. Kortan, A.J. Muller, A.M. Mujsce, M.J. Rosseinsky, S.M. Zahurak, A.V. Makhija, F.A. Thiel, K. Raghavachari, E. Cockayne and V. Elser, *Nature*, 350 (1991) 46.
18 S.W. McElvany, M.M. Ross and J.H. Callahan, *Acc. Chem. Res.*, 25 (1992) 162.
19 D.M. Cox, S. Bethal, M. Disko, S.M. Gorun, M. Greaney, C.S. Hsu, E.B. Kollin, J. Millar, J. Robbins, W. Robbins, R.D. Sherwood and P. Tindall, *J. Am. Chem. Soc.*, 113 (1991) 2940.
20 J.M. Hawkins, T.A. Lewis, S.D. Loren, A. Meyer, J.R. Health, Y. Shibato and R.J. Saykally, *J. Org. Chem.*, 55 (1990) 6250.
21 C.J. Welch and W. Pirkle, *J. Chromatogr.*, 609 (1992) 89.
22 F. Mikes, G. Boshart and E. Gil-Av, *J. Chromatogr.*, 122 (1976) 205.
23 Y.S. Klausner and M. Bodansky, *Synthesis*, 333 (1981) 453.
24 O. Sinanoglu and S. Abbdulnur, *Proc. Am. Soc. Exp. Biol.*, 24 (1965) 12.
25 D.C. Locke, *J. Chromatogr. Sci.*, 11 (1973) 120.
26 K. Jinno, T. Ibuki, N. Tanaka, M. Okamoto, J.C. Fetzer, R. Biggs, P.R. Griffiths and J.M. Olinger, *J. Chromatogr.*, 461 (1989) 209.
27 G.B.M. Vaughan, P.A. Heiney, J.E. Fischer, D.E. Luzzi, D.A. Ricketts-Foot, A.R. McGhie, Y.W. Hui, A.L. Smith, D.E. Cox, W.J. Romanow, B.H. Allen, N. Coustel, J.P. McCauley, Jr. and A.B. Smith III, *Science*, 254 (1992) 1350.
28 W.R. Melander, A. Nahum and Cs. Horváth, *J. Chromatogr.*, 185 (1979) 129.
29 W.H. Pirkle and C.J. Welch, *J. Org. Chem.*, 56 (1991) 6973.
30 W.H. Pirkle, *J. Chromatogr.*, 558 (1991) 1.
31 Y. Arai, M. Hirukawa and T. Hanai, *J. Chromatogr.*, 384 (1987) 279.
32 A. Nahum and Cs. Horváth, *J. Chromatogr.*, 203 (1981) 53.
33 W.A. Scriven, P.W. Bedworth and J.M. Tour, *J. Am. Chem. Soc.*, 114 (1992) 7917.

Journal of Chromatography, 639 (1993) 141–149
Elsevier Science Publishers B.V., Amsterdam

CHROM. 24 936

Chiral packing materials for high-performance liquid chromatographic resolution of enantiomers based on substituted branched polysaccharides coated on silica gel

Guy Félix* and Tong Zhang

ENSCPB/CNRS–URA 35, Laboratoire de Chimie Organique et Organometallique, 351 Cours de la Libération, F-33 405 Talence (France)

(First received December 8th, 1992; revised manuscript received February 2nd, 1993)

ABSTRACT

The preparation of amylopectin-based chiral stationary phases coated on an achiral support, according to a process similar to that reported for substituted cellulose or amylose carbamate derivatives, is reported. The influence of the different synthesis parameters on chiral discrimination is discussed.

INTRODUCTION

Resolution of enantiomers by liquid chromatography on chiral stationary phases (CSPs) has become a practically useful method for obtaining optical isomers and determining their purities [1]. Several different types of chiral stationary phases have been developed and a wide range of applications have been published during the last decade [2].

Among the numerous chiral stationary phases that have been investigated, polysaccharide-based phases have been identified as versatile and useful chiral sorbents for the separation of enantiomers [3]. Numerous applications have been reported on microcrystalline cellulose triacetate used in the pure polymer form [2,3]. A variety of cellulose and amylose derivatives have been introduced for the same purpose by Okamoto and co-workers as a coating of polymer on large-pore silica gel [2,3]. Most of these coated silica materials are commercially available and they show different selectivities depending on the type of polysaccharide and on the derivatizing groups on the polysaccharide. More recently, benzoylcellulose beads in the pure cellulosic form have been shown to have remarkable chiral recognition abilities [4,5].

All these polysaccharide CSPs are produced from linear polysaccharides. No work has been published on branched polysaccharides except the use of pure starch to resolve atropoisomers containing polar substituents [6–10] and soluble starch derivatized with 3,5-dimethylphenyl isocyanate and supported on silica gel, which exhibited similar but slightly lower recognition compared with amylose tris(3,5-dimethylphenylcarbamate) [11]. However, starch is in reality a mixture of polysaccharides containing, for example, 20% amylose and 80% amylopectin in the case of maize starch. Of these two polysaccharides, amylose CSPs are well known [11–17],

* Corresponding author.

but amylopectin CSPs have not been described and studied.

We report here the synthesis of and chromatographic studies on chiral discrimination of CSPs based on substituted amylopectin triphenylcarbamates.

EXPERIMENTAL

Chemicals and solvents

Amylopectins were commercially available under the trade name Glucidex, from Roquette (Lestrem, France). Silica gels were obtained from Macherey–Nagel (Strasbourg, France). The physical characteristics of the different silica gels (data from manufacturer) are reported in Table I.

Triaminosilane, N-aminoethyl-3-aminopropyltrimethoxysilane and 3-aminopropyl trimethoxysilane were obtained from Hüls (Paris, France). Isocyanates and racemates were purchased from Aldrich Chemicals (Strasbourg, France) and HPLC solvents from CIL (Sainte-Foy la Grande, France).

Apparatus

Separations were carried out on an HPLC system composed of a Philips Model 4015 pump, a Philips Model 4025 multi-wavelength UV detector (Philips Science et Industrie, Bobigny, France) and a Kipp & Zonen BD 40 recorder (Enraf-Nonius, Gagny, France). The columns (250 × 4.6 mm I.D.) were packed by Silichrom (Pessac, France). The prepared bonded materials were sent for carbon content analysis to the Service Central d'Analyses du CNRS (Vernaison, France).

TABLE I

PHYSICAL CHARACTERISTICS OF SILICA GEL

Silica gel	Pore size (Å)	Specific surface area (m^2/g)	Pore volume (ml/g)	Particle size (μm)
N-100-5	100	350	1.0	5
N-300-5	300	100	0.8	5
N-1000-5	1000	25	0.8	5
N-4000-5	4000	10	0.7	5

Chromatographic conditions

Chromatography was performed using the same mobile phase composition [hexane–2-propanol (90:10, v/v)] at a constant flow-rate of 0.5 ml/min. The dead time of the columns was determined by injection of 1,3,5-tri-*tert.*-butylbenzene used as non-retained compound. Typically, 10 μl of a 1% solution of racemate dissolved in hexane were injected.

In order to investigate the influence of the different parameters on the recognition ability, five racemates having the structures presented in Fig. 1 were chromatographed: *trans*-stilbene oxide (SO), Tröger base (TB), benzoin (Bz), benzoin methyl ether (BME) and flavanone (Fla).

Preparation of the chiral phases

General procedure for the silanization of silica gel. A 10-g amount of silica gel, dried under vacuum (0.1 Torr) (1 Torr = 133.322 Pa) at 180 °C, is made to react with the silane in 80 ml of xylene. The mixture is heated under reflux for 24 h and the product is filtered off and washed successively with xylene (50 ml), tetrahydrofuran (THF) (100 ml), THF–water (50:50) (50 ml), water (100 ml), THF (200 ml) and hexane (50 ml). The bonded material is dried at 80 °C under vacuum (0.1 Torr).

General procedure for the preparation of substituted amylopectin triphenylcarbamates. A 5-g amount of amylopectin dissolved in freshly distilled pyridine (50 ml) is dried by a Dean and Stark procedure. After removing water, 0.28 mol of isocyanate is added dropwise and refluxed at

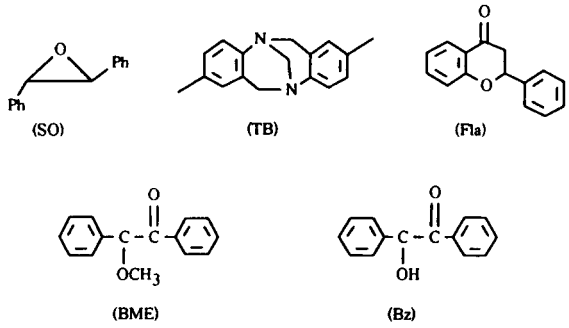

Fig. 1. Structures of test compounds.

110 °C for 24 h. After cooling, 30 ml of methanol are added and the resulting solution is poured into 400 ml of methanol with stirring. The precipitate is filtered and washed twice with methanol. The product is dissolved in methylene chloride and precipitated with 400 ml of methanol. This process is repeated three times, at room temperature, to give a brown solid.

IR (KBr): ν(NH) 3400, 3300, 1530 cm^{-1}; ν(CO) 1740 cm^{-1}; ν(C–O–C) 1030–1100 cm^{-1} (no adsorption at 3470 cm^{-1}, hydroxyl groups of polysaccharides). Elemental analyses were satisfactory.

General procedure for the coating. A 3.2-g amount of bonded silica gel is added to 0.8 g of amylopectin carbamate dissolved in dioxane (30 ml). The mixture is stirred for 15 min, then the solvent is removed with a rotary evaporator.

RESULTS AND DISCUSSION

Description of amylopectin

As for the cellulose CSPs, the polysaccharides cannot be used as they are because their molecular mass is too high for them to be soluble. Hence it is necessary to cut them into lower molecular mass soluble moieties [18]. The same applies to amylopectin but fortunately degraded amylopectin is readily available under the trade name Glucidex, used as a sugar food. Glucidex is a mixture of "nutritive saccharides" obtained by a sparing hydrolysis of starch maize, followed by purification and spray drying.

Starch maize is a mixture containing 78% amylopectin and 22% amylose [19]. Amylose is composed of about 250–300 glucose units linked by 1,4-α-disaccharide bridges [20]. The amylopectin chain composition is similar to that of amylose, but the molecular structure is more complex. Amylopectin is a branched structure constituted of about 1000 glucose units. Several hundred side-chains, having 20–25 glucose units each, are linked to the major chain by 1,6-α-disaccharide bridges (Fig. 2) [21].

During hydrolysis (acidic or enzymic) of starch, amylose is degraded to maltose and then to glucose [22,23] and amylopectin is slightly degraded giving a lower molecular mass ramified polysaccharide [21]. When the degradation of starch is substantial, the breakdown products are named dextrins.

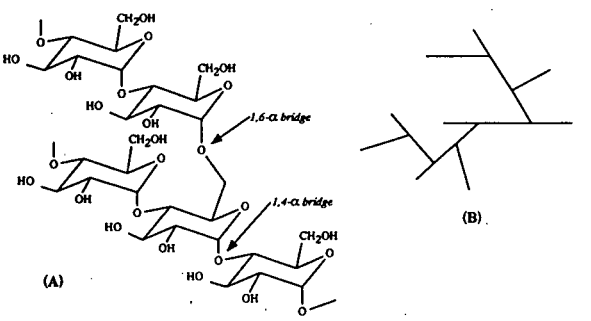

Fig. 2. (A) Structure of amylopectin; (B) simplified structure of amylopectin.

The final product (Glucidex) used here is a mixture of glucose (1%), maltose (2%) and higher polysaccharides (97%) having a polydispersity of 8500, a mass-average molecular mass of 12 800 and a number-average molecular mass of 1500 [24].

Preparation of the chiral agent

The Glucidex is easily converted into carbamates by adding isocyanate derivatives under the usual conditions (Fig. 3). The crude carbamate is purified by a series of precipitations followed by solubilization to remove glucose, maltose and oligosaccharide carbamates, giving a purer amylopectin carbamate with a narrow molecular distribution, measured by gel permeation chromatography. For example, amylopectin triphenylcarbamate has a polydispersity of 2550 and a mass-average molecular mass of 9000, indicating loss of material. Then amylopectin carbamate is coated on an amino-bonded silica, packed in a 250 × 4.6 mm I.D. stainless-steel

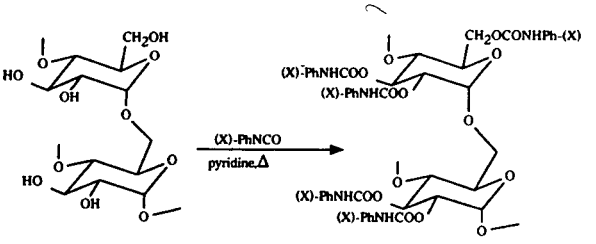

Fig. 3. Preparation of amylopectin carbamates.

column by a slurry method [18] and used as chiral support.

To have a large range of amylopectin CSPs, several substituents listed in Table II were introduced onto the phenyl group of derivatized amylopectin.

Before discussing the chiral behaviour of the different amylopectin CSPs, several achiral parameters such as the type of aminosilane, the pore size of the bonded aminosilica and the percentage of chiral agent coated have to be studied in order to establish their influence on chiral discrimination.

Influence of the aminosilane

Okamoto *et al.* [18] used γ-aminopropyltrimethoxysilane to deactivate silica gel because amino groups have the property of forming hydrogen bonds with carbamate functions, stabilizing the coating. In this way, to have a more stable coating, it would be of interest to increase the hydrogen bonds by using a di- or a triaminosilane for silanization. However, it is not certain that all amino groups form hydrogen bonds and as a consequence they can have undesirable effects on the elution.

Therefore, in order to establish the best aminosilane, silica gel (N-1000-5) was derivatized with 3-aminopropyltrimethoxysilane (1N), N - aminoethyl - 3 - aminopropyltrimethoxysilane (2N) and triaminosilane (3N) and coated with amylopectin triphenylcarbamate (PhAMY) as chiral agent using the procedure described Experimental. Their influences on chiral recognition are reported Fig. 4.

In general, the capacity factors are slightly better with monoaminosilane derivatization and

TABLE II

LIST OF DIFFERENT AMYLOPECTIN CSPs

Phase	Substituent
pMeOPhAMY	4-OCH_3
pMePhAMY	4-CH_3
3,5MePhAMY	3,5-$(CH_3)_2$
PhAMY	H
pFPhAMY	4-F
3,4ClPhAMY	3,4-Cl_2

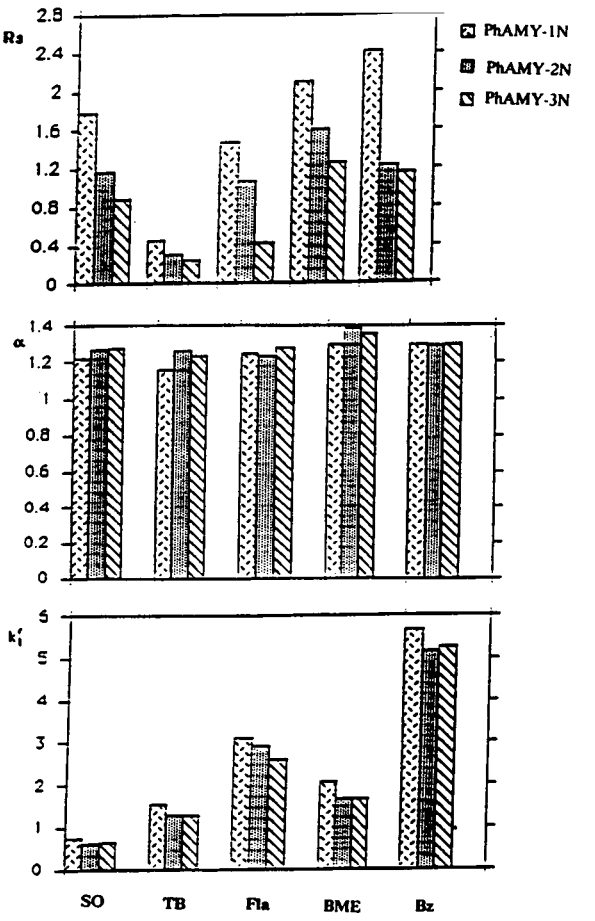

Fig. 4. Influence of the nature of aminosilane on the chiral discrimination.

the α values are almost the same for the three amino-bonded silicas, showing the weak influence of the type of amino chain on the discrimination power. However, for all racemates, the resolution is higher with monoamino-bonded silica gel and the decrease in chiral resolution is comparatively greater with increase in the number of amino groups and the longer the arm. Therefore, silica gel was subsequently derivatized with γ-aminopropyltrimethoxysilane.

Influence of the silica gel pore size

To prepare cellulose phases, Okamoto *et al.* [18] used large-pore silica gel with a diameter ≥1000 Å because celluloses have a molecular mass of about 32 000. As amylopectins have a lower molecular mass (about 10 000), the use of

large-pore silica gel is not obvious. Hence, to define the exact type of silica gel, PhAMY CSPs were made with four silica gels having pore sizes of 100, 300, 1000 and 4000 Å. The studies under the usual conditions are reported in Fig. 5.

All the CSPs show a chiral recognition power, but silica gel of 100 Å pore size has a poor ability. It seems to be difficult for the macromolecules of substituted amylopectin to penetrate the pores, giving a heterogeneous coating of the surface, closing more or less the pores. Considering the changes in enantioselectivities, resolutions and the specific surface areas, it appears that a 300 Å pore-size silica gel is the best compromise.

Percentage of chiral agent coated

The chiral ability of the CSP depends on the thickness of the coating. Usually, the greater the amount of chiral agent, the better is the chiral discrimination. For the coated cellulose CSP, Okamoto and co-workers [18,25,26] chose a rate of coating of about 20–25% by mass.

To have an exact view of the amount of chiral agent, several PhAMY CSPs coated with different percentages on a 300 Å pore-size aminosilica gel were studied (Figs. 6 and 7).

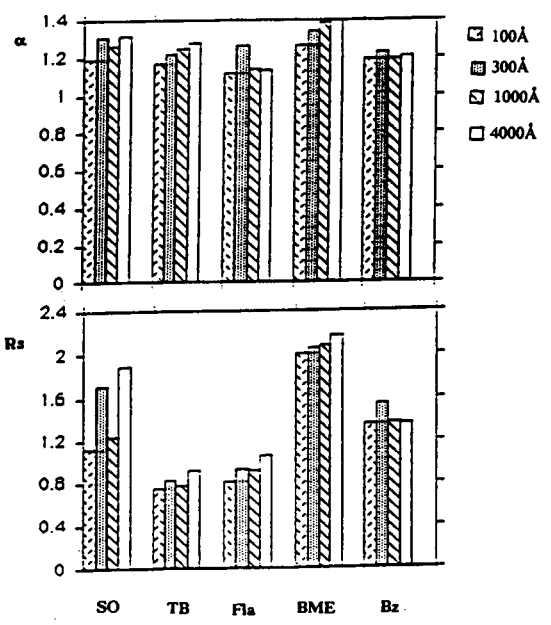

Fig. 5. Influence of silica gel pore size on the chiral discrimination.

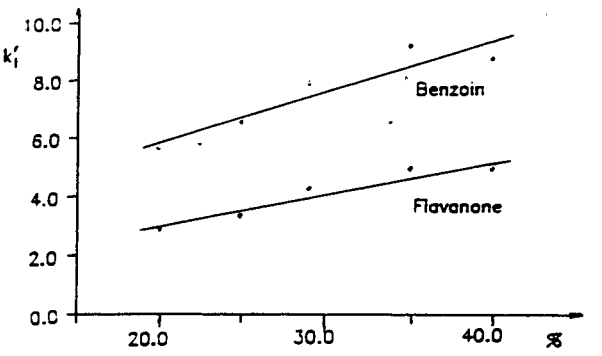

Fig. 6. Influence of percentage of PhAMY coated on the capacity factor.

As the percentage of PhAMY coated on silica gel increases, the capacity factors increase (Fig. 6) and do not affect the enantioselectivity (Fig. 7). This is a normal phenomenon in chromatography. However, the resolution increases rapidly with a coating rate between 20 and 25%, beyond which the effect is small. It appears that resolution increases when the capacity factors increase, but for values higher than 25% the efficiency of the column decreases because the substituted polysaccharides close the pores. Hence a coating of 25% by mass appears to be the best average.

Therefore, in subsequent work, a 25% coating of substituted amylopectin on 300 Å silica gel derivatized with 3-aminopropyltrimethoxysilane was used.

Influence of the substituent present on phenyl group

As for the other polysaccharide CSPs, the chiral recognition ability depends largely on the substituent attached to the phenyl moiety [11–17,25,26]. In order to investigate the influence on chiral discrimination, the racemates used above were chromatographed on the substituted amylopectin phenylcarbamates listed in Table II. (No discrimination ability was observed with benzolamylopectin like that for benzoylpullulan [27]. Amylopectin 4–nitrophenylcarbamate and 4-chlorophenylcarbamate were also synthesized, but they are soluble in hexane, as mobile phase,

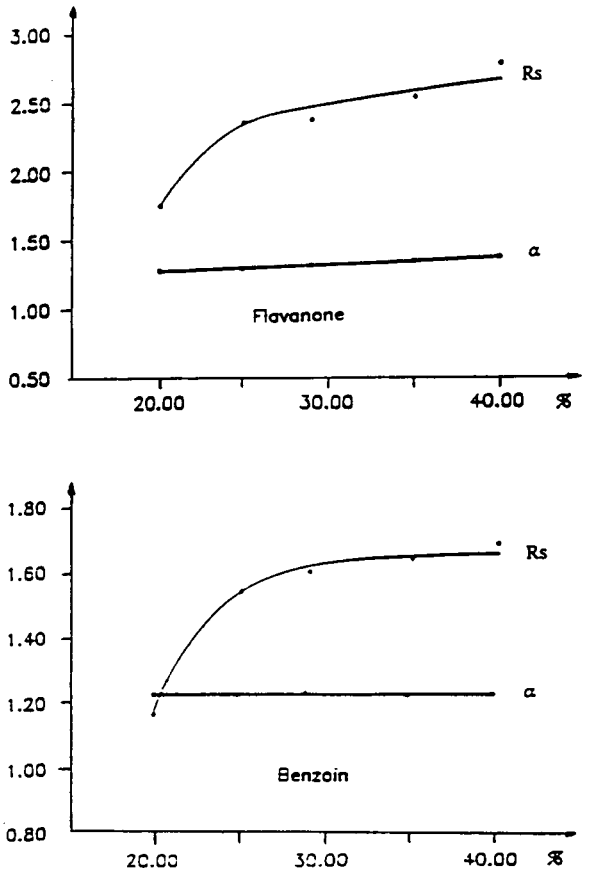

Fig. 7. Influence of the percentage of PhAMY coated on enantioselectivity.

containing 2% of 2-propanol.) The results are summarized in Table III.

With polysaccharide carbamate derivatives, the polar interaction centre of the CSP is the urethane group. The inductive effect of substituents on the phenyl group of the urethane moiety depends on the nature, position and number of substituents. Hence a chromatographic system with a non-polar eluent, hydrogen bond and dipole–dipole interactions between the urethane moiety of amylopectin triphenylcarbamate and the polar groups of racemic compounds are considered to be the dominant forces for chiral recognition. Both CO and NH of the carbamate moiety can interact with the solute through a hydrogen bond.

The introduction of an electron-withdrawing substituent such as a halogen increases the acidity of the NH proton [26]. On the one hand, the increase in the acidity of the NH proton should enhance the capability for hydrogen bond formation of this proton with an electron-donating group such as carbonyl. On the other hand, an electron-donating group such as an alkyl increases the electron density of the carbonyl group, strengthening the hydrogen bond. Hence the introduction of an alkyl or halogen group is expected to improve the chiral recognition ability of cellulose or amylose triphenylcarbamates [11–17,26].

TABLE III

CAPACITY FACTORS OF THE LESS STRONGLY RETAINED ENANTIOMER AND SELECTIVITIES

CSP	Parameter	Racemate				
		SO	TB	Fla	BME	Bz
pMeOPhAMY	k'_1	0.72	1.60	2.82	1.95	5.87
	α	1.18	1.00	1.08	1.18	1.19
pMePhAMY	k'_1	0.57	1.36	2.10	1.43	4.29
	α	1.30	1.00	1.18	1.47	1.19
3,5MePhAMY	k'_1	0.67	1.00	1.82	4.64	1.33
	α	1.46	1.38	1.33	1.18	2.47
PhAMY	k'_1	0.72	1.44	2.84	1.94	5.68
	α	1.31	1.22	1.27	1.34	1.23
pFPhAMY	k'_1	0.62	1.64	2.68	2.08	5.70
	α	1.13	1.14	1.22	1.11	1.00
3,4ClPhAMY	k'_1	0.61	2.70	3.50	3.20	7.11
	α	1.00	1.00	1.27	1.00	1.00

This mechanism, well established for cellulose and amylose CSP, is not completely valid for amylopectin triphenylcarbamates. For example, the 3,4ClPhAMY CSP shows no discriminating power whereas the similar cellulose type exhibits a high chiral recognition [26] and MeOPhAMY CSP gives separations of the racemates (except Tröger base) whereas the cellulose type does not improve chiral recognition [17]. The best separations are observed when the substituents are weak electron donors (PhAMY and 3,5MePhAMY), giving similar results to those obtained on the cellulose and amylose CSPs [11–17,26]. The ramified structure of amylopectin is probably responsible for the difference in behaviour, by increasing the inclusion phenomenon and changing the environment of the glucose unit. Examples of separations of racemic com-

pounds on 3,5MePhAMY CSP are given in Fig. 8.

Comparison of the chiral recognition abilities of cellulose, amylose and amylopectin CSPs

Capacity factors of the less strongly retained enantiomers and selectivities for four racemates (SO, TB, Fla and Bz) on cellulose, amylose and amylopectin CSPs are listed in Table IV. The data for cellulose and amylose CSPs were obtained from the literature [11, 26]. For racemates of *trans*-stilbene oxide and Tröger base, amylose and cellulose CSPs appear to have a better chiral recognition ability. For flavanone and benzoin, it is less evident. In general, AMY CSPs exhibit a better discriminating power than cellulose CSPs (Fla and Bz) and amylose CSPs (Bz). This ability is particularly true when the substituents of the phenyl group have a donor effect.

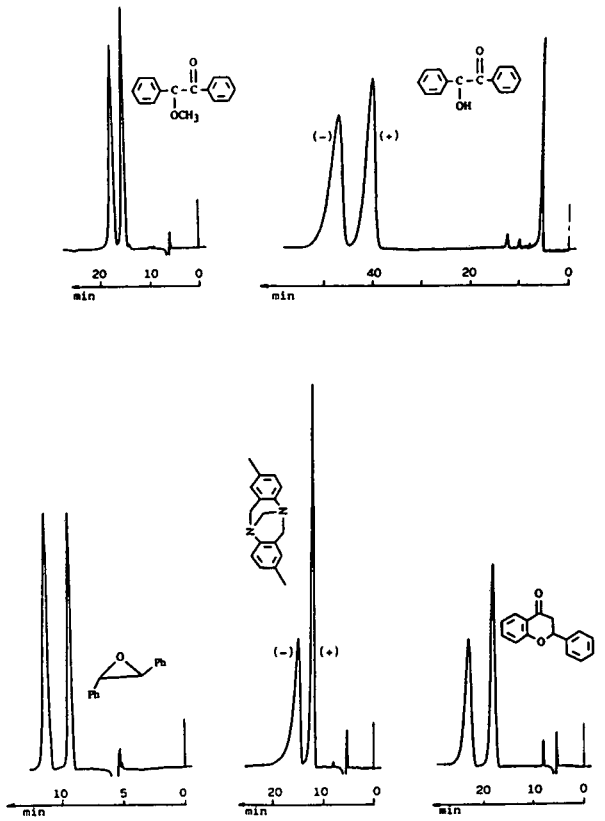

Fig. 8. Examples of separation of racemic compounds on 3,5MePhAMY CSP. Mobile phase, hexane–2-propanol (95:5); flow-rate, 0.5 ml/min.

In fact, each polysaccharide CSP has its own chiral properties; the discriminating power depends largely on the structure of the polysaccharide but also on the structure of the racemates.

Study of the separation mode

The cellulose CSP can be used in normal and reversed modes [28]. Effectively, the carbamate group gives polar interactions (hydrogen bonds and dipole–dipole interactions) and the phenyl moiety hydrophobic (apolar) and $\pi-\pi$ interactions. Hence, in the reversed-phase chromatographic mode hydrophobic interactions occurred and in the normal mode polar or $\pi-\pi$ interactions were responsible for the separations.

To examine the effect of the chromatographic mode on chiral discrimination, 3,5MePhAMY CSP was studied in normal and reversed modes. The results are given in Table V.

In the normal mode, racemates were eluted in the order Bz > Fla > BME > TB > SO, showing the relationship between enantiomer structures and polar strength intensities. *trans*-Stilbene oxide enantiomers are the least retained owing to the deficiency of polar interaction centres and benzoin enantiomers are the most retained because they have two polar groups (OH and C = O), able to form strong hydrogen bonds. However, the enantioselectivity values increase in the opposite order (Bz < BME < Fla < TB < SO), showing that a long retention time does not lead to the best chiral separation. The solute affinities for the CSP do not contribute to the chiral discrimination.

With the reversed mode, the polar interactions are destroyed and replaced by hydrophobic interactions, giving the order SO > Fla > TB > Bz > BME for capacity factors and Bz < BME < SO < TB < Fla for enantioselectivities. The AMY CSP can be used in both modes, but its behaviour is different.

CONCLUSIONS

Preparations of substituted amylopectin CSPs coated at 25% by mass on an achiral support of 300 Å pore size and derivatized with 3-aminopropyltrimethoxysilane were described. Chiral

TABLE IV

COMPARISON OF RECOGNITION ABILITIES OF CELLULOSE (Cel), AMYLOSE (Am) AND AMYLOPECTIN (AMY) CSPs

CSP		Racemate							
		SO		TB		Fla		Bz	
		k'_1	α	k'_1	α	k'_1	α	k'_1	α
p-MeO	Cel	0.56	1.34	1.09	1.01	2.23	1.01	0.48	1.01
	AMY	0.72	1.18	1.60	1.00	2.82	1.08	5.87	1.19
p-Me	Cel	0.51	1.55	0.75	1.48	1.57	1.16	3.00	1.12
	AMY	0.57	1.30	1.36	1.00	2.10	1.18	4.29	1.19
3,5-Me	Cel	0.74	1.68	0.97	1.32	1.47	1.41	2.43	1.58
	Am	0.42	3.04	0.53	1.58	0.93	1.12	3.14	1.21
	AMY	0.67	1.46	1.00	1.38	1.82	1.33	1.33	2.47
H	Cel	0.67	1.46	1.12	1.37	2.22	1.10	5.28	1.01
	Am	0.39	1.46	0.77	1.28	2.21	1.51	3.72	1.00
	AMY	0.72	1.31	1.44	1.22	2.84	1.27	5.68	1.23
p-F	Cel	0.52	1.38	1.00	1.14	1.89	1.13	4.26	1.14
	AMY	0.62	1.13	1.64	1.14	2.68	1.22	5.70	1.00
3,4-Cl	Cel	0.38	1.93	0.79	1.47	1.29	1.04	3.24	1.10
	AMY	0.61	1.00	2.70	1.00	3.50	1.27	7.11	1.00

TABLE V

EFFECT OF SEPARATION MODE WITH 3,5MePhAMY CSP

Mobile phase	Parameter	SO	TB	Fla	BME	BZ
Hexane–2-propanol (90:10), 1 ml/min	k'_1	0.67	1.00	1.82	1.24	4.64
	α	1.46	1.38	1.33	1.23	1.18
Ethanol–water (75:25), 1 ml/min	k'_1	1.44	0.57	1.34	0.19	0.30
	α	1.17	1.40	1.46	1.11	1.00

recognition of amylopectin triphenylcarbamate derivatives depended greatly on the type, position and number of substituents on the phenyl groups. Racemic compounds considered in this work are resolved with 3,5-dimethylphenylcarbamate; however, 3,4-dichlorophenylcarbamate has a very low chiral recognition whereas 4-methoxyphenylcarbamate exhibits a real discriminating power. The branched structure of amylopectin induces different mechanisms to those for cellulose or amylose, requiring further studies to explain the retention mechanisms.

REFERENCES

1 G. Blaschke, *Angew. Chem., Int. Ed. Engl.*, 19 (1980) 13.
2 S.G. Allenmark, *Chromatographic Enantioseparation*, Wiley, New York, 1988.
3 T. Shibata, K. Mori and I. Okamoto, in A.M. Krstulovic (Editor), *Chiral Separation by HPLC —Applications to Pharmaceutical Compounds*, Wiley, New York, 1989, pp. 336–398.
4 E. Francotte and R.M. Wolf, *Chirality*, 3 (1991) 43.
5 E. Francotte and R.M. Wolf, *J. Chromatogr.*, 595 (1992) 63.

6 H. Krebs, J.A. Wagner and J. Diewald, *Chem. Ber.*, 89 (1956) 1875.
7 H. Krebs and W. Schumacher, *Chem. Ber.*, 99 (1966) 1341.
8 W. Steckelberg, M. Block and H. Musso, *Chem. Ber.*, 101 (1968) 1519.
9 R.K. Haynes, H. Hess and H. Musso, *Chem. Ber.*, 107 (1974) 3733.
10 H. Hess, G. Burger and H. Musso, *Angew. Chem.*, 90 (1978) 645.
11 Y. Okamoto, R. Aburatani, K. Fukumoto and K. Hatada, *Chem. Lett.*, (1987) 1857.
12 Y. Okamoto, R. Aburatani, Y. Kaida and K. Hatada, *Chem. Lett.*, (1988) 1125.
13 Y. Okamoto, R. Aburatani, K. Hatano and K. Hatada, *J. Liq. Chromatogr.*, 11 (1988) 2163.
14 Y. Okamoto, T. Senoh, H. Nakane and K. Hatada, *Chirality*, 1 (1989) 216.
15 Y. Okamoto, R. Aburatani, Y. Kaida, K. Hatada, N. Inotsume and M. Nakuro, *Chirality*, 1 (1989) 239.
16 Y. Okamoto, R. Aburatani and K. Hatada, *Bull. Soc. Chem. Jpn.*, 63 (1990) 955.
17 Y. Okamoto and Y. Kaida, *J. High Resolut. Chromatogr.*, 13 (1990) 708.
18 Y. Okamoto, K. Hatada, T. Shibata, I. Okamoto, H. Namikoshi and Y. Yuki, *Eur. Pat. Appl.*, EP 147 804 (1984).
19 C.T. Greenwood, *Adv. Carbohydr. Chem.*, 11 (1956) 335.
20 S. Coffey, *Rodd's Chemistry of Carbon Compounds*, Elsevier, Amsterdam, 1967, p. 678 and references cited therein.
21 S. Coffey, *Rodd's Chemistry of Carbon Compounds*, Vol. I, part F, Elsevier, Amsterdam, 1967, p. 680 and references cited therein.
22 H. Baum and G.A. Gilbert, *Chem. Ind. (London)*, (1954) 489.
23 W. Banks, C.T. Greenwood and J.T. Thompson, *Makromol. Chem.*, 31 (1959) 197.
24 *Technical Notes*, Roquette Compagnie, Lestrem.
25 Y. Okamoto, M. Kawashima and K. Hatada, *J. Am. Chem. Soc.*, 106 (1984) 5357.
26 Y. Okamoto, M. Kawashima and K. Hatada, *J. Chromatogr.*, 363 (1986) 173.
27 S.G. Allenmark, *Chromatographic Enantioseparation*, Wiley, New York, 1988, p. 101.
28 K. Ikeda, T. Hamasaki, H. Kohno, T. Ogawa, T. Matsumoto and J. Sakai, *Chem. Lett.*, (1989) 1089.

Journal of Chromatography, 639 (1993) 151–157
Elsevier Science Publishers B.V., Amsterdam

CHROM. 25 007

Tandem supercritical fluid extraction and liquid chromatography system for determination of chlorinated phenols in solid matrices

M.H. Liu, S. Kapila* and K.S. Nam

Environmental Trace Substances Research Center, University of Missouri, Columbia, MO 65203 (USA)

A.A. Elseewi

Environmental Division, Southern California Edison Company, Rosemead, CA (USA)

(First received January 13th, 1992; revised manuscript received February 22nd, 1993)

ABSTRACT

A tandem supercritical fluid extraction–liquid chromatography system for determination of chlorinated phenols in various solid matrices is described. The system permitted direct introduction of supercritical fluid extracts into the liquid chromatograph, allowing quantitation down to the sub-parts per million (w/w) levels without any sample clean-up. The system performance compared favorably with the traditional methodologies in terms of both the analysis speed and the selectivity.

INTRODUCTION

Supercritical fluids with the low viscosities and relatively high densities are efficient solvents for a number of compounds. These fluids can be made selective solvents through change in density, brought about by relatively simple temperature and pressure manipulations. Due to rapid equilibration periods and variable solvating strength of these fluids, there has been considerable interest in the application of supercritical fluid extraction (SFE) in analytical chemistry. SFE has been used for rapid extraction of a variety of xenobiotics and extraction efficiencies ranging from 70–98% have been obtained for non-polar and moderately polar analytes such as polychlorinated biphenyls, chlorinated pesticides and phenols [1–3]. The extractions can be accomplished in much shorter periods than the liquid solvent-based extraction methods. In addition, SFE extracts are cleaner due to lower concentrations of interfering co-extractants. This last feature permits the direct introduction of extracts into analytical systems such as gas chromatography (GC), supercritical fluid chromatography (SFC), liquid chromatography (LC) and mass spectrometry (MS) [4–10].

The coupling of SFE and LC results in an integrated system which is suitable for a number of moderately polar and polar chemicals and a few applications of such systems have been reported in literature. Nieass *et al.* [11,12] used a coupled SFE–LC system for solubility assessment of organic compounds. Evaluation of a similar system for extraction and determination of valtrate and didrovaltrate from *Radix valerianae* was reported by Unger and Roumeliotis

* Corresponding author. Present address: Department of Chemistry, 142 Schrenk Hall, University of Missouri–Rolla, Rolla, MO 65401-0249, USA.

0021-9673/93/$06.00

[13]. Schneiderman *et al.* [14] used a SFE–HPLC system with electrochemical detector for the determination of anthraquinone in paper and wood. Direct coupling of SFE with microcolumn LC has recently been described by Cortes *et al.* [15]. In this system micro-LC was used as a clean up (fractionation) step prior to GC separation and analysis.

Solvation and extraction of chlorinated phenols from solid matrices such as soil, wood and biological tissue have been under investigation in our laboratory. These studies have been facilitated by a tandem SFE–LC system. The system also performed well in the determination of phenols at trace levels, details of this application are presented in this article.

EXPERIMENTAL

A schematic of the SFE–LC system is shown in Fig. 1. The system consisted of a pneumatic amplifier (Model AAD-30; Haskel Engineering, Burbank, CA, USA), a pressure surge tank, extraction vessels and a liquid chromatograph. The pressure surge tank and extraction vessels were placed in a thermostated water bath. Carbon dioxide from the cylinder was compressed to desired pressure with the pneumatic amplifier. The compressed CO_2 was introduced into the 660-ml capacity surge tank. The surge tank acted as a reservoir for compressed CO_2 and also served to bring the CO_2 temperature down to the operating level. Samples were loosely packed into a glass wool lined wire mesh sample holder. The sample holders were placed in the extraction vessel and extraction vessel sealed. Extraction vessels were pressured by opening the inlet valve. The contents were allowed to equilibrate for periods ranging from 30 min to 2 h. After a set equilibration period on aliquate of equilibrated CO_2 was transferred to LC by operating the appropriate three-way valve and a vessel selection valve (V-3) and the sampling loop valve (V-2). Extraction vessels with internal volume of 150 ml were used. These vessels were designed to operate at pressures up to 400 atm (1 atm = 101 325 Pa) and were fabricated at the Science Instrument Shop, University of Missouri–Columbia. Three-way stainless-steel valves were purchased from High Pressure Equipment (Erie, PA, USA). The vessel selection valve (V-3) and sampling loop valves (V-1 and V-2) were ob-

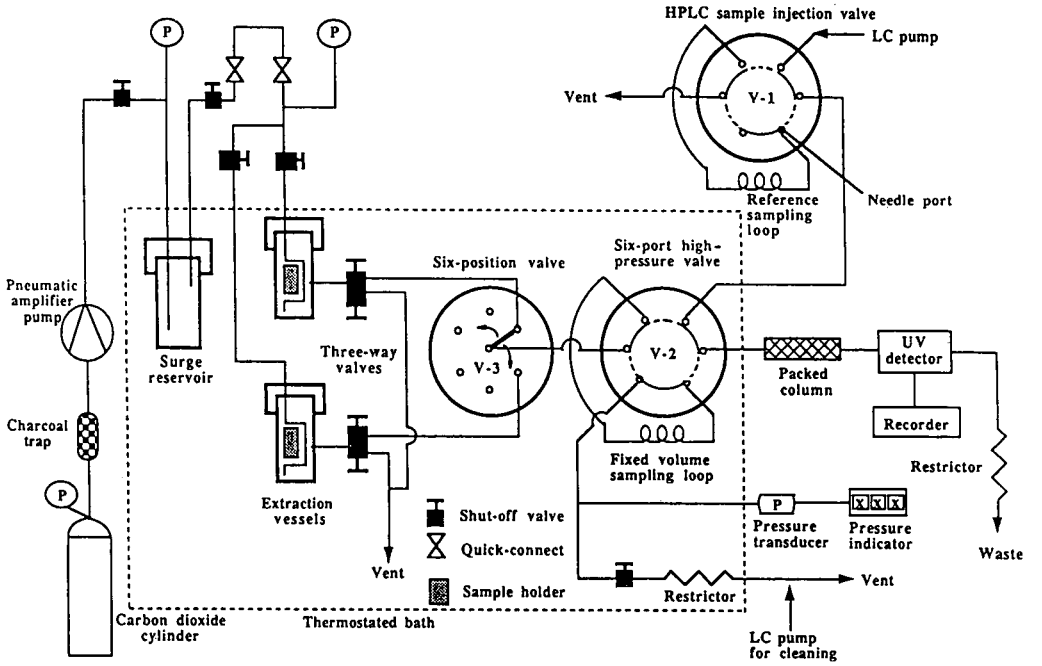

Fig. 1. A schematic of the on-line SFE–HPLC system.

tained from Rheodyne (Cotati, CA, USA). Incorporation of valve V-3 permitted sequential sampling of up to six extraction vessels. The details of sample preparation and SFE apparatus have been presented elsewhere [16].

A 20-μl loop (V-1) was used for introducing samples during the routine LC mode of operation, whereas a 50-μl loop (V-2) was used for introduction of the SFE extract. The LC system consisted of a bonded C_{18} column, a LC pump (Model series 4; Perkin-Elmer, Norwalk, CT, USA) and a UV–Vis detector (Model LC-85, Perkin-Elmer). To prevent formation of CO_2 bubbles, two linear restrictors consisting of 8 cm $\times$ 25 μm I.D. fused-silica tubing were attached at the end of the detector and the vent tube. The restrictor tubing was obtained from Polymicro Technologies (Tucson, AZ, USA). The selection of restrictors was based on the pressure limit of the detector cell, mobile phase flow-rate and composition. A low-volume pressure transducer (void volume *ca.* 10 μl) was installed in the back of sample loop restrictor to ascertain the pressure difference between the extraction vessel and the sampling loop.

The separation of chlorinated phenols was accomplished by reversed-phase chromatography with a 250 $\times$ 4.6 mm I.D. stainless-steel column with 5 μm C_{18} bonded silica packing (Supelcosil; Supelco, Supelcopark, PA, USA). Water–acetonitrile was used as the mobile phase, the composition being changed from 100% A (water–acetonitrile–acetic acid, 94:5:1) to 100% B (acetonitrile–acetic acid, 99:1) in 35 min using a linear solvent gradient. The absorbance of separated components was measured at 275 nm.

The initial evaluation of the SFE–LC system was carried out with a mixture of chlorinated phenols spiked on glass beads. However, optimal partition parameters were established for each matrix separately. This optimization involved selection of equilibration pressure, temperature, modifier, modifier concentration. The minimum detection limit (MDL) and linearity of response were determined by spiking different matrices with the phenol mixture over a concentration range of 1–500 ppm (w/w). For comparative purposes soil and wood shaving samples were also extracted by conventional liquid solvent

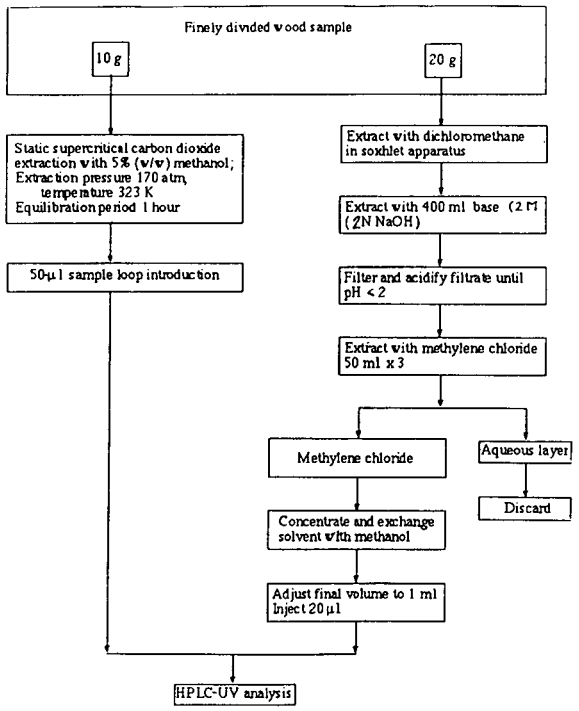

Fig. 2. Flow scheme for the determination of chlorinated phenols in wood shavings.

based methods which entailed Soxhlet extraction followed by partitioning of phenols and other acidic components into a strong base, neutralization of the base and back extraction of the phenols into methylene chloride. The extraction and clean-up schemes are outlined in the flow schemes in Fig. 2.

RESULTS AND DISCUSSION

The optimization of the system involved selection of SFE and LC parameters. These parameters were first selected independently through off-line extraction experiments and collection of extracts in methanol. Extracted phenols were analyzed by introduction of methanol into the liquid chromatograph through valve V-1. The objective of optimization experiments as to establish conditions which permitted highest selectivity, *i.e.*, where recovery of components of interest was highest and amount of coextractants lowest. In earlier studies it was pointed that optimal conditions are dependent not only on

the analytes but also on the matrix. For instance, while the non-polar analytes such as polychlorinated biphenyls (PCBs) and chlorinated biphenyls can be readily removed from biological matrices with carbon dioxide, recoveries of the same analytes is much worse from soil or sediments. These differences arise from the fact that these non-polar analytes are generally associated with non-polar portions of the biological tissues with which carbon dioxide exhibits better wetting properties than polar humic portions of soil and sediments. Distribution coefficients for a number of non-polar and moderately polar organics in different supercritical fluids and matrices have been determined in our laboratory. Most of these studies were conducted with an off-line extraction set-up [17]. These experiments showed that optimal extraction parameters for all matrices were in the near critical region, *i.e.*, the extraction temperature of 40°C and the pressure of approximately 170 atm. Under these conditions a minimum equilibration period of 30 min was required to reach steady state concentration. As a result, in all experimental extractions, an equilibration period of 1 h was employed.

Under the optimized LC parameters separation of all phenols of interest was achieved in approximately 25 min. The first step in the evaluation of tandem SFE–LC was to monitor the integrity of the chromatographic separation. The introduction of pressurized carbon dioxide led to considerable deterioration in the chromatographic performance. The primary cause of this deterioration was bubble formation (entrapment of CO_2) at the exit end of the chromatographic column and the detector cell. High diffusivities of solutes molecules in the CO_2 band also led to peak broadening (Fig. 3). The band broadening problem was addressed through the modification of solvent gradient which entailed a longer initial hold and lowering of acetonitrile concentration in the eluent A from 30% to 5%. These changes allowed CO_2 band to elute away from most solutes of interest. The overall effect of these changes was an elongation of elution time from 25 min to 35 min. The problem of CO_2 bubble formation was eliminated by installing a restrictor at the outlet of the detector.

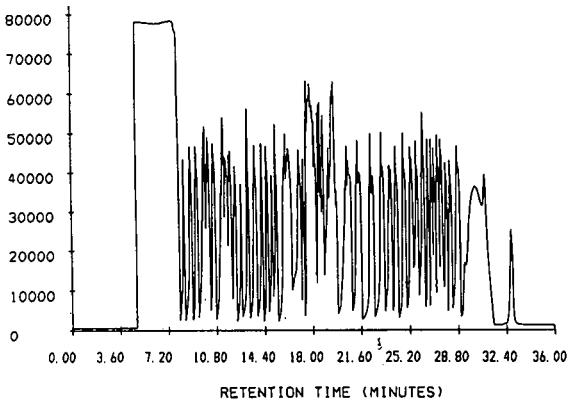

Fig. 3. Output of UV–Vis detector in the integrated system without outlet restrictor. *y*-Axis is reponse in arbitrary units.

Linear restrictors with 50 μm I.D. were used for the purpose. The back pressure was determined by the length of the restrictor and the flow-rate. In the present study an over pressure of 850 p.s.i. (1 p.s.i. = 6894.76 Pa) was found to be adequate for preventing bubble formation. The chromatographic separation of phenols obtained with the integrated SFE-LC is shown in Fig. 4. This separation was achieved by introducing 250 μg of phenols on 10 g of glass beads. Spiked glass beads were placed in extraction vessels and equilibrated with CO_2 at 170 atm and 40°C for 1 h. A 50-μl aliquot of CO_2 extract was introduced into the LC system through the sampling valve (V-2). The chromatographic performance of the system remained largely unchanged except for peaks co-eluting of CO_2 or immediately after it.

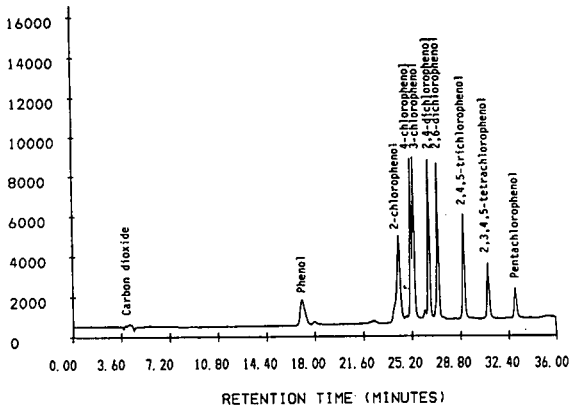

Fig. 4. Chromatogram of chlorinated phenols obtained with SFE–HPLC system under optimized gradient conditions and with outlet restrictors. *y*-Axis is reponse in arbitrary units.

The performance of the system was evaluated over a concentration range of 1–500 ppm with two other solid matrices: soil and wood shavings. A linear response was obtained over the entire range for each analyte with all three matrices. The calibration curves obtained with glass beads are shown in Fig. 5. A high degree of precision was obtained with the system. The standard deviation for six replicate analyses was less than 2%. It should be pointed out that detection limit and linear range in the system are interrelated and are depended on a number of parameters which include sample size, extraction vessel volume and the sampling loop volume. These parameters are in turn depended on partition ratios of the analyte in the given matrix/supercritical fluid system. The MDL of the system can be calculated through the following expression.

$$\text{MDL (ppm)} = d_1 \cdot \frac{V_{EX}}{V_L} \cdot \frac{1}{K} \cdot \frac{1}{S_w}$$

where d_1 is the instrument detection limit (μg), V_L is the volume of sampling loop (ml), V_{EX} is the volume of the extraction vessel (ml), K is the partition ratio of the analyte and S_W is the sample mass (g).

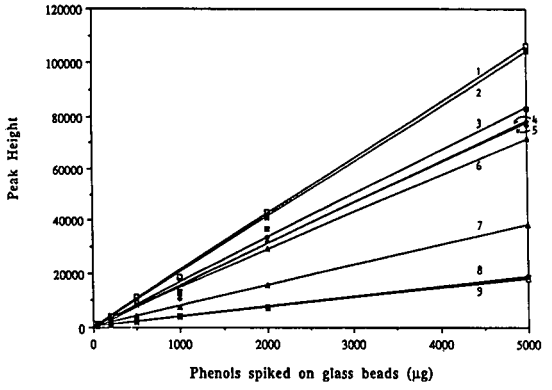

Fig. 5. Calibration curves for chlorinated phenol. Lines: 1 = phenol ($y = 499.62 + 3.4372x$, $R^2 = 0.999$); 2 = 2,4-dichlorophenol ($y = -775.79 + 15.790x$, $R^2 = 0.995$); 3 = 4-chlorophenol ($y = 95.502 + 16.680x$, $R^2 = 0.995$); 4 = 2-chlorophenol ($y = -81.644 + 15.496x$, $R^2 = 0.995$); 5 = 3-chlorophenol ($y = -570.43 + 20.923x$, $R^2 = 0.999$); 6 = 2,4,5-trichlorophenol ($y = -142.98 + 21.288x$, $R^2 = 0.999$); 7 = tetrachlorophenol ($y = 227.97 + 14.250x$, $R^2 = 0.999$); 8 = pentachlorophenol ($y = 253.30 + 75623x$, $R^2 = 1.000$); 9 = 2,6-dichlorophenol ($y = 279.73 + 3.6365x$, $R^2 = 0.999$).

While little difference in chromatographic performance was observed in case of soil samples, the recoveries were generally low, falling in 60–65% range. To achieve better extraction efficiencies (≥80%) a polar modifier such as methanol had to be introduced into the extraction vessel, and 5% (w/w) methanol was found to give optimal results. Under these conditions the complete analysis was performed in 1.5 h which compared favorably to the *ca.* 15 h required for traditional analytical methodologies.

System performance was found to be decidedly superior in case of complex matrices which contain high levels of interfering compounds, *e.g.*, wood samples with high pigment content. The analyses of chlorinated phenols in such

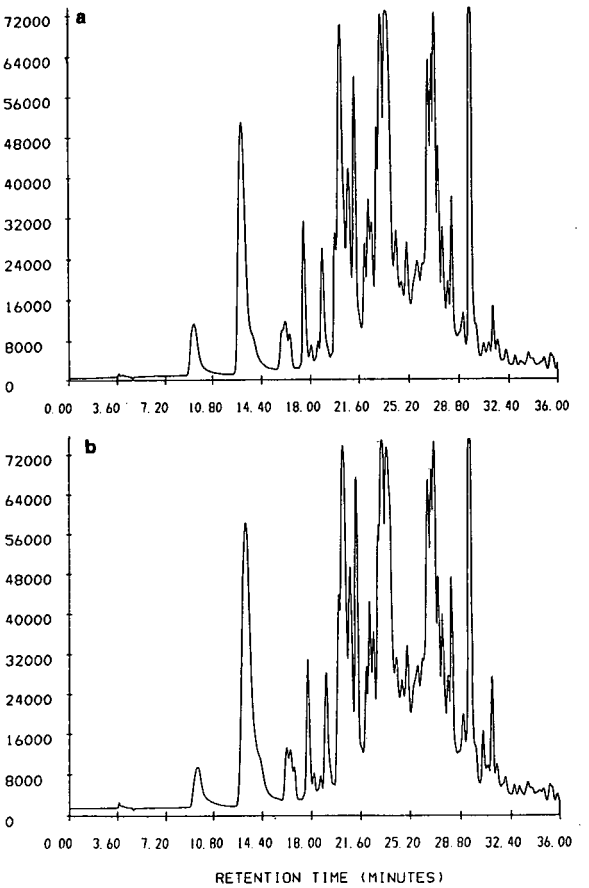

Fig. 6. (a) Chromatogram of liquid solvent extract of a wood shaving sample. (b) Chromatogram of liquid solvent extract of a wood shaving samples spiked with chlorinated phenols; spike concentration 20 ppm. *y*-Axes represent response in arbitrary units.

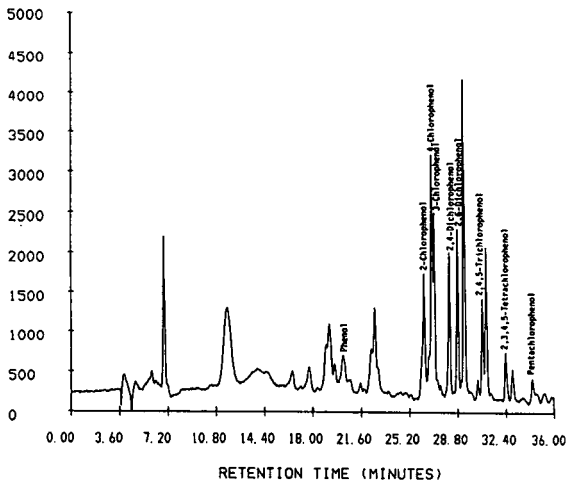

Fig. 7. Chromatogram of supercritical fluid extract of a wood shavings sample spiked with chlorinated phenols. Spike concentration 20 ppm. *y*-Axis is response in arbitrary units.

matrices are exceedingly difficult due to the presence of interferents. The chromatography of a wood shaving extract obtained by Soxhlet extraction, followed by extraction with a base, neutralization and black extraction into methylene chloride is shown in Fig. 6a. The complexity of the chromatographic data is self evident and prevented quantitation of spiked phenols (Fig. 6b). By contrast, the supercritical fluid extracts were decidedly cleaner with considerably less pigment load. Results obtained with SFE–LC system for wood shaving samples are shown in Fig. 7; all of the phenols could be quantitatively determined to sub ppm level. A summary of spike recoveries and detection limits are given in Table I.

TABLE I

DETECTION OF PHENOLS BY SFE–HPLC IN WOOD SAMPLE

Components	Recovery (%)[a]	Detection limit (in 15 g sample) (ppm)
Phenol	106.4	2.5
2-Chlorophenol	93.3	1.0
4-Chlorophenol	94.6	1.0
3-Chlorophenol	96.1	1.0
2,4-Dichlorophenol	100.7	1.0
2,6-Dichlorophenol	101.1	1.0
Trichlorophenol	85.2	1.0
Tetrachlorophenol	85.0	2.5
Pentachlorophenol	84.7	3.3

[a] Based on the reference standard spiked on the glass beads for SFE.

CONCLUSIONS

Quantitative recoveries for chlorinated phenols can be obtained with CO_2 under near critical conditions. The CO_2 extract can be easily and directly introduced into a LC system for rapid determination of these analytes.

ACKNOWLEDGEMENTS

The research described in this article was funded in part by the US Environmental Protection Agency under assistance agreement R-815709. Partial support for the work was also provided by the Environmental Division, Southern California Edison Company, Rosemead, CA, USA.

REFERENCES

1 K.M. Dooley, C.C. Kao, R.P. Gambrell and F.C. Knopf, *Ind. Eng. Chem. Res.*, 26 (1987) 2058.
2 K.S. Nam, S. Kapila, D.S. Viswanath, T.E. Clevenger, J. Johansson and A.F. Yanders, *Chemosphere*, 19 (1989) 33.
3 R.K. Roop, R.K. Hess and A. Akgerman, in K.P. Johnston and J.M.L. Penninger (Editors), *Supercritical Fluid Science and Technology*, American Chemical Society, Washington, DC, 1989.
4 B.W. Wright, S.R. Frye, D.G. McMinn and R.D. Smith, *Anal. Chem.*, 59 (1987) 640.
5 S.B. Hawthorne, D.J. Miller and M.S. Krieger, *J. Chromatogr. Sci.*, 27 (1989) 347.
6 J.M. Levy and A.C. Rosselli, *Chromatographia*, 28 (1989) 613.
7 K.S. Nam, S. Kapila, A.F. Yanders and R.K. Puri, *Chemosphere*, 23 (1991) 1109.
8 W. Gmuer, J.O. Bosset and E. Plattner, *J. Chromatogr.*, 388 (1987) 143.
9 J.B. Nair and J.W. Huber, III, *LC · GC*, 6 (1988) 1071.
10 H.T. Kalinoski, H.R. Udseth, B.W. Wright and R.D. Smith, *Anal. Chem.*, 58 (1986) 2421.
11 C.S. Nieass, M.S. Wainwright and R.P. Chaplin, *J. Chromatogr.*, 194 (1980) 335.
12 C.S. Nieass, R.P. Chaplin and M.S. Wainwright, *J. Liq. Chromatogr.*, 5 (1982) 2193.

13 K.K. Unger and P. Roumeliotis, *J. Chromatogr.*, 282 (1983) 519.
14 M.A. Schneiderman, A.K. Sharma and D.C. Locke, *J. Chromatogr.*, 409 (1987) 343.
15 H.J. Cortes, L.S. Green and R.M. Cambell, *Anal. Chem.*, 63 (1991) 2719.
16 K.S. Nam, S. Kapila, A.F. Yanders and R.K. Puri, *Chemosphere*, 20 (1990) 873–880.
17 M.H. Liu, *Ph.D. Dissertation*, University of Missouri–Columbia, Columbia, MO, August 1992.

Journal of Chromatography, 639 (1993) 159–164
Elsevier Science Publishers B.V., Amsterdam

CHROM. 24 961

High-performance size-exclusion chromatography of wood hemicelluloses on a poly(2-hydroxyethyl methacrylate–co-ethylene dimethacrylate) column with sodium hydroxide solution as eluent

T.E. Eremeeva* and T.O. Bykova

Cellulose Laboratory, Institute of Wood Chemistry, Latvian Academy of Sciences, 27 Akademijas Str., Riga 226006 (Latvia)

(First received October 9th, 1992; revised manuscript received January 2nd, 1993)

ABSTRACT

The determination of the molecular mass parameters of wood hemicelluloses by high-performance size-exclusion chromatography (HPSEC) using a poly(2-hydroxyethyl methacrylate–co-ethylene dimethacrylate) (Separon S HEMA 1000) column and 0.5 *M* NaOH as solvent and eluent is described. It is shown that universal calibration between dextran and xylan is valid. The Mark–Houwink equation for xylan in 0.5 *M* NaOH was found to be $[\eta] = 2.67 \cdot 10^{-4} M^{0.73}$, where M = molecular mass. A direct method of characterization of hemicelluloses extracted with 18% NaOH from different celluloses and pulps by HPSEC is described.

INTRODUCTION

Hemicelluloses are a type of polysaccharide that is widespread together with cellulose in land plants. Large amounts are present in wood tissues, and some of them remain in the wood pulp, therefore influencing the pulp properties.

The degree of polymerization (*DP*) and polydispersity of wood hemicelluloses have been investigated by numerous workers over many years [1–3]. The molecular mass (M_r) parameters of wood hemicelluloses have been studied by viscometry [4–6], osmometry [1,4–7] and ultracentrifugation [1,4]. Hemicelluloses are established to have a *DP* of 300–30, and polydispersity values are quoted from monodisperse to highly polydisperse [1–6].

Size-exclusion chromatography has been the most popular method for determining the molecular mass distribution (MMD) of hemicelluloses, traditionally carried out using soft organic gels as column packing materials [8–12]. Today for the determination of the MMD of polymers the time-consuming gel permeation chromatography has generally been replaced by high-performance size-exclusion chromatography (HPSEC). However, the determination of the MMD of hemicelluloses utilising HPSEC columns is still very limited.

In a previous paper [13], the feasibility of determining the MMD of the 4-O-methyl-D-glucuronoxylan in aprotic solvents (dimethyl sulphoxide, dimethylformamide (DMF) by HPSEC, using a poly(2-hydroxyethyl methacrylate–co-ethylene dimethacrylate) (Separon S HEMA 1000) column, was investigated. The results showed that fractionation according to MM was achieved, using DMF containing appropriate amounts of H_3PO_4 and LiBr as eluent. Further experiments demonstrated that the Separon S HEMA 1000 packing is a stable in

* Corresponding author.

0021-9673/93/$06.00

strongly alkaline media and it is possible to determine the MMD of hemicelluloses using cadoxen (pH ≈ 13) as eluent [14,15]. A disadvantage of this method is that large amounts of cadoxen, an expensive and laborious way to prepare eluent, are needed.

In this work, in order to develop a more convenient and rapid method for the determination of the MMD of hemicelluloses by HPSEC, the use of a prepacked Separon S HEMA 1000 column with 0.5 *M* NaOH as eluent was investigated.

EXPERIMENTAL

Chemicals and materials

Analytical reagent-grade sodium hydroxide (Lachema, Brno, Czech Republic) and doubly distilled water were used. Dextran standards T 10, T 20, T 40, T 70, T 110, T 500 and T 2000 were obtained from Pharmacia (Uppsala, Sweden). Oat husk xylans were obtained from Sigma (St. Louis, MO, USA) and Serva (Heidelberg, Germany).

Isolation of the hemicelluloses

The preparation and characterization of the xylan fractions were described elsewhere [13]. The isolation procedures for birch and beech xylans and arabinogalactan were described previously [13,16,17]. Spruce glucomannan was isolated from spruce chlorite holocellulose by the usual procedure, as described for the glucomannan [3].

Extraction of the hemicelluloses fractions

A 400-mg amount of milled pulp fibres or holocellulose was placed in a 10-ml tube, 4 ml of 18% NaOH were added and the mixture was left for 1 h at room temperature. The sample was quickly squeezed and filtered through an N2 glass filter and then immediately analysed by HPSEC.

Solution preparation

The solvent for all samples was 0.5 *M* NaOH, except for larch arabinogalactan, for which water was used as the solvent. The time for complete dissolution was 10–20 min. To calibrate the chromatographic system and to analyse isolated hemicelluloses samples, 25 μl of 0.2% solutions were injected. The hemicelluloses were found to be stable in 0.5 *M* NaOH at least for 6 h; the chromatograms after this time were virtually identical with these obtained immediately after the dissolution.

HPSEC

The analyses were performed on a size-exclusion chromatograph from Laboratory Instruments (Prague, Czech Republic) with a refractometric detector, equipped with a Rheodyne Model 7125 fixed-loop (100 μl) injector. A prepacked stainless-steel column (250 × 8 mm I.D.) containing Separon S HEMA 1000 (10 μm) (Tessek, Prague, Czech Republic) was used. The eluent was 0.5 *M* NaOH and analyses were carried out at the room temperature. The analysis time was 20 min at a flow-rate 0.4 ml/min.

Intrinsic viscosity measurement

Viscosities were determined at 25 ± 0.05°C in cadoxen using an Ubbelohde viscometer. The DP_v of the hemicelluloses samples was obtained from viscometric measurements using the following equation, established for xylan [4]; $[\eta] = 9.2 \cdot 10^{-3}\ DP_v^{0.84}$ dl/g.

RESULTS AND DISCUSSION

Calibration of column

A series of dextrans were used to obtain the calibration graph and to check the range of retention volume for chromatographic separation. The M_r parameters of dextran standards provided by the manufacturer are given in Table I.

Fig. 1 shows typical elution curves for dextran standards under the conditions applied. The fractionation of dextrans T 10, T 20, T 40, T 70 and T 110 is resulted in symmetrical curves; dextrans T 500 and T 2000 were only partially resolved since a portion of them have M_r values higher than the column exclusion limit. A plot of 0.5 log $(\bar{M}_w\bar{M}_n)$ against retention volume (V_e) gives a straight line over the range $3 \cdot 10^5$–$2 \cdot 10^3$ (Fig. 2).

TABLE I

MOLECULAR MASS AND ELUTION CHARACTERISTICS OF DEXTRAN STANDARDS AND XYLAN FRACTIONS

$\bar{M}_w$ = mass-average molecular mass; $\bar{M}_n$ = number-average molecular mass; M_p = peak molecular mass calculated by 0.5 ln $(\bar{M}_w\bar{M}_n)$.

No.	Sample	$\bar{M}_w$	$\bar{M}_n$	M_p	V_e (ml)	Log $M_p[\eta]$
1	Dextran T 2000	2 000 000			3.96	6.21
2	Dextran T 500	506 000	190 000	310 000	4.08	5.24
3	Dextran T 110	116 000	56 000	81 700	4.87	4.38
4	Dextran T 70	66 300	36 400	49 100	5.25	4.05
5	Dextran T 40	39 400	23 400	30 400	5.58	3.75
6	Dextran T 20	20 900	14 000	17 100	6.00	3.38
7	Dextran T 10	9 500	4 900	6 800	6.58	2.78
8	Xylan I	26 200	20 800	23 300	5.33	3.98
9	Xylan II	22 300	17 700	19 900	5.47	3.87
10	Xylan III	17 600	13 100	15 200	5.70	3.66
11	Xylan IV	13 000	9 600	11 170	5.94	3.43
12	Xylan V	11 000	7 900	9 300	6.09	3.29
13	Xylan VI	5 800	4 200	4 900	6.62	2.81
14	Xylan 0	19 000	14 000	16 300	5.64	3.72
15	Raffinose	504			7.25	
16	Cellobiose	342			7.40	
17	Glucose	180			7.52	

The xylan fractions were used to obtain a calibration graph for evaluation the MMD of hemicelluloses. The M_r and retention volumes of the fractions are given in Table I. As can be seen from Fig. 2, the calibration graph for xylans is linear over the range examined.

The investigation of the elution behaviour of hemicelluloses showed that there are no non-exclusion effects observed on the Separon S HEMA 1000 column in 0.5 *M* NaOH.

The possibility of universal calibration applied to the calculation of the MMD of hemicelluloses was examined. For this purpose, the Mark–Houwink constants for xylan fractions in 0.5 *M* NaOH were calculated using combined SEC and viscometric data according to the principle described by Dobbin *et al.* [18]. The Mark–Houwink equation was $[\eta] = 2.67 \cdot 10^{-4} M^{0.73}$ dl/g, where M = molecular mass. It has been found that when using for dextran the constants $K = 13.2 \cdot 10^{-2}$ and $\alpha = 0.478$ [19], and the evaluated constants for xylan, the universal calibration {log

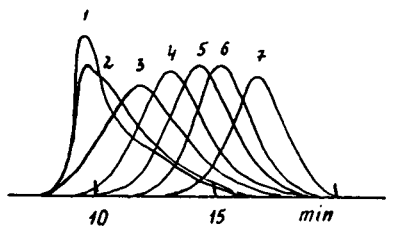

Fig. 1. Experimental chromatograms of dextran standards (numbers as in Table I).

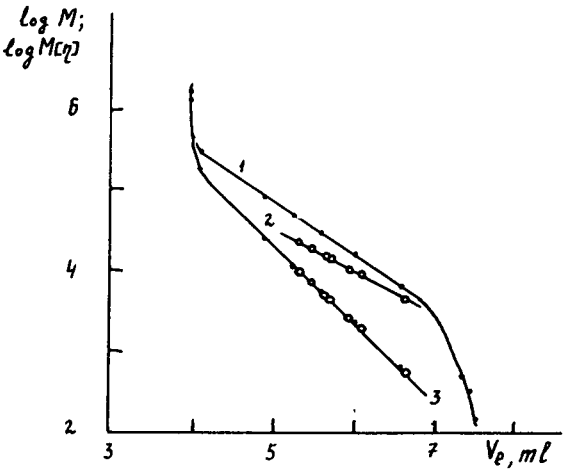

Fig. 2. Calibration graphs of log $M = f(V_e)$ for (1) dextran and (2) xylan and (3) universal calibration of log $M[\eta] = f(V_e)$ obtained on the Separon S HEMA 1000 column with 0.5 *M* NaOH.

$M[\eta] = f(V_e)\}$ is valid, as shown in Fig. 2. Hence the universal calibration procedure can be used to calculate the M_r parameters of hemicelluloses if characterized hemicellulose fractions are unavailable.

Analysis of isolated hemicelluloses

In order to demonstrate the ability of the column to fractionate hemicelluloses according to M_r, the following hemicelluloses samples were used: two wood xylans isolated from birch and beech holocelluloses, two oat husk xylans supplied by Sigma and Serva, glucomannan isolated from spruce holocellulose, arabinogalactan from larch and two hemicellulose fractions from spruce sulphite and pine kraft viscose-grade bleached celluloses isolated at the mercerization stage.

As Fig. 3 shows, the chromatograms of the investigated hemicelluloses are nearly symmetrical. The M_r parameters of these samples calculated by calibration of xylan fractions are given in Table II. The xylans from oat husks have a higher M_r than those isolated from hardwood holocelluloses. Thus, the mass-average molecular mass $\bar{M}_w$ of the Sigma and Serva xylans are *ca.* 25 000, whereas those of beech and birch xylans are *ca.* 20 000 and 17 000, respectively. The pine kraft hemicelluloses differ from those obtained from spruce sulphite cellulose. They have a higher M_r values and are less polydisperse: $\bar{M}_w = 8900$, $M_w/M_n = 1.30$ and $\bar{M}_w = 5900$, $M_w/M_n = 1.42$, respectively.

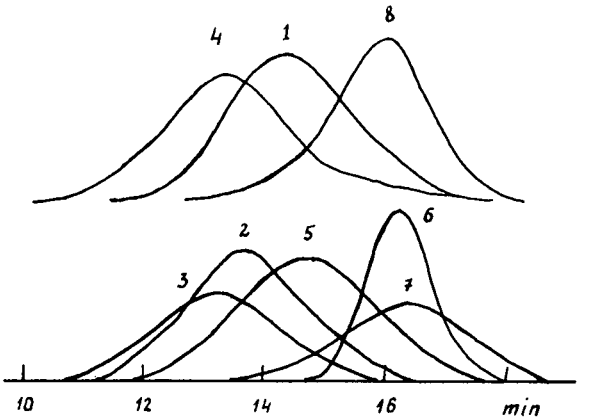

Fig. 3. Experimental chromatograms of isolated hemicelluloses (numbers as in Table II).

The M_r data for reference xylans obtained by SEC are in good agreement with $\bar{M}_v$ (viscosity-average molecular mass) estimated by viscometry in cadoxen and are closely comparable to the results obtained by the other investigators for the corresponding hemicelluloses [1–3]. The data obtained show that the calibration graph evaluated for xylans is applicable to the M_r calculation of softwood glucomannan, giving reliable results. Thus, the DP_w values of softwood glucomannan have been reported to be from 60 to 90 and $\bar{M}_w$ from 10 000 to 15 000, respectively [1–3]; these results are in good agreement with ours (Table II).

TABLE II

MOLECULAR MASS PARAMETERS OF ISOLATED HEMICELLULOSES

No.	Sample	$\bar{M}_w$	$\bar{M}_n$	M_w/M_n	Viscometry in cadoxen	
					$\bar{M}_v$	DP_v
1	Xylan, birch	17 510	12 600	1.39	17 000	109
2	Xylan, beech	20 650	14 440	1.43	20 000	133
3	Xylan, oat husks (Sigma)	27 500	20 500	1.34	26 100	174
4	Xylan, oat husks (Serva)	26 270	17 170	1.53	25 000	166
5	Glucomannan, spruce	14 600	11 000	1.45	14 000	86
6	Arabinogalactan, larch	6 600	5 500	1.21	–	–
7	Hemicelluloses from spruce sulphite cellulose	5 900	4 150	1.42	5 350	33
8	Hemicelluloses from pine sulphate cellulose	8 900	6 830	1.30	8 500	53

For the larch arabinogalactan M_r data, it should be noted that no reliable data have been reported previously and the estimated earlier M_r values seems to be too high [11,20]. It is our suggestion that these values for arabinogalactan M_r are high owing to the polyelectrolyte expansion and the M_r of arabinogalactan in fact does not exceed 10 000 [16].

Analysis of alkaline extracts

The species of hemicelluloses are traditionally obtained by extraction with basic solutions; commonly 10–24% KOH or NaOH are used, followed by precipitation and purification [1–3]. In this work, the analysis of alkaline extracts from wood pulps was performed without isolation of the hemicelluloses from the solution; no sample treatment other than extraction and filtration was required. This procedure shortens the analysis time considerably and minimizes any changes in the hemicelluloses fractions due to sample preparation.

Fig. 4 shows the SEC of the hemicelluloses extracted with 18% NaOH from birch holocellulose, spruce sulphite paper- and viscose-grade pulps and beech and pine kraft viscose-grade pulps. The volume injected for extracts from holocellulose and paper-grade samples was 25 μl and for viscose-grade samples 100 μl.

The M_r parameters of the extracted hemicelluloses are given in Table III. These data are compared with the corresponding values for hemicelluloses presented in Table II. The average M_r and polydispersity of extracted birch xylan and isolated by the usual procedure from holocellulose are virtually identical. The hemicelluloses extracted from pine kraft and spruce sulphite viscose-grade bleached celluloses have higher average M_r values than the isolated compounds. Obviously the extracted hemicelluloses suffer less extensive changes than those isolated at the mercerization stage.

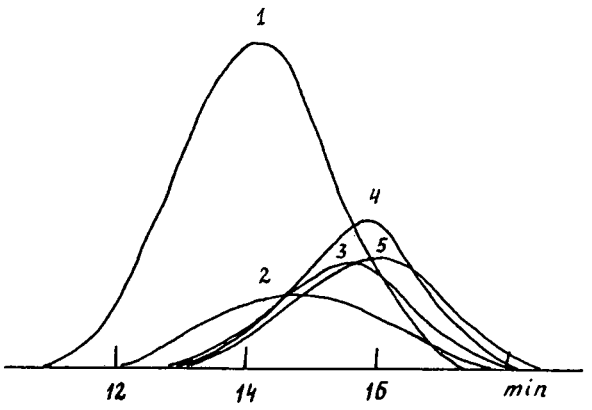

Fig. 4. Experimental chromatograms of wood hemicelluloses extracted with 18% NaOH from (1) birch holocellulose, (2) beech sulphate viscose-grade, (3) spruce sulphite paper-grade, (4) pine sulphate and (5) spruce sulphite viscose-grade celluloses.

It should be pointed out that simultaneously in addition to the determination of the MMD of the hemicelluloses, it is also possible by HPSEC to determine the hemicellulose content in the extracts obtained from different wood celluloses.

TABLE III

MOLECULAR MASS PARAMETERS AND AMOUNTS OF HEMICELLULOSES EXTRACTED WITH 18% NaOH FROM CELLULOSES

No.	Cellulose sample	Solubility in 18% NaOH (%)		$\bar{M}_w$	$\bar{M}_n$	M_w/M_n
		Standard method	HPSEC			
1	Birch holocellulose	33.0[a]	30.0	17 470	12 640	1.38
2	Spruce sulphite paper-grade cellulose	13.0	13.5	8 240	5 500	1.50
3	Beech sulphate viscose-grade cellulose	3.9	4.2	10 120	6 910	1.46
4	Spruce sulphite viscose-grade cellulose	5.0	5.1	9 100	6 250	1.46
5	Pine sulphate viscose-grade cellulose	4.2	4.3	9 410	6 580	1.43

[a] Pentosan content determined according to ref. 3.

For this purpose calibration graphs for the corresponding hemicelluloses with known concentrations *vs.* chromatographic peak area obtained by refractive index detection were constructed. The calculated amounts of hemicelluloses in the investigated wood celluloses are summarized in Table III. The data obtained by HPSEC are in good agreement with the hemicellulose content determined by standard analytical methods [3].

Further investigations in this direction are in progress, and more detailed information on the HPSEC analysis of alkali-soluble fractions from different wood celluloses will be published.

CONCLUSIONS

An HPSEC method for the determination of the MMD of hemicelluloses, both isolated by a commonly used procedure and directly extracted with 18% NaOH, has been described. The method suggested for the characterization of wood hemicelluloses is very simple, because stages such as neutralization, precipitation and purification, which are usually required in hemicellulose isolation procedures, are omitted. All changes in and losses of hemicelluloses connected with the traditional scheme of isolation in this instance are eliminated.

Further, the HPSEC method can be used to determine the hemicellulose content in different wood celluloses and pulps when the corresponding calibration graph has been obtained. The method presented is useful for measurements of numerous samples in routine work.

The Separon S HEMA 1000 column is particularly suitable for the determination of the MMD of different hemicelluloses. The possibility of using this SEC technique for studies of any alkali-soluble polymer is evident.

ACKNOWLEDGEMENT

The authors gratefully thank Dr. A. Ebringerova for providing some of the hemicelluloses samples.

REFERENCES

1 T.E. Timell, *Adv. Carbohydr. Chem.*, 19 (1964) 247; 20 (1965) 409.
2 Z. Kin, *Hemicellulozy, Chemia i Wykorzystanie*, Panstwowe Wydawnictwo Rolnicze i Lesne, Warsaw, 1980, p. 231.
3 V.I. Sharkow and N.I. Kuibina, *Khimiya Gemitscellulozh*, Lesnaya Promyshlennost, Moscow, 1972, p. 440.
4 R. Wikstrom, *Sven. Papperstidn.*, 10 (1968) 399.
5 L.G. LeBell, A.J. Goring and T.E. Timell, *J. Polym. Sci., Part C*, 2 (1963) 9.
6 R.J. Sturgeon, *Carbohydr. Res.*, 30 (1973) 175.
7 M. Zinbo and T.E. Timell, *Sven. Papperstidn.*, 70 (1967) 695.
8 K. Kringstad and O. Ellefsen, *Papier (Darmstadt)*, 18 (1964) 583.
9 K. Kringstad, *Acta Chem. Scand.*, 19 (1965) 1493.
10 K.-E. Eriksson, B.A. Pettersson and B. Steenberf, *Sven. Papperstidn.*, 71 (1968) 695.
11 B.W. Simson, W.A. Cote and T.E. Timell, *Sven. Papperstidn.*, 71 (1968) 699.
12 B.V. Ettling and M.F. Adams, *Tappi*, 51 (1968) 116.
13 T.E. Eremeeva and O.E. Khinoverova, *Cellul. Chem. Technol.*, 24 (1990) 439.
14 T. Eremeeva and A. Ebringerova, *Application Note, F321*, Tessek, Prague, 1990.
15 T. Eremeeva, A. Ebringerova, A. Treimanis and O. Khinoverova, *Abstracts of 4th Bratislava Symposium on Saccharides, Smolenice, August–September, 1988*, p. 59.
16 T.E. Eremeeva and T.O. Bykova, *Carbohydr. Polym.*, 18 (1992) 217.
17 A. Ebringerova, T.E. Eremeeva, O.E. Khinoverova and B.G. Ershov, *Carbohydr. Polym.*, 15 (1991) 255.
18 J. Dobbin, A. Rudin and M.F. Tchir, *J. Appl. Polym. Sci.*, 27 (1982) 1081.
19 A. Bose and J. Rollings, *J. Appl. Polym. Sci.*, 27 (1982) 795.
20 A.A. Salyers, R. Arthur and A. Kuritza, *J. Agric. Food Chem.*, 29 (1981) 475.

Journal of Chromatography, 639 (1993) 165–173
Elsevier Science Publishers B.V., Amsterdam

CHROM. 24 934

Liquid chromatography–mass spectrometry of fatty acids including hydroxy and hydroperoxy acids as their 3-methyl-7-methoxy-1,4-benzoxazin-2-one derivatives

Takashi Kusaka*

Department of Clinical Nutrition, Kawasaki University of Medical Welfare, 288 Matsushima Kurashiki, Okayama 701-01 (Japan)

Mitsunori Ikeda

Department of Biochemistry, Kawasaki Medical School, 577 Matsushima Kurashiki, Okayama 701-01 (Japan)

(First received September 30th, 1992; revised manuscript received January 25th, 1993)

ABSTRACT

Many kinds of authentic fatty acids, including hydroperoxy and hydroxy acids, were found to be not only detectable by liquid chromatography–mass spectrometry (LC–MS) with an atmospheric pressure chemical ionization interface system, but also measurable quantitatively by LC–MS installed with a spectrophotometer. We used LC–MS with spectrophotometry to analyse fatty acids split from lecithins after phospholipase A_2 treatment. Thus, some hydroperoxy fatty acids split from photo-oxidized lecithin could be identified.

INTRODUCTION

Recently, we reported the development of a new method of analysing fatty acids [1,2]. With this method the amide derivatives of hydroxy and non-hydroxy fatty acids were sensitively detected by liquid chromatography–mass spectrometry with an atmospheric pressure chemical ionization interface system (LC–APCI-MS). The method was applied to the simultaneous analysis of hydroxy and non-hydroxy fatty acids in rat brain [2] and to the analysis of fatty acids with a wide range of carbon chain lengths (C_{14}–C_{54}) in some mycobacteria [3].

We further attempted to quantitatively analyse labile fatty acids such as polyunsaturated hydroxy and hydroperoxy fatty acids. As a result, 3-bromomethyl-7-methoxy-1,4-benzoxazin-2-one (BrMB), known as a fluorescence labelling reagent for carboxylic acid, was found to be useful for detecting hydroperoxy and hydroxy fatty acids by LC–MS.

EXPERIMENTAL

Chemicals

Heptadecanoic acid ($C_{17:0}$), oleic acid ($C_{18:1}$), linoleic acid ($C_{18:2}$), α- and γ-linolenic acids ($C_{18:3}$), eicosatetraenoic acid ($C_{20:4}$), docosadienoic acid ($C_{22:2}$) and docosahexaenoic acid ($C_{22:6}$) were purchased from Nu-Chek-Prep. through Funakoshi Pharmaceutical (Tokyo, Japan). 12-Hydroxystearic acid (12-OH-$C_{18:0}$) was obtained from Serdary Research Labs., 2-hydroxystearic acid (2-OH-$C_{18:0}$) was purchased from Larodan Fine Chemicals, 15-hydroxyeicosatetraenoic acid (15-HETE or 15-OH-

* Corresponding author.

0021-9673/93/$06.00

$C_{20:4}$), 15-hydroperoxyeicosatetraenoic acid (15-HPETE or 15-OOH-$C_{20:4}$) and 5-hydroperoxy-eicosatetraenoic acid (5-HPETE or 5-OOH-$C_{20:4}$) were obtained from Cascade Biochemistry and 1-palmitoyl-2-arachidonoyl-*sn*-glycero-3-phosphocholine and bovine liver lecithin were purchased from Avanti Polar Lipids through Funakoshi Pharmaceutical. A standard mixture of eight kinds of fatty acids ($C_{14:0}$, $C_{16:0}$, $C_{16:1}$, $C_{18:0}$, $C_{18:1}$, $C_{18:2}$, γ-$C_{18:3}$, $C_{20:0}$) was purchased from Funakoshi Pharmaceutical. High-performance liquid chromatography (HPLC) grades of methanol and acetonitrile and N,N-diisopropylethylamine (DPEA) were purchased from Nakarai Tesque (Kyoto, Japan). Redistilled water was used for HPLC. BrMB was obtained from Tokyo Kasei (Tokyo, Japan). Bee venom phospholipase (PLase) A_2 (E.C.3.1.1.4) (Sigma, St. Louis, MO, USA) was further purified by reversed-phase HPLC according to the method of Hara *et al.* [4].

Equipment

A Hitachi (Tokyo, Japan) M-2000-type double-focusing mass spectrometer–computer system, equipped with a Hitachi L-6200-type HPLC instrument through a Hitachi APCI interface system, was used. HPLC was performed using a reversed-phase Cosmosil $5C_{18}$-packed column with 5-μm particles (250 mm × 4.6 mm I.D., Nakarai Tesque). The column temperature was maintained at 37°C in the column oven. The eluate from the LC column was conducted to the mass spectrometer via a photometric cell and the APCI interface system. Spectrophotometric chromatograms at a wavelength (λ) of 355 nm [λ_{max} for the 7-methoxy-1,4-benzoxazin-2-one-3-methyl (MB) ester of fatty acid] were processed with a 7000-B-type chromatogram processor (System Instrument, Tokyo, Japan). The drift voltage of APCI was 100 V and the temperatures of the vaporizer and desolvator were 250 and 385°C, respectively. The multiplier voltage of the mass spectrometer was 1700 V.

Derivatization of fatty acids with BrMB

Derivatization of fatty acids with BrMB was performed according to a slight modification of the method of Naganuma *et al.* [5] (Fig. 1). To 0.3 ml of acetonitrile containing 10–50 nmol of fatty acids were added 0.2 ml of 2.0 m*M* BrMB in acetonitrile and 30 nmol of DPEA as a catalyser. The reaction mixture was left at room temperature for 30 min, and then evaporated to dryness *in vacuo*. The residue was dissolved in 20–50 μl of acetonitrile. It was measured by the LC–MS immediately or stored at −70°C until use.

Photo-oxidation of unsaturated fatty acids and lecithin

Photo-oxidation of unsaturated fatty acids and lecithin was performed according to the method of Terao *et al.* [6]. Briefly, 100–200 μg of each authentic fatty acid ($C_{18:1}$, $C_{18:2}$, α- and γ-$C_{18:3}$, $C_{20:2}$, $C_{20:4}$, $C_{22:2}$, $C_{22:6}$) or bovine liver lecithin were dissolved in 0.5 ml of chloroform–methanol (1:1, v/v) containing 20 μg of methylene blue in test tubes. Each tube was irradiated with a tungsten lamp (40 W) at a distance of 10 cm for 2–3 h. The temperature of the reaction mixture was maintained at 20°C during the reaction. After the irradiation, the methylene blue in the medium was removed by column chromatog-

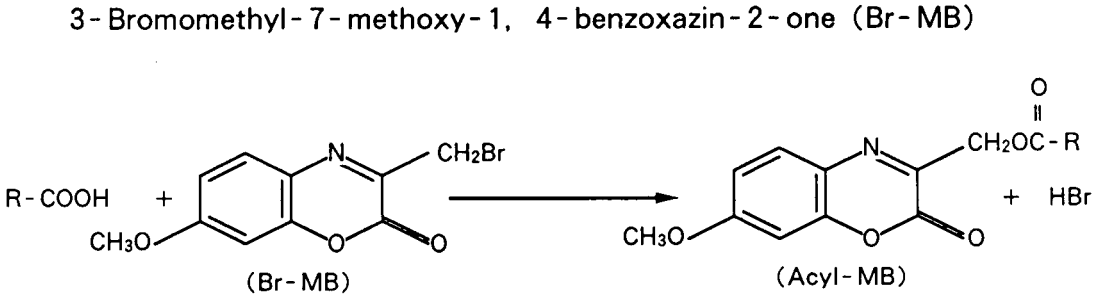

Fig. 1. Equation for the acyl MB preparation.

raphy with silica gel G (Merck, Darmstadt, Germany) using a mixture of chloroform and methanol (1:1, v/v) as the elution system.

Splitting of fatty acids from lecithin with PLase A_2

Splitting of fatty acids from lecithin with PLase A_2 was performed according to the method of Hara *et al.* [4]. Briefly, 100–200 μg of lecithin from bovine liver or 1-palmitoyl-2-arachidonoyl-*sn*-glycero-3-phosphocholine were incubated with 10 units of purified PLase A_2 for 10 min at room temperature in 1 ml of 10 m*M* Tris–HCl (pH 8.9) containing 0.1 ml of diethyl ether, 0.1 m*M* EDTA, 2 m*M* calcium chloride and 20 m*M* sodium chloride. The split fatty acids were extracted with hexane–diethyl ether (1:1, v/v).

Reduction of hydroperoxy fatty acids with sodium borohydride

Reduction of hydroperoxy fatty acids with sodium borohydride was performed according to the method of Van Rollins and Murphy [7]. An aliquot of 10–50 nmol of authentic 15-HPETE, 5-HPETE or photo-oxidized unsaturated fatty acids prepared as described above was dissolved in 1 ml of methanol, after which sodium borohydride (1 mg) was added. The solutions were incubated on ice for 15 min and at room temperature for 10 min. Then 1 ml of water was

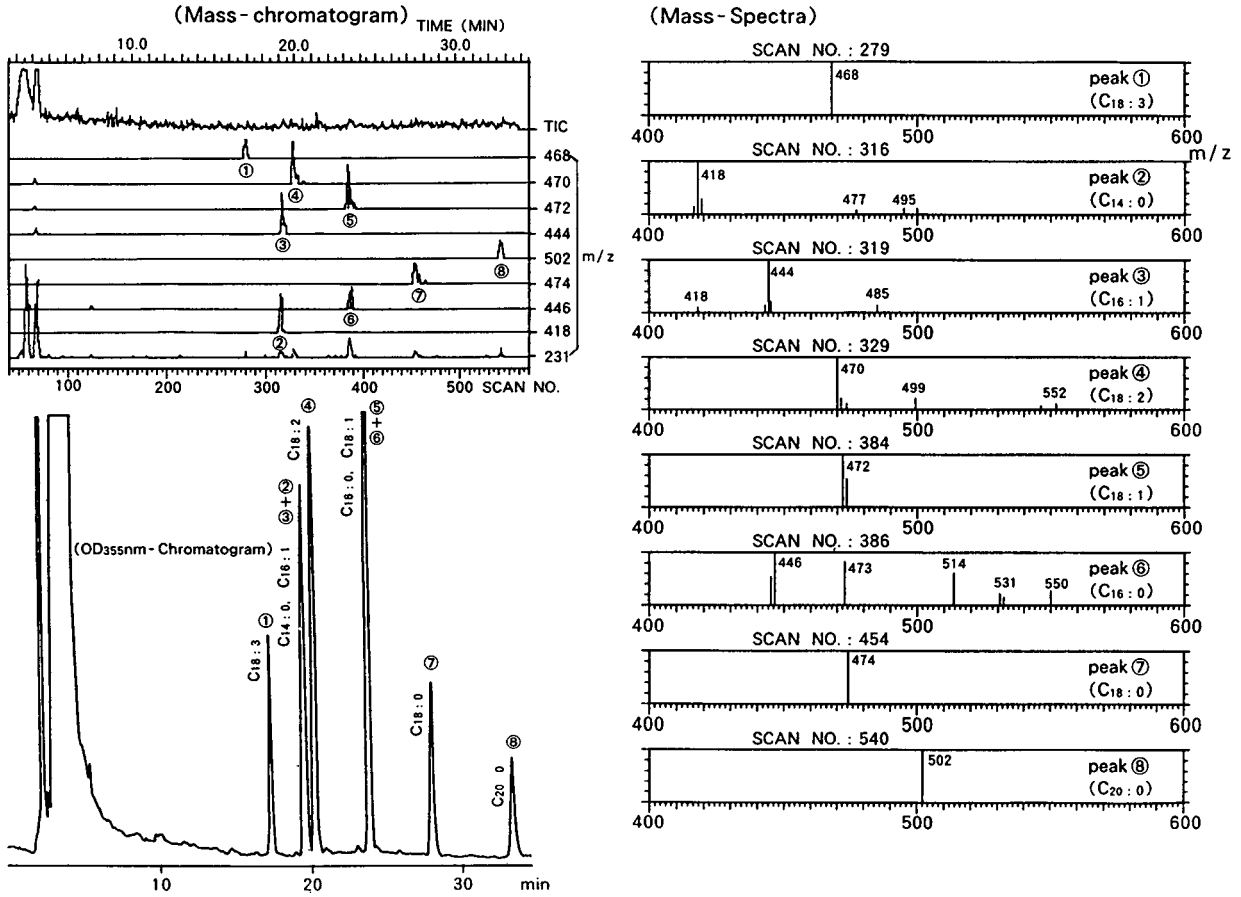

Fig. 2. LC–MS of the MB derivatives of standard fatty acids. A mixture of eight kinds of fatty acids (approximately 10 nmol each of $C_{14:0}$, $C_{16:0}$, $C_{16:1}$, $C_{18:0}$, $C_{18:1}$, $C_{18:2}$, $C_{18:3}$, $C_{20:0}$) was the starting material. The mobile phase was acetonitrile–water (80:20, v/v) with acetonitrile increasing linearly at the rate of 1%/min.

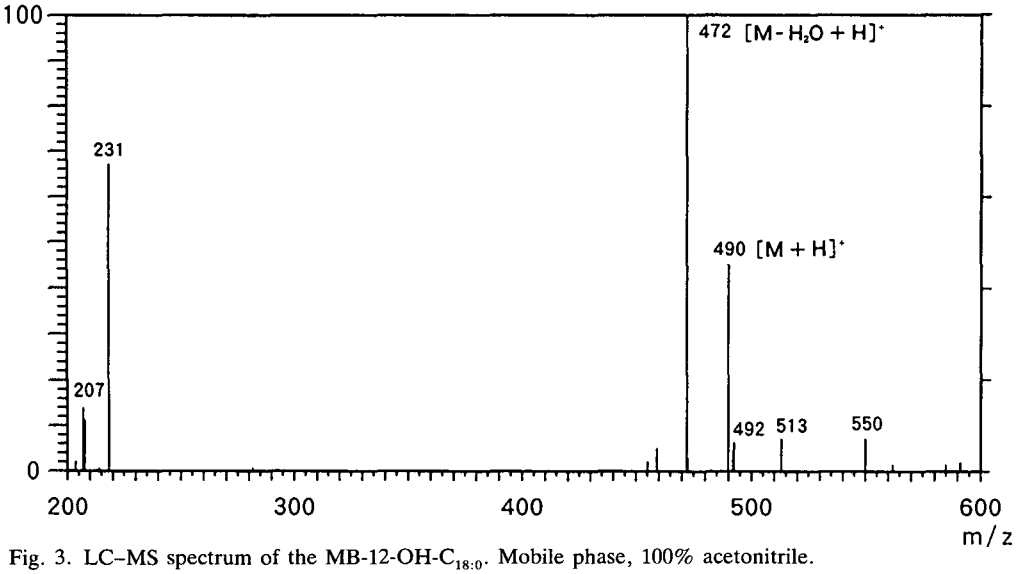

Fig. 3. LC–MS spectrum of the MB-12-OH-$C_{18:0}$. Mobile phase, 100% acetonitrile.

added and the solutions were adjusted to pH 4 with 5% hydrochloric acid. The fatty acids in the solutions were extracted with methylene chloride.

RESULTS

LC–MS of MB derivatives of authentic fatty acids

First, we examined whether the MB derivatives of fatty acids could be detected by LC–MS.

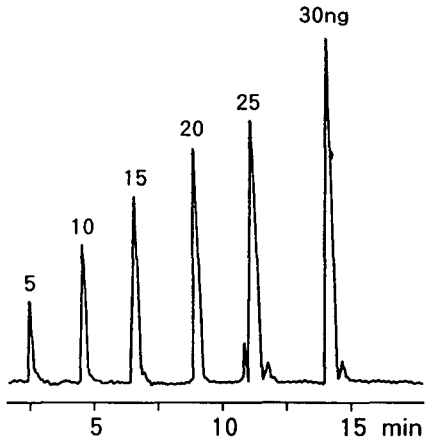

Fig. 4. Sensitivity of the MB derivative of palmitic acid. The mass spectrometer–computer system was set to detect a single ion $[M+H]^+$ with the maximum sensitivity for the derivative.

The MB derivatives of a mixture of eight kinds of authentic fatty acids were measured by the LC–MS with spectrophotometry. As shown in Fig. 2, we observed the mass spectra and mass chromatograms of MB derivatives of fatty acids. The pseudomolecular ions $[M+H]^+$ in these derivatives are the base peaks. Ions observed at

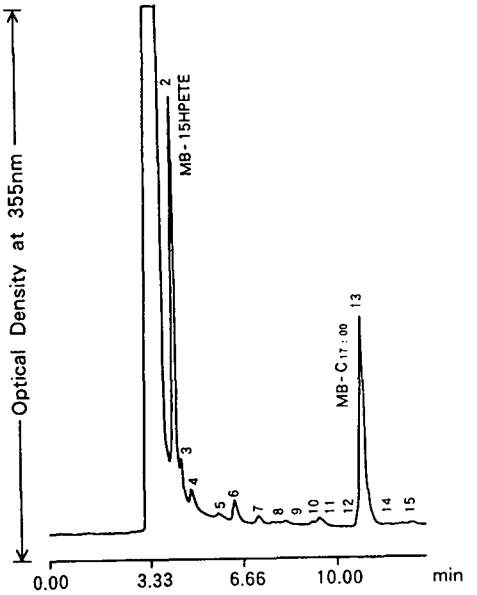

Fig. 5. HPLC of MB-15-HPETE and $C_{17:0}$. A mixture of 3 nmol each of 15-HPETE and $C_{17:0}$ was derivatized with BrMB. Mobile phase, 100% acetonitrile.

m/z 231 in these MB derivatives are assumed to be ions of [7-methoxy-1,4-benzoxazin-2-one-3-methyl + CH_3CN]. No significant difference could be observed between the spectra of saturated and unsaturated fatty acids. Peaks in the spectrophotometric chromatogram at 355 nm synchronized with those in the mass chromatogram. The mass spectrum of the MB derivative of authentic 12-OH-$C_{18:0}$ was also observed (Fig. 3). In this spectrum, an ion $[M - H_2O + H]^+$ (base peak) accompanying a smaller pseudomolecular ion $[M + H]^+$ was observed. The spectrum of the MB derivative of 2-OH-$C_{18:0}$ was similar (data not shown).

Sensitivity of MB derivative for detection by LC–MS

The sensitivity of the MB derivative of palmitic acid for detection by LC–MS was determined by monitoring a single ion $[M + H]^+$ (Fig. 4). Even 5 ng of palmitic acid could be observed.

Derivatization of hydroperoxy fatty acids with BrMB

Derivatization of 15-HPETE with BrMB was examined. The MB derivative of a mixture of 15-HPETE and $C_{17:0}$ was prepared according to the method described in the Experimental sec-

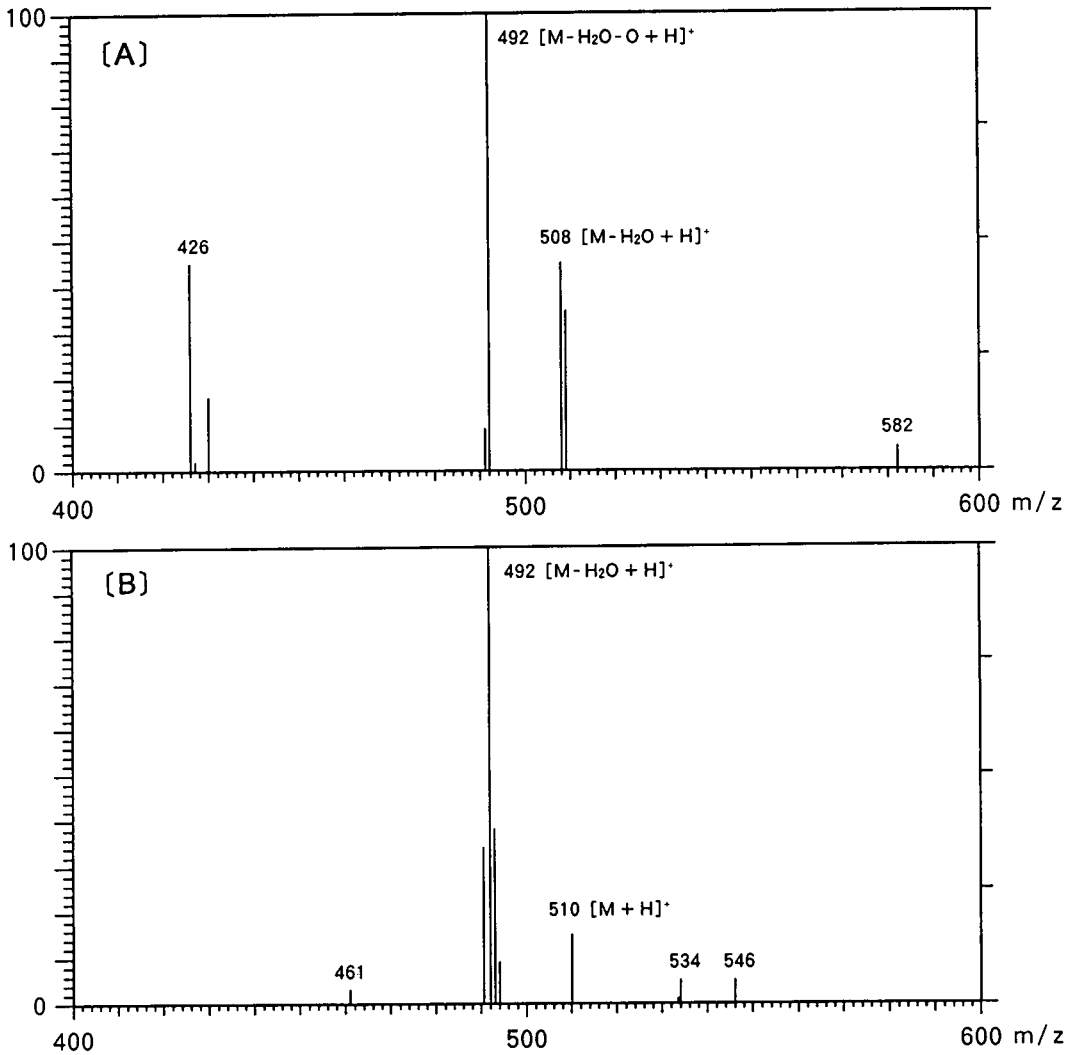

Fig. 6. LC–MS spectra of MB derivatives of 15-HPETE (A) and 15-HETE (B).

tion. Then, LC–MS with spectrophotometry was performed (Fig. 5). Fig. 6A shows a mass spectrum from peak 2 in Fig. 5. In the spectrum, no pseudomolecular ion could be observed, but ions $[M - H_2O + H]^+$ and $[M - H_2O - O + H]^+$ (base peak) were noted. This spectrum was confirmed to be distinguishable from that of 15-HETE representing a pseudomolecular ion $[M + H]^+$ and an ion $[M - H_2O + H]^+$ (base peak) (Fig. 6B). The time courses for the preparation of the MB derivatives of 15-HPETE and $C_{17:0}$ were examined by HPLC with spectrophotometry (Fig. 7). $C_{17:0}$ was derivatized quantitatively after 30 min, and derivatization of 15-HPETE showed the best yield at 30 min. Therefore, derivatization was thereafter carried out by incubation for 30 min. The derivatization yield of hydroperoxy fatty acids was determined using various amounts (2–8 nmol) of 15-HPETE and 3 nmol of $C_{17:0}$ as an internal standard. Then, 15-HPETE was found to be derivatized quantitatively (data not shown).

To confirm further MB derivatization of hydroperoxy fatty acids, several kinds of unsaturated fatty acids ($C_{18:1}$, $C_{18:2}$, α-$C_{18:3}$, γ-$C_{18:3}$, $C_{20:2}$, $C_{20:4}$, and $C_{22:6}$) were photo-oxidized separately to prepare hydroperoxy fatty acids and were derivatized after or without reduction to hydroxy fatty acids with sodium borohydride as described in the Experimental section. Then,

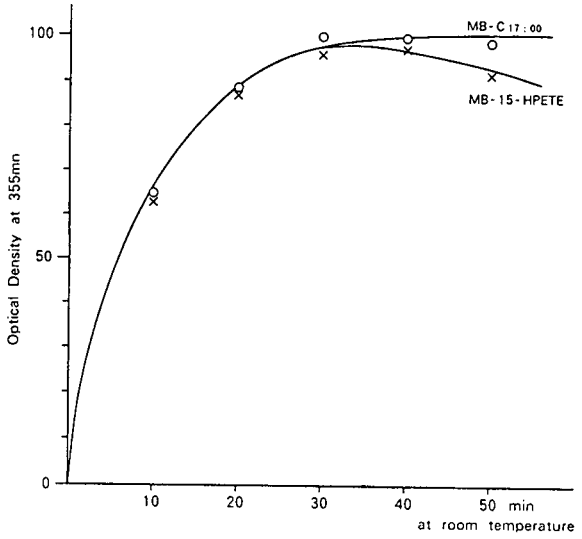

Fig. 7. Time course for MB derivatization. Aliquots of 20 nmol each of $C_{17:0}$ (○) and 15-HPETE (×) were used.

LC–MS with spectrophotometry was performed. Fig. 8 shows data thus obtained from $C_{20:2}$ and $C_{20:4}$. Similar data were obtained from the other acids (data not shown). Clusters of peaks appeared in the spectrophotometric chromatograms of photo-oxidized and reduced photo-oxidized fatty acids. These clusters of peaks should be from the isomers of each hydroperoxy or hydroxy fatty acid, because the LC–MS spectra of individual peaks in the clusters were similar to each other. The spectra from the MB derivatives of photo-oxidized fatty acids showed a characteristic combination of ions $[M - H_2O - O + H]^+$ (base peak) and $[M - H_2O + H]^+$. On the other hand, spectra from the MB derivatives of reduced photo-oxidized fatty acids showed peaks of ions $[M - H_2O + H]^+$ (base peak) and $[M + H]^+$ which are characteristic of the MB derivatives of hydroxy fatty acids.

Analysis of hydroperoxy fatty acids in photo-oxidized lecithin

Fatty acids split from lecithin by PLase A_2 with or without photo-oxidation were analysed by the above method. The splitting yield of fatty acids from the 2-position of authentic 1-palmitoyl-2-arachidonoyl-*sn*-glycero-3-phosphocholine was about 95 ± 5% (mean ± S.D., $n = 5$) (HPLC with spectrophotometry, $C_{17:0}$ as an internal standard). The MB derivatives of the fatty acids were measured by LC–MS with spectrophotometry and several kinds of hydroperoxy fatty acids could be identified (Fig. 9).

DISCUSSION

We successfully analysed labile fatty acids such as hydroperoxy and hydroxy polyunsaturated fatty acids quantitatively and qualitatively by LC–MS with spectrophotometry. However, the sensitivity of MB derivatives of fatty acids for detection by LC–MS was not as high as that of the amide derivatives [1,2] (Fig. 4). Therefore, a choice between the derivatization methods has to be made depending on the purpose.

There have been numerous studies on lipid hydroperoxides in relation to the possible cause of ageing, adult diseases, etc. [8,9], but there seem to have been only a few studies aimed at improving the analysis of lipid hydroperoxides. It

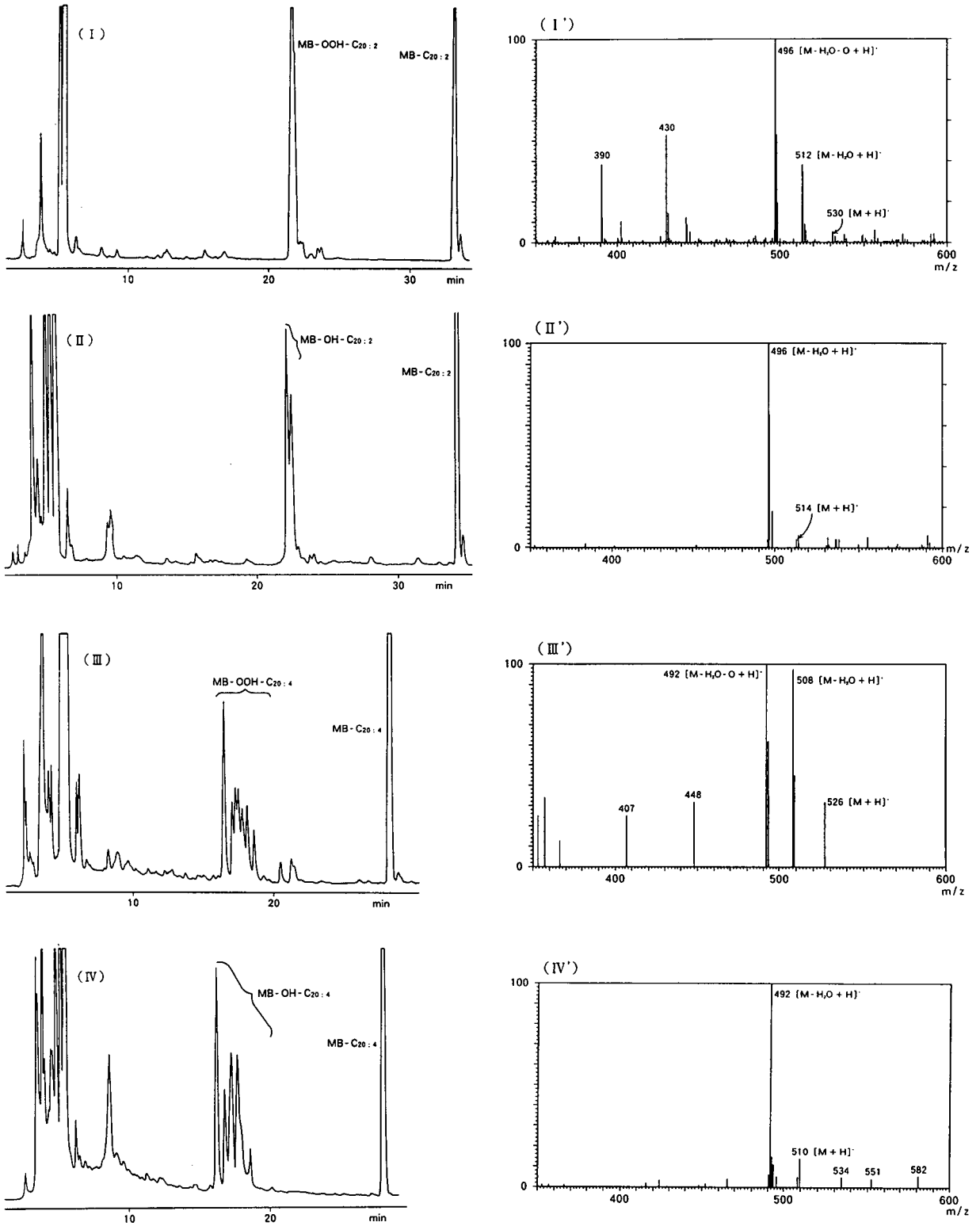

Fig. 8. HPLC profiles by spectrophotometric detection at 355 nm and LC–MS spectra of MB derivatives of photo-oxidized and reduced photo-oxidized fatty acids. I–IV: Spectrophotometric chromatograms at 355 nm. I′–IV′: LC–MS spectra. The mobile phase was acetonitrile–water (70:30, v/v) with acetonitrile increasing linearly at the rate of 1%/min.

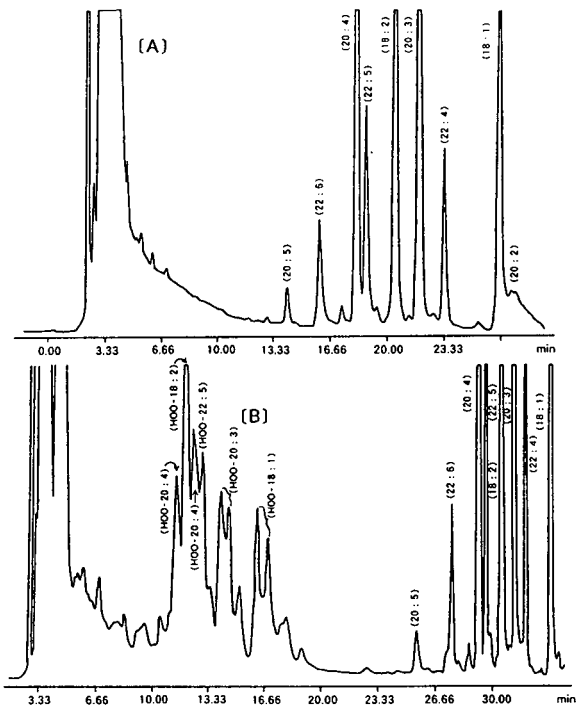

Fig. 9. Identification of fatty acids split from bovine liver lecithin (A) without or (B) with 2.5 h photo-oxidation by PLase A_2. The numerals in parentheses in (A) indicate the numbers of carbon atoms and unsaturated bonds in the fatty acids. The HOO numerals in parentheses in (B) indicate monohydroperoxy fatty acids and the numbers of their carbon atoms and unsaturated bonds. The mobile phase in (A) was acetonitrile–water (85:15, v/v) with acetonitrile increasing linearly at the rate of 0.5%/min. That of (B) was acetonitrile–water (80:20, v/v) and it was fixed during the first 15 min, then acetonitrile increased linearly at a rate of 2%/min.

is almost impossible to detect hydroperoxy fatty acids by gas chromatography (GC) or GC–MS, tools which are still very widely used in the analysis of common fatty acids. Some studies on the analysis of oxygenated products of docosahexaenoic acid and other polyunsaturates by LC–MS have been developed [10,11], but these analyses are unquantitative or only useful for a limited number of species of fatty acids. Although other kinds of approach to the analysis of lipid peroxides, such as HPLC with chemiluminescence detection [12,13] and HPLC with UV and electrochemical detection [14,15] are highly specific and sensitive to hydroperoxy phospholipids or hydroperoxy cholesterol esters, they are not useful for the identification of individual hydroperoxy fatty acids in lipids.

This study was also concerned with analysis of hydroperoxy fatty acids split from photo-oxidized lecithin by PLase A_2. Since polyenoic fatty acids in the biomembrane are preferentially located at the 2-position of the *sn*-glycero-3-phosphor skeleton of phospholipids [16,17] and are thought to be prominent targets of naturally occurring radical or non-radical peroxidation, the method in this paper may be useful for experimental studies on lipid peroxidation in biomembranes.

ACKNOWLEDGEMENTS

We wish to thank Mr. H. Nakano for his help in carrying out LC–MS. This study was supported in part by Research Project Grant No. 3-411 from Kawasaki Medical School.

REFERENCES

1 T. Kusaka, M. Ikeda, H. Nakano and Y. Numajiri, *J. Biochem.*, 104 (1988) 495.
2 M. Ikeda and T. Kusaka, *J. Chromatogr.*, 575 (1992) 197.
3 T. Kusaka and M. Ikeda, in I. Yano (Editor), *Proceedings of Japanese Medical Mass Spectrometry*, Vol. 14, Kanazawa, Japan, 1989, p. 209.
4 S. Hara, I. Kudo, H.W. Chung, K. Matsuta, T. Miyamoto and K. Inoue, *J. Biochem.*, 105 (1989) 395.
5 H. Naganuma, A. Nakanishi, J. Kondo, K. Watanabe and Y. Kawahara, *Sankyo Kenkyusho Nenpo*, 40 (1988) 51.
6 J. Terao, I. Asano and S. Matsushita, *Lipids*, 20 (1985) 312.
7 M. Van Rollins and R.C. Murphy, *J. Lipid Res.*, 25 (1984) 507.
8 J. Terao and S. Matsushita, *Lipids*, 16 (1981) 98.
9 E.N. Frankel and W. Neff, *Biochim. Biophys. Acta*, 754 (1983) 264.
10 J.A. Yergey, H. Kim and N. Salem, Jr., *Anal. Chem.*, 58 (1986) 1344.
11 H. Kim and N. Salem, Jr., *Prostaglandins*, 37 (1989) 105.
12 Y. Yamamoto, M.H. Brodsky, J.C. Baker and B.N. Ames, *Anal. Biochem.*, 160 (1987) 7.
13 T. Miyazawa, K. Yasuda and K. Fujimoto, *Anal. Lett.*, 20 (1987) 915.

14 S. Terao, S. Shibata and S. Matsushita, *Anal. Biochem.*, 169 (1988) 415.
15 W. Korytowsky, G.J. Bachowski and A.W. Girotti, *Anal. Biochem.*, 197 (1991) 149.
16 S. Yasuda, Y. Kitagawa, E. Sugimoto and M. Kito, *J. Biochem.*, 87 (1980) 1511.
17 M. Ishinaga, J. Sato, Y. Kitagawa and E. Sugimoto, *J. Biochem.*, 92 (1982) 253.

Journal of Chromatography, 639 (1993) 175–184
Esevier Science Publishers B.V., Amsterdam

CHROM. 25 009

Reversed-phase high-performance liquid chromatography of phospholipids with fluorescence detection

S.L. Abidi*, T.L. Mounts and K.A. Rennick

Food Quality and Safety Research, National Center for Agricultural Research, Agricultural Research Service, US Department of Agriculture, 1815 N. University Street, Peoria, IL 61604 (USA)

(First received December 22nd, 1992; revised manuscript received February 16th, 1993)

ABSTRACT

Reversed-phase high-performance liquid chromatographic (HPLC) behavior of fluorescent labeled phospholipids (PLs) was studied. Molecular species of phosphatidylethanolamine (PE) derivatized with fluorescein-, thiocarbamoyl-, pyrenesulfonyl-, and dimethylaminonaphthalenesulfonyl (dansyl)-fluorophores were separated on octadecylsilica with a mobile phase of acetonitrile–methanol–water in the presence of tetraalkylammonium phosphates (TAAPs). Under similar HPLC conditions, dansylated phosphatidylserines and PE plasmalogens (ether-linked PLs) were also resolved. Incorporation of the fluorescein moiety to the parent PE appeared to facilitate further resolution of its subcomponents. Subcomponents of dansylated PE derived from egg phosphatidylcholines were quantifiable. Effects of the type and concentration of TAAP on capacity factors of PL solutes were indicative of an ion-pair separation processes. HPLC with high-molecular-mass TAAPs favored the separation of the components that remained unresolved with mobile phases containing low-molecular-mass TAAPs. The HPLC–fluorescence detection method provided a useful approach to quantitative analyses of various PL structures. Compositions of PL subcomponents were determined directly from peak areas.

INTRODUCTION

Separations and quantitative measurements of phospholipids (PLs) in crude and degummed soybean oil are important analytical procedures in studying effects of oil storage on the polar lipid compositions. Normal-phase high-performance liquid chromatography (HPLC)–evaporative light scattering detection techniques (ELSD) have been used to monitor the changes in all soybean PL classes as well as in molecular species subclasses of phosphatidylcholine (PC) and phosphatidylethanolamine (PE) [1–5]. For negatively charged PLs, molecular species have been separated by reversed-phase (RP) ion-pair HPLC with UV detection [6–9].

As demonstrated in a recent study [10], detection of neutral PLs (*e.g.* PE and PC) by normal-phase HPLC–ELSD was considerably less efficient and less sensitive than by RP-HPLC–UV with mobile phases containing tetraalkylammonium phosphate (TAAP) additives. However, limitations inherent with the RP-HPLC–UV detection systems are: (a) its inability to quantify molecular species simultaneously from the UV detector signals [11], (b) its requirement of fraction collection of individual molecular species, and (c) quantitative analysis of each fraction by phosphorimetry [12,13]. In other words, compositions of PL subcomponents can not be determined by direct computer integration of individual peak areas on chromatograms. An additional drawback of the RP-HPLC system with mobile phase electrolytes is the incompatibility of the mobile phases with an ELSD or a mass

* Corresponding author.

0021-9673/93/$06.00

spectrometer for quantitation or characterization of molecular species.

In common analytical practice, derivatization of PLs with fluorescent materials should allow not only quantitative analyses of the products with specific fluorescence detection, but also lead to substantial enhancement in detection sensitivity. Few publications are available in the literature on the analysis of PL subclasses using fluorescence-labeled derivatives. In several known procedures [14–19], the PL structure is disrupted for the removal of the polar head group prior to HPLC analysis. Thus, fluorescent derivatives of diradylglycerols prepared from treatment of PLs with phospholipase C were the analyte fragments produced by molecular cleavage at the glycerol oxygen–phosphorus bond of PLs. Although a few other papers [20–22] have dealt with fluorescent derivatives of PLs, quantitative analyses of intact PL molecular species by HPLC–fluorescence detection have not been thoroughly investigated. This paper reports the RP-ion-pair HPLC behavior of fluorescence-labeled PLs. Examples of utilizing the ion-pair HPLC-fluorescence detection (FL) technique for the quantitative determination of molecular species compositions are presented.

EXPERIMENTAL

Chemicals and reagents

Dansylated egg PE was purchased from Molecular Probes (Eugene, OR, USA). Dansyl-, pyrenesulfonyl- and fluoresceinthiocarbamoyl-PE obtained by transphosphatidylation of egg PC were purchased from Avanti Polar Lipids (Pelham, AL, USA). Dansylated brain PE (mainly PE plasmalogen) and brain PS were also products of Avanti. Dansylated plant PE was prepared from plant PE (Avanti) by the procedure described in the following paragraph. Tetramethylammonium phosphate (TMAP) was prepared by treating tetramethylammonium hydroxide (Aldrich, Milwaukee, WI, USA) with phosphoric acid (Fisher, Fair Lawn, NJ, USA) until reaching pH 6.5. Tetrabutylammonium phosphate (TBAP), pentyltriethylammonium phosphate (PTAP), heptyltriethylammonium phosphate (HPTAP), octyltriethylammonium phosphate (OTAP), and dodecyltriethylammonium phosphate (DTAP) were purchased from Regis Chemicals (Morton Grove, IL, USA). HPLC solvents acetonitrile and methanol were obtained from J.T. Baker (Phillipsburg, NJ, USA). HPLC water was obtained by filtering distilled water through a Millipore (Bedford, MA, USA) Milli-Q water purifier.

General procedure for the preparation of dansylated phospholipids

A previously reported procedure [23] was modified as follows: PE (10 mg) dissolved in 0.5 ml chloroform in a reacti-vial was treated with dansyl chloride (4 mg) and triethylamine (50 μl) in 0.5 ml chloroform. The mixture was stirred at room temperature for two hours and then chromatographed onto a Varian (Sunnyvale, CA, USA) Bond Elut-Si column for purification of products. The column was extracted with methanol–chloroform (1:1). After evaporation, the residue was dissolved in 1 ml methanol (or chloroform) to exact volume for quantitative HPLC analysis. For qualitative analysis, the residual crude reaction mixture was streaked on a HP-TLC plate coated with silica gel-60 (E.M. Science, Gibbstown, NJ, USA) and developed in ethyl acetate. The product band was scraped off and extracted with methanol–chloroform (1:1) to give samples suitable for analyses.

High-performance liquid chromatography

A Spectra-Physics (San Jose, CA, USA) Model SP8800 liquid chromatograph coupled with an Applied Biosystems (Foster City, CA, USA) Model 980 programmable fluorescence detector was used in all HPLC experiments. PL analytes were detected at various wavelengths depending on the type of fluorophores used: dansyl-PL, excitation 338 nm, emission 470 nm; fluorescein-PL, excitation 489 nm, emission 550 nm; pyrene-PL, excitation 342 nm, emission 389 nm. Mobile phases were prepared by mixing desired amounts of tetraalkylammonium phosphates (TAAP) to acetonitrile–methanol–water. The ternary solvents were adjusted to suit different structural types of fluorescent PL. The mobile phase solutions were filtered, degassed,

and pumped through a RP column at a flow-rate of 1 ml/min. All samples were freshly prepared from frozen materials prior to analysis. Aliquots (10 μl) of the samples containing 1–2 mg/ml of PL analytes were injected onto the column via a Rheodyne (Cotati, CA, USA) Model 7125 injector fitted with 10-μl loop. Two different RP columns were used. These include (1) a Beckman Instruments (San Ramon, CA, USA) Ultrasphere ODS column, 150 × 4.6 mm I.D., 5 μm, and (2) a Waters (Milford, MA, USA) NovaPak C18 column, 300 × 3.9 mm I.D., 4 μm.

In HPLC experiments where the analyte components were well resolved, individual chromatographic peaks were isolated, and converted to fatty acid methyl esters by a published HCl–methanol method [24]. Fatty aldehyde liberation from PE plasmalogens were performed following a known procedure [25]. Both fatty aldehyde and fatty acid determinations were carried out on a Varian (Sugarland, TX, USA) Model 3400 gas chromatograph interfaced with a flame ionization detector. Fatty acid components were separated on a 30 m × 0.25 mm I.D. fused-silica capillary column coated with 0.2 μm SP 2330 (Supelco, Bellefonte, PA, USA), using helium as the carrier gas. The column temperature was programmed by holding initially at 200°C then increasing to 220°C at 10°C/min. Peak areas were automatically integrated by a built-in data processor.

RESULTS AND DISCUSSION

In RP-HPLC with mobile phases containing TAAP quaternary ammonium salts, subcomponents of neutrally charged PLs (PC and PE) were presumably separated via an ion-suppression mechanism [10]. Derivatization of the amino group in PE with fluorescent materials (fluoresceinthiocarbamoyl, pyrenesulfonyl, and dansyl compounds) yielded the corresponding fluorescent labeled PE as shown in Fig. 1. Each of the derivatized polar lipids was consequently left with a negative charge in the molecule. As expected, the retention behavior of these fluorescent compounds was different from that of the parent PE, but was very similar to that of negatively charged PLs [phosphatidylinositol (PI), phosphatidic acid (PA), phosphatidylserine (PS), phosphatidylglycerol (PG) and diphosphatidylglycerol (DPG)] reported previously [6–9].

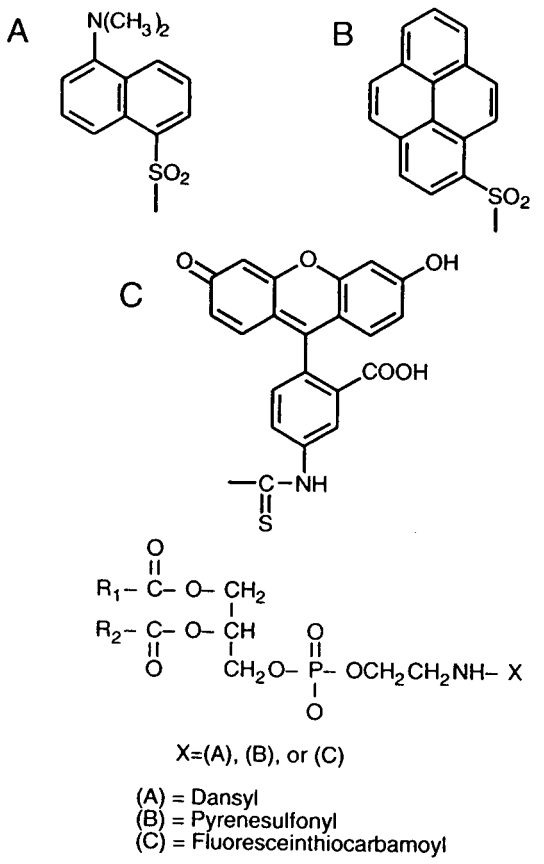

Fig. 1. Structures of investigated fluorescent derivatives of phosphatidyl ethanolamine (PE).

The purpose of introducing three fluorescent groups (dansyl, fluorescein, and pyrene) to the underivatized parent polar lipids was to see if these fluorescent substituents would contribute some degrees of differential selectivity for PL subcomponents. Although hydrophobicity of the parent PL was enhanced as a result of derivatization, HPLC without the use of the TAAP electrolytes in mobile phases normally led to little retention of PL solutes on octadecylsilica.

It was of interest to note that HPLC separations of subcomponents of PLs were dramatically influenced by the nature of fluorophores attached to the head groups. As illustrated in Fig. 2A and B, only three major egg PC species were

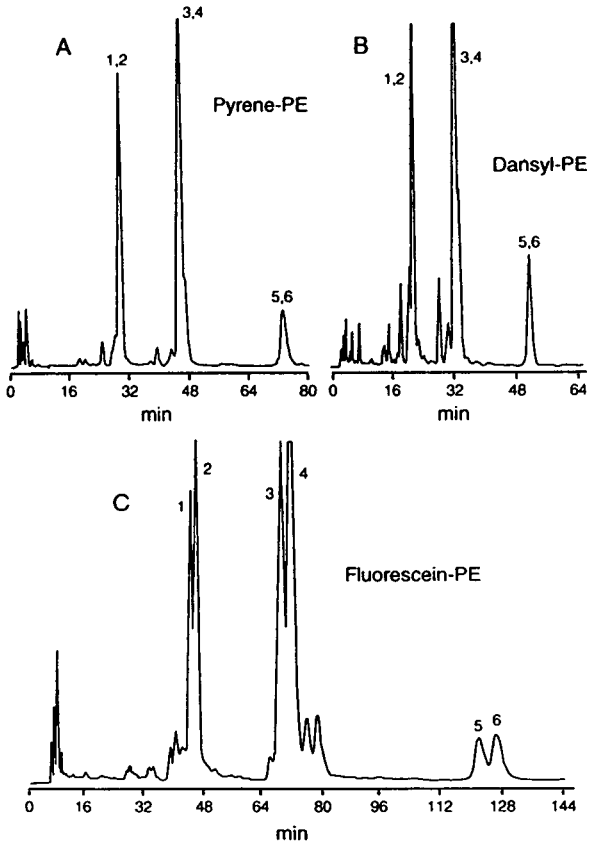

Fig. 2. RP-ion pair-HPLC separations of fluorescence-labeled PE derived from egg PC. Column, NovaPak C18; mobile phases, 5 m*M* DTAP in acetonitrile–methanol–water [(A) and (B) 70:28:2; (C) 70:22:8]. For peak identification, see footnote to Table I.

resolved on a NovaPak C18 phase, when the PE amino group was derivatized with either pyrene- or dansyl-fluorophores. However, upon conversion of the parent PE to the fluoresceinthiocarbamoyl derivative, each of the three components was further split into two subcomponents as shown in Fig. 2C. The chromatograms shown in Fig. 2 are obtained under optimized HPLC conditions where the mobile phase for Fig. 2A and B is different from that for Fig. 2C. When the HPLC experiments for all three derivatives of PE were carried out under the same conditions as for Fig. 2C (fluorescein-PE), separations of subcomponents of pyrene- and dansyl-PE (retention times were too long to be of any practical value) were not improved. Thus, the observed differences in component resolution among the three PE derivatives investigated were not simply due to the use of a different mobile phase containing a high percentage of water (Fig. 2C *vs.* Fig. 2A and B). This is the first example of substituent effects of the PL head group on the RP separation processes. The results of the present study appeared to contradict earlier findings that hydrophobic interactions of analyte solutes with a hydrocarbonaceous stationary phase were confined to the tail groups of perbenzoylated PI [6], which is also a negatively charged PL. In a PE molecule, the fluorescein substituent on the amino group is situated two carbons remote from the phosphorus center where the inositol group of PI is attached.

Inspection of the retention data in Table I and II revealed a decreasing order of retention characteristics of analyte components: k'(pyrene-PE) > k'(dansyl-PE) > k'(fluorescein-PE). This follows the reverse order of polarity of the fluorescent moieties: pyrenesulfonyl < dansyl < fluoresceinthiocarbamoyl irrespective of that of the total number of carbon atoms of the fluorescent ring systems.

Three sets of plots were selected to show linear relationships between ln k' of fluorescent-labeled PL and the total number (N) of carbon atoms in TAAP and are presented in Fig. 3. Solvophobic interactions in RP-ion pair-HPLC of the compounds of interest were found to discriminate different structure types (*i.e.* symmetrically substituted TAAP *vs.* unsymmetrically substituted TAAP) of TAAP employed. As noted in the figure, a deviant of each set of linear correlation lines is located at $N = 16$ where TBAP was used as the counter ion. This is due to the fact that TBAP is in a different structural series from the primary alkyltriethylammonium phosphate series investigated (Table III). The observations are parallel to earlier results [7–9] from HPLC studies of PA, PS, and DPG. However, the results of the present study are in contrast with the linear correlation data for PI and PG [6,9] that showed independence of ln k' values on TAAP structural types. It is not clear whether the hydroxy functionalities of PI and PG at the close proximity to the phosphorus center

TABLE I

HPLC SEPARATION OF SUBCOMPONENTS OF FLUORESCEIN-LABELED PE DERIVED FROM EGG PC (ON A BECKMAN ULTRASPHERE ODS, 150 × 4.6 mm I.D. COLUMN)

Mobile phase			Capacity factor (k') of component[b]								
Ratio[a]	TAAP	Concentration (mM)	1	2	α_{1-2}	3	4	α_{3-4}	5	6	α_{5-6}
70:28:2	TMAP	10.0	0.0	0.0	1.0	0.0	0.0	1.0	0.1	0.1	1.0
70:28:2	PTAP	5.0	0.1	0.1	1.0	0.1	0.1	1.0	0.2	0.2	1.0
70:28:2	HPTAP	10.0	0.3	0.3	1.0	0.5	0.5	1.0	1.1	1.1	1.0
70:22:8	PTAP	10.0	0.5	0.5	1.0	1.2	1.2	1.0	2.2	2.2	1.0
70:22:8	OTAP	10.0	3.8	3.8	1.0	6.7	6.7	1.0	11.7	11.7	1.0
		20.0	150	152	1.01	175	178	1.02	287	296	1.03
70:22:8	DTAP	2.5	0.2	0.2	1.0	0.5	0.5	1.0	1.1	1.1	1.0
		5.0	4.5	4.8	1.07	7.7	8.2	1.07	13.8	14.7	1.07
		7.5	17.2	18.0	1.05	28.5	30.2	1.06	54.8	63.5	1.16
		10.0	39.0	41.5	1.06	71.3	76.2	1.07	139	159	1.15

[a] Ratio acetonitrile–methanol–water.
[b] Component identification: (1) + (2) 16:0–18:2, (3) + (4) 16:0–18:1, and (5) + (6) 18:0–18:2 corresponding to fatty acid chains with R_1 and R_2 groups in PE derivatives (Fig. 1). Fatty acid designations: 16:0 = palmitic; 18:0 = stearic; 18:1 = oleic; 18:2 = linoleic. Exact structures within component pairs 1–2, 3–4, and 5–6 were not determined.

TABLE II

HPLC SEPARATIONS OF SUBCOMPONENTS OF DANSYLATED AND PYRENE-LABELED PE DERIVED FROM EGG PC (ON A BECKMAN ULTRASPHERE ODS, 150 × 4.6 mm I.D. COLUMN)

Mobile phase conditions[a]		Capacity factor (k') of component[b]					
TAAP	Concentration (mM)	1	2	3	4	5	6
Dansylated PE							
TMAP	10.0	2.2	2.2	3.8	3.8	6.5	6.5
HPTAP	5.0	1.2	1.2	2.0	2.0	2.7	2.7
	10.0	4.5	4.5	7.2	7.2	11.6	11.6
Pyrene-labeled PE							
TMAP	10.0	3.0	3.0	4.8	4.8	7.9	7.9
HPTAP	5.0	2.2	2.2	2.3	2.3	6.3	6.3
	10.0	5.3	5.3	8.2	8.2	13.2	13.2

[a] Mobile phase: TAAP in acetonitrile–methanol–water (70:28:2).
[b] All component pairs 1–2, 3–4, and 5–6 were not resolved ($\alpha = 1.0$). For component identification, see footnote to Table I.

have any bearing on the availability of the total area of tetraalkyl groups in TAAP for solvophobic interactions [26,27]. The linear plots are useful for the prediction of k' values of PL components analyzed under HPLC conditions where an unknown member of TAAP within the same structural series is present in a mobile phase.

As previously observed in HPLC work involving negatively charged PL, retention times or capacity factors (k') values of subcomponents of fluorescent-labeled PE derived from egg PC (Table I and II) were invariably longer in HPLC with mobile phases containing TAAP of larger size and higher concentration (positive concentration effects). Evidently, the RP separation

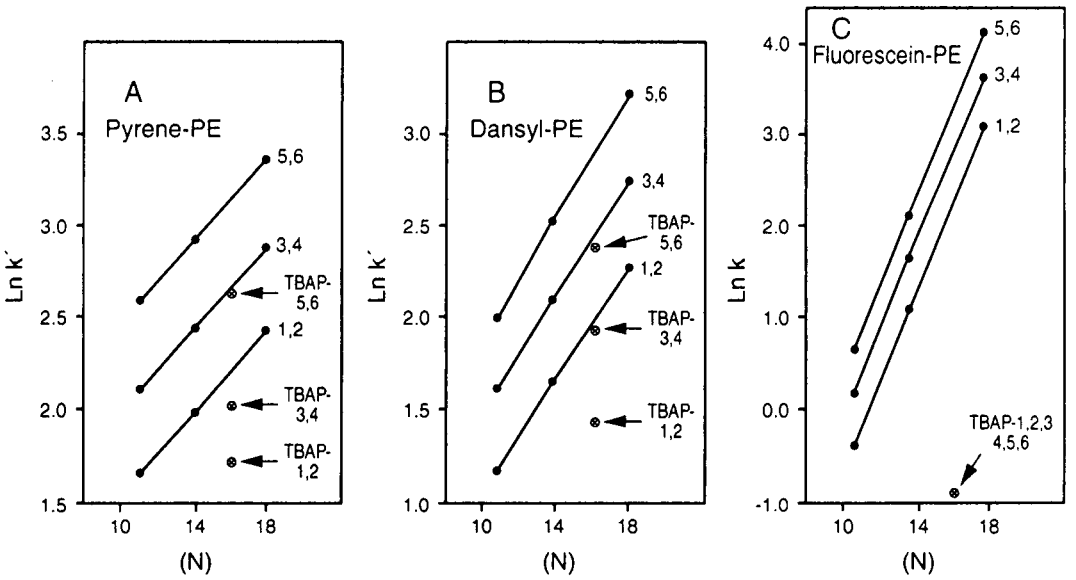

Fig. 3. Linear correlation between the total number (N) of carbon atoms in TAAP and ln k' of fluorescence-labeled PE derived from egg PC. HPLC conditions are same as in Fig. 2 except various TAAP were used. The deviant points for TBAP are shown for components 1, 2, 3, 4, and 5 of the three different derivatives studied.

TABLE III

EFFECTS OF TAAP STRUCTURES ON CAPACITY FACTORS, k', OF SUBCOMPONENTS OF FLUORESCENT DERIVATIVES OF PE DERIVED FROM EGG PC (ON A NOVAPAK C_{18}, 300 × 3.9 mm I.D. COLUMN)

TAAP[a]	Capacity factor (k') of component					
	1	2	3	4	5	6
Fluorescein-labeled PE [acetonitrile–methanol–water (70:22:8)]						
TBAP	0.4	0.4	0.4	0.4	0.4	0.4
PTAP	0.6	0.6	1.2	1.2	2.0	2.0
OTAP	3.1	3.1	5.4	5.4	9.0	9.0
DTAP[b]	21.8	22.6	36.0	37.2	61.5	65.3
Dansyl-labeled PE [acetonitrile–methanol–water (70:28:2)]						
TBAP	4.2	4.2	7.0	7.0	11.0	11.0
PTAP	3.2	3.2	5.0	5.0	8.0	8.0
OTAP	5.2	5.2	8.2	8.2	12.6	12.6
DTAP	9.8	9.8	15.6	15.6	25.0	25.0
Pyrene-labeled PE [acetonitrile–methanol–water (70:28:2)]						
TBAP	5.6	5.6	7.6	7.6	14.1	14.1
PTAP	5.2	5.2	8.2	8.2	13.4	13.4
OTAP	7.2	7.2	11.5	11.5	33.6	33.6
DTAP	11.5	11.5	18.0	18.0	29.3	29.3

[a] Concentration of TAAP is 5 mM.

[b] The α values of component pairs 1–2, 3–4, and 5–6 are 1.04, 1.03 and 1.06, respectively. All other component pairs 1–2, 3–4, and 5–6 shown in this table were not resolved ($\alpha = 1.0$). For component identification, see footnote to Table I.

processes were typical of an ion-pair retention mechanism. Interestingly, fluorescein-labeled PE complex was inadequately resolved into three major components, when a low member of TAAP in the series was present at a low concentration in the mobile phase of relatively low water content (*e.g.* 2% water shown in Table I). Examples of the poor resolution of the PE mixture can also be seen in the table where 2.50 m*M* of DTAP or 10 m*M* of PTAP (or OTAP) was used in mobile phases containing 8% of water. Separation factors (α) for the unresolved component pairs 1–2, 3–4, and 5–6 were 1.00. However, a total of six major components (three sets of doublets each having α values greater than 1.00) were obtained with mobile phases containing either 20 m*M* of OTAP or DTAP at concentrations greater than 5 m*M* in acetonitrile–methanol–water (70:22:8). For dansyl- and pyrene-labeled PE, resolution of subcomponents was apparently incomplete because only three major components (each unresolved pair has an α value of 1.00) are visible from the HPLC data in Table II.

Table IV shows the positive concentration effects of TAAP on the k' values of the subcompo-

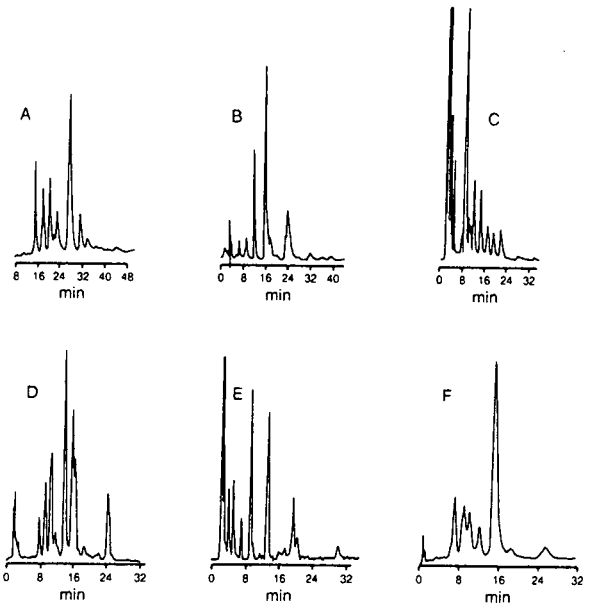

Fig. 4. Comparisons of HPLC–UV chromatograms of underivatized parent phospholipids (PLs) [(A) Egg-PE; (B) soybean-PE; (C) brain-PS] with HPLC–fluorescence chromatograms of the corresponding dansylated PLs (D, E, F). Columns, (A, B, C) NovaPak C18; (D, E, F) Beckman Ultrasphere ODS. Mobile phases, acetonitrile–methanol–water [(A, B, D, E) 70:28:2; (C, F) 70:22:8] containing (A, B) 25 m*M* TMAP; (C) 5 m*M* TMAP; (D, E, F) 10 m*M* HPTAP.

TABLE IV

HPLC SEPARATIONS OF SUBCOMPONENTS OF DANSYLATED EGG PE AND BRAIN PS (ON A BECKMAN ULTRASPHERE ODS COLUMN, 150 × 4.6 mm I.D. COLUMN)

Mobile phase conditions		Capacity factor (k') of component					
TAAP	Concentration (m*M*)	1	2	3	4	5	6
Dansylated egg PE							
TMAP[a]	10.0	1.8	2.2	2.7	3.8	4.6	7.5
HPTAP[a]	5.0	1.2	1.3	1.7	2.5	3.1	5.0
	10.0	2.2	2.8	3.3	4.6	5.7	9.1
Dansylated brain PS							
HPTAP[b]	5.0	2.5	3.3	3.7	4.5	7.8	9.8
	7.5	9.0	11.5	13.6	16.3	20.2	25.7
	10.0	21.0	26.3	31.8	39.2	48.5	79.2

[a] Mobile phase TAAP in acetonitrile–methanol–water (70:28:2).

[b] Mobile phase: HPTAP in acetonitrile–methanol–water (70:22:8).

[c] Component identification: PE, (1) 18:2–18:2, (2) 16:0–20:4, (3) 16:0–18:2, (4) 18:0–20:4, (5) 16:0–18:1 + 18:0–18:2, (6) 18:0–18:1. PS, (1) 16:0–20:4, (2) 18:0–20:4, (3) 16:0–18:1, (4) 18:0–18:2, (5) 18:0–18:1, (6) 18:0–20:1. Fatty acid designations: 20:1 = eicosenoic, 20:4 = arachidonic; for others, see footnote to Table I.

nents of dansylated egg PE and brain PS. Negative concentration effects have been observed in HPLC of the underivatized parent PE or PC [10], in which the charge is internally neutralized. Conversion of the parent neutral PL to negatively charged fluorescent derivatives led to a corresponding change in a retention mechanism from ion-suppression to an ion-pair separation processes. Such a mechanistic change reflected opposite effects of the counter ion conconcentrations. Comparisons of HPLC–UV chromatograms of underivatized parent egg PE, soybean PE, and brain PS shown in respective Fig. 4A, B, and C with corresponding HPLC–FL chromatograms of their dansylated derivatives (Fig. 4D, E, and F) indicated that generally the component peak patterns are fairly simple and quite similar despite obvious differences in peak intensities. On the other hand, the HPLC–FL chromatogram of dansylated brain PE (Fig. 5B) is much more complex than the HPLC–UV chromatogram of the parent brain PE (Fig. 5A). In Fig. 5, the later-eluting peaks of both the parent and dansylated materials correspond to the subcomponents of PE plasmalogen as confirmed by the characterization of the major components (Table V). Interestingly, the retention behavior of PE plasmalogens exhibiting increased retention times relative to the corresponding diacyl PE is similar to that of alkenylacyl acetylglycerols relative to the diacyl analogues [28]. Most of the peaks attributable to the dansylated brain PE are significantly more intense than those of corresponding underivatized components. Apparently the UV absorptions of the ether lipids having large alkyl mem-

TABLE V

COMPOSITION DATA FOR COMPONENTS OF DANSYLATED PHOSPHOLIPIDS DERIVED FROM NATURAL SOURCES

A Beckman Ultrasphere ODS (150 × 4.6 mm I.D.) was used; mobile phases varied depending on the PL structural type. Values in parentheses are coefficients of variation. Major component identification: brain PE plasmalogen, (3) 18:1–22:6, (4) 18:1–20:4, (5) 18:0–22:6, (7) 18:0–20:1, (9) 18:1–18:1, (10) 16:0–18:1; egg PE, (3) 18:2–18:2, (4) 16:0–20:4, (5) 16:0–18:2, (7) 18:0–20:4, (8) 16:0–18:1, (9) 18:0–18:2, (16) 18:0–18:1; soybean PE, (1) 18:2–18:2, (3) 16:0–18:2, (6) 16:0–18:1, (10) 18:0–18:2; egg PC, (1) 16:0–20:4, (2) 16:0–18:3, (3) 18:1–18:2, (4) 16:0–18:2, (5) 16:0–18:1, (6) 18:0–18:2, (10) 18:0–18:1; for PS components, see footnote to Table IV. Fatty acid designation: 22:6 = docosahexaenoic; for others, see footnotes to Table I and IV.

Component	Composition (%)[a]				
	Brain PS	Brain PE	Egg PE	Soybean PE	Egg PC
1	11.9 (1.5)	2.9 (6.0)	0.1 (9.5)	29.3 (2.0)	3.0 (5.5)
2	12.8 (5.0)	3.8 (4.5)	0.3 (9.0)	1.8 (9.0)	4.2 (5.0)
3	12.3 (3.0)	8.7 (4.0)	4.2 (7.0)	37.7 (1.0)	26.3 (0.5)
4	9.6 (1.5)	10.6 (4.0)	7.6 (6.0)	1.1 (9.5)	7.5 (5.0)
5	47.8 (0.5)	13.4 (3.5)	14.3 (4.0)	1.8 (9.0)	41.3 (0.5)
6	1.7 (9.0)	4.8 (5.0)	4.2 (8.0)	17.6 (2.5)	6.2 (4.5)
7	3.9 (5.5)	8.2 (5.0)	22.5 (1.5)	6.0 (5.0)	0.8 (8.0)
8		6.5 (5.0)	24.5 (1.0)	0.1 (9.5)	0.1 (9.5)
9		10.8 (3.5)	6.1 (3.0)	0.1 (9.5)	0.3 (9.5)
10		11.1 (4.0)	0.6 (8.5)	4.2 (5.0)	10.4 (3.0)
11		4.3 (6.5)	2.5 (6.0)		
12		2.8 (8.0)	0.6 (7.5)		
13		3.1 (6.5)	0.3 (9.5)		
14		3.6 (7.0)	0.7 (9.0)		
15		1.2 (9.5)	1.0 (9.5)		
16		1.7 (9.5)	10.2 (3.0)		
17		2.7 (8.5)	0.2 (9.0)		
18			0.3 (9.0)		

[a] Mean values of triplicate determinations.

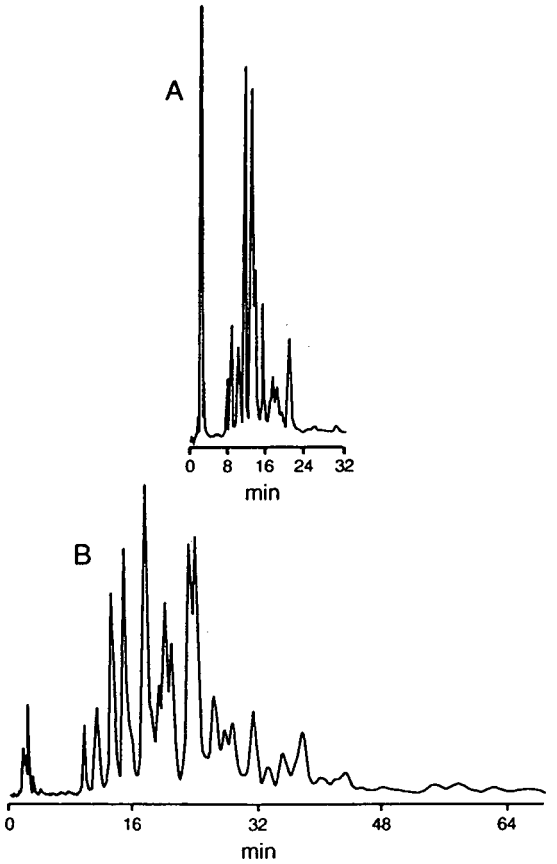

Fig. 5. Comparison of (A) HPLC–UV chromatogram of underivatized parent brain PE and (B) HPLC–fluorescence chromatogram of the dansylated brain PE. Columns, (A) NovaPak C18; (B) Beckman. Mobile phases, acetonitrile–methanol–water (70:28:2) containing (A) 25 m*M* TMAP; (B) 5 m*M* TMAP.

bers of the non-polar tail groups (Fig. 1) were relatively weak.

Compositions of subcomponents of fluorescent-labeled PL were determined directly by computer data processing of the FL detector signals as shown in Table V and Table VI. This is the first report on sensitive, reliable quantitative analyses of intact molecular species of negatively charged PLs. The analytical data for peak integration gave coefficients of variation ranging from 0.5 to 9.5%. On the contrary, direct computation of UV detector responses has proved futile because of variations in absorbance of different molecular species at a given UV wavelength. In HPLC with FL detection, peak areas

TABLE VI

COMPARISONS OF COMPOSITION DATA FOR SUBCOMPONENTS OF VARIOUS FLUORESCENT LABELED PE DERIVED FROM EGG PC

A Beckman Ultrasphere ODS column (150 × 4.6 mm I.D.) was used; mobile phases varied depending on the PL structural type. Values in parentheses are coefficients of variation. Major component identification: pyrene-PE, (1) 16:0–20:4, (2) 16:0–18:3, (3) 16:0–18:2, (6) 16:0–18:1, (9) 18:0–18:2; fluorescein-PE, (3) 16:0–20:4, (4) 16:0–18:2, (5) 16:0–18:2, (8) 16:0–18:1, (9) 16:0–18:1, (10) 18:0–18:2; dansyl-PE, (1) 16:0–20:4, (2) 16:0–18:3, (3) 16:0–18:2, (5) 16:0–18:1, (8) 18:0–18:2. For fatty acid designations, see footnotes to Table I and IV.

Component	Composition (%)[a]		
	Pyrene-PE	Fluorescein-PE	Dansyl-PE
1	2.5 (5.5)	0.8 (7.5)	3.3 (5.0)
2	2.5 (5.5)	0.9 (7.0)	4.5 (5.5)
3	27.7 (1.5)	3.1 (5.0)	26.8 (2.0)
4	1.1 (9.0)	15.3 (4.0)	6.2 (5.0)
5	2.2 (6.0)	21.9 (2.0)	48.2 (1.0)
6	50.5 (0.5)	0.7 (8.5)	0.6 (8.5)
7	4.8 (4.5)	0.3 (9.0)	0.4 (9.0)
8	0.6 (8.0)	20.0 (2.0)	10.1 (4.0)
9	7.9 (5.0)	23.1 (1.5)	
10		3.9 (6.0)	
11		4.4 (5.5)	
12		2.5 (7.5)	
13		3.1 (6.0)	

[a] Mean values of triplicate determinations.

of individual lipid subcomponents were linearly correlatable within the normal range 5 ng–50 μg of analytical samples assayed. The fluorophores of individual analytes were solely responsible for the linearity of peak integrals with the amounts injected as well as for the detection specificity and sensitivity. The minimum FL detection limit at a signal-to-noise ratio of 4/1 was 4 ng, which was substantially lower than that of UV detection (100 μg).

CONCLUSION

In conclusion, the FL detection techniques developed in this study facilitate a convenient means for the analysis of a variety of PL structures. In addition to PE, subcomponents (or molecular species) of PC may be quantified in

the forms of PA, PG, and PS via sequential transphosphatidylation and derivatization with a suitable fluorigenic compound. If a high degree of component resolution is required, fluorescein is the preferred derivatizing agent because of its unusual tendency to resolve structurally similar subcomponents. In view of the abundant occurrence of PC and PE in the nature, the RP-ion pair-HPLC–FL detection method may provide a useful alternative approach to the analysis of these compounds with high reproducibility, sensitivity, and specificity.

REFERENCES

1 W.W. Christie, *J. Lipid Res.*, 26 (1985) 507.
2 H.A. Norman and J.B. St. John, *J. Lipid Res.*, 27 (1986) 1104.
3 L. Breton, B. Serkiz, J.P. Volland and J. Lepagnol, *J. Chromatogr.*, 497 (1989) 243.
4 M.D. Grieser and J.N. Geske, *J. Am. Oil Chem. Soc.*, 66 (1989) 1484.
5 T.L. Mounts, S.L. Abidi and K.A. Rennick, *J. Am. Oil Chem. Soc.*, 69 (1992) 438..
6 S.L. Abidi, T.L. Mounts, and K.A. Rennick, *J. Liq. Chromatogr.*, 14 (1991) 573.
7 S.L. Abidi, *J. Chromatogr.*, 587 (1991) 193.
8 S.L. Abidi and T.L. Mounts, *J. Liq. Chromatogr.*, 15 (14) 2487.
9 S.L. Abidi and T.L. Mounts, *J. Chromatogr. Sci.*, (1993) in press.
10 S.L. Abidi and T.L. Mounts, *J. Chromatogr.*, 598 (1992) 209.
11 N. Sotirhos, C.T. Ho and S.S. Chang, *Fette Seifen Anstrichm.*, 88 (1986) 6.
12 G.M. Patton, J.M. Fasulo and S.J. Robins, *J. Lipid Res.*, 23 (1982) 190.
13 M. Seewald and H.M. Eichinger, *J. Chromatogr.*, 469 (1989) 271.
14 J. Kruger, H. Rabe, G. Reichmann and B. Rustow, *J. Chromatogr.*, 307 (1984) 384.
15 H. Takamura and M. Kito, *J. Biochem.*, 109 (1991) 436.
16 P.J. Ryan, K. McGoldrick, D. Stickney and T.W. Honeyman, *J. Chromatogr.*, 320 (1985) 421.
17 P.J. Ryan and T.W. Honeyman, *J. Chromatogr.*, 331 (1985) 177.
18 H. Mita, H. Yasueda, T. Hayakawa and T. Shida, *Anal. Biochem.*, 180 (1989) 131.
19 A. Rastegar, A. Pelletier, G. Duportail, L. Freysz and C. Leray, *J. Chromatogr.*, 518 (1990) 157.
20 O.C. Martin and R.E. Pangano, *Anal. Biochem.*, 159 (1986) 101.
21 A.D. Postle, *J. Chromatogr.*, 415 (1987) 241.
22 M. Kitsos, C. Gandini, G. Massolini, E. De Lorenzi and G. Caccialanza, *J. Chromatogr.*, 553 (1991) 1.
23 A.S. Waggoner and L. Stryer, *Proc. Natl. Acad. Sci. USA*, 67 (1970) 579.
24 W.W. Christie, *Lipid Analysis*, Pergamon, New York, 1973, p. 85.
25 W.J. Ferrell, D.M. Radloff and J.E. Radloff, *Anal. Biochem.*, 37 (1970) 227.
26 H. Colin and G. Guiochon, *J. Chromatogr.*, 141 (1977) 289.
27 M.C. Hennion, C. Picard and M. Cande, *J. Chromatogr.*, 166 (1978) 21.
28 Y. Nakagawa and L.A. Horrocks, *J. Lipid. Res.*, 24 (1983) 1268.

Journal of Chromatography, 639 (1993) 185–191
Elsevier Science Publishers B.V., Amsterdam

CHROM. 25 015

Liquid chromatography–thermospray mass spectrometric assay for trenbolone in bovine bile and faeces

S.A. Hewitt, W.J. Blanchflower, W.J. McCaughey, C.T. Elliott and D.G. Kennedy*

Veterinary Sciences Division, Department of Agriculture for Northern Ireland, Stoney Road, Stormont, Belfast BT4 3SD, Northern Ireland (UK)

(First received December 15th, 1992; revised manuscript received February 25th, 1993)

ABSTRACT

A liquid chromatography–thermospray mass spectrometric assay was developed and validated to confirm the presence of illegal residues of the synthetic androgenic growth promoter, trenbolone acetate, in cattle. The assay was specific for 17α-trenbolone, the major bovine metabolite of trenbolone acetate. Methods were developed for the determination of 17α-trenbolone in both bile and faeces, the most appropriate matrices for the control of trenbolone acetate abuse. The clean-up procedure developed relied on enzymatic hydrolysis, followed by sequential liquid–liquid and liquid–solid extraction. The extracts were then subjected to immunoaffinity chromatography. 17α-Trenbolone was detected by selected ion monitoring at m/z 271 using positive ion thermospray ionisation. The limit of detection was approximately 0.5 ng/g in faeces and 0.5 ng/ml in bile.

INTRODUCTION

17β-Trenbolone (17β-TBOH) is a synthetic androgen which has important anabolic activity. In the form of trenbolone acetate (17β-TBOAc) it has been used as a solid implant to promote growth, usually in combination with 17β-estradiol, in steers, heifers and veal calves [1]. Although the use of 17β-TBOAc has been banned in the European Community [2], it is still legally used in many other parts of the world.

Previous studies on the metabolism of 17β-TBOAc in cattle [3–5] have demonstrated that it is rapidly hydrolysed to the active compound 17β-TBOH. Free trenbolone can bind to both testosterone and estrogen receptors, altering the rates of protein synthesis and degradation. The net result of these interactions in an increase in skeletal muscle mass [6]. The 17β-TBOH undergoes oxidation to trendione leading to reduction to epi-TBOH (17α-TBOH) which, in the form of a glucuronide or sulphate conjugate, is the major biliary metabolite of trenbolone [5].

To control the illegal use of 17β-TBOAc, analytical methods must be sensitive and specific for the determination of 17α-TBOH in biological samples. Bile is the sample of choice in animals presented for slaughter in abattoirs, since it is in bile that the highest levels of 17α-TBOH have been found [5]. However, in follow-up investigations on farms, faeces are frequently the only samples which are readily available.

A number of analytical methods for the determination of trenbolone in urine and tissue have been described which employ HPLC [7], enzyme immunoassay [8], GC–MS [9] and LC–MS–MS [10]. Other workers have reported the use of immunoaffinity chromatography as one of the clean-up steps in the analysis of 17α-TBOH

* Corresponding author.

0021-9673/93/$06.00

in urine and tissue [11]. However, none of these assays have described the quantitative determination of 17α-TBOH in either bile or faeces.

We wish to report a procedure which uses immunoaffinity chromatography coupled with liquid chromatography–thermospray mass spectrometry (LC–MS) for the specific detection of trenbolone residues in bile and faeces. LC–MS offers several advantages to the determination of polar drugs in biological matrices. Firstly, derivatization is not necessary. Secondly, the sensitivity of LC–MS is highly compound dependent enhancing the response from a sensitive analyte over that obtained from matrix effects.

EXPERIMENTAL

Chemicals and equipment

Acetonitrile, diethyl ether and methanol were HPLC grade, other reagents were analytical-reagent grade. β-Glucuronidase/aryl sulphatase (type H2 from *Helix pomatia* was purchased from Sigma (Poole, UK). This was used without dilution for the enzymatic hydrolysis of glucuronide conjugates in faeces and bile samples. [^{3}H]17β-TBOH was prepared by Amersham International (Amersham, UK). 17α-TBOH was obtained from RIVM (Bilthoven, Netherlands). A stock standard (1 mg/ml) in methanol was prepared. The stock standard was stored at 4°C and was stable for several months. Working standards were prepared daily as described below by dilution of the stock standard in mobile phase.

Immunoaffinity columns

The antiserum used was a polyclonal antiserum (titre 1:60 000 by radioimmunoassay) which was produced in this laboratory (by W.J. McC.) by immunising a New Zealand White rabbit with a conjugate of 17β-TBOH hemisuccinyl ester and bovine serum albumin. The specificity of the antisera was investigated by measuring the crossreactivity of other, structurally related compounds. Crossreactivity was defined as 100 times the amount of 17β-TBOH required to displace 50% of a tracer quantity of [^{3}H]17β-TBOH from a fixed amount of antibody divided by the amount of competitor required to produce the same displacement. The antibodies showed 85% crossreactivity with 17α-TBOH and 15% crossreactivity with 19-nortestosterone. The antibody exhibited $<0.01\%$ crossreactivity with a wide range of other compounds including testosterone, 17α- and 17β-oestradiol, progesterone, zeranol, hexoestrol, diethylstilboestrol, cortisol, corticosterone and hydroxyprogesterone. The immunoglobulin G (IgG) fraction was isolated from the antiserum by precipitation with caprylic acid [12]. The protein content of the IgG fraction was estimated using the method of Lowry *et al.* [13], and was then adjusted to 2 mg/ml with 0.1 mol/l sodium hydrogencarbonate buffer pH 8.3 containing 0.5 mol/l sodium chloride. The antibodies were coupled to cyanogen bromide-activated Sepharose (Pharmacia, Uppsala, Sweden) according to the suppliers' instructions to give a matrix containing 1 mg IgG per ml of swollen gel. Aliquots of the immunoaffinity matrix (1 ml) were placed in open glass columns (10×0.7 cm) in isotonic phosphate-buffered saline (PBS) and washed with 5 ml of the same solvent. Columns were stored at 4°C in the presence of PBS containing merthiolate (50 μg/ml). Before use, the columns were washed with 0.1 mol/l sodium acetate buffer, pH 4.0, containing 0.5 mol/l sodium chloride (5 ml) followed by 1.0 mol/l sodium carbonate (5 ml). They were then rinsed with PBS (5 ml), and the samples were applied. After

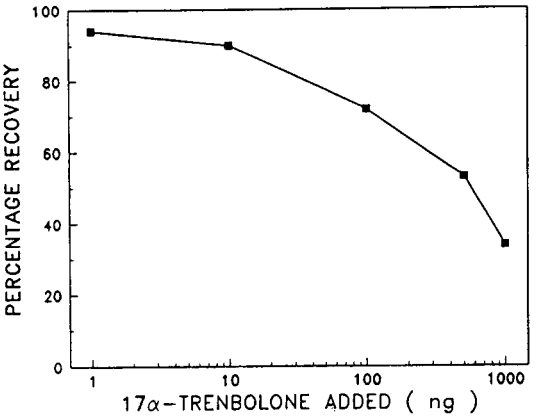

Fig. 1. Capacity of a typical immunoaffinity column for 17α-trenbolone.

use, the columns were rinsed with ethanol–water (70:30, v/v) (10 ml), water (5 ml) and stored with PBS–merthiolate as described above.

The immunoaffinity columns are stable, when stored as described above, for at least 4 months. During a 4-month period a column was spiked on 12 separate occasions with 10 ng 17α-TBOH. The recovery of 17α-TBOH did not alter during this period, being 73.7% on the first occasion and 71.1% on the last.

The capacity of the immunoaffinity columns was measured by applying a trace quantity of [^{3}H]17β-TBOH, along with varying amounts of non-radioactive 17β-TBOH, to a column and irrigating it as described below. The capacity of the columns varied somewhat from batch to batch. Fig. 1 shows a typical result obtained for one preparation.

Biological samples

Known trenbolone-free samples of bile and faeces were collected from animals born and fattened on a farm owned and maintained by the Department of Agriculture for Northern Ireland. Incurred material was obtained by implanting 15 pellets, containing a total of 300 mg 17β-TBA into the base of the left ear of a six-month old calf. Faeces and bile samples were taken 6 weeks after implantation.

Extraction procedure

The procedures developed to hydrolyse the samples and to perform the liquid–liquid extraction differed for bile and faeces. These are described separately. Thereafter all samples were treated identically.

Hydrolysis and liquid–liquid extraction: faeces. A series of negative and fortified samples (10 g each) were prepared by adding between 0 and 50 ng of 17α-TBOH to a known negative faeces sample. These, along with a series of test samples (10 g each) were incubated with β-glucuronidase (100 μl) and 0.2 mol/l sodium phosphate buffer, pH 5.5 (25 ml) either overnight at ambient temperature or for 4 h at 37°C.

Methanol (60 ml) was added to the hydrolysates which were then shaken on a reciprocating mixer for 1 h. The sample was centrifuged at 2000 *g* for 10 min at 4°C and an aliquot of the supernatant (50 ml) removed. The methanol was evaporated under vacuum in a rotary evaporator at 40°C and 0.1 mol/l glycine–sodium hydroxide buffer, pH 12.5, containing 0.1 mol/l sodium chloride (10 ml) added. The extract was then shaken vigorously for 1 min each with two portions (10 ml) of *tert.*-butyl methyl ether (t-BME) and then centrifuged at 2000 × *g* for 10 min at 4°C to enhance separation of the layers. The pooled t-BME extracts were then taken to dryness under a stream of nitrogen at 40°C.

Hydrolysis and liquid–liquid extraction: bile. A series of negative and fortified samples (5 ml each) were prepared by adding between 0 and 100 ng of 17α-TBOH to a known negative bile sample. These, along with a series of test samples (5 ml each) were incubated with β-glucuronidase (50 μl) and 0.2 mol/l sodium phosphate buffer, pH 7.0 (12.5 ml) either overnight at ambient temperature or for 4 h at 37°C.

The hydrolysates were loaded onto Extrelut 20 columns (Merck, Poole, UK) and allowed to stand for 20 min. The columns were irrigated with diethyl ether (2 × 20 ml) and the eluates were collected in round-bottomed flasks. It was found beneficial to allow the column to run dry between each addition of diethyl ether. The diethyl ether was removed under vacuum at 30°C.

Liquid–solid extraction: faeces and bile. The residues in the flasks were dissolved in diethyl ether (3 ml) with the aid of ultrasonication and aliquots of petroleum spirit (3 ml, 40–60°C) were added to each. These solutions were then loaded onto a Bond-Elut CN cartridge (Analytichem International, Harbor City, CA, USA) which had been preconditioned by washing with chloroform (4 ml) followed by petroleum spirit (5 ml). The flasks were then washed with aliquots (1 ml) of petroleum spirit–diethyl ether (50:50, v/v). These washings were also applied to the Bond-Elut cartridges. The cartridges were then washed with petroleum spirit (3 ml), and petroleum spirit–chloroform (50:50, v/v) (4 ml). The cartridges were then irrigated with chloroform (4 ml) to elute the 17α-TBOH. The solvent was concentrated to dryness under a gentle stream of nitrogen at 40°C and dissolved in methanol (500

μl) with the aid of ultrasonication. Finally, isotonic PBS (2 ml) was added with vortexing.

Immunoaffinity chromatography: faeces and bile. The sample solutions derived from the liquid–solid extraction were then applied to the immunoaffinity columns, which were then washed with water (3 ml). The adsorbed 17α-TBOH was eluted with ethanol–water (70:30, v/v) (3 ml). The eluate was concentrated to dryness under a gentle stream of nitrogen at 70°C. The columns were washed and stored as described above.

LC–MS system

The LC–MS system consisted of a Merck–Hitachi (BDH, Dagenham, UK) Model L-6000 pump, a Rheodyne (Rheodyne, Cotati, CA, USA) Model 7125 injector fitted with a 50-μl sample loop and a LiChrosorb (Merck, Poole, UK) RP-18, endcapped, 125 × 4 mm reversed-phase cartridge with holder. The mobile phase consisted of acetonitrile–0.1 mol/l ammonium acetate (45:55, v/v). It was degassed and filtered under vacuum through a 0.45-μm filter using a solvent filtration system (Millipore–Waters, Harrow, UK). The mobile phase was pumped at a rate of 1.0 ml/min. This system was directly coupled to a Vestec (Houston, TX, USA) Model 201A thermospray LC–MS system complete with a Technivent workstation.

The instrument was operated in two modes, the positive ion pure thermospray mode and the negative ion chemical ionisation (CI) mode using filament-assisted ionisation with a electron beam current of 250 μA. The electron multiplier voltage was 1600 V. The temperatures of the source block, tip heater and lens assembly were 260, 260 and 135°C, respectively. The vaporizer probe was operated at about 15°C below the take-off point. This was optimized for each probe used, but was typically in the region of 190°C. The instrument was operated either in the full scan mode to collect spectra, or in the selected ion monitoring mode (SIM) for maximum sensitivity. For the former, a dwell time of 3 ms was used, and for the latter the dwell time was 100 ms. In each case the sweep window was set at 0.5 u. The tuning parameters were checked daily according to the manufacturers instructions using a 50 mg/l solution of polyethylene glycol 300 in acetonitrile–water (50:50, v/v), containing 0.1 mol/l ammonium acetate.

LC–MS confirmation: faeces and bile

The residues from the immunoaffinity chromatography step were dissolved in acetonitrile (100 μl) with the aid of ultrasonication (10 min). Water (100 μl) was added with vortexing. Aliquots (50 μl) were then injected onto the LC–MS system. Both identification and quantification were carried out by SIM of ions characteristic of 17α-TBOH in the positive and negative ionisation modes. The positive mode was operated in pure thermospray and the [M + 1] ion (*m/z* 271) monitored. This was the normal mode of operation for trenbolone analyses. However, negative mode, filament-assisted ionization was also sensitive when the [M] ion (*m/z* 270) was monitored. Calibration curves were constructed using least-squares linear regression analysis. For quantification of 17α-TBOH, the area of either the [M + 1] or the [M] peak was compared to a range of calibration standards equivalent to 0, 0.4, 2, 4, 10, 20, 30 and 40 ng/ml 17α-TBOH.

RESULTS AND DISCUSSION

LC–MS analysis of 17α-TBOH

Full-scan spectra were easily achievable using 100 ng 17α-TBOH. In the negative ion mode,

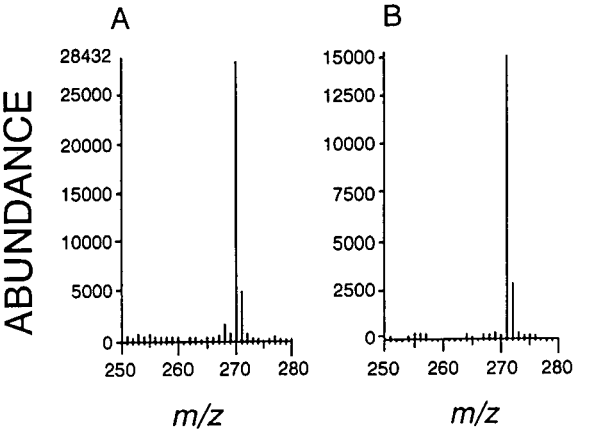

Fig. 2. Full scan spectra of 17α-trenbolone using either negative ion filament-assisted ionisation (A) or positive ion thermospray ionisation (B).

filament-assisted ionisation gave as base peak, the molecular ion at m/z 270 (Fig. 2A), while in the positive ion mode, in pure thermospray, the base peak was the protonated molecular ion at m/z 271 (Fig. 2B). No observable fragmentation was found in either mode. On SIM of m/z 270 or m/z 271, 500 pg 17α-TBOH injected onto the column were readily detectable.

The signals obtained in both modes were consistent during a run but were variable from day to day. One explanation may be the alteration of the spray characteristics of the probe as a result, perhaps, of contamination. This did not present a problem if standards were carried through with each set of samples. This could have been overcome by the use of an internal standard. However, we did not have access to deuterated trenbolone. Another possibility would have been to have employed 19-nortestosterone (19-NT). However, this was found not to be practical for two reasons. Firstly, the response produced by 19-NT on LC–MS is only approximately 10% of that produced by 17α-TBOH. Consequently, high concentrations of 19-NT would have had to be carried through the assay. Secondly, the crossreactivity of our antibody with 19-NT was only 15%, which would also have required the use of high concentrations of 19-NT. These two factors would thus have substantially reduced the capacity of the immunoaffinity columns for 17α-TBOH.

Assay development and validation

To enhance the specificity of the procedure for the isolation of 17α-TBOH from the complex matrices of bile and faeces, immunoaffinity chromatography was combined with the orthodox procedures of solvent extraction and solid-phase extraction.

In the case of faeces, adjustment of the pH to 12.5 ensured that unwanted acidic compounds were ionised and extracted into the aqueous phase while 17α-TBOH remained in the neutral form and was retained in the t-BME fraction. The use of a Bond-Elut CN cartridge in the normal phase mode, separated 17α-TBOH from any non-polar matrix components. The cleanliness of the sample after the final immunoaffinity chromatography step removed any variability caused by matrix components altering the efficiency of the thermospray ionisation mechanism.

Although 17α-TBOH produced a sensitive signal in both the positive and negative modes, positive ion thermospray was the method chosen for use throughout this study. The calibration graphs relating the peak areas of m/z 271 with the concentration of 17α-TBOH in prepared standards were linear in the range 0–40 ng/ml. The regression characteristics were, typically, $y = 209x + 33.6$, (correlation coefficient 0.9998). The accuracy and precision of this method were evaluated by analysis of fortified bile and faeces samples at concentrations of 5 and 20 ng/ml bile, and 2 and 5 ng/g faeces. Table I shows that the R.S.D. of the assay is between 4 and 8.5% for bile and between 10 and 11% for faeces. The recovery of 17α-TBOH from fortified bile or faeces ranged from 60–75%.

Sample analysis

This assay has been used to provide evidence of the illegal use in cattle of 17β-TBA-containing

TABLE I

RECOVERY OF 17α-TRENBOLONE FROM FORTIFIED SAMPLES ($n = 5$) OF BILE AND FAECES

Matrix	17α-TBOH added (mean ± S.D.) (ng/ml or ng/g)	17α-TBOH recovered (mean ± S.D.) (ng/ml or ng/g)	Recovery (%)	R.S.D. (%)
Bile	5.00	3.12 ± 0.26	62.4	8.3
Bile	20.00	14.50 ± 0.60	72.5	4.1
Faeces	2.00	1.50 ± 0.16	75.0	10.7
Faeces	5.00	3.10 ± 0.30	62.0	9.7

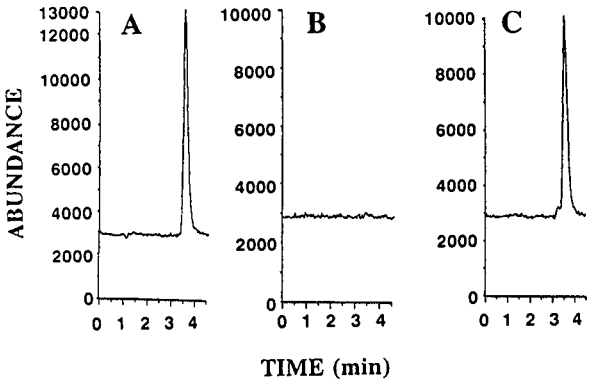

Fig. 3. Selected ion monitoring (m/z 271) for the detection of 17α-trenbolone in a standard solution containing the equivalent of 3.6 ng 17α-TBOH per g (A), a known negative faeces sample (B) and an incurred faeces sample (C) using positive ion thermospray LC–MS.

implant pellets to promote growth. Typical SIM chromatograms of standard, negative and incurred faeces samples are shown in Fig. 3. There were no co-eluting components in the negative faeces samples which could have caused interference in the assay. This shows the power of immunoaffinity chromatography as a clean-up procedure in the analysis of faeces, a particularly dirty matrix. The 17α-TBOH concentration in the faeces sample shown in Fig. 3 was 2.5 ng/g. The SIM chromatograms obtained for bile were similar to those of faeces (data not shown). In bile the limit of detection of the assay was approximately 0.5 ng/ml, and in faeces 0.5 ng/g, based on a signal to noise ratio of 3:1.

The Commission of the European Communities (EC) has produced criteria to determine the suitability of various analytical techniques for the chemical confirmation of veterinary drug residues [14]. However, the EC criteria have not, as yet, drafted specific criteria for the suitability of LC–MS. An alternative approach was adopted by an EC panel of experts which undertook a desk-top evaluation of the components of an analytical method [15]. They assigned partial selectivity indices to each step of a procedure and concluded that a confirmatory assay should have a minimum selectivity index of 7. The described assay consists of a liquid–liquid extraction (score 0), a liquid–solid extraction (score 2), immunoaffinity chromatography (score 3) and detection of a pseudomolecular ion (score 4). Thus, the described assay has a selectivity index of 9, making it suitable for use as a confirmatory assay. We believe that this is probably an underestimate of the selectivity of LC–MS because of the very marked compound-dependent sensitivity of this technique. For example, as mentioned above, 19-NT gives very poor responses on LC–MS. Thus, although the described assay does not measure 4 diagnostic ions, the approach advocated by the EC for low-resolution GC–MS [14], the selectivity achieved by the combination of immunoaffinity chromatography and LC–MS makes this method eminently suitable for the confirmation of 17α-TBOH residues in bile and faeces.

In conclusion, the described assay is reproducible and is sufficiently sensitive to be useful as a method for the independent chemical confirmation of trenbolone in bile and faeces, which are of most value in controlling the illegal use of this compound. Bile samples are preferred from dead animals, because bile is a cleaner matrix and because analysis is faster and more economical, with up to 10 samples being processed in one working day. The equivalent figure for faeces is 5 samples in 2 working days. The described assay has now been used in this laboratory for over 2 years to confirm the presence of 17α-TBOH in bile and faeces taken from cattle in Northern Ireland, following screening by enzyme immunoassay.

REFERENCES

1 B. Hoffmann and P. Evers, in A.G. Rico (Editor), *Drug Residues in Animals*, Academic Press, London, 1986, p. 111.
2 Commission of the European Communities, *Off. J. Europ. Comm.*, L191 (1985) 46.
3 M.W.A. Phillips and D.G. Harwood, *J. Vet. Pharm. Ther.*, 5 (1982) 285.
4 J. Pottier, M. Busigny and J.A. Grandadam, *J. Animal Sci.*, 41 (1975) 962.
5 J. Pottier, C. Cousty, R.J. Heitzman and I.P Reynolds, *Xenobiotica*, 11 (1981) 489.
6 R.J. Heitzman and K.H. Chan, *Br. Vet. J.*, 130 (1974) 532.
7 E.H.J.M. Jansen, P.W. Zoontjes, H. van Blitterswijk, R. Both-Miedema and R.W. Stephany, *J. Chromatogr.*, 319 (1985) 436.

8 G. Degand, P. Schmitz and G. Maghuin-Rogister, *J. Chromatogr.*, 489 (1989) 235.
9 D. de Boer, M.E. Gainza Bernal, R.D. van Ooyen and R.A.A. Maes, *Biol. Mass Spectrom.*, 20 (1991) 459.
10 S.-S. Hsu, T.R. Covey and J.D. Henion, *J. Liq. Chromatogr.*, 10 (1987) 3033.
11 L.A. van Ginkel, H. van Blitterswijk, P.W. Zoontjes, D. van den Bosch and R.W. Stephany, *J. Chromatogr.*, 445 (1988) 385.
12 B.A.L. Hurn and S.M. Chantler, *Methods Enzymol.*, 70 (1980) 104.
13 O.H. Lowry, N.J. Rosebrough, A.L. Farr and R.J. Randall, *J. Biol. Chem.*, 193 (1951) 265.
14 Commission of the European Communities, *Off. J. Europ. Comm.*, L223 (1987) 18.
15 *Proceedings of EC Workshop "The use of Immunoaffinity Chromatography in Multi-Residue and Confirmation Analysis of β-Agonists in Biological Samples"*, RIVM, Bilthoven, Netherlands, 1991, pp. 81–87.

Journal of Chromatography, 639 (1993) 193–196
Elsevier Science Publishers B.V., Amsterdam

CHROM. 24 975

Enantiomeric separation of amino alcohols on dinitrobenzoyl-diaminocyclohexane chiral stationary phases

B. Gallinella and F. La Torre

Istituto Superiore di Sanita', Laboratorio di Chimica del Farmaco, Viale Regina Elena 299, 00185 Rome (Italy)

R. Cirilli and C. Villani*

Dipartimento di Studi di Chimica e Tecnologia delle Sostanze Biologicamente Attive, Universita' "La Sapienza", Piazzale A. Moro 5, 00185 Rome (Italy)

(First received December 3rd, 1992; revised manuscript received February 15th, 1992)

ABSTRACT

A silica-bonded chiral stationary phase, containing the N,N'-3,5-dinitrobenzoyl derivative of 1*R*,2*R*-diaminocyclohexane, was used to separate the enantiomers of some amino alcohols with β-blocking activity after their conversion to oxazolidin-2-ones. The influence of mobile phase composition (mixtures of hexane with dichloromethane, chloroform, dioxane and isopropanol) on the enantioselectivity and efficiency of the column was evaluated. Furthermore, a tandem arrangement of the chiral column and its racemic version was used to resolve all the stereoisomers of one amino alcohol containing two stereogenic centres.

INTRODUCTION

The development of adrenergic blocking agents (β-blockers) has been one of the most important pharmacological and therapeutic innovations in recent years. These drugs are widely used in the treatment of angina, cardiac arrhythmias, hypertension [1] and anxiety [2].

The stereoisomerism of β-blockers is due to the presence of a stereogenic centre in the arylpropanolamine side-chain. Owing to the different pharmacological activity of the enantiomers (*S*-propranolol is about 100 times more active than the *R* enantiomer [2]), there is an increasing need to separate racemic mixtures of such compounds at analytical and preparative levels.

Resolution by HPLC of racemic β-blockers has been achieved, after cyclization to oxazolidin-2-ones, using Pirkle-type chiral stationary phases (CSPs) [3,4]. Microbore and standard analytical columns packed with a CSP derived from *trans*-1,2-diaminocyclohexane have been employed in the resolution of a large series of β-blockers and related compounds after conversion to oxazolidin-2-ones with phosgene or 1,1-carbonyldiimidazole [5,6]. Underivatized enantiomers of β-blockers have been separated on columns packed with tris(3,5-dimethylphenylcarbamate) cellulose supported on silica gel [7], immobilized bovine serum albumin [8], α_1'-acid glycoprotein [9] and ovomucoid [10]; recently, a CSP derived from a 3,5-dinitrobenzoyl-aminophosphonate has been developed for the direct separation of underivatized β-blockers [11].

In the present communication we describe the

* Corresponding author.

results obtained in the direct HPLC resolution of the enantiomers of two β-blocking agents using a π-acid CSP containing the N,N′-3,5-dinitrobenzoyl derivatives of *trans*-1,2-diaminocyclohexane covalently bonded to a silica matrix (DACH–DNB CSP). This kind of stationary phase is obtained by a three-step modification of silica microparticles consisting of covalent binding of chiral (or racemic) *trans*-1,2-diaminocyclohexane via reactive epoxy groups and subsequent derivatization with 3,5-dinitrobenzoyl chloride. A large number of racemic compounds have been separated on this CSP, including sulphoxides, selenoxides, phosphinates, phosphinoxides, derivatized acids, amines and amino acids containing at least one π-basic function in their structure [12].

EXPERIMENTAL

Apparatus

Chromatography was performed using a Waters M510 HPLC pump, a U6K injector, and an M490 programmable multi-wavelength detector and temperature control module; chromatographic data were collected and processed on a Waters 840 data and chromatography control station.

The following columns were used: *R,R*-DACH–DNB CSP (250 × 4 mm I.D.) and its racemic version (150 × 4 mm I.D.) at a flow-rate of 1 ml/min at 25°C; the wavelength used was 275 nm. Synthesis, column packing and kinetic evaluation are described elsewhere [5,6,12].

Chemicals

HPLC-grade solvents were obtained from Merck (Darmstadt, Germany); 1,1′-carbonyldiimidazole and 20% phosgene solution in toluene were from Fluka (Buchs, Switzerland); the racemic analytes were supplied by the following manufacturers: (2*RS*, 3*RS*)-1-(2,3-dihydro-7-methyl-1H-inden-4-yl)oxy-3-(1-methylethyl)-amino-butan-2-ol hydrochloride from ICI-Pharma (Milan, Italy) and (2*RS*)-1-(2-(1-pyrrolyl)-phenoxy)-3-isopropylamino propan-2-ol hydrochloride from Ciba-Geigy (Basle, Switzerland). Conversion of racemic amino alcohols into oxazolidin-2-ones was accomplished as previously described [6] with 90% yield.

RESULTS AND DISCUSSION

All the racemic mixtures of amino alcohols (compounds **1–3**) could be efficiently separated after their conversion to oxazolidin-2-ones; chromatographic data pertinent to these resolutions are listed in Table I. No separations were observed when chromatography of the underivatized amino alcohols was attempted because of the strong interaction between the amino group and the stationary phase. Cyclization to the

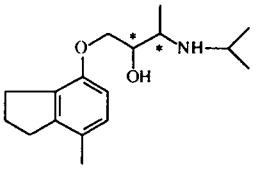

compound 1 : *erythro*
compound 2 : *threo*

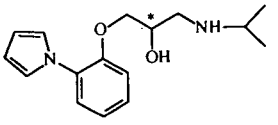

compound 3

TABLE I

CHROMATOGRAPHIC DATA FOR THE RESOLUTION OF COMPOUNDS **1–3** AS OXAZOLIDIN-2-ONES ON THE *R,R*-DACH–DNB CSP

Eluents employed are: (A) *n*-hexane–dioxane (50:50); (B) *n*-hexane–dichloromethane (40:60); (C) *n*-hexane–chloroform (25:75); (D) *n*-hexane–2-propanol (40:60).

Entry	Compound	k_1' [a]	α [b]	R_s [c]	Eluent
1	**1**	7.69	1.30	2.6	A
2	**1**	7.69	1.20	1.6	B
3	**1**	8.12	1.22	1.2	C
4	**1**	10.15	1.20	1.1	D
5	**2**	8.19	1.57	5.2	A
6	**2**	8.12	1.36	3.9	B
7	**2**	8.63	1.40	2.8	C
8	**2**	10.51	1.38	2.2	D
9	**3**	9.93	1.29	2.2	A
10	**3**	8.30	1.26	1.6	B
11	**3**	8.56	1.27	1.5	C
12	**3**	8.95	1.30	1.4	D

[a] The capacity factor of the first eluted enantiomer.
[b] The enantioselectivity factor.
[c] The resolution factor.

oxazolidin-2-ones reduces both the basicity of the analytes and their conformational flexibility, thus leading to good values of enantioselectivity and chromatographic efficiency. The enantioselectivity factors (α) for compounds **1** and **2** show a significant dependence on eluent composition, higher values being observed when 1,4-dioxane is used as polar modifier in the mobile phase (Fig. 1); for compound **3** the degree of enantioselectivity observed is almost constant with the four eluents used. Resolution factors (R_s) show a greater dependence on the nature of the mobile phase as a consequence of variations in both α and efficiency of separation: the lowest R_s values are obtained using 2-propanol as a polar modifier, because of the higher viscosity of the eluent and thus lower diffusion coefficients of the analytes: passing from dichloromethane to chloroform or 2-propanol results in a loss of resolution in spite of similar α and k_1' values (Table I, entries 2, 3, 4; 6, 7, 8; 10, 11, 12).

Of the two diastereoisomers of compounds **1** and **2**, only the erythro form is active: it is therefore desirable to have a stereoselective method able to separate and quantify all four possible isomers, *e.g.* to check the stereochemical stability (*in vitro* and/or *in vivo*) of both stereogenic centres of the drug. From the data listed in Table I it is clearly seen that the chiral column does not afford the required diastereoselectivity: in fact, the separation factors between the first eluted enantiomers of the erythro and threo forms (ratio of the k' values listed in Table I) are always smaller than 1.10, leading to incomplete resolution of the four stereoisomers (overlapping of the first two eluting peaks); a common practice to improve global selectivity in such situations is to connect in series columns with different, complementary selectivities and similar mobile phase requirements [12,13]: by using two columns in series, one packed with the *R,R*-DACH–DNB CSP and the other with its racemic analogue, the complete separation of the four stereoisomers of compounds **1** and **2** is achieved using a ternary mobile phase (chromatogram C, Fig. 2). The composition of the mobile phase was chosen in order to obtain the highest values of enantioselectivity together with a good chromatographic efficiency.

It is worth noting that the tandem arrangement between the chiral column DACH–DNB CSP and a silica column (LiChrosorb Si 60), successfully employed to resolve the four stereoisomers of the racemic ephedrine and ψ-ephedrine [6], it is not feasible in the present

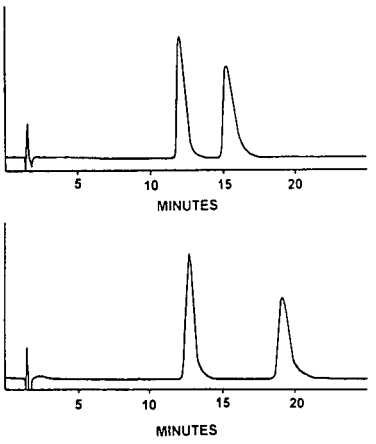

Fig. 1. Chromatographic analysis of compounds **1** (top) and **2** (bottom) using eluent A. See Table 1 for other conditions.

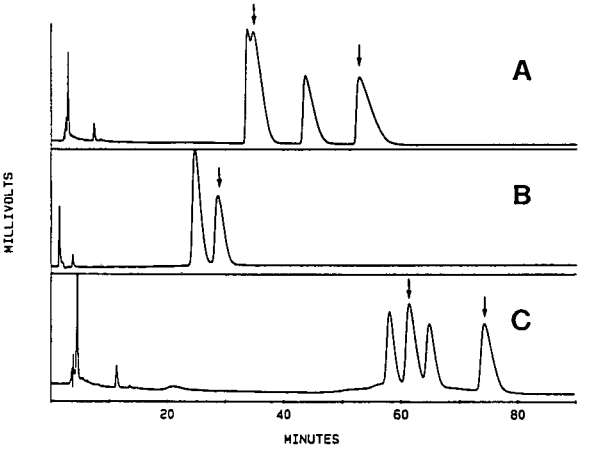

Fig. 2. Chromatographic analysis of the four stereoisomers of compounds **1** and **2**. Eluent: *n*-hexane–dioxane–dichloromethane (60:30:10); (A) *R,R*-DACH–DNB CSP; (B) Racemic version of the CSP; (C) tandem arrangement: *R,R*-DACH–DNB and the racemic version coupled in series. Arrows indicate peaks relative to the *threo* isomer.

case because of the opposite diastereoselectivities afforded by the two phases (the erythro isomer is most retained on the silica column).

CONCLUSIONS

In conclusion, a method for the separation and quantization of the optical isomers of β-blocking agents is reported. The separation of the enantiomers of chiral drugs having more than one stereogenic centre is, in principle, not significantly different from that for compounds with a single stereogenic centre. However a coupled achiral–chiral system is often necessary to compensate for the weak diastereoselectivity of a chiral column.

REFERENCES

1 R.G. Shanks, *Trends Pharm. Sci.*, 5 (1984) 405.
2 P.C. Waldmeier, M. Williams, P.A. Bauman, S. Bischoff, M.A. Sills and R.F. Neale, *Arch. Pharmacol.*, 337 (1988) 609.
3 A.M. Krstulovic, *J. Pharm. Biomed. Anal.*, 6 (1988) 641.
4 I. Wainer and T. Doyle, *J. Chromatogr.*, 306 (1984) 405.
5 F. Gasparrini, D. Misiti, C. Villani, F. La Torre and M. Sinibaldi, *J. Chromatogr.*, 457 (1988) 235.
6 F. Gasparrini, D. Misiti, C. Villani and F. La Torre, *J. Chromatogr.*, 539 (1991) 25.
7 Y. Okamoto, M. Kawashima, R. Aburatani, K. Hatada, T. Nishiyama and M. Masuda, *Chem. Lett.*, (1986) 1237.
8 S. Allenmark, in A.M. Krstulovic (Editor), *Chiral Separation by HPLC: Applications to Pharmaceutical Compounds*, Wiley/Ellis Horwood, New York, 1989, p. 285.
9 G. Schill, I. Wainer and S. Barkan, *J. Liq. Chromatogr.*, 9 (1986) 621.
10 J. Haginaka, J. Wakai, K. Takahashi, H. Yasuda and T. Katagi, *Chromatographia*, 29 (1990) 587.
11 W.H. Pirkle and J.A. Burke, *J. Chromatogr.*, 557 (1991) 173.
12 F. Gasparrini, D. Misiti and C. Villani, *Chirality*, 4 (1992) 447.
13 W.H. Pirkle, R. Dappen and D. Reno, *J. Chromatogr.*, 407 (1987) 211.

Journal of Chromatography, 639 (1993) 197–205
Elsevier Science Publishers B.V., Amsterdam

CHROM. 25 062

Separation and determination of trace metals in concentrated salt solutions using chelation ion chromatography

O.J. Challenger, S.J. Hill and P. Jones*

Department of Environmental Sciences, University of Plymouth, Drake Circus, Plymouth PL4 8AA (UK)

(First received October 13th, 1992; revised manuscript received March 2nd, 1993)

ABSTRACT

A high-performance ion chromatography system using chelating dye coated columns for the determination of trace metals in high-ionic-strength media is described. All the preconcentration and separation studies of metal ions were carried out using a single chelating column. Spectrophotometric detection using 4-(2-pyridylazo)resorcinol and Pyrocatechol Violet post-column reagent was employed to investigate divalent and trivalent metal ions. A number of metal ion determinations in 1 *M* laboratory salt solutions, concentrated brines and sea waters were achieved under isocratic and step gradient elution conditions, where up to nine metal ions could be separated in a single injection. Standard addition was used for calibration and good linearity was obtained in the low $\mu g\ l^{-1}$ range.

INTRODUCTION

Present ion chromatography techniques for the determination of trace metals work well if the sample is relatively low in ionic strength. If the ionic strength is too high, the salt ions may "swamp" the ion-exchange sites, seriously affecting any separation. Thus, direct analysis of important samples such as concentrated brines and sea waters is extremely difficult by conventional ion chromatography. This problem can be overcome by using chelating exchange groups instead of ion exchange groups on the stationary phase substrate. Metal ion separations will then be dependent on the conditional stability constants of each metal chelate, and are much less affected by the ionic strength of the sample.

Chelating resins have been used for some time for preconcentration of metal ions. One of the first to demonstrate this for preconcentrating trace metals from sea waters were Riley and Taylor in 1968 [1]. They used Chelex 100 which contains covalently bonded chelating groups to the surface of the substrate. Since then, many chelating groups have been synthesized beforehand and covalently bonded to the substrate. However, they have predominantly been used for matrix elimination and preconcentration before determination by another technique. Siriraks *et al.* [2] used a chelating column for trace metal preconcentration in trace elemental analysis in various environmental and biological samples before separation by conventional ion chromatography, but the ion chromatography system used was rather complex. Fritz *et al.* [3] prepared a number of chemically bonded chelating substrates and demonstrated their use for separation of trace metals, however efficiency was low. Toei [4] has used a covalently bonded chelating column employing iminodiacetic acid functional groups for the analytical separation of magnesium and calcium in sea water with high efficiency. A recent review highlights many

* Corresponding author.

0021-9673/93/$06.00

bonded chelating polymers suitable for trace metal separation and preconcentration of environmental samples [5].

An alternative approach to chemical bonding is to coat the substrate with a chelating dye. This avoids the need to synthesise and bond the chelating group onto the substrate, which can be a very time-consuming and difficult procedure. Most chelation exchange coatings have been on anion exchange resins with very few on neutral resins as shown in a review of this area by Marina *et al.* [6]. Again the majority of these coated resins have been used for preconcentration and matrix elimination. For example, recently a Xylenol Orange column coated onto Dowex 1-X8 anion-exchange resin has been used as a preconcentration column as part of an automated HPLC system for trace metal determinations in concentrated brines [7]. However, little work has been carried out using coated chelating columns to investigate trace metal separations on high performance grade substrates. Jones and Schwedt [8] investigated a dyestuff-coated HPLC resin for chelation exchange separation of metal ions. Although a range of chelating dyes were initially examined for their depth of coating and chemical stability, Chrome Azurol S was chosen for further study and coated onto a neutral Benson BPI-10 resin. Separations of divalent and trivalent metals in 1 *M* potassium nitrate was achieved, though the efficiency was relatively low.

Recently, we have reported [9] a more detailed investigation into dyestuff-coated columns using a range of chelating dyes coated onto a number of resins of varying particle size. The chelating performance was found to vary markedly depending on the type of substrate and chelating dye employed. Xylenol Orange was then chosen to coat onto a neutral small-particle-size HPLC-grade resin, and a separation of all four alkaline earth metals in 1 *M* potassium nitrate was achieved. Further work using these columns enabled separations of other divalent metals, and separations from high concentrations of alkaline earth metals using gradient elution [10].

This paper reports on further developments in combined preconcentration and high-performance separations of trace metals in various high-ionic-strength matrices, using a single dye-coated HPLC grade chelation exchange column. The application of this column for the determination of trace metals in concentrated brines and sea waters is also reported.

EXPERIMENTAL

Instrumentation

The chelation ion chromatography post-column reaction system employed is shown in Fig. 1. Two injection valves were used to enable either preconcentration or a direct injection onto the column.

The instrumentation used consisted of two ConstaMetric Model III pumps (Laboratory Data Control, Riviera Beach, FL, USA) for the eluent and post-column reagent. Injector 1 was a stainless-steel injector with 100-μl sample loop (Rheodyne, Cotati, CA, USA) and used for direct injections. The preconcentration system was composed of entirely inert materials which comprised an Eldex Labs. (Menlo Park, CA, USA) Model AA pump with PTFE-lined pump heads and check valves, and titanium injector (number 2) (Valco, Schenkon, Switzerland). All connecting tubing and junctions were composed of PTFE. The UV–visible detector was a Spectroflow Monitor SF770 (Schoeffel, Westwood, NJ, USA).

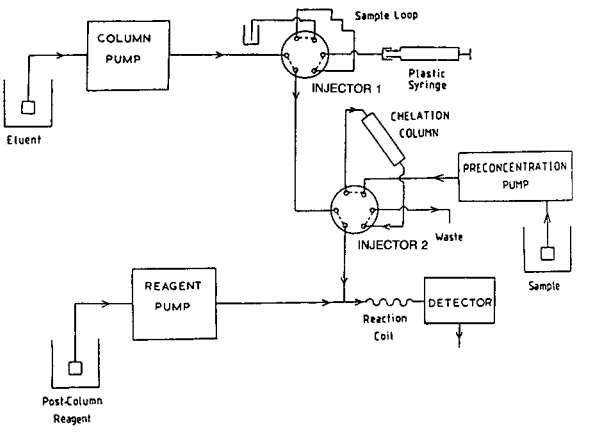

Fig. 1. Chelation ion chromatography post-column reaction system.

Chelating columns

Two dye-coated columns were investigated. These were Xylenol Orange (5,5′-bis-NN-bis(carboxymethyl)aminomethyl-4′-hydroxy-3,3′-dimethylfuchsone-2″-sulphonic acid (tetrasodium salt)] (BDH, Poole, UK), and Chrome Azurol S [2″,6″-Dichloro-4′-hydroxy-3,3′-dimethyl-3″-sulphofuchsone-5,5-dicarboxylic acid (Trisodium salt), (Sigma, St. Louis, MO, USA) coated onto 8 μm, 100 Å polystyrene–divinylbenzene neutral PLRP-S resin (Polymer Labs., Church Stretton, UK). These columns were 10 cm × 4.6 mm I.D., metal free and inert, being made of poly ether ether ketone (PEEK), (Alltech, Carnforth, UK). These columns were coated by pumping a 0.2% solution of the dye through a packed PLRP-S column.

Materials

All chemicals were obtained from BDH except 4-(2-pyridylazo)resorcinol (PAR), ZnEDTA and sodium sulphate which were obtained from Fluka (Buchs, Switzerland). Metal stock solutions were Spectrosol atomic absorption standards obtained from BDH. All reagents and working standards were prepared using distilled deionized water obtained from a Milli-Q system (Millipore, Bedford, MA, USA).

To reduce the levels of metal impurities, the eluents and buffers were pumped through a Xylenol Orange coated XAD-2 (BDH) chelating column (10 cm × 4.6 mm I.D.). This off-line clean up process considerably reduced levels of metal ions which are likely to build up on the analytical column during preconcentration and step gradient elution processes.

Eluents and post-column reagents

Divalent metal ion determinations. The eluent used in all cases was 1 *M* potassium nitrate containing 0.05 *M* lactic acid, adjusted to the appropriate pH with dilute nitric acid or dilute ammonia. The post-column reagent employed was $1.2 \cdot 10^{-4}$ *M* PAR–$2 \cdot 10^{-4}$ *M* ZnEDTA in 2 *M* ammonia for all samples except sea water where $1.2 \cdot 10^{-4}$ *M* PAR in 2 *M* ammonia without the ZnEDTA was used. Absorbance was monitored at 490 nm.

Trivalent metal ion determinations. The eluent used here was 1 *M* potassium nitrate, and the post-column reagent employed was 0.004% Pyrocatechol Violet in 0.5 *M* hexamine adjusted to pH 6. Absorbance was monitored at 580 nm.

Samples and sample treatment

Samples. Sodium chloride and potassium chloride brines were obtained from ICI Chemicals and Polymers, Runcorn, UK. The sea water sample was obtained from Plymouth Sound. Laboratory chemicals were made up as 1 *M* solutions. A pH meter was used to monitor all pH adjustments as detailed below. Blank determinations showed negligible contamination from the small volumes of acid or alkali used to adjust the pH.

Sample analysis

Direct injection. The pH of the sample was adjusted to the same pH as the eluent using dilute nitric acid or dilute ammonia before injection. A 100-μl volume of sample was then injected using injector 1.

Preconcentration. The sample was adjusted to an appropriate pH using dilute nitric acid or dilute ammonia, depending on the metals of interest. Before preconcentration it was necessary to equilibrate the column to the same pH as the sample by pumping 10 ml of the appropriate buffer (0.1 *M* borate for pH 10 or pH 11, and 0.1 *M* hexamine for pH 6). This was followed by 10 ml of the sample, and finally 3 ml of distilled deionized water. This was all carried out with the potassium nitrate eluent bypassing the column as shown in Fig. 1. The gradient program was initiated by switching the titanium injector to allow the potassium nitrate eluent to pass through the preconcentration column. The pH of the 1 *M* potassium nitrate eluent was then changed in a series of steps at specified times as described in the Results and Discussion section.

RESULTS AND DISCUSSION

The stability of the columns after coating proved to be very good. There was an initial bleed of the dye during the cleaning process directly after coating the column, but only a

large sudden change in ionic strength would produce any further slight bleeding of the dye. To illustrate the different chelating strengths of the two dyes, the pH required to completely retain various metal ions on small particle size coated columns was investigated. Initial studies showed that these two columns were distinctly different (Table I), the Chrome Azurol S showing much weaker chelation than Xylenol Orange, not retaining alkaline earth metals until pH 11 or above.

Since pH is a major controlling factor on chelating strength, various groups of metal ions can be selectively eluted in the order of increasing stability constants. However, under isocratic conditions the peaks become quite broad after a relatively short time and therefore only three or four metal species can reasonably be determined this way. To separate a greater number of metals a pH gradient is necessary. Peak compression occurs and even the last eluting peaks are relatively sharp. We found that step gradients gave better results than a continuous gradient, though in some cases this caused steps in the chromatogram baseline. An example of a nine metal separation on a Xylenol Orange coated column using three step gradients is shown in Fig. 2. The metal mixture was directly injected at pH 10 where every metal would be retained on the column. By stepping the eluent to pH 6.5 the alkaline earth metals were eluted, then a change to pH 3 after 15 min eluted manganese, cadmium and zinc, and a final step to pH 0.5 after 30 min to elute nickel and copper which form the strongest chelates.

TABLE I

MINIMUM pH REQUIRED FOR COMPLETE RETENTION OF 5 mg l^{-1} METAL STANDARDS (10 mg l^{-1} FOR BARIUM), ON SMALL-PARTICLE-SIZE DYE-COATED COLUMNS, USING 1 *M* POTASSIUM NITRATE MOBILE PHASE

Standard	Xylenol Orange-coated PLRP-S	Chrome Azurol S-coated PLRP-S
Ba^{2+}	10	>11
Mg^{2+}	9	11
Sr^{2+}	9	>11
Ca^{2+}	8	>11
Mn^{2+}	6	8
Co^{2+}	4	7
Zn^{2+}	4	7
Cd^{2+}	5	7
Pb^{2+}	4	6
Ni^{2+}	3	6
Cu^{2+}	2	5

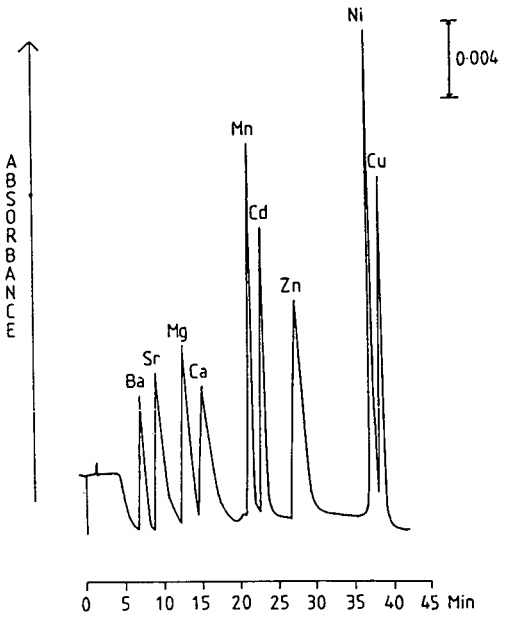

Fig. 2. Chromatogram showing separation of nine metals on a Xylenol Orange-coated PLRP-S dye-coated column, using three step gradients. Sample conditions were direct injection of 100 μl of 1 *M* KNO_3 containing 0.05 *M* lactic acid adjusted to pH 10, spiked with the following concentrations of metal ions: 5 mg l^{-1} Mg^{2+}, Ca^{2+}, Mn^{2+}, Ni^{2+}, Cu^{2+}, 10 mg l^{-1} Cd^{2+} and Zn^{2+}, and 20 mg l^{-1} Ba^{2+} and Sr^{2+}.

Preconcentration and separation of trace metals

As described above, many metal ions can be separated in a single injection using pH step gradients. However, in order to investigate samples containing metals at low parts per billion levels, a preconcentration step was needed prior to the analytical separation. In the following work the preconcentration and separation is carried out on the same column. Because of the much lower concentration of metals, it is important that the preconcentration system is composed of inert materials as described in the Experimental section. No observable contamination was found from the steel pumps pumping 1

M potassium nitrate eluent, even in acidic media. However, the major contamination occurred with impurities in the potassium nitrate itself and the buffer solutions. This necessitated clean-up with a Xylenol Orange-coated XAD-2 column as described in the Experimental. In all cases blank runs were carried out using the same step gradient program, but omitting the sample. All quantitative data was blank corrected if necessary.

Concentrated brines

Actual industrial samples of concentrated sodium and potassium chloride brines used in the chloralkali industry, obtained from ICI, were analyzed for trace metal content using the Xylenol Orange column. The actual concentrations of these samples determined by titration was 2.4 *M* for KCl and 5.1 *M* for NaCl brine.

Fig. 3 shows a typical separation of alkaline earth metals in KCl brine, using a single-step gradient from pH 11 to pH 6. Some degree of selectivity is possible by changing the starting pH of the gradient. Thus, by starting at a lower pH the separation of some transition metals is possible while the alkaline earth metals pass straight through on the solvent front. A calibration series for alkaline earth and some transition metals in KCl brine was carried out by the method of standard addition. Good linear results were obtained with the correlation coefficient, *r*, ranging from 0.991 to 0.999.

If the full range of metal species need to be studied in a single determination then a more complex step gradient programme can be used. The chromatogram in Fig. 4 shows the separation of nine metals in 2.4 *M* KCl brine achieved with a three-step gradient. A step gradient from pH 10 to pH 6 eluted the alkaline earth metals, followed by a step to pH 3 after 7 min to elute manganese, cadmium and zinc, then a final step to pH 0.7 after 15 min to elute nickel and copper.

A calibration series for alkaline earth metals in saturated NaCl brine (5.1 *M*) was also carried out and the results compared to those obtained for KCl brine (Table II). It can be seen that the KCl brine contains higher levels of calcium, but the NaCl brine as expected, contains much higher levels of strontium, due to the high levels naturally occurring in rock salt. For comparison a separation of alkaline earth metals in a NaCl brine sample using the same step gradient as KCl, is shown in Fig. 5.

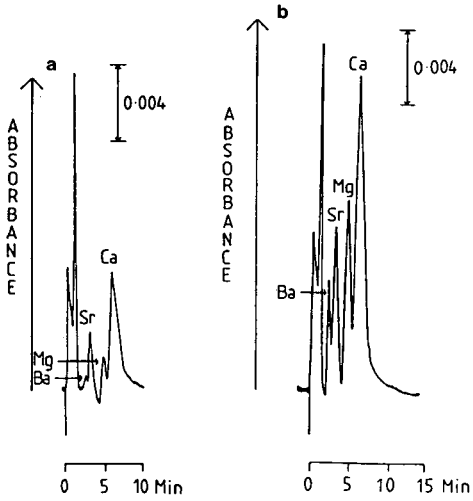

Fig. 3. Chromatograms showing preconcentration and separation of alkaline earth metals in KCl brine using the Xylenol Orange coated column. (a) KCl brine sample, (b) KCl brine spiked with 25 $\mu g\ l^{-1}$ Mg^{2+}, 50 $\mu g\ l^{-1}$ Ca^{2+}, Sr^{2+} and Ba^{2+}. Sample volumes were 10 ml adjusted to pH 11.

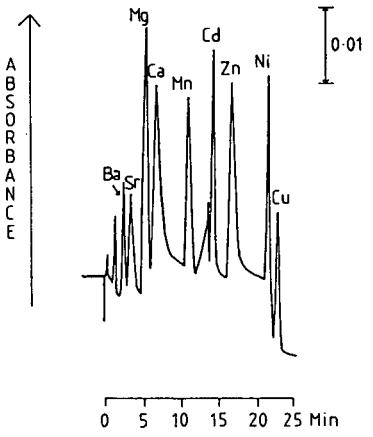

Fig. 4. Chromatogram showing preconcentration and separation of nine metal ions in 2.4 *M* KCl brine using the Xylenol Orange-coated column with a three-step gradient. Spiked metal concentrations were 50 $\mu g\ l^{-1}$ Mg^{2+}, Ca^{2+}, Zn^{2+}, Ni^{2+}, Cu^{2+} and 0.1 mg l^{-1} Sr^{2+}, Ba^{2+}, Mn^{2+} and Cd^{2+}. Sample volume was 10 ml adjusted to pH 10.

TABLE II

CONCENTRATION OF TRACE METALS IN KCl AND NaCl BRINES

ND = Not determined. Reproducibilities were determined on samples spiked at the midpoint of each calibration range. The relative standard deviations on six replicates all ranged between 2 and 5%.

	Concentration ($\mu g\ l^{-1}$)		
	NaCl	KCl	Approx. detection limit[a]
Mg^{2+}	3	1	0.5
Ca^{2+}	6	18	2
Sr^{2+}	95	28	4
Ba^{2+}	9	3	2
Mn^{2+}	ND	8	0.5
Zn^{2+}	ND	17	1
Ni^{2+}	ND	4	2
Cu^{2+}	ND	<1	1

[a] Detection limits are for a 10-ml preconcentration volume and for 2× baseline noise level.

Impurities in laboratory chemicals

The successful use of these columns in the determination of trace metals in concentrated brines encouraged further work with other matrices. One such area is the investigation of trace metal impurity levels in laboratory reagents. Three laboratory chemicals were selected, these were potassium nitrate, sodium sulphate and caesium iodide. These were made up as 1 *M* solutions for analysis. Using a step gradient from pH 6 to pH 3.7, then pH 2 after 1 min and pH 0.7 after 6 min, six metal species could be separated, namely manganese, cadmium, zinc, lead, nickel and copper. A typical example of the separation achieved by this gradient programme on a spiked sample is shown in Fig. 6 and Fig. 7 shows the actual trace metal impurity profiles obtained for the three laboratory chemicals. It can be seen that the potassium nitrate used as our eluent contains relatively high levels of zinc, and shows the necessity for clean-up of this reagent as described in the experimental section. There were some problems in quantifying copper in caesium iodide, probably due to

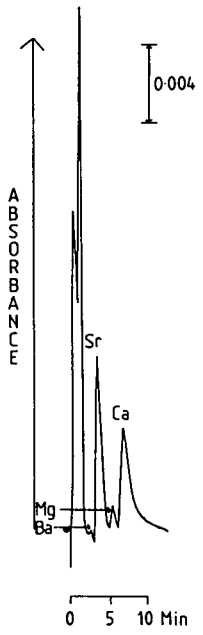

Fig. 5. Chromatogram showing preconcentration and separation of alkaline earth metals in a saturated (5.1 *M*) NaCl brine sample using the Xylenol Orange-coated column. Sample volume was 10 ml adjusted to pH 11.

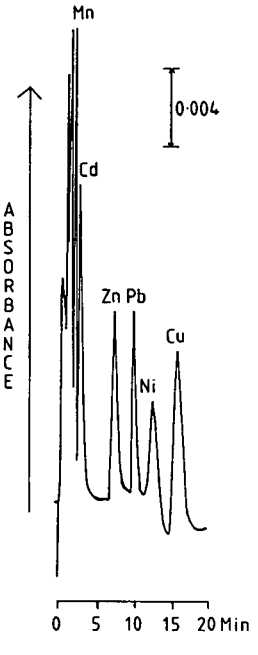

Fig. 6. Chromatogram showing preconcentration and separation of trace metals in 1 *M* Na_2SO_4 sample spiked with 10 $\mu g\ l^{-1}$ Mn^{2+}, 25 $\mu g\ l^{-1}$ Zn^{2+} and 0.1 mg l^{-1} Cd^{2+}, Pb^{2+}, Ni^{2+} and Cu^{2+}. Sample volume was 10 ml adjusted to pH 6.

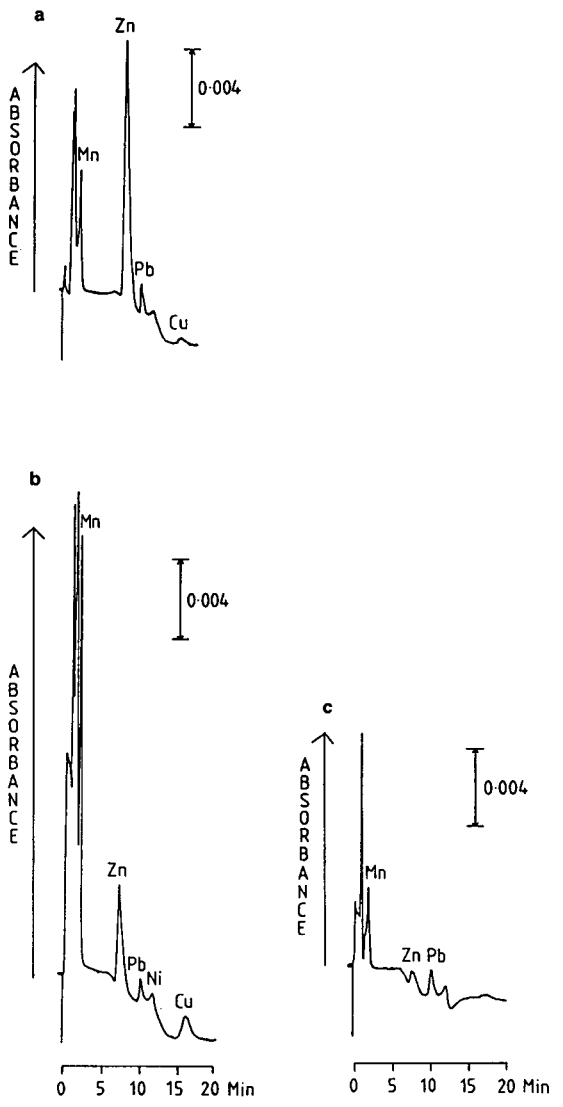

Fig. 7. Chromatograms showing preconcentration and separation of trace metal ions in laboratory chemical samples using the Xylenol Orange-coated column. (a) 1 *M* KNO_3 sample, (b) 1 *M* Na_2SO_4 sample and (c) 1 *M* CsI sample. Sample volumes were 10 ml adjusted to pH 6.

interference of iodide which is known to reduce Cu^{2+} to Cu^{+}. Approximate impurity levels in all three chemicals are shown in Table III.

Analysis of trace metals in sea waters

The Chrome Azurol S-coated column although more suitable for sea waters because of its weak affinity for calcium and magnesium, was not as efficient as the Xylenol Orange-coated column

TABLE III

APPROXIMATE IMPURITY LEVELS IN THREE LABORATORY CHEMICALS

X = Not quantified (see text).

	Concentration ($\mu g\ l^{-1}$)		
	1 *M* KNO_3	1 *M* Na_2SO_4	1 *M* CsI
Mn^{2+}	5	28	4
Cd^{2+}	–	–	–
Zn^{2+}	60	21	2
Pb^{2+}	10	10	15
Ni^{2+}	–	5	–
Cu^{2+}	3	12	X

and could not separate all of the metals investigated. However, it was still possible to use the Xylenol Orange-coated column by adjusting the sea water to pH 6 when most of the magnesium and calcium present will not be retained. Also by using PAR alone, which does not react well with alkaline earth metals, as the post-column reagent, the magnesium/calcium peak can be further reduced.

Sea water from Plymouth Sound, filtered before use to remove particulate matter, was investigated for traces of cadmium, zinc, lead, nickel and copper. This separation was achieved with a step gradient from pH 6 to pH 3.7, then to pH 2 after 5 min and pH 0.7 after 10 min. Fig. 8a shows Plymouth Sound sea water, whilst Fig. 8b shows a spiked sample. A large peak due to magnesium and calcium still occurs at the solvent front as PAR does react slightly with these ions [11]. Zinc and copper were shown to be present at 1 $\mu g\ l^{-1}$ and 3 $\mu g\ l^{-1}$, respectively, with a slight hint that lead may be present in the sea water. Higher preconcentration volumes will be needed to quantify this. The level of copper present is significantly higher than would normally be expected as several rivers feeding into Plymouth Sound are enriched with copper due to the local geology.

Trivalent metal ion separation

The work so far demonstrates the suitability of the chelation chromatography approach for the determination of divalent metal ions. However,

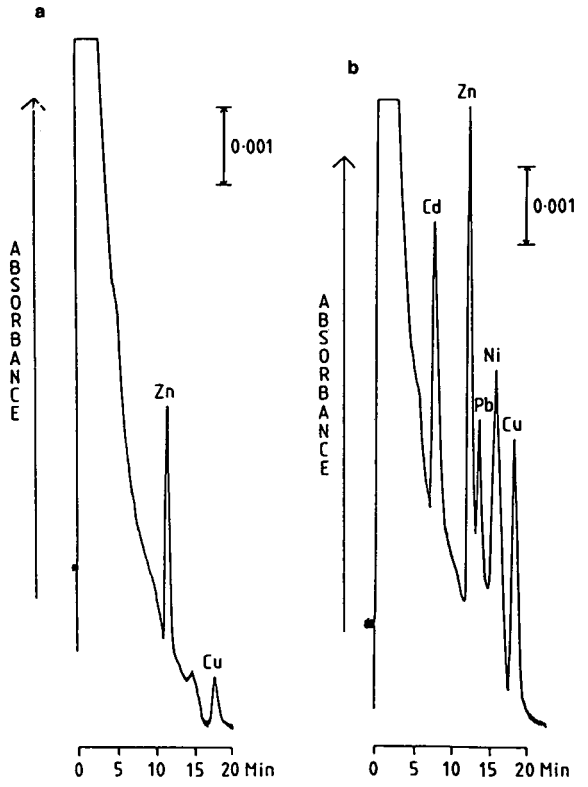

Fig. 8. Chromatograms of trace metals in Plymouth Sound sea water preconcentrated and separated using the Xylenol Orange-coated column. (a) Plymouth Sound sea water showing Zn^{2+} (1 μg l^{-1}) and Cu^{2+} (3 μg l^{-1}) present in the sample, (b) Plymouth Sound sea water spiked with 5 μg l^{-1} Zn^{2+}, 20 μg l^{-1} Cu^{2+} and 50 μg l^{-1} Cd^{2+}, Pb^{2+} and Ni^{2+} Sample volumes were 10 ml adjusted to pH 6.

trivalent metal ions in general form much stronger chelates than divalent metal ions. The Xylenol Orange-coated column would require much more acidic eluents for desorption, therefore it was decided to investigate these ions using the weaker chelating Chrome Azurol S column.

Fig. 9 shows an isocratic separation of aluminium, gallium and indium in 1 *M* potassium nitrate achieved at pH 2.2. Because the exchange kinetics are slow, the column was operated at an elevated temperature of 60°C. The separation profile is similar to previous work [8], but the elution order is different, gallium eluting before indium. Further studies are underway including other trivalent metal ions such as iron and bismuth.

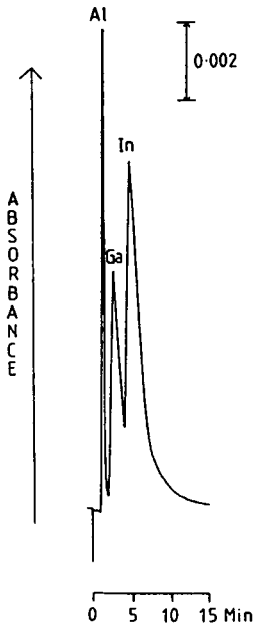

Fig. 9. Chromatogram showing isocratic separation of 2 mg l^{-1} Al^{3+}, 10 mg l^{-1} Ga^{3+} and 20 mg l^{-1} In^{3+} in 1 *M* KNO_3, at pH 2.2, using the Chrome Azurol S-coated column at 60°C. Direct injection of 100 μl sample.

CONCLUSIONS

This work shows that chelation ion chromatography using dye-coated columns shows clear potential for the determination of trace metals in high-ionic-strength media. They give high efficiencies and can be used to separate selective groups of metal ions, or a larger range using a series of step gradients.

Combined preconcentration and separation of trace metals in various high-ionic-strength media including concentrated brines, sea waters and laboratory chemicals can be achieved using a single chelating column. A separation of nine metal ions in 1 *M* potassium nitrate and concentrated KCl brine has also been successfully achieved.

These chelating dye-coated columns are much easier to prepare than chemically bonded chelating columns, and so far the Xylenol Orange-coated column has proved to be very stable, having been used for over 1.5 years without any apparent loss of efficiency.

Chelation ion chromatography can only de-

velop further in the future as a relatively simple and inexpensive method of directly determining trace metals in various high-ionic-strength media.

ACKNOWLEDGEMENTS

The authors would like to thank the Trustees of the Royal Society of Chemistry Analytical Division Trust Fund, and ICI Chemicals & Polymers, Runcorn, for the provision of a studentship (to O.J.C.) and for their financial support of this work. Also we would like to thank P. Norman (ICI Chemicals & Polymers, Runcorn) for his support.

REFERENCES

1 J.P. Riley and D. Taylor, *Anal. Chim. Acta*, 40 (1968) 479–485.
2 A. Siriraks, H.M. Kingston and J.M. Riviello, *Anal. Chem.*, 62 (1990) 1185–1193.
3 J.S. Fritz, D.T. Gjerde and C. Pohlandt, in W. Bertsch, W.G. Jennings and R.E. Kaiser (Editors), *Ion Chromatography (Chromatographic Methods Series)*, Hüthig, Heidelberg, 1982, pp. 19–23 and 179–184.
4 J. Toei, *Fresenius' Z. Anal. Chem.*, 331 (1988) 735–739.
5 C. Kantipuly, S. Katragadda, A. Chow and H.D. Gesser, *Talanta*, 37 (1990) 491–517.
6 M.L. Marina, V. Gonzalez and A.R. Rodriguez, *Microchem. J.*, 33 (1986) 275–294.
7 L. Ebdon, H.W. Handley, P. Jones and N.W. Barnett, *Mikrochim. Acta*, II (1991) 39–47.
8 P. Jones and G. Schwedt, *J. Chromatogr.*, 482 (1989) 325–334.
9 O.J. Challenger, S.J. Hill, P. Jones and N.W. Barnett, *Anal. Proc.*, 29 (1992) 91–93.
10 P. Jones, O.J. Challenger, S.J. Hill and N.W. Barnett, *Analyst*, 117 (1992) 1447–1450.
11 J.R. Jezorek and H. Freiser, *Anal. Chem.*, 51 (1979) 373–376.

Journal of Chromatography, 639 (1993) 207–214
Elsevier Science Publishers B.V., Amsterdam

CHROM. 24 991

Indirect introduction of liquid samples in gas correlation chromatography

D.J. Louwerse and H.C. Smit*

University of Amsterdam, Laboratory for Analytical Chemistry, Nieuwe Achtergracht 166, 1018 WV Amsterdam (Netherlands)

(First received December 16th, 1992; revised manuscript received February 18th, 1993)

ABSTRACT

An injection device, indirectly introducing liquid samples, for gas correlation chromatography is described. It introduces the liquid sample without disturbing the constant gas flow necessary for correlation chromatography. This is achieved by separation of the evaporation from the actual injection. An interesting feature of this system is the ease of performing correlation chromatography in a differential mode.

INTRODUCTION

Correlation chromatography (CC) or multiplex chromatography has been known for several decades. Compared with conventional chromatography, a lower detection limit can be achieved without preconcentration of the sample. Injections are performed according to a pseudo-random binary sequence (PRBS), containing $2^n - 1$ periods of which $I = 2^{n-1}$ injections (n being a positive integer). Theoretically the detection limit can be reduced by $\sqrt{(I/2)}$ when the injection time of a single injection is equal to the PRBS period time at the cost of a doubled analysis time. The reason is that the sequence time length has to be equal to or larger than the chromatogram time length, and at least two sequences have to be injected successively. After the first sequence, called the presequence, the detector signal becomes circular, and the detector signal of the second sequence can be used to calculate the so-called correlogram with *e.g.*, a cross-correlation procedure.

Much effort has been applied to develop these techniques for determining (very) low concentrations [1–13]. Most applications were published in the field of correlation gas chromatography (CGC) [1–3,6–9,13]. All CGC applications, however, concern gaseous samples, headspace samples or liquid samples that were made gaseous first. This is in contrast to the common practice in gas chromatography (GC), where in most methods liquid samples are injected as such. Up to now this direct introduction of liquid samples has not been used in CGC, as specific problems arise.

Apart from the large amount of solvent introduced by the semi-continuous injections, probably the most important problem is the appearance of a pressure pulse caused by the evaporation of the liquid. This evaporation pulse disturbs the constant gas flow for a certain period of time. In conventional GC an evaporation pulse occurs only once, at the start of the chromatogram. The detector may give a response and a few moments after the injection the GC system stabilizes again. The separation process itself is hardly disturbed, and a detector response, if present, is of no value because components had not yet

* Corresponding author.

0021-9673/93/$06.00

arrived at the detector. In CGC, however, sample is injected semi-continuously. A disturbance of the gas flow with every injection is unacceptable, as it disrupts the stationary state of the system. For an optimally performing CC system, a stationary state is an important requirement.

In this paper, an injection device that does not disturb the stationary state of the system is described, being intermediate between the direct introduction of liquid samples and the introduction of gaseous samples. First the sample is (partly) evaporated, then the vapour of this sample is injected without disturbing the gas flow.

Liquid injection system

Fig. 1 shows a system for the indirect introduction of liquid samples in CGC. The important parts for CGC are the sample compartment located outside the gas chromatograph, the evaporation compartment and the injector. The evaporation compartment and the injector are located in an injector oven separated from the column oven. The sample and evaporation compartments are connected with a capillary used to introduce a liquid sample into the evaporation compartment. When the sample compartment is pressurized, liquid will be transported through the capillary from the sample compartment to the evaporation compartment. The temperature and the heat capacity of the evaporation compartment have to be high enough to evaporate the sample completely and immediately. The pressure of the evaporation compartment rises owing to the evaporation of the sample until an equilibrium is reached. When vapour is injected into the column, the pressure of the evaporation compartment falls. Liquid is transported through the capillary and evaporates owing to the high temperature until equilibrium is reached again. Only very small volumes of liquid need to be evaporated to replace a certain volume of gas because of the large difference in density between the liquid and gas phases.

As mentioned before, for CGC a constant gas flow through the GC column is required. It should not make any difference whether sample is injected or not. For this reason, it is necessary to tune the pressure of the nitrogen gas supply in such a way that the pressure in the evaporation compartment is equal to the pressure of the nitrogen carrier gas.

In the system described here, large amounts of vapour are injected (up to half of the time vapour may be injected). It can be expected that the separation conditions will be influenced and non-linearities will arise owing to the large differences in concentration of carrier gas and vapour, especially at the top of the column.

Mainly for reasons of pressure tuning and changes in separation, first a more symmetrical system was developed, which is outlined in Fig. 2. In this system both the sample and reference compartments contain liquid; the reference compartment contains, *e.g.*, pure solvent and the other compartment contains the sample. Nitrogen as a carrier gas is replaced with solvent vapour. Nitrogen is only used to maintain an adjustable pressure. After equilibrium, both evaporation compartments will have the same pressure.

The system under consideration can easily be used in a differential CC mode, as described by Laeven *et al.* [14] for liquid chromatography.

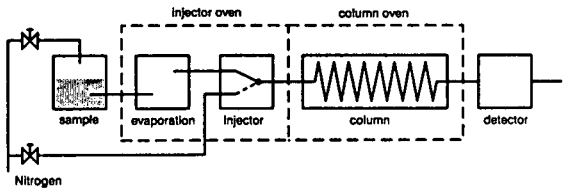

Fig. 1. Correlation gas chromatograph equipped with an indirect asymmetric device for liquid sample introduction.

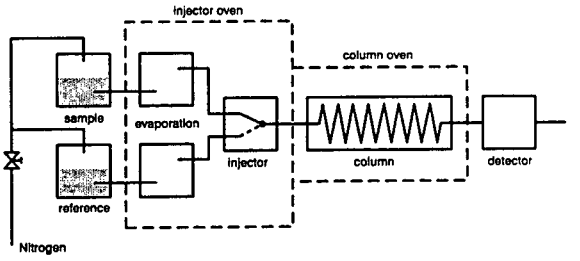

Fig. 2. Correlation gas chromatograph equipped with an indirect symmetrical device for liquid sample introduction.

When instead of pure solvent a known (standard) sample is used as a reference, only differences between the "unknown" sample and the other sample are measured.

A constant and equal pressure in both evaporation compartments can only be achieved when there is no significant pressure drop in one of the compartments when it starts to deliver gas to the chromatographic column. Assuming the evaporation of liquid is fast and a pressure drop due to a time consuming evaporation can be neglected, the pressure drop is negligible when the mass flow resistance of the capillary supplying the liquid is small compared with the mass flow resistance of the chromatographic column. The pressure drop over this liquid-supplying capillary can be described by the Hagen–Poiseuille law. This law is applicable for a laminar flow profile and an incompressible fluid:

$$\Delta P = \frac{8\Phi_m \eta l}{\pi r^4 \rho} \quad (1)$$

where:

ΔP = pressure difference (N m^{-2})
Φ_m = mass flow (kg s^{-1})
η = viscosity (kg m^{-1} s^{-1})
l = capillary length (m)
r = capillary radius (m)
ρ = density (kg m^{-3})

For gases eqn. 1 is not valid as they are compressible, the density ρ being dependent on pressure. However, to obtain a rough impression, eqn. 1 can be of limited use. When capillary GC columns are used, preferably the column inside diameter should not be larger than the diameter of the capillary supplying the liquid, as the pressure drop and the inside diameter are related to the fourth power. The length of the capillary supplying the liquid under normal conditions can easily be at least a factor of 100 smaller than that of a capillary GC column (which is usually 20 m or longer). The difference in density between liquids and gases is at least a factor of 100 when the pressure is low. Finally, the difference in viscosity can be a factor of 10–50 (28 for CS_2 liquid at 20°C and CS_2 vapour at 114°C [15]) between liquids and their vapour, depending on pressure and temperature. In most common cases the pressure drop over the capillary supplying the liquid can be small or negligible.

Separation/detection

In both systems described the separation conditions will change compared with conventional chromatography. In the first, asymmetric, system (Fig. 1), a large number of injections also introduce substantial amounts of solvent vapour. Depending on the actual amounts injected, up to 50% of the mobile phase is solvent vapour. This may give rise to non-linear chromatographic behaviour because of very large differences in concentration between sample, containing solvent vapour, and reference, containing carrier gas. The changed mobile phase composition of CGC compared with GC may also cause a separation difference between a single injection chromatogram and a correlogram. When the detector is sensitive to the solvent vapour, a very large solvent peak in the correlogram appears, which may cause so called correlation noise in the correlogram [14]. Correlation noise can be defined as noise present in the correlogram that does not originate from detector noise. This correlation noise caused by the solvent peak may disturb the determination of the other peaks, especially when the other peaks are small compared with the solvent peak.

The second, symmetrical, system (Fig. 2) differs even more from a conventional chromatographic system. The mobile phase only consists of liquid vapour. Instead of, *e.g.*, nitrogen, solvent vapour is used as the carrier gas. The use of solvent vapour as a carrier gas has been reported previously [16–21]. Large concentration differences between solvent vapour and mobile phase are eliminated. Therefore, non-linear chromatographic behaviour will not appear as quickly in this symmetrical system as in the other asymmetric system.

The detector must be able to cope with the large amounts of vapour involved. Therefore, if possible, a solvent is used that gives only a very small detector signal or does not respond at all. Another possibility is to use a differential detector, such as a heat conductivity detector.

EXPERIMENTAL

An existing CGC system, developed and tested for CC [22] in our laboratory, was used for the experiments. This system was modified to an indirect symmetrical liquid injection system as outlined in Fig. 2. Table I lists the equipment. As the injection device a pair of MOVPT-1/100 pneumatic needle valves (Scientific Glass Engineering) were used, controlled by a computer with an optocoupler as a circuit breaker. The valves were connected to the column by a 0.8-mm T-piece (Valco). The evaporation compartments, laboratory-made 300-cm^3 glass vessels, were connected to the needle valves by a 3 cm × 1.6 mm O.D. steel capillary. Glass vessels, as described above, were also used as sample and reference compartments. A piece of steel capillary connected the inlet of the sample and reference compartment to the nitrogen gas supply, without a significant pressure drop.

Fused-silica capillaries (50 cm × 0.2 mm I.D.) were connected between the sample compartment and its evaporation compartment and the reference compartment and its evaporation compartment. The injector oven, containing the injection device and the evaporation compartments, was a rebuilt temperature-controlled PV 4000 GC oven (Philips). The separations were performed on a 50 m × 0.32 mm I.D. open-tubular GC column, coated with 1.13-μm CP-Sil 5 CB (Chrompack). Table II gives the separation conditions.

Three samples were prepared; Table III gives the volume fractions of the compounds in carbon disulphide. 2-Methyl-2-butanol was purchased from BDH and other chemicals from Merck.

TABLE I

LIST OF EQUIPMENT

Apparatus	Type
GC	Packard Becker Model 421 with flame ionization detector
Injector	Laboratory-made
i–v converter	Atlas MAT DC60CH
Filter	24-dB low-pass filter, laboratory made
CC computer	Tulip dc386 with DAS-16 DAC/ADC controlled by Assyst
Data-handling computer	HP-9000/350

TABLE II

CHROMATOGRAPHIC CONDITIONS

Gas	Pressure (10^5 kPa)	Temperature control	Temperature (°C)
H_2	0.6	Injector	118
N_2	1.9	Column	110
Air	1.4	Detector	180

TABLE III

VOLUME FRACTION OF COMPOUNDS

Compound	Volume fraction (ml l^{-1})		
	1	2	3
Ethanol	0.5	0.5	0.5
2-Propanol	0.5	0.6	0.5
1-Propanol	0.5	0.5	0.5
2-Butanone	0.5	0.5	0.6
2-Methyl-2-butanol	0.5	0.5	0.5

The CC experiments were carried out with a PRBS of 511 elements and a clock period (the time length of one element) of 0.3 s. The data were collected with equal sampling time periods. A filter frequency of 1.2 Hz was chosen to avoid aliasing. To produce a correlogram at least two PRBSs were injected and the data collected during the last injection sequence were used to calculate the correlogram. For single-injection experiments, the data sampling period and filter frequency were chosen to be equal to those in the CC experiments.

RESULTS AND DISCUSSION

As already mentioned, the experiments were performed with the indirect symmetrical liquid injection system. A single-injection chromatogram (Fig. 3), a normal correlogram (Fig. 4a), an inverse-bit correlogram (Fig. 4b) and the inverse-bit subtracted from the normal correlogram (Fig. 4c) are shown for sample mixture 1 against a reference of pure carbon disulphide.

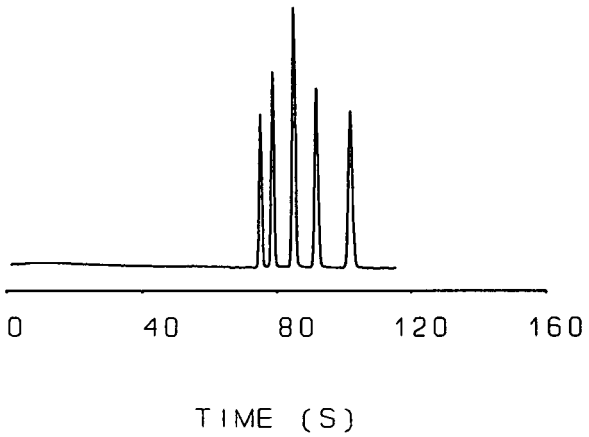

Fig. 3. Single-injection chromatogram obtained with the symmetrical system. A mixture of ethanol, 2-propanol, 1-propanol, 2-butanone and 2-methyl-2-butanol in carbon disulphide was analysed with carbon disulphide functioning as the carrier gas.

Carbon disulphide vapour functions as a carrier gas and has a low detector (flame ionization detector) response. The inverse-bit correlogram is obtained by inverting the injection-bits of the PRBS. A "1" represents "no injection" instead of an "injection" in case of a normal correlogram, and a "0" represents an "injection" instead of "no injection" [22].

The small peaks at 143, 147, 153, 6 and 16 s in the correlogram and the inverse-bit correlogram (Fig. 4a and b) are ghost peaks of the five main eluting components. The average time difference between a component peak and its corresponding ghost peak is 236.2 clock periods or 70.9 s. This corresponds very well with a theoretical expected value of 237 clock periods (71.1 s) for a first-order non-complementary ghost peak [22], also known as a λ3 ghost peak. This λ3 ghost peak may appear when a memory effect is present in the injection sequence. Comparing the normal correlogram with the inverse-bit correlogram, the sign of the ghost peaks with respect to the main peaks has changed. Theoretically, this is expected for first-order non-complementary ghost peaks. The ghost peaks disappear when the inverse-bit correlogram is subtracted from the normal correlogram in Fig. 4c. The noise level in Fig. 4c has been considerably reduced. Probably other small non-complementary effects are also present, as they are neutralized with subtraction [22,23]. Reproducible small pressure variations and injection errors due to the small clock period (the injector could not cope with smaller clock periods) might have caused these reproducible effects.

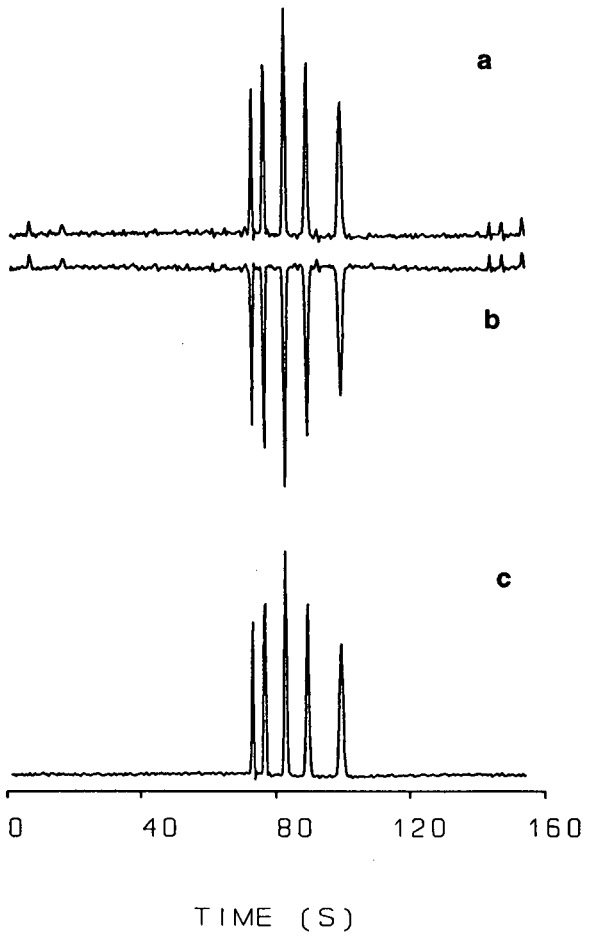

Fig. 4. (a) Correlogram, (b) inverse-bit correlogram and (c) the correlogram subtracted from the inverse-bit correlogram. The system used and the mixture analysed are identical with those in Fig. 3.

Comparing the retention times of the single-injection chromatogram with the correlogram, the components of the single injection elute on average 2.1 s later. This phenomenon has been observed and explained before in CC [23]. Owing to the many injections, the concentration level of the components is relatively high all over the column during a CC experiment, whereas

during a single injection this is not the case. These high concentrations act as a modifier of the mobile phase, making the components elute sooner. In this instance, however, it cannot explain the retention time shift, as exactly the same shift is also observed in the experiments below, where high component concentrations are present both in the sample and in the reference.

An undesired pressure drop in the evaporation compartments can explain this phenomenon and it is assumed that this causes the retention shift. When a pressure drop in the evaporation compartments is caused by the supply of gas to the column, during a CC experiment the pressure drop will be approximately the same in both the sample and reference compartments, as the injector often switches from sample to reference and both evaporation compartments supply gas to the column for an equal amount of time. In a single-injection experiment, most of the time the gas is supplied by the reference evaporation compartment. Assuming the pressure drop in this compartment is small compared with the total pressure over the column, it can be estimated to be approximately double the pressure drop in the CC experiments. The observed time shift was 2.1 s (this equals a time shift of ±2.5%). When the preceding assumptions are correct, and it is also assumed that within a small pressure range the column pressure is inversely related to the retention time, a pressure drop of ±2.5% is expected for CC experiments and ±5% for a single-injection chromatogram.

Differential CC experiments are shown in Figs. 5 and 6. Sample mixture 2 was measured against reference mixture 3. A single-injection chromatogram (Fig. 5), a normal correlogram (Fig. 6a), an inverse-bit correlogram (Fig. 6b) and the inverse-bit subtracted from the normal correlogram (Fig. 6c) are shown. The same ghost peaks appear as described before at exactly the same places relative to the main components. They also are identified as first-order non-com-

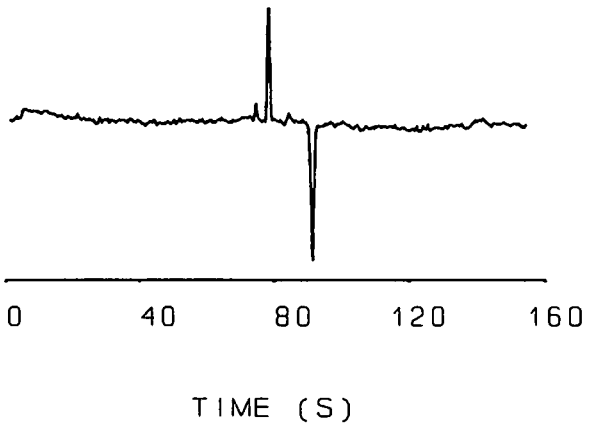

Fig. 5. Differential single-injection chromatogram obtained with the symmetrical system. A mixture of ethanol, 2-propanol, 1-propanol, 2-butanone and 2-methyl-2-butanol in carbon disulphide was analysed (sample). A mixture with the same components present in equal or changed amounts was used as the carrier gas (reference).

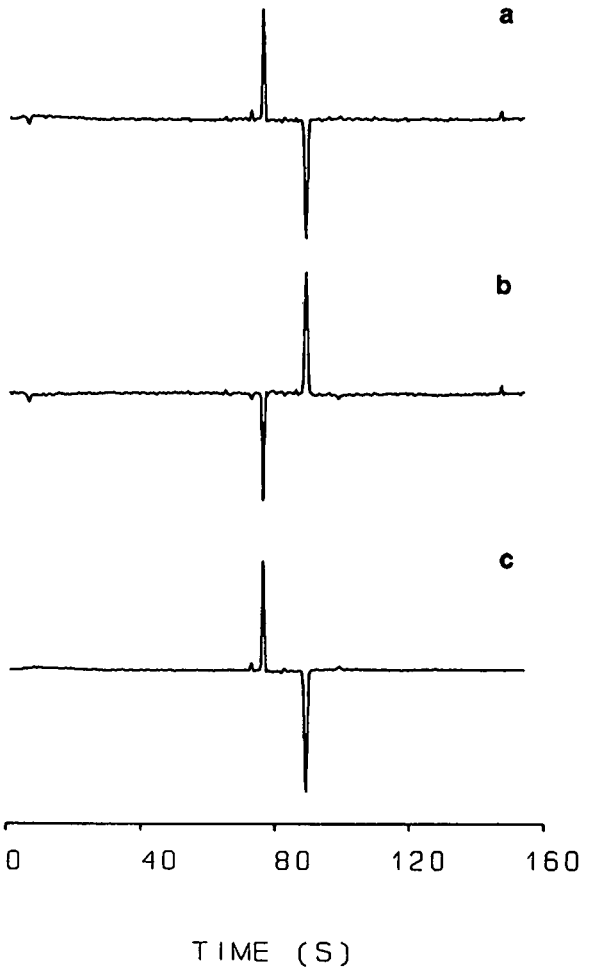

Fig. 6. Differential correlograms. (a) Correlogram, (b) inverse-bit correlogram and (c) the correlogram subtracted from the inverse-bit correlogram. The system used and the mixtures analysed are identical with those in Fig. 5.

plementary ($\lambda 3$) ghost peaks; the ghost peaks disappear when the inverse-bit correlogram is subtracted from the normal correlogram (Fig. 6c). The positive peak in Figs. 5 and 6 relates to the extra 0.1 ml l^{-1} of 2-propanol in mixture 2 relative to mixture 3. The opposite is valid for butanone: mixture 2 contains 0.1 ml l^{-1} less than mixture 3, so a negative peak appears in the chromatogram and correlogram. The other three components are hardly present in the correlogram, except possibly for ethanol. Taking the peak heights in Figs. 3–6 concerning ethanol and 2-propanol into consideration, the ethanol content in mixture 2 is estimated to be 0.01 ml l^{-1} higher compared with mixture 3.

CONCLUSIONS

The results demonstrate that the indirect introduction of liquid samples in CGC is not only possible in theory but also in practice. An existing CGC system can be extended without much difficulty to the use of indirect liquid injection. For this purpose the injector together with the evaporation compartments have to be placed in an injector oven apart from the column oven in order to maintain separate temperature control. Experiments show that even if a small pressure drop in the evaporation compartments is present during the CC process, still very reasonable results can be obtained with CGC. Both evaporation compartments will have approximately the same pressure drop, as there is a continuous switching due to the PRBS injection pattern. If needed, the pressure drop can be decreased by using a capillary with a larger diameter to supply the liquid to the evaporation compartment. When an injection device is developed especially dedicated for indirect liquid sample introduction in CGC, special attention has to be paid to preventing a significant pressure drop.

Compared with conventional GC, the system has been changed. The carrier gas consists completely of solvent vapour when a symmetrical system is used. One should be aware of the fact that the separation may change, which might complicate the analyses. On the other hand, an extra dimension is added when the content of a solvent (mixture) is used to optimize the separation. A solvent (mixture), however, always has to be chosen in agreement with the detector in order to avoid a non-linear detector response or an overloaded detector.

One of the main advantages of the symmetrical system is the possibility of determining differences in concentration that are small with respect to the total concentration between two samples using differential CC. It can therefore be a powerful tool for monitoring the concentrations of various components in process control. A process sample can be measured against an "optimum" reference sample. The level of the components present in this reference sample can be chosen in such a way that it represents the optimum process conditions. The resulting correlogram will only show the components of the process sample that have a different concentration level with respect to the reference sample, and only differential peaks (positive or negative) appear in the correlogram. Because of the multiplex advantage of CC, more accurate results may be obtained compared with conventional chromatography. Differences between a sample and an (optimum) reference sample that can hardly be distinguished or not at all by conventional chromatography can be determined accurately using differential CC. Therefore, the introduction of an indirect liquid injection system for CGC opens up a new field of applications in CC, which could not previously be achieved.

REFERENCES

1 H.C. Smit, *Chromatographia*, 3 (1970) 515.
2 G.C. Moss and K.R. Godfrey, *Instrum. Technol.*, 20 (1973) 33.
3 R. Annino, M.F. Gonnord and G. Guiochon, *Anal. Chem.*, 51 (1979) 379.
4 H.C. Smit, *Anal. Chim. Acta*, 122 (1980) 201.
5 H.C. Smit, T.T. Lub and W.J. Vloon, *Anal. Chim. Acta*, 122 (1980) 267.
6 R. Annino and J. Leone, *J. Chromatogr. Sci.*, 20 (1982) 19.
7 J.R. Valentin, G.C. Carle and J.B. Phillips, *Anal. Chem.*, 57 (1985) 1035.
8 J.B. Phillips, D. Luu, J.B. Pawliszyn and G.C. Carle, *Anal. Chem.*, 57 (1985) 2779.
9 M. Kaljurand and E. Küllik, *Trends Anal. Chem.*, 4 (1985) 200.

10 T.T. Lub, H.C. Smit and H. Poppe, *J. Chromatogr.*, 149 (1978) 721.
11 C. Mars and H.C. Smit, *Anal. Chim. Acta*, 228 (1990) 193.
12 D.P. Carney and J.B. Phillips, *Anal. Chem.*, 58 (1986) 1251.
13 E. Küllik and M. Kaljurand, *Anal. Chim. Acta*, 181 (1986) 51.
14 J.M. Laeven, H.C. Smit and J.C. Kraak, *Anal. Chim. Acta*, 194 (1987) 11.
15 R.C. Weast (Editor), *Handbook of Chemistry and Physics*, CRC Press, Cleveland, OH, 64th ed., 1983, pp. F40–F43.
16 K.L. Wagaman and T.G. Smith, *J. Chromatogr. Sci.*, 9 (1971) 241.
17 A. Nonaka, *Anal. Chem.*, 45 (1973) 483.
18 B.A. Rudenko, M.A. Baydarovtseva and V.A. Kuzovkin, *J. Chromatogr.*, 112 (1975) 373.
19 T. Tsuda, N. Tokoro and D. Ishii, *J. Chromatogr.*, 46 (1970) 241.
20 T. Tsuda and D. Ishii, *J. Chromatogr.*, 87 (1973) 554.
21 T. Tsuda, H. Yanagihara and D. Ishii, *J. Chromatogr.*, 101 (1974) 95.
22 R. Mulder, P.J. Hoogerbrugge and H.C. Smit, *Chemometr. Intell. Lab. Syst.*, 1 (1987) 243.
23 M. Engelsma, D.J. Louwerse, H.F.M. Boelens, W.Th. Kok and H.C. Smit, *Anal. Chim. Acta*, 228 (1990) 209.

Journal of Chromatography, 639 (1993) 215–220
Elsevier Science Publishers B.V., Amsterdam

CHROM. 24 986

Quantitative comparisons using gas chromatography–mass spectrometry and dual-isotope techniques for detection of isotope and impurity interferences

Lawrence C. Thomas*, Kathleen M. Fiehrer and John A. Edwards

Department of Chemistry, Seattle University, Broadway and Madison, Seattle, WA 98122 (USA)

(First received September 11th, 1992; revised manuscript received February 17th, 1993)

ABSTRACT

Dual-isotope methods for special quantitative comparisons using GC–MS are evaluated for assessing interferences in reaction experiments. The procedure is suitable for detecting interferences from impurities in reactants, errors due to isotope exchange and effects of kinetic differences between labeled and non-labeled forms. Combined reaction of both isotopic forms of test compounds in the same reaction system, followed by concurrent pretreatment and GC–MS measurements, allow for special ratios to be tested statistically to determine if the interferences are significant.

The comparisons may be relatively unaffected by large uncertainties in pretreatment and measurement steps and thus may yield greatly improved results relative to corresponding conventional assessments. Moreover, concentrations of the individual eluates need not be known and eluate identifications may not be required for proper use of this approach.

INTRODUCTION

Dual-isotope methods can be used for quantitative analyses or comparisons [1–4]. Radioactive isotopes are used in dual-label studies to take advantage of the good selectivity and high sensitivity of radiometric measurements, but are typically restricted to only special procedures, partly due to potential health hazards or regulations. Alternatively, non-radioactive isotopic labels may be preferred, and mass spectrometry (MS) measurements may be useful with them if sufficient mass discrimination and sensitivities may be attained.

Dual-isotope MS methods which mimic isotope dilution, using equilibrated mixtures of isotopically labeled target compounds have been used for years [5] and have been adapted to important environmental determinations [6]. A known amount of that analyte's selected isotopically labeled form is added to samples before pretreatment and measurement and the two analyte forms thereby undergo identical treatment. An appropriate subsample is then analyzed by GC–MS with each analyte and its corresponding isotopically labeled form measured via characteristic m/z values.

GC–MS measurements are especially helpful in experiments involving many analytes, partly because GC–MS can provide excellent selectivity and high sensitivity. Resulting low limits of detection and freedom from many interferences can thus make GC–MS procedures powerful quantitative methods. The use of GC–MS for complicated analyses is well-established, and a variety of versatile commercial instruments are available. However, several factors plague GC–MS procedures for analyte measurements from complex sample matrices, predominantly in pretreatment steps [7]. Variations in extraction efficiencies, variable losses during solvent volume

* Corresponding author.

0021-9673/93/$06.00

reductions and other factors can be partially compensated by traditional recovery standard and internal standard techniques [8], sometimes using added compounds which are isotopically labeled but otherwise identical to target analytes [5,6]. Consequently, those techniques require both availability and careful characterization of appropriate reference materials for *every* measured component. Unfortunately, for complex systems such as studies of metabolisms or environmental exposures, several reaction product analytes may be measured for each sample, which exacerbates difficulties associated with use of internal standard methods, especially if pure reference materials are not available for every analyte. Moreover, identities of the reaction product analytes are not always known, which precludes use of conventional internal or external standard methods [2–4].

In previous work, compounds labeled with two different radioactive isotopes were used with high performance liquid chromatography (HPLC) for special dual-label procedures which mimic multiple internal standard methods [1–4,9,10]. The dual-label approaches allow for compensation for: (a) variations in extraction efficiencies, (b) variable losses during concentration of extracts, (c) imprecisions of volume measurements, and (d) uncertainties in specific activities of reactant compounds and reaction products. Moreover, the procedures may greatly obviate difficulties caused by unavailability of pure reference compounds. For special cases [3,10] dual-isotope GC–MS procedures may be used for quantitative comparisons to evaluate: (a) effects of impurities on reaction product formation experiments, (b) effects of isotope exchange upon those experiments, and (c) effects of kinetic differences between the forms which may be caused by their different respective masses. Moreover, theoretically valid comparisons which may be tested statistically are allowed by those methods and show dramatic increases in quality of results when compared to conventional procedures [4,10]. The dual-label techniques are powerful for comparing reaction efficiencies for multiple pathway reactions [2,4] and for assessing complications caused by impurities or isotope effects [3,10].

Dual-isotope GC–MS procedures reported in this study show many of the advantages of dual-label radiometric methods described above, but avoid use of radioactive materials.

THEORY

A main advantage of the dual-isotope procedures for GC–MS measurements for assessing isotope and impurity effects is that special ratios may yield well-defined, theoretically predictable results which can be tested statistically [2–4,10]: one may concurrently react in the same solution both an isotopically labeled (X-labeled) test compound and the same compound which is unlabeled, (herein called Y-labeled) with perhaps one or both being of unknown concentration. If the two differently labeled reactant compounds are chemically identical, their respective reaction products also typically will be identical, except for their respective molecular masses; this equivalence is a reasonable assumption unless isotope exchange occurs during reaction, or if kinetics are affected as a result of differences in isotopic masses. Moreover, if the reaction products are pretreated together in the same solution prior to measurement, the pretreatments will typically have equivalent extraction/concentration/dilution efficiencies, E, for the two forms of each reaction product i, *i.e.*, $E_{X,i} = E_{Y,i}$. Thus, if V_a is the volume of the pretreated sample solution derived from the reaction mixture, V_{ss} is the volume of the prepared subsample used for chromatographic separation, and M is the mass of specified analyte in the original sample, then $A_{X,i} = (V_{ss}/V_a)M_{X,i}E_{X,i}S_{X,i}$ and $A_{Y,i} = (V_{ss}/V_a)M_{Y,i}E_{Y,i}S_{Y,i}$, where $A_{X,i}$ and $A_{Y,i}$ are measured GC–MS areas, respectively, for the X-labeled and unlabeled forms of eluate component i from volume V_{ss}, and $S_{X,i}$ and $S_{Y,i}$ are the integrated response factors for GC–MS measurement of the m/z values characteristic for the respective measured species [11].

Intrasample comparisons

To evaluate isotope or impurity effects for reaction systems, special intrasample ratios can be defined for X *vs.* unlabeled reaction products.

For this, V_a and V_{ss} are respectively identical for both labeled and unlabeled forms of each reaction product taken together from the same sample solution. Accordingly, as $E_{X,i} = E_{Y,i}$, a ratio of respective masses can be calculated and $M_{X,i}M_{Y,i}^{-1} = (A_{X,i}S_{Y,i})(A_{Y,i}S_{X,i})^{-1}$ for any component i. Furthermore, separated reaction products, i *vs.* j, derived from the same reaction experiment can then be compared.

$$Q_{ij} = (M_{X,i}M_{Y,i}^{-1})(M_{X,j}M_{Y,j}^{-1})^{-1}$$
$$= (A_{X,i}A_{Y,j})(A_{Y,i}A_{X,j})^{-1}(S_{Y,i}/S_{X,i})$$
$$\times (S_{Y,j}/S_{X,j})^{-1}$$

If relative integrated response factors for components i and j are known, then Q_{ij} may be calculated from GC–MS area data in combination with those appropriate $S_{Y,i}/S_{Y,j}$ and $S_{X,i}/S_{X,j}$ ratios. Moreover, if the relative integrated response factors for both i and j are directly proportional to their relative injected amounts [11], *i.e.*, fulfill a basic assumption for common internal standard procedures, then $Q_{ij} = (A_{X,i}A_{Y,i})(A_{Y,i}A_{X,j})^{-1}$. Thus, Q_{ij} may be computed from measured GC–MS area data of the dual-isotope chromatograms only.

If there has been neither isotope exchange nor differences in kinetics, nor contributions to the specific components due to impurities and the data used are sufficiently precise, then $Q_{ij} = 1$; that is, the relative isotopic composition for the components is the same. If isotope effects or impurities cause interferences, then Q_{ij} may be significantly different than unity, and one may test Q_{ij} statistically for each i,j pair through replications and a null hypothesis that the measured reaction products are unaffected by impurities or isotope effects: If, statistically, $Q_{ij} \neq 1$ one may not accept the null hypothesis.

Intersample comparisons

Similarly, one may compare intersample Q-ratios to ascertain intersample differences due to impurities or isotope effects; for compound i, $Q_{12,i} = (M_{X,i,1}M_{Y,i,1}^{-1})(M_{X,i,2}M_{Y,i,2}^{-1})^{-1}$ for comparisons for samples 1 *vs.* 2, both resulting from reactions of identical aliquots of the same test solution containing both X- and Y-labeled reactant. Conveniently, if the relative integrated response factors do not vary, *i.e.*, $(S_{X,i,1}/S_{Y,i,1}) = (S_{X,i,2}/S_{Y,i,2})$, for those intersample comparisons, then $Q_{12,i} = (A_{X,i,1}A_{Y,i,2})(A_{X,i,2}A_{Y,i,1})^{-1}$, which can be readily calculated from GC–MS area data only and can be tested statistically for $Q_{12,i} = 1$, as above.

Likewise, intrasample comparisons can be extended to comparisons of two or more component concentration ratios relative to the same components in intersample sets of measurements, *e.g.*, $Q_{ij,1}/Q_{ij,2} = Q_{ij,12}$. This might correspond to comparing products of two reaction pathways and $Q_{ij,12} = 1$ if the reaction product profiles are unaffected by impurities or isotope effects. Again, the Q-ratio can be calculated from GC–MS area data only and replications can be tested statistically.

EXPERIMENTAL

Reagents

Anthracene and decadeuterated anthracene were purchased from Aldrich, both at >99% purity. All solvents used were of ChromAR grade from Mallinckrodt and helium carrier gas was >99.9995% pure.

Apparatus

A Hewlett-Packard Model 5971A mass-selective detector interfaced to a Hewlett-Packard Model 5890 Series II gas chromatograph was used, controlled and monitored by a Hewlett-Packard Model QS-20 Vectra computer. Automated MS optimizations were performed daily using provided algorithms. Helium was used as the carrier gas at 50 kPa pressure in the split-splitless inlet, yielding a 1.0 ml min^{-1} flow-rate out of the 12 m × 0.2 mm I.D. (0.33-μm film thickness) cross-linked methylsilicone fused-silica capillary column at 25°C. A splitting ratio of 60:1 was used, with a 1.0-min splitless period after each injection. Injection volumes of 1.0 μl were used, as indicated below.

Procedures

Solutions of anthracene and [$^2H_{10}$]anthracene were prepared in methanol, $4.1 \cdot 10^{-4}$ M and $3.8 \cdot 10^{-4}$ M, respectively. Measured volumes of

the two solutions were mixed to 10 ml total volume, yielding relative concentrations, [anthracene]/[[$^2H_{10}$]anthracene], varying between 10^{-3} and 10^3. The mixed solutions were exposed to sunlight through window glass for 35 days and then stored at 0°C in darkness until used.

Four subsamples for each dilution of the methanolic reactants and their photolysis products were measured via GC–MS. Over several days' duration, 1-μl subsamples were injected into the 325°C injector, in splitless mode, with oven temperature at 60°C. The 60°C initial temperature was maintained for 5 min, then raised to 120°C at 10°C min^{-1}, held at 120°C for 2 min, raised to 160°C at 2°C min^{-1}, held at 160°C for 2 min, raised to 250°C at 5°C min^{-1} and maintained at 250°C for 2 min. The GC–MS transfer line was isothermal at 285°C.

Eluates were measured by selected-ion monitoring (SIM) unless stated otherwise. Between retention times of 15 min and 30 min, ions at m/z = 178, 180, 188, 190, 208 and 216 were monitored every 0.81 s with 100 ms measurement times for each. Between retention times of 30 min and 45 min, ions at m/z = 194, 202, 203, 208, 216 and 217 were monitored every 0.69 s with 100 ms measurement times for each. Selected ion chromatograms were produced and integrated via provided algorithms, and statistical calculations were made by conventional techniques. For tentative eluate identifications using full m/z scanning detector currents for m/z values between 50 and 250 were measured at a rate of 2.4 scans s^{-1}, between retention times of 15 min and 45 min.

RESULTS AND DISCUSSION

Several subsamples of anthracene–[$^2H_{10}$]anthracene mixtures and their respective photolysis products were separated by GC–MS with m/z scanning. Anthracene (parent ion = 178 m/z) and [$^2H_{10}$]anthracene (parent ion = 188 m/z) were identified by their mass spectra at elution times of 27.2 min and 27.1 min, respectively. Similarly, 9,10-anthracenedione (anthraquinone, parent ion = 208 m/z) and its corresponding octadeuterated species (parent ion = 216 m/z) were tentatively identified at elution times of 35.9 min and 35.7 min, respectively. None of the identifications were confirmed by supplemental methods, as true identities need not be known for Q-ratio evaluations. Other eluates were present but showed significant peak overlaps or insufficient ion currents for reliable measurements.

The selected eluate pairs measured by SIM (see Fig. 1) fulfilled the basic relative sensitivity assumption for use with Q-ratios. They showed linear relative response *vs.* relative initial reactant concentration relations, *i.e.*, linear log/log relations with slope = 1, over approximately three orders of magnitude (see Fig. 2). These individual GC–MS measurements had good relative precisions of approximately ±10% with nonlinearities at extremes due to one of the amounts being near its limit of reliable measurement and hence showing Poisson data distributions for non-zero entries. Although the initial reactant concentrations were controlled, none of the

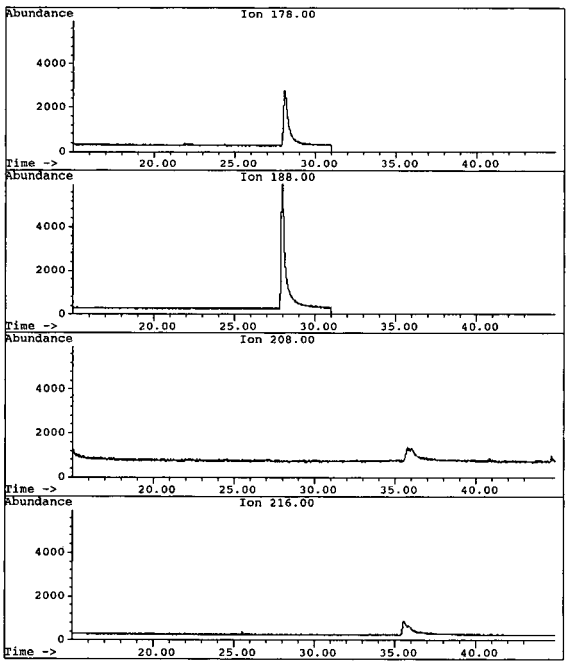

Fig. 1. Selected-ion (SIM) chromatograms for m/z values 178, 188, 208, 216 for 1-μl subsample of a photolyzed solution with [[$^2H_{10}$]anthracene]/[anthracene] = 2.0. Time in min.

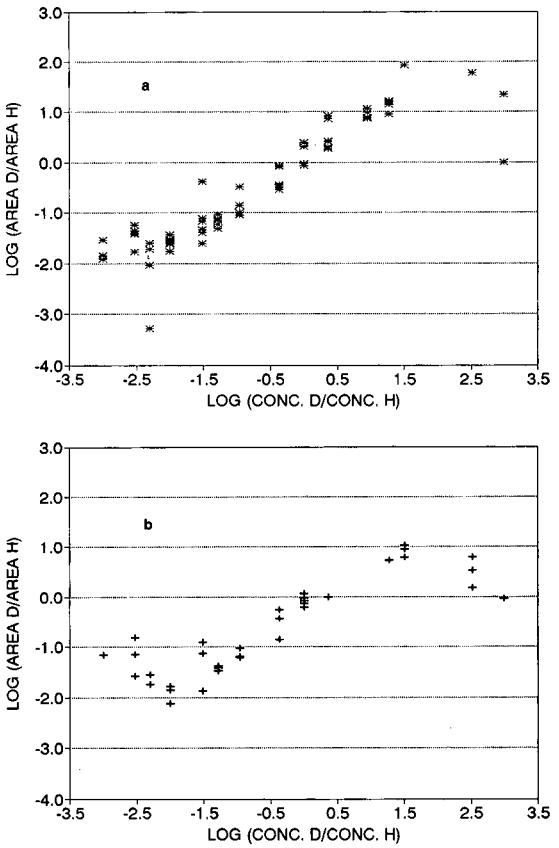

Fig. 2. Relative GC–MS areas log ($Area_{[^2H_{10}]anthracene\ product}$ $Area_{anthracene\ product}$) *vs.* log of relative concentrations of reactants prior to reaction, pretreatment and measurements: (a) $[^2H_{10}]$anthracene/anthracene, (b) probable $[^2H_8]$anthraquinone/anthraquinone.

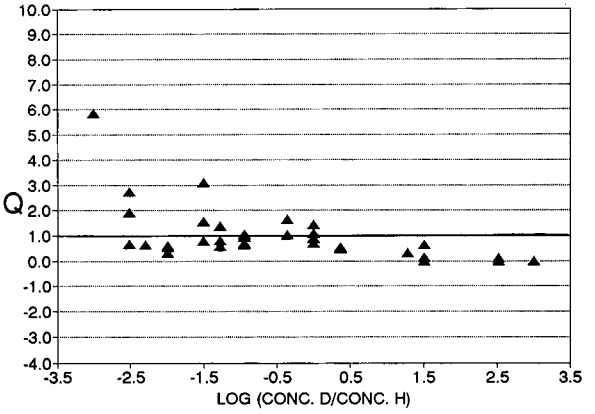

Fig. 3. *Q*-ratios *vs.* log of relative concentrations of reactants prior to reaction, pretreatment and measurements. *Q*-ratio here is $(A_{[^2H_8]anthraquinone}/A_{anthraquinone})/(A_{[^2H_{10}]anthracene}/A_{anthracene})$.

postreaction concentrations were known. However, the relative integrated responses for corresponding labeled and non-labeled species varied directly (see Fig. 2) with initial reactant concentrations, which indicates compatibility with the use of the *Q*-ratios described above.

Q-ratios for anthracenes *vs.* tentatively identified anthraquinones were not statistically different than unity (Fig. 3) over the 2 1/2 orders of magnitude, $10^{-2.0}$ to $10^{0.5}$, spanning reliable measurements for all included components. Results in that range were consistent with the theoretical prediction, *i.e.*, acceptance of the null hypothesis, for reactions in the absence of impurity interferences or isotope effects.

The *Q*-ratio methods for GC–MS described herein are compatible with eluates of unknown concentrations and perhaps of unknown identities and therefore may be used when conventional techniques such as standard additions and isotope dilution are not feasible. They use well-accepted statistical tests and are useful for comparing relative concentrations, especially for evaluating interferences in dual-isotope reaction systems. The required GC–MS assumptions are similar to those accepted for dual-isotope GC–MS procedures which mimic isotope dilution. However, use with eluates of unknown identities has the risk of improper pairing of eluates and improper selection of appropriate m/z values for measurements.

ACKNOWLEDGEMENT

We thank the Petroleum Research Foundation for support of this work with grant PRF No. 25307-B5.

REFERENCES

1 T.R. Roberts, *Radiochromatography*, Elsevier, Amsterdam, 1978.
2 L.C. Thomas and T.L. Ramus, *Anal. Chim. Acta*, 154 (1983) 143. .
3 L.C. Thomas and T.L. Ramus, *Anal. Lett.*, 17 (1984) 2001.
4 L.C. Thomas and C.L. Wood, *J. Chromatogr.*, 522 (1990) 117.

5 A.V. Grosse, S.G. Hindin and A.D. Kirshenbaum, *Anal. Chem.*, 21 (1949) 386.
6 *Method 1624, Revision C and Method 1625, Revision C*, US Environmental Protection Agency, Washington, DC, 1988.
7 W.D. MacLeod, Jr., A.J. Friedman and D.W. Brown, *Marine Environ. Res.*, 26 (1988) 209.
8 W.D. MacLeod, Jr., P.G. Prohaska, D.D. Genero and D.W. Brown, *Anal. Chem.*, 54 (1982) 386.
9 L.C. Thomas, W.D. MacLeod and D.C. Malins, *Publ. No. 519*, National Bureau of Standards, Gaithersburg, MD, 1979, p. 79.
10 L.C. Thomas, *Talanta*, 39 (1992) 599–607.
11 L.C. Thomas and W. Weichmann, *J. Chromatogr.*, 587 (1991) 255.

Journal of Chromatography, 639 (1993) 221–226
Elsevier Science Publishers B.V., Amsterdam

CHROM. 25 030

Analysis of carbon monoxide by molecular sieve trapping

R.T. Talasek* and K.E. Daugherty

Department of Chemistry, University of North Texas, Denton, TX (USA)

(First received December 29th, 1992; revised manuscript received March 1st, 1993)

ABSTRACT

The determination of carbon monoxide is demonstrated trapping CO on preconditioned molecular sieve and thermal desorption. Analysis in this case is performed by gas chromatography–mass spectrometry, although the trapping technique is applicable to other suitable GC techniques. Storage of the trapped sample for an indefinite time is possible with no degradation, even at several tenths of mg m^{-3}. Detection limits of 100 $\mu g\ m^{-3}$ are reported with a linear dynamic range that permits analysis in the mg m^{-3} range. Balance gas interferences are reduced, but not eliminated.

INTRODUCTION

Carbon monoxide is one of many common pollutants that has come under increasing scrutiny in the last several years [1,2]. Carbon monoxide is most often produced from incomplete combustion of carbonaceous fuels such as coal, natural gas, and gasoline. Carbon monoxide is also suspected of contributing to ozone production [3]. To understand the total contribution of carbon monoxide to the environment, it is important to be capable of determining the high (mg m^{-3}) concentration associated with combustion emissions as well as the lower ($\mu g\ m^{-3}$) concentration associated with ambient or indoor measurements. Often it is necessary to determine instantaneous pollutant concentration to correlate with specific events, as well as an average measurement over a defined time period.

Carbon monoxide is often determined in source sampling using remote optical sensing [4], but this method is inconvenient for ambient or indoor sampling. Fourier transform infrared spectroscopy has been used to determine carbon monoxide concentrations in air [5], as well as CO-specific sensors of SnO_2 and other materials [6–10], but these usually require a continuous sample stream. Direct analysis of air using bombs or bags is often used to determine carbon monoxide in air. Gas chromatography has been used in many instances to determine carbon monoxide [11–14], but the most universal stationary phases for this type application are porous polymer materials such as the Porapak series (Waters Assoc.) and the Chromosorb "Century Series" (Johns-Manville) [15]. This separation technique cannot be used directly for air samples since at ambient temperature, carbon monoxide coelutes with air, making quantitation with a universal detector extremely difficult even at subambient GC temperatures. Carbon monoxide can be separated from air on molecular sieves, but the carbon dioxide and water content of most air samples makes frequent thermal conditioning necessary. A flame ionization detector in conjunction with a methanizer is capable of detecting carbon monoxide at low levels. Unfortunately, the metal catalysts used in methanizers are poisoned by exposure to large

* Corresponding author. Present address: Texas Instruments, Inc., P.O. Box 655012, M/S 301, Dallas, TX 75265, USA.

0021-9673/93/$06.00

quantities of oxygen, making them impractical for repeated air analysis. Also, percent level quantities of oxygen have been known to produce positive responses with a flame ionization detector, making quantitation of a coeluting carbon monoxide impossible. Carbon monoxide is also reactive with many materials including metals and plastics, making the storage of air samples with trace amounts of carbon monoxide in any container suspect.

Trapping of carbon monoxide may offer a solution to chromatographic interferences mentioned above, as well as potentially offering a stable method of storing samples while in transit to the laboratory for analysis. A passive sampler utilizing the trapping of carbon monoxide on specially treated zeolites has demonstrated quantitative recoveries [16]. Short-term immobilization has also been demonstrated on a molecular sieve porous-layer open tubular (PLOT) column [17]. It is possible that a suitable trap could be constructed to allow remote sampling by trapping, and subsequent laboratory analysis.

Detection by mass spectrometry offers a possible solution to coelution problems mentioned above. Operation of a mass spectrometer in the selective ion monitoring (SIM) mode may offer sufficient sensitivity for ambient air analysis. However, most gas analysis applications require relatively high carrier flow-rates necessary for packed columns and gas sampling valves. Typically, the pressure reduction required for the high vacuum of the mass spectrometer source is achieved by one of several interface types [18–32]. Unfortunately, none of these interfaces provide the desired sensitivity with low-molecular-mass compounds ($m/z < 50$), either due to poor discrimination or dilution in the interface. Direct interfacing of capillary columns to the ion source [33,34] was one of the first methods developed for sample introduction into the mass spectrometer, however smaller-diameter columns are incompatible with typical sample volumes (>0.1 ml) and flow-rates (*ca.* 10–30 ml min^{-1}) associated with the use of gas sampling valves, requiring sample splitting [35] and severely limiting sensitivity. Also the loss of column efficiency due to the "vacuum effect" is well documented [36,37].

The advent of fused-silica PLOT columns [38] with the porous polymer and molecular sieve stationary phases typically used in the analysis of low-molecular-mass gases [39–42] offers a possible compromise to a number of these problems. Wide-bore (0.53 mm) PLOT columns operate well at carrier flows compatible with gas sampling valves. By using a deactivated fused silica interface of sufficiently small internal diameter (0.2 mm) and sufficient length, the analytical column can be maintained at near atmospheric pressure, thereby preventing the loss of column efficiency mentioned above. This approach requires a differentially pumped mass spectrometer with sufficient pumping capacity to prevent high-pressure ionization effects such as chemical ionization. Two approaches that provide an appropriate combination of chromatography with mass-selective detection to achieve this determination are described here.

EXPERIMENTAL

A Hewlett-Packard (Avondale, CA, USA) 5988A quadrupole mass spectrometer equipped with a 5890A gas chromatograph was used for this study. This mass spectrometer is differentially pumped with an electron impact (EI) ion source. While pumping capacity in this configuration is more than adequate for typical narrow-bore capillary carrier flows, it is marginal for a minimum carrier flow of *ca.* 10 ml min^{-1} necessary for flushing a sample loop of sufficient volume in a short enough time to prevent severe band broadening. By separating the forelines of the two diffusion pumps, and using a separate 400 l min^{-1} foreline pump for the source diffusion pump, pumping capacity was increased significantly. This modified vacuum system is capable of maintaining a nominal source vacuum pressure of $2 \cdot 10^{-5}$ Torr (1 Torr = 133.322 Pa) at carrier flows of 10–15 ml min^{-1}. Carrier flows were calculated from averaged linear velocity measurements and column volume, since actual flow-rates are expected to be significantly different with the column end at atmospheric pressure and high vacuum. Average linear velocity was determined from the retention time of neon,

which is virtually unretained on these column materials.

A PoraPLOT Q (Chrompack, Raritan, NJ, USA) column 25 m × 0.53 mm was utilized for this application. A 5 m × 0.2 mm I.D. deactivated fused-silica capillary was used to directly interface the PLOT column to the mass spectrometer source and maintain the PLOT column at atmospheric pressure or above throughout the column, thereby avoiding loss of column efficiency. The butt connection was achieved with a zero dead volume union using special fused-silica adapter fittings (Valco Instruments). The typical chromatographic configuration used for gas samples was modified by inserting an additional 4-port valve between the injection valve and the column (Fig. 1). This configuration allows the trap to be inserted in the chromatographic flow, purged with carrier gas, heated independently of the gas chromatograph to desorb the carbon monoxide, and injected onto the column through appropriate sequencing of valves and heaters. Timing of valve switching was controlled by a digital valve sequence programmer combined with digital valve interfaces for each valve (Valco Instruments, Houston, TX, USA). The programmer also controlled the start of the mass spectrometer and chromatograph programs. Carrier gas was purified with a rare earth metal getter (SAES Getters, Colorado Springs, CO, USA) to reduce air impurities below detectable levels.

The trap was constructed from a Valco 4-port valve and fittings, and 1/16 in. O.D. × 0.03 in. I.D. (1 in. = 2.54 cm) 316L stainless-steel tubing. The empty trap volume in each case was approximately 1 ml. The tubing was packed with 180–220-mesh molecular sieves 3A, 4A, 5A and 13X (Alltech, Deerfield, IL, USA), and wrapped around a temperature-controlled column mandrel (Valco). Air samples were drawn through the sampler with a PAS-3000 battery-operated variable volume sampling personal air sampler (Supelco, Bellefonte, PA, USA). Fig. 2 schematically illustrates the trapping device.

Detection limit and linearity evaluations were conducted using a single stage dynamic blender using mass flow controllers to dilute NIST traceable standards [100 ppm (v/v) CO in nitrogen] (Scott Specialty Gas, Houston, TX, USA). The dilution gas was air.

Mass tuning and signal optimization for the most common GC–EI–MS applications (organic mixture analysis) are typically performed with a compound such as perfluorotri-*n*-butylamine (PFTBA), often utilizing a computerized optimization routine. These routines are typically designed to optimize performance at m/z values significantly larger than those of interest for this application. While mass calibration is usually still adequate, a significant gain in sensitivity was obtained by manually optimizing tuning parameters using molecular ions of air components (m/z

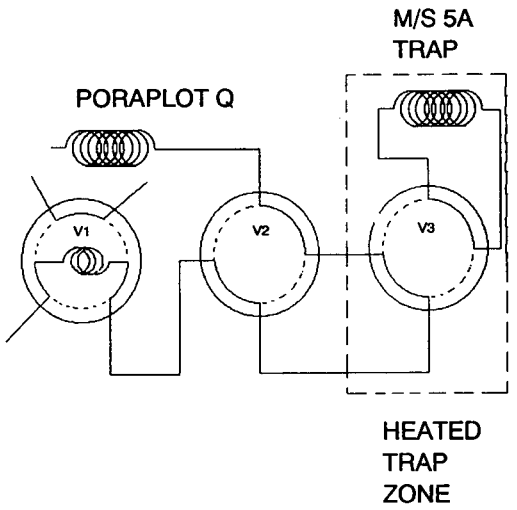

Fig. 1. Plumbing configuration for chromatographic utilization of molecular sieve (M/S) trap.

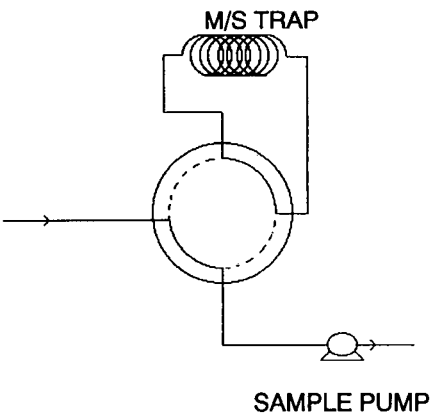

Fig. 2. Molecular sieve trap.

18, 28, 32). This is only possible with a system in which extreme care has been taken to maintain the air background at a sufficiently low level by minimizing leaks and maintaining sufficient carrier purity. A decrease in electron energy from 70 to 60 eV served to increase the molecular ion with respect to other fragments in all cases. Filament current was also increased from 300 to 400 μA to produce the maximum number of ions. Lens voltages were adjusted to attain maximum responses at these masses.

RESULTS AND DISCUSSION

The properties of molecular sieves when used as chromatographic stationary phases can be modified significantly by varying the water content of the media [43,44]. By modifying the conditioning temperature, carrier gas, and moisture content of the carrier gas, water content and therefore retention properties of the media can be drastically modified. Similar effects would be expected when molecular sieve is being used as a trapping media. Trapping efficiencies were evaluated for molecular sieves 3A, 4A, 5A and 13X. All materials were conditioned under flowing gettered helium for 24 h at 350°C to remove as much water as possible without affecting the molecular sieve structure. Recoveries were determined for each trap as a function of desorption temperature for a 1 mg m^{-3} concentration of carbon monoxide flowed over the trap for 1 min at 10 ml min^{-1}. Analysis was performed using the chromatographic configuration described earlier, and the timing sequence shown in Table I. The results are shown in Fig. 3. Both 3A and 13X show little propensity to act as effective trapping media. This was not unexpected, since carbon monoxide (3.12 Å molecular diameter) is larger than the effective diameter of 3A, and much smaller than 13X. Molecular sieve 4A shows a definite tendency to trap carbon monoxide, however adequate recoveries are never reached, indicating that perhaps carbon monoxide is too strongly bound. Only molecular sieve 5A shows reasonable recovery, therefore it was selected as the trapping media.

One of the improvements desired from this method is the elimination of the matrix gas (air in the case of environmental samples) from the trapped sample. Fig. 4 shows the SIM chromatograms at m/z 12, 28 and 32 for the molecular sieve 5A sample at 200°C from the above evaluation. Unfortunately, significant levels of oxygen and nitrogen apparently remain adsorbed to the trapping material. While the matrix is drastically reduced, it is not eliminated, thereby precluding the use of this method with universal detectors without adequate chromatographic separation. Also, m/z 28 (the molecular ion for CO, which occurs in the mass spectra at higher abundance than any other ion) cannot be used for quantitation by GC–MS, limiting the sensitivity of the

TABLE I

VALVE SEQUENCE AND TEMPERATURE PROGRAM FOR DESORPTION AND ANALYSIS FOR PLUMBING CONFIGURATION IN FIG. 1

Time (min)	Trap temperature	Valve position		
		V1	V2	V3
0.0	Ambient	1	2	1
0.1	Ambient	1	1	1
0.5	Ambient	1	1	2
2.0	Ambient	1	1	1
10.0	200°C	1	1	1
10.1	200°C	1	1	2
15	200°C	1	1	1
30	Ambient	1	1	1

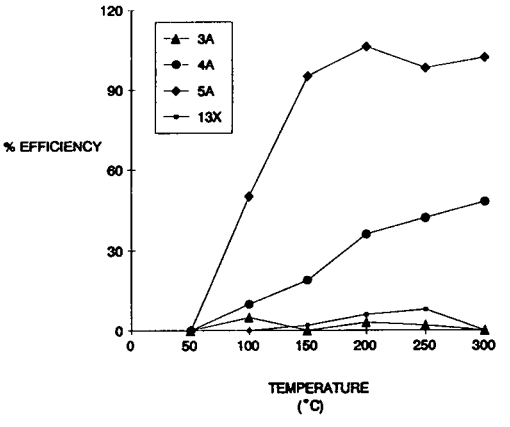

Fig. 3. Trapping performance for several common molecular sieves.

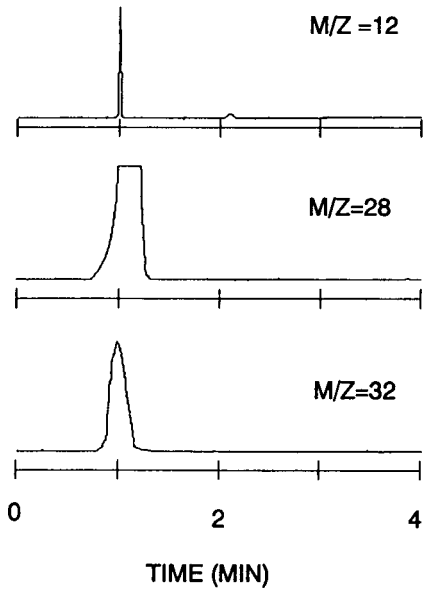

Fig. 4. Selected ion chromatograms for m/z 12, 28 and 32.

technique. The technique still provides acceptable results by monitoring m/z 12, and provides approximately a 100-fold improvement over direct analysis of CO in air using m/z 12. Other selective detectors, such as flame ionization detector–methanizer, should be applicable, although this was not evaluated here.

Since it was suspected that the trapping process was not totally irreversible at ambient temperature, the trapping efficiency was studied

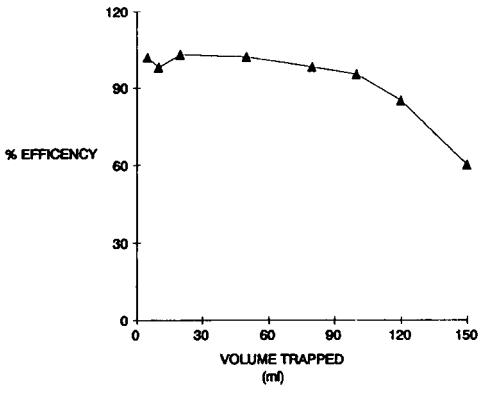

Fig. 5. Trapping efficiency *vs.* sample volume for molecular sieve 5A trap.

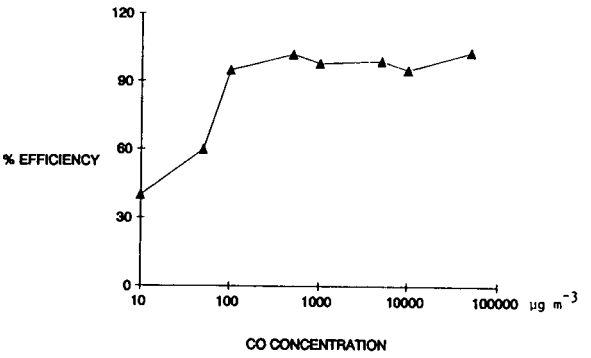

Fig. 6. Trapping efficiency *vs.* carbon monoxide concentration for molecular sieve 5A trap.

as a function of total air volume passed through the trap. The results are shown in Fig. 5. Non-linearity was observed at approximately 100 times the volume of the trapping material for 180–220-mesh 5A at ambient temperature. Mesh size, flow-rate and temperature are all expected to affect maximum trapping volume, but were not explored further. An evaluation of efficiency over four orders of magnitude of concentration of carbon monoxide using a constant volume of air demonstrated linear response with a negative deviation observed below about 100 μg m^{-3} as shown in Fig. 6. Sample stability over time was also a concern. To evaluated the stability of trapped samples, 1 mg m^{-3} of carbon monoxide in air was sampled with the 5A trap for 1 min and allowed to sit for 1–7 days. The trap was desorbed and analyzed by GC–MS. All results were found to be within 10% of the mean of the group.

CONCLUSIONS

The results summarized here demonstrate that trapping carbon monoxide on molecular sieve allows the collection of the analyte with elimination of most of the sample matrix, in the case of air. Carbon monoxide can be concentrated on the molecular sieve to achieve approximately a 100-fold increase in sensitivity with compatible techniques. Samples can be collected remotely and stored for an adequate period of time to allow transportation to a laboratory.

REFERENCES

1 P.J. Lioy, *Environ. Sci. Technol.*, 25 (1991) 1361.
2 R. Henrichs, *Res. J. Water Pol.*, 63 (1991) 310.
3 R. Crouse and H. Jeffries, *Proc. 1991 EPA/AWMA Int. Symp. Meas. Toxic Relat. Air Pollut.*, (1991) 10.
4 W.B. Grant, R.H. Kagann and W.A. McClenny, *J. Air Waste Manage. Assoc.*, 42 (1992) 18.
5 A.Q. McArver, *Proc. 1991 EPA/AWMA Int. Symp. Meas. Toxic Relat. Air Pollut.*, (1991) 58.
6 R. Ionescu, V. Vasilescu and A. Vancu, *Sens. Actuators B (Chem.)*, B8 (1992) 151.
7 J. Huusko, H. Torvela and V. Lantto, *Sens. Actuators B (Chem.)*, B7 (1992) 700.
8 N. Miura, H. Minamoto, G. Sakai and N. Yamazoe, *Sens. Actuators B (Chem.)*, B5 (1991) 211.
9 K. Marcinkoska, M.P. McGauley and E.A. Symons, *Sens. Actuators B (Chem.)*, B5 (1991) 91.
10 T. Maruyama, *Matl. Sci. Eng. A (Struc. Eng.)*, A146 (1991) 81.
11 R.N. Dietz, *Anal. Chem.*, 40 (1968) 1576.
12 A. Fish, N.H. Franklin and R.T. Pollard, *J. Appl. Chem.*, 13 (1963) 506.
13 A. Lawson and H.G. McAdie, *J. Chromatogr. Sci.*, 8 (1970) 731.
14 W.L. Thronsbury, *Anal. Chem.*, 43 (1971) 452.
15 O.L. Hollis, *Anal. Chem.*, 38 (1966) 309.
16 K. Lee, Y. Yanaglsawa, M. Hishinuma, J.D. Spengler and I.H. Billick, *Environ. Sci. Technol.* 26 (1992) 697.
17 R.T. Talasek and K.E. Daugherty, *J. Chromatogr.*, 635 (1993) 265.
18 E.J. Bonelli, M.S. Story, J.B. Knight, *Dyn. Mass Spectrom.*, 2 (1971) 177.
19 R. Rhyage, *Anal. Chem.*, 36 (1964) 759.
20 M. Blumer, *Anal. Chem.*, 40 (1968) 1590.
21 C. Brunee, H.J. Bultemann and G. Kappus, *17th Annual Conference on Mass Spectrometry and Applied Topics*, No. 46, Dallas (1969).
22 J. Copet and J. Evans, *Org. Mass. Spectrom.*, 3 (1970) 1457.
23 M.A. Grayson and R.L. Levey, *J. Chromatogr. Sci.*, (1971) 687.
24 M.A. Grayson and J.J. Bellina, *Anal. Chem.*, 45 (1973) 487.
25 P.M. Krueger and J.A. McCloskey, *Anal. Chem.*, 41 (1969) 1930.
26 J.T. Watson and K. Biemann, *Anal. Chem.*, 36 (1964) 1135.
27 M.A. Grayson and C.J. Wolf, *Anal. Chem.*, 42 (1970) 426.
28 P.M. Llewellyn and D.P. Littlejohn, presented at the *Pittsburgh Conf. Anal. Chem. Spectr. Pittsburgh, PA*, (1966).
29 W.H. McFadden, *J. Chromatogr. Sci.*, 17 (1979) 2.
30 R.F. Arrendale, R.F. Severson and D.T. Chortyk, *Anal. Chem.*, 56 (1984) 1533.
31 D. Henneberg, U. Henrichs, H. Husmann and G. Schromburg, *J. Chromatogr.*, 167 (1978) 139.
32 J.J. Stern and B. Abraham, *Anal. Chem.*, 50 (1978) 2161.
33 J.C. Holmes and F.A. Morrell, *Appl. Spectr.*, 11 (1957) 86.
34 R.S. Golke, *Anal. Chem.*, 31 (1959) 535.
35 S. Jacobsson and O. Falk, *J. Chromatogr.*, 497 (1989) 194.
36 P.A. Leclercq, G.J. Scherpenzeel, E.A.A. Vermeer and C.A. Cramers, *J. Chromatogr.*, 241 (1982) 61.
37 F.W. Hatch and M.E. Parrish, *Anal. Chem.*, 50 (1978) 1164.
38 J. de Zeeuw, R.C.M. de Nijs and L.T. Henrich, *J. Chromatogr. Sci.*, 25 (1987) 71.
39 K. Bachmann and F.J. Reineke, *J. Chromatogr.*, 323 (1985) 323.
40 N. Pelz, N.M. Dempster and P.R. Shore, *J. Chromatogr. Sci.*, 28 (1990) 230.
41 L.H. Henrich, *J. Chromatogr. Sci.*, 26 (1988) 198.
42 L. Do and F. Raulin, *J. Chromatogr.*, 19 (1965) 249.
43 R. Aubeau, J. LeRoy and L. Champeix, *J. Chromatogr.*, 19 (1965) 249.
44 B.M. Karlsson, *Anal. Chem.*, 38 (1966) 668.

Journal of Chromatography, 639 (1993) 227–238
Elsevier Science Publishers B.V., Amsterdam

CHROM. 25 012

Automatic on-line gas chromatographic monitoring of mixing of natural gas with liquefied petroleum gases under high pressure

Gary K.-C. Low

Division of Coal and Energy Technology, Lucas Heights Research Laboratories, Commonwealth Scientific and Industrial Research Organisation (CSIRO), PMB 7, Menai, N.S.W. 2234 (Australia)

(First received December 1st, 1992; revised manuscript received February 22nd, 1993)

ABSTRACT

An automated system was constructed for the on-line monitoring of the mixing of natural gas with liquefied petroleum gases under different temperature (10–45°C) and pressure (5–20 MPa) regimes. After the system was equilibrated, compressed samples from gas and liquid phases were isolated into high-pressure sampling loops through a series of switching valves before their expansion into variable-volumes syringes. The expanded samples were then analysed by a rapid-scanning, dual-channel gas chromatograph to give the distribution of hydrocarbon components in the respective phases.

The system was devised to overcome the problems associated with on-line sampling and GC monitoring of mixtures from reactions of low-molecular-mass hydrocarbons under high pressure where phase changes can occur. This system features rapid sampling under pressure from the phases; accurate sampling of small volumes (50–500 μl) from these phases without disturbing the reaction equilibrium; volume expansion of the compressed samples (maximum pressure at 20 MPa) so they are amendable to GC analysis; transport of the expanded gases to GC with minimum peak broadening; and finally, very rapid GC analysis (<1 min).

The system is computer-controlled to enable fully automatic operation. Data points from the respective phases of a mixture under a temperature and pressure regime can be obtained in a fraction of time required with conventional procedures.

INTRODUCTION

The phase behaviour of a hydrocarbon mixture depends on the temperature and/or pressure of the system. The mixture can exist in a single phase as a liquid or a gas, or a gas–liquid binary phase, or even a single supercritical fluid phase when the operating temperature and pressure is greater than the critical point of the mixture [1]. Therefore in examining a mixture of hydrocarbons under different temperature–pressure regimes it is important to know how many phases are present and the distribution of the components in these phases.

The automation of on-line GC monitoring of reaction of hydrocarbons under high pressure has always been a difficult area in that a number of obstacles have to be overcome: rapid and accurate sampling from different phases from the system under pressure; *in situ* volume expansion of the compressed samples without selectively precipitating the heavier components from the mixture in a phase (caused by the Joule–Thomson effect [2]); transport of expanded gases for GC analysis without loss of separation efficiency (due to large dead volume along the chromatographic circuit); and rapid GC analyses.

Previous studies [3,4] on gas mixtures under pressure usually involved separate manual operations of sampling, expansion and analysis. A preferred method was to trap the sample from a phase into a gas bag that resided inside a water-filled container [5]. The amount of sample taken was then estimated from the mass of the water

0021-9673/93/$06.00

displaced from the container after its expansion. The gas bag was then removed and an aliquot of the expanded gas was analysed by GC. This procedure, while it gave accurate results, was still cumbersome and time-consuming, sometimes requiring large volumes being sampled from the phases. The reaction equilibrium was often disturbed which prevented subsequent samples being taken from the same experiment. To obtain a complete reaction profile within a temperature–pressure range, it was necessary sometimes to run several parallel experiments that could be curtailed at different reaction intervals.

In the past, studies [6,7] on mixtures of hydrocarbons at different temperature and pressure regimes mostly have been confined to the phenomena of vapour–liquid equilibria. Recently, O'Brien *et al.* [8] have reported that the solubility of methane in low-molecular-mass hydrocarbons can be increased at moderately elevated pressure (<8 MPa). An implication to this finding is the possible enhancement of storage of natural gas (NG) in liquefied petroleum gases (LPG).

In Australia about 5% of vehicles are already fuelled by LPG comparing to the relatively fewer vehicles that are using NG (as compressed NG). The reasons for this are largely due to the low amounts of the fuel which can be carried onboard and the danger perceived by the public of carrying a highly pressurised gas in a vehicle. An increase in the usage of NG will only come when both the storage capacity and onboard transport safety can be improved. Australia has one of the largest reserves of NG in the world. An increase in its usage for transport purposes will not only reduce the expenditure for imported oils, but also will have positive impact to the environment since NG-powered vehicles emit lower hydrocarbons, carbon oxides, and smokes.

LPG is well-suited as a storage solvent for NG. It is abundant, being a cheap offcut in oil refining and also as an "impurity" from natural gas wells. Under moderate pressure and at normal temperature, LPG can be transported in a liquid form, and when released at atmospheric pressures at relatively low temperature it vaporises and can be handled as a gas. It is therefore far safer to store NG in LPG at relatively low pressure than the pressure required in compressed NG. Further, instead of using LPG only as a storage solvent, LPG–NG mixtures may be used as an alternative transport fuel. This would overcome the costly operation of having to separate the NG from the storage medium before its use. In using these mixtures it is envisaged that only minor modifications would be required to the existing technology for LPG and NG. As a combined fuel, LPG–NG mixtures would also have higher energy densities than NG or LPG alone [9].

This project at CSIRO is a study on the storage capacity of NG in LPG at different temperatures and pressures. The work will also examine whether LPG–NG mixtures can be used as vehicular fuels, in particular the phase and composition changes during the emptying of the storage tank! This is the first of a series of papers on the storage of NG in LPG. This paper concentrates on the construction of an automated system that can monitor the changes in distribution of hydrocarbons in the different phases of mixtures in a reaction vessel under varying temperature and pressure regimes. The work reports the obstacles involved in interfacing of a rapid-scan GC to a high-pressure gas mixing system. *In situ* GC is an integral part of the automated system.

EXPERIMENTAL

Materials

Propane (>99% purity) and a standard gas mixture consisting of carbon monoxide (4.5 mol%), carbon dioxide (8.99%), methane (28.28%), ethane (5.11%), propane (29.0%), propene (9.42%) and butane (14.7%) were obtained from Matheson (CA, USA). The NG was obtained from AGL Sydney (Sydney, Australia) and was compressed in the laboratory to 20 MPa. LPG was purchased from Elgas (Sydney, Australia).

Two other gas standards were used: an *n*-alkane mixture (C_1–C_6, 1 ppm (v/v) of each in helium), and a mixture containing carbon dioxide, carbon monoxide, oxygen and hydrogen. Both were purchased from Alltech (Sydney, Australia).

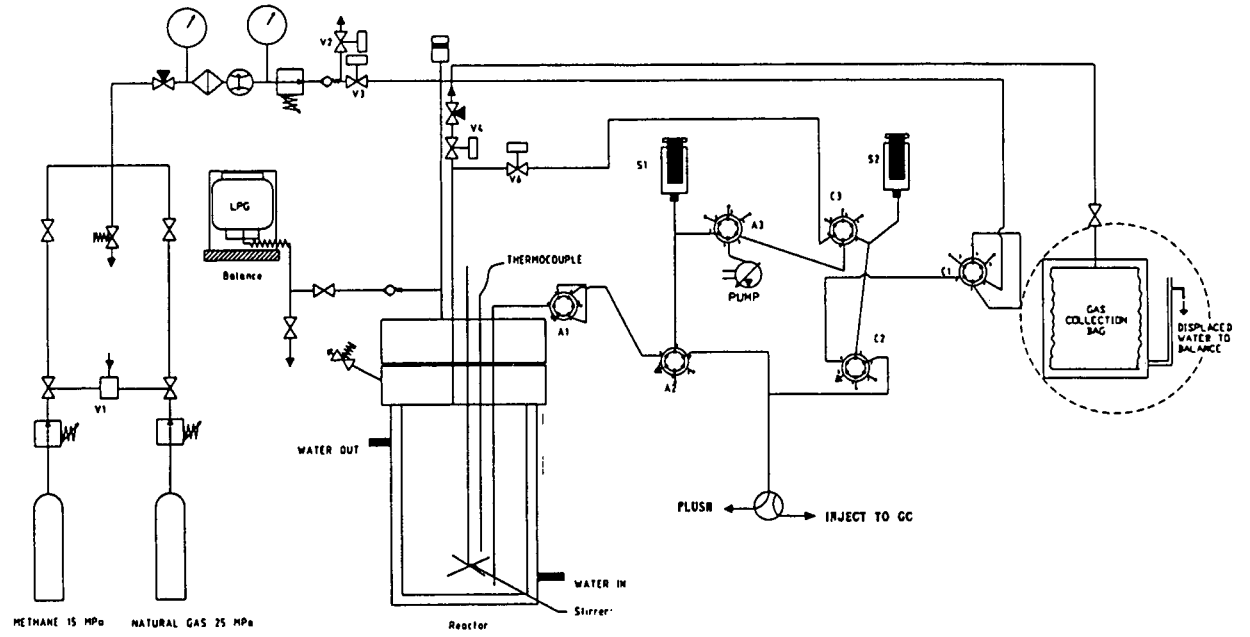

Fig. 1. The schematic of the GLS rig used for this work. Two sets of two way switching valves (A1/A2/A3 and C1/C2/C3) are used for manipulating samples from the liquid and gas phase of the mixture. S1 and S2 are variable-volume syringes. For gas discharge experiments the gas collection system is connected to V_4 as showed by the broken circle in the figure.

Equipment

The schematic of the apparatus constructed for this study is shown in Fig. 1. The storage solvent such as propane, butane or LPG was introduced first into the reaction vessel (316 stainless steel 300 ml packless autoclave from Autoclave Engineers, Erie, PA, USA). To ensure that only the liquid phase was used, the hydrocarbon was metered into the reaction chamber through a valve from an inverted cylinder sitting on a Mettler PM 34 Delta Range balance (Mettler Instrument Co., NJ, USA). NG or methane was then used to fill the reaction vessel to a preset pressure via a Brooks Mass Flow Meter (5850E 1-l CH_4/min, Brooks Instrumental Division, Hatfield, PA, USA). The exact mass ($M = ftd$) of the latter gas used was calculated from its flow rate at the set pressure (f), the duration of filling (t), and density (d). The temperature of the autoclave was maintained at a constant temperature by recirculating water from a Model SPE. TBC Thermoline waterbath (Thermoline Scientifics Equipments, Sydney, Australia) through a water jacket surrounding the autoclave. A 1.5-mm diameter type "T" thermocouple was used to monitor the temperature.

The mixture in the reaction vessel was stirred to equilibrate the reaction. The stirrer in the autoclave was driven by a 1/2 Hp DC shunt motor (Aust. Balder, Sydney, Australia) with a Multi-Driver speed controller (K. B. Electronics, NY, USA). Changes in pressure were monitored during stirring and the reaction is equilibrated when there is no further change in pressure. Fig. 2 shows a typical pressure–time profile. Although the reaction was equilibrated in few minutes, stirring was maintained throughout the duration of the experiment to ensure that there was no phase change.

Samples from the phases were trapped separately into fixed-volume loops (250 and 500 μl) of switching valves (Rheodyne 7000ARV with actuator, Rheodyne, Cotati, CA, USA). The sampling lines and loops were flushed twice before actual sampling. The samples in the loops then were expanded into previously evacuated variable-volume syringes (VVSs) after equilibration. Aliquot of the expanded phases was then inject-

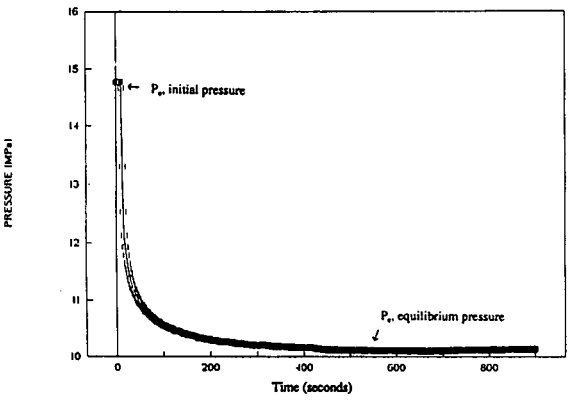

Fig. 2. Pressure–time profile of LPG–NG mixture during stirring (473 rpm) at 15 MPa and 20°C. The masses of LPG and NG are 40.2 and 34.54 g, respectively.

ed into the rapid-scan M200-D gas chromatograph (MTI, Fremont, CA, USA). Separate transfer lines and expansion syringes were used for the two phases to avoid cross contamination.

The VVSs were laboratory-made for expanding compressed samples from the two phases. Glass airtight syringes (SGE, Australia) of 50 and 100 ml were used respectively for expanding samples from the gas and liquid phase. The movement of the syringes was controlled by stepmotor drivers (200 steps/revolution) via lead screws. A set of two "safety" microswitches were positioned at the upper and lower expansion limits of the syringe. The first limit was the software control of syringe movement and the second was connected to the interlock of the motor that cuts off the motor once the microswitch has been activated. This double safety feature was necessary to ensure that the plunger of either syringe does not travel beyond the extreme limits.

Venting experiment

For the gas discharge experiment the gas collection system (showed by the broken circle in Fig. 1) was connected to valve V4 of the rig (hence referred as the gas–liquid solubility rig (GLS) in Figure 1). As the gas was discharged from the reaction chamber into the gas bag an equal volume of waster was displaced from the Perspex box.

Operation of the switching valves

Venting/flushing of the transfer lines and sample loops, evacuation, filling and emptying of syringes, and transport of expanded samples for GC analyses were controlled by two separate sets of serially linked 2-way switching valves. Each set of three valves controlled all the operations on a phase. Table I gives an example of

TABLE I

COMBINED VALVE CONFIGURATIONS FOR SAMPLING FROM THE LIQUID PHASE OF THE GAS–LIQUID SOLUBILITY RIG AND INJECTION OF ALIQUOT ONTO THE GC SYSTEM

Operation sequence	Switching valve configuration						Syringe movement	GC inlet valve	Function
	A1	A2	A3	C1	C2	C3			
1[a]	1	0	0	0	0	1	None	Flush	Fill sampling loop
2[a]	0	0	0	0	0	1	None	Flush	Expel sampling loop
3	1	1	1	0	0	1	Up	Flush	Fill loop and devacuate syringe and sampling line
4	1	1	0	0	0	1	None	Flush	Isolate syringe from pump
5	0	1	0	0	0	1	None	Flush	Expand liquid from loop to syringe
6	0	0	0	0	0	1	Down	Inject[b]	Inject expanded gas to GC system
7	0	0	0	0	0	0	None	Flush	Reset valve configuration and flush GC system
8	0	0	0	0	0	0	Up	Flush	Reset syringe to maximum volume

[a] The combined operation of sequences 1 and 2 is used for flushing the sampling loop.
[b] The GC inlet is switched to "Inject" after the sampling lines have been flushed with expanded gas.

the configurations of a set of valves for manipulating a liquid phase from the reaction chamber of the GLS rig. The movement of a valve is given as either "0" or "1" in the table, representing the valve configurations shown in Fig. 3. A similar sequence of operations was required for manipulation of samples from the gas phase. As indicated in Fig. 1, valves A_1, A_2, and A_3 control all the operations on the liquid phase and C_1, C_2, and C_3, on the gas phase.

The movements of the valves were computer-synchronized. Fig. 4 shows the combined movements of the valves during the filling of the sampling loop from the liquid phase (top) and the simultaneous evacuation of the transfer lines and the VVS just before the expansion of the compressed sample (bottom). One or more valves can be switched during an operation.

Evacuation of the syringes and transfer lines was actuated by switching the appropriate valves in-line with the pump that was left on throughout the experiment.

Operating conditions for M200-D gas chromatograph

The M200-D GC system can be operated isothermally only and therefore required two separate columns for complete separation of all the hydrocarbon components in the LPG–NG mixtures. GC analysis under isothermal conditions gives a faster turnaround time than temperature programming since no column temperature re-equilibration is required. On entering the GC system, the sample is split for analysis on the

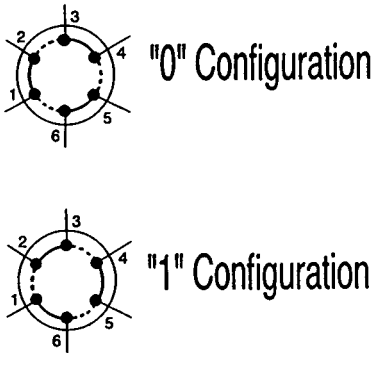

Fig. 3. "0" and "1" configurations representing position of switching valves are referred in Table I.

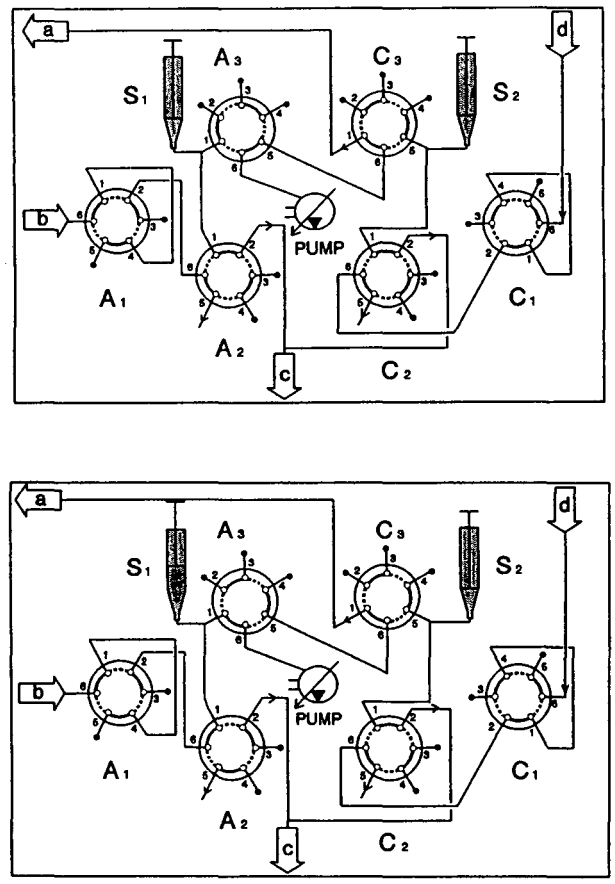

Fig. 4. Combined movements (top) of valves for filling of sampling loop (connecting ports 1 and 4 of A_1) from the liquid phase and (bottom) evacuation of transfer lines and syringe before the expansion of the trapped sample in the loop. Line connectors in the figure, "b" and "d", are connections from liquid and gas phases. Connector "c" comes from the GC system and "a" from the transfer line joining V_6.

two columns. Channel A of the M200-D has a 4-m MS-5 column which was operated at 100°C with column head pressure of 14.5 p.s.i. (1 p.s.i. = 6894.75 Pa), and channel B, an 8-m PoraPlot Q column operated at 135°C and a column head pressure of 27.5 p.s.i. The analysis times for channel A and B were 60 and 80 s, respectively, and the sampling time (equivalent to the amount injected to the microchamber) was 5 ms.

A 2-μl A315 precolumn filter (Upchurch Scientific, Oak Harbor, WA, USA) was placed between the GC inlet switching valve and the

inlet of the M200-D GC system. This is important in preventing the blockage of the fine orifice of the columns by particulate matter.

No special setting of the detector condition was needed for the M200-D; the only requirement was the switching on of the detector with the sensitivity set on low, medium, or high level. These functions are controlled through the EZ-Chrom software.

Sampling of expanded gases from VVSs to the M200-D GC system

The M200-D GC system has a built-in 8-μl microchamber which is filled by drawing sample from the flowing stream by the built-in micro vacuum pump only when the GC is activated. In the GLS rig, the expanded gas from either of the two VVSs was expelled to waste through an adjustable needle valve via a 2-way switching valve (Fig. 5). In the "inject" mode (top) the GC inlet was positioned in-line with the flowing stream of the expelling gas and an aliquot was then extracted into the GC system for analysis. Otherwise, the GC inlet valve was left in the "flush" mode where the expanded gas was vented to waste continuously out the needle valve (bottom). The switching of the GC inlet valve to the GC system was computer synchronised with

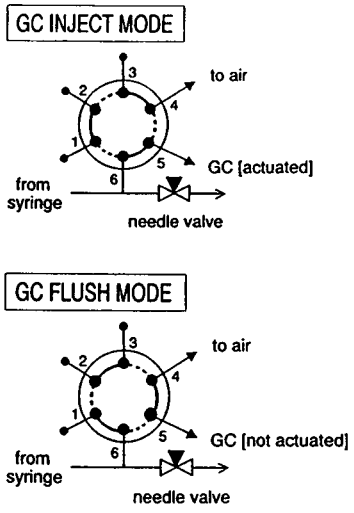

Fig. 5. The configuration of the GC inlet valve can be either in "inject" or "flush" mode. In the "inject" mode, the GC was connected directly to the flowing stream whereas in the "flush" mode it was diverted away.

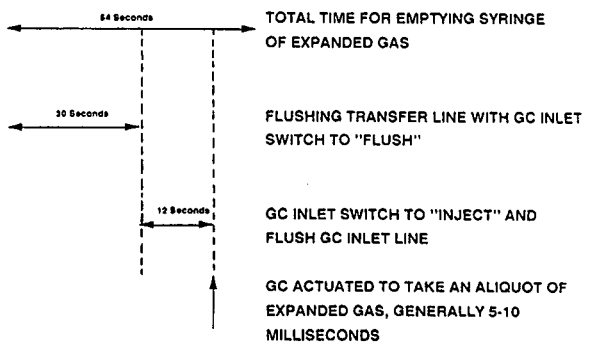

Fig. 6. Segmentation of events during the emptying of the expanded gas from the syringe.

the opening/closing of the microchamber of the M200-D. As shown in Fig. 6 the switching of the GC inlet valve to the "inject" mode occurs only after both the transfer line to the GC system and the GC inlet valve have been flushed with the incoming gas. The volume of expanded gas injected onto the GC columns depends on sampling time into the sample chamber of the M200-D and this is usually 5–10 ms.

Sampling from the expelling stream of the expanded gas at the immediate entrance of the GC system minimises peak broadening arisen from extra column effects.

Computer control

A software package (referred here as GLS software) was developed to synchronise switching of valves and for controlling various functions of the phases on the GLS rig. Fig. 7 summarizes the functions of the software. Manu-

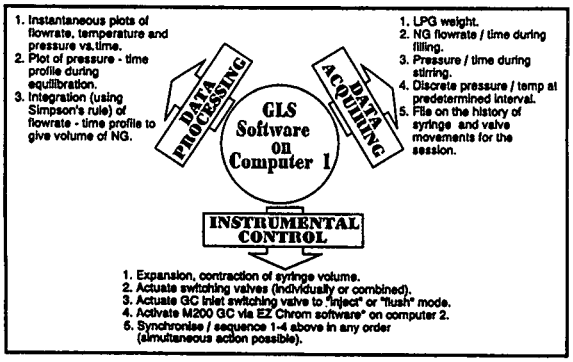

Fig. 7. GLS software used for controlling various functions on the GLS rig. *Commerical software from MTI, Freemont, CA, USA.

al operation of the system was automated through the instrument control section of the GLS software. In-build macros in the software allow considerable flexibility (point 5 under Instrumental Control in Fig. 7) in manipulating the action sequences during an automated run. Each macro is equivalent to a unique action and entails a line of valve operations such as that showed in Table I. These operations are carried out simultaneously. Macros can be sequenced in any order in a block to allow different combinations of actions in an automated run. For example, a sequence of eight actions listed in Table I can be programmed in macros and placed into a single block which then can be actuated by a single keystroke in the GLS software. Typically, for an automated run the program can be structured similarly to the flowchart given in Fig. 8.

Under the automatic mode the progress of a run can be viewed from a single screen. The experiment can be paused, stopped or even skipped to other sections of the program.

The GLS software provides an additional facility for low level testing of the interface boards. It was rarely used and employed mainly for fault finding and correction. The GLS software also provides a manual "screen" which shows the status of various parts of the GLS rig and allows the operator to interrupt the operation of the rig by pressing keystrokes on the computer.

A 640K XT computer (HYPEC, Sydney, Australia) was used to run the GLS software with special commercially available boards (I/O and ACD cards) for the controlling of the valves, stepping motors, and for data gathering. A separate computer (HPEC 386) was used for the gathering and analysis of GC data. The EZ-CHROM 200 version 3.1 (MTI) software was used for processing the GC data.

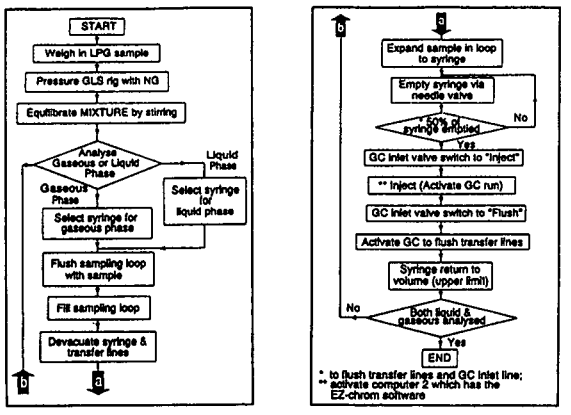

Fig. 8. The flowchart for the GLS software.

GC for analysing gas samples manually trapped in gas bags

A stand-alone GC system (Shimadzu 9C-9A) was used for analysing samples of gas mixtures which were trapped manually from the vapour and liquid phases. The GC system is a dual-injection system with both thermal conductivity and flame ionization detectors. For hydrocarbons, a 3-m alumina column (Alumina F-1, 80–100 mesh) was used with following GC conditions: helium carrier gas flow-rate at 25 ml/min, oven temperature 85°C and flame ionization detector at 280°C. For carbon dioxide, a 3-m Carbosphere (80–100 mesh) was used with the thermal conductivity detector with the following GC conditions: helium carrier gas flow-rate at 40 ml/min, oven temperature at 80°C and detector temperature 150°C (bridge current 150 mA).

RESULTS AND DISCUSSION

System automation

A number of obstacles have to be overcome to automate the system. Sampling from phases under pressure was carried out using fixed volume loops on high-pressure switching valves that have been used for HPLC. Since only a relatively small amount of sample was taken, there was no perceptible change of pressure in the reaction chamber during sampling and therefore there was a minimal disturbance of reaction equilibrium. Samples from phases were taken from different points in the reaction chamber, with the liquid phase drawn from the bottom and the gas phase from the top of the chamber. Separate sampling loops and switching valves were used for the two phases to minimise possible cross contamination. There was a notable drop of temperature of 4–6°C during the flushing of the sampling loops. An elapsing time of 3 min therefore was included in the automated cycle

for reestablishing the loop temperature before the actual sampling from the phases.

The compressed samples in the sampling loops were expanded in separate VVSs. The volumes of those syringes were fixed with respect to the sizes of the loops used. There was no notable change of temperature in the VVS during expansion, but a waiting period was included in the automated cycle to allow temperature equilibration.

Samples for GC were taken during the expelling mode of the VVSs. The actual sampling occurred immediately at the inlet orifice of the M200-D GC system after it had been switched in-line with the outgoing stream of the expanded gas from either of the VVSs. Sampling at this point minimised peak broadening since there was little or no dead volume along the chromatographic circuit.

Fig. 6 shows the actual sampling of the GC system from the expelling stream occurred during the emptying of the last 20% of the expanded gas from the syringe. The early portion of the expanded gas in the syringe was mainly to flush the GC inlet valve and transfer lines to the GC system. To gauge how representative was the sample taken from this segment of the syringe, samples were taken at the beginning, the middle, and near the end portion of the syringe during emptying. The peak area of these samples were compared and a maximum deviation of 2% was found. There was no evidence for the selective precipitation of the heavier components from the hydrocarbon mixtures. However, sampling from the early portion of the syringe did indicate that cross contamination occasionally occurred, especially when concentrations were varied widely between successive samples. Flushing was required to avoid this. Fig. 9 clearly illustrates the decrease of ghost peaks in the chromatograms after the system has been repeatedly flushed.

Finally, the M200-D rapid-scan GC system was used to provide rapid analysis. Samples from different phases of the reaction mixture in the GLS rig have to be analysed almost instantaneously once they have been sampled into the loops since prolonged waiting could cause phase separation [3]. Using two columns under isothermal condition, the M200-D GC system can analyse a mixture typically containing N_2, O_2,

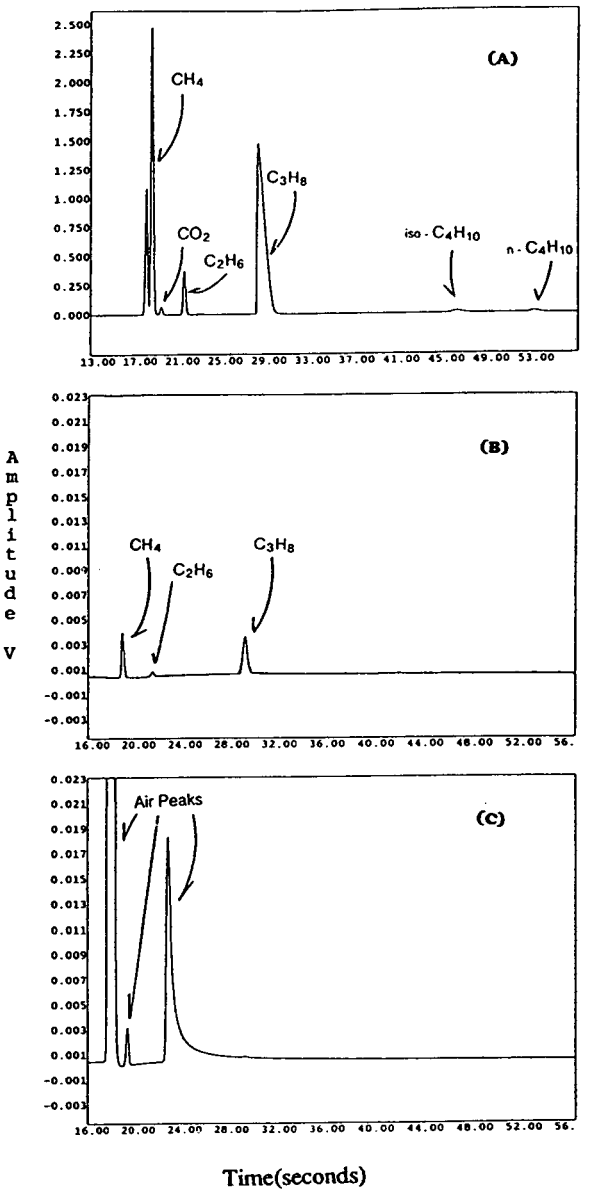

Fig. 9. Chromatograms illustrate the contamination problem: (A) is an injection of sample from the liquid phase of the reaction mixture; (B) shows ghost peaks from previous injection; and (C) after flushing the GC system with air.

CO, CO_2, CH_4, C_2H_6, C_3H_6, C_3H_8, n-C_4H_{10} and iso-C_4H_{10} in less than 80 s. This compares with a 50–60-min cycle time (reconditioning time for next run) required for the separation of the same gas mixture using conventional gas chromatographs. Fig. 10 shows a typical separation of a sample from the gas phase of the LPG–NG mixture. The column in channel A of the M200-

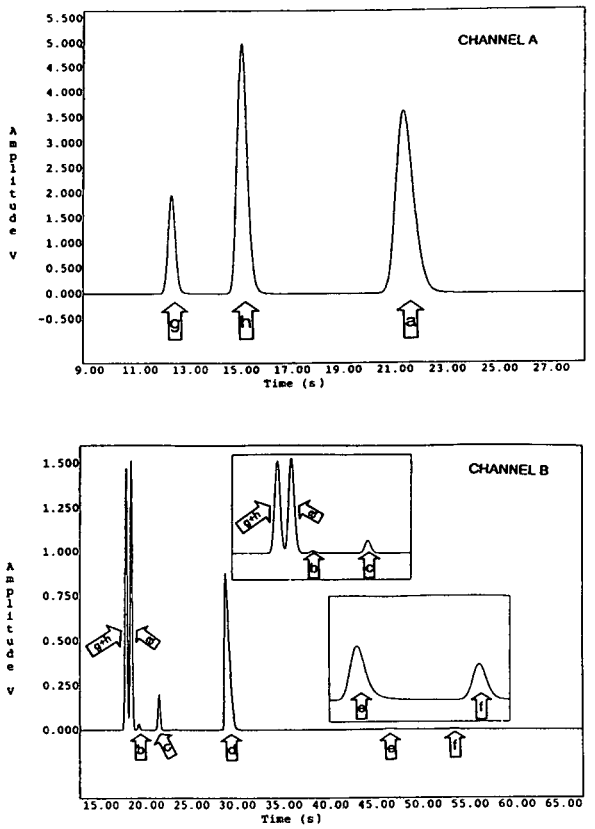

Fig. 10. Separation of sample from the gas phase of a LPG–NG mixture. The conditions of mixing was 12 MPa and 10°C using 59.9 g LPG and 22.21 g NG. a = Methane; b = carbon dioxide; c = ethane; d = propane; e = *n*-butane; f = isobutane; g = oxygen; h = nitrogen. The insets to the bottom figure show disproportionally small peaks that can be adequately handled by the EZ-CHROM software.

D was used for mainly detecting N_2, O_2 and CO. The CO peak, if present in the mixture, eluted immediately after the methane peak in channel A, and propene before propane in channel B. The EZ-CHROM software used with the M200-D gave a good dynamic range that allowed the detection of peaks of vastly different concentrations. This again is well illustrated in Fig. 10 where the concentration of *n*-butane and isobutane is approximately 100 times less than propane.

Automated cycle for determination of phase compositions

After mixing, samples from the respective phases of the reaction chamber were analysed. An automated cycle was then set up entailing the following actions: flushing of the sample loops and transfer lines; sampling from the phases; fixing the volumes of the VVSs; evacuation of the syringes; expansion of the samples in the loops into the VVSs; flushing of the GC inlet lines; transporting samples for GC analysis; and resetting of the switching valves and VVSs for the next run. Successive runs of a standard hydrocarbon mixture gave a maximum deviation of 3% for the smallest peak in the mixture.

Each cycle consisted of the actual GC analyses of the samples from the two phases plus flushing of the GC system after each analysis. For flushing, a sample of air was run through the system. Fig. 11 shows four sets of chromatograms resulted from each automated cycle. The complete cycle takes only 14 min.

The components of gases in the final mixture (using both phases) were mass balanced against those in the initial mixtures before mixing. Typically, in mixing NG with LPG at 10 MPa and 20°C, mass balances >99% was found for methane and propane, and >95% for ethane, *n*-butane and isobutane, and carbon dioxide. The good mass balances obtained here were mainly due to the closed nature of the automated GLS system, where losses were minimised, and the precise manipulations of the samples during its operation.

Results from the automated setup were also compared with those obtained using the conventional procedure where the gases from the phases were trapped into gas bags and analysed by a stand-alone GC system. A maximum deviation of 2% was found for the major components (methane and propane) and 4% for minor components of the mixture.

NG solubility in LPG

The reaction chamber of the GLS rig was never filled completely with liquid phase. Most of the time two phases existed in the chamber, with a liquid at the bottom and a vapour phase that occupies the space above the liquid. When the chamber is vented, some vapour leaves the chamber and immediately a certain amount of the liquid is evaporated to replace the lost vapour. However, the mixture in the chamber can become a single gas phase by reducing the

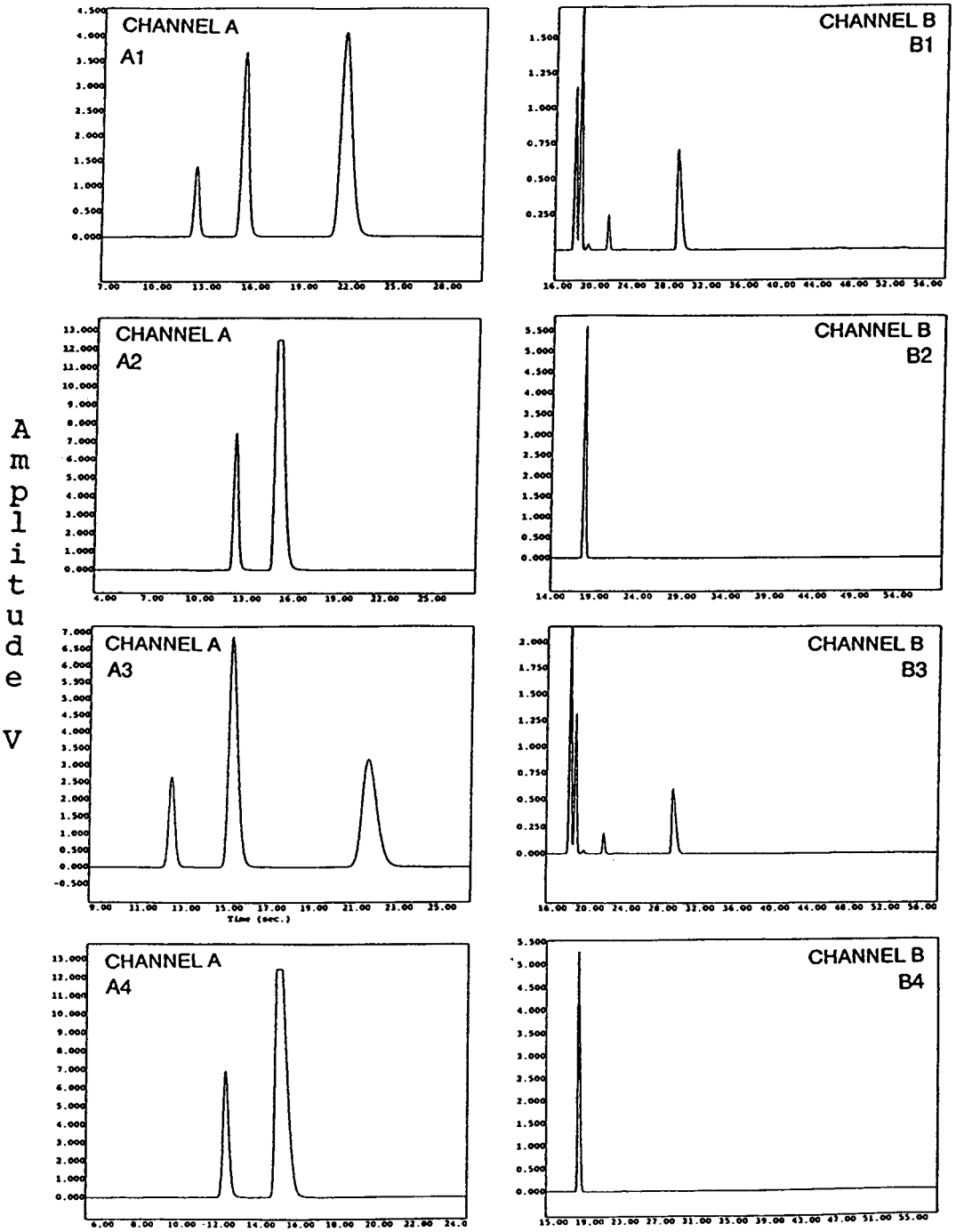

Fig. 11. Chromatograms from an automated cycle run: A1 and B1 are chromatograms of the liquid phase from channels A and B of the M200-D GC systems; A3 and B3 from the vapour phase; and A2, B2, A4 and B4 are chromatograms after the GC system has been flushed after each analysis.

pressure and/or increasing the temperature of the reaction chamber.

The dissolution of NG in LPG was calculated using the differential pressure profile of the stirring NG–LPG mixture similar to the one shown in Fig. 2. The formula used was:

$$n_g^i - n_g^f = \frac{(P_0 - P_s)(V_s^i)}{Z_0 R T_0} - \frac{(P_e - P_{sm})(V - V_s^f)}{Z_f R T_f}$$

where P_0 and P_e are pressures of reaction chamber before and after mixing; V is the volume of the vessel; V_s^i and V_s^f are volumes of liquid phase before and after mixing; P_s and P_{sm} are vapour pressure of the solvent before and after mixing; Z_0 and Z_f are compressibility factors before and after stirring; T_0 and T_f are temperature before and after stirring; n_g^i and n_g^f are the moles of the mixture in the gas phase before and after mixing; and R is the universal gas constant.

The above equation was further simplified to

$$C = \left[\frac{(M_r)_s}{W_s}\right]\left\{\left[\frac{W_g}{(M_r)_g}\right] - 273.15(P_e - P_{sm}) \times \left(\frac{V - \left(\frac{W_s}{d_f}\right)}{22.414 Z_f T_f}\right)\right\}$$

where $(M_r)_g$ and $(M_r)_s$ are the mean molecular masses of the gas and solvent mixtures; W_g and W_s are the masses of gas and solvent used initially; d_f is the density of the final solvent; and C is the dissolution concentration expressed in mol/mol.

The derivation of these formulae and a more detailed discussion on the solubility results will be the subject of a later publication. The second equation was used to calculate the solubility of NG in LPG with a given NG–LPG ratio (w/w) at a particular temperature and pressure. The saturated solubility was obtained by increasing the NG–LPG ratio until no more gas dissolved. Generally, the dissolution of NG at 20°C in LPG in a pressure range of 4 to 20 MPa increased the amount of gas stored. Enhancement factors were generally in the range of 1.4 to 1.65. That is, the amount of NG in a given volume could increase by half as much again when dissolved in a hydrocarbon solvent under the conditions specified. The increase in NG storage found here is less than that obtained when activated carbon was used as a storage medium [10]. An enhancement factor of 3 was obtained at 4 MPa using the best available activated carbon.

An example of solution of NG in LPG is demonstrated in Table II. At the equilibrium pressure of 3.31 MPa, the ratio of phase concentration of methane ($[CH_4]_{vap}/[CH_4]_{liq}$) was 2.43 but decreased to 1 at 11.49 MPa. While the ratio of phase concentration of propane ($[C_3H_8]_{vap}/[C_3H_8]_{liq}$) was 0.58 at the low pressure but increased to 1 at the higher pressure. Therefore, at pressure greater than 10.0 MPa the distribution of the components in both phases is the same. The finding here has important implication for how the stored mixture could be used. If the total mixture was to be used as a fuel then it would be preferable to mechanically maintain the system under high pressure (>10 MPa) so that the major components of the mixtures were evenly distributed in both liquid and gas phases. However, if the aim was to use the methane only and to cycle the hydrocarbon solvent as the storage medium then the operating pressure

TABLE II

DISTRIBUTION OF MAIN COMPONENTS IN RESPECTIVE PHASES OF MIXTURES AT DIFFERENT PRESSURE

Mixtures	Main components (in mol%)			
	CH_4	CO_2	$C_2H_6C_3H_8$	
NG (Initial)	90	1.6	8.2	0.2
LPG (Initial)	–	–	5.3	94
NG–LPG mixture at 3.31 MPa and 20°C				
Liquid phase	20.2	0.6	2.38	76.79
Vapour phase	49.1	1.2	2.4	47.31
NG–LPG mixture at 8.06 MPa and 20°C				
Liquid phase	47.78	1.16	4.45	46.62
Vapour phase	65.95	1.29	4.09	28.66
LPG–NG mixture at 11.49 MPa and 20°C				
Liquid phase	55.06	1.27	5.06	38.61
Vapour phase	56.78	1.34	5.37	36.38

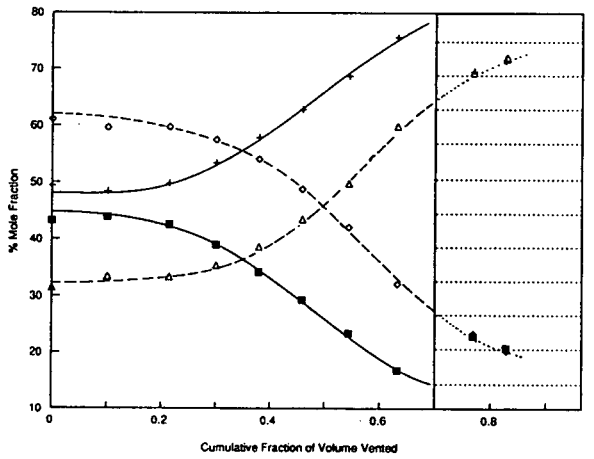

Fig. 12. Discharging profile of a NG–LPG mixture. The mixture was equilibrated at 8 MPa and 20°C using 60 g of LPG and 29 g of NG. The shaded area represents a change from a binary to single phase. ■ = CH_4(liq); + = C_3H_8(liq); ◇ = CH_4(vap); △ = C_3H_8(vap).

should be lower than the convergence pressure of the mixture.

Venting gas from the various two phase systems generally resulted in large variations in the vent gas molar composition until pressure fell to a point where a single gas phase existed. Fig. 12 shows a typical example. After gas was vented from the system there was a decrease of lighter hydrocarbon, CH_4, and an increase of the heavier gas, C_3H_8, in the remaining mixture. Both phases behaved similarly. A phase change occurred when 70% of the mixture had been vented and this is indicated in Fig. 12 by the abrupt coincidence of methane and propane concentrations for the two phases.

CONCLUSIONS

Studies on the dissolution of gases in hydrocarbon solvents must consider phase changes. Automation of *in situ* GC monitoring of the distribution of hydrocarbons in the different phases entailed the compressed samples from both phases to be in gaseous form at ambient temperature and pressure before they can be handled by GC. The use of rapid-scan GC and sampling at strategic locations in the system ensured rapid analysis with good sensitivity and minimum peak diffusion from reduced extra chromatographic effects. The automated system allowed the solubility of NG in LPG to be studied in one tenth of the time as that required with conventional procedures.

At equivalent temperature–pressure regimes the storage of NG was shown to be enhanced by more than 50% by dissolving it in LPG than when it was stored alone. However, NG was found to separate out the solvent during discharge when the system is continuously depressurised.

ACKNOWLEDGEMENTS

The financial assistance from the National Energy Research Development and Demonstration Council for this work is gratefully acknowledged. I am also indebted to the technical assistance of L. Leipa, J. Wong, K. Wong and D. Chivers.

REFERENCES

1 T. Ahmed, *Hydrocarbon Phase Behaviour*, Gulf Publ. Co., Houston, TX, 1989, Ch. 1.
2 R.A. Budenholzer, B.H. Sage and W.N. Lacey, *Ind. Eng. Chem.*, 31 (1939) 369–374.
3 C.J. Cowper and A.J. DeRose, *The Analysis of Gases by Chromatography* (*Pergamon Series in Analytical Chemistry*, Vol. 7), Pergamon Press, Oxford, 1983, Ch. 6.
4 K.J. Rygle, G.P. Feulmer and R.F. Scheideman, *J. Chromatogr. Sci.*, 22 (1984) 514–519.
5 G.C. Wall, *Proceedings of the 1st Australian Workshop on Oil Shale, Lucas Heights*, CSIRO Division of Energy Chemistry, Sydney, 1983, pp. 105–108.
6 S.K. Shibata and S.I. Sandler, *J. Chem. Eng. Data*, 34 (1989) 291–298.
7 C.-H. Kim, A.B. Clark, P. Vimalchand and M.D. Donohue, *J. Chem. Eng. Data*, 34 (1989) 391–395.
8 R.N. O'Brien, B. Turnham and S. Visaisouk, *Proceedings of the 1st International Conference and Exhibition on NGV —The New Direction in Transportation, Sydney, 1988*, pp. 1–9.
9 A. Melvin, *Natural Gas: Basic Science and Technology*, British Gas, Bristol, 1988, Ch. 6.
10 A. Chaffee and A. Pandolfo, *Extended Abstracts and Programme of International Carbon Conference, Paris, 1990*, pp. 246–247.

Journal of Chromatography, 639 (1993) 239–253
Elsevier Science Publishers B.V., Amsterdam

CHROM. 25 040

Improved gas chromatography procedure for speciated hydrocarbon measurements of vehicle emissions

S. Kent Hoekman

Chevron Research and Technology Company, 100 Chevron Way, Richmond, CA 94802 (USA)

(First received January 5th, 1993; revised manuscript received March 5th, 1993)

ABSTRACT

A dual-column gas chromatography (GC) procedure was developed for speciated analysis of hydrocarbons in automobile exhaust emissions. Light hydrocarbons (C_1–C_3) are analyzed using a 30 m × 0.53 mm GS-Q column; heavier hydrocarbons (C_3–C_{12}) are analyzed using a 60 m × 0.32 mm DB-1 column. The two columns are operated simultaneously within a single GC oven. Variable temperature adsorption traps (VTATs) are used to concentrate samples prior to GC analysis. The detection limits for individual hydrocarbon species are approximately 5–10 ppb (v/v) C. The GC procedure was used to analyze exhaust emissions from both gasoline- and methanol-fueled vehicles. Sample instability was shown to be a problem for diene species in exhaust mixtures —including 1,3-butadiene.

INTRODUCTION

In recent years, increasingly sophisticated analytical techniques have been employed to measure hydrocarbon emissions from motor vehicles. In part, this has been driven by regulations which consider the propensity of hydrocarbons to contribute to the formation of tropospheric ozone [1,2]. Since hydrocarbon compounds vary in their ozone-formation reactivity, highly detailed, speciated analyses are necessary to assess the overall impact of an emissions mixture.

We recently reported the use of a relatively simple, single-column GC procedure for speciating hydrocarbon compounds from C_1 to C_{12} [3]. Similar procedures have been reported by others [4–6]. While advantageous in terms of simplicity and speed, such single-column techniques lack the degree of resolution which is necessary to adequately characterize all hydrocarbon species of interest.

This report describes the development and application of a dual-column GC procedure for hydrocarbon speciation. Multiple-column procedures have also been used by others [7–14], but none incorporates all three advantages offered by our approach: (1) use of "built-in" sample concentration devices, (2) simultaneous analysis on two columns contained within a single GC instrument, and (3) automation of the sampling and analysis procedures.

EXPERIMENTAL

GC equipment

All chromatographic analyses were performed using a Varian Model 3600 GC (Varian, Sunnyvale, CA, USA). The instrument was equipped with an automatic gas sampling valve, two heated sample loops, two variable temperature adsorption traps (VTATs), two analytical columns, and two flame ionization detection (FID) systems. A simple schematic drawing showing all these components is given in Fig. 1. Control of instrument parameters was accomplished by an on-board microprocessor. Data collection and

0021-9673/93/$06.00

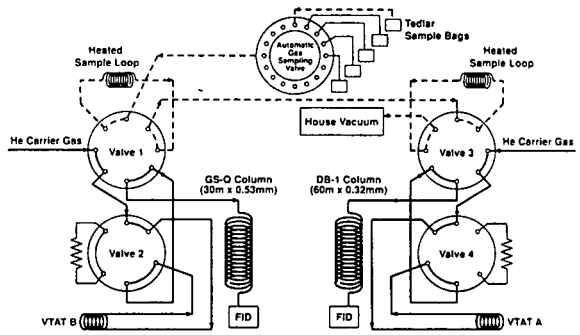

Fig. 1. Plumbing diagram of Varian Model 3600 GC used for speciated hydrocarbon measurements. Configuration shown is for start of run (filling sample loops).

manipulation were done with a Varian Model DS651 data station.

One analytical column was a 60 m × 0.32 mm DB-1 fused-silica capillary column, having a film thickness of 1.0 μm (J & W Scientific, Folsom, CA, USA). This column was used to measure most of the hydrocarbon species in emissions samples (C_3–C_{12}). The other column was a 30 m × 0.53 mm GS-Q Megabore column (J & W Scientific). This was used to measure only a few light hydrocarbons (C_1–C_3).

Vehicle exhaust samples

Vehicle exhaust samples were obtained during standard emissions testing —generally using the 1975 Federal Test Procedure (FTP) [15]. Diluted vehicle exhaust was collected during each of three phases: cold start, stabilized, and hot start (bag 1, bag 2, and bag 3, respectively). A sampling system was used whereby 3-l Tedlar bags for speciated GC analysis were filled simultaneously with the 100-l bags which are generally used for criteria pollutant measurements. This represents an improvement over our previous sampling techniques in which the GC Tedlar bags were filled by transferring samples from the larger bags [3].

Background air samples were routinely obtained during each phase of the FTP emissions test, but only the bag 2 background sample was analyzed by GC. The background composition determined from this sample was assumed to apply for all three FTP bag samples. The predominant hydrocarbon constituent in background air is methane, which is generally observed at concentrations of 2–3 ppm (v/v). In our testing facility, trace levels (0.01–0.10 ppm C) of major gasoline constituents are also seen. These include *n*-butane, 2-methylbutane, methylpentanes, toluene and xylenes.

House vacuum was used to draw diluted exhaust from the Tedlar bags through two 5.0-ml sample loops that were heated at 125°C (see sampling conditions listed in Table I). Larger sample loops could be used to further improve sensitivity, but 5.0 ml is the largest size that could conveniently fit in the temperature-controlled zones of the GC instrument.

VTAT operation

VTATs were used to concentrate diluted emissions samples prior to injection onto the GC columns. They consisted of 3 ft. × 1/16 in. (1 ft. = 30.48 cm; 1 in. = 2.54 cm) stainless-steel tubing in which the middle 2-ft. section was packed with a polymeric adsorbent material, Hayesep D (60–80 mesh). This adsorbent is preferred over Chromosorb 106 which was used previously [3], since it could be subjected to a higher desorption temperature without releasing objectionable amounts of contaminants.

Operating conditions for the VTATs are summarized in Table II. Although the two VTATs were loaded simultaneously, they were desorbed and injected onto the two analytical columns at different times —injection onto the DB-1 column occurred at 7.0 min; injection onto the GS-Q column occurred at 32.0 min. This was done to coordinate injection timing with optimum temperature conditions for each column.

Chromatographic conditions

The chromatographic conditions used for speciation of emissions samples are summarized in Table I. The initial column temperature of −40°C provided optimal separation of propane and propene on the DB-1 column. The multiple-gradient column temperature conditions were empirically selected as a compromise between maximum peak resolution and minimum analysis time. The entire analysis time —including sampling, VTAT operation, chromatographic sepa-

TABLE I

CONDITIONS FOR SPECIATED ANALYSIS OF HYDROCARBON EMISSIONS

Sampling conditions

Sample draw:	house vacuum
Sampling rate:	40–50 ml/min
Sampling time:	4–6 min
Sample loops:	5.0 ml; heated at 125°C
Sampling valve:	Valco Model A16 automatic gas sampling valve

GC conditions	Side A	Side B
Column type	DB-1	GS-Q
Column dimensions	60 m × 0.32 mm	30 m × 0.53 mm
Film thickness	1.0 μm	–
Carrier gas type	Helium	Helium
Carrier gas flow-rate[a]	4 ml/min	8 ml/min
Makeup gas type	Nitrogen	Nitrogen
Makeup gas flow-rate	26 ml/min	22 ml/min
Detector type	FID	FID
Detector temperature	275°C	275°C
Switching valve temperature	125°C	125°C

Column oven temperature program

Initial temperature of −40°C (hold 12 min)
Increase 3°C/min to 125°C (no hold)
Increase 6°C/min to 185°C (no hold)
Increase 20°C/min to 220°C (hold 2 min)

[a] Flow controllers were used to maintain a constant flow-rate throughout chromatographic runs.

TABLE II

OPERATION OF VARIABLE TEMPERATURE ADSORPTION TRAPS (VTATs)

Time (min)	Function	VTAT A (DB-1 column)		VTAT B (GS-Q column)	
		Temp. (°C)	Direction of flow through VTAT	Temp. (°C)	Direction of flow through VTAT
0.0–0.2	Equilibrate pressure in sample loops	−60	Normal	−99	Normal
0.2–4.0	Load VTATs	−60	Normal	−99	Normal
4.0–5.0	Desorb VTAT A	−60→180	No flow	−99	No flow
5.0–7.0	Equilibrate VTAT A	180	No flow	−99	No flow
7.0–28.0	Inject VTAT A	180	Reverse	−99	No flow
28.0–30.0	Desorb VTAT B	180	Reverse	−99→180	No flow
30.0–32.0	Equilibrate VTAT B	180	Reverse	180	No flow
32.0–81.0	Inject VTAT B	180	Reverse	180	Reverse

ration, and cool down period —was about 90 min.

Compound identification

Hydrocarbon identifications were assigned by comparing retention times of chromatographic peaks from emissions samples with those from known standard mixtures. A peak library, consisting of 164 compounds, is shown in Table III. The peak numbers given in this table are based upon an in-house nomenclature system which was developed to characterize gasolines. Gaso-

TABLE III

GC PEAK LIBRARY FOR SPECIATED HYDROCARBON ANALYSES

GC conditions are given in Table I.

Peak ID	Compound name	CAS No.	Retention time (min)[a]	Retention index[b]
1	Methane	00074-82-8	32.91	100.0
300	Ethylene	00074-85-1	34.16	163.5
550	Ethyne	00074-86-2	34.80	195.0
2	Ethane	00074-84-0	34.90	200.0
301	Propylene	00115-07-1	11.68	290.0
3	Propane	00074-98-6	11.89	300.0
500	Propadiene	00463-49-0	13.36	326.0
551	Propyne	00074-99-7	13.50	328.3
5	2-Methylpropane	00075-28-5	15.73	362.3
305	2-Methylpropene	00115-11-7	17.85	390.6
302	1-Butene	00106-98-9	17.93	391.6
502	1,3-Butadiene	00106-99-0	18.22	395.1
4	*n*-Butane	00106-97-8	18.62	400.0
1000	Methanol	00067-56-1	18.80	402.5
304	*trans*-2-Butene	00624-64-6	19.63	413.6
552	1-Butyne	00107-00-6	20.43	423.9
303	*cis*-2-Butene	00590-18-1	20.88	429.5
310	3-Methyl-1-butene	00563-45-1	23.65	461.5
1003	Ethanol	00064-17-5	25.05	476.4
7	2-Methylbutane	00078-78-4	25.14	477.3
554	2-Butyne	00503-17-3	26.37	489.5
306	1-Pentene	00109-67-1	26.52	491.0
309	2-Methyl-1-butene	00563-46-2	27.15	497.1
6	*n*-Pentane	00109-66-0	27.46	500.0
509	2-Methyl-1,3-butadiene	00078-79-5	27.78	504.5
308	*trans*-2-Pentene	00646-04-8	28.22	510.5
327	3,3-Dimethyl-1-butene	00558-37-2	28.55	514.9
307	*cis*-2-Pentene	00627-20-3	28.82	518.6
311	2-Methyl-2-butene	00513-35-9	29.19	523.4
505	*trans*-1,3-Pentadiene	02004-70-8	29.35	525.6
530	Cyclopentadiene	00542-92-7	29.95	533.3
12	2,2-Dimethylbutane	00075-83-2	30.25	537.2
450	Cyclopentene	00142-29-0	31.50	552.6
319	4-Methyl-1-pentene	00691-37-2	32.10	559.9
800	Cyclopentane	00287-92-3	32.33	562.6
13	2,3-Dimethylbutane	00079-29-8	32.69	566.9
1412	2-Methoxy-2-methylpropane (MTBE)	01634-04-4	32.80	568.2
326	2,3-Dimethyl-1-butene	00563-78-0	32.88	569.1
10	2-Methylpentane	00107-83-5	33.17	572.4
324	4-Methyl-*trans*-2-pentene	00674-76-0	33.36	574.6

TABLE III *(continued)*

Peak ID	Compound name	CAS No.	Retention time (min)[a]	Retention index[b]
11	3-Methylpentane	00096-14-0	34.22	584.4
317	2-Methyl-1-pentene	00763-29-1	34.69	589.6
312	1-Hexene	00592-41-6	34.77	590.5
9	*n*-Hexane	00110-54-3	35.64	600.0
315	*cis*-3-Hexene/*trans*-3-Hexene	07642-09-3	35.88	603.6
314	*trans*-2-Hexene	04050-45-7	36.05	606.1
320	2-Methyl-2-pentene	00625-27-4	36.22	608.7
321	3-Methyl-*cis*-2-pentene	00922-62-3	36.37	610.8
313	*cis*-2-Hexene	07688-21-3	36.70	615.6
322	3-Methyl-*trans*-2-pentene	00616-12-6	37.17	622.4
1450	2-Ethoxy-2-methylpropane (ETBE)	00637-92-3	37.27	623.9
801	Methylcyclopentane	00096-37-7	37.38	625.4
18	2,2-Dimethylpentane	00590-35-2	37.55	627.7
20	2,4-Dimethylpentane	00108-08-7	37.91	632.8
600	Benzene	00071-43-2	39.09	649.3
451	1-Methylcyclopentene	00693-89-0	39.09	649.3
2006	2,3-Dimethyl-2-pentene	10574-37-5	39.38	653.2
2004	2,4-Dimethyl-1-pentene	02213-32-3	39.59	656.0
825	Cyclohexane	00110-82-7	39.73	657.9
2033	2-Methyl-*trans*-3-hexene	00692-24-0	40.21	664.3
2031	5-Methyl-*trans*-2-hexene	07385-82-2	40.55	668.7
15	2-Methylhexane	00591-76-4	40.69	670.6
19	2,3-Dimethylpentane	00565-59-3	40.71	671.0
460	Cyclohexene	00110-83-8	40.90	673.4
1413	2-Methoxy-2-methylbutane (TAME)	00994-05-8	40.92	673.6
16	3-Methylhexane	00589-34-4	41.27	678.1
806	*cis*-1,3-Dimethylcyclopentane	02532-58-3	41.59	682.2
807	*trans*-1,3-Dimethylcyclopentane	01759-58-6	41.78	684.6
805	*trans*-1,2-Dimethylcyclopentane	00822-50-4	41.97	687.1
37	2,2,4-Trimethylpentane	00540-84-1	42.13	689.2
2038	1-Heptene	00592-76-7	42.61	695.2
2042	*trans*-3-Heptene	14686-14-7	42.90	698.7
14	*n*-Heptane	00142-82-5	43.00	700.0
2034	3-Methyl-*cis*-3-hexene	04914-89-0	43.34	705.4
2040	*trans*-2-Heptene	14686-13-6	43.57	709.1
2008	2,3-Dimethyl-2-pentene	10574-37-5	43.88	714.0
826	Methylcyclohexane	00108-87-2	44.18	718.8
811	1,1,3-Trimethylcyclopentane	04516-69-2	44.45	723.0
802	Ethylcyclopentane	01640-89-7	45.02	731.9
31	2,5-Dimethylhexane	00592-13-2	45.20	734.6
30	2,4-Dimethylhexane	00589-43-5	45.31	736.4
817	1,2,4-Trimethylcyclopentane	02815-58-9	45.63	741.3
814	1,2,3-Trimethylcyclopentane	15890-40-1	46.12	748.7
39	2,3,4-Trimethylpentane	00565-75-3	46.32	751.6
38	2,3,3-Trimethylpentane	00560-21-4	46.52	754.6
601	Toluene	00108-88-3	46.52	754.6
815	1,2,4-Trimethylcyclopentane	02815-58-9	46.88	759.9
1414	2-Methoxy-2-methylpentane (THEME)	38772-53-1	47.06	762.7
29	2,3-Dimethylhexane	00584-94-1	47.13	763.7
24	2-Methylheptane	00592-27-8	47.47	768.8
26	4-Methylheptane	00589-53-7	47.57	770.2
25	3-Methylheptane	00589-81-1	47.96	775.9

(Continued on p. 244)

TABLE III *(continued)*

Peak ID	Compound name	CAS No.	Retention time (min)[a]	Retention index[b]
831	*cis*-1,3-Dimethylcyclohexane	00638-04-0	48.14	778.4
828	1,1-Dimethylcyclohexane	00590-66-9	48.49	783.4
42	2,2,5-Trimethylhexane	03522-94-9	48.66	786.0
861	1-Ethyl-1-methylcyclopentane	16747-50-5	48.90	789.4
2193	1-Octene	00590-66-9	48.95	790.0
830	*trans*-1,2-Dimethylcyclohexane	06876-23-9	49.26	794.5
832	*trans*-1,3-Dimethylcyclohexane	02207-03-6	49.48	797.5
23	*n*-Octane	00111-65-9	49.66	800.0
2198	*cis*-4-Octene	07642-15-1	50.02	806.3
2194	*cis*-2-Octene	07642-04-8	50.39	812.6
43	2,3,5-Trimethylhexane	01069-53-0	50.69	817.8
829	*cis*-1,2-Dimethylcyclohexane	02207-01-4	50.82	820.0
52	2,4-Dimethylheptane	02213-23-2	51.17	825.8
827	Ethylcyclohexane	01678-91-7	51.53	831.9
53	2,3-Dimethylheptane	01072-05-5	51.74	835.4
55	3,5-Dimethylheptane	00926-82-9	51.96	839.0
602	Ethylbenzene	00100-41-4	52.60	849.6
956	1,3,5-Trimethylcyclohexane	01839-63-0	52.80	852.8
604	*m*-Xylene	00108-38-3	53.13	858.2
605	*p*-Xylene	00106-42-3	53.19	859.3
62	4-Methyloctane	02216-34-4	53.72	867.7
60	2-Methyloctane	03221-61-2	53.73	867.9
61	3-Methyloctane	02216-33-3	54.13	874.3
712	Styrene	00100-42-5	54.20	875.4
603	*o*-Xylene	00095-47-6	54.49	880.0
405	1-Nonene	00124-11-8	54.62	882.1
4651	2,2,4-Trimethylheptane	14720-74-2	55.03	888.6
41	*n*-Nonane	00111-84-2	55.77	900.0
607	Isopropylbenzene	00098-82-8	56.45	912.5
151	2,2-Dimethyloctane	15869-87-1	56.80	919.0
835	*n*-Propylcyclohexane	01678-92-8	57.31	928.2
161	4,4-Dimethyloctane	15869-95-1	57.42	930.2
155	2,6-Dimethyloctane	02051-30-1	57.82	937.4
644	*n*-Propylbenzene	00103-65-1	58.16	943.4
609	1-Ethyl-3-methylbenzene	00620-14-4	58.58	951.0
610	1-Ethyl-4-methylbenzene	00622-96-8	58.70	953.1
613	1,3,5-Trimethylbenzene	00108-67-8	59.02	958.7
86	4-Methylnonane	17301-94-9	59.47	966.6
608	1-Ethyl-2-methylbenzene	00611-14-3	59.57	968.4
84	2-Methylnonane	00871-83-0	59.87	973.5
85	3-Methylnonane	05911-04-6	60.16	978.6
612	1,2,4-Trimethylbenzene	00095-63-6	60.42	982.9
960	1-Methyl-2-propylcyclohexane	04291-79-6	60.78	989.2
615	Isobutylbenzene	00538-93-2	60.93	991.6
616	*sec*-Butylbenzene	00135-98-8	61.15	995.4
100	*n*-Decane	00124-18-5	61.42	1000.0
611	1,2,3-Trimethylbenzene	00576-73-8	61.93	1010.0
650	Indan	00496-11-7	62.55	1022.2
658	Indene	00095-13-6	62.95	1029.9
646	1,3-Diethylbenzene	00141-93-5	63.42	1038.9
647	1-Methyl-3-propylbenzene	01074-43-7	63.57	1041.8
648	1-Methyl-4-propylbenzene	01074-55-1	63.79	1045.8
651	1,2-Diethylbenzene	00135-01-3	63.92	1048.4

TABLE III *(continued)*

Peak ID	Compound name	CAS No.	Retention time (min)[a]	Retention index[b]
653	1-Methyl-2-propylbenzene	01074-17-5	64.39	1057.4
654	1,4-Dimethyl-2-ethylbenzene	01758-88-9	64.92	1067.2
655	1,3-Dimethyl-4-ethylbenzene	00874-41-9	65.03	1069.2
163	2-Methyldecane	06975-98-0	65.23	1073.0
656	1,2-Dimethyl-4-ethylbenzene	00934-80-5	65.34	1075.0
657	1,3-Dimethyl-2-ethylbenzene	02870-04-4	65.71	1082.0
659	1,2-Dimethyl-3-ethylbenzene	00933-98-2	66.38	1094.3
101	*n*-Undecane	01120-21-4	66.69	1100.0
635	1,2,4,5-Tetramethylbenzene	00095-93-2	67.01	1107.5
634	1,2,3,5-Tetramethylbenzene	00527-53-7	67.19	1111.7
7800	Methylindan A	27133-93-3	68.03	1131.4
7801	Methylindan B	27133-93-3	68.50	1142.4
633	1,2,3,4-Tetramethylbenzene	00488-23-3	68.70	1146.8
755	1-Methyl-3-butylbenzene	01595-04-6	68.11	1133.2
714	Naphthalene	00091-20-3	69.81	1172.1
102	*n*-Dodecane	00112-40-3	71.05	1200.0
796	2-Methylnaphthalene	00091-57-6	73.89	1285.4
795	1-Methylnaphthalene	00090-12-0	74.39	1299.5
103	*n*-Tridecane	00629-50-5	74.40	1300.0

[a] The first four compounds listed were measured from GS-Q column; all other compounds were measured from DB-1 column.
[b] Retention index (I) is defined as follows:

$$I = 100 \cdot \frac{\log X_i - \log X_{nz}}{\log X_{nz+1} - \log X_{nz}} \cdot 100z$$

where:
z = Number of carbon atoms in *n*-alkane which immediately precedes peak i.
X_i = Retention time of peak i.
X_{nz} = Retention time of *n*-alkane (having z carbon atoms) which precedes peak i.
X_{nz+1} = Retention time of *n*-alkane (having $z+1$ carbon atoms) which follows peak i.

line analysis —using conventional GC as well as GC–MS— was also used to confirm the identities of compounds detected in emissions samples. A DB-1 chromatogram of a reference gasoline sample is shown in Fig. 2.

Another material used for compound identification was a gas standard from the Auto/Oil Air Quality Improvement Research Program [6]. This standard (CLM 3218) contained 21 hydrocarbon species, most at concentrations near 5 ppm C (Scott Specialty Gases, Troy, MI, USA). Chromatograms of this material are shown in Fig. 2 (DB-1 column) and Fig. 3 (GS-Q column). The GS-Q column provided good resolution of C_1–C_3 hydrocarbons, but was not able to resolve completely the C_4 and higher compounds.

Compound quantification

Both GC detectors were calibrated daily using a propane standard with an approximate concentration of 5 ppm C. This standard is traceable to one prepared by the National Institute for Standards and Technology (NIST) and has an accuracy within 2% of the stated concentration. All hydrocarbons (other than oxygenated compounds) were assumed to give a detector response equivalent to that of propane (on a per-carbon basis). This assumption is typically used for speciated emissions measurements, and is implicitly used in the routine measurement of total hydrocarbon emissions.

Oxygenated compounds give lower detector response than hydrocarbons. Based upon analy-

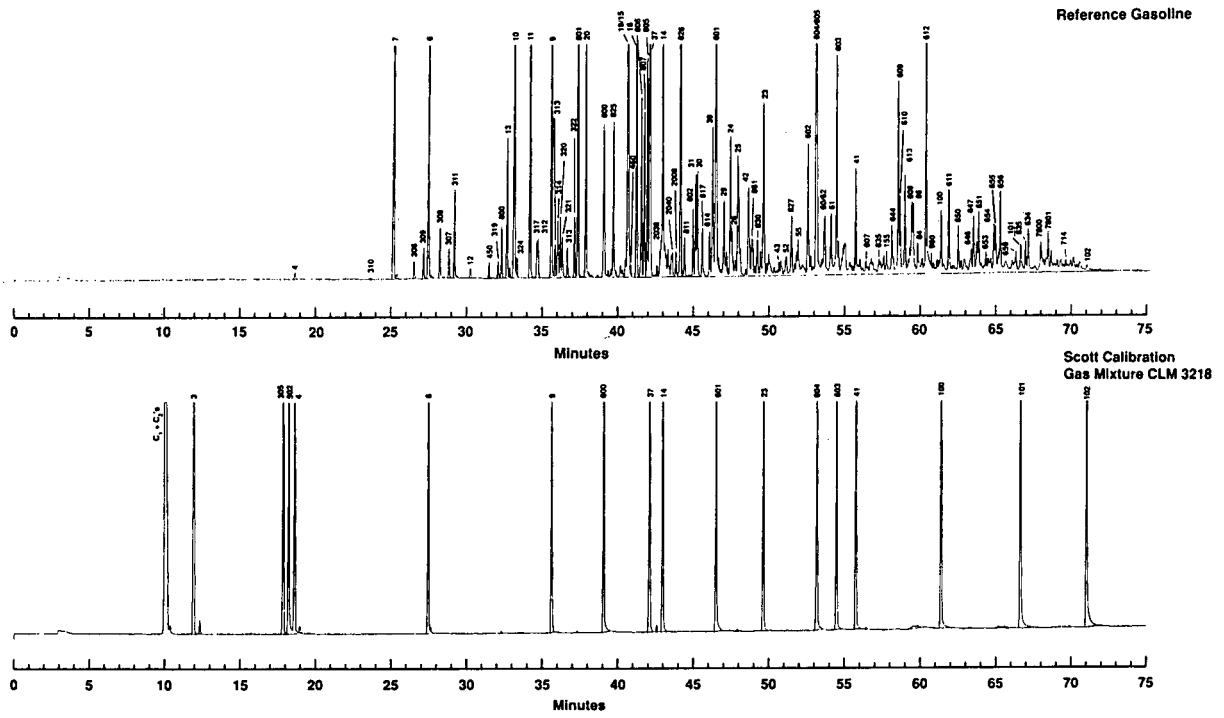

Fig. 2. Capillary column analyses of reference gasoline and calibration gas mixture. GC conditions are given in Table I. Peak identifications are given in Table III.

sis of known liquid samples (gasoline blends) detector responses were determined for several oxygenated compounds. Relative to a propane response of 1.00, a response of 0.87 was measured for methyl *tert.*-butyl ether (MTBE), 0.89 for *tert.*-amyl methyl ether (TAME), and 0.91 for *tert.*-hexyl methyl ethers (THEME). These lower response factors were used when quantifying the corresponding oxygenates in emissions samples.

Detector response variability was determined by repetitive analysis of the 21-component gas standard. Fig. 4 shows representative control charts generated from 29 analyses of this stan-

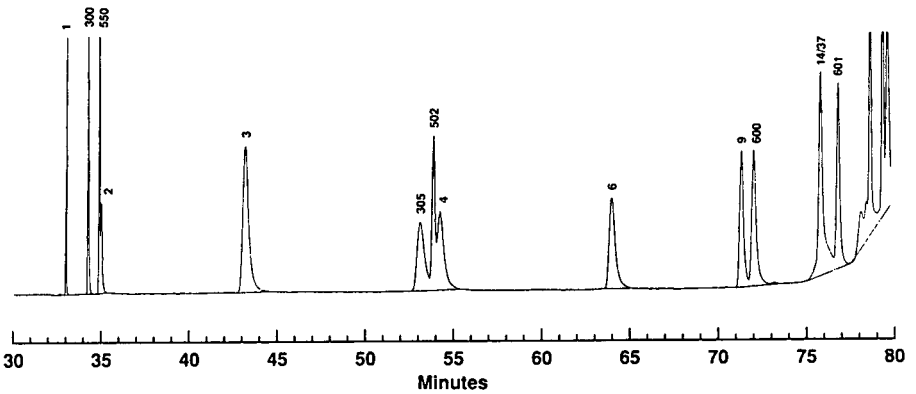

Fig. 3. GS-Q megabore column analysis of Scott calibration gas mixture CLM 3218. GC conditions are given in Table I. Peak identifications are given in Table III.

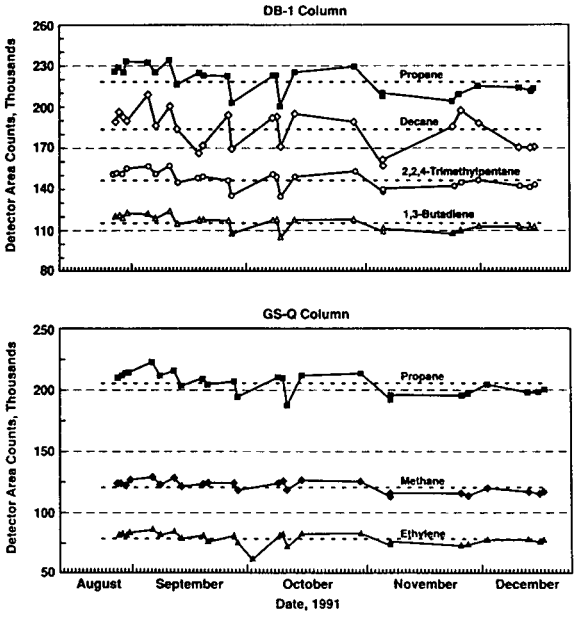

Fig. 4. Detector response control charts for analysis of Scott calibration gas mixture CLM 3218. Dashed lines represent average values.

dard over a 4-month period. These data illustrate that the detector response variability was largely systematic —that is, similar profiles were observed for all compounds. (Slight exceptions are apparent in the control charts for decane and ethylene.) This is attributed in large part to variability in preparing and sampling the Tedlar bags each day, rather than to actual changes in response of the detectors. When analyzing vehicle emissions samples, the effect of these variations was minimized by using a running weighted average response factor, comprising 3/4 of the historical response factor and 1/4 of the current day's factor.

Variability results for all 21 components are summarized in Table IV. For most compounds, the relative standard deviation (R.S.D.) was less than 5% on an absolute basis, and 1–3% when normalized to the propane response. The higher variability measured for ethane was due to the close retention times for acetylene and ethane, and the atypical composition of this standard gas mixture. (In emissions samples from modern vehicles, ethane is generally present at comparable or higher concentrations than acetylene, while in this standard mixture, ethane's concentration is only about 25% of acetylene's.) The higher variability for the heaviest alkanes ($\geq C_{10}$) is not surprising due to difficulties in sampling and analysis of such materials at low concentration.

Given uncertainties in the composition of this standard mixture, these results also confirm that most compounds give equivalent detector responses. The significantly higher responses measured for the heaviest alkanes ($\geq C_{10}$) are surprising, and remain unexplained. However, this finding is of little consequence since emissions samples generally contain only trace amounts of hydrocarbons in this range.

Detection limit

The GC detection limit was estimated from the same set of replicate analyses described above. Although this gas standard contained only 21 intentionally added hydrocarbons, trace levels of several other compounds were also present. Three of these impurities [*cis*-2-butene (peak 303; retention time of 20.9 min), 2-methyl-2-butene (peak 311; retention time of 29.2 min), and methylcyclopentane (peak 801; retention time of 37.4 min)] were used to calculate the Method Detection Limit (MDL) as defined by the US EPA [16]. The MDLs for these three compounds varied from 0.004 to 0.007 ppm C. Using the upper value of 0.007 ppm C and our normal emissions testing conditions, this translates to an emission rate detection limit of approximately 0.10 mg/mile for FTP bags 1 and 3, and 0.17 mg/mile for FTP bag 2.

Co-eluting compounds

Co-elution of some compounds is unavoidable with samples as complex as vehicle emissions. As was demonstrated by GC–MS analyses, many of the heavier hydrocarbons ($\geq C_6$) co-elute from the DB-1 column with others. The compounds listed in Table III represent our best estimate of the predominant constituents in most emissions samples.

For several important cases, calculational procedures are used to resolve co-eluting pairs. As described previously [3] the basis for these resolutions is a separate, completely resolved analy-

TABLE IV

GC RESPONSE FACTORS FOR HYDROCARBON COMPOUNDS

29 Replicate analyses of Scott Mixture CLM 3218. GC conditions shown in Table I.

Peak ID No.	Name	Conc. (ppm C)	GC column	Raw results			Propane-normalized results	
				Avg. area counts	Area counts per ppm C	R.S.D. (%)	Avg. response	R.S.D (%)
1	Methane	4.20	GS-Q	120 731	28 745	4.37	1.058	2.01
300	Ethylene	2.79	GS-Q	78 047	27 974	5.22	1.029	1.55
550	Acetylene	4.09	GS-Q	115 031	28 125	5.88	1.035	3.32
2	Ethane	0.89	GS-Q	27 477	30 873	9.78	1.136	5.23
3	Propane	7.56	GS-Q	205 415	27 171	4.45	1.000	–
3	Propane	7.56	DB-1	219 593	29 047	4.49	1.000	–
305	2-Methylpropene	4.93	DB-1	135 623	27 510	4.32	0.947	0.63
502	1 2-Butadiene	3.99	DB-1	115 149	28 859	4.33	0.994	0.69
4	*n*-Butane	4.46	DB-1	122 909	27 558	3.91	0.949	0.97
6	*n*-Pentane	4.71	DB-1	143 280	30 420	4.21	1.047	1.08
9	*n*-Hexane	4.78	DB-1	139 486	29 181	4.01	1.005	1.02
600	Benzene	4.98	DB-1	148 289	29 777	4.47	1.025	0.69
37	2,2,4-Trimethylpentane	4.88	DB-1	147 140	30 152	4.23	1.038	1.29
14	*n*-Heptane	4.68	DB-1	145 182	30 956	4.12	1.066	1.19
601	Toluene	5.29	DB-1	143 122	27 055	4.87	0.931	1.46
23	*n*-Octane	5.11	DB-1	149 829	29 321	4.10	1.010	1.42
604	*p*-Xylene	5.06	DB-1	148 659	29 403	5.35	1.012	2.11
603	*o*-Xylene	4.95	DB-1	146 401	29 576	5.44	1.018	2.39
41	*n*-Nonane	5.16	DB-1	161 580	31 314	4.48	1.078	2.67
100	*n*-Decane	4.99	DB-1	184 056	36 885	7.28	1.270	5.86
101	*n*-Undecane	5.14	DB-1	234 560	45 634	10.65	1.570	7.56
102	*n*-Dodecane	5.89	DB-1	234 300	39 779	10.88	1.372	9.48

sis of the fuels used to generate the emissions samples. In three cases where the co-eluting pairs are chemically similar, the ratio of the two in the fuel is applied directly to the emissions: (1) 2-methylhexane/2,3-dimethylpentane (peaks 15/19; retention time of 40.7 min), (2) *m*-xylene/*p*-xylene (peaks 604/605; retention time of 53.1 min), and (3) 4-methyloctane/2-methyloctane (peaks 62/60; retention time of 53.7 min).

In two other cases, the co-eluting pairs are not chemically similar: benzene/1-methylcyclopentene (peaks 600/451; retention time of 39.1 min) and toluene/2,3,3-trimethylpentane (peaks 601/38; retention time of 46.5 min). In these cases, the measurement of a third compound is used to apportion the co-eluting peak into two parts. For instance, the ratio of 2,3,4-trimethylpentane/2,3,3-trimethylpentane measured in the fuel is assumed to be the same in emissions. Thus, from analysis of 2,3,4-trimethylpentane in emissions samples, the amount of 2,3,3-trimethylpentane is calculated, and toluene is computed by difference.

APPLICATIONS

Gasoline vehicle emissions

Representative chromatograms from analysis of a bag 1 exhaust emissions sample from a 1989 gasoline vehicle are shown in Fig. 5. As is typical of emissions from catalyst-equipped vehicles, the bag 1 sample contained a much higher concentration of total hydrocarbons (70 ppm C) than did the bag 2 or bag 3 samples (11 and 17 ppm C, respectively).

The GS-Q chromatogram (bottom of Fig. 5) shows excellent resolution of all C_1–C_3 hydrocarbons. In addition, a small peak attributed to CO_2 is seen at 33.4 min. The DB-1 capillary chromatogram (top of Fig. 5) shows all major

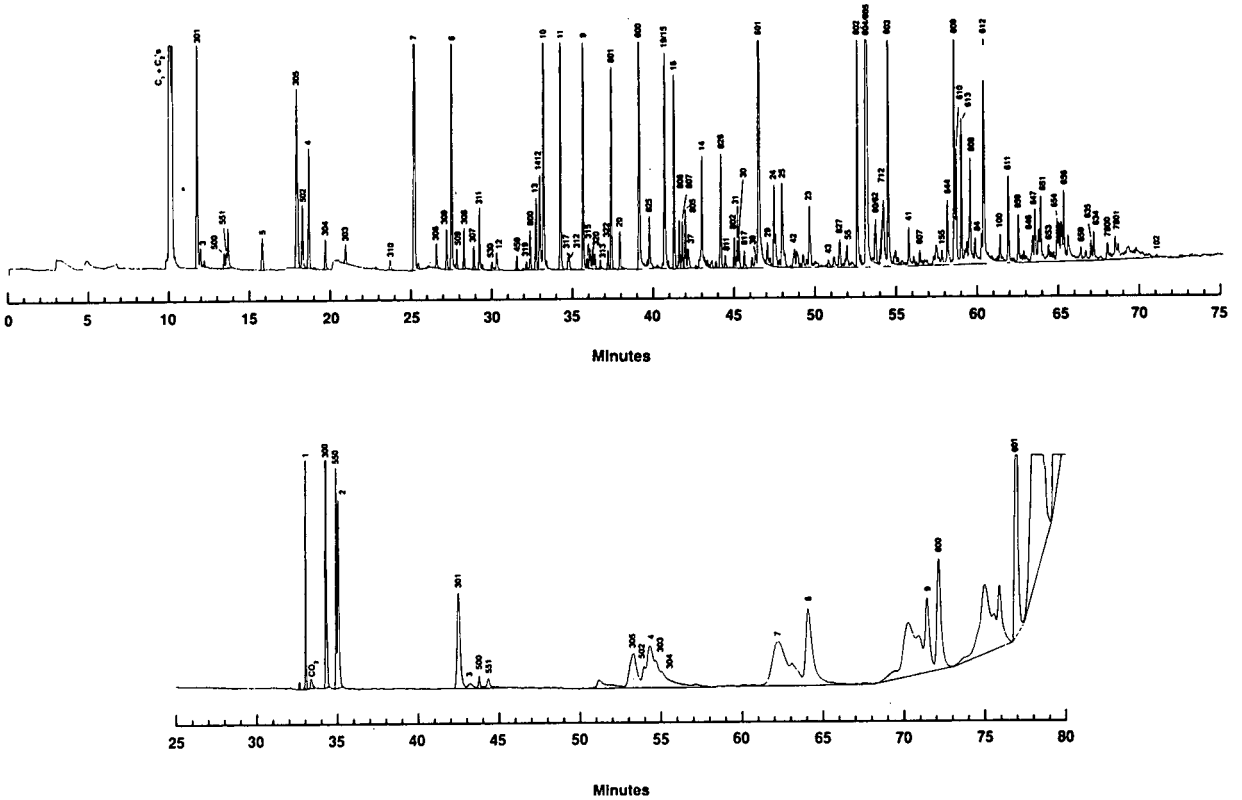

Fig. 5. GC analysis of bag 1 exhaust emissions sample from a gasoline vehicle. Total hydrocarbon concentration of 71.2 ppm C. Top: DB-1 capillary column. Bottom: GS-Q Megabore column. Peak identifications are given in Table III.

TABLE V

STABILITY OF SELECTED SPECIES IN BAG 1 EXHAUST EMISSIONS SAMPLE FROM NONCATALYST VEHICLE

Results are expressed as concentration relative to propylene.

Peak No.	Compound name	Injection No.												
		1	2	3	4	5	6	7	8	9	10	11	12	13
		Aging time (h)												
		0.0	1.6	3.3	4.9	6.6	8.2	9.9	11.6	13.2	14.9	16.5	18.2	19.8
1	Methane	0.500	0.511	0.507	0.506	0.523	0.518	0.524	0.525	0.530	0.539	0.541	0.546	0.550
300	Ethylene	1.143	1.163	1.162	1.152	1.175	1.167	1.174	1.172	1.175	1.173	1.171	1.173	1.163
550	Acetylene	0.457	0.466	0.468	0.469	0.475	0.470	0.477	0.468	0.484	0.468	0.487	0.471	0.470
301-GSQ	Propylene	1.000	1.000	1.000	1.000	1.000	1.000	1.000	1.000	1.000	1.000	1.000	1.000	1.000
301-DB1	Propylene	1.000	1.000	1.000	1.000	1.000	1.000	1.000	1.000	1.000	1.000	1.000	1.000	1.000
500	Propadiene	0.062	0.060	0.061	0.061	0.061	0.060	0.061	0.061	0.061	0.062	0.062	0.062	0.061
551	Propyne	0.092	0.081	0.093	0.084	0.081	0.097	0.080	0.080	0.079	0.080	0.080	0.079	0.080
502	1,3-Butadiene	0.188	0.142	0.102	0.083	0.073	0.058	0.053	0.046	0.042	0.040	0.037	0.034	0.032
4	*n*-Butane	0.412	0.414	0.414	0.418	0.411	0.411	0.413	0.417	0.416	0.418	0.417	0.421	0.420
309	2-Methyl-1-butene	0.097	0.096	0.091	0.094	0.093	0.093	0.091	0.092	0.093	0.093	0.093	0.093	0.092
6	*n*-Pentane	0.216	0.218	0.213	0.219	0.218	0.217	0.220	0.221	0.219	0.222	0.221	0.222	0.222
509	2-Methyl-1,3-butadiene	0.095	0.034	0.014	0.010	0.009	0.009	0.007	0.011	0.009	0.009	0.008	0.009	0.010
505	*trans*-1,3-Pentadiene	0.016	0.009	0.005	0.003	0.003	0.002	0.002	0.000	0.000	0.000	0.000	0.000	0.000
530	Cyclopentadiene	0.038	0.004	0.001	0.001	0.001	0.001	0.001	0.001	0.001	0.001	0.001	0.001	0.001
9	*n*-Hexane	0.144	0.142	0.144	0.145	0.144	0.145	0.145	0.144	0.151	0.148	0.151	0.150	0.151
600	Benzene	0.846	0.841	0.841	0.847	0.829	0.843	0.835	0.840	0.842	0.845	0.844	0.849	0.847
37	2,2,4-Trimethylpentane	0.723	0.716	0.718	0.732	0.713	0.726	0.719	0.726	0.729	0.732	0.738	0.739	0.741
601	Toluene	2.891	2.884	2.870	2.916	2.833	2.836	2.856	2.876	2.872	2.887	2.882	2.892	2.892
604/605	*m*/*p*-Xylene	1.177	1.178	1.163	1.162	1.159	1.143	1.149	1.151	1.151	1.155	1.151	1.149	1.151
712	Styrene	0.135	0.109	0.090	0.076	0.067	0.065	0.048	0.042	0.039	0.035	0.030	0.026	0.026
611	1,2,3-Trimethylbenzene	0.129	0.135	0.125	0.127	0.127	0.123	0.125	0.122	0.125	0.125	0.124	0.121	0.122

fuel constituents as well as a number of combustion-produced hydrocarbons. Of particular note is 1,3-butadiene (peak 502; retention time of 18.2 min) which previously was difficult to resolve [3], but is now baseline-separated.

Resolution of 2-methylpropene and 1-butene (peaks 305 and 302; retention time of 17.9 min) from the DB-1 capillary column is problematic. The graphical capabilities of the chromatography data station are used to magnify this region, thereby permitting the two peaks to be distinguished. In cases where significant levels of MTBE are present in the fuel (as in Fig. 5), 2-methylpropene generally predominates over 1-butene. Use of MTBE in fuels is known to increase emissions of 2-methylpropene [3,17,18].

MTBE itself is seen in the DB-1 chromatogram of Fig. 5 (peak 1412; retention time of 32.8 min). Although the fuel contained approximately 10% MTBE, the relative concentration in the emissions sample was much lower. This preferential removal of MTBE has also been documented before [3,19].

Methanol vehicle emissions

Fig. 6 presents typical chromatograms of a bag 1 exhaust emissions sample produced from a 1989 flexible-fueled vehicle operating on M-85 [methanol–gasoline (85:15, v/v)]. In addition to the major species found in gasoline vehicle exhaust, these chromatograms each show a dominant peak due to methanol. On both the DB-1 and GS-Q columns, methanol elutes very near to *n*-butane, thereby making the quantification of *n*-butane difficult. This is normally a problem only with bag 1 samples, where the methanol concentrations are high. Significantly, methanol does not interfere with measurement of 1,3-butadiene.

The DB-1 chromatogram in Fig. 6 shows a peak with retention time of 24.5 minutes that is attributed to acetonitrile. This is not an emis-

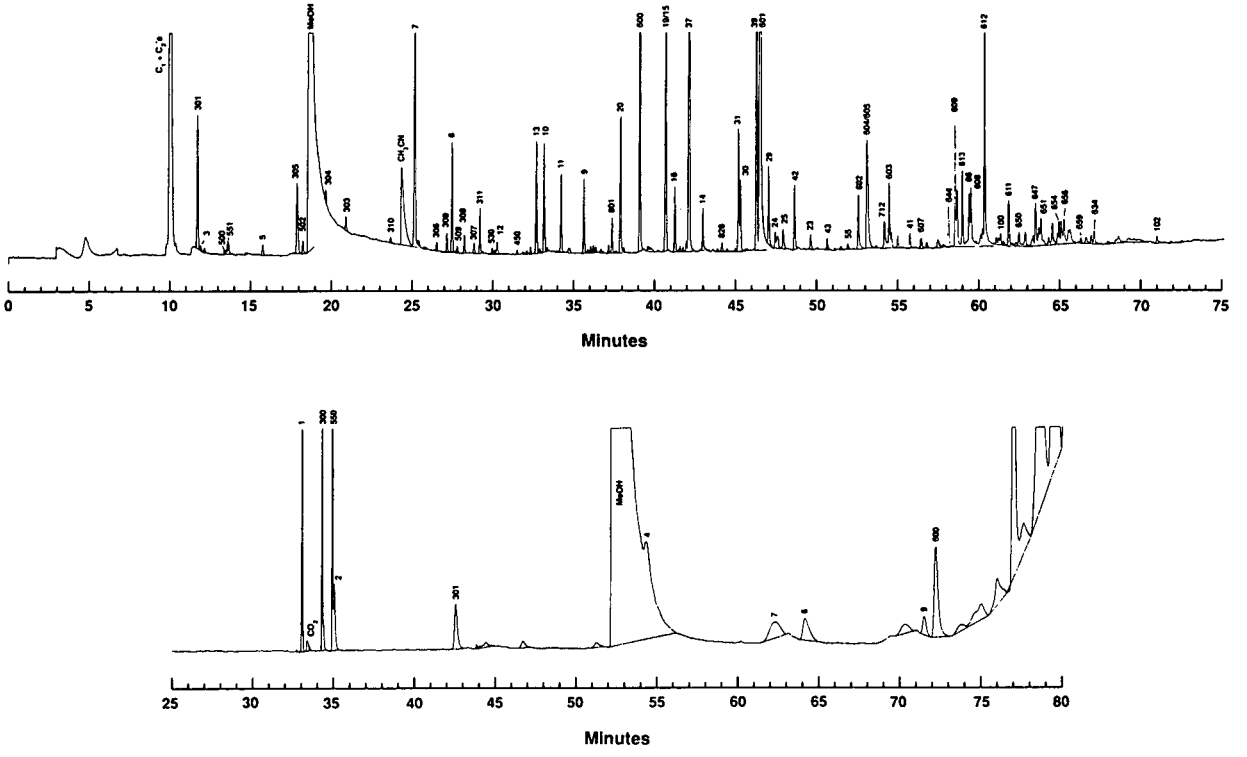

Fig. 6. GC analysis of bag 1 exhaust emissions sample from M-85 vehicle. Total hydrocarbon concentration of 140 ppm C. Top: DB-1 capillary column. Bottom: GS-Q Megabore column. Peak identifications are given in Table III.

sions species, but is a contaminant that arises from impinger techniques that are used to collect aldehydes during vehicle emissions testing.

Stability of emissions species

In recent years, there has been concern about the stability of certain exhaust emissions species when stored in Tedlar bags —particularly 1,3-butadiene. Lipari [4] reported a 25% loss of 1,3-butadiene in a bag 1 emissions sample after storing 24 h, and 70% loss after 48 h. Dempster and Shore [20] reported that "1,3-butadiene deteriorates rapidly when stored in dilute exhaust". Kaiser *et al.* [21] have recently observed degradation of 1,3-butadiene in exhaust samples from a single-cylinder engine [21].

This issue was investigated by generating and repeatedly analyzing a bag 1 exhaust emissions sample. To provide high initial concentrations of the unstable species, the vehicle that was used (1987 Chevrolet Celebrity; 2.8-l engine, 6-cylinder, port fuel injection) had its catalyst removed. This high concentration sample (270 ppm C) enabled accurate monitoring of degradation of several dienes (including 1,3-butadiene) which are normally present at only trace levels.

The exhaust emissions sample was attached to the automatic gas sampling valve on the GC instrument and was analyzed at approximately 90-min intervals until the Tedlar bag was empty. The concentrations of 20 selected compounds were measured at each analysis time. These compounds included all five dienes which are routinely measured in vehicle emissions, as well as representative *n*-alkanes, isoalkanes, alkenes, and aromatics in the range of C_1–C_9.

The results summarized in Table V are expressed as concentrations relative to the concentration of propylene. Propylene is a convenient choice for internal normalization since it can be measured reliably from both GC columns. This normalization eliminates sampling variability and compensates for sample dilution which was unavoidable using our automatic sampling technique. It has been reported that propylene itself is stable in such emissions samples for up to 1 day [4,21]. We independently established propylene's stability in samples aged for 3 days [22].

Clear differences in stability among the emissions species were seen. The 20 compounds can be broadly categorized as stable (*n*-alkanes, isoalkanes, propylene, acetylene, aromatics and most alkenes), moderately unstable (styrene and 1,3-butadiene), and highly unstable (C_{5+} dienes). Degradation of the unstable species is further illustrated in Fig. 7, with *n*-butane included as a point of reference.

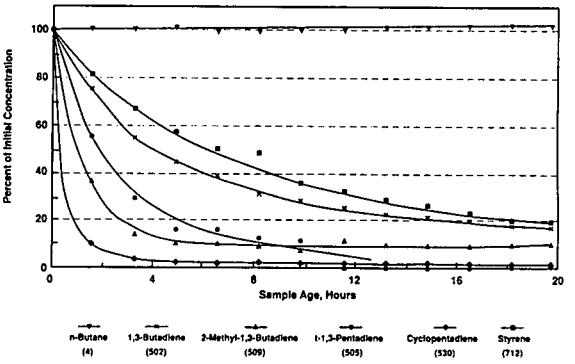

Fig. 7. Degradation of species in bag 1 exhaust emissions sample from non-catalyst gasoline vehicle.

In theory, such degradation curves could be used to adjust the measured concentrations of these unstable compounds in aged samples. However, similar analyses of other emissions samples showed the rates of degradation to be quite variable —although the relative ranking of stability was always similar to that shown in Fig. 7. In particular, lower degradation rates were observed in emissions from catalyst-equipped vehicles. It is not known whether this is due to lower levels of total hydrocarbons, lower NO_x, or other factors. Varying degradation rates for 1,3-butadiene and cyclopentadiene have been reported by others as well [21].

SUMMARY AND CONCLUSIONS

An improved GC methodology has been developed for speciated analysis of C_1–C_{12} hydrocarbons in vehicle exhaust emissions. The simultaneous use of two columns allows for complete analysis of emissions samples using a single GC instrument. Detection limits for individual hydrocarbons are $\leq$10 ppb C, which corresponds to an emission rate of approximately 0.1 mg/mile for a typical FTP bag sample. While this is

adequate to provide thorough characterization of exhaust emissions from current vehicles, additional sensitivity may be necessary for future, low-emitting vehicles.

This improved GC procedure has been satisfactorily used to analyze exhaust emissions from both gasoline- and methanol-fueled vehicles. The presence of methanol in emissions samples does not seriously hinder measurement of hydrocarbons. Sample instability was found to be a general problem for diene compounds in exhaust mixtures. The rates of degradation are sample dependent, and may be influenced by the amount of other components in emissions. To minimize concerns about sample integrity, exhaust emissions should be analyzed promptly after collection.

ACKNOWLEDGEMENTS

The efforts of the following individuals are gratefully acknowledged: Ms. A.N. Tiedemann conducted all GC analyses; Mr. G. Hemighaus assisted in constructing the GC peak library; and Messrs. J.A. Cembura and W.E. Warren generated all vehicle emissions samples.

REFERENCES

1 California Air Resources Board Staff Report, *Proposed Regulations for Low-Emission Vehicles and Clean Fuels*, Air Resources Board, Sacramento, CA, August 13, 1990.
2 California Air Resources Board Technical Support Document, *Proposed Reactivity Adjustment Factors for Transitional Low-Emission Vehicles*, Air Resources Board, Sacramento, CA, September 27, 1991.
3 S.K. Hoekman, *Environ. Sci. Technol.*, 26 (1992) 1206.
4 F. Lipari, *J. Chromatogr.*, 503 (1990) 51.
5 N. Pelz, N.M. Dempster and P.R. Shore, *J. Chromatogr. Sci.*, 28 (1990) 230.
6 T.E. Jensen, W.O. Siegl, J.F.O. Richert, F. Lipari, J.F. Loo, A. Prostak and J.E. Sigsby, *SAE Tech. Pap. Ser.*, 920320 (1992).
7 F.M. Black, L.E. High and J.E. Sigsby Jr., *J. Chromatogr. Sci.*, 14 (1976) 257.
8 H.E. Dietzman, *Final Report EPA 600-1-79-017*, US EPA, Research Triangle Park, NC, February 1979.
9 L.R. Smith and C. Urban, *Final Report EPA 460-3-82-004*, US EPA-Research Triangle Park, NC, March 1982.
10 P.F. Nelson and S.M. Quigley, *Atmos. Environ.*, 18 (1984) 79.
11 F.D. Stump and D.L. Dropkin, *Anal. Chem.*, 57 (1985) 2629.
12 J.E. Sigsby Jr., S. Tejada, W. Ray, J.M. Lang and J.W. Duncan, *Environ. Sci. Technol.*, 21 (1987) 466.
13 P. Rieger and W. McMahon, *84th Annual Meeting of the Air and Waste Management Association, Vancouver, BC, June 1991, AWMA Paper 91-107.3.*
14 E.G. Sweeny, J.H. Baudino and C.H. Schmidt, *SAE Tech. Pap. Ser.*, 922253 (1992).
15 *Code of Federal Regulations*, Title 40, Part 86; Revision 40 CFR 86.101 to 86.144-90, July 1989.
16 *Fed. Reg.*, 49, No. 209 (1984) 43430.
17 A.M. Hochhauser, R.A. Gorse, R.M. Reuter, J.D. Benson, W.J. Koehl, J.A. Rutherford, V.R. Burns and L.J. Painter, *SAE Tech. Pap. Ser.*, 920325 (1992).
18 P.A. Weber, L.R. Smith and J.E. Kubsh, *SAE Tech. Pap. Ser.*, 922245 (1992).
19 W.R. Leppard, R.A. Gorse, L.A. Rapp, J.C. Knepper, V.R. Burns and W.J. Koehl, *SAE Tech. Pap. Ser.*, 920329 (1992).
20 N.M. Dempster and P.R. Shore, *SAE Tech. Pap. Ser.*, 900354 (1990).
21 E.W. Kaiser, W.O. Siegl, D.F. Cotton and R.W. Anderson, *Environ. Sci. Technol.*, 26 (1992) 1581.
22 S.K. Hoekman, Chevron Research and Technology Company, unpublished report, 1992.

Journal of Chromatography, 639 (1993) 255–259
Elsevier Science Publishers B.V., Amsterdam

CHROM. 24 990

Gas chromatography of Titan's atmosphere

IV. Analysis of permanent gases in the presence of hydrocarbons and nitriles with a Molsieve PLOT capillary column

E. de Vanssay*, P. Capilla, D. Coscia, L. Do, R. Sternberg and F. Raulin

Équipe Physico-Chimie Organique Spatiale, LPCE, URA 1404 du CNRS, Université Paris 12, Val de Marne, F-94010 Créteil Cedex (France)

(Received January 11th, 1993)

ABSTRACT

A Molsieve 5A wide-bore capillary column was systematically studied for the separation of CO and N_2 in the presence of other permanent gases, including noble gases, light hydrocarbons and nitriles, which are all plausible constituents of Titan's atmosphere. This column has a chromatographic behaviour similar to that of a molecular sieve 5A packed column. The efficiency of the column, the detection limit of CO in N_2 and the effect of the presence of nitriles in the injected samples on the chromatographic performance of the column were characterized by determining Van Deemter curves for CO, N_2 and noble gases at different temperatures. This column offers a rapid separation of the selected solutes under isothermal conditions, with about 1000 theoretical plates/m at 60°C for most of the solutes.

INTRODUCTION

As reported in previous papers in this series [1–3], we are systematically studying GC columns that could provide the separation of most of the constituents of Titan's atmosphere and of the pyrolytic products of its organic aerosols, for integration in the GC–MS instrument of the Cassini–Huygens mission. One of the objectives with this instrument is to determine the vertical concentration profile of several of the organic and inorganic species present in the atmosphere, including hydrocarbons, nitriles, CO, N_2, CH_4, Ar and other noble gases. The GC subsystem should be able to achieve the separation of these compounds in a relatively short time (*i.e.*, within less than, say, 10 min), under conditions fully compatible with the constraints of space instrumentation. These include the constraints induced by GC–MS coupling such as low carrier gas inlet pressure, low flow-rate and simple column temperature cycle (the easiest being isothermal conditions). The previous papers reported studies of GC columns for analysing organic compounds. This present paper deals with the analysis of CO and permanent gases. Such an analysis is of paramount importance, as the GC–MS instrument will have to confirm and determine the depletion of CO in Titan's stratosphere, relative to the troposphere [4], the origin of which is still not clearly understood [5]. To achieve such an objective, it is crucial that the GC stage provides a good separa-

* Corresponding author.

0021-9673/93/$06.00

tion of CO from N_2, as the MS subsystem will not be able to perform direct determination of CO because of the presence of large amounts of N_2, the main atmospheric component, and because of the limited mass resolution of the instrument.

To achieve such a separation, we have carried out studies in two complementary directions: small and short columns packed with microparticles and wide-bore capillary columns, both using a molecular sieve. This packing material has been widely used in the GC analysis of permanent gases with conventional packed columns, including GC devoted to space instrumentation [6,7]. A molecular sieve has also been used recently as a coating material in wide-bore fused-silica capillary columns, such as the Molsieve 5A column (Chrompack, Middelburg, Netherlands). The characteristics and chromatographic performance of this capillary column have already been published [8].

A wide-bore Molsieve 5A column seems to offer the advantages of both capillary columns, *i.e.*, combining the possibility of high resolution and relatively fast analysis, and those of conventional packed columns, with a high charge capacity [8]. However, no detailed studies of this column, including Van Deemter curves, have been reported. In addition, no data were available on the separation limit of CO in N_2 or on the possible effect of the injection of non-eluted compounds such as nitriles on the behaviour of this column. To obtain such crucial information (in particular in terms of reproducibility of the chromatograms, and eventual degradation of its performance due to the injection of compounds of high polarity), we have systematically studied a Molsieve 5A capillary column and the results are reported in this paper.

EXPERIMENTAL

Column and gas chromatograph

The Molsieve 5A column was a 10 m × 0.53 mm I.D. PLOT fused-silica capillary column coated with a 50-μm film of molecular sieve 5A. It was mounted on a Hewlett-Packard Model HP 5890 Series II gas chromatograph equipped with a micro thermal conductivity detector, an electro-pneumatic six-port gas sampling valve (Valco) with a 0.25- or 2-ml sample loop and a Spectra-Physics Model SP 4100 integrator–recorder.

The GC column was operated isothermally at temperatures in the range 30–130°C. The temperatures of the detector, injector and gas sample valve were chosen as a function of the column temperature. Hydrogen was used as the carrier gas because for equivalent HETP values it can provide faster analyses. In addition, it is more convenient for GC–MS instrumentation in space, as it is much more easily pumped out than other carrier gases. Its flow-rate was adjusted around 2 ml/min (except when determining HETP values).

In most of the studies, the gas chromatograph was used in the split mode (splitting ratio from 10:1 to 100:1). For studying the effect of the dilution of CO in N_2, the splitless mode was chosen. In that case, to obviate any effect of the injector dead volume, a purge septum flow of hydrogen was maintained at 1 ml/min.

Sampling

Standard gas mixtures of known composition, including CO, N_2, CH_4, C_2H_6 and noble gases (He, Ne, Ar, Kr and Xe), were prepared and stored in a sampling glass reservoir connected to a vacuum line and equipped with a high-vacuum stopcock (SVT, Ris Orangis, France). This reservoir was initially evacuated, then a commercial CH_4–Ar mixture and each component were successively introduced by expanding a known volume at a known and precalculated pressure, as described previously [1]. A similar method was used for preparing the samples used to study the effect of CO dilution. The loop of the gas sampling valve was also connected to the vacuum line. It was directly sampled, at a known pressure, by expanding the contents of the reservoir to the loop, initially evacuated.

The vacuum line through the primary pump was able to reach a vacuum as good as 10^{-2} mbar, checked with a Pirani vacuum gauge (MKS, Andover, MA, USA). Absolute pressures were measured with a pressure gauge (Schlumberger, Montrouge, France) with a relative precision of better than 1%.

Reagents

Cyanogen was obtained from Matheson (East Rutheford, NJ, USA) and helium (grade C) from AGA (Toulouse, France). All other gases, *i.e.*, argon–methane mixture (90:10, pure), nitrogen, neon and ethane (grade N30), krypton (grade N35), xenon, carbon monoxide and methane (grade N45), were purchased from Alphagaz–L'Air Liquide (Bois d'Arcy, France).

Determination of Van Deemter curves

To determine experimentally the height equivalent to a theoretical plate (HETP), H, *versus* the mean linear velocity of the carrier gas, $\bar{u}$, the different selected solutes were injected with helium at different inlet pressures of the carrier gas and different column temperatures. The outlet flow-rate was measured with a bubble flow meter.

The value of $\bar{u}$ was calculated from the relationship $\bar{u} = L/t_m$, where L is the length of the column and t_m is the retention time of helium. For the selected solutes, H was calculated from the classical relationship:

$$H = \frac{Lw_h^2}{5.54(t_r - t_m)^2} \quad (1)$$

where t_r is the retention time of the solute and w_h is the peak (assumed to be Gaussian) width at half-height.

The fitting of the Van Deemter curve with the experimental data was performed by using a polynomial regression program based on an extended Golay–Giddings equation:

$$H = B/\bar{u} + C\bar{u} + D\bar{u}^2 \quad (2)$$

where the term $D\bar{u}^2$ represents the apparatus contribution [9].

To verify the influence of these coefficients on the fitting, we studied two other polynomial regression programs. The first uses the classical Golay equation:

$$H = B/\bar{u} + C\bar{u} \quad (3)$$

and the second, because of the small effect of C, uses the equation

$$H = B/\bar{u} + D\bar{u}^2 \quad (4)$$

Optimization of detector response

In preliminary work, we studied and optimized the response of the thermal conductivity detector, particularly for CO. This response can be characterized by $R = (A/w)P$, where A is the integrated area of the chromatographic peak, w its half-width and P the pressure of the injected solute. R was studied as a function of the ratio of the detector to column temperature, T_d/T_c, and as a function of the duration of the splitless mode for various sample pressures. The highest responses were obtained for a splitless duration of about 30 s and a T_d/T_c value of about 2.

RESULTS AND DISCUSSION

The Molsieve column provides a good separation of most of the selected solutes within a relatively short time. For instance, at 90°C, as shown in Fig. 1, with the exception of He and Ne which are co-eluted, all the permanent gases and CH_4 are measured in about 8 min. Under these conditions, the higher molecular mass organic compounds are not eluted before 22 min (ethane).

In order to characterize quantitatively the performance of the column and its behaviour after injection of nitriles, we determined Van Deemter curves at different temperatures with and without injection of nitriles. Fig. 2 presents

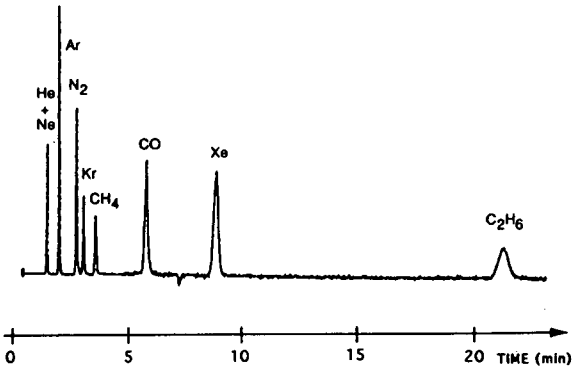

Fig. 1. Gas chromatogram of a gaseous mixture of He, Ne, Ar, N_2, Kr, CH_4, CO, Xe and C_2H_6 on a 10 m × 0.53 mm I.D. Molsieve 5A (film thickness 50 μm) fused-silica PLOT column at 90°C. Carrier gas, H_2; outlet flow-rate, 2 ml/min; amount injected, *ca.* 3 nmol of each constituent; splitting ratio, 40:1; thermal conductivity detector.

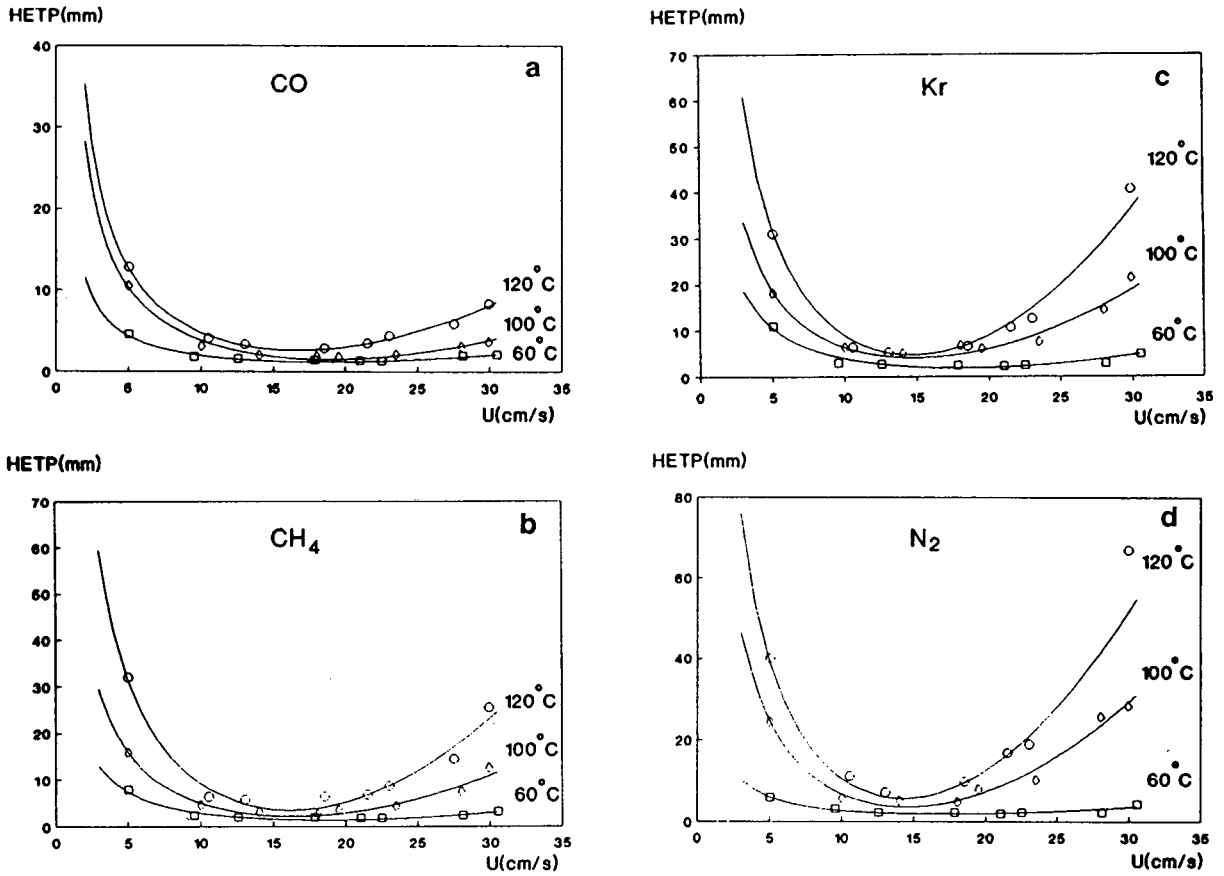

Fig. 2. Plots for (a) CO, (b) CH_4, (c) Kr and (d) N_2 of the height equivalent to a theoretical plate (HETP) versus the mean linear velocity ($\bar{u}$) of the carrier gas (H_2) at 60, 100 and 120°C on a 10 m × 0.53 mm I.D. Molsieve 5A (film thickness 50 μm) fused-silica PLOT column. The points correspond to experimental data and the curves to the best theoretical fit based on the extended Golay–Giddings' equation: $H = B/\bar{u} + C\bar{u} + D\bar{u}^2$.

the results relating to N_2, CH_4, Kr and CO (Fig. 2A, B, C and D, respectively), for three column temperatures. They were obtained by injection of about 3 nmol of each solute in the injector. There is a satisfactory fit between the experimental results (points) and the extended theoretical fitting curves $H = B/\bar{u} + C\bar{u} + D\bar{u}^2$. For all these solutes, the minimum HETP (H_m) is reached for an optimum $\bar{u}$ ($\bar{u}_m$) of about 20 cm/s at 60°C and 15 cm/s at 120°C, corresponding to 1.9 and 1.4 ml/min, respectively. This H_m ranges between 1 mm (CO at 60°C) and 8 mm (N_2 at 120°C) and it increases with temperature, as is usually observed. The part of the curve corresponding to $\bar{u}$ values higher than $\bar{u}_m$ has a slope that also increases with increasing temperature. This can be easily explained by an increase in the diffusion coefficient of the solute with temperature.

The HETP values thus determined are of the same order of magnitude (1.4 mm at 60°C for methane) as those indicated by Chrompack, the column manufacturer (1.3 mm at 30°C for methane). These values are high probably because of the relatively large film thickness (50 μm).

The possible influence of the presence of nitriles in the injected samples on the behaviour of this column was studied by injecting various amounts of cyanogen, simultaneously with constant amounts (about 3 nmol) of CO and N_2, and by measuring the HETP for the two permanent gases. In each series of experiments, the amount

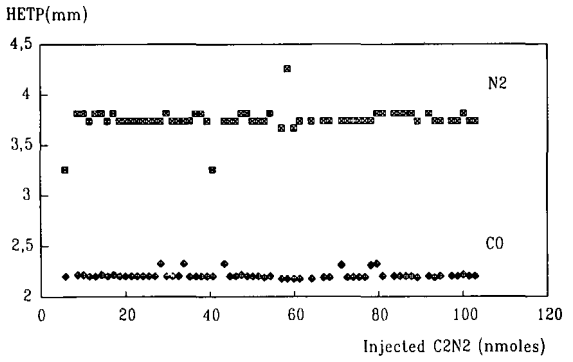

Fig. 3. Plot of the height equivalent to a theoretical plate (HETP) versus the amount of cyanogen (C_2N_2) injected for CO and N_2 at 100°C. Carrier gas, H_2; column, 10 m × 0.53 mm I.D. Molsieve 5A (film thickness 50 μm) fused-silica PLOT.

of cyanogen was systematically increased from the first to the last injection. The column was then conditioned at 270°C for 16 h, before carrying out a new series of experiments. The results show that the retention times of the eluted solutes are not modified by the presence of cyanogen in the sample, even after several injections of large amounts (several micromoles) of nitrile. Further, the HETP is not affected by the irreversible adsorption of these amounts in the column, as shown in Fig. 3.

CONCLUSIONS

The Molsieve 5A wide-bore capillary column allows a good and rapid separation of permanent gases, including CO, N_2 and noble gases, in the presence of hydrocarbons and nitriles. It is important to note that the injection of relatively large amounts (several micromoles) of cyanogen does not degrade or modify markedly the performance and behaviour of the column. The maximum mole fraction of nitriles in the low atmosphere of Titan is less than about 10^{-4} [10,11]. The sampling volume of the GC subsystem of the GC–MS set-up in the Cassini–Huygens mission will be less than 1 ml. Hence the absolute amount of nitrile in one sample (even at the maximum Titan atmosphere pressure of 1.5 bar) will be less than about 10^{-8} mol. Even after ten injections (which will peak during the descent of the probe), clearly the total amount of nitrile adsorbed in the column will still be one to two orders of magnitude below the currently tested conditions. Hence it can be assumed that such a column will not be affected by the chemical conditions of Titan's environment. In addition, the chromatographic conditions, in terms of temperature (about 100°C), flow-rate (less than about 2 ml/min) and inlet relative pressure (0.5 bar), are fully compatible with the constraints of MS coupling and space instrumentation.

However, the mechanical resistance of this column has not yet been tested under the acceleration and vibration conditions of a rocket launch. If such a test shows that it cannot withstand these intense vibrations, as has recently been observed for other PLOT columns [3], then one should consider the other option, *viz.*, the use of a short capillary column packed with a molecular sieve. The study of such packed columns (similar to the present one) is in progress.

ACKNOWLEDGEMENTS

Thanks are due to Dr. Vidal-Madjar for her help during this work and comments during the preparation of the manuscript. This research was supported by a grant from the Centre National d'Etudes Spatiales.

REFERENCES

1 L. Do and F. Raulin, *J. Chromatogr.*, 481 (1989) 45.
2 L. Do and F. Raulin, *J. Chromatogr.*, 514 (1990) 65.
3 L. Do and F. Raulin, *J. Chromatogr.*, 591 (1992) 297.
4 A. Marten, D. Gautier, L. Tanguy, A. Lecacheux, C. Rosolen and G. Paubert, *Icarus*, 76 (1988) 558.
5 E. Chasséfiere and M. Cabane, *Geophys. Res. Lett.*, 18 (1991) 467.
6 B.G. Gelman, V.G. Zolutukhin, L.M. Mukin, N.I. Lamonov, B.V. Levchuk, D.F. Nenarov, B.P. Okhotnikov, V.A. Kotin and A.N. Lipatov, *Space Res.*, 20 (1980) 219.
7 F. Raulin, E. de Vanssay, L.J. Do and P. Paillous, *LC·GC*, 5, No. 7 (1992) 22.
8 J. de Zeews, *J. Chromatogr. Sci.*, 25 (1987) 71.
9 G. Gaspar, C. Vidal-Madjar and G. Guiochon, *Chromatographia*, 15 (1982) 125.
10 Y.L. Yung, *Icarus*, 72 (1987) 468.
11 A. Coustenis, B. Bézard, D. Gautier, A. Martin and R. Samuelson, *Icarus*, 89 (1991) 152.

Journal of Chromatography, 639 (1993) 261–271
Elsevier Science Publishers B.V., Amsterdam

CHROM. 24 989

Simultaneous analysis of 25 pesticides in crops using gas chromatography and their identification by gas chromatography–mass spectrometry

Jongki Hong, Yunwoo Eo, Jaeseong Rhee and Taekjae Kim*

Advanced Analysis Center, Korea Institute of Science and Technology, Seoul 131 (South Korea)

Kangjin Kim

Department of Chemistry, Korea University, Seoul 131-701 (South Korea)

(Received November 24th, 1992)

ABSTRACT

The simultaneous analysis of 25 pesticides in soy beans and rices was performed by gas chromatography with dual electron-capture detection and nitrogen–phosphorus detection. The pesticides were extracted from the samples with solvent and the Bio-Beads S-X3 clean-up procedure was used. Recovery studies were performed at the 1-ppm level of pesticides added to each crop. Their recoveries ranged between 83 and 105% with coefficient of variations of 0.5–8.2%. The gas chromatographic properties of the 25 pesticides were also investigated. Conformation analysis was achieved by the retention time and characteristic fragment ions using the technique of gas chromatography–mass spectrometry–selected-ion monitoring.

INTRODUCTION

The monitoring of pesticides in crops is of importance in public health, because of the inherent toxicity of pesticides. Many analysts have contributed to the methodological development for analysis of pesticide residues in crops. Several chromatographic methods have been reported for the separation, detection and quantitative measurement of pesticides in food [1,2], water [3–5] and soil [6,7]. Published methods include those based on gas–liquid chromatography [8,9], gas chromatography (GC)–mass spectrometry (MS) [10–12], high-performance liquid chromatography (HPLC) [13,14] and liquid chromatography (LC)–MS [15–17].

GC methods have been based on the chemical structure of pesticides containing nitrogen, phosphorus or chlorine atoms, and so high sensitivity has been obtained with electron-capture detection (ECD) and nitrogen–phosphorus detection (NPD). LC systems have been applied to thermally unstable and non-volatile pesticides, which have proved to be difficult to quantify by GC. Many procedures for sample preparation prior to GC analysis have been reported using extraction by organic solvents [18,19], distillation systems [20,21] on column chromatography [22,23]. Recently, Bio-Beads have been widely used in column chromatography for the analysis of samples containing fat and oil [24,25]. Mattern *et al.* [26] described a GC–MS method for detection and quantitation of twelve pesticides in fruits and vegetables. And Roach and Carson [12] reported

* Corresponding author.

0021-9673/93/$06.00

the MS behaviour of organopesticides in food using the collisionally activated decomposition mode.

In this paper, we describe a GC–ECD–NPD procedure for the simultaneous separation and determination of 25 pesticides regulated in our country [27]. Each pesticide was confirmed using GC–MS–selected-ion monitoring (SIM) mode.

EXPERIMENTAL

Chemicals

All reagents were of residual pesticide grade. Acetone, methanol, ethylacetate, hexane and methylene chloride purchased from J.T. Baker (Phillisburg, NJ, USA). Bio-Beads S-X3 (200–400 mesh) for chromatography was from Bio-Rad (Richmond, CA, USA). Purified water was

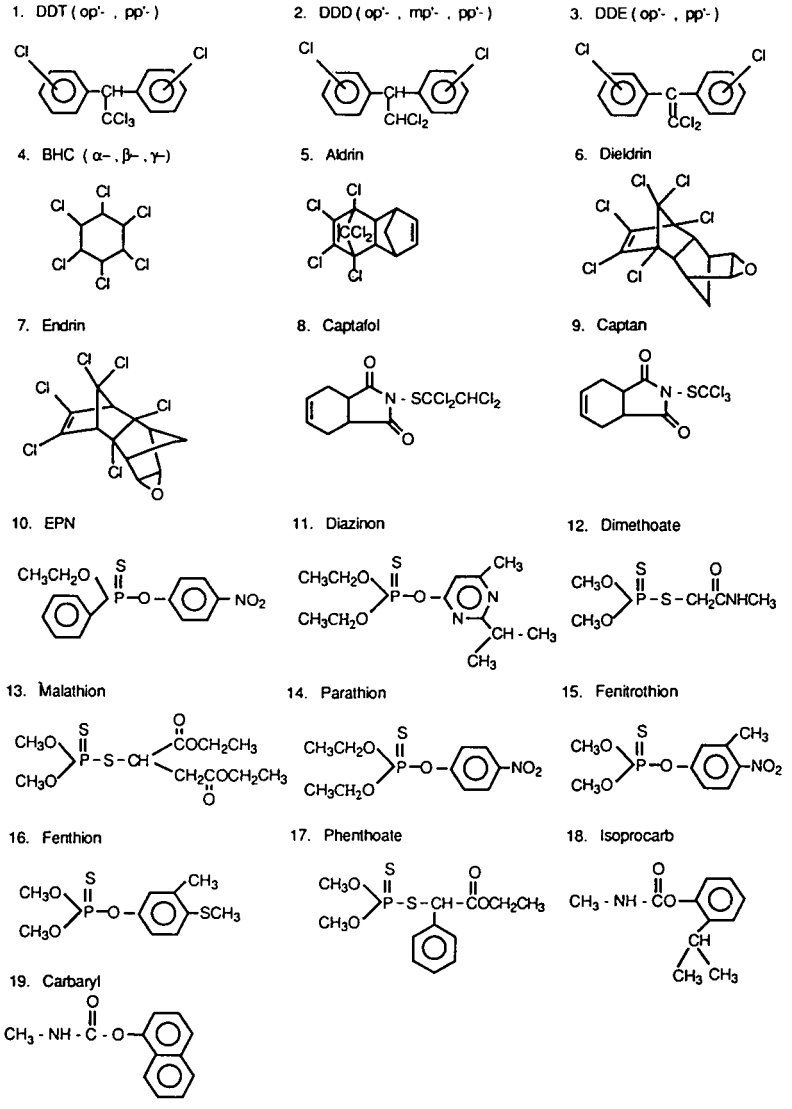

Fig. 1. Chemical structures of pesticides.

obtained with a Milli-Q system (Millipore, USA). Twenty-five pesticide standards were obtained from Chem. Service (West Chester, PA, USA) and from Aldrich (Milwaukee, WI, USA). Standard stock solutions in hexane and acetone were stored at 4°C. Triphenyl phosphate (TPP) and 24,-dichloronitrobenzene (DCNB) from Merck (Darmstadt, Germany) were used as internal standards and dissolved in hexane. The chemical structures of the pesticides tested in this study are shown in Fig. 1.

Gas chromatography

The gas chromatographic analysis was carried out on a Varian Vista 6000/6500 gas chromatograph (Sunnyvale, CA, USA) equipped with a dual nitrogen–phosphorus detector and ^{63}Ni electron-capture detector. A Varian Vista 402 chromatograph data system was used for the data processing. All extracts were injected onto an on-column capillary inlet designed for fused-silica columns. Separation was achieved with an HP-1 capillary column with cross-linked methylsilicone (SE-30, 50 m × 0.32 mm I.D., 0.32 μm film thickness). The capillary column was installed and connected to both detectors via the variable effluent splitter from Varian. The chromatographic conditions were as follows: detector temperature, 280°C, column temperature, 150°C at 6°C/min to 260°C, held for 10 min; carrier gas, nitrogen at a flow of 0.4 ml/min for ECD and 4.0 ml/min for NPD.

Gas chromatography–mass spectrometry

The Hewlett-Packard GC–MS system consisted of a Model 5890A gas chromatograph, a Model 5970B mass-selective detector, an HP 5970C MS Chemstation and an HP 7946 disc drive. A fused-silica capillary column coated with HP-1 cross-linked metylsilicone (SE-30, 25 m × 0.25 mm I.D., 0.17 μm film thickness) was also used. The GC temperature programme was as follows: initial temperature was 100°C, held for 4 min, increased by 8°C/min to 280°C, and held for 5 mins. Samples were injected in the split mode with a splitting ratio of 1:10. The carrier gas was helium (99.999%) at 0.9 ml/min. Injector temperature was 250°C, transfer line temperature was 270°C and ion source temperature was 200°C. The mass spectrometer was operated at 70 eV in the electron-impact (EI) mode using scan or SIM. The selected ion groups for the identification of 25 pesticides in SIM mode are listed in Table I. The dwell time for each ion was set at 50 ms.

Extraction and partitioning

Samples of 25 g were ground and extracted with a mixed solvent of 100 ml of acetone and 50 ml of methanol in a blender jar for 10 min at high speed. The mixture was filtered with suction through a 12-cm Büchner funnel. The filtrate was transferred to a 500-ml round-bottomed flask. The volume of this solution was reduced to about 100 ml by a rotary evaporator and then 50 ml of water and 30 ml of saturated sodium chloride solution added. To this mixture, 100 ml of methylene chloride were added, followed by vigorous shaking in a separatory funnel. The

TABLE I

FOUR ION GROUPS ACCORDING TO RETENTION TIME IN THE SIM MODE

Ion groups	Selected ions
Group A (6 min to 12.5 min)	
Isoprocarb	121, 136
BHC isomers	181, 183, 219
Dimethoate	93, 125
Diazinon	137, 179
Group B (12.5 min to 15 min)	
Carbaryl	144, 115
Fenitrothion	125, 109
Aldrin	66, 263
Malathion	125, 173
Fenthion	278
Parathion	291, 97
Captan	79, 149
Group C (15 min to 17.4 min)	
Phenthoate	274, 121
DDE isomer	246, 248
Endrin, dieldrin	261, 263, 265
DDD	235, 237
Group D (17.4 min to 22 min)	
DDT isomers	235, 237
Captafol	79, 311, 313
EPN	157

extracted organic phase was collected in a 200-ml round-bottomed flask. The aqueous phase was re-extracted with 50 ml of methylene chloride in the same way. The organic phase was combined with the first extract in a 200-ml round-bottomed flask. The organic phase was evaporated to dryness by a rotary evaporator.

Clean-up

Bio-Bead S-X3 was slurried into a 30 cm × 1 cm I.D. column to *ca.* 15 cm height and was washed with 5 ml of methylene chloride–cyclohexane (1:1). Extracted residue was dissolved in methylene chloride–cyclohexane (1:1) and then placed on the column. Methylene chloride–cyclohexane was used as eluent solvent at a flow-rate of 2 ml/min. The eluate was collected in two fractions: the first fraction (9 ml) containing lipids was discarded, while the second fraction (11 ml) was collected and then evaporated under a nitrogen stream. The dried residue was dissolved with 2 ml of hexane.

RESULTS AND DISCUSSION

Analysis by GC–NPD–ECD

GC with dual NPD and ECD in parallel is able to identify residual pesticides and achieve the simultaneous determination of compounds containing chlorine, phosphorus or nitrogen atoms. The GLC separation of 25 standard pesticides on an SE-30 fused-silica capillary column using dual

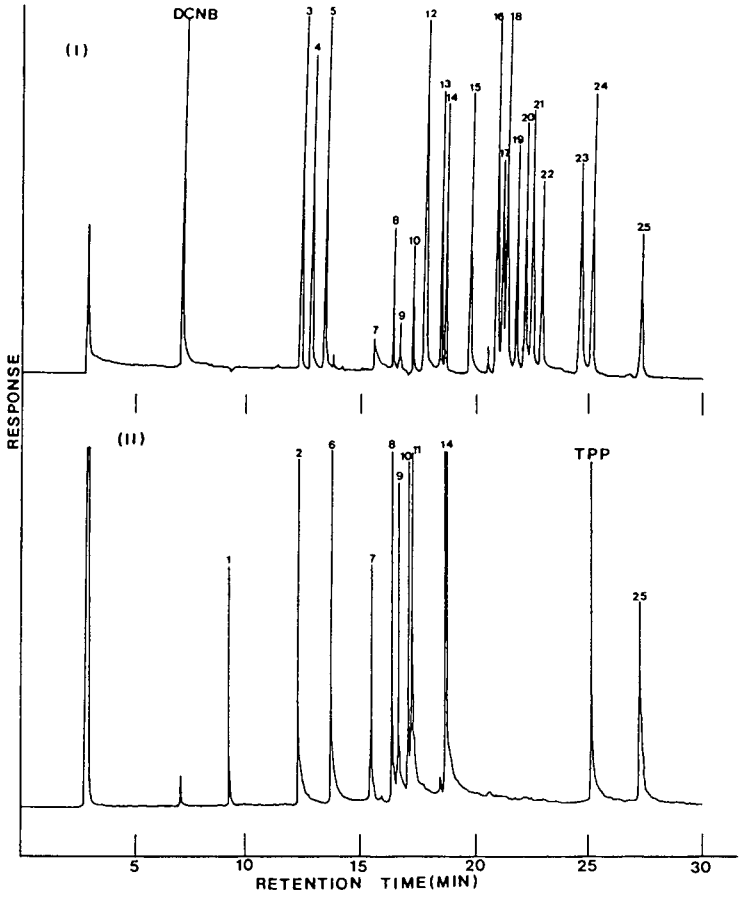

Fig. 2. Dual ECD (I) and NPD (II) chromatograms of 25 standard pesticides. Peaks: 1 = isoprocarb; 2 = dimethoate; 3 = α-BHC; 4 = β-BHC; 5 = γ-BHC; 6 = diazinon; 7 = carbaryl; 8 = fenitrothion; 9 = malathion; 10 = fenthion; 11 = parathion; 12 = aldrin; 13 = captan; 14 = phenthoate; 15 = *o,p'*-DDE; 16 = *p,p'*-DDE; 17 = *o,p'*-DDD; 18 = dieldrin; 19 = *m,p'*-DDD; 20 = endrin; 21 = *p,p'*-DDD; 22 = *o,p'*-DDT; 23 = *p,p'*-DDT; 24 = captafol; 25 = EPN.

NPD and ECD is shown in Fig. 2. As shown in Fig. 2, 25 pesticides were successfully separated within 30 min. Noticeably, each peak exhibited no significant peak tailing. Baseline separation was achieved for each pesticide in the standard mixture. In general, N-methylcarbamates are thermally unstable at the temperatures required for GC analysis. For example, carbaryl and isoprocarb underwent thermal decomposition and lost their carbamates in the hot insert liner, which contained glass beads or OV-101. Typically, 75% of carbaryl and 15% of isoprocarb were converted into naphthol and *o*-isopropylphenol, respectively. So it was difficult to quantify by GC with a hot packed injector. To circumvent this problem, we used the cold on-column injector instead of the hot packed injector in GC and used the split liner which contained only the silanized glass wool in GC–MS analysis.

The relative retention time (RRT) and relative molar response (RMR) of pesticide with respect to internal standard DCNB and TPP are listed in Table II. As indicated in Table II, excellent precision in RRT and RMR of each pesticide was observed. The retention times of dimethoate and α-BHC were very close (12.992 and 12.993 min, respectively). Nevertheless, these compounds could still be analysed, because dimethoate and α-benzene hexachloride (BHC) should be detected by NPD and ECD, respectively.

In the RMR study, captan and captafol

TABLE II

RELATIVE RETENTION TIME (RRT) AND RELATIVE MOLAR RESPONSE (RMR) OF PESTICIDES IN RICE AND SOY BEANS USING GC–NPD–ECD ($n = 3$)

Pesticide	ECD		NPD	
	RRT (R.S.D., %)	RMR (R.S.D., %)	RRT (R.S.D., %)	RMR (R.S.D, %)
DCNB (I.S.)[a]	1.000 (0.98)	1.00	–	–
Isoprocarb	–	–	0.356 (0.46)	0.13 (3.9)
Dimethoate	–	–	0.494 (0.15)	1.01 (4.6)
α-BHC	1.780 (0.18)	4.45 (4.8)	–	–
β-BHC	1.925 (0.13)	1.11 (4.5)	–	–
γ-BHC	1.945 (0.13)	4.09 (4.6)	–	–
Diazinon	–	–	0.527 (0.09)	1.92 (8.6)
Carbaryl	–	–	0.623 (0.06)	0.12 (4.4)
Fenitrothion	–	–	0.641 (0.03)	1.50 (2.0)
Malathion	–	–	0.648 (0.02)	1.26 (3.1)
Fenthion	–	–	0.666 (0.02)	1.22 (3.4)
Parathion	–	–	0.670 (0.02)	1.88 (6.1)
Aldrin	2.495 (0.03)	3.79 (4.1)	–	–
Captan	2.733 (0.02)	0.53 (6.4)	–	–
Phenthoate	–	–	0.730 (0.01)	0.80 (3.6)
o,p'-DDE	2.821 (0.01)	1.52 (3.6)	–	–
p,p'-DDE	2.995 (0.01)	2.64 (3.7)	–	–
o,p'-DDD	3.058 (0.01)	1.40 (3.9)	–	–
Dieldrin	3.011 (0.01)	3.69 (3.8)	–	–
m,p'-DDD	3.170 (0.01)	1.46 (4.0)	–	–
Endrin	3.208 (0.01)	2.28 (5.1)	–	–
p,p'-DDD	3.279 (0.01)	2.17 (3.9)	–	–
o,p'-DDT	3.306 (0.01)	1.35 (3.9)	–	–
p,p'-DDT	3.561 (0.01)	2.08 (3.8)	–	–
TPP(I.S.)[a]	–	–	1.000 (0.01)	1.00
Captafol	3.789 (0.01)	0.87 (6.5)	–	–
EPN	–	–	1.089 (0.02)	1.52 (0.7)

[a] Retention times of DCNB and TPP are 6.687 and 25.123 min, respectively.

showed a slightly lower response than other chlorinated pesticides. In particular, β-BHC of the BHC isomers showed a significantly lower response on ECD than α- or γ-BHC. It is suggested that the six chlorine atoms on the cyclohexane ring are located in an equatorial position in β-BHC, whereas in α- and γ-BHC three and four of the six chlorine atoms, respectively, are positioned axially. Presumably, the different response of BHC isomers on ECD is caused by the difference in stereochemical structure. DDE, DDD and DDT isomers also showed different responses depending on the position of the chlorine atoms on the benzene ring.

The NPD response of pesticides is also dependent on the structure and is particularly affected by substituents bonded at the nitrogen atom. Isoprocarb and carbaryl showed slightly lower sensitivity than other nitrogen-containing compounds because the nitrogen of carbamates bonded to a carbonyl group is known to be less effective in NPD response [28]. Although, of chlorinated pesticides, captan and captafol contain a nitrogen atom, these compounds exhibited very low sensitivity in the NPD chromatogram. This could be attributed to the fact that the nitrogen atom in captan and captafol is bonded to two carbonyl groups. Some pesticides, such as carbaryl, fenitrothion, malathion, fenthion, phenthoate and O-ethyl O,4-nitrophenyl phenylphosphonothioate (EPN), could be detected with both ECD and NPD. These results can be used to identify pesticide peaks.

Extraction and clean-up

It is necessary to pretreat the specimens in order to extract the pesticide of interest and to remove inferences from the fatty sample. Therefore, clean-up including solvent partitioning and column chromatography were required to remove the fatty materials.

In this study, methylene chloride was chosen in the solvent partitioning and Bio-Beads S-X3 was used for column chromatography. In general, Florisil clean-up in column chromatography is known to be unsuitable for the elution of polar pesticides and the removal of fatty materials. However, Bio-Bead S-X3 clean-up removes interfering lipids from the initial methylene chloride extract, so it is particularly valuable for the analysis of the residual pesticides in fatty samples. The methylene chloride extracts containing pesticides and lipids were chromatographed on a 15-cm Bio-Beads S-X3 column to determine the pesticide recovery. The elution curves of pesticides and rice oils with Bio-Beads S-X3 are shown in Fig. 3. The effluent from 11 to 20 ml was collected, concentrated and analysed for pesticide contents by gas chromatography. As shown in Fig. 3, more than 75% of lipid was removed through this column, whereas most pesticides were recovered.

Typical chromatograms obtained from the control rice and soy bean extracts using the methylene chloride partition and Bio-Beads S-X3 are shown in Fig 4. No interferences were detected in the dual chromatograms.

Recovery studies were performed three times at the 1-ppm (w/w) level for each pesticide spiked in rices and soy beans. These samples were prepared by adding 0.5 ml of 50 μg/ml pesticide stock solutions to 25 g of ground rices or by adding 0.1 ml of 50 μg/ml stock solution to 5 g of ground soy beans before extraction. The extracts were analysed as previously described. Fig. 5 shows the chromatograms obtained from the spiked rices and soy beans. The ratios of peak area obtained from extracted pesticides were compared with those of standard solutions containing the same concentration of pesticide and internal standards.

The recoveries of pesticide in crops are listed in Table III. Recoveries for rices were between

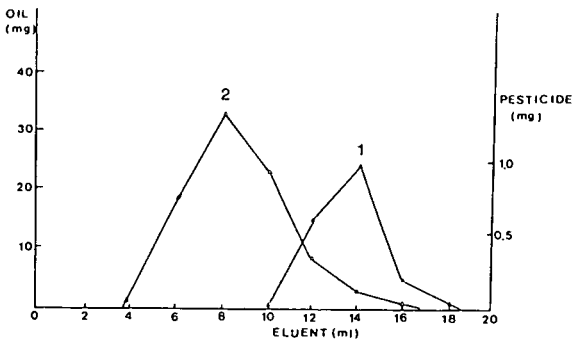

Fig. 3. Elution curves of (1) pesticides and (2) rice oil with a Bio-Beads S-X3 column.

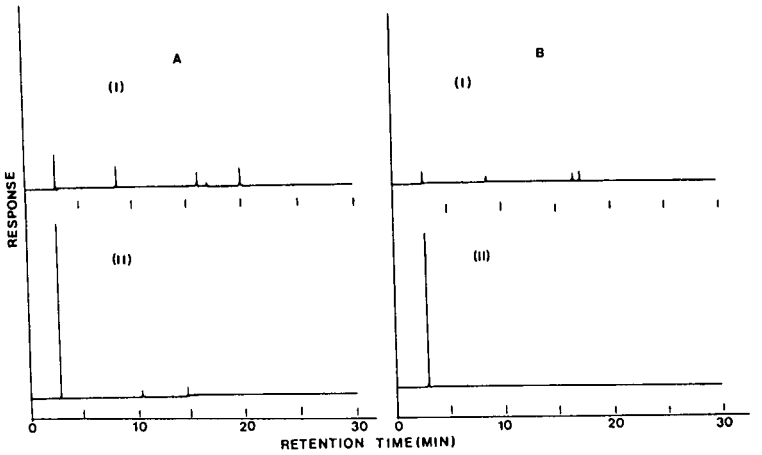

Fig. 4. Dual ECD (I) and NPD (II) chromatograms of (A) control rices and (B) control soy bean extract.

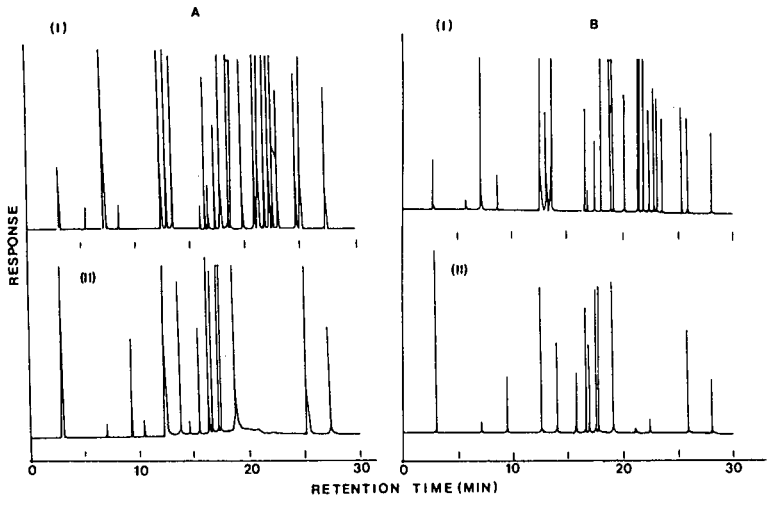

Fig. 5. Dual ECD (I) and NPD (II) chromatograms of (A) rice extract and (B) soy bean extract (peaks same as in Fig. 2).

83 and 105%, and the coefficients of variation were 0.5–7.2%, with an average of 94%, and for soy beans were between 63 and 102% with coefficients of variation of 0.9–8.2%, with an average of 88%.

The limits of detection of all pesticides in the crops tested are also listed in Table III. Of the 25 pesticides, isoprocarb and carbaryl had a limit of detection of 0.3 ppm in soy beans. The other pesticides had a limit of detection between 0.002 and 0.05 ppm in soy beans and rices.

In view of their recoveries and removal of interference peaks, methylene chloride partition and Bio-Beads S-X3 column clean-up was good for the reliable conformation and quantitation analysis of pesticides.

Analysis by GC–MS

In principle, the analysis of pesticides by GC–NPD–ECD may be falsified by a compound with the same retention time as one of the pesticides. In this case, the reliability of analysis can be greatly improved by GC–MS.

In Fig. 6, the total-ion chromatogram of the mixture of pesticides is shown, demonstrating good GC separation of 25 pesticides. Under the

TABLE III

RECOVERIES (%) AND LIMIT OF DETECTION OF PESTICIDES IN RICE AND SOY BEANS USING GC–NPD–ECD ($n = 3$)

R.S.D.s are given in parentheses.

Pesticide	Rice		Soy beans	
	Recovery	Limit of detection (ppm)	Recovery	Limit of detection (ppm)
Isoprocarb	95.4 (3.7)	0.05	81.8 (3.6)	0.3
Dimethoate	101.2 (2.8)	0.01	100.5 (2.1)	0.03
α-BHC	101.8 (2.7)	0.002	88.4 (1.4)	0.01
β-BHC	91.3 (0.8)	0.009	91.9 (1.8)	0.04
γ-BHC	95.6 (2.5)	0.002	96.2 (2.8)	0.01
Diazinon	83.4 (1.5)	0.01	62.7 (8.6)	0.05
Carbaryl	99.8 (2.6)	0.05	101.7 (4.4)	0.3
Fenitrothion	95.3 (2.2)	0.005	96.1 (3.3)	0.03
Malathion	91.4 (3.8)	0.02	79.5 (7.2)	0.08
Fenthion	89.6 (4.1)	0.008	98.7 (3.0)	0.04
Parathion	86.8 (1.2)	0.007	91.3 (1.2)	0.04
Aldrin	87.4 (4.3)	0.006	84.8 (2.0)	0.03
Captan	84.9 (3.7)	0.02	85.2 (0.6)	0.07
Phenthoate	100.4 (4.6)	0.03	86.1 (3.6)	0.1
o,p'-DDE	99.6 (7.2)	0.007	89.7 (4.4)	0.04
p,p'-DDE	97.6 (2.7)	0.007	84.3 (0.9)	0.04
o,p'-DDD	97.0 (5.0)	0.01	91.2 (1.9)	0.05
Dieldrin	96.7 (3.3)	0.006	89.2 (1.5)	0.03
m,p'-DDD	97.4 (2.6)	0.01	91.9 (3.2)	0.05
Endrin	99.1 (2.4)	0.01	91.7 (2.3)	0.05
p,p'-DDD	97.3 (2.6)	0.01	90.2 (3.2)	0.05
o,p'-DDT	92.9 (0.5)	0.01	90.1 (8.2)	0.05
p,p'-DDT	91.7 (2.2)	0.01	87.4 (1.6)	0.05
Captafol	83.4 (0.7)	0.03	77.2 (1.6)	0.1
EPN	96.2 (1.8)	0.02	91.2 (1.0)	0.08

GC–MS conditions specified in the experimental section, the mass spectra of pesticides were obtained in the electron-impact mode. Table IV summarizes the retention times, the molecular weights, base peak and characteristic ions of the mass spectra. For organochlorinated pesticides, their mass fragment [M] ions are accompanied by [M + 2] and/or [M + 4] ions, because of the isotopic effect of chlorine. For example, the isomers of DDD and DDT yielded a base peak m/z 235 from the loss of the $-CHCl_2$ and $-CCl_3$ group, respectively, and this fragment is accompanied by two isotopic peaks, m/z 237 and m/z 239. Of the pesticides containing six chlorine atoms, BHC isomers, aldrin, endrin and dieldrin show a weak intensity of molecular ion. The fragmentation of these compounds exhibited the loss of HCl and Cl in stepwise pattern from the molecular ion. In particular, aldrin, endrin and dieldrin containing a cyclohexene ring produced the ion cluster m/z 261, 263 and 265 by the retro-Diels–Alder (RDA) fragment. Captan and captafol showed the very weak intensity of molecular ion and also produced the base peak, m/z 79 (cyclohexadiene) by the RDA fragment.

For organophosphorus pesticides, the typical fragmentation patterns of phosphorus groups are explained in most part by Fig. 7. This fragmentation patterns are in good agreement with those represented by Pritchard [29]. These fragments appeared with strong intensity in the mass spectra of organophosphorus pesticides. In the case

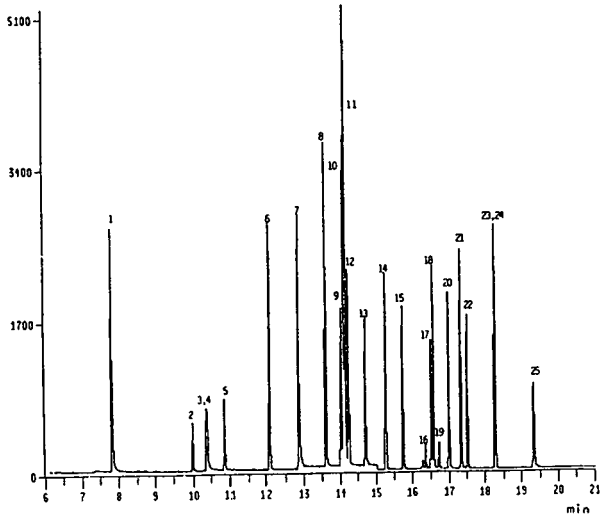

Fig. 6. Total-ion chromatogram of standard pesticides using SIM mode. Peaks: 1 = isoprocarb; 2 = α-BHC; 3 = dimethoate; 4 = β-BHC; 5 = γ-BHC; 6 = diazinon; 7 = carbaryl; 8 = fenitrothion; 9 = aldrin; 10 = malathion; 11 = fenthion; 12 = parathion; 13 = captan; 14 = phenthoate; 15 = *o,p'*-DDE; 16 = dieldrin; 17 = *p,p'*-DDE; 18 = *o,p'*-DDD; 19 = endrin; 20 = *m,p'*-DDD; 21 = *p,p'*-DDD; 22 = *o,p'*-DDT; 23 = *p,p'*-DDT; 24 = captafol; 25 = EPN. *y*-Axis: abundance; *x*-axis: retention time (min).

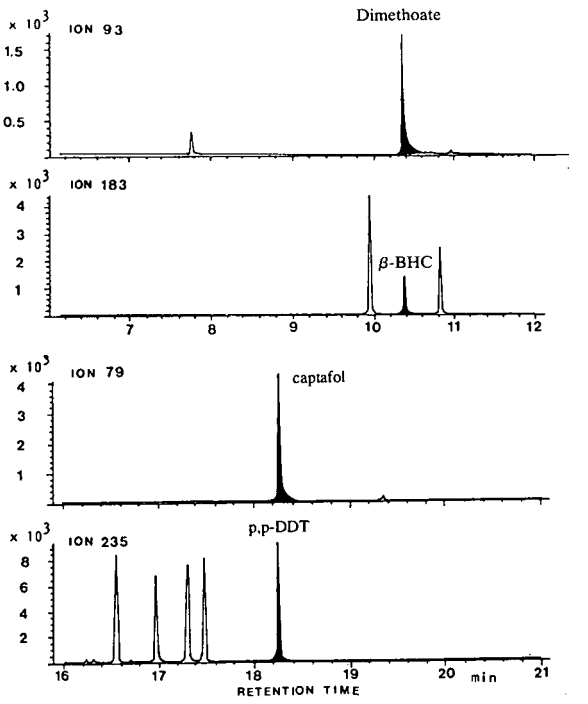

Fig. 8. Selected-ion chromatograms of some co-eluting pesticides. *y*-Axis: abundance.

of N-methylcarbamate pesticides, isoprocarb and carbaryl, the base peak of carbaryl was produced by the loss of N-methyl carbamate group from the molecular ion and that of isoprocarb was formed by the loss of the methyl group from ($M-O=C=N=CH_3$) ion. On the basis of this fragment information, various pesticides could be identified and complementary structural information would be obtained.

In this study, the determination of the pesticides at trace level in crops was achieved by GC–MS using selected-ion monitoring (SIM) model with two or three ions. The SIM mode may be used to improve the detection limit by producing the strongest intensity and to improve the specificity for the compound of interest by reducing the interference peaks. As shown in Fig. 6, although some pesticides were co-eluted, they could still be analysed because of the specificity of SIM, as typically demonstrated in Fig. 8 for β-BHC (*m/z* 181 or 183) and dimethoate (*m/z* 93) co-eluting at 10.5 min and *p,p*-DDT (*m/z* 235) and captafol (*m/z* 79) at 18.4 min. The ion *m/z* 93 instead of *m/z* 87 for dimethoate was selected to obtain the precise analysis by SIM mode because the ion *m/z* 87 also appeared in the mass spectrum of β-BHC.

The detection limits of some pesticides were around 10 ng as an injection amount in the scan mode. However, the detection limits in the SIM mode using only the base peak of each pesticide were about 0.05 ng, except for dieldrin and endrin, whose detection limits were about 0.2 ng

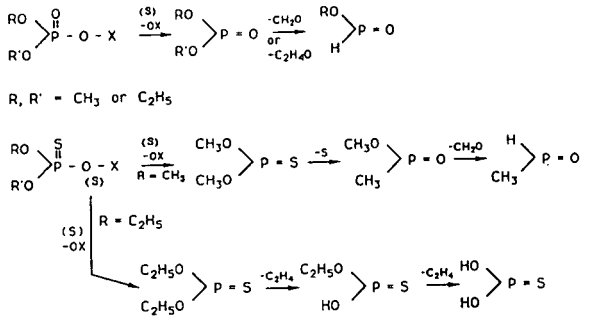

Fig. 7. Basic fragmentation patterns of organophosphorus compounds.

TABLE IV

RETENTION TIMES (t_R) AND CHARACTERISTIC MASS FRAGMENT IONS FOR PESTICIDES

Relative abundance (%) is given in parentheses.

Compound	t_R (min)	Molecular mass mass	Mass fragment ion (m/z)					
Isoprocarb	7.929	193	121 (100)	136 (57)	91 (17)	77 (11)	193 (2)	
α-BHC	10.119	291	181 (100)	183 (94)	217 (52)	219 (74)	109 (60)	111 (57)
Dimethoate	10.518	229	87 (100)	93 (77)	125 (43)	63 (17)	79 (16)	229 (12)
β-BHC	10.520	291	183 (100)	181 (95)	217 (44)	219 (65)	109 (36)	111 (40)
γ-BHC	10.989	291	181 (100)	183 (94)	109 (92)	111 (91)	217 (52)	219 (62)
Diazinon	12.289	304	137 (100)	179 (74)	152 (56)	93 (44)	66 (28)	304 (21)
Carbaryl	13.021	201	144 (100)	115 (48)	89 (12)	63 (6)	201 (5)	
Fenitrothion	13.747	277	125 (100)	109 (93)	277 (34)	93 (31)	79 (28)	
Aldrin	14.175	365	66 (100)	261 (40)	263 (58)	265 (54)	91 (38)	
Malathion	14.225	330	125 (100)	93 (76)	173 (57)	158 (42)	99 (32)	79 (18)
Fenthion	14.287	278	278 (100)	109 (92)	125 (86)	93 (51)	169 (40)	79 (10)
Parathion	14.369	291	109 (100)	97 (93)	139 (41)	153 (34)	291 (32)	
Captan	14.830	300	79 (100)	149 (26)	117 (20)	119 (19)	77 (14)	
Phenthoate	15.432	320	125 (100)	93 (76)	121 (64)	274 (55)	246 (24)	
o,p'-DDE	15.896	318	246 (100)	248 (72)	316 (45)	318 (55)	320 (48)	176 (38)
Dieldrin	16.509	380	79 (100)	261 (28)	263 (45)	265 (24)	279 (18)	
p,p'-DDE	16.673	316	246 (100)	248 (68)	316 (42)	318 (53)	320 (48)	176 (45)
o,p'-DDD	16.740	320	235 (100)	237 (59)	165 (38)	199 (13)	318 (5)	320 (6)
Endrin	16.899	380	81 (100)	261 (41)	263 (59)	265 (38)	289 (25)	
m,p'-DDD	17.154	320	235 (100)	237 (71)	165 (48)	199 (15)	318 (4)	320 (5)
p,p'-DDD	17.491	320	235 (100)	237 (59)	165 (42)	199 (18)	318 (2)	320 (3)
o,p'-DDT	17.665	354	235 (100)	237 (58)	165 (38)	199 (12)	136 (7)	
p,p'-DDT	18.425	354	235 (100)	237 (70)	165 (31)	199 (9)	136 (5)	
Captafol	18.426	349	79 (100)	311 (18)	313 (23)	183 (10)	149 (7)	
EPN	19.491	323	157 (100)	169 (51)	141 (32)	185 (27)	63 (25)	323 (15)

at a signal-to-nose ratio of 5. But the detection limits by GC–ECD, for dieldrin and endrin, were noticeably lower than those by SIM. The base peak m/z 79 of dieldrin and m/z 81 of endrin could not be distinguished at times between 15 and 17.4 min (group C) in the SIM mode because these ions were subject to interference from fatty species likely to be present in the sample matrix. The ion cluster m/z 261, 263 and 265, instead of m/z 79 and 81, could be monitored to enhance specificity for endrin and dieldrin but with a reduction in sensitivity. For most pesticides, the detection limits with the GC–MS–SIM method were similar to those with GC–NPD–ECD. However, the GC–MS–SIM method provided much higher sensitivity for carbamates, which was shown by the low sensitivity of the NPD response. The detection limits using SIM were seven times lower for isoprocarb and 12.5 times lower for carbaryl than those using NPD. In many cases of GC analysis, the detection limits could also be decreased by adjusting the sample volume and splitless mode.

CONCLUSIONS

The screening of 25 pesticides in rice and soy beans with GC–NPD–ECD has been achieved within 30 min using an SE-30 capillary column. For the simultaneous determination of 25 pesticides, the solvent partition and Bio-Beads S-X3 column method appears to be suitable for removal of the interferences from the fatty matrix components. The present method for the analysis of various pesticides in the fatty crops gave good recoveries with reasonable precision and seemed to be suitable for multiresidue analysis. Each pesticide was identified by its retention time and characteristic mass fragment ions using GC–MS–SIM. The GC–MS–SIM was proved to be a reliable means of identification and confirmation of a variety of pesticide residues. Although the response of dual detection alone does not give enough evidence of the presence of the pesticides, the appearance of two or three ions at a specific retention time using the GC–MS–SIM technique can be a good evidence that a specific pesticide is present.

REFERENCES

1 M.A. Luke, H.T. Masumoto, T. Cairns and H.K. Hundley, *J. Assoc. Off. Anal. Chem.*, 71 (1988) 415.
2 D.K. Verma, *Int. J. Environ. Anal. Chem.*, 42 (1990) 79.
3 E.E. McNeil, R. Otson, W.F. Miles and F.J.M. Rajabalee, *J. Chromatogr.*, 132 (1977) 277.
4 J.P. Hsu, H.G. Wheeler, Jr., D.E. Camann and H.J. Schattenberg, *J. Chromatogr. Sci.*, 26 (1988) 181.
5 W.E. Pereira, C.E. Rostad and T.J. Leiker, *Anal. Chim. Acta*, 228 (1990) 69.
6 G.H. Fujie and D.H. Fullmer, *J. Agric. Food Chem.*, 26 (1978) 395.
7 A. Ambrus, J. Lantas, E. Visi, I. Cstals and L. Sarvari, *J. Assoc. Anal. Chem.*, 64 (1981) 735.
8 G.S. Durell and T.C. Sauer, *Anal. Chem.*, 62 (1990) 1867.
9 A. DiMuccion, A. Ausili, L. Vergori, I. Camoni, R. Dommarco, L. Gambetti, A. Sanilio and F. Vergori, *Analyst*, 115 (1990) 1167.
10 H.J. Satn, *J. Chromatogr.*, 467 (1989) 85.
11 E.E. Hargensheimer, *J. Assoc. Off. Anal. Chem.*, 67 (1984) 1067.
12 J.A. Roach and L.J. Carson, *J. Assoc. Off. Anal. Chem.*, 70 (1987) 439.
13 W.P. Cochrane and M. Lanouette, *J. Assoc. Off. Anal. Chem.*, 64 (1981) 724.
14 C.H. Marvin, I.D. Brihdle, R.P. Singh, C.D. Hall and M. Chiba, *J. Chromatogr.*, 518 (1990) 242.
15 C.H. Liu, G.C. Mattern, X. Yu, R.T. Rosen and J.D. Rosen, *J. Agric. Food Chem.*, 39 (1991) 718.
16 T.A. Beller and W.L. Buddle, *Anal. Chem.*, 60 (1988) 2076.
17 D. Barcelo, F.A. Maris, R.B. Geerdink, R.W. Frei, G.J. De Jong and U.A. Th. Brinkman, *J. Chromatogr.*, 394 (1987) 65.
18 M.C. Goldberg, L. Delong and M. Sinclair, *Anal. Chem.*, 45 (1973) 89.
19 M. Ahnoff and B. Josefsson, *Anal. Chem.*, 45 (1974) 658.
20 A.J. Nunez and J.M.H. Bemelmans, *J. Chromatogr.*, 294 (1984) 361.
21 J. Curvers, T. Noij, C. Cramers and J. Rijks, *Chromatographia*, 19 (1986) 225.
22 H. Steinwandter, *Fresenius' Z. Anal. Chem.*, 312 (1982) 342.
23 J.J. Blaha and P.J. Jackson, *J. Assoc. Off. Anal. Chem.*, 68 (1985) 1095.
24 D.L. Stalling, G.C. Tindle and J.L. Johnson, *J. Assoc. Off. Anal. Chem.*, 55 (1972) 32.
25 M.L. Hopper, *J. Agric. Food Chem.*, 30 (1982) 1038.
26 G.C. Mattern, G.M. Singer, J. Louis, M. Robson and J.D. Rosen, *J. Agric. Food Chem.*, 38 (1999) 402.
27 *Sikpoom Kongjun*, Korea Food Industrial Agency, Leemoon Public Press, 1989, p. 35.
28 B. Kolb, M. Auer and P. Pospisil, *J. Chromatogr. Sci.*, 15 (1977) 53.
29 J.G. Pritchard, *Org. Mass Spectrom.*, 3 (1970) 163.

Journal of Chromatography, 639 (1993) 273–279
Elsevier Science Publishers B.V., Amsterdam

CHROM. 24 982

Gas chromatographic separation of diastereoisomeric and enantiomeric forms of some fluorinated amino acids on glass capillary columns

V. Vlasáková*, V. Tolman and K. Živný

Institute of Nuclear Biology and Radiochemistry, Czech Academy of Sciences, Vídeňská 1083, 142 20 Prague 4 (Czech Republic)

(First received October 21st, 1992; revised manuscript received February 5th, 1993)

ABSTRACT

The monofluorinated analogues of 2-aminocarboxylic acids up to C_7 were efficiently separated into the diastereomers on glass capillary columns coated with achiral phases BP-1, BP-10 and OV-330. In addition, some difluoro and trifluoro analogues were also measured. Chiral resolution was achieved on capillary well-coated open tubular fused-silica columns coated with chiral phases XE-60–L-Val–L-(1-phenylethyl)amide, Chirasil–L-Val and Behenoyl–L-Val–*tert.*-butylamide. The separation factors and the Kovats indices of the fluorinated amino acids were determined and compared. The *erythro* racemates display a higher degree of resolution than the *threo* ones. The order of elution was found to be the L- after the D-solute on all L-phases.

INTRODUCTION

Gas chromatographic methods using chiral stationary phases have been used for efficient separations of a number of racemic substances. A large body of work has been reported since the first studies describing a direct resolution of amino acid enantiomers on chiral phases by Gil-Av and co-workers [1–5]. Bayer and co-workers [6–10] have introduced polymeric siloxane phases of low volatility and high thermal stability, such as Chirasil–L-Val, formed by coupling of the L-Val–*tert.*-butylamide moiety to a copolymer of dimethylsiloxane and carboxyalkylmethylsiloxane units. Analogously, König and co-workers [11–14] have prepared a chiral phase by connecting L-Val–L-(1-phenylethyl)amide to a methylcyanoethyl-polysiloxane XE-60 and obtained a highly heat-resistant polymeric phase with high enantioselectivity that was used to resolve amines, amino alcohols, amino acids, hydroxy acids, carbohydrates and other substances. Also, some monoamine phases, such as N-lauroyl-D-[1-(1′-naphthyl)ethyl]amine, are conveniently used for the resolution of 2-halogenocarboxylic acids and other compounds [15].

There is a rapidly increasing demand from many scientific branches for analytical methods capable of a rapid and efficient enantiomeric separation of diverse compounds. These methods are indispensable for the resolution of drugs whose individual enantiomers exhibit different pharmacological properties and have a considerable clinical importance. A wide group of chiral compounds with biological and/or pharmaceutical importance is constituted by many fluorinated analogues of amino acids. The GC study of some of them is the subject of this paper.

The analysed fluoro derivatives of amino acids are divided into three groups. The first group is

* Corresponding author.

0021-9673/93/$06.00

formed by five linear-chain amino acids with one fluorine atom at C-3, which form a homologous series: 3-fluoroalanine, 2-amino-3-fluorobutyric acid, 3-fluoronorvaline, 3-fluoronorleucine and 2-amino-3-fluoroheptanoic acid. The second group consists of three amino acids containing a terminal trifluoromethyl: 3,3,3-trifluoroalanine, 4,4,4-trifluorovaline and 5,5,5-trifluoroleucine. In addition, three other amino acids were measured separately: 3-fluorovaline, 5-fluoronorleucine and 5,5-difluoronorleucine.

EXPERIMENTAL

Chemicals

The standards of fluorinated amino acids were received from the authors who described their syntheses: 3-fluoroalanine, 2-amino-3-fluorobutyric acid, 3-fluoronorvaline, 3-fluoronorleucine, 2-amino-3-fluoroheptanoic acid and 3-fluorovaline [16] were kindly provided by H. Gershon, 5-fluoronorleucine [17] and 5,5-difluoronorleucine [18] by M. Hudlický, 3,3,3-trifluoroalanine [19] by A. Uskert, 4,4,4-trifluorovaline [20,21] and 5,5,5-trifluoroleucine [21] by H.M. Walborsky. Methanol and other organic solvents were of analytical grade and were supplied by Lachema (Brno, Czech Republic).

Gas chromatographic analysis

The fluorinated amino acids were converted into the N-trifluoroacetylated methyl esters according to Darbre and Islam [22]. A Varian Model 3700 (Palo Alto, CA, USA) gas chromatograph equipped with a flame ionization detector was used. All achiral measurements were performed on glass capillary columns (12 m × 0.32 mm) coated with phases BP-1 (phase I), $d_f = 0.25$ μm; BP-10 (phase II), $d_f = 0.25$ μm; and OV-330 (phase III), $d_f = 0.20$ μm. Chiral separations were carried out on capillary wall-coated open tubular fused-silica columns coated with XE-60–L-Val–L-(1-phenylethyl)-amide (phase IV), 50 m × 0.25 mm, $d_f = 0.12$ μm; Chirasil-L-Val (phase V), 25 m × 0.25 mm, $d_f = 0.12$ μm; and with Behenoyl–L-Val–*tert.*-butylamide (phase VI), 25 m × 0.25 mm, $d_f =$ 0.20 μm. Phases I and II were manufactured by SGE, Sydney, Australia, phases III and VI by Serva, Heidelberg, Germany, and phases IV and V by Chrompack, Middelburg, Netherlands. Nitrogen was used as carrier gas. Sample volumes of 1 μl were injected onto the columns using the splitting technique; the split ratio was 1:100. The retention times t'_R are corrected for the dead column volume. Separation factors are defined as $\alpha = t'_{R_2}/t'_{R_1}$, where R_1 refers to the first peak and R_2 to the second one. The Kovats indices I were calculated for the separation temperatures indicated; for the temperatures, the optimal values were chosen, taking into account the measured temperature dependence of separation factors, the time of analysis and the peak width. Chromatograms were quantitatively evaluated using a Varian integrator CDS 111.

RESULTS AND DISCUSSION

GC separation of diastereoisomers

The presence of two chiral centres in the 2-amino-3-fluoro carboxylic acids (with the exception of 3-fluoroalanine and 3-fluorovaline) gives rise to two racemic diastereoisomers. Separation of the diastereoisomers was performed on glass capillary columns coated with achiral phases of different polarity, *i.e.* phases I–III. The highest values of the separation factors α were found on phase II at 110°C ($\alpha = 1.22$–1.24), lower on III at 150°C ($\alpha = 1.16$–1.18) and the lowest on phase I at 90°C ($\alpha = 1.07$–1.10).

The elution sequence of the *erythro* and *threo* forms was deduced partly from analogy with 4-fluoroglutamic acid diastereoisomers [23], partly from their chromatographic behaviour. The *erythro* forms of all compounds within this study exhibited shorter retention times than the corresponding *threo* forms on all phases. The same sequence of diastereoisomers was described, for example, by Rose *et al.* [24] in the separation of diastereoisomeric esters and by Abalain *et al.* [25] for the diastereomers of alkane-2,3-diols. The separation mechanism was deduced from the conformation immobility along the C–C bond bearing the asymmetric centres. In addition, the *threo* isomers of monofluorinated

aliphatic amino acids present a greater spatial bulk than the *erythro* forms.

The retention characteristics of the individual diastereoisomers, *i.e.* the retention times and Kováts indices (I), along with the values of the separation factors on phases I–III are summarized in Table I. The logarithms of retention times of both the *erythro* and *threo* forms in the homologous series were plotted against the number of carbon atoms, yielding two parallel lines that confirmed the linear relationship between these two quantities. This relationship was found on all three phases (Fig. 1).

A comparison of the separation factor values in the homologous series of 2-amino-3-fluoro carboxylic acids reveals that these values are nearly identical for all members of the series on each one of the phases used. On the other hand, comparison of the separation factors of 3-fluoronorleucine and 5-fluoronorleucine under the same chromatographic conditions shows the value of the latter to be much lower than that of the former (Table I). This is in accordance with the concept of Karger and co-workers [24,26] concerning the effect of the distance between the two chiral centres on the separation of a dia-

TABLE I
GC SEPARATION OF FLUORINATED AMINO ACIDS ON ACHIRAL PHASES

Compound	Isomer	Phase I BP-1 (90°C)			Phase II BP-10 (110°C)			Phase III OV-330 (150°C)		
		t'_R	α	I_{90}	t'_R	α	I_{110}	t'_R	α	I_{150}
3-Fluoroalanine	–	1.01	–	922	1.56	–	1187	3.63	–	1398
2-Amino-3-fluoro-butyric acid	*erythro*	1.36	1.07	966	1.57	1.24	1187	2.83	1.17	1344
	threo	1.46		977	1.94		1224	3.31		1378
3-Fluoronorvaline	*erythro*	2.41	1.07	1054	2.46	1.22	1267	3.78	1.16	1408
	threo	2.59		1064	3.01		1300	4.40		1441
3-Fluoronorleucine	*erythro*	4.27	1.10	1140	4.00	1.24	1351	5.22	1.17	1477
	threo	4.68		1152	4.95		1388	6.13		1511
2-Amino-3-fluoro-heptanoic acid	*erythro*	7.98	1.10	1236	6.92	1.24	1444	7.80	1.18	1563
	threo	8.79		1251	8.57		1481	9.18		1598
3-Fluorovaline	–	1.95	–	1021	2.00	–	1229	2.64	–	1330
5-Fluoronorleucine	*erythro*	6.50	1.07	[a]	8.52	1.11	[a]	12.97	1.07	[a]
	threo	6.97			9.45			13.92		
5,5-Difluoro-norleucine	–	5.54	–	[a]	8.50	–	[a]	12.79	–	[a]
3,3,3-Trifluoro-alanine	–	0.27	–	840	0.45	–	966	0.50	–	974
4,4,4-Trifluoro-valine	–	1.34	–	979	1.92	–	1224	2.10	–	1282
5,5,5-Trifluoro-leucine	–	2.77	–	1042	4.70	–	1378	4.88	–	1463

[a] For 5-fluoronorleucine and 5,5-difluoronorleucine the I values were not estimated.

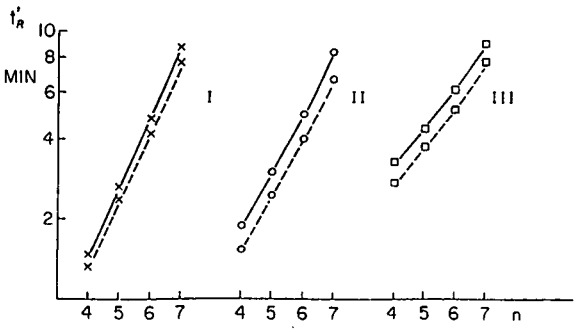

Fig. 1. Homologous 2-amino-3-fluoro carboxylic acids: logarithms of retention times (t'_R) on achiral phases I–III plotted against the number of carbon atoms (n). Solid lines = *threo* forms; dashed lines = *erythro* forms.

stereoisomeric pair. According to the proposed separation mechanism the distance between the chiral centres affects the conformational mobility of groups along the C–C bond; the lower the distance the higher the immobility of the groups and the higher the chromatographic difference between the diastereoisomers. The constant distance between the chiral centres in a homologous series is reflected in the constant values of separation factors, whereas the larger distance in 5-fluoronorleucine lowers the separation factor (1.11 as compared with 1.24 for 3-fluoronorleucine on phase II).

TABLE II

GC RESOLUTION OF THE HOMOLOGOUS SERIES OF 2-AMINO-3-FLUORO CARBOXYLIC ACIDS ON CHIRAL PHASES

Compound	Isomer	Phase IV (140°C) XE-60-S-Val-S-PEA			Phase V (100°C) Chirasil-L-Val			Phase VI (110°C) Behenoyl-L-Val		
		t'_R	α	I_{140}	t'_R	α	I_{100}	t'_R	α	I_{110}
3-Fluoroalanine	D	2.90		1412	1.80		1146	1.20		1010
			1.03			1.00			1.13	
	L	3.00		1419	1.80		1146	1.35		1027
2-Amino-3-fluoro-butyric acid	*erythro*-D	2.35		1368	1.80		1146	1.15		1004
			1.04			1.08			1.22	
	erythro-L	2.45		1377	1.94		1161	1.40		1032
	threo-D	2.87		1410	2.55		1199	1.62		1051
			1.06			1.00			1.06	
	threo-L	3.05		1422	2.55		1199	1.71		1060
3-Fluoronorvaline	*erythro*-D	3.23		1434	2.92		1225	2.01		1084
			1.04			1.07			1.15	
	erythro-L	3.37		1443	3.11		1234	2.31		1104
	threo-D	4.09		1483	4.21		1284	3.00		1142
			1.04			1.00			1.05	
	threo-L	4.25		1491	4.21		1284	3.15		1149
3-Fluoronorleucine	*erythro*-D	4.72		1513	4.92		1312	3.49		1164
			1.05			1.08			1.17	
	erythro-L	4.95		1523	5.29		1322	4.08		1187
	threo-D	6.00		1562	6.99		1368	5.25		1222
			1.04			1.01			1.06	
	threo-L	6.25		1571	7.09		1378	5.55		1230
2-Amino-3-fluoro-heptanoic acid	*erythro*-D	7.35		1605	8.80		1405	6.56		1254
			1.05			1.08			1.16	
	erythro-L	7.70		1614	9.47		1417	7.60		1275
	threo-D	9.40		1656	12.58		1463	9.95		1314
			1.04			1.02			1.06	
	threo-L	9.80		1664	12.78		1466	10.55		1322

The effect of length of the aliphatic chain is perceptible in the separation only by slightly higher α values of 3-fluoronorleucine and 2-amino-3-fluoroheptanoic acid, this being found only on the non-polar phase I (Table I).

GC resolution of enantiomers

Separation of enantiomers of the fluorinated amino acids under study was investigated on three types of chiral phases, IV–VI. The values of separation factors were determinated and the Kováts indices calculated (Tables II and III). The complete separation of all measured enantiomeric pairs was observed on phase IV under isothermal conditions at 140°C (Fig. 2) and on phase VI at 110°C. Phase V failed to resolve 3-fluoroalanine and the *threo* isomers of 2-amino-3-fluorobutyric acid and 3-fluoronorvaline at 100°C. However, the resolution of all *erythro* enantiomeric pairs was complete also on this phase (Fig. 3).

We also investigated the effect of various chiral phases on the resolution of racemic *erythro* and *threo* forms of the 2-amino-3-fluoro carboxylic acids. The results, summarized in Table II, clearly show larger α values for enantiomers of the *erythro* forms than for those of the *threo* forms. Separation factors were nearly identical for all members of the homologous series with each type of chiral phase.

Optical isomers of the trifluoro derivatives of alanine, valine and leucine were separated on all three phases, IV–VI. In all cases the α values increased from 3,3,3-trifluoroalanine to 5,5,5-tri-

TABLE III

GC RESOLUTION OF MISCELLANEOUS FLUORINATED AMINO ACIDS ON CHIRAL PHASES

Compound	Isomer	Phase IV (140°C) XE-60-S-Val-S-PEA			Phase V (100°C) Chirasil-L-Val			Phase VI (110°C) Behenoyl-L-Val		
		t'_R	α	I_{140}	t'_R	α	I_{100}	t'_R	α	I_{110}
3,3,3-Trifluoro-alanine	D	0.72	1.04	1123	0.76	1.07	1002	0.36	1.03	837
	L	0.75		1131	0.81		1017	0.37		841
4,4,4-Trifluoro-valine	D	2.38	1.08	1371	2.80	1.09	1215	1.47	1.11	1039
	L	2.56		1386	3.04		1232	1.63		1054
5,5,5-Trifluoro-leucine	D	6.11	1.10	1566	8.48	1.14	1398	3.75	1.21	1174
	L	6.70		1585	9.66		1420	4.54		1201
3-Fluorovaline	D	2.30	1.03	1364	1.55	1.05	1047	1.55	1.05	1047
	L	2.38		1371	1.63		1054	1.63		1054
5-Fluoronorleucine	*erythro*-D	11.03	1.09	[a]	11.51	1.16	[a]	7.44	1.13	[a]
	erythro-L	12.01			13.40			8.37		
	threo-D	12.00	1.08	[a]	13.38	1.08	[a]	9.61	1.12	[a]
	threo-L	12.93			14.50			10.81		
5,5-Difluoro-norleucine	D	10.84	1.09	[a]	12.01	1.13	[a]	7.06	1.30	[a]
	L	11.86			13.57			9.19		

[a] Not estimated (see footnote in Table I).

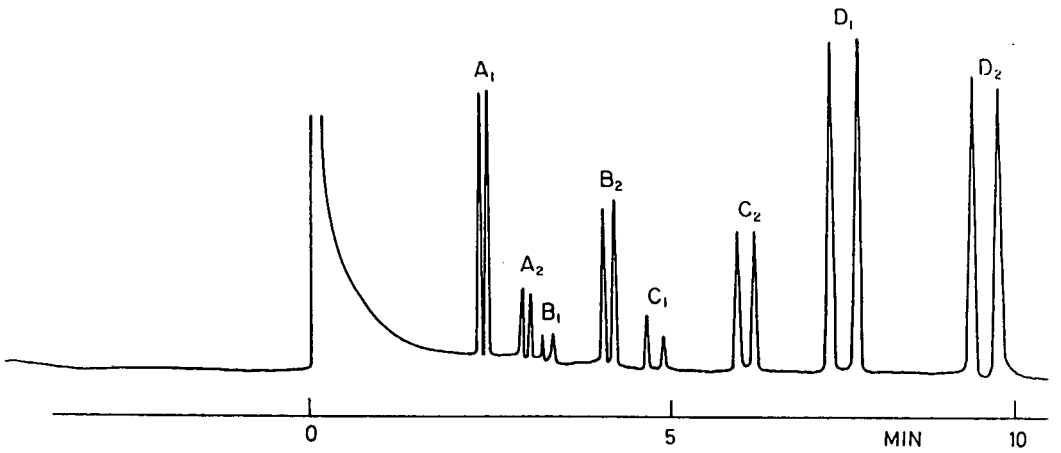

Fig. 2. Homologous 2-amino-3-fluoro carboxylic acids: GC separation of the four enantiomers on chiral phase IV at 140°C. (A) 2-Amino-3-fluorobutyric acid; (B) 3-fluoronorvaline; (C) 3-fluoronorleucine; (D) 2-amino-3-fluoroheptanoic acid. The *erythro* forms are indexed by 1, the *threo* forms by 2. In each pair of peaks the left one represents the D-antipode.

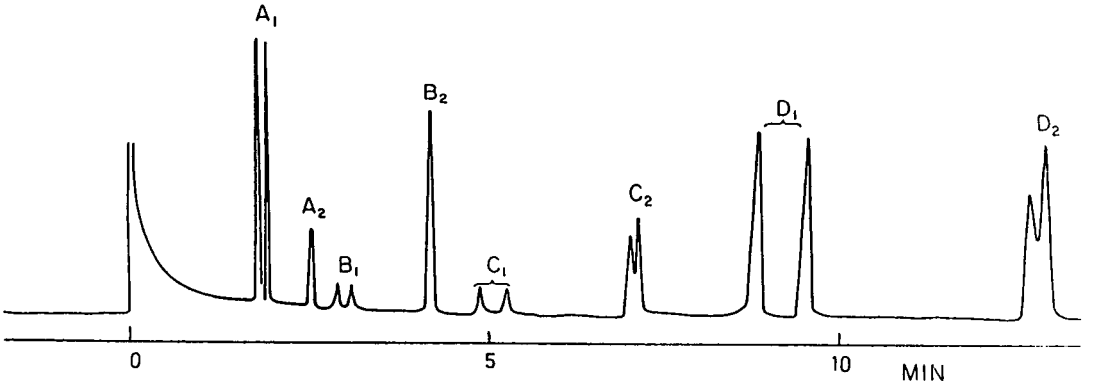

Fig. 3. Homologous 2-amino-3-fluoro carboxylic acids: GC separation of the four enantiomers on chiral phase V at 100°C. Legend as at Fig. 2; A_2 and B_2 are unresolved *threo*-D,L-2-amino-3-fluorobutyric acid and *threo*-D,L-3-fluoronorvaline, respectively.

fluoroleucine. Table III summarizes the retention characteristics and the α values.

The sequence of eluted enantiomers on all chiral phases was derived from analogy with the same types of aliphatic non-fluorinated 2-amino acids of known steric relevance and by comparison with isolated optical isomers of 4-fluoroglutamic acid [23]. On all L-phases the D-isomers were eluted first. The same sequence was observed for the esters of 3-fluoroalanine on phase V by Wagner *et al.* [27].

The linear relationship between the logarithms of retention times of the individual enantiomers and the number of carbon atoms in both the *erythro* and *threo* series was documented (Fig.

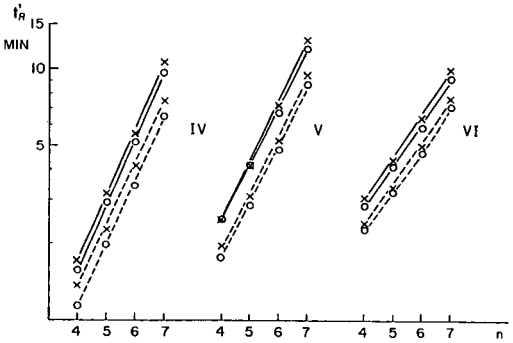

Fig. 4. The four individual enantiomers of homologous 2-amino-3-fluoro carboxylic acids: logarithms of retention times on chiral phases IV–VI plotted against the number of carbon atoms. Solid lines = *threo* forms; dashed lines = *erythro* forms; × = L; ○ = D.

4). This relationship was confirmed on all three phases, IV–VI.

REFERENCES

1 E. Gil-Av, B. Feibush and R. Charles-Sigler, *Tetrahedron Lett.*, (1966) 1009.
2 E. Gil-Av, B. Feibush and R. Charles-Sigler, in A.B. Littlewood (Editor), *Gas Chromatography*, Institute of Petroleum, London, 1967, p. 227.
3 S. Nakaparksin, P. Birrell, E. Gil-Av and J. Oró, *J. Chromatogr. Sci.*, 8 (1970) 177.
4 B. Feibush and E. Gil-Av, *Tetrahedron*, 26 (1970) 1361.
5 R. Charles, U. Beitler, B. Feibush and E. Gil-Av, *J. Chromatogr.*, 112 (1975) 121.
6 W. Parr, J. Pleterski, C. Yang and E. Bayer, *J. Chromatogr. Sci.*, 9 (1971) 141.
7 W.A. König, W. Parr, H.A. Lichtenstein, E. Bayer and J. Oró, *J. Chromatogr. Sci.*, 8 (1970) 183.
8 H. Frank, G.J. Nicholson and E. Bayer, *J. Chromatogr. Sci.*, 15 (1977) 174.
9 H. Frank, G.J. Nicholson and E. Bayer, *Angew. Chem.*, 90 (1978) 396.
10 H. Frank, G.J. Nicholson and E. Bayer, *J. Chromatogr.*, 146 (1978) 197.
11 W.A. König, S. Sievers and I. Benecke, in R.A. Kaiser (Editor), *Proceedings of the IVth Symposium on Capillary Chromatography, Hindelang, 1981*, Institut für Chromatographie, Bad Dürkheim and Hüthig, Heidelberg, 1981, p. 703.
12 W.A. König, I. Benecke and S. Sievers, *J. Chromatogr.*, 217 (1981) 71.
13 W.A. König, I. Benecke and S. Sievers, *J. Chromatogr.*, 238 (1982) 427.
14 W.A. König, W. Francke and I. Benecke, *J. Chromatogr.*, 239 (1982) 227.
15 K. Watabe and E. Gil-Av, *J. Chromatogr.*, 318 (1985) 235.
16 H. Gershon, M.W. McNeil and E.D. Bergmann, *J. Med. Chem.*, 16 (1973) 1407.
17 M. Hudlický and B. Kakáč, *Coll. Czech. Chem. Commun.*, 31 (1966) 1101.
18 M. Hudlický, *Coll. Czech. Chem. Commun.*, 32 (1967) 453.
19 A. Uskert, A. Néder and E. Kasztreiner, *Magyar Kémiai Folyóirat*, 79 (1973) 333; *Chem. Abstr.*, 79 (1973) 79147r.
20 D.F. Loncrini and H.M. Walborsky, *J. Med. Chem.*, 7 (1964) 369.
21 H.M. Walborsky, M. Baum and D.F. Loncrini, *J. Am. Chem. Soc.*, 77 (1955) 3637.
22 A. Darbre and A. Islam, *Biochem. J.*, 106 (1968) 923.
23 V. Tolman, V. Vlasáková and K. Živný, *J. Chromatogr.*, 315 (1984) 421.
24 H.C. Rose, R.L. Stern and B.L. Karger, *Anal. Chem.*, 38 [3] (1966) 469.
25 J.H. Abalain, D. Picart and F. Berthou, *J. Chromatogr.*, 274 (1983) 305.
26 B.L. Karger, R.L. Stern, W. Keane, B. Halpern and J.W. Westley, *Anal. Chem.*, 39 (1967) 229.
27 J. Wagner, E. Wolf, B. Heinzelmann and C. Gaget, *J. Chromatogr.*, 392 (1987) 211.

Journal of Chromatography, 639 (1993) 281–285
Elsevier Science Publishers B.V., Amsterdam

CHROM. 25 069

Boronic esters as derivatives for supercritical fluid chromatography of ecdysteroids

Jae-Han Shim[☆], Ian D. Wilson and E. David Morgan*

Department of Chemistry, Keele University, Keele, Staffordshire ST5 5BG (UK)

(First received November 23rd, 1992; revised manuscript received March 8th, 1993)

ABSTRACT

The use of boronic ester derivatives for the recognition of ecdysteroids possessing a 20,22-diol group in supercritical fluid chromatography is demonstrated for some model systems and for insect and plant extracts. Derivative formation with methyl-, butyl- and phenyl-boronic acids occurs rapidly under mild conditions with excess boronic acid to give products of significantly shorter retention than the parent ecdysteroids with supercritical CO_2–methanol mobile phase.

INTRODUCTION

The importance of ecdysteroids (insect moulting hormones) in insect development, and their identification and quantification is a matter of great interest to insect physiologists and biochemists looking for new ways to control insect pests.

Ecdysteroids are found in insect tissues and eggs in μg/g to pg/g quantities [1]. Such small amounts of ecdysteroids require either selective methods of extraction providing sufficient material with high purity for analysis or a method of analysis with sensitive and selective detection [2]. Some of these same compounds and others, known as phytoecdysteroids are found in plants scattered throughout the plant kingdom [3]. The development of sensitive and specific analytical methods for the ecdysteroids, was of fundamental importance in the advance of ecdysteroid research [4].

The ecdysteroids are a family of polyhydroxylated sterols. They are interesting for chromatographic studies because they all have the same rigid 5β-cholestane skeleton, with a 7-ene-6-one UV chromophore and a variety of other substituent groups. We have already demonstrated the advantages of supercritical fluid chromatography (SFC) with CO_2–methanol for the analysis of ecdysteroids [5,6].

Boronic acids can react selectively with 1,2- and 1,3-diols, enediols, 2-hydroxy acids and other such groups to form cyclic derivatives. Brooks and co-workers [7,8] have thoroughly explored the use of boronic acids, including phenylboronic acid to give volatile cyclic boronate derivatives of steroids for gas chromatography. Poole and Morgan [9] explored the use of cyclic phenylboronates as gas chromatographic derivatives for ecdysteroids coupled with the use of the nitrogen-specific detector for selective detection of the boron. Poole *et al.* [10] also suggested phenanthreneboronic acid as a fluorescence label in the HPLC and TLC analysis of ecdysteroids. More recently, we have used phenylboronic acid immobilized on silica gel for the solid-phase extraction of ecdysteroids

* Corresponding author.
☆ On leave from Department of Agricultural Chemistry, Chonnam National University, Kwangju, South Korea.

0021-9673/93/$06.00

[11,12]. Phenylboronic acid has also been used as derivatization agent in HPLC and TLC [13,14]. These boronic esters have selective mass spectral fragmentations that are helpful in structure identification [13]. The appearance of a chromatogram before and after treatment with a boronic acid spotlights the presence of ecdysteroids with the side-chain diol group.

Because of the constant demand to determine sensitive and specific analytical methods for the ecdysteroids, we have investigated here a number of boronate esters which are formed exclusively from the diol in the side chain of ecdysteroids (Fig. 1), even if an excess of reagent is present in the reaction mixture. The reaction is quantitative and ecdysteroid boronates are stable in supercritical carbon dioxide–methanol mobile phase. The derivatization reaction results in a decrease in polarity of the ecdysteroids. This property can be utilized for simple checking of the presence of the 20,22-diol system in the ecdysteroid molecule and might be extended to SFC–electron-capture detection.

EXPERIMENTAL

Ecdysteroids are obtained from the collection of I.D. Wilson or were purchased from Simes (Milan, Italy). The samples of plant extracts of *Silene otites* and *Ajuga* (tentatively identified as *A. iva*) were gifts of R. Lafont. Ecdysteroids and boronic acids were prepared as dilute solutions in methanol. Varying amounts of methyl, butyl or phenylboronic acid were added to a methanol solution of an ecdysteroid and the reaction mixture was left for 3 min at room temperature before chromatography.

SFC experiments were performed on a purpose-built system (LDC Analytical, Stone, UK) containing guard and analytical columns (LDC Analytical, 150 × 4.6 mm I.D. packed with 5 μm cyanopropyl silica) with carbon dioxide–methanol (9:1) as mobile phase at a flow-rate of 1.8 ml/min and a pressure of 320 bar and temperature of 55°C.

Samples (10 μl) were injected into the system through a Rheodyne 7125 injection valve with a 20-μl injection loop (Anachem, Leek, UK). UV detection was set to monitor at 240 nm.

RESULTS AND DISCUSSION

The formation of boronic esters was explored with four representative ecdysteroids. 20-Hydroxyecdysone (**I**) (for structures, see Fig. 1), 20-hydroxyecdysone-2-cinnamate (**II**) and cyasterone (**III**) all possess 20,22-diols and all formed cyclic boronates. Ecdysone (**IV**) which possesses a 2,3-diol but not a 20,22-diol showed no evidence of formation of a cyclic ester under mild conditions even with a large excess of reagent. This is consistent with our earlier finding in a study of the use of immobilized boronic acids for solid-phase extraction of ecdysteroids [11] (see also refs. 13 and 14). Only those ecdysteroids with a 20,22-diol were selectively retained on the boronic acid column through cyclic ester formation [11,12]. The distance between the hydroxyl groups on C-20 and C-22 is suitable for formation of the cyclic boronate

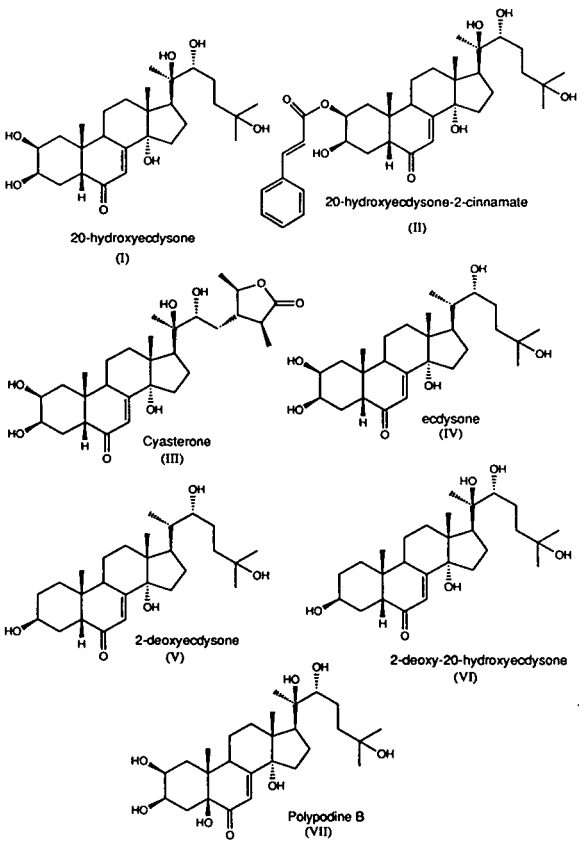

Fig. 1. Structures of ecdysteroids studied here.

ester, however *cis* fusion of the A and B rings of ecdysteroids causes the C-2 and C-3 β-hydroxyl groups to be too far apart for easy formation of a cyclic boronate, so, for example, ecdysone was not absorbed onto the immobilized boronic acid column [11]. The same effect appears to be operating here. Ecdysteroid 2,3-*cis*-diols do not give cyclic boronates under the conditions explored.

Addition of an excess of 1% solution of methyl-, butyl- or phenyl-boronic acid to a dilute (micromolar) solution of an ecdysteroid possessing a 20,22-diol gave rapid formation of a stable cyclic boronate ester (Fig. 2) which had a shorter retention time than the parent ecdysteroid. The excess of boronic acid required to convert a known quantity of ecdysteroid to its cyclic ester in 3 min at room temperature was explored with the three boronic acids and 20-hydroxyecdysone. Plots of extent of conversion to boronic ester against quantity of boronic acid added are given in Fig. 3. The formation of the phenylboronic ester occurred much more readily than either the methyl or butyl esters (Fig. 4), which required a ten-fold greater excess of reagent for complete conversion. The electron-donating effect of the phenyl ring evidently assisted ester formation.

Raising the temperature of reaction had little effect on the rate of reaction, but leaving the mixture together for a longer time at room temperature before chromatography gave more complete reaction with amounts of boronic acid below the optimum (Table I).

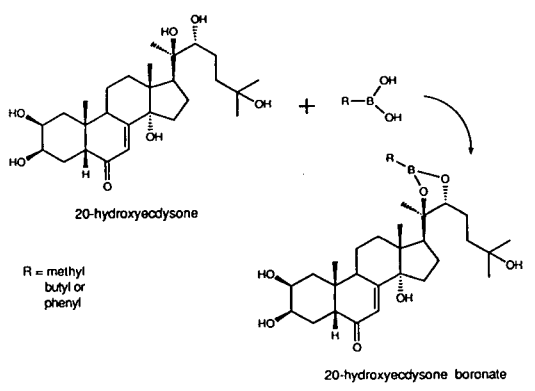

Fig. 2. Formation of a cyclic boronic ester of 20-hydroxyecdysone.

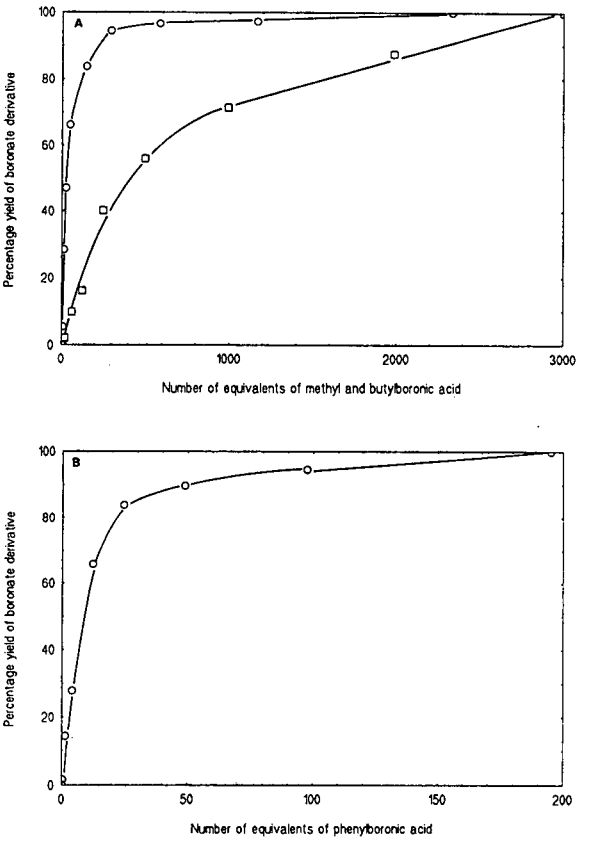

Fig. 3. Plots of extent of reaction of 20-hydroxyecdysone with differing amounts of (A) methyl- and butyl- and (B) phenylboronic acids to show the amount required for complete conversion in 3 min at room temperature. (A) □ = Methylboronate; ○ = butylboronate.

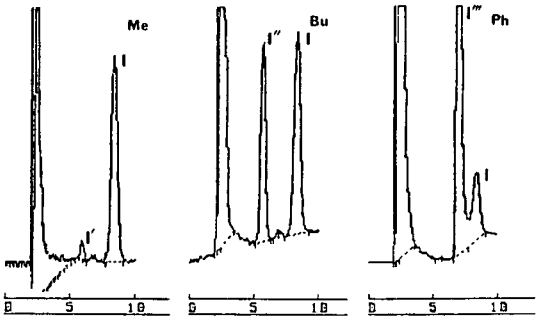

Fig. 4. SFC chromatograms of 20-hydroxyecdysone (I) after reaction with 10 molar excess of methyl-, butyl- and phenylboronic acids for 3 min at room temperature. I′ = Methylboronate; I″ = butylboronate; I‴ = phenylboronate. Time scale in min.

TABLE I

EFFECT OF TIME AND TEMPERATURE ON EXTENT OF REACTION BETWEEN 20-HYDROXYECDYSONE ($4.2 \cdot 10^{-10}$ mol) AND METHYLBORONIC ACID ($4.17 \cdot 10^{-9}$ mol) OR PHENYLBORONIC ACID ($4.0 \cdot 10^{-9}$ mol) IN DILUTE SOLUTION IN METHANOL

Boronic acid	Molar excess	Temperature (°C)	Time (min)	Conversion (%)
Methyl	993	Room	3	67
		Room	5	75
		Room	12	87
		50	3	78
Phenyl	9.5	Room	3	71
		Room	5	78
		Room	30	100
		50	3	74

The three ecdysteroids of varying structure were chosen to observe the change in retention on conversion to the boronic esters. Their relative retentions are shown in Table II. Conversion to a particular boronic ester had very similar effects upon each of the ecdysteroids. For example, the methylboronic esters of all three ecdysteroids (I to III) had retention times 24% shorter than the corresponding free ecdysteroids in the chromatographic system chosen. The butyl esters had shortest retentions and the phenyl esters were the closest to the parent ecdysteroids (Fig. 4).

To test the use of these boronic esters with natural materials, we have examined crude extracts of desert locust (*Schistocerca gregaria*) eggs, which, after enzymic hydrolysis, contain ecdysone (**IV**) and 2-deoxyecdysone (**V**), and extracts of *Ajuga iva* (tentative identification) which contains 20-hydroxyecdysone (**I**), 2-deoxy-20-hydroxyecdysone (**VI**) and polypodine B (**VII**) and an extract of *Silene otites* which we have already examined by SFC [6] and which contains polypodine B (**VII**), and 20-hydroxyecdysone (**I**). The *Schistocerca* eggs contain ecdysteroids which do not form boronic esters, however, although the main peaks were unaffected on addition of boronic acid, a small new peak appeared at 5.5 min, which suggested there was a small amount of complex-forming ecdysteroid in the mixture (Fig. 5A). In the case of the *Ajuga* and *Silene* plant extracts, all the components were shifted to shorter retention times when sufficient boronic acid was added (Fig. 5B, C) showing that all the components in the extract contained the 20,22-diol structure, although compounds **VI** and **VII** eluted as one unresolved peak, as did their boronic esters, under the conditions used (Fig. 5B).

These experiments demonstrate that boronic esters can be formed in neutral media without catalysis and with impure mixtures. These less polar esters can give a rapid indication of 20,22-diol ecdysteroids in crude plant or animal ex-

TABLE II

RELATIVE RETENTION TIMES OF ECDYSTEROIDS AND THEIR CYCLIC BORONATE ESTERS ON A CYANOPROPYL SILICA COLUMN USING SUPERCRITICAL CARBON DIOXIDE–METHANOL (9:1) AS MOBILE PHASE

Ecdysteroid (Fig. 1)	Boronic acid	t_r ecdysteroid[a]	t_r ester	t_r ester/ t_r ecdysteroid
I	Methyl	7.45	5.66	0.76
	Butyl	7.63	5.52	0.72
	Phenyl	7.65	6.48	0.85
II	Methyl	6.51	4.97	0.76
	Butyl	6.51	4.88	0.75
	Phenyl	6.77	5.86	0.87
III	Methyl	8.75	6.64	0.76
	Butyl	8.83	6.50	0.74
	Phenyl	8.87	7.84	0.88

[a] Retention times vary slightly with time, therefore relative retentions are quoted.

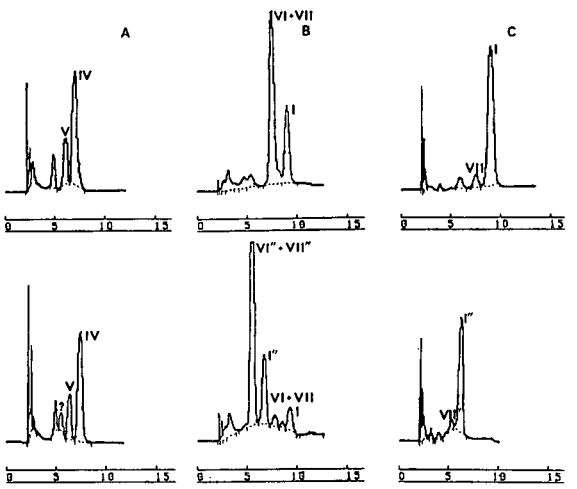

Fig. 5. SFC chromatograms of (A) *Schistocerca* eggs, (B) *Ajuga* (*iva*?) extract and (C) *Silene otites* plant extracts, before (above) and after treatment with butylboronic acid (below). (B) shows incomplete conversion, when using a larger excess of butylboronic acid the residual peaks at 8 and 10 min disappeared. Roman numerals correspond to those in Fig. 1. Roman numerals with double prime indicate the corresponding butylboronate esters. Time scale in min.

tracts and can be a useful guide in the screening of plant materials. For rapid formation, the phenylboronic esters is preferred, but if a larger shift in retention is required, the butylboronic ester is recommended.

ACKNOWLEDGEMENT

We thank the Korea Science and Engineering Foundation for a Fellowship to J.-H.S. and R. Lafont, Ecole Normale Superieure, Paris, for gifts of plant extracts.

REFERENCES

1 H.H. Rees, in J. Koolman (Editor), *Ecdysone*, Georg Thieme Verlag, Stuttgart, 1989, p. 28.
2 E.D. Morgan and I.D. Wilson, in J. Koolman (Editor), *Ecdysone*, Georg Thieme Verlag, Stuttgart, 1989, p. 114.
3 R. Lafont and D.H.S. Horn, in J. Koolman (Editor), *Ecdysone*, George Thieme Verlag, Stuttgart, 1989, p. 39.
4 G.B. Russell and D.R. Greenwood, in J. Koolman (Editor), *Ecdysone*, George Thieme Verlag, Stuttgart, 1989, p. 97.
5 E.D. Morgan, S.J. Murphy, D.E. Games and I.C. Mylchreest, *J. Chromatogr.*, 441 (1988) 165.
6 M.W. Raynor, J.P. Kithinji, K.D. Bartle, D.E. Games, I.C. Mylchreest, R. Lafont, E.D. Morgan and I.D. Wilson, *J. Chromatogr.*, 467 (1989) 292.
7 C.J.W. Brooks and D.J. Harvey, *J. Chromatogr.*, 54 (1971) 193.
8 G.M. Anthony, C.J.W. Brooks, I. Maclean and I. Sangster, *J. Chromatogr. Sci.*, 7 (1969) 623.
9 C.F. Poole and E.D. Morgan, *Scan*, 6 (1975) 19.
10 C.F. Poole, S. Singhawangcha, A. Zlatkis and E.D. Morgan, *J. High Resolut. Chromatogr. Chromatogr. Commun.*, 1 (1978) 96.
11 S.J. Murphy, E.D. Morgan and I.D. Wilson, in A.L. McCaffery and I.D. Wilson (Editors), *Chromatography and Isolation of Insect Hormones and Pheromones*, Plenum, New York, 1990, p. 131.
12 I.D. Wilson, E.D. Morgan and S.J. Murphy, *Anal. Chim. Acta*, 236 (1990) 145.
13 J. Pis and J. Harmatha, *J. Chromatogr.*, 596 (1992) 271.
14 I.D. Wilson, *J. Planar Chromatogr.*, 5 (1992) 316.

Journal of Chromatography, 639 (1993) 287–294
Elsevier Science Publishers B.V., Amsterdam

CHROM. 24 928

On the precise estimation of R_M values in reversed-phase thin-layer chromatography including aspects of pH dependence

Karl Dross and Christoph Sonntag

C. and O. Vogt Institute for Brain Research, Heinrich-Heine-Universität, Universitätsstrasse 1, 4000 Düsseldorf 1 (Germany)

Raimund Mannhold*

Biomedical Research Center, Molecular Drug Research Group, Heinrich-Heine-Universität, Universitätsstrasse 1, 4000 Düsseldorf 1 (Germany)

(First received November 9th, 1992; revised manuscript received January 29th, 1993)

ABSTRACT

In order to improve the application of reversed-phase thin-layer chromatography (RP-TLC) for the chromatographic estimation of drug lipophilicity, some aspects of measuring true R_M values [log $(1/R_F - 1)$] are considered in the present investigation:

(1) An optimization of experimental conditions, including the importance of temperature and humidity, as well as densitometric evaluation of spots is presented.

(2) The estimation of thermodynamically true R_M values is described; it is shown that in case of high modifier contents preloading effects induce pronounced deviations of R_F from R_F' values. Only the latter allow the calculation of true R_M values.

(3) The influence of solvent pH on R_M values is negligible for pure partition chromatography in the case of low modifier contents; with increasing modifier contents polar adsorption becomes more prominent; under these conditions an influence of pH on R_M in the case of strong bases is detected.

INTRODUCTION

Chromatographic estimation of drug lipophilicity is predominantly undertaken by means of RP-18 HPLC, while reversed-phase TLC is less frequently used. This reduced acceptance of the latter [1] may be because of improperly designed experimental protocols. To the authors' knowledge, investigators almost always neglect relevant experimental factors such as temperature and humidity despite their well-known importance for chromatographic behaviour [2]. Most often running distances are measured "by hand" under UV light and corresponding R_F values —related to the observed visible front— are used to calculate R_M values. In the present investigation densitometric estimation of spot positioning is used, as also applied by Dingenen and Pluym [3], and, in addition, a procedure for estimating the "thermodynamically true" front is presented for RP-18 TLC.

The pH dependence of chromatographic data in normal-phase TLC was demonstrated by Stahl and Dumont [4] a long time ago. It deserves mention here that Stahl and Dumont varied the pH of the stationary phase and not that of the solvent. Several authors assume that this pH dependence is equally valid in reversed-phase chromatography [2,5–7]. This is in contrast to

* Corresponding author.

0021-9673/93/$06.00

reports [8–10] that indicate a lack of influence of solvent pH in RP-18 TLC on R_F or R_M in which pH varied between 2 and 11. In a recently published paper Dross *et al.* [11] reported on investigations using silanized silica gel plates, in which application of the commonly used pK correction [5] yielded poorly plausible results. Accordingly, it was concluded that no, or a different pH/pK correction seems necessary. In continuation of such experiments we investigated the pH dependence of "thermodynamically true" R_M values using RP-18 silica gel.

EXPERIMENTAL

For the chromatographic experiments described here, we used precoated TLC plates RP-18 F_{254S}, 10×20 cm in size, purchased from Merck (Darmstadt, Germany). A 0.5-μl volume of an ethanolic solution of the test compounds (1 mg/ml) was applied to the plates with the aid of a Nanomat II (Camag, Muttenz, Switzerland). Before use, plates were preconditioned by heating on a Thermoplate S (Desaga, Heidelberg, Germany) for 15 min at 120°C. The starting points of the test compounds were positioned 10 mm from the bottom edge of the plate and at least 25 mm from the side of the plate with 5 mm between. As front markers we used potassium bromide, potassium iodide and sodium nitrate; 50 mg of these front markers were dissolved in 10 ml of a water–ethanol mixture (25:75, v/v), 0.5 μl of which were applied to the plate in the middle and at the two lateral positions. The Nanomat II does not allow an exact positioning of starting points; accordingly they were exactly evaluated with the aid of a CD50 densitometer (Desaga, Heidelberg, Germany) in remission mode. Compounds were measured at appropriate wavelengths.

Running of the plates was performed in twin trough chambers (Camag) which were lined with blotting paper in order to guarantee a saturation of the gas phase. Chambers were placed in an incubator adjusted to 30°C; the incubator contained a water-filled glass to ensure constant humidity. In some cases horizontal sandwich chambers (Camag) were used.

As solvent we used methanol–buffer mixtures of varying composition. For preparation of Tris buffer pH 7.4, purest water from a Milli-Q plus water system (Millipore, Bedford, MA, USA) was used; in some cases commercially available buffers (pH 3, 10 and 12) from Riedel-de Haen (Seelze, Germany) were applied. Plates were run up to 1 cm below the upper end of the plate,

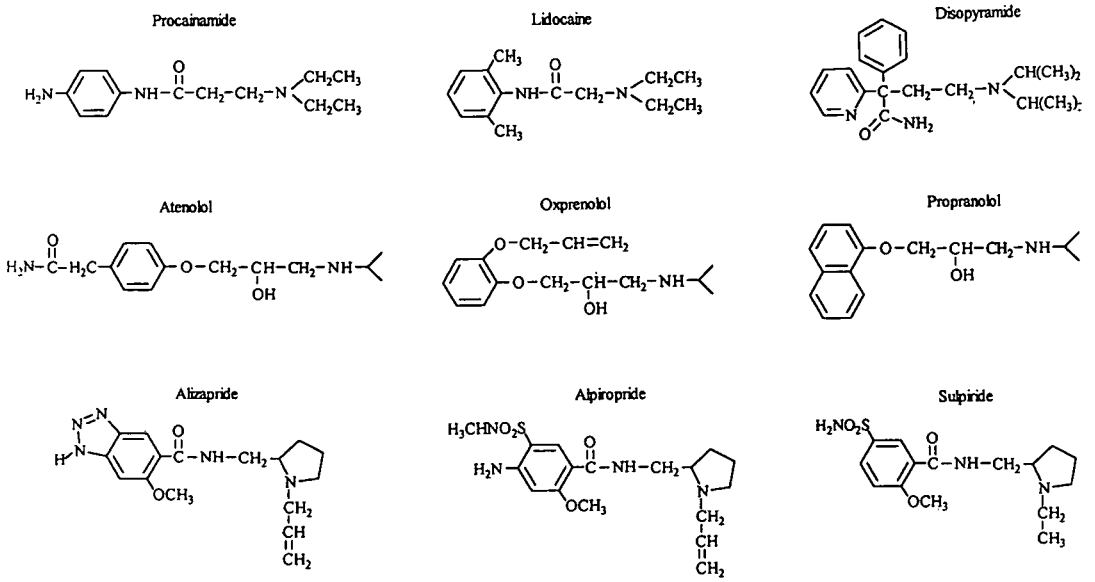

Fig. 1. Structural formulae of tested drug molecules.

which corresponds to a start–front distance of about 8 cm. After the run the plates were dried in a cold stream of air; afterwards the runs were evaluated densitometrically as described above.

Test compounds

Benzoic acid, 4-iodobenzoic acid, biphenyl and 2,6,2′,6′-tetramethylbenzophenone were kindly provided by R.F. Rekker (Department of Pharmacochemistry, Vrije Universiteit, Amsterdam, Netherlands). Resorcin, naphthoresorcin, diphenylamine and N-phenylnaphthylamine were obtained from Aldrich (Milwaukee, WI, USA). The following drugs were kindly supplied by pharmaceutical companies: procainamide, lidocaine, disopyramide, atenolol, oxprenolol, propranolol, alizapride, alpiropride and sulpiride. Their structural formulae are given in Fig. 1. All other chemical compounds, if not indicated otherwise, were analytical-reagent grade and were obtained from Merck.

RESULTS AND DISCUSSION

The importance of the densitometric evaluation of starting and running points

In the case of manual estimations of R_F values, some error (up to ±1 mm) is unavoidable; in contrast, a densitometer is accurate to about ±0.01 mm. Correspondingly, in the range of R_F values lower than 0.1 a significant improvement in the accuracy of R_M calculations is achieved. Nevertheless, this improvement is only valid if at the same time an exact estimation of the starting point position is performed densitometrically. For technical reasons, the Nanomat II is only adjustable to within about 0.5 mm; in addition, the support for the microcapillary pipette contributes position uncertainty of up to 0.3 mm (see Table I).

The experimental conditions described here prevent, in the case of low R_F values resulting in high R_M values, errors in calculating R_M of up to ±0.5.

The estimation of the "thermodynamically true" R_M

"Thermodynamically true" R_M values in TLC can only be obtained if it is possible to determine the thermodynamically true position of the front. It is known [2,12,13] that the visible front is not identical to the "true front". According to Geiss [2,12] two factors in particular have to be considered for correction in conventional TLC: the "preloading effect" and the "front gradient". The "preloading effect" causes the stationary phase to adsorb volatile mobile phase molecules

TABLE I

MEAN POSITION (mm) OF SPOTS ON FOURTEEN RP-TLC PLATES

The second column gives the maximum deviation of 30 spots, applied to each of the fourteen plates with the aid of a Nanomat II applicator, adjusted to about 10 mm.

9.80 ± 0.20	10.46 ± 0.28
10.09 ± 0.15	10.00 ± 0.20
9.95 ± 0.20	9.98 ± 0.16
9.92 ± 0.16	10.07 ± 0.10
9.59 ± 0.20	9.56 ± 0.16
9.83 ± 0.13	9.88 ± 0.30
9.88 ± 0.25	9.86 ± 0.30

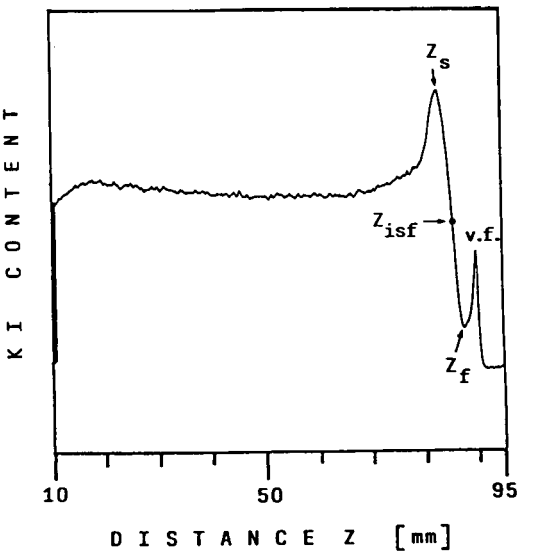

Fig. 2. Densitogram of a TLC plate which runs with buffer–methanol (30:70, v/v) and 0.05% potassium iodide in the buffer. Marked are the visible front (v.f.), the position until which stationary phase is solvent saturated (Z_s) and the mobile phase front of unsaturated flow (Z_f). Half-way between Z_s and Z_f the front of idealized saturated flow (Z_{isf}) is also indicated. According to Bolotov [13] Z_{isf} is the position of the thermodynamically true front. The distance between Z_f and v.f. is the area of preloading.

TABLE II

OBSERVED hR_F VALUES OF THE THREE FRONT MARKERS POTASSIUM BROMIDE, POTASSIUM IODIDE AND SODIUM NITRATE, ON RP-18 TLC USING VARIABLE MIXTURES OF METHANOL AND BUFFER, pH 7.4.

The higher the methanol content, the lower the hR_F due to larger preloading of stationary phase with increasing methanol content in the solvent. Above 65% methanol the hR_F of potassium iodide is the highest of the markers tested.

	Methanol concentration (%)					
	60	65	70	75	80	85
$hR_{F_{obs}}$, KBr	93.8	92.6	91.6	90.6	89.6	88.6
$hR_{F_{obs}}$, KI	93.6	93.0	92.9	91.6	91.1	90.8
$hR_{F_{obs}}$, $NaNO_3$	93.7	92.3	91.0	89.9	88.9	87.7

(*e.g.* methanol molecules from methanol–buffer mixtures) from the gas phase in the chamber before or during chromatographic runs. On the other hand, the mobile phase moves through the porous thin layer as an unsaturated flow, the mobile phase content in the layer varying along the distance from the source to the front and producing in the front region a gradient from fully saturated mobile phase content to zero content (see Fig. 2).

Almost all previous investigators [2,12,13] have tested the importance of these factors on silica gel or aluminium oxide layers. Accordingly, front markers used in these cases were rather lipophilic dyes such as Sudan Red with an anticipated R_F of 1.0.

The "front" in TLC is approximately equivalent to the "dead volume" (t_0) in HPLC. Therefore we investigated inorganic salts such as potassium bromide, potassium iodide and sodium nitrate as putative front markers, which were proposed by Braumann [14] as probes for estimating the dead volume in RP-HPLC. In a horizontal sandwich chamber, with and without water saturation, the three above-mentioned front markers were run in a methanol–buffer mixture of 1:1 (v/v) as well as in pure methanol. In all cases the front markers ran almost identically with the front; the difference amounted to less than 0.3 mm at a running distance of 80 mm ($R_F > 0.996$).

In the case of chamber saturation with methanol instead of water, the difference between the visible front and the marker position increased by up to 4 mm ($R_F = 0.95$). This observation might indicate that in RP-TLC correction of the "front gradient" is of marginal importance, while the "preloading effect" demands correction.

In a further series of experiments performed under the above-described conditions, *i.e.* twin trough chambers with solvent saturation and a temperature of 30°C, the apparent R_F values of the three front markers were estimated. Because of some residual free silanol groups in the stationary phase one has to consider a limited adsorption, which explains the lack of identity of front and marker positioning. As can be seen from Table II, of the three investigated compounds, potassium iodide exhibits the highest R_F values, at high methanol concentrations; thus we consider this salt to be the most convenient marker of the salts tested.

To further characterize the "front gradient"-related corrections, we performed investigations under standard conditions; potassium iodide (0.05%, w/v) was added to the buffers which were used as solvent in varying mixtures with methanol. Fig. 2 exemplifies typical results of such chromatograms.

For calculating the position of Z_{isf} (idealized solvent front, see also Fig. 2) in the gradient a modification of the procedure of Bolotov [13] was used. On standard silica gel plates Bolotov observed a gradient curve that could be described by an elliptical equation, while in case of RP-TLC, as shown in Fig. 2, the gradient exhibits a sigmoidal shape. Therefore, the thermodynamically true front position that equals Z_{isf} is exactly half-way between Z_s and Z_f and can be calculated with the equation

TABLE III

OBSERVED R_F VALUES, RELATED TO THE VISIBLE FRONT, OF POTASSIUM IODIDE AND OF THE FRONT OF IDEALIZED SATURATED FLOW, Z_{isf} (SEE FIG. 2)

From the last row it can be seen that their ratio varies only slightly around 0.99.

	Methanol concentration (%)					
	60	65	70	75	80	85
$R_{F_{obs}}$, KI	0.940	0 926	0.912	0.901	0.889	0.873
$R_{F_{obs}}$, Z_{isf}	0.950	0.936	0.921	0.910	0.897	0.884
R_F, KI/R_F, Z_{isf}	0.989	0.989	0.990	0.990	0.991	0.988

$$Z_{isf} = (Z_s + Z_f)/2 \quad (1)$$

In Table III the apparent R_F values as related to the visible front, of the front gradient ($R_{F_{obs}}$, Z_{isf}) and of potassium iodide ($R_{F_{obs}}$, KI) are listed for varying methanol contents. As can be seen from the data, the front gradient always surmounts the potassium iodide peak. The most accurate estimation of the thermodynamically true R'_F —and thereby of R_M— would obviously be represented by adding potassium iodide to all modifier mixtures and a direct estimation of the values with the thermodynamically true front. However, orientating experiments revealed some limitations in this respect. Many compounds, namely amines, exhibit a rather different chromatographic behaviour in iodide-containing modifiers as compared with iodide-free conditions. This is presumably due to the formation of adducts with iodide. Thus, we used a simplified procedure to calculate the thermodynamically true R_M values. As can be derived from Table III (third row) the ratio of potassium iodide peak to thermodynamically true front amounts to 0.99. Accordingly, using potassium iodide as a front marker, one has to divide the observed potassium iodide migration distance by 0.99. Formally, the observed apparent R_F of the compound X is:

$$R_{F_{obs},X} = (z_X - z_0)/(z_f - z_0) \quad (2)$$

The R_F value of the compound X when the potassium iodide peak is considered to indicate the front is:

$$R_{KI,X} = (z_X - z_0)/(z_{KI} - z_0) \quad (3)$$

The "thermodynamically true" R'_F value is then given by:

$$R'_{F,X} = [(z_X - z_0)/(z_{KI} - z_0)] \times 0.99 \quad (4)$$

R_M values have been calculated according to Bate-Smith and Westall [15]:

$$R_{M,X} = \log(1/R'_{F,X} - 1) \quad (5)$$

All R_M values have been calculated in this manner. R_M calculation with and without front correction causes differences of up to ±0.25, especially at high modifier contents. The differences between estimated true R_M values (*i.e.* related to the idealized solvent front) and uncorrected, apparent R_M values (*i.e.* related to the visible front) can be seen in Fig. 3. True R_M values are always lower than apparent R_M values; this difference increases with increasing modifier content, as also shown in Tables II and III. Consequently, linear regression is improved (see Fig. 3A).

The influence of solvent pH on R_M values

In recent investigations [11] it was shown that the commonly applied pH/pK correction of R_M leads to poorly plausible results. The above-mentioned investigations were performed on silanized silica gel plates and acetonitrile was used as modifier. We felt it necessary to prove the importance of these corrections also under the experimental conditions used in the present paper. For this purpose, investigations were

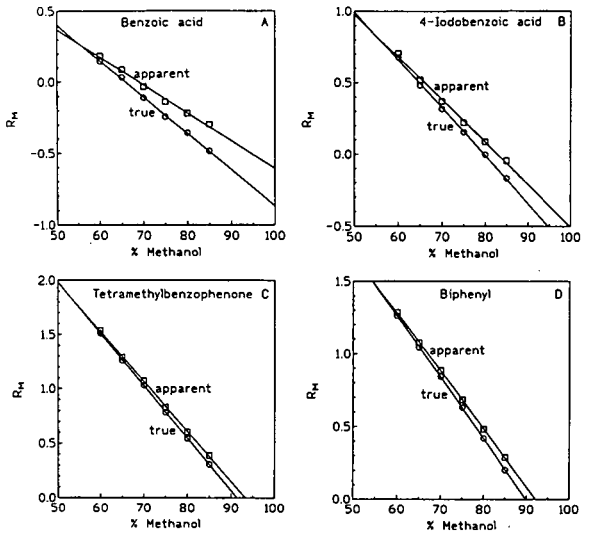

Fig. 3. Plots of linear regression analyses of true (○) and apparent (□) R_M values *versus* methanol concentration (v/v, %); buffer pH is 7.4.

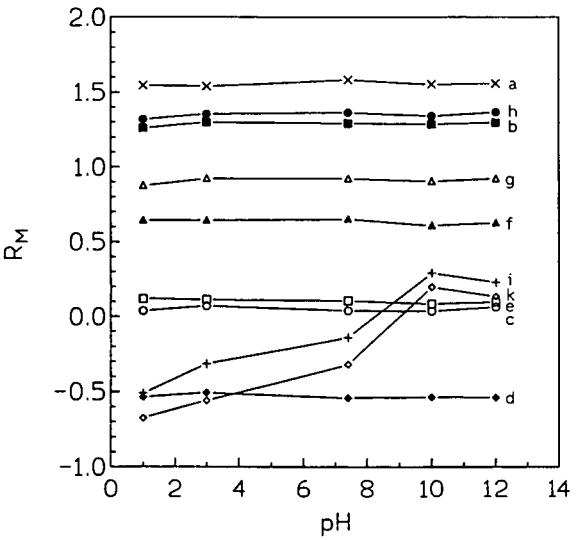

Fig. 4. Plot of R_M *versus* pH of some compounds on RP-18 silica gel plates using buffer–methanol mixtures (40:60, v/v). Only stronger amines such as atenolol (k, ◇) and procainamide (i, +) show variation between pH 1 and pH 10, but no further increase to pH 12. All other compounds show no variation: biphenyl (b, ■), tetramethylbenzophenone (a, ×), resorcin (d, ◆), naphthoresorcin (c, ○), benzoic acid (e, □), iodobenzoic acid (f, ▲), diphenylamine (g, △), N-phenylnapthylamine (h, ●).

carried out with a constant methanol:buffer ratio of 60:40; buffer pH was varied between 1 and 12.

The following ten test compounds were included: the non-polar biphenyl; the polar, non-ionizable tetramethylbenzophenone; the weak acids resorcin and naphthoresorcin (pK_a *ca.* 9.5); the strong acids benzoic and iodobenzoic acid (pK_a 4.2 and 4.0, respectively); the two weak bases diphenylamine and naphthylphenylamine (pK_a *ca.* 0.85) and the two strong bases procainamide (pK_a 9.4) and atenolol (pK_a 9.6).

The results, shown in Fig. 4, allow the conclusion that there is no need for a pK correction except for the strong bases. For example, for benzoic acid the above-described commonly used scheme for correction [5] leaves the measured value at pH 1 unaltered, while at pH 12 the measured value is to be corrected by +7.7 units. In contrast, the difference in the values obtained at pH 1 and 12 amounts to only 0.02 units. With a total of four hydroxybenzoic acids (pK_a about 3.0) Wilson [8] also did not detect variations in R_M within a pH range of 2–11. Similarly, for strong bases corrections that are far too high are calculated with the commonly used correction procedure. In this case, corrections at pH 12 should be negligible, while for atenolol at experimental pH 1, for example, as much as 8.6 units should be added for correction. In contrast to this theoretical consideration, the measured difference amounts to 0.81 units. The corresponding values for procainamide are 8.4 (theoretical) and 0.74 (experimentally obtained).

From our point of view, these examples convincingly prove the failure of the commonly used pK correction procedure. On the other hand, reasons for the observed weak pH dependence of strong bases remain to be clarified. One might speculate that R_M variation in these cases is a function of the modifier concentration. As shown by Horvath and co-workers [16–18] in RP-HPLC, the so-called silanophilic effect becomes prominent in cases of high modifier content. El Tayar *et al.* [19] have demonstrated the pH dependence of this silanophilic effect.

With these data in mind, we performed investigations with nine strong bases (pK_a values between 8.0 and 10.7) including procainamide

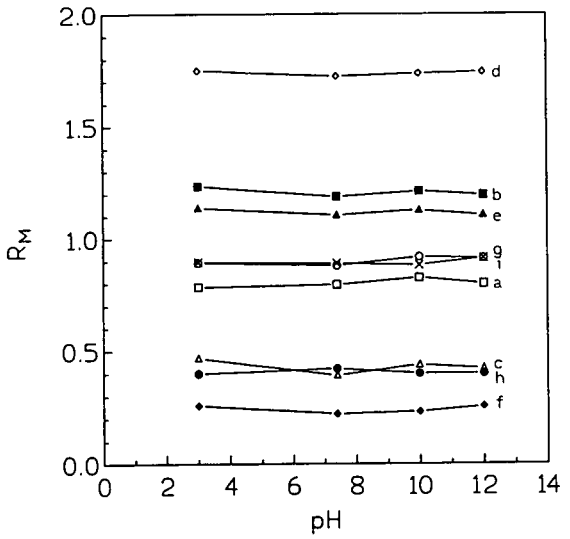

Fig. 5. Plot of R_M *versus* pH using solvent buffer–methanol (75:25, v/v) on RP-18 TLC plates showing the absence of any variation of the stronger organic bases (pK_a: 8.0–10.7) in low modifier mixtures. Key: lidocaine (a, □), disopyramide (b, ■), procainamide (c, △), propranolol (d, ◇), oxprenolol (e, ▲), atenolol (f, ◆), alizapride (g, ○), sulpiride (h, ●), alpiropride (i, ×).

and atenolol; modifier content was reduced to 25%.

As shown in Fig. 5, at this modifier concentration pH dependence of R_M is no longer observed; data differ only within the range of experimental variance. At this modifier content the chromatographic process is almost exclusively determined by partitioning. Obviously, the dissociation of solutes plays a negligible role in the partitioning process in RP-TLC. From similar observations in RPLC [20], Taylor [1] concluded that dissociated organic molecules will also be distributed into the stationary lipid phase. In our opinion this is because the dissociation velocity is much higher than compared to the distribution velocity (it takes time to reach a steady-state equilibrium in the shake-flask method).

With increasing methanol content the chromatographic process is, beyond lipophilic partitioning, increasingly due to polar adsorption, when the importance of ionization becomes more prominent. The pH dependence of this process was shown by Cserháti and Szögyi [21], while Dingenen and Pluym [3] speculated on the influence of silanol dissociation in this context. Our data with respect to atenolol and procainamide (Fig. 4) are not in conflict with this view. The small but continuous increase in R_M of these two amines between pH 1 and pH 10 and the lack of further increase to pH 12 may well reflect dissociation of silicon hydroxide. On the other hand the lack of pH dependence of benzoic acids (pK_a 4–4.2), as shown in Fig. 4, and salicylic acid [8] (pK_a 3.0), even at high modifier content, may well substantiate our interpretation. As mentioned above, the classic study of Stahl and Dumont [4] was performed by varying the pH of the stationary phase. Thus, our findings and those of Dingenen and Pluym [3] closely correspond to those in ref. 4.

REFERENCES

1 P.J. Taylor, in C. Hansch (Editor), *Comprehensive Medicinal Chemistry*, Pergamon Press, Oxford, 1990.
2 F. Geiss, *Fundamentals of Thin Layer Chromatography*, Hüthig, Basel, 1987.
3 J. Dingenen and A. Pluym, *J. Chromatogr.*, 475 (1989) 95.
4 E. Stahl and E. Dumont, *J. Chromatogr. Sci.*, 7 (1969) 517.
5 E. Tomlinson, *J. Chromatogr.*, 113 (1975) 1.
6 A. Hulshoff and J.H. Perrin, *J. Chromatogr.*, 120 (1976) 65.
7 J.K. Seydel and K.J. Schaper, *Chemische Struktur und biologische Aktivität von Wirkstoffen*, Verlag Chemie, Weinheim, 1979.
8 I.D. Wilson, *J. Chromatogr.*, 354 (1986) 99.
9 T. Cserháti, B. Bordás and G. Ösapay, *Chromatographia*, 23 (1987) 184.
10 K. Kovács-Hadady and J. Szilágyi, *J. Chromatogr.*, 553 (1991) 459.
11 K.P. Dross, R. Mannhold and R.F. Rekker, *Quant. Struct.–Act. Relat.*, 11 (1992) 36.
12 F. Geiss, *Parameter der Dünnschichtchromatographie*, Verlag Vieweg, Braunschweig, 1972.
13 S.L. Bolotov, *Kontakte (Darmstadt)*, 2 (1990) 36.
14 T. Braumann, *J. Chromatogr.*, 373 (1986) 191.
15 E.C. Bate-Smith and R.G. Westall, *Biochim. Biophys. Acta*, 4 (1950) 427.
16 Cs. Horváth, W.R. Melander and I. Molnár, *J. Chromatogr.*, 125 (1976) 129.
17 A. Nahum and Cs. Horváth, *J. Chromatogr.*, 203 (1981) 53.
18 K.E. Bij, Cs. Horváth, W.R. Melander and A. Nahum, *J. Chromatogr.*, 203 (1981) 65.

19 N. El Tayar, H. van de Waterbeemd and B. Testa, *J. Chromatogr.*, 320 (1985) 293.
20 S.H. Unger, P.S. Cheung, G.H. Chiang and J.R. Cook, in W.J. Dunn, III, J. Block and R.S. Pearlman (Editors), Partition Coefficient: Determination and Estimation, Pergamon Press, Oxford, 1986, p. 69.
21 T. Cserháti and M. Szögyi, *J. Chromatogr.*, 520 (1990) 249.

Journal of Chromatography, 639 (1993) 295–302
Elsevier Science Publishers B.V., Amsterdam

CHROM. 24 970

Thin-layer and high-performance liquid chromatographic analyses of limonoids and limonoid glucosides in *Citrus* seeds

Hideaki Ohta*

Chugoku National Agricultural Experiment Station, Ministry of Agriculture, Forestry and Fisheries, Fukuyama City, Hiroshima 721 (Japan)

Chi H. Fong, Mark Berhow and Shin Hasegawa

Fruit and Vegetable Chemistry Laboratory, Agricultural Research Service, US Department of Agriculture, 263 South Chester Avenue, Pasadena, CA 91106 (USA)

(First received August 31st, 1992; revised manuscript received February 9th, 1993)

ABSTRACT

A routine method for the analysis of limonoids and limonoid glucosides in citrus seeds, which utilizes thin-layer chromatography (TLC) and high-performance liquid chromatography (HPLC), is described. Seed meals were washed with *n*-hexane to remove oily materials, after which limonoids and limonoid glucosides were extracted with acetone and then methanol. The methanol extract contains the remainder of the limonoid aglycones and all limonoid glucosides. After the methanol was evaporated off, the residue was extracted with methylene chloride–water (1:1). The limonoids of both the acetone and methylene chloride fractions were separated and quantified by HPLC. The total limonoid glucoside content of the water fraction was determined by silica gel TLC. Each of the limonoid glucosides was then eluted from the reversed-phase HPLC column by a linear gradient system starting at 15% acetonitrile in 3 m*M* phosphoric acid and ending with 26% acetonitrile after 35 min, and quantitated by spectrophotometric detection at 210 nm. The limonoid aglycones and limonoid glucosides in two kinds of citrus seeds, Shiikuwasha (*Citrus depressa*) and Iyo (*Citrus iyo*), were determined. The content of limonoid glucosides in Shiikuwasha was found to be approximately two-fold higher than that of Iyo.

INTRODUCTION

The limonoids are a group of chemically related triterpenoid derivatives present in the Rutaceae and Meliaceae families. Limonoids are one of two major bitter principles in citrus juices. Among the 37 limonoids isolated from *Citrus* and its hybrids, limonin is the major cause of the bitterness in a variety of citrus juices. Recently, limonoids have been shown to be also present as glucoside derivatives in *Citrus* [1]. Nineteen limonoid glucosides have been isolated from *Citrus* and, significantly, they are all non-bitter in taste.

Limonoids possess important biological activities such as the inhibition of the growth of cancerous tumours in laboratory animals [2–4] and antifeedant activity against insects and termites [5,6]. The demand for limonoids has increased significantly in recent years. Citrus seeds are major sources of both limonoid aglycones and their glucosides and could be utilized as a source of these important compounds.

Methods for the determination of limonoid aglycones, such as limonin and nomilin, using

* Corresponding author.

0021-9673/93/$06.00

thin-layer chromatography (TLC) and high-performance liquid chromatography (HPLC) have been reported [7–14]. In particular, Van Beek and Blaakmeer [14] performed a detailed analytical investigation of limonin in citrus juice. In this HPLC method the combination of reversed-phase columns and spectrometric detection was successfully applied to limonoid aglycone assays. Recently, limonoid glucosides in citrus juices have been also analysed using TLC [15] and HPLC [16].

The objective of this study was to establish a routine procedure for the extraction, isolation and characterization of limonoid aglycones and limonoid glucosides in citrus seeds by TLC and HPLC. For this study, the seeds of Shiikuwasha (*Citrus depressa* Hayata) and Iyo (*Citrus iyo* hort. Tanaka) were examined. The structures of major limonoids and limonoid glucosides are shown in Fig. 1.

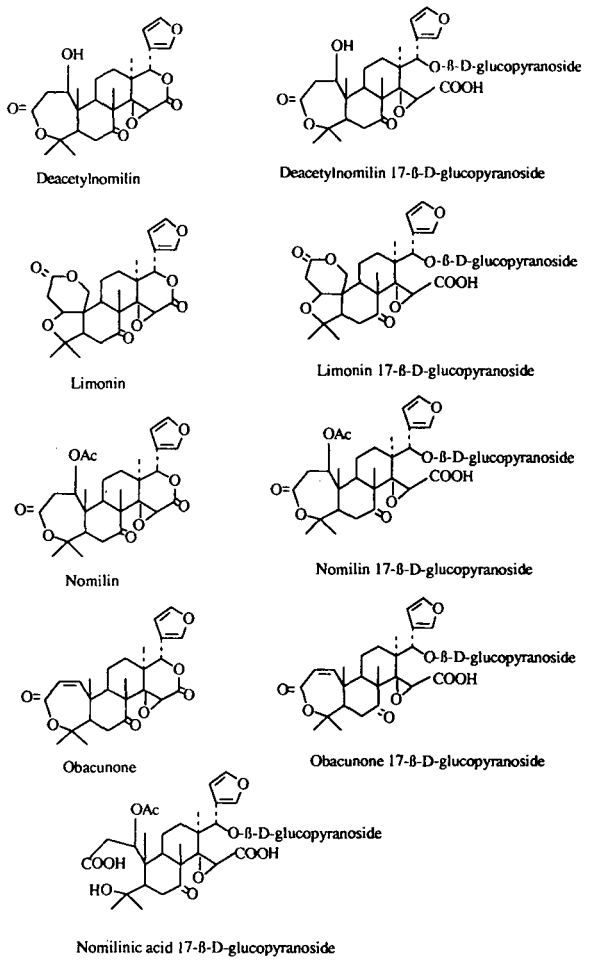

Fig. 1. Structures of major limonoids and limonoid glucosides.

EXPERIMENTAL

Materials

Shiikuwasha (*Citrus depressa* Hayata) was harvested in November, 1991, from trees grown at the Agricultural Product Processing Factory, Agricultural Cooperative Association of Okinawa, Japan. Iyo (*Citrus iyo* hort. ex Tanaka) was sampled in October, 1991, at the Tree Research Station of Saga Prefecture, Japan. The seeds were ground with a Retsch mill (Brinkmann, Westbury, NY, USA) after drying at 60°C for 3 days.

Chemicals

Silica gel HLF plates were purchased from Analtech (Newark, DE, USA). A preparative HPLC column, C_{18} reversed-phase, Partisil ODS-3, 25 cm × 2.2 cm, particle size 10 μm (Whatman, Hillsboro, OR, USA) was used. DEAE-Sephacel, Amberlite XAD-2 resin (20–60 mesh), hesperidinase and naringinase were obtained from Sigma (St. Louis, MO, USA). Sep-Pak silica cartridges, used for sample clean-up, were obtained from Waters (Milford, MA, USA).

Standards of limonoids and limonoid glucosides

Limonoid aglycones such as limonin, nomilin, deacetylnomilin and obacunone, and 17-β-D-glucopyranosides of limonin, deacetylnomilin, nomilin, nomilinic acid and obacunone, which were isolated and characterized by NMR at the Fruit and Vegetable Chemistry Laboratory, US Department of Agriculture, Agricultural Research Service, Pasadena, CA, USA, were used as standards in this study.

Apparatus for HPLC

The system consisted of two Waters 510 LC pumps, a Waters Automated Gradient Control-

ler, a C_{18} reversed-phase analytical HPLC column (250 mm × 4.6 mm, 5 μm particle size, Alltech Associates, Deerfield, IL, USA), a Perkin Elmer LC-75 spectrophotometric detector and a Shimadzu C-R3A integrator (Shimadzu, Kyoto, Japan).

Extraction of limonoid aglycones and glucosides

Aliquots of 100 g of each seed meal obtained from the dried seeds were placed in a Soxhlet extractor and washed thoroughly with *n*-hexane to remove oily materials, then extracted sequentially with acetone and methanol. The acetone extract (fraction 1) contained approximately 50% of total limonoid aglycones. The methanol extract (fraction 2) contained the remainder of limonoid aglycones and all the limonoid glucosides. This fraction was evaporated to dryness and the residue was re-extracted with methylene chloride–water (1:1). The methylene chloride fraction (fraction 3) contained aglycones, and the water fraction (fraction 4) contained glucosides.

TLC identification and HPLC analysis of limonoid aglycones

Both the acetone (fraction 1) and methylene chloride (fraction 3) fractions were combined and evaporated to analyse the limonoid aglycones. The dried material was resuspended in methanol and a portion was spotted onto silica gel TLC plates, which were developed in one dimension. The following three solvent systems were used in saturated chambers: cyclohexane–ethyl acetate (2:3), methylene chloride–methanol (49:1) and ethyl acetate–methylene chloride (2:3). The developed plate was sprayed with Ehrlich's reagent and colour was developed in a hydrochloric acid chamber [9]. R_F values were compared with those of standards for identification purposes. Another portion of the resuspended sample was injected into a C_{18} reversed-phase HPLC column, the column being eluted isocratically with acetonitrile–methanol–water (10:41:49). The limonoid aglycones were separated and identified by monitoring UV absorption at 210 nm.

HPLC and TLC analyses of the limonoid glucosides

The content of limonoid glucosides in the seeds was determined by both TLC and HPLC methods.

For the TLC, the water extract (fraction 4) was evaporated, dissolved in a measured volume of methanol and spotted on a plate, which was developed in one dimension with an ethyl acetate–methyl ethyl ketone–formic acid–water (5:3:3:1) system. Limonoid glucosides were visualized by spraying with Ehrlich's reagent followed by exposure to hydrogen chloride gas [17]. The spots were compared with those of a standard compound, and the total limonoid glucosides were determined by the relative intensity of the colour. This analysis was done in duplicate and average values were reported. Limonin glucose standards ranging from 1 to 5 μg at increments of 0.2 μg were used [15]. A preliminary analysis was needed to determine the approximate concentration of the sample to be used on TLC.

For the HPLC, a portion of the water extract (fraction 4) was treated with hesperidinase [0.010 units mg^{-1} solid: one unit was defined as 1.0 μmol of reducing sugar (as glucose) from hesperidin per min at pH 3.8 at 40°C] and naringinase [365 units g^{-1} solid: one unit was defined as 1.0 μmol of reducing sugar (as glucose) from naringin per min at pH 4.0 at 40°C] in a 0.1 *M* sodium formate buffer at pH 3.8 for 20 h at room temperature. This treatment was necessary to obtain good peak resolution by cleaving the sugars from interfering flavonoids. The sample was then loaded onto a Sep-Pak column, washed with water and eluted with methanol. This methanol fraction was evaporated in a test tube; 250 μl of 15% acetonitrile in 3 m*M* phosphoric acid were added and analysed by HPLC. For each sample extracted, duplicate 100-μl injections were made on a C_{18} reversed-phase analytical HPLC column. The flow-rate was 1 ml min^{-1} with a linear gradient system, starting with 15% acetonitrile in 3 m*M* phosphoric acid and ending with 26% at 35 min. The elution was monitored by UV absorption at 210 nm and a standard curve was run for each of the limonoid glucosides.

Isolation and characterization of limonoid glucosides

The water fraction of a seed meal extraction (fraction 4) (pH 6.5) was transferred on to a DEAE-Sephacel column (25 cm × 2.5 cm I.D.), followed by a thorough washing with water. The limonoid glucosides were eluted by an increasing linear gradient of sodium chloride in water. Fractions containing glucosides were combined, desalted by passing through a Dowex 50 column (H^+ form, 20 cm × 1.5 cm I.D.), and refractionated on an XAD-2 column (75 cm × 2.5 cm I.D.). The column was eluted with methanol. After the solvent was evaporated, the residue was dissolved in water and fractionated on a C_{18} reversed-phase preparative HPLC column. The column was eluted at 6 ml min^{-1} with a linear gradient starting with 15% and ending with 55% methanol in water over 75 min [18]. Fractions containing each limonoid glucoside were characterized by NMR [1,19] and analytical HPLC. NMR spectra were recorded on a JEOL GSX-270 NMR spectrometer in [$^2H_6$] dimethyl sulphoxide at 90°C, at 270 MHz for ^1H and 67.8 MHz for ^{13}C. NMR spectral assignments were made on the basis of ^1H-^1H COSY (correlation spectroscopy) and NOESY (nuclear Overhauser enhancement and exchange spectroscopy), DEPT (distortionless enhancement by polarization transfer) and ^{13}C-^1H COSY spectra [1,19].

RESULTS AND DISCUSSION

Determination of limonoid aglycones

Identification of limonoid aglycones by silica gel TLC. Limonoids in citrus tissue and juice have been customarily detected by TLC [7]. For identification purposes, we first examined R_F values of the major standard limonoids by TLC, using the three solvent systems described above. Table I lists the R_F values of major limonoids, including limonin, nomilin, deacetylnomilin and obacunone. Although these R_F values are a useful indicator with which to identify each of the limonoids, it is recommended that standard compounds be co-chromatographed on the same TLC plate.

Qualitative and quantitative analyses of limonoid aglycones by HPLC. The individual limonoid aglycones in the acetone and methylene chloride extracts were separated and quantified by HPLC. We used a C_{18} reversed-phase column and the column was eluted isocratically with acetonitrile–methanol–water (10:41:49). A typical chromatogram of standard limonoids is shown in Fig. 2, the retention times for limonin, deacetylnomilin, nomilin and obacunone being 15.1, 18.8, 26.3 and 43.2 min, respectively.

TABLE I

R_F VALUES OF LIMONOID AGLYCONES ANALYSED BY TLC

Limonoid aglycone	R_F value		
	Solvent system		
	1[a]	2[b]	3[c]
Limonin	0.32	0.53	0.55
Deacetylnomilin	0.12	0.33	0.36
Nomilin	0.23	0.60	0.58
Obacunone	0.57	0.74	0.81

[a] Cyclohexane–ethyl acetate (2:3).
[b] Methylene chloride–methanol (49:1).
[c] Ethyl acetate–methylene chloride (2:3).

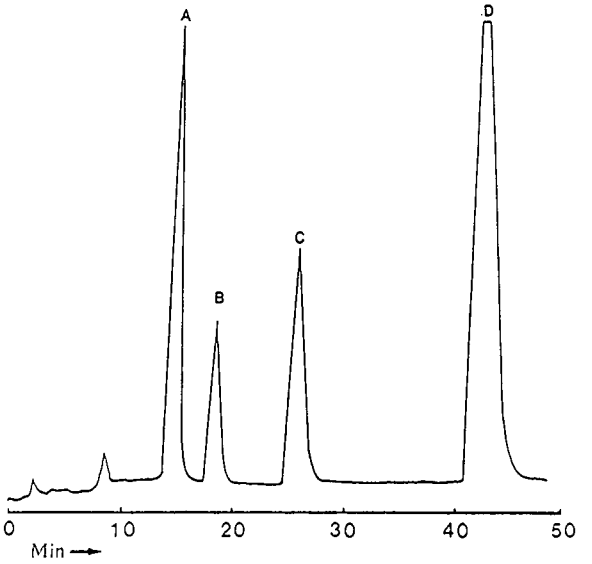

Fig. 2. High-performance liquid chromatogram of limonoid aglycones. Peaks: A = limonin (5 μg); B = deacetylnomilin (2.5 μg); C = nomilin (5 μg); D = obacunone (5 μg). See text for the HPLC conditions.

These retention times are also useful indicators for the identification of each limonoid.

In order to check the linearity of the relationship between the limonoid levels and peak area using the above separation and detection system, various amounts of dissolved limonoid standards were injected into the HPLC column in the concentration range of 0–4 μg. Except for obacunone, all the graphs exhibited good linearity and obeyed Beer's law. For the regression equation $y = ax + b$, where x is the amount of limonoid (μg) and y is the peak area, the correlation coefficients (r) of the limonoids were as follows: for limonin, $y = (4.814 \cdot 10^5)x - 2.174 \cdot 10^4$ ($r = 0.999$); for deacetylnomilin, $y = (4.216 \cdot 10^5)x - 1.221 \cdot 10^4$ ($r = 0.999$); for nomilin, $y = (4.209 \cdot 10^5)x - 4570$ ($r = 1.000$); for obacunone, $y = (1.372 \cdot 10^6)x + 1.661 \cdot 10^4$ ($r = 0.999$). These results suggest that these HPLC conditions are sufficiently sensitive to detect the levels of the major limonoids.

Determination of limonoid glucosides

Estimation of total limonoid glucosides by TLC. A portion of the water extract (fraction 4) described above was spotted on TLC plates and developed with ethyl acetate–methyl ethyl ketone–formic acid (88%)–water (5:3:3:1). The plate was then developed in the same manner mentioned above. The R_F values were compared with standards run in most cases on the same plate.

R_F values of the major 17-β-D-glucopyranosides of limonin, deacetylnomilin, nomilin and obacunone were 0.34, 0.26, 0.37 and 0.54, respectively. In the determination of the total limonoid glucosides, two judges provided estimates of the glucosides by comparing the size and colour intensity of spots with those of the standards as described above.

Qualitative and quantitative analyses of limonoid glucosides by HPLC. The standard limonoid glucosides were separated by a C_{18} reversed-phase HPLC column. The column was eluted at 1 ml min^{-1} using a linear gradient starting with 15% acetonitrile in 3 m*M* phosphoric acid and concluding with 26% after 35 min. A typical HPLC chromatogram is shown in Fig. 3, retention times for the 17-β-D-glucopyranosides of limonin, deacetylnomilin, nomilin, nomilinic acid and obacunone being 16.2, 23.4, 29.6, 30.5 and 33.8 min, respectively.

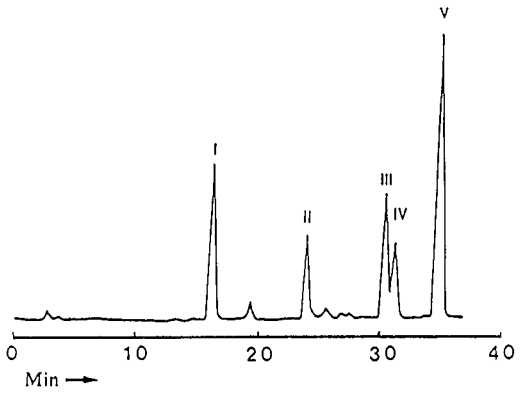

Fig. 3. High-performance liquid chromatogram of limonoid glucosides. 17-β-D-Glucopyranosides of limonin (I, 2.4 μg), deacetylnomilin (II, 1.6 μg), nomilin (III, 1.6 μg), nomilinic acid (IV, 1.6 μg) and obacunone (V, 1.6 μg).

The calibration curves for the 17-β-D-glucopyranosides of limonin, deacetylnomilin, nomilinic acid and obacunone showed good linearity in the concentrations range 0–4 μg, except for obacunone glucosides. For the regression equation $y = ax + b$, where x is the amount of limonoid glucosides (μg) and y is the peak area, the correlation coefficients (r) of the limonoid glucosides were as follows: for limonin glucoside, $y = (1.675 \cdot 10^5)x - 289.2$ ($r = 0.999$); for deacetylnomilin glucoside, $y = (1.378 \cdot 10^5)x - 7794$ ($r = 0.999$); for nomilin glucoside, $y = (1.963 \cdot 10^5)x - 1121$ ($r = 0.999$); for nomilinic acid glucoside, $y = (1.515 \cdot 10^5)x + 7795$ ($r = 0.999$); for obacunone glucoside, $y = (6.042 \cdot 10^5)x - 1677$ ($r = 0.999$). These results indicated that this HPLC condition was sufficiently sensitive to detect the limonoid glucosides.

Recovery of limonoid glucosides. Five limonoid glucosides, limonin glucoside, deacetylnomilin glucoside, nomilin glucoside, nomilinic acid glucoside and obacunone glucoside, were added at 100 mg l^{-1} to a sample water fraction (fraction 4) of Iyo containing known levels of the compounds (see Table II), followed by analysis by the HPLC method described in the Experimental section after Sep-Pak clean-up. The recoveries were 97% for limonin glucoside, 98% for deacetyl nomilin glucoside, 97% for nomilin

glucoside, 95% for nomilinic acid glucoside and 98% for obacunone glucoside. Several experiments gave recoveries in the range 93–100%. These recoveries were certainly within acceptable limits.

Application

Seeds of Shiikuwasha (Citrus depressa Hayata). TLC analysis with the three solvent systems described in Experimental section showed that Shiikuwasha contains three limonoid aglycones. They were identified as limonin, nomilin and obacunone. These are the major limonoid constituents in *Citrus* and its hybrids, and are widely spread in many species [20]. Like many other species, limonin is the predominant limonoid in the seeds of Shiikuwasha, followed by nomilin and obacunone. Limonin, which is the major cause of limonoid bitterness in a variety of citrus juices, has been shown to be biosynthesized from nomilin via obacunone, obacunoate and ichangin [21,22].

NMR analysis of the isolates showed that Shiikuwasha contains the 17-β-D-glucopyranosides of limonin, deacetylnomilin, nomilin, nomilinic acid and obacunone. Fig. 4 shows a chromatogram of limonoid glucosides in the seeds of Shiikuwasha. Table II gives the results expressed as mg g^{-1} (dried seeds). As expected, nomilin 17-β-D-glucopyranoside was the predominant limonoid glucoside, followed by obacunone 17-β-D-glucopyranoside, nomilinic acid 17-β-D-glucopyranoside, limonin 17-β-D-glucopyranoside and deacetylnomilin 17-β-D-glucopyranoside in order of decreasing concentration. This order is very common in many *Citrus* species [20].

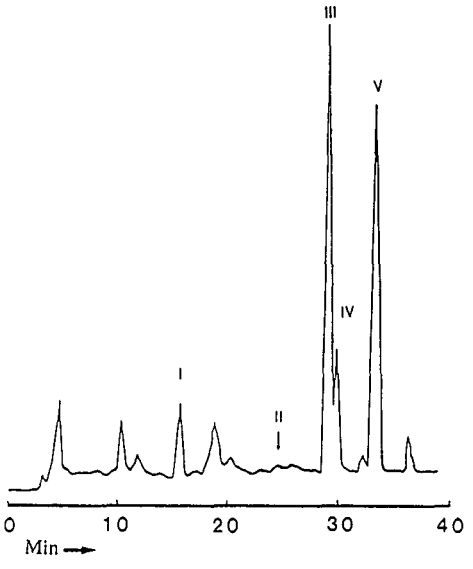

Fig. 4. High-performance liquid chromatogram of water extract from Shiikuwasha (*Citrus depressa*) seeds. 17-β-D-Glucopyranosides of limonin (I), deacetylnomilin (II), nomilin (III), nomilinic acid (IV) and obacunone (V).

TABLE II

LIMONOID AND LIMONOID GLUCOSIDES IN SEEDS OF SHIIKUWASHA (*CITRUS DEPRESSA* HAYATA) AND IYO (*CITRUS IYO* HORT. EX TANAKA)

Limonids	Content[a] (mg per g dried seed)	
	Shiikuwasha	Iyo
Limonin	1.87	4.57
Deacetylnomilin	–	0.72
Nomilin	0.96	2.53
Obacunone	0.45	0.91
Total	3.28	8.73
17-β-D-glucopyranoside of		
Limonin	1.16	0.53
Deacetylnomilin	0.18	0.48
Nomilin	7.59	2.24
Nomilinic acid	1.85	0.34
Obacunone	1.96	0.87
Total[b]	12.74	4.46
Total[c]	11.82	4.41

[a] Average values of duplicate measurements.
[b] Determined by HPLC.
[c] Determined by TLC.

Table II also shows the limonoid glucoside content as analysed by TLC. The values for total amount of limonoid glucosides determined by TLC and HPLC correlated very closely. A paired-sample *t*-test gave no significant variance at the $p = 0.05$ confidence level. Quantitative analyses by TLC and HPLC showed that the contents of limonoid glucosides in the seeds of Shiikuwasha are approximately twofold higher than that of other citrus seeds [20], whereas the content of limonoid aglycones analysed by HPLC is lower than that of others. The conversion of limonoid aglycones to their corre-

sponding glucosides occurs in *Citrus* during late stages of fruit growth and maturation [23]. This conversion may continue until fruit is harvested. The Shiikuwasha fruits used in this study were harvested at the early season of November. Thus, fruit harvested in the late season should have higher concentrations of limonoid glucosides.

Citrus limonoids have been shown to possess biological activities such as anticancer activity in laboratory animals [2–4] and antifeedant activity against insects and termites [5,6]. Thus the demand for seeds as a source of limonoids has increased significantly in recent years. Shiikuwasha is mainly grown in Okinawa, the most southern part of Japan, and is used mainly as a flavour enhancer. This work shows that its seeds are also excellent sources of limonoids, particularly their glucoside derivatives.

Seeds of Iyo (Citrus iyo hort. ex Tanaka). Four limonoid aglycones were identified. They were limonin, nomilin, obacunone and deacetylnomilin in order of decreasing concentration (Table II). As in many other *Citrus* species, limonin was the predominant limonoid aglycone in the seed of Iyo.

Analyses of the isolates by NMR spectra resulted in the identification of five limonoid glucosides from the seeds of Iyo. They are the 17-β-D-glucopyranosides of nomilin, obacunone, limonin, deacetylnomilin and nomilinic acid. Fig. 5 presents a typical chromatogram of limonoid glucosides in the seeds of Iyo. As shown in Table II, data on the total limonoid glucoside contents obtained from the two methods, TLC and HPLC, also agreed very well.

The composition and relative concentrations of limonoid aglycones and their glucosides are very similar to those of the common *Citrus* species [20]. Like the others, the ratio of aglycones to glucosides was about 2. The 17-β-D-glucopyranoside of nomilin is the predominant limonoid glucoside. This supports the previous suggestion [24] that limonoids and limonoid glucosides in seeds are biosynthesized there, independent from the biosynthesis occurring the fruit tissue.

From these results, we recommend this TLC and HPLC procedure as a convenient method for the analysis of the limonoid aglycones and limonoid glucosides in citrus seeds. We also expect that this method will be a useful in any chemotaxonomic analysis of Rutaceae and Meliaceae families and as a method for the purification of limonoids and limonoid glucosides from citrus seeds.

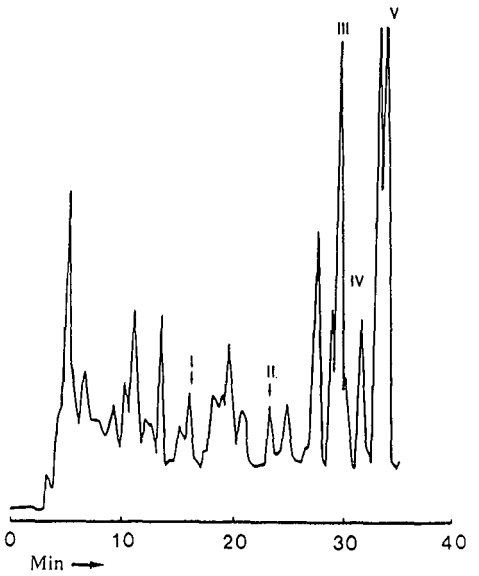

Fig. 5. High-performance liquid chromatogram of water extract from Iyo (*Citrus iyo*) seeds. 17-β-D-Glucopyranosides of limonin (I), deacetylnomilin (II), nomilin (III), nomilinic acid (IV) and obacunone (V).

ACKNOWLEDGEMENTS

This research was supported in part by a Grant-in-Aid from the Science and Technology Agency of Japan. S.H. was a recipient of Research Awards for specialists from Japanese Government.

REFERENCES

1 S. Hasegawa, R.D. Bennett, Z. Herman, C.H. Fong and P. Ou, *Phytochemistry*, 28 (1989) 1717.
2 L.K.T. Lam and S. Hasegawa, *Nutr. Cancer*, 12 (1989) 43.
3 L.K.T. Lam, Y. Li and S. Hasegawa, *J. Agric. Food Chem.*, 37 (1989) 378.
4 E.G. Miller, R. Fanous, F.R. Hidalgo, W.H. Binnie, S. Hasegawa and L.K.T. Lam, *Carcinogenesis*, 10 (1989) 1535.

5 A.R. Alford and M.D. Bentley, *J. Econ. Entromol.*, 79 (1987) 35.
6 A.R. Alford, J.A. Cullen, R.H. Stoch and M.D. Bentley, *J. Econ. Entromol.*, 80 (1987) 575.
7 V.P. Maier and E.R. Grant, *J. Agric. Food Chem.*, 18 (1970) 250.
8 J.H. Tatum and R.E. Berry, *J. Food Sci.*, 38 (1973) 1244.
9 H. Ohta, A. Watanabe, K. Iino and S. Kimura, *J. Jap. Soc. Food Sci. Technol.* (Nippon Shokuhin Kogyo Gakkaishi), 28 (1981) 91.
10 J.F. Fisher, *J. Agric. Food Chem.*, 23 (1975) 1199.
11 J.F. Fisher, *J. Agric. Food Chem.*, 26 (1978) 497.
12 R.L. Rouseff and J.F. Fisher, *Anal. Chem.*, 52 (1980) 1228.
13 P.E. Shaw and C.W. Wilson, *J. Food Sci.*, 49 (1984) 1216.
14 T.A. Van Beek and A. Blaakmeer, *J. Chromatogr.*, 464 (1989) 375.
15 C.H. Fong, S. Hasegawa, Z. Herman and P. Ou, *J. Food Sci.*, 54 (1989) 1505.
16 Z. Herman, C.H. Fong, P. Ou and S. Hasegawa, *J. Agric. Food Chem.*, 38 (1990) 1860.
17 D. Dreyer, *J. Org. Chem.*, 30 (1965) 749.
18 H. Ohta, M. Berhow, R.D. Bennett and S. Hasegawa, *Phytochemistry*, 31 (1992) 3905.
19 R.D. Bennett, S. Hasegawa and Z. Herman, *Phytochemistry*, 28 (1992) 2777.
20 Y. Ozaki, C.H. Fong, Z. Herman, H. Maeda, M. Miyake, Y. Ifuku and S. Hasegawa, *Agric. Biol. Chem.*, 55 (1991) 137.
21 S. Hasegawa, R.D. Bennett and V.P. Maier, *Phytochemistry*, 23 (1984) 1601.
22 S. Hasegawa and Z. Herman, *Phytochemistry*, 24 (1985) 1973.
23 S. Hasegawa, P. Ou, C.H. Fong, Z. Herman, C.W. Coggins, Jr. and D.K. Atkin, *J. Agric. Food Chem.*, 39 (1991) 262.
24 C.H. Fong, S. Hasegawa, Z. Herman and P. Pu, *J. Sci. Food Agric.*, 54 (1991) 393.

Journal of Chromatography, 639 (1993) 303–316
Elsevier Science Publishers B.V., Amsterdam

CHROM. 24 992

Optimization of capillary zone electrophoresis–electrospray mass spectrometry for cationic and anionic laser dye analysis employing opposite polarities at the injector and interface

Johnson Varghese and Richard B. Cole*

Department of Chemistry, University of New Orleans, Lakefront Campus, New Orleans, LA 70148 (USA)

(First received November 10th, 1992; revised manuscript received February 11th, 1993)

ABSTRACT

On-line capillary zone electrophoresis–electrospray mass spectrometry (CZE–ES-MS) has been used to investigate the purity of laser dyes. A CZE–ES-MS interface linking a Dionex CE System I and a Vestec 201 electrospray mass spectrometer was constructed and employed for this purpose. Interface optimization studies revealed that maximum sensitivity conditions are significantly different from maximum stability conditions. Use of a cationic surfactant, cetyltrimethylammonium chloride, proved effective at reducing the interaction between the cationic laser dye, Rhodamine 6G, and the wall of the silica capillary, a problem which can otherwise persist even at low pH. To direct electroosmotic flow towards the detector, negative voltages were applied to the CZE source vial. This enabled efficient separation of Rhodamine 6G from low level isomeric and analogue impurities which were detected using positive voltages at the mass spectrometer ion source. Despite intrinsic difficulties associated with negative-ion ES-MS, negative-ion detection was used in combination with positive CZE potentials to separate and characterize analogue impurities found in the anionic laser dye Eosin Y. Impurities present in such laser dyes can have profound effects on the operating efficiencies of dye lasers and the usable lifetime of the dye.

INTRODUCTION

Interest in capillary electrophoresis (CE) from both the research and commercial standpoints has increased dramatically within the last five years. Capillary electrophoresis may be subdivided into several categories including capillary zone electrophoresis (CZE) [1], micellar electrokinetic capillary chromatography (MECC) [2], gel CE [3], isotachophoresis [4] and isoelectric focusing [5]. These techniques can provide separation of closely related structures in a relatively short time period [6] as compared to conventional liquid separation techniques such as high-performance liquid chromatography [7].

Information regarding the structures of unknown analytes present in sample mixtures can be obtained with highest specificity when a mass spectrometer is used as the detector. Coupling of capillary electrophoresis with mass spectrometry (MS) is aided by the prerequisite of both techniques that analytes be present in ionic form. From a mass spectrometry perspective, CE–MS interfacing has relied upon electrospray (ES) [8], "ion-spray" [9], and fast atom bombardment (FAB) [10,11] ionization techniques which have been adapted to allow efficient on-line transfer of materials eluting from an electrophoretic column into the gas phase. The "spray" ionization techniques, in particular electrospray and ion-spray, have been utilized in the liquid sheath

* Corresponding author.

0021-9673/93/$06.00

electrode [8] and the liquid-junction [9] interfaces. These approaches offer the capability to interface a variety of capillary types to mass spectrometers, thus accommodating a wide range of samples.

The challenge of CE–MS interfacing is to maintain proper operating conditions on both sides of the interface, *e.g.*, fixed potentials of sufficient magnitude at the CZE source vial and the electrospray needle to permit reproducible, high-efficiency CE separations, and allow high ion currents at the mass spectrometer. The incorporation of a make-up flow just prior to MS analysis has allowed stable ionization of the column eluent. In the case of electrospray [8] or "ion-spray" [9] techniques, typically methanol and acetonitrile are used, whereas glycerol or other liquid matrix materials are essential in flow-FAB [10,11] experiments.

Olivares *et al.* [12] reported the first successful coupling of CZE and MS. This initial work evolved into the liquid sheath electrode interface [8] where electrical contact is made at the capillary terminus via a steady liquid flow. Proper mixing of the sheath liquid and the CZE eluent allows the use of aqueous buffers of relatively high ionic strength which cannot be used in the absence of sheath flow. The operation of the interface was found to be relatively unaffected by variations in CZE flow-rates. The CZE capillary was placed in the interior of the stainless-steel electrospray needle such that the capillary terminus protruded approximately 0.1 to 0.2 mm, in order to minimize zone broadening. At the needle voltage corresponding to the onset of electrospray, the liquid sheath enables formation of the characteristic "Taylor cone" [13] at the tip of the protruding capillary. This arrangement allows adequate mixing of the CZE eluent and the sheath flow, permitting a stable electrospray current.

This paper describes the in-house construction, optimization, and application of a CZE–MS interface linking two commercially available instruments, *i.e.*, a capillary electrophoresis System I (Dionex, Sunnyvale, CA, USA) and a 201 electrospray mass spectrometer (Vestec, Houston, TX, USA). The combined instrumentation has been used to investigate the purity of selected cationic and anionic laser dyes. Solutions of such organic dyes are used in laser sources to offer both pulsed and continuous laser operation over a continuum of wavelengths from the near-UV to the near-IR [14]. Such dye lasers not only offer tunability of wavelength, but also a facility in cooling (largely due to the fact that the dyes are present in solution) that permits intense laser pumping at high pulse repetition rates [15]. The purity of such laser dyes can profoundly affect the laser efficiency and the usable lifetime of the dye. Secondary products generated in the manufacture of laser dyes are quite likely to be of inferior efficiency for laser operation. Furthermore, impurities may quench laser activity at variable rates, leading to a deterioration of laser power. For these reasons, assessment of laser dye purity can be of high importance to the large constituency of dye laser users.

EXPERIMENTAL

Chemicals

Rhodamine 6G (95% and 99% purity levels) was purchased from Eastman Kodak (Rochester, NY, USA) and Aldrich (St. Louis, MO, USA). Eosin Y (92%) was also purchased from Aldrich, as was cetyltrimethyl ammonium chloride (CTAC). CZE buffers utilized ammonium acetate and ammonium hydroxide from J.T. Baker (Phillipsburg, NJ, USA); sodium chloride was purchased from EM Industries (Gibbstown, NJ, USA). All solvents used (*i.e.*, water and methanol from EM Industries) were HPLC grade.

Capillary zone electrophoresis

Both CZE–UV and on-line CZE–ES-MS were performed using the Dionex CE System I. For all applications reported, the constant-voltage CE mode was employed. For off-line work, UV–Vis absorbance detection was used. Flexibility was provided by the three modes of sample introduction: electrokinetic, gravity and pressure. Vitreous silica capillaries were employed in all analyses; 50 μm I.D., 220 μm O.D. were purchased from SGE (Austin, TX, USA); 100

μm I.D., 235 μm O.D. from Polymicro (Phoenix, AZ, USA).

Electrospray mass spectrometry

A Vestec 201 electrospray mass spectrometer was employed for all mass spectral analyses [16]. Collisionally induced dissociations were minimized in all experiments by maintaining a low skimmer–collimator voltage difference. A Sage syringe pump (Orion Research, Boston, MA, USA) was used for direct infusion of solutions during off-line ES-MS work and for the delivery of the sheath flow of liquid during CZE–ES-MS.

CZE–ES-MS interface

The manufacturer's electrospray probe was replaced by a CZE–ES-MS interface probe constructed in-house at the University of New Orleans (Fig. 1) which allowed for delivery of a "make-up" fluid and an electrical contact at the capillary exit, in an analogous fashion to the sheath flow set-up described previously by Smith *et al.* [8]. In order to introduce the sheath flow (typically 100% methanol at 2.9 μl/min), a portion of the CZE capillary (17 cm) was placed inside a stainless-steel capillary via a 1/16 in. (1 in. = 2.54 cm) stainless-steel make-up "tee". To avoid terminology confusion, stainless-steel capillaries used for ES-MS are hereafter referred to as "needles", in order to distinguish them from silica capillaries. The electrospray voltage (+2.45 to 2.85 kV for cation analysis) was applied directly to this tee rather than to the needle tip. For cation analysis, the counter electrode (nozzle), skimmer and collimator were maintained at 200 to 300 V, 9 to 14 V, and 10 V, respectively. Negative voltages of similar magnitude were used during analyses of anions. The Dionex CE System I was directly coupled to the MS system without additional modifications. The dual polarity power supply can deliver a constant voltage to the source vial (up to ±30 kV) with the CZE capillary removed from the destination vial. The CZE source vial was typically maintained between 20 and 25 kV (−20 and −25 kV for reversed-polarity work) while ensuring that the CZE current drawn from the power supply did not exceed 10–15 μA, to maintain electrospray stability. Cleaning (with 0.1 *M* NaOH) and filling of the capillaries (with fresh buffers) were made easy by the pressure inject facility on the CE instrument. The problem of continuous siphoning during sample introduction or CZE operation was avoided by maintaining the source buffer and the capillary exit at approximately the same levels.

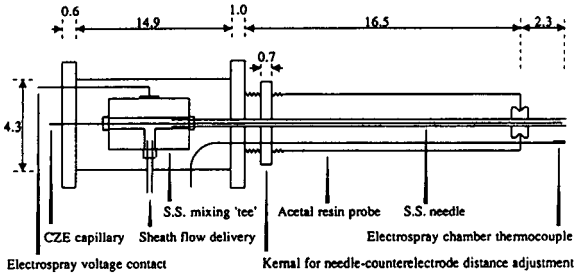

Fig. 1. Schematic diagram of the interface constructed to couple the Dionex CE System I to the Vestec 201 electrospray mass spectrometer. All dimensions are given in centimetres. For all applications reported, the CZE capillary tip was held (*ca.* 1.0 mm) inside the stainless-steel (S.S.) needle. During operation the platform supporting the tee is covered by a plexiglass case for safety purposes.

RESULTS AND DISCUSSION

Construction of the liquid sheath electrode interface

The liquid sheath flow [8] type CZE–MS coupling was chosen for the Vestec electrospray mass spectrometer mainly due to design and positioning constraints of the electrospray chamber. The theory of CZE, as first described by Jorgenson and Luckacs [1], proposes that column efficiencies are not dependent upon capillary length. Rapid, high-resolution separations are thus possible using rather short capillaries. Since the electrospray source has a 16.5 cm probe shaft leading to the nozzle (counter electrode), the terminal end of the CZE–sheath flow system had to be fitted with a retractable probe of this length (Fig. 1) which was constructed in-house at the University of New Orleans. The probe dimensions and the physical geometry of the CZE instrument necessitated the use of capillaries of at least 100 cm in length for on-line CZE–MS analysis. Although non-ideal for CZE purposes, the use of longer capillaries reduced the problem of voltage fluc-

tuations at the electrospray needle because of the greater resistance between the CZE source vial and the ES-MS needle.

Optimization of the CZE–MS interface

Placement of the CZE silica capillary relative to the ES needle has a large effect on ES-MS signal characteristics. Smith *et al.* [8] reported that when the exit of the CZE capillary was pulled back inside of the stainless-steel needle tip, a loss of analyte signal resulted, possibly due to electrochemical processes taking place on the metallic needle surface. In order to systematically investigate the manner in which electrospray signals are affected by changes in the CZE capillary size and position within a given stainless-steel needle, two CZE capillaries (50 and 100 μm I.D.; both 220 to 235 μm O.D.) were tested in conjunction with three different needle sizes (250, 300, and 350 μm I.D.; all 500 μm O.D.). For each combination of stainless-steel needle and silica capillary, several arrangements were adopted: silica capillary tip approximately 1 mm inside the needle, silica capillary tip adjacent with the stainless-steel needle exit, and silica capillary tip approximately 0.2 mm outside the stainless-steel needle exit.

Rhodamine 6G, the most widely used laser dye in the world as of 1990 [14], was selected as the test compound. A 100 ng/μl solution was electroosmotically infused through the vitreous silica capillary, and a sheath flow of methanol (100%) was introduced at a flow-rate of 2.9 μl/min. Application of CZE voltage initiated electroosmotic flow and movement of Rhodamine 6G towards the detector end. Electrospray parameters were optimized to obtain the maximum stable current for the "parent" cation (m/z 443). Successful mixing of the CZE eluent and sheath flow, hence, the establishment of a stable potential gradient along the capillary, was verified by monitoring the electrospray current measured at the nozzle. At the onset of CZE voltage the electrospray current was observed to increase.

Plots of m/z 443 ion current at the detector *vs.* capillary position appear in Fig. 2. Each data point represents the integrated ion current obtained over 118 s. Data for the 100 μm and 50 μm I.D. silica capillaries were acquired on consecutive days. For a particular capillary and stainless-steel needle size, data for the various capillary positions were acquired in rapid sequence. This procedure was repeated at the next needle size. The use of unconventionally large I.D. electrospray needles was necessitated by the requirement of "housing" fused-silica capillaries having O.D.s near 240 μm. Blockage of the silica capillary prevented the acquisition of the final data points for the 300 μm I.D. stainless-

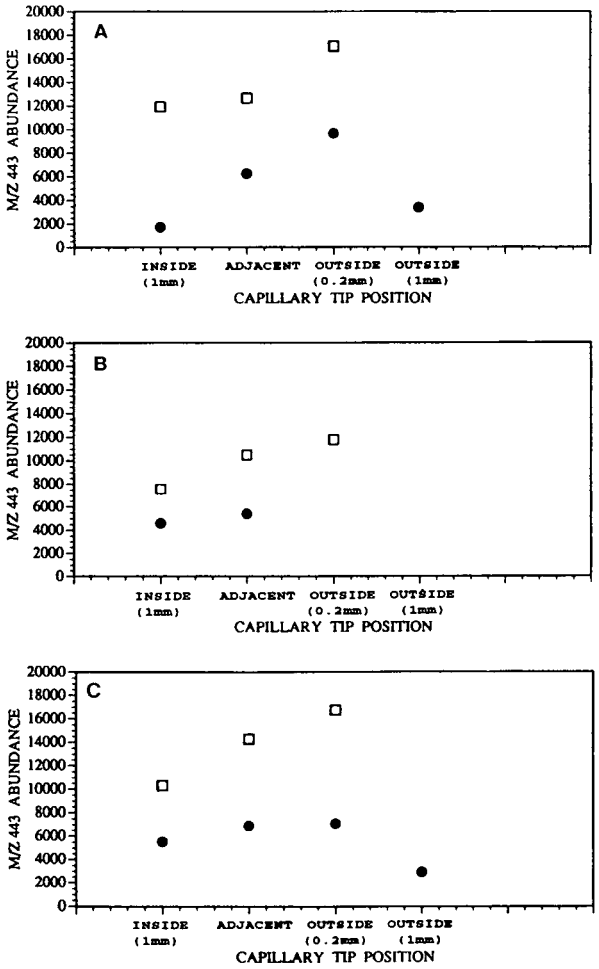

Fig. 2. Plots of m/z 443 abundance from Rhodamine 6G *vs.* CZE capillary tip position relative to the fixed stainless-steel needle having an I.D. of: (A) 250 μm, (B) 300 μm, and (C) 350 μm. The laser dye (100 ng/μl) was electroosmotically infused (-20 kV) through vitreous silica capillaries [50 μm (●) and 100 μm (□) I.D., both 100 cm in length] in the presence of cetyltrimethylammonium chloride.

steel needle in combination with the 50 μm I.D. capillary.

From Fig. 2, certain conclusions can be drawn regarding the stability and ease of generating high ES-MS signals. In all cases, the higher throughput of the larger (100 μm) silica capillary resulted in a higher m/z 443 ion current. Furthermore, for all the needles tested, as the silica tip was moved from inside the stainless-steel needle to outside, the ion current at the detector was observed to increase. When the tip extended beyond the needle by 0.1 to 0.2 mm, optimum sensitivity was obtained. At more extreme extensions (*e.g.*, 1 mm outside, for the 50 μm I.D. capillaries in combination with 250 or 350 μm needles, Fig. 2), signal intensity was observed to decrease.

The initial increase in ion current observed when the silica capillary begins to protrude from the stainless-steel needle can be attributed to a decrease in mixing volume leading to less dilution by the sheath liquid. Furthermore, with the silica protruding slightly, it is likely that finer droplets will be formed via the electrospray process, leading to more efficient ion production, as compared to the case where electrospray occurs directly from the tip of a wide-bore needle. Beyond a certain point, however, the silica tip protrudes too far to enable adequate mixing.

Although optimum sensitivities could be obtained with the tip protruding 0.1 to 0.2 mm outside the capillary, certain disadvantages existed for this configuration. When the CZE buffer exceeded a critical concentration, conductance down the CZE capillary created excess charging at the electrospray needle tip, resulting in inherent instability and a tendency toward electric discharge. This effect became more pronounced as the silica capillary was moved further outside the stainless-steel needle or when larger I.D. capillaries were used. In addition, after approximately one hour of constant operation, the silica tip invariably experienced deterioration causing loss of signal and necessitating removal of the affected region of the capillary. In coupling a CZE system to a Vestec electrospray source, Parker *et al.* [17] used silica capillaries having larger outer diameters (360 μm O.D., 75 μm I.D.) than those used in this investigation. This necessitated the use of wide-diameter stainless-steel needles (700 μm O.D., 425 μm I.D.) to house the large-diameter capillaries and provide a make-up flow. In their set-up, the silica tip was always placed outside of the stainless-steel needle and degradation of the silica was not observed, presumably due to the greater material thickness of the larger silica capillaries.

In order to characterize the relationship between CZE voltage and generated electrospray current, a capillary (100 μm I.D., total length 100 cm) filled with an electrolyte (5 m*M* NaCl) was placed in a 300 μm I.D. stainless-steel needle. A series of voltages (0 to 30 kV) was then applied to the anodic (source) reservoir also containing the electrolyte. As before, a sheath flow of methanol (100%) was introduced at the interface. Using a constant electrospray voltage, the total ion current (measured at the nozzle) due purely to liquid sheath flow was recorded. The CZE voltage was then increased by increments of 4 kV while the generated electrospray currents were recorded. The complete operation was repeated using three different silica capillary tip positions (1 mm inside, adjacent, and 0.2 mm outside, relative to the stainless-steel needle); findings are plotted in Fig. 3. This figure shows that regardless of capillary tip position, electrospray current increases with CZE voltage. Optimal operating conditions of the electrospray mass spectrometer, however, necessitate a low contribution to electrospray current from corona discharge processes [18,19]. The manufacturer recommends that current at the counter electrode should be maintained below 250 nA, to avoid electric discharge conditions. One can conclude that placement of the capillary tip inside the stainless-steel needle allows operation at higher CZE voltages before discharge conditions are reached. Of course the electrospray needle voltage can be lowered somewhat to alleviate the electric discharge problem, but this often has adverse effects upon electrospray sensitivity and stability.

Despite some loss in ultimate sensitivity, placement of the capillary inside the needle afforded ruggedness to the interface, hence, this

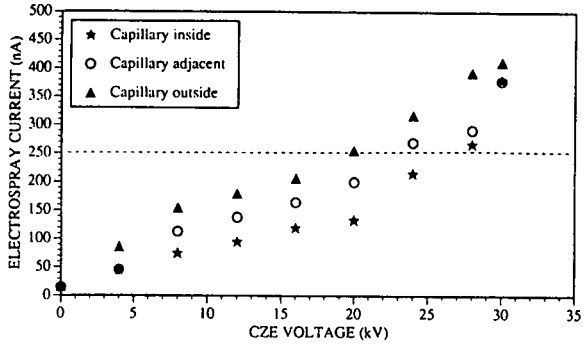

Fig. 3. Plot of total electrospray current (measured at the "nozzle" counterelectrode) as a function of applied CZE voltage for a CZE–MS interface employing a 300 μm I.D. stainless-steel needle with a 100 μm I.D. silica column whose exit tip was placed within (*ca.* 1 mm), adjacent to, and outside (0.2 mm) the needle. Aqueous NaCl (5 m*M*) was employed as the buffer with a sheath flow (2.9 μl/min) of methanol (100%). The dashed line signifies the manufacturer's suggested current limit at the counterelectrode, such that electric discharge processes are minor.

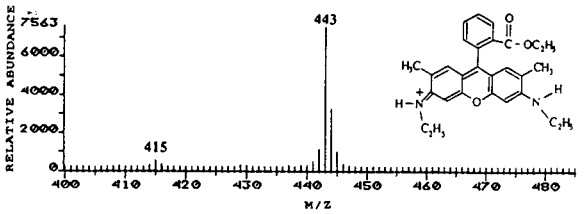

Fig. 4. Electrospray mass spectrum of Rhodamine 6G in the presence of cetyltrimethylammonium chloride, obtained by electroosmotic infusion employing CZE and MS conditions typically used during on-line CZE–ES-MS (see Fig. 6).

configuration was adopted for analyses where sensitivity was not the limiting issue. Under these conditions, fluctuations in the applied voltages or variation in buffer properties (including uneven liquid sheath flow-rates) did not degrade electrical contact at the interface. Furthermore, long periods of analysis were possible with no loss in stability. Although dilution of the buffer and the potential for zone broadening are greater with the silica capillary inside, the ability to use high ionic strength buffers (*e.g.*, 10 m*M*) is improved (electrospray stability is maintained). Presumably the current due to capillary conductance is dissipated more efficiently when the silica capillary is within the stainless-steel needle.

Normal-polarity CZE–MS of Rhodamine 6G

Displayed in Fig. 4 is the ES-MS spectrum (parent ion region only) of Rhodamine 6G, obtained by electroosmotically infusing a 100 ng/μl solution through the CZE–ES-MS interface. The Rhodamine 6G cation (structure shown in Fig. 4) appears at *m/z* 443; in addition, under minimal fragmentation conditions, ions were also noted at *m/z* 415. In examining Rhodamine 6G of various grades available from different manufacturers, it became clear that contaminants were prevalent even among "high-purity" products. From direct MS measurements alone, it is not possible to evaluate whether isomeric impurities are present, hence, the development of on-line CE–MS methodology was pursued to clarify the purity issue.

A common problem encountered in CZE analysis is that of adsorption of cationic molecules (*e.g.*, polypeptides [20]) onto the wall of the fused-silica capillary. An attempt was made to reduce this effect by employing acetic acid (1% glacial, pH 2.9) to selectively protonate fixed anionic sites on the capillary. However, direct CZE using this approach (Fig. 5a) was found to be unsuccessful due to a failure to achieve complete wall deactivation. Although wall adsorption is an anticipated problem when switching to a borate buffer (pH adjusted to alkaline), peak tailing can be alleviated by the presence of electroosmotic flow. Despite significant tailing, in addition to the main component at *m/z* 443 (peak 1, Fig. 5b), the selected-ion electropherogram reveals that a second *m/z* 443 component (peak 2, presumably an isomer of the main component, Fig. 5b) appeared in four scans. It is possible that the shape of peak 2 was narrowed by the presence of other cationic species in the sample solution, i.e., those comprising the tailing portion of the major peak. Operation at pH 8.9, of course, did not permit deactivation of anionic sites on the silica capillary, hence, alternative buffer systems were investigated.

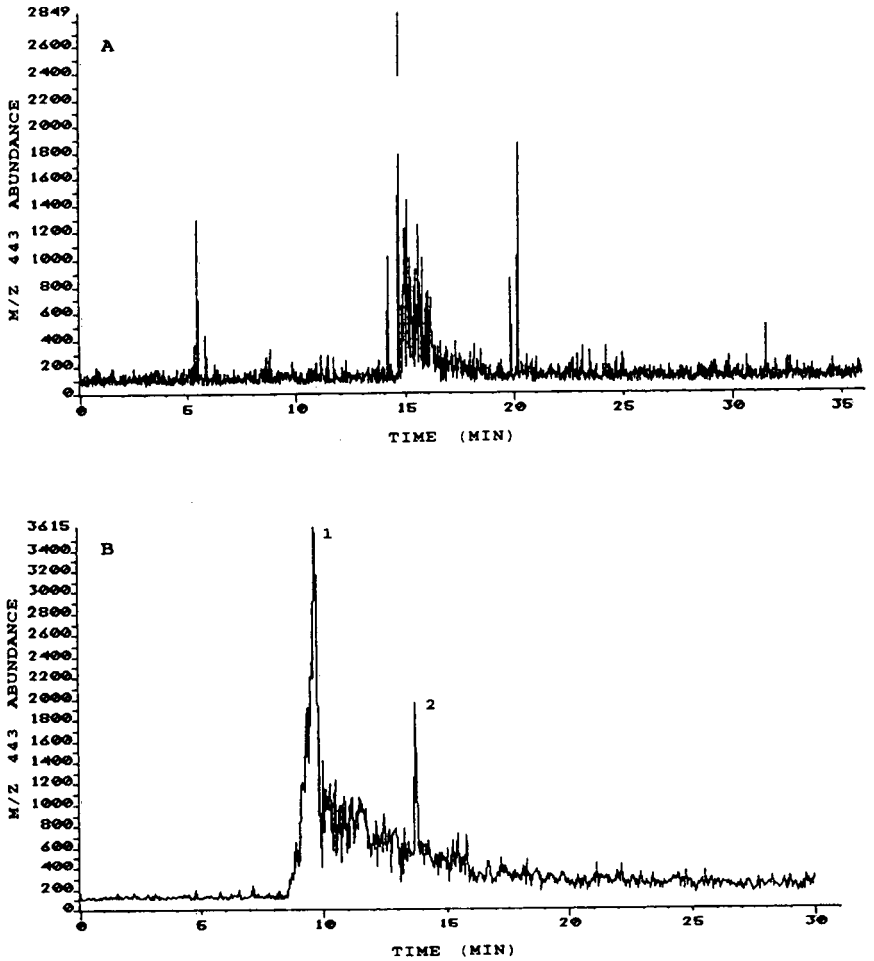

Fig. 5. Selected-ion electropherogram (m/z 443) from the CZE–ES-MS analysis of Rhodamine 6G (100 ng/μl), employing: (A) buffer: glacial acetic acid (1%, v/v), pH 2.9; capillary: 50 μm I.D., 220 μm O.D., 100 cm in length; sample injection: 10 kV/10 s; CZE voltage: 25 kV; ES voltage: 2.44 kV; MS scan rate: 1.16 s/scan (m/z 100 to 500). (B) Conditions as for (A) except, buffer: sodium borate (10 mM), pH 8.9; MS scan rate: 3.03 s/scan (m/z 100 to 600). Both electropherograms display raw data.

Reversed-polarity CZE–ES-MS of Rhodamine 6G

Minimization of the interaction between cationic analytes and the silica wall is best achieved by chemically deactivating fixed anionic sites on the wall, or by creating a positively charged layer on the inner surface of the wall. However, electroosmotic flow towards the detector is only possible if CZE is performed in the reversed-polarity mode [21] (negative polarity at the source vial). Recently, the utilization of aminopropyl-silylated (APS) fused-silica capillaries for on-line CZE–MS analysis has been reported by Mosely and co-workers [22,23]. In that reversed-polarity work, with the bonded phase positively charged at or below pH 3.4 (corresponding to the pK_a value of APS), the electroosmotic flow was reversed in direction and increased in velocity relative to normal-polarity fused-silica capillaries. Efficient peptide separations were reported utilizing these columns in conjunction with low pH buffers and a coaxial interface.

Other studies have shown that certain electrolytes can alter the rate of electroosmotic flow and even reverse the direction of flow in fused-

silica capillaries. In particular, quaternary ammonium surfactants have been shown to be effective in this regard. Terabe *et al.* [21] first reported the utilization of cetyltrimethylammonium bromide (CTAB) to reverse electroosmotic flow via formation of a positively charged layer on the inner surface of the silica capillary. Altria and Simpson [24] showed that under equivalent conditions, an increase in flow-rate by one order of magnitude occurred for capillaries filled with CTAB (2 m*M*) as compared to bare silica capillaries containing phosphate buffers (2 m*M*). A homologue of CTAB, tetradecyltrimethylammonium bromide (TTAB), was also used by Huang *et al.* [25] to separate a series of low-molecular mass carboxylic acids. Again, reversed-polarity conditions were employed allowing separation of six acids within 3.5 min. In that study, reversal of flow was initiated at a minimum TTAB concentration of 0.4 m*M*.

In an effort to improve upon electropherograms shown in Fig. 5, the cationic surfactant, cetyltrimethylammonium chloride (CTAC) was added to the CZE buffer (0.5 m*M*). Selected-ion electropherograms for the analysis of a solution of Rhodamine 6G (100 ng/μl), corresponding to 6.41 pmol loaded on column, appear in Fig. 6. The mass spectrometer was scanned from *m/z* 442 to 445. Close inspection of the "blow-up" of the *m/z* 443 electropherogram (inset in Fig. 6) reveals that a minimum of three, maybe four, peaks were present in addition to the main component. These impurities were estimated to represent approximately 3 to 4% of the total observed ion current. Most likely, these later eluting peaks correspond to isomers of Rhodamine 6G. To improve the signal-to-noise ratio for the minor components, the concentration of Rhodamine 6G was increased by a factor of ten (to 1 μg/μl, representing 64.1 pmol on column). The analysis was repeated under the same conditions, except that the mass spectrometer was scanned over a larger range (from *m/z* 300 to 600) in order to detect other (non-isomeric) contaminants. "Overloading" of the column for the main component, resulted in a baseline width of 1 min (Fig. 7, top), compared to 20 s for the more dilute sample (Fig. 6).

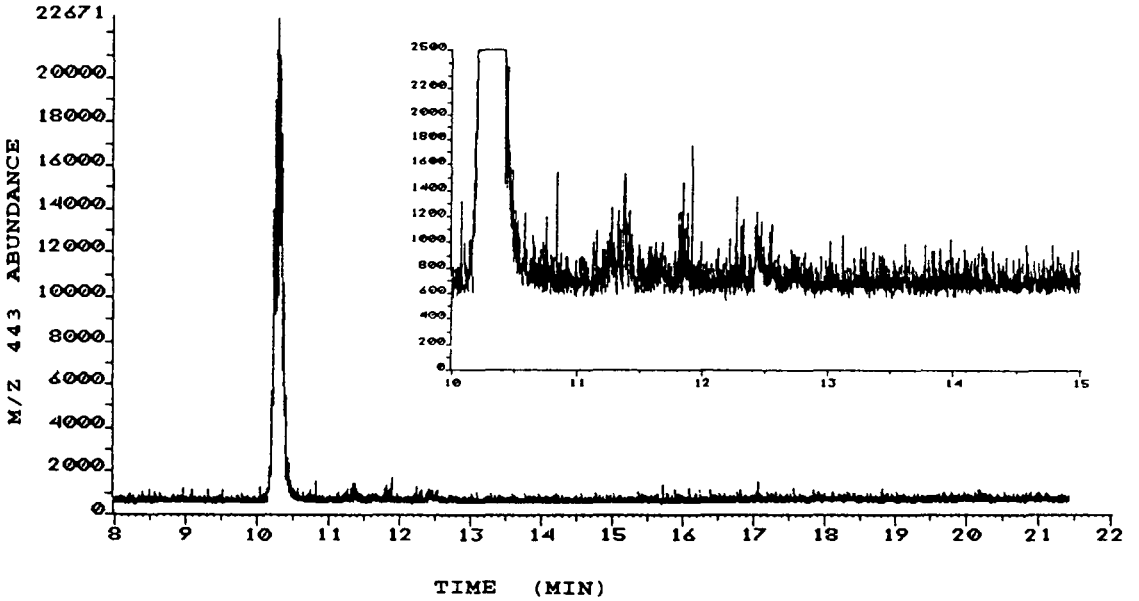

Fig. 6. Selected-ion electropherogram (*m/z* 443) showing raw data from the CZE–ES-MS analysis of Rhodamine 6G (100 ng/μl solution/6.41 pmoles on column). Buffer: CTAC (0.5 m*M*) and NaCl (5 m*M*), pH 6.2; capillary: 100 μm I.D.; 235 μm O.D.; 100 cm in length; sample injection: 100 mm/10 s; CZE voltage: 20 kV; ES voltage: 2.8 kV; MS scan rate: 0.07 s/scan (*m/z* 442 to 445). Inset shows magnified view of response between 10 and 15 min.

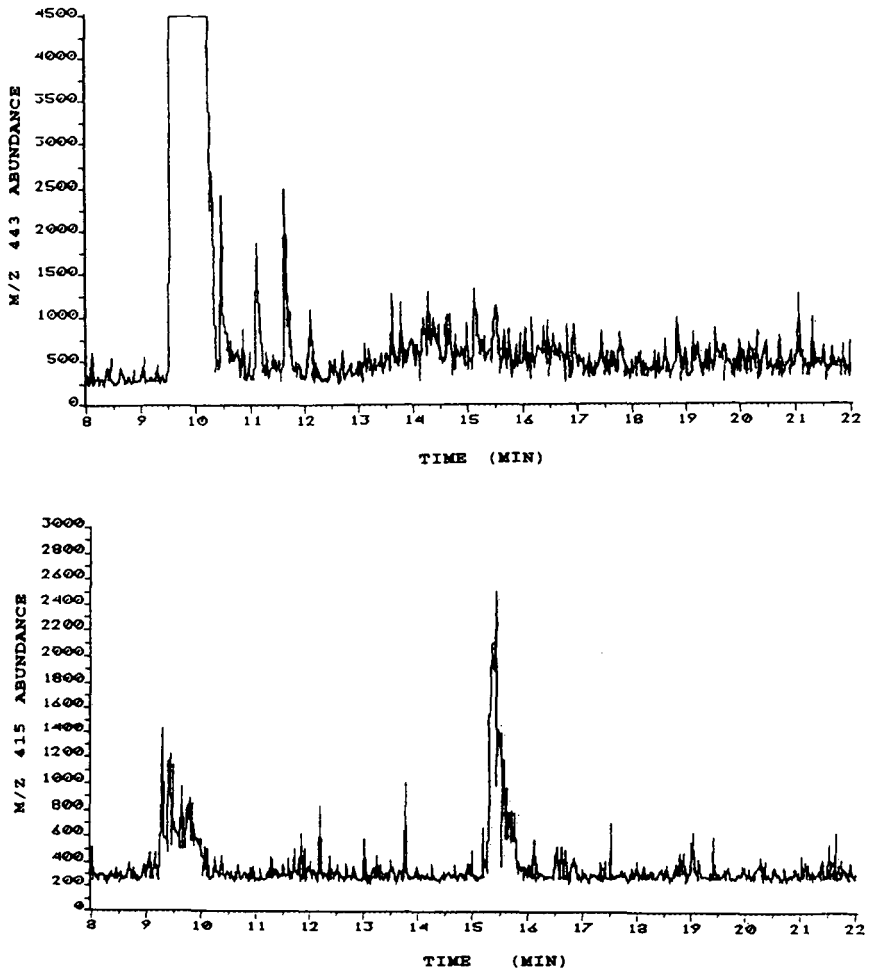

Fig. 7. Selected-ion electropherograms of m/z 443 (top) and m/z 415 (bottom) from the CZE–ES-MS analysis of Rhodamine 6G. Conditions as for Fig. 6, except concentration of Rhodamine 6G is now 1000 ng/μl (64.1 pmoles on column) and MS scan rate is 1.21 s/scan (m/z 300 to 600). Both electropherograms display raw data.

However, this exercise did have the desired effect of pulling the minor peaks out of the noise background. Four definite, reproducible peaks consisting of several (1.2 s) mass spectrometer scans each, clearly appear between 10.5 and 12.5 min.

The increase in sample concentration and scan range also enabled detection of peaks at m/z 415 which have heights similar to the m/z 443 impurities. Two components at m/z 415, separated by approximately 6 min appeared in the electropherogram (Fig. 7, bottom) of Rhodamine 6G purchased from one manufacturer. Other Rhodamine 6G from different manufacturers showed only one impurity at m/z 415, eluting at approximately 15.5 min. It is plausible that the early eluting m/z 415 impurity corresponds to a hydrolyzed form of Rhodamine 6G, where the ethyl ester has been converted to a carboxylic acid. Appearance of the carboxylate anion (zwitterionic) form could cause the m/z 415 peak to elute in front of Rhodamine 6G, as was indeed observed in Fig. 7. The empirical formula of the later eluting m/z 415 impurity is also likely to be the same as that of Rhodamine 6G less C_2H_4; this may arise via deficiency of an ethyl substituent (replaced by a hydrogen atom) at either nitrogen site.

The high level of reproducibility of all data with minor variations in retention times, and the evidence of adequate separations were sufficient to validate the analysis. Rhodamine 6G must be prepared in solutions containing the same concentration of CTAC as the buffer. This insures that the silica sites will retain positively charged cetyltrimethylammonium cations, thus minimizing adsorption of analyte onto the capillary walls. It should be noted that a large bulk flow of any reagent into the ES ion source will often degrade sensitivity for analytes. Furthermore, adsorption of reagents onto the nozzle and other electrospray source components contribute to the degradation of all signals at the MS detector, necessitating cleaning of the ES counter electrode after each full day of use. The CTAC cation has a molecular mass of 284. Under the employed conditions, the abundance of m/z 284 ions is high enough to saturate the detector, thus, MS scanning over this background peak was avoided.

Normal-polarity CZE–ES-MS of Eosin Y

Certain commercially important laser dyes such as Eosin Y contain anionic functional groups, hence, ES-MS in the negative ion mode can best be used to optimize detection of impurities which may be present. On-line normal-mode CZE–negative ion-MS has already been applied to the analysis of negatively charged species using a liquid-junction interface [26]. The physical gap of 10 to 20 μm which comprises the liquid junction effectively decoupled the CZE from the MS and allowed the use of a positive voltage at the CZE source vial and a negative voltage at the electrospray needle.

CZE–UV analysis revealed the reproducible presence of two major components of the Eosin Y laser dye (Fig. 8). Off-line negative-ion ES-MS (Fig. 9) offered more information concerning the composition of the mixture. In the mass spectrum, singly charged (m/z 647) and doubly charged (m/z 323) species representative of Eosin Y were apparent (Fig. 9A and B, respectively). A clear isotope distribution pattern reveals the presence of four bromines in both the singly and doubly charged species. Also present in the low fragmentation mass spectrum of Eosin

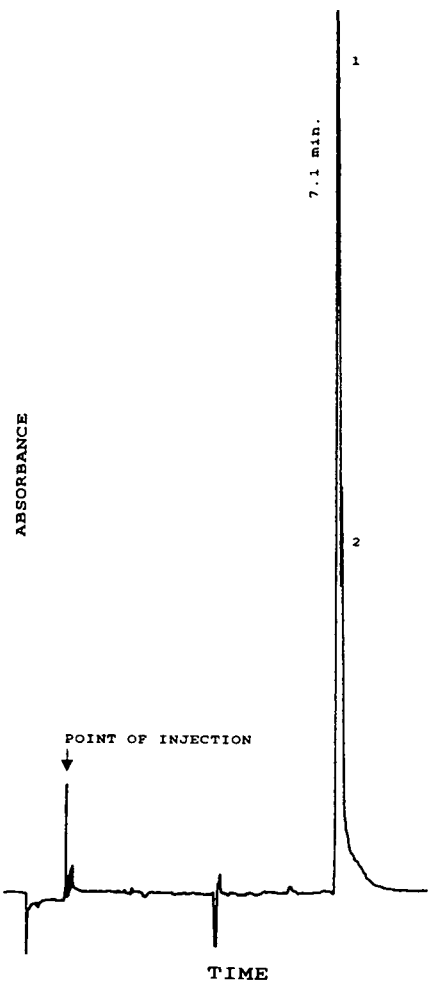

Fig. 8. CZE–UV trace displaying the presence of two components in Eosin Y (100 ng/μl). Column: 75 μm I.D., 65 cm in length; buffer: sodium borate (5 mM), pH 9.05; sample injection: 100 mm/7 s; CZE voltage: 25 kV; detection: 254 nm.

Y were ions yielding an isotope distribution pattern characteristic of an impurity containing three bromine atoms. These signals appeared at m/z 567 and m/z 283 (Fig. 9C and D) corresponding to singly and doubly charged molecules, respectively.

In developing a normal-polarity CZE method to analyze negatively charged compounds, the use of normal bare silica columns is highly suited for creating a satisfactory electroosmotic flow and allowing minimal wall interaction. This arrangement again demands the use of opposite

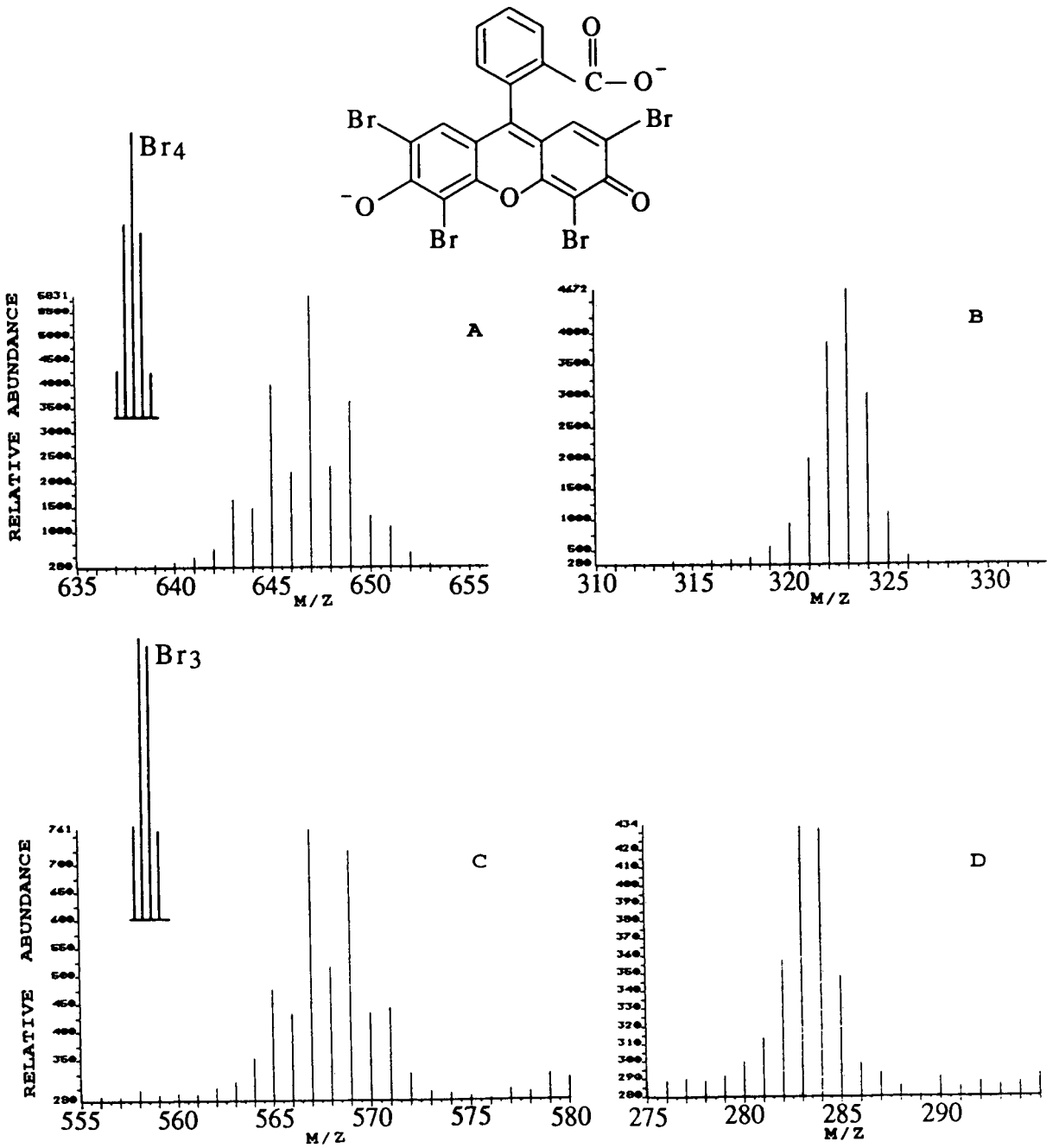

Fig. 9. Negative-ion electrospray mass spectrum of 100 ng/μl Eosin Y (dianion $M_r = 646$) sample generated by direct infusion. (A) Singly charged Eosin Y wherein one anionic site has been protonated. (Inset shows the natural isotopic distribution pattern for a compound containing four bromine atoms [28].) (B) Doubly charged Eosin Y. (C) Singly charged impurity of Eosin Y. (Inset shows the natural isotopic distribution pattern for a compound containing three bromine atoms [28].) (D) Doubly charged impurity of Eosin Y.

polarities for CZE separation (positive) and electrospray ionization (negative). Even with direct infusion of sample, negative-ion electrospray mass spectrometry of aqueous solutions can be wrought with instability problems created by a high tendency toward electric discharge. The corona discharge problem is most severe in the negative-ion mode because electrons can emanate from the edges of the stainless-steel needle held at high negative potentials [19]. Stability of operation at each juncture, of course, is crucial to the success of CZE–MS. The electrical contact established between the source vial at positive potential and the electrospray needle at negative potential during sheath flow CZE–MS can aggravate an already tenuous situation.

Employing the same type of silica capillary (100 μm I.D.) as for the Rhodamine 6G application, no signals were observed for Eosin Y when electroosmotic infusion of the compound was conducted. This situation was found to be independent of the position of the silica capillary tip in the electrospray needle. Apparently, conductance in the capillary was too great to permit the electrospray needle to sustain a stable negative voltage. Since the capillary was already 100 cm long, increasing the capillary length would lead to unacceptably long analysis times. The

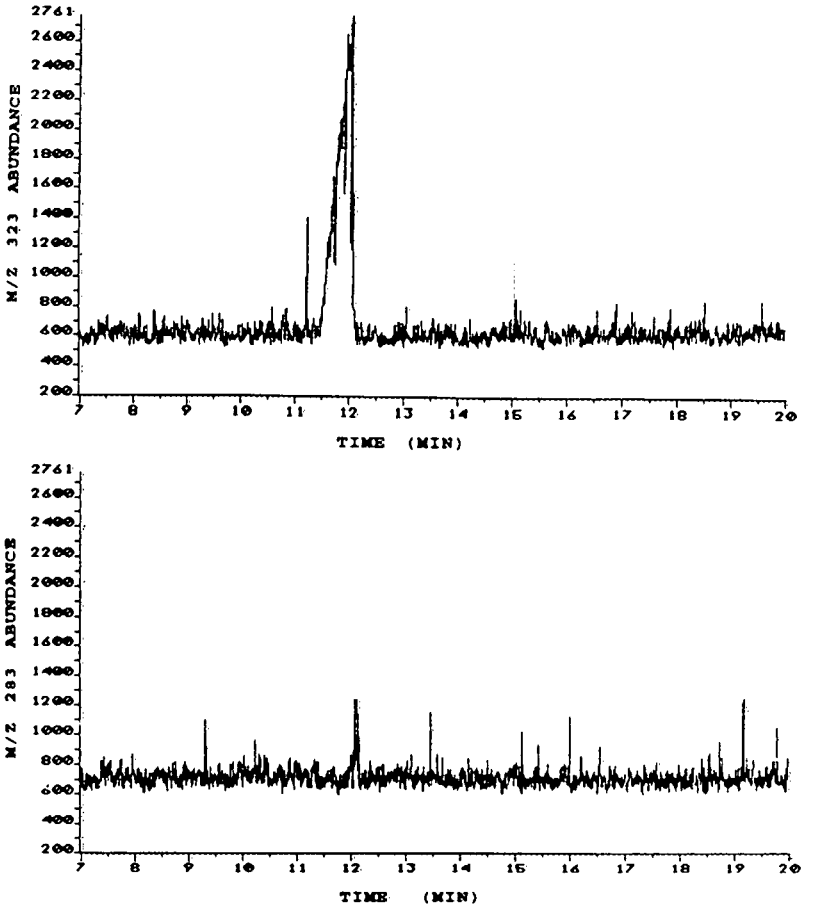

Fig. 10. Single-ion monitoring electropherograms of m/z 323 (top) and m/z 283 (bottom) from 600 ng/μl Eosin Y sample. Buffer: ammonium acetate (5 mM) and ammonium hydroxide (1%, v/v), pH 10.3; capillary: 50 μm I.D., 220 μm O.D., 100 cm in length; sample injection: 10 kV/10 s; CZE voltage: 20 kV; ES voltage: 2.75 kV; MS scan speed: 0.12 s/scan. The data in this figure only have been taken through a "de-spiking" routine.

concentration of the buffer was already too low (5 mM) to consider dilution.

The most effective and practical option to increase the resistance between the two operating voltages was via reduction of the capillary I.D. The utilization of a 50 μm I.D. capillary instead of the 100 μm I.D. capillary (same length) added considerable stability to the negative-ion electrospray current. As was done for Rhodamine 6G, the capillary exit was placed within the electrospray needle to allow greater mixing with the sheath liquid. After examining various buffers, an ammonium acetate–ammonium hydroxide combination was found to be the best suited volatile alkaline buffer (pH 10.3). Under the conditions employed, formation of doubly charged ions occurred in preference to singly charged ions. In the single-ion monitoring (SIM) mode, signals corresponding to the four species viewed in Fig. 9 were acquired as functions of time.

The SIM electropherograms for the doubly charged ions (m/z 323 and 283) are displayed in Fig. 10. Although the electrophoretic peak shape for the m/z 323 ion was poor, separation of the two components was achieved with near baseline resolution. The peak shape for m/z 283 was much better due to a combination of factors. Since this peak corresponds to a minor sample component in the mixture, overloading was avoided. Secondly, as expected, the smaller molecule eluted after the major zone, hence, fronting of the zone was avoided due to the mobility effects of the preceding zone. Fronting of the first zone was probably due to an incompatibility of the buffer wherein the mobility of the analyte was too high in comparison to the mobility of the carrier [27].

The reproducibility of the on-line analysis was found to be quite satisfactory, including the peak distortion for the main zone. Alternative buffers, *e.g.*, sodium borate, were found to be unsuccessful in improving the shape of the main zone. Nevertheless, the separation was adequate to distinguish the two components (their different peak shape was further evidence of heterogeneity). Normal-polarity CZE with negative ion ES-MS detection thus allowed confirmation of the presence of an analogous compound containing three bromine atoms as the main impurity in Eosin Y, where the fourth bromine atom has been replaced by a hydrogen atom.

ACKNOWLEDGEMENTS

The authors thank Dionex Corporation for providing CE instrumentation for this project. We also thank Drs. Joseph H. Boyer and Piotr Piotrowiak for sharing with us their expertise on the subject of laser dyes. Research funding from the Louisiana Education Quality Support Fund [grant No. (1991–93)-RD-B-15] is gratefully acknowledged.

REFERENCES

1 J.W. Jorgenson and K.D. Luckacs, *Anal. Chem.*, 53 (1981) 1298.
2 S. Terabe, K. Otsuka and T. Ando, *Anal. Chem.*, 57 (1985) 834.
3 A.S. Cohen and B.L. Karger, *J. Chromatogr.*, 397 (1987) 409.
4 P. Bocek, M. Deml, B. Kaplanova and J. Janak, *J. Chromatogr.*, 160 (1978) 1.
5 S. Hjerten and M.D. Zhu, *J. Chromatogr.*, 346 (1985) 265.
6 C.A. Monnig and J.W. Jorgenson, *Anal. Chem.*, 63 (1991) 802.
7 I.J. Haleem, G.M. Janini, I.Z. Atamna and G.M. Muschik, *J. Liq. Chromatogr.*, 14 (1991) 817.
8 R.D. Smith, C.J. Barinaga and H.R. Udseth, *Anal. Chem.*, 60 (1988) 1948.
9 E.D. Lee, W. Muck, J.D. Henion and T.R. Covey, *Biomed. Environ. Mass Spectrom.*, 18 (1989) 844.
10 R.M. Caprioli, W.T. Moore, M. Martin and B.B. DaGue, *J. Chromatogr.*, 480 (1989) 247.
11 M.A. Moseley, L.J. Deterding, K.B. Tomer and J.W. Jorgenson, *Rapid. Commun. Mass Spectrom.*, 3 (1989) 87.
12 J.A. Olivares, N.T. Nguyen, C.R. Yonker and R.D. Smith, *Anal. Chem.*, 59 (1987) 1232.
13 G.I. Taylor, *Proc. R. Soc. London A*, 280 (1964) 383.
14 F.J. Duarte and L.W. Hillman (Editors), *Dye Laser Principles With Applications*, Academic Press, Boston, 1990.
15 F.J. Duarte and J.A. Piper, *Appl. Opt.*, 23 (1984) 1391.
16 M.H. Allen and M.L. Vestal, *J. Am. Soc. Mass Spectrom.*, 3 (1992) 18.
17 C.E. Parker, J.R. Perkins, K.B. Tomer, Y. Shida, K. O'Hara and M. Kono, *J. Am. Soc. Mass Spectrom.*, 3 (1992) 563.

18 M.G. Ikonomou, A.T. Blades and P. Kebarle, *J. Am. Soc. Mass Spectrom.*, 2 (1991) 497.
19 R.B. Cole and A.K. Harrata, *Rapid Commun. Mass Spectrom.*, 6 (1992) 536.
20 J.W. Jorgenson and K.D. Lukacs, *Science*, 222 (1983) 266.
21 S. Terabe, K. Ishikawa, K. Utsuka, A. Tsuchiya and T. Ando, *Proceedings of the 26th International Liquid Chromatography Symposium, Kyoto, Japan, Jan., 25–26, 1983.*
22 M.A. Moseley, L.J. Deterding, K.B. Tomer and J.W. Jorgenson, *Anal. Chem.*, 63 (1991) 109.
23 M.A. Moseley, J.W. Jorgenson, J. Shabanowitz, D.F. Hunt and K.B. Tomer, *J. Am. Soc. Mass Spectrom.*, 3 (1992) 289.
24 K.D. Altria and C.F. Simpson, *Anal. Proc. (London)*, 23 (1986) 453.
25 X. Huang, J.A. Luckey, M.J. Gordon and R.N. Zare, *Anal. Chem.*, 61 (1989) 766.
26 E.D. Lee, W. Muck, J.D. Henion and T.R. Covey, *Biomed. Environ. Mass Spectrom.*, 18 (1989) 253.
27 W. Thormann, *Electrophoresis*, 4 (1983) 383.
28 F.W. McLafferty, *Interpretation of Mass Spectra*, University Science Books, Mill Valley, CA, 3rd Ed., 1980.

Journal of Chromatography, 639 (1993) 317–321
Elsevier Science Publishers B.V., Amsterdam

CHROM. 24 996

Analytical capillary isotachophoresis of bis(2-ethylhexyl) hydrogenphosphate and 2-ethylhexyl dihydrogenphosphate

Rubén Velásquez

Department of Gastroenterology and Hepatology, Hannover Medical School, Konstanty-Gutschow-Strasse 8, W-3000 Hannover 61 (Germany)

Dimitrios Tsikas*

Department of Clinical Pharmacology, Hannover Medical School, Konstanty-Gutschow-Strasse 8, W-3000 Hannover 61 (Germany)

Gorig Brunner

Department of Gastroenterology and Hepatology, Hannover Medical School, Konstanty-Gutschow-Strasse 8, W-3000 Hannover 61 (Germany)

(First received December 8th, 1992; revised manuscript received February 16th, 1993)

ABSTRACT

Bis(2-ethylhexyl) hydrogenphosphate (H2DEHP) and 2-ethylhexyl dihydrogenphosphate (HDEHP) are widely used liquid cation exchangers. An analytical capillary anionic isotachophoretic method was developed for the determination of H2DEHP and HDEHP in methanolic and aqueous phosphate-buffered solutions. The detection limit of the method was 3 nmol for H2DEHP and 0.16 nmol for HDEHP. H2DEHP was determined in aqueous phases at concentrations down to 15 μmol/l when it was previously ion-pair extracted by use of tetrabutylammonium hydrogensulphate. The recovery and the intraassay relative standard deviation of the method including the ion-pair extraction procedure were 78% and 6.8%, respectively.

INTRODUCTION

Organic phosphates such as bis(2-ethylhexyl) hydrogenphosphate (H2DEHP) and 2-ethylhexyl dihydrogenphosphate (HDEHP) (Fig. 1) are widely used liquid ion exchangers for selective ion-pair extraction of inorganic cations such as zinc, uranium and trace rare-earth elements [1–4]. Also, H2DEHP has been shown to be remarkably selective with respect to organic cations such as various biogenic amines [5] including histamine [6], a potent mediator of allergy and hypersensitivity. The high selectivity of H2DEHP with respect to histamine is utilized in our laboratory for the selective extracorporeal removal of histamine from blood of patients with acute hepatic failure by means of hollow-fibre-supported liquid membranes (HFSLM) which contain H2DEHP.

In order to study quantitatively the stability of H2DEHP-containing HFSLM, an accurate and sensitive analytical method is required. Both the acidimetric and the photometric picrate method

* Corresponding author.

0021-9673/93/$06.00

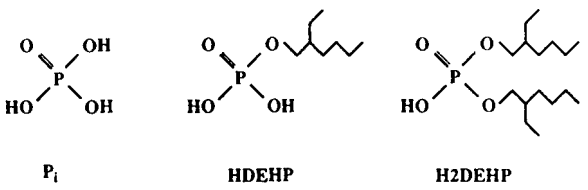

Fig. 1. Structures of inorganic phosphate (P_i), 2-ethylhexyl dihydrogenphosphate (HDEHP) and bis(2-ethylhexyl) hydrogenphosphate (H2DEHP).

[7] were found to be inapplicable for our purposes. Analytical capillary anionic isotachophoresis (ITP) has been shown to be an excellent analytical tool for the determination of inorganic and organic phosphates [8]. In this paper, an anionic ITP method for the determination of H2DEHP and HDEHP in organic and aqueous solution is described. For the sensitive determination of H2DEHP in aqueous buffered solutions, an ion-pair extraction procedure using the phase-transfer catalyst tetrabutylammonium hydrogensulphate (TBAHS) in chloroform was developed.

EXPERIMENTAL

Apparatus and materials

Anionic ITP analyses were performed on a Model 2127 Tachophor (LKB, Bromma, Sweden) using the conditions given in Table I. Isotachopherograms were recorded with an LKB Model 2120 line recorder at a chart speed of 0.5 mm/s. The terminator passed the detector at a potential of about 5 kV. H2DEHP and TBAHS were obtained from Serva (Heidelberg, Germany). A mixture of HDEHP and H2DEHP (45:55, w/w) was obtained from Merck–Schuchardt (Hohenbrunn, Germany). These and all other chemicals were of the highest quality available and used as received. Because of the low water solubility of H2DEHP and HDEHP, methanol was used to prepare stock solutions.

Ion-pair extraction procedure

H2DEHP was ion-pair extracted from potassium phosphate-buffered aqueous solutions (10–100 mmol/l, pH 7.4) as follows: TBAHS (0.8 g in the main experiments) was added to a 45-ml sample of a potassium phosphate-buffered aqueous solution of H2DEHP. After shaking with 5 ml of chloroform for 5 min the layers were allowed to separate for 15 min and a 4.5-ml aliquot of the organic phase was transferred into a conical centrifuge tube. The solvent was completely evaporated under reduced pressure and the residue was dissolved in 100 μl of methanol. Up to 5 μl of this solution were injected into the Tachophor instrument.

Hollow-fibre experiments

A liquid membrane preparation that contained paraffin oil, *n*-dodecanol and H2DEHP (75:20:5, w/w/w) was supported on polysulphone hollow fibres (Fresenius, Bad Homburg, Germany) by a similar procedure to that described elsewhere [9]. A potassium phosphate-buffered (10 mmol/l, pH 7.4) solution of histamine (100 ml small scale; 5000 ml large scale) was circulated in the internal compartment and a potassium phosphate-buffered (100 mmol/l, pH 7.4) solution

TABLE I

ITP CONDITIONS FOR THE DETERMINATION OF BIS(2-ETHYLHEXYL) HYDROGENPHOSPHATE AND 2-ETHYLHEXYL DIHYDROGENPHOSPHATE

Tachophor	LKB, Model 2127
Capillary	Polytetrafluoroethylene, 20 cm × 0.5 mm I.D.
Leading electrolyte	10 mmol/l HCl, pH 3.3 (β-alanine) 0.25% (w/w) hydroxypropylmethylcellulose
Terminating electrolyte	10 mmol/l hexanoic acid
Detector	UV (254 nm) and conductivity
Driving current	50 μA
Solvent	Water
Sample volume	3–5 μl
Temperature	Ambient

(20 ml small scale; 1000 ml large scale) in the external compartment of the HFSLM reactor. Samples (20 or 45 ml) were taken from both compartments of the HFSLM reactor after 5 h and H2DEHP was ion-pair extracted and analysed by ITP as described above.

RESULTS AND DISCUSSION

Fig. 2 shows an isotachopherogram from the analysis of the commercially available mixture of H2DEHP and HDEHP. In Table II the reciprocal reference unit (RRU) values and the specific zone lengths of inorganic phosphate (P_i), H2DEHP and HDEHP are summarized. RRU values were calculated from the relative step heights of the conductivity signal relative to the terminating ion applying the following expression:

$$R_{rel} = (h_T - h_L)/(h_C - h_L)$$

where R_{rel} is the RRU value of a compound C, relative to that of the terminating ion; h_T, h_L and h_C are the heights of the conductivity signals for terminating, leading ion and compounds C, respectively.

As can be seen in Fig. 2, P_i, H2DEHP and HDEHP were completely separated from one another. These compounds appear as non-UV-absorbing zones resolved by UV-absorbing peaks from impurities. The UV-absorbing zone from

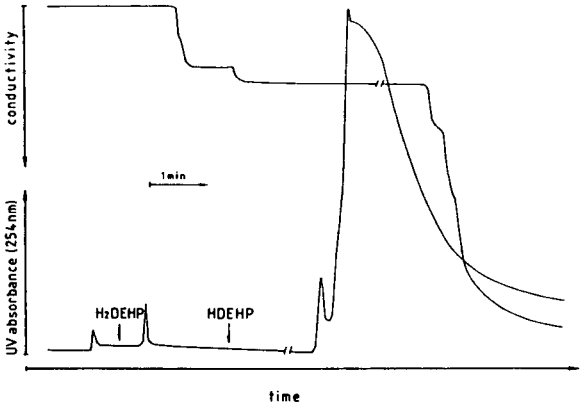

Fig. 2. Isotachopherogram from the analysis of 5 μl of a commercially available mixture of H2DEHP and HDEHP (55:45, w/w) in methanol (16 mg/ml). ITP conditions as described in Table I.

TABLE II

SPECIFIC ZONE LENGTHS AND RECIPROCAL REFERENCE UNIT (RRU) VALUES FOR INORGANIC PHOSPHATE (P_i), HDEHP AND H2DEHP USING THE CONDITIONS GIVEN IN TABLE I

Substance	Specific zone length (s/nmol)	RRU (mean ± S.D., $n = 6$)
P_i	5.37	6.24 ± 0.21
H2DEHP	0.29	4.60 ± 0.41
HDEHP	5.93	3.79 ± 0.13

an unknown compound that migrated behind HDEHP was always obtained when methanol was injected into the system. The specific zone lengths were obtained from the slopes of the calibration graphs obtained by injection of standard solutions of H2DEHP and HDEHP in methanol. The calibration graphs were linear in the range 5–50 mmol/l for H2DEHP and 0.3–3.0 mmol/l for HDEHP. From the calibration graphs the detection limit of the method was calculated to be 3 nmol for H2DEHP and 0.16 nmol for HDEHP. The precision of the method was determined by analysing monthly within a time of period of 6 months 100 nmol of H2DEHP. The mean specific zone length was 0.285 ± 0.008 (S.D.) s/nmol, and the interassay R.S.D. was 2.9%. The within-day ($n = 6$) R.S.D. was 1.8%.

Very low concentrations of H2EDHP and the presence of large amounts of phosphate in phosphate-buffered solutions used in HFSLM experiments make direct determination difficult and result in extremely long analysis times. These problems could be overcome by ion-pair extraction of H2DEHP from potassium phosphate-buffered aqueous solutions into chloroform by using TBAHS as ion-pairing agent. This procedure eliminates the interference by P_i (Fig. 3) as P_i is not extractable by TBAHS into chloroform. Also, the preconcentration effect significantly decreases the detection limit of the method. The recovery of H2DEHP and HDEHP from their phosphate-buffered solutions (250 and 15 μmol/l, respectively) was found to depend on the concentration of TBAHS in the buffer (Fig. 4). Sufficient recovery (75%) for H2DEHP was

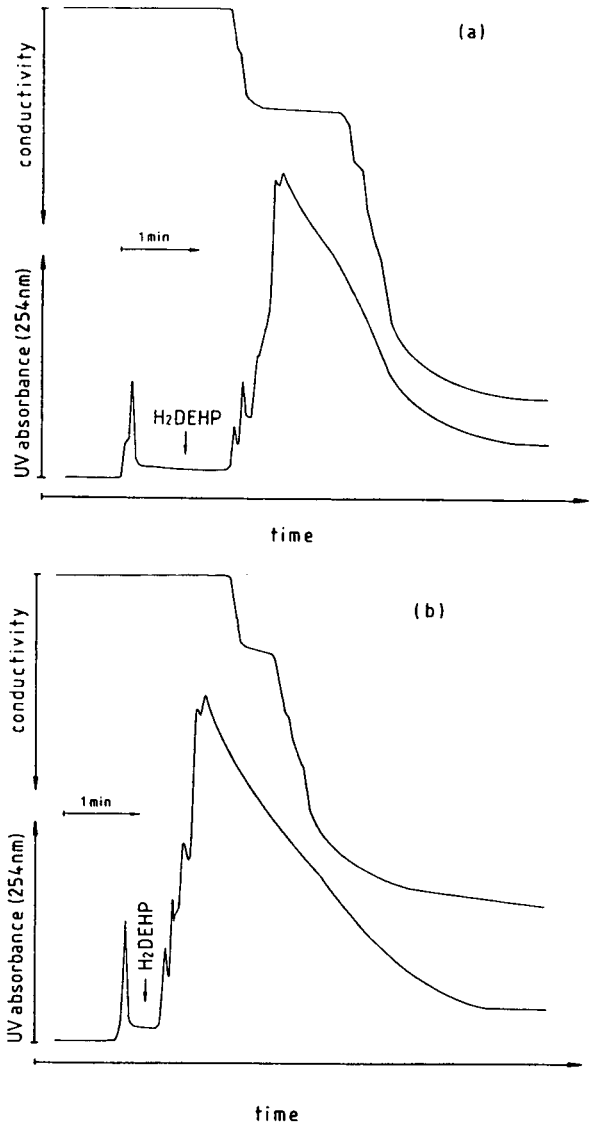

Fig. 3. Isotachopherograms from the separate analysis of H2DEHP following ion-pair extraction with TBAHS (a) from a standard solution (200 μmol/l) in phosphate-buffered solution and (b) from the internal compartment solution of a small-scale HFSLM experiment.

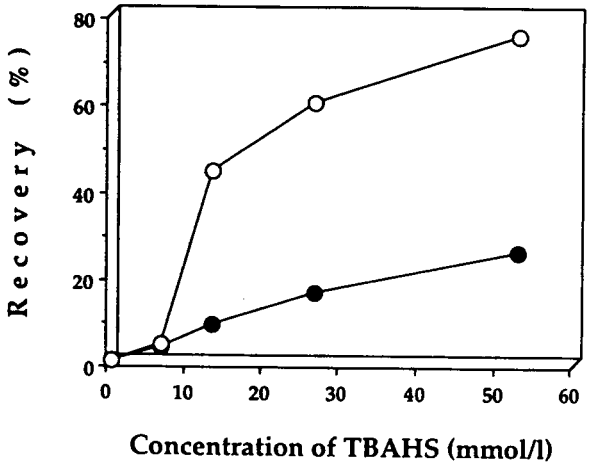

Fig. 4. Effect of the concentration of TBAHS on the recovery of (○) H2DEHP and (●) HDEHP (15 and 250 μmol/l, respectively) from potassium phosphate-buffer solutions (10 mmol/l, pH 7.4). The ion-pair extraction procedure is described under Experimental.

achieved by using 0.8 g of TBAHS in a 45-ml sample volume (final concentration 50 mmol/l). When H2DEHP (24–240 μmol/l) was ion-pair extracted using 50 mmol/l TBAHS, a straight line was observed with the regression equation $y = 0.777x - 3.702$, $r > 0.997$, where y is the measured and x the initial concentration of H2DEHP in the buffer. The slope of this line gives the recovery of the ion-pair extraction for H2DEHP, which amounted to 77.7%. Under these conditions, up to a 300-fold preconcentration of H2DEHP was achieved. The ion-pair extraction enables H2DEHP to be determined in aqueous solutions at concentrations down to 15 μmol/l. The intra-assay R.S.D. of the overall procedure was determined by analysing six samples of H2DEHP in buffer (100 μmol/l) and was found to be 6.8%.

In HFSLM experiments on both small and large scales, no H2DEHP was detectable in the external compartment of the reactor after 5 h. At this time the concentrations of H2DEHP in the internal compartment of the reactor were 55 ± 10 μmol/l for the small-scale and 180 ± 17 μmol/l for the large-scale experiments (mean ± S.D., $n = 3$). These values correspond to about 10% of the initial amount of H2DEHP in the HFSLM in both experiments. The release of H2DEHP from the HFSLM may be due to shear forces rather than physical solubility. Preliminary results show that the stability of the liquid membrane mainly depends on the composition of the liquid membrane, especially on its *n*-dodecanol content, and on other experimental conditions such as pores size and membrane

thickness of the hollow fibres and flow-rate through the hollow fibres.

The ITP method described here is currently used in our laboratory for stability studies on HFSLM in order to find the optimum composition of the liquid membrane and the experimental conditions for *in vivo* application. This ITP method should also be equally suitable in other fields in which H2DEHP, HDEHP and other related organic phosphates are involved, *e.g.*, in determining formation/dissociation constants of ion pairs between H2DEHP and inorganic or organic cations in two-phase systems [5].

ACKNOWLEDGEMENTS

R.V. is the recipient of a graduate scholarship from the Deutscher Akademischer Austauschdienst (DAAD). The authors acknowledge the skilful technical assistance of Miss A. Hofrichter and Mr. K. Jordanidis.

REFERENCES

1 J. Sandblom, *J. Phys. Chem.*, 73 (1969) 257.
2 M.B. Shabani, T. Akagi and A. Masuda, *Anal. Chem.*, 62 (1990) 2709.
3 M.B. Shabani, T. Akagi and A. Masuda, *Anal. Chem.*, 63 (1991) 2099.
4 M.B. Shabani, T. Akagi and A. Masuda, *Anal. Chem.*, 64 (1992) 737.
5 R. Modin and M. Johansson, *Acta Pharm. Suec.*, 8 (1971) 561.
6 R. Velásquez, D. Tsikas and G. Brunner, *Fresenius' J. Anal. Chem.*, 343 (1992) 78.
7 K. Gustavii and G. Schill, *Acta Pharm. Suec.*, 3 (1966) 241.
8 C.J. Holloway, S. Husmann-Holloway and G. Brunner, *J. Chromatogr.*, 188 (1980) 235.
9 G. Brunner and F. Tegtmeier, *Artif. Organs*, 8 (1984) 161.

Journal of Chromatography, 639 (1993) 323–328
Elsevier Science Publishers B.V., Amsterdam

CHROM. 24 957

Determination of coptisine, berberine and palmatine in traditional Chinese medicinal preparations by capillary electrophoresis

Ying-Mei Liu and Shuenn-Jyi Sheu*

Department of Chemistry, National Taiwan Normal University, 88, Sec. 5, Roosevelt Road, Taipei (Taiwan)

(First received January 5th, 1993; revised manuscript received February 5th, 1993)

ABSTRACT

A capillary electrophoresis method for the determination of coptisine, berberine and palmatine in traditional Chinese medicinal preparations was established. The buffer solution used in this method was 0.2 *M* sodium acetate solution–acetonitrile (1:1). The linear calibration range was 0.003–0.128 mg/ml ($r = 0.9998$) for coptisine, 0.016–0.640 mg/ml ($r = 0.9999$) for berberine and 0.006–0.240 mg/ml ($r = 0.9999$) for palmatine. The recovery was 98.1–101.9% for coptisine, 98.0–100.4% for berberine and 99.7–101.0% for palmatine. The relative standard deviation was 0.96% (intraday) and 2.56% (interday) for coptisine, 1.50% (intraday) and 2.68% (interday) for berberine and 1.12% (intraday) and 2.22% (interday) for palmatine. This method is simple, rapid and reproducible. The contents of these three alkaloids in 23 Coptidis Rhizoma- and/or Phellodendri Cortex-containing Chinese medicinal preparations could easily be determined within 8 min without any pretreatment or any inference.

INTRODUCTION

Coptidis Rhizoma and Phellodendri Cortex are commonly used Chinese herbal drugs with the effects of clearing heat, drying up dampness, purging toxicosis and detoxification [1]. The former is known to contain coptisine, berberine and palmatine (Fig. 1) [2] and the latter contains mainly berberine and palmatine [3]. They may combine with other herbs to form tonic, surface-internal, coordinative, blood regulating, fire purging and astringent formulas [4]. At present, the best method of evaluating the quality of Coptidis Rhizoma- and/or Phellodendri Cortex-containing Chinese medicinal preparations is to determine the contents of coptisine, berberine and palmatine by HPLC [5]. However, owing to complicated components in Chinese medicinal formulas, the use of HPLC is restricted by its lengthy analysis time (at least 30 min until the next injection) and the presence of potentially interfering alkaloidal peaks and because the chromatographic column is easily to contaminated and hard to clean. CE is a recently developed technique that requires a short analysis time, uses a small amount of sample, and can be used for autosampling; in addition, the capillary can easily be thoroughly cleaned. Used in the analysis of Chinese herbs, it gives very good results [6–9]. This study has also found that the use of the CE to analyse various Coptidis Rhizoma- and/or Phellodendri Cortex-containing formulas can offer very satisfactory results. Hence, it is a suitable method for analyses of Chinese medicinal preparations, especially when large numbers of samples are involved and for quality control in pharmaceutical plants.

* Corresponding author.

0021-9673/93/$06.00

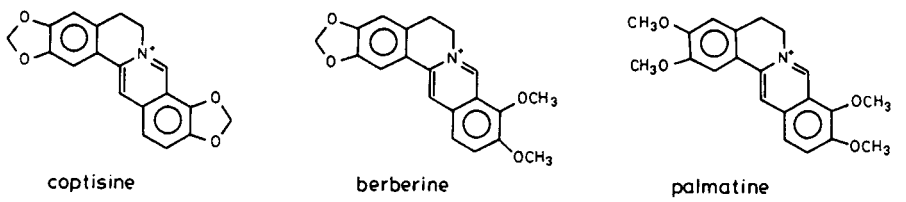

Fig. 1. Structures of marker substances.

EXPERIMENTAL

Reagents and materials

Berberine chloride was purchased from Sigma (St. Louis, MO, USA), coptisine chloride from Nacalai (Kyoto, Japan) and sodium acetate from Osaka (Osaka, Japan). Palmatine was isolated from *Phellodendron amurense* Pupr. [3]. Methyltriphenylphosphonium iodide was prepared from triphenyl phosphine and methyl iodide [10]. Deionized water from a Milli-Q system (Millipore, Bedford, MA, USA) was used to prepare all buffer and sample solutions. Methanol and acetonitrile were HPLC grade. Coptidis Rhizoma- and/or Phellodendri Cortex-containing Chinese medicinal preparations were provided by a Chinese pharmaceutical company in Taipei, Taiwan.

Preparation of Chinese medicinal preparations extracts

A 0.5-g sample of Chinese medicinal preparation was extracted with 70% aqueous methanol (3 ml) by stirring at room temperature for 30 min, then centrifuged at 1500 *g* for 5 min. Extraction was repeated three times. The extracts were combined and filtered through a No. 1 filter paper. After the addition of a 1.0 ml of internal standard solution (6.0 mg of methyltriphenylphosphonium iodide in 1 ml of 70% aqueous methanol), the Chinese medicinal preparation extract was diluted to 10 ml with 70% aqueous methanol. This solution was passed through a 0.45-μm filter and *ca.* 1.7 nl (10-s hydrostatic sampling) of the filtrate were injected into the capillary electrophoresis system directly.

Apparatus and conditions

All analyses were carried out on a Waters Quanta 4000 capillary electrophoresis system equipped with a UV detector set at 254 nm and a 80 cm × 75 μm I.D. uncoated capillary (Millipore, USA) with the detection window placed at 72.5 cm. The conditions were as follows: sampling time, 10 s hydrostatic; run time, 8 min; applied voltage, 25 kV (constant voltage, positive to negative polarity); temperature, 24.5–25.0°C. The electrolyte was a buffer solution consisting of 0.2 *M* sodium acetate solution–acetonitrile (1:1).

Solution for linearity response

Seven solutions of coptisine, berberine and palmatine, which ranged from 0.003 to 0.128 mg/ml for coptisine, 0.016 to 0.640 mg/ml for berberine and 0.006 to 0.240 mg/ml for palmatine, were prepared. Each concentration was analysed three times.

Solution for recovery studies

Different amounts of coptisine, berberine and palmatine standard were added to two samples of Chinese medicinal preparations of known alkaloid content and the mixtures were extracted and analysed using the proposed procedure.

RESULTS AND DISCUSSION

Analytical conditions

In the studies of Coptidis Rhizoma and Phellodendri Cortex crude drugs [7,8], we found that a mixture of sodium acetate solution and organic solvent (methanol or acetonitrile) could give a good resolution of the quaternary alkaloids (for Coptidis Rhizoma, they were coptisine, berberine, epiberberine, palmatine, columbamine, berberastine, jatrorrhizine and magnoflorine; for Phellodendri Cortex, they were berberine, palmatine, jatrorrhizine, magnoflorine and phellodendrine). However, surveys of a number of

commercial Coptidis Rhizoma- and/or Phellodendri Cortex-containing Chinese medicinal preparations, showed that usually only berberine, palmatine and coptisine existed in the text solutions. Actually, one of these three compounds is now used as the marker substance for the evaluation of different Chinese medicinal preparations by HPLC [5]. Therefore, it would be desirable to find a far simpler method that will lead to a shorter analysis time and could be applied to many various Coptidis Rhizoma- and/or Phellodendri Cortex-containing formulas, though it may only be able to separate coptisine, berberine and palmatine well.

From the analysis of quaternary alkaloids [7,8], we knew that carboxylate was a good counter ion for the positively charged nitrogen of the alkaloids, and organic solvent (methanol or acetonitrile) could make the peaks sharper. Hence, we tried to prepare buffer solutions with sodium acetate solutions and methanol (or acetonitrile). After a series of experiments, it was found that 0.2 *M* sodium acetate solution–acetonitrile (1:1) could resolve coptisine, berberine and palmatine within 8 min. At a lower concentration of sodium acetate (0.1 *M*), the peaks were found to be partially overlapped. At lower concentrations of acetonitrile (40, 30, 20 and 10%), the resolution was not good, Acetonitrile was found to be better than methanol in this experiment.

An electrolyte consisting of 0.2 *M* sodium acetate solution–acetonitrile (1:1) was chosen as the buffer solution of this study. Fig. 2 is an electropherogram showing the separation of the authentic compounds with migration times of 6.2 min for the internal standard (methyltriphenylphosphonium iodide), 6.4 min for coptisine, 6.6 min for berberine and 7.0 min for palmatine. As the methanol–water extracts of Chinese medicinal preparations were injected directly and analysed, the results were as good as those obtained with pure chemical samples without interference with each peak and the analysis could also be completed within 8 min, as shown in Fig. 3.

Calibration graphs for coptisine, berberine and palmatine

Calibration graphs (peak-area ratio, *y*, *vs.* concentration, *x*, mg/ml) were constructed in the range 0.003–0.128 mg/ml for coptisine, 0.006–

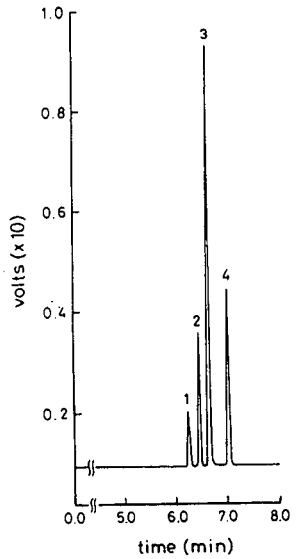

Fig. 2. Capillary electropherogram of authentic compounds of coptisine, berberine and palmatine. Peaks: 1 = internal standard (methyltriphenylphosphonium iodide), 0.600 mg/ml; 2 = coptisine, 0.048 mg/ml; 3 = berberine, 0.240 mg/ml; 4 = palmatine, 0.090 mg/ml.

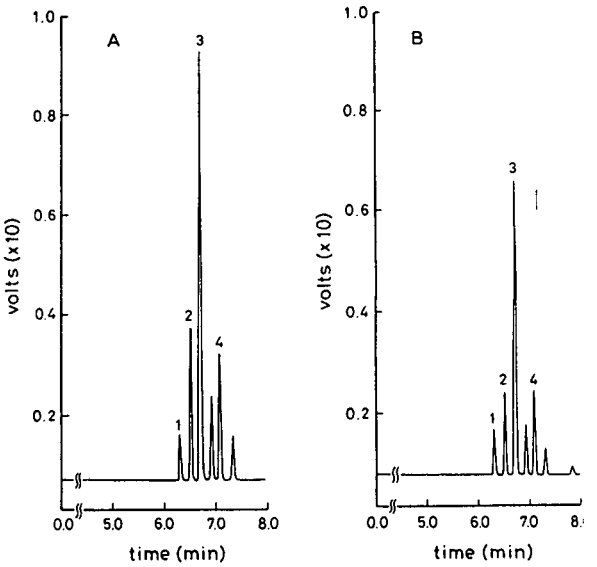

Fig. 3. Capillary electropherograms of Chinese medicinal preparations: (A) *Huang-lien-tang*; (B) *Pu-chi-hsiao-tu-yin*. Peaks as in Fig. 2.

0.240 mg/ml for berberine and 0.006–0.240 mg/ml for palmatine. The regression equations of these curves and their correlation coefficients were calculated as follows:

Coptisine $y = 30.84x + 0.01$ ($r = 0.9998$)
Berberine $y = 32.14x - 0.03$ ($r = 0.9999$)
Palmatine $y = 33.41x - 0.01$ ($r = 0.9999$)

System suitability test

The reproducibility (relative standard deviation) of this proposed method, on the basis of peak-area ratios for six replicate injections, was 0.96% (intraday) and 2.56% (interday) for coptisine, 1.50% (intraday) and 2.68% (interday) for berberine and 1.12% (intraday) and 2.22% (interday) for palmatine.

The results of standard addition recovery studies of coptisine, berberine and palmatine from sample composites of Chinese medicinal preparations are calculated. The recovery was 98.1–101.9% for coptisine, 98.0–100.4% for berberine and 99.7–101.0% for palmatine. All

TABLE I

CONTENTS OF COPTISINE, BERBERINE AND PALMATINE IN COPTIDIS RHIZOMA-CONTAINING CHINESE MEDICAL PREPARATIONS (mg/g)

Sample[a]	Coptisine	Berberine	Palmatine	Total
1	0.71	2.45	0.80	3.96
2	0.90	3.43	1.02	5.35
3	0.52	2.18	0.58	3.28
4	1.81	6.52	1.69	10.02
5	2.84	8.80	2.77	14.41
6	0.56	1.84	0.41	2.81
7	1.32	4.10	1.17	6.59
8	0.95	3.60	1.06	5.61
9	2.21	8.99	3.06	14.26
10	0.81	3.57	0.95	5.33
11	0.61	2.19	0.62	3.42
12	0.85	3.15	0.80	4.80

[a] Names and compositions of the Coptidis Rhizoma-containing Chinese medicinal formulas: **1** = *Chai-hsien-tang*: Pinelliae Tuber, Trichosanthis Fructus, Bupleuri Radix, Coptidis Rhizoma, Scutellariae Radix, Ginseng Radix, Glycyrrhizae Radix, Zingiberis Rhizoma, Zizyphi Fructus; **2** = *Ching-wei-tang*: Moutan Radicis Cortex, Angelicae Radix, Rehmanniae Radix, Coptidis Rhizoma, Cimicifugae Rhizoma; **3** = *Ching-yin-li-ke-tang*: Lonicerae Flos, Forsythiae Fructus, Schizonepetae Herba, Menthae Herba, Ledebouriellae Radix, Scrophulariae Radix, Coptidis Rhizoma, Platycodi Radix, Scutellariae Radix, Niter, Rhei Rhizoma, Gardeniae Fructus, Arctii Fructus, Glycyrrhizae Radix; **4** = *Huang-lien-tang*: Coptidis Rhizoma, Glycyrrhizae Radix, Zingiberis Siccatum Rhizoma, Ginseng Radix, Cinnamomi Ramulus, Zizyphi Fructus, Pinelliae Tuber; **5** = *Ko-ken-huang-lien-huang-chin-tang*: Puerariae Radix, Coptidis Rhizoma, Scutellariae Radix, Glycyrrhizae Radix; **6** = *Pan-hsia-hsieh-hsin-tang*: Pinelliae Tuber, Scutellariae Radix, Coptidis Rhizoma, Zingiberis Siccatum Rhizoma, Ginseng Radix, Glycyrrhizae Radix, Zizyphi Fructus; **7** = *Pan-hsieh-liu-chun-tzu-tang*: Pinelliae Tuber, Zingiberis Siccatum Rhizoma, Scutellariae Radix, Atractylodis Rhizoma, Coptidis Rhizoma, Citri Leiocarpae Exocarpium, Ginseng Radix, Glycyrrhizae Radix, Poria, Ostreae Testa; **8** = *Pu-chi-hsiao-tu-yin*: Scutellariae Radix, Coptidis Rhizoma, Baphicacanthis Rhizoma et Radix, Forsythiae Fructus, Arctii Fructus, Scrophulariae Radix, Glycyrrhizae Radix, Platycodi Radix, Cimicifugae Rhizoma, Bupleuri Radix, Lashiosphaera, Citri Leiocarpae Exocarpium, Menthae Herba, Bombyx Batryticatus; **9** = *San-huang-hsieh-hsin-tang*: Rhei Rhizoma, Scutellariae Radix, Coptidis Rhizoma; **10** = *Shao-yao-tang*: Paeoniae Radix, Cinnamomi Cortex, Saussureae Radix, Scutellariae Radix, Glycyrrhizae Radix, Angelicae Radix, Rhei Rhizoma, Arecae Semen, Coptidis Rhizoma; **11** = *Tien-wang-pu-hsin-tan*: Rehmanniae Radix, Ginseng Radix, Poria, Polygalae Radix, Scrophulariae Radix, Salviae Miltiorrhizae Radix, Platycodi Radix, Thujae Orientalis Semen, Asparagi Radix, Ophiopogonis Tuber, Zizyphi Spinosi Semen, Angelicae Radix, Schizandrae Fructus, Cinnabaris, Acori Rhizoma, Coptidis Rhizoma; **12** = *Tzu-sheng-ming-mu-tang*: Angelicae Radix, Paeoniae Radix, Ligustici Rhizoma, Rehmanniae Radix, Platycodi Radix, Ginseng Radix, Gardeniae Fructus, Coptidis Rhizoma, Angelicae Dahuricae Radix, Viticis Fructus, Chrysanthemi Flos, Glycyrrhizae Radix, Junci Caulis Medulla, Camelliae Folium.

the tailing factors of the four peaks (internal standard, coptisine, berberine and palmatine) are very close to 1.

Determination of coptisine, berberine and palmatine in Chinese medicinal preparations

When the test solutions of Chinese medicinal preparations extracts were analysed by CE under the selected conditions, the calculated contents of coptisine, berberine and palmatine as shown in Tables I–III were obtained. There was no interference with any peak of the extracts in various Chinese medicinal preparations (including Coptidis Rhizoma containing, Phellodendri Cortex containing as well as Coptidis Rhizoma and Phellodendri Cortex containing). These data indicate that the proposed CE method is relatively suitable for the determination of coptisine, berberine and palmatine in Chinese medicinal preparations. Moreover, this analytical method not only needs no pretreatment, but also offers autosampling. In addition to its rapid and accurate performance, it allows the next injection to be given within 8 min with a thoroughly cleaned capillary too. Therefore, it should be especially useful for bulky samples and also quality control in pharamaceutical plants.

TABLE II

CONTENTS OF COPTISINE, BERBERINE AND PALMATINE IN PHELLODENDRI CORTEX-CONTAINING CHINESE MEDICINAL PREPARATIONS (mg/g)

Sample[a]	Berberine	Palmatine	Total
13	0.42	0.24	0.66
14	0.61	0.35	0.96
15	0.25	0.15	0.40
16	0.25	0.11	0.36
17	0.51	0.24	0.75

[a] Names and compositions of the Phellodendri Cortex-containing Chinese medicinal formulas: **13** = *Chih-po-pa-wei-wan*: Anemarrhenae Rhizoma, Phellodendri Cortex, Rehmanniae Radix, Batatatis Rhizoma, Corni Fructus, Poria, Alismatis Rhizoma, Moutan Radicis Cortex; **14** = *I-chi-chung-ming-tang*: Astragali Radix, Ginseng Radix, Puerariae Radix, Viticis Fructus, Paeoniae Radix, Phellodendri Cortex, Cimicifugae Rhizoma, Glycyrrhizae Radix; **15** = *Pai-tu-san*: Rehmanniae Radix, Platycodi Radix, Forsythiae Fructus, Moutan Radicis Cortex, Trichosanthis Radix, Scrophulariae Radix, Lonicerae Flos, Bupleuri Radix, Glycyrrhizae Radix, Phellodendri Cortex, Menthae Herba, Paeoniae Radix, Gypsum Fibrosum, Arctii Fructus; **16** = *Pan-hsia-pai-chu-tien-ma-tang*: Pinelliae Tuber, Atractylodis Rhizoma, Poria, Citri Leiocarpae Exocarpium, Atractylodis Lanceae Rhizoma, Hordei Germinatus Fructus, Gastrodiae Rhizoma, Monasco Cum Oryzae Semen, Astragali Radix, Ginseng Radix, Alismatis Rhizoma, Phellodendri Cortex, Zingiberis Siccatum Rhizoma, Zingiberis Rhizoma; **17** = *Tzu-yin-chiang-huo-tang*: Angelicae Radix, Paeoniae Radix, Asparagi Radix, Ophiopogonis Tuber, Atractylodis Rhizoma, Rehmanniae Radix, Citri Leiocarpae Exocarpium, Phellodendri Cortex, Anemarrhenae Rhizoma, Glycyrrhizae Radix.

TABLE III

CONTENTS OF COPTISINE, BERBERINE AND PALMATINE IN COPTIDIS RHIZOMA AND PHELLODENDRI CORTEX-CONTAINING CHINESE MEDICAL PREPARATIONS (mg/g)

Sample[a]	Coptisine	Berberine	Palmatine	Total
18	0.62	2.92	0.91	4.45
19	1.03	5.51	1.43	7.97
20	1.44	3.38	2.19	7.01
21	4.42	17.79	5.30	27.51
22	1.32	4.16	1.34	6.82
23	0.85	3.39	0.86	5.10

[a] Names and compositions of the Coptidis Rhizoma and Phellodendri Cortex-containing Chinese medicinal formulas: **18** = *Chai-hu-ching-kan-tang*: Bupleuri Radix, Angelicae Radix, Paeoniae Radix, Ligustici Rhizoma, Rehmanniae Radix, Coptidis Rhizoma, Scutellariae Radix, Phellodendri Cortex, Gardeniae Fructus, Forsythiae Fructus, Platycodi Radix, Arctii Fructus, Trichosanthis Radix, Menthae Herba, Glycyrrhizae Radix; **19** = *Chih-cho-ku-pen-wan*: Nelumbinis Stamen, Coptidis Rhizoma, Phellodendri Cortex, Alpiniae Oxyphyllae Fructus, Amomi Semen, Pinelliae Tuber, Poria, Polyporus, Glycyrrhizae Radix; **20** = *Huang-lien-chieh-tu-tang*: Coptidis Rhizoma, Phellodendri Cortex, Scutellariae Radix, Gardeniae Fructus; **21** = *Pai-tou-weng-tang*: Pulsatillae Radix, Coptidis Rhizoma, Phellodendri Cortex, Fraxini Cortex; **22** = *Sanhuang-shih-kao-tang*: Gypsum Fibrosum, Scutellariae Radix, Coptidis Rhizoma, Phellodendri Cortex, Gardeniae Fructus, Ephedrae Herba, Sojae Semen Praeparatum, Zingiberis Rhizoma, Zizyphi Fructus, Camelliae Folium; **23** = *Wen-ching-yin*: Angelicae Radix, Rehmanniae Radix, Paeoniae Radix, Ligustici Rhizoma, Coptidis Rhizoma, Scutellariae Radix, Phellodendri Cortex, Gardeniae Fructus.

ACKNOWLEDGEMENT

Financial support from the National Science Council Taiwan, is gratefully acknowledged.

REFERENCES

1 H.Y. Hsu, Y.P. Chen, S.J. Sheu, C.H. Hsu, C.C. Chen and H.C. Chang, *Chinese Materia Medica —A Concise Guide*, Modern Drug Press, Taipei, 1984, pp. 112–113, 117–118.
2 M. Tomita and S. Kura, *J. Pharm. Soc. Jpn.*, 76 (1956) 1425.
3 M. Tomita and J. Kunitomo, *Yakugaku Zasshi*, 78 (1958) 1444.
4 S.Y. Huang, *A Collective Commentary to Herbal Formulas*, Ba-Teh Education and Culture Press, Taipei, 1987, pp. 1–10.
5 T. Misaki, K. Sagara, M. Ojima, S. Kakizawa, T. Oshima and H. Yoshizawa, *Chem. Pharm. Bull*, 30 (1982) 354.
6 Y.M. Liu and S.J. Sheu, *J. Chromatogr.*, 600 (1992) 370.
7 Y.M. Liu and S.J. Sheu, *J. Chromatogr.*, 623 (1992) 196.
8 Y.M. Liu and S.J. Sheu, *J. Chromatogr.*, 634 (1993) 329.
9 Y.M. Liu, S.J. Sheu, S.H. Chiou, H.C. Chang and Y.P. Chen, *Planta Medica*, in press.
10 H.E. Baumgarten, *Organic Syntheses*, Collective Volume 5, Wiley, New York, 1973, pp. 751–752.

Journal of Chromatography, 639 (1993) 329–332
Elsevier Science Publishers B.V., Amsterdam

CHROM. 25 075

Short Communication

Comments on a report of the separation of the enantiomers of π-donor analytes on π-donor chiral stationary phases

William H. Pirkle*, Christopher J. Welch☆ and Qing Yang

School of Chemical Sciences, University of Illinois, 1209 West California Street, Urbana, IL 61801 (USA)

(Received February 5th, 1993)

ABSTRACT

A report by Oliveros *et al.* [*J. Chromatogr.*, 589 (1992) 53] concerning the separation of the enantiomers of several π-basic analytes on π-basic chiral stationary phases was investigated. Claims for the separation of the enantiomers of two of these analytes are believed to be erroneous, the confusion in one instance presumably arising from the presence of an impurity in the commercially available material. Several methods for verifying the assignment of two chromatographic peaks as arising from enantiomers are also presented.

INTRODUCTION

A recent report by Oliveros *et al.* [1] concerns the separation of the enantiomers of compounds **1–8** (Fig. 1) using a series of π-donor chiral stationary phases (CSPs). Most of these CSPs are similar to analytes whose enantiomers are separable on N-(3,5-dinitrobenzoyl)amino acid-derived CSPs [2]. The reported separations of the enantiomers of the N-(3,5-dinitrobenzoyl)amino acid derivatives **1–3** (Fig. 1) on these CSPs comes as no great surprise given the reciprocal nature of chiral recognition. However, in our experience, π-donor CSPs typically show little or no ability to separate the enantiomers of π-donor analytes (unless the latter contain functionality capable of serving as hydrogen bond donors). It was thus with considerable interest that we read of the rather large separation factors ($\alpha > 20$ in one case) which were reported for the enantiomers of nitrile **7** and epoxide **8**, analytes which possess neither π-acidic functionality nor hydrogen bond donor groups. Such enantioselectivities suggested that some as yet undiscovered chiral recognition principle might be operative, and prompted us to further investigate some of these separations.

RESULTS AND DISCUSSION

From previous studies, we have available a column containing the naproxen-derived CSP first reported by Doyle *et al.* [3,4] and designated

* Corresponding author.
☆ Present address: Regis Chemical Company, 8210 Austin Avenue, Morton Grove, IL 60053, USA.

0021-9673/93/$06.00

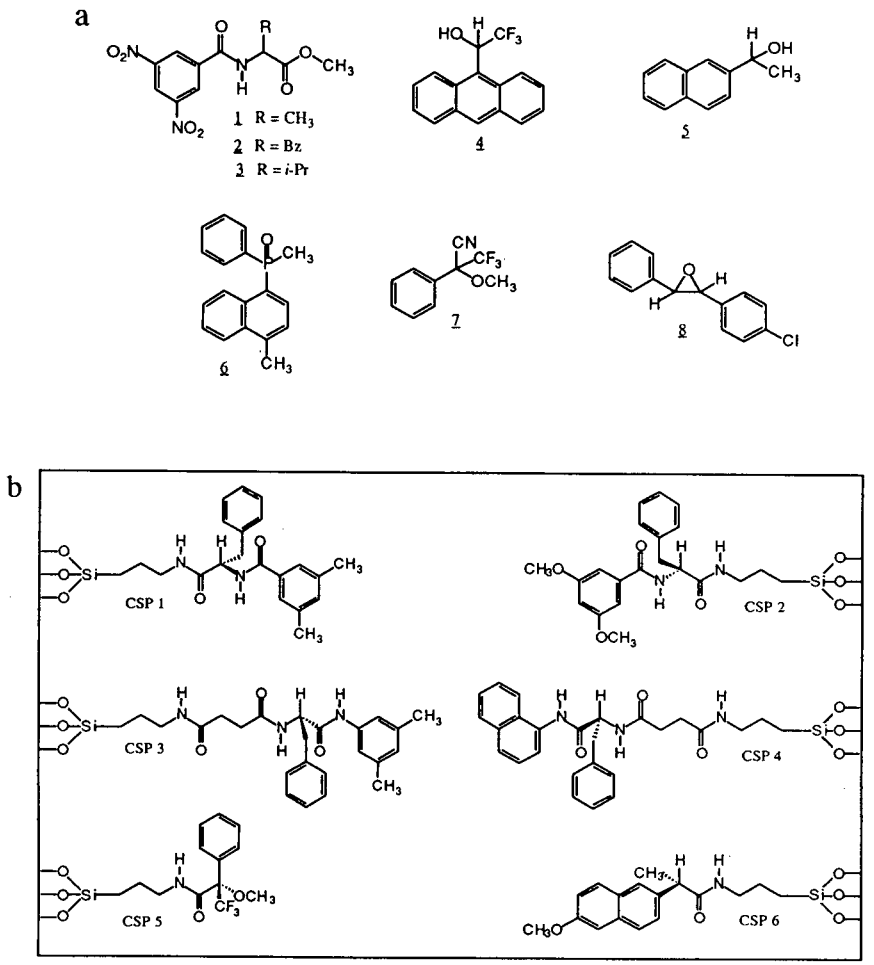

Fig. 1. (a) Analytes and (b) CSPs utilized in the study by Oliveros *et al.* [1].

as CSP 6 by Oliveros *et al.* We also have a column containing CSP 7, which is similar to CSP 3, the major differences being that CSP 7 is derived from leucine, whereas CSP 3 is derived from phenylalanine, and that CSP 7 is bonded to silica using a rather less complicated tether.

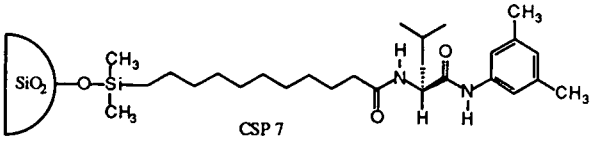

In our hands, the enantiomers of the ethyl ester of N-(3,5-dinitrobenzoyl)phenylalanine are separated on our CSP 6 ($\alpha = 1.94$, $k_1' = 0.85$) and CSP 7 ($\alpha = 2.46$, $k_1' = 0.79$) using the mobile phase described. These values compare favorably with the values reported for CSP 6 ($\alpha = 1.51$, $k_1' = 1.37$) and for CSP 3 ($\alpha = 2.10$, $k_1' = 0.65$) for the enantiomers of the methyl ester of N-(3,5-dinitrobenzoyl)phenylalanine, suggesting that our CSP 6 and CSP 7 are reasonable approximations of CSP 6 and CSP 3 used by Oliveros *et al.*

When samples of racemic nitrile **7** and racemic epoxide **8** were obtained from the vendor cited in the work by Oliveros *et al.* [1] and chromatographed on columns containing our CSP 6 and CSP 7, the results were inconsistent with the findings reported in the original study. Using the mobile phase reported by Oliveros *et al.* [1] (and several other mobile phases as well) nitrile **7**

affords but a single, scarcely retained peak. Epoxide **8** affords two peaks of comparable area on both CSP 6 and CSP 7. However, one of the peaks stems from an impurity since the same two peaks are noted on an achiral nitrile column. A trace of the more strongly UV absorbing 4-chlorostilbene, a logical precursor for **8**, was suspected to be present. However, gas chromatography–mass spectrometry shows the chlorine-containing impurity to have a molecular mass of 216/218 rather than the expected 214/216. The expected value of 230/232 was obtained for the epoxide. When epoxide **8** is chromatographed on a π-acidic CSP which *is* capable of separating its enantiomers [5], three peaks are observed: one giving a strong positive response from a polarimetric detector, one giving no response, and the last giving a strong negative response. No polarimetric response is noted when **8** is similarly chromatographed on CSP 6 or CSP 7.

Although we realize that preparation of the same CSP in two different laboratories will result in non-identical products, it seems likely that the separation factors of 3.55 and 4.20 reported for the enantiomers of nitrile **7** and the values 1.70 and 1.50 reported for epoxide **8** on CSPs 3 and 6 are erroneous. It seems likely that Oliveros *et al.* misinterpreted peaks arising from impurities as an indication of enantiomer separation when, in fact, no such separations were occurring.

One additional set of observations supports the view that the reported separations of the enantiomers of **7** are erroneous. On the strength of the large separation factors (*e.g.* 14.86, 23.00) they believed they were encountering on CSP 1 and CSP 2, Oliveros *et al.* prepared CSP 5 with the expectation that this reciprocal CSP would afford significant levels of enantioselectivity. In fact, in the series of analytes **1–8**, CSP 5 is reported to separate only the enantiomers of epoxide **8**. Since our sample of **8** (obtained from the same vendor as that of Oliveros *et al.*) is contaminated with an impurity, we suspect the claimed resolution of **8** by CSP 5 is also incorrect. The poor performance of CSP 5 was noted but no inference was drawn by Oliveros *et al.* from this observation.

Apparent separations of enantiomers are frequently encountered in chromatographic enantioseparation, particularly when multicomponent samples are investigated. Determining whether two chromatographic peaks arise from enantiomers can be facilitated by a variety of methods including:

(i) Use of a chiroptic detector. Many enantiomers can be detected using a polarimetric or circular dichroism detector, neither of which afford a response for a nonresolved racemate or an achiral sample.

(ii) Use of a racemic version of the CSP: the two peaks corresponding to the separated enantiomers typically show up as a single peak on a racemic version of the CSP [6]. In several instances [7,8] enantiofractionation has been observed during chromatography of enantioenriched analytes on an achiral CSP. However, this phenomenon is rarely encountered in practice. Chromatography of the sample on an achiral stationary phase (*e.g.* silica, amino, nitrile) affords a minimum estimate of the number of components in the sample, information relevant to the number of peaks to be expected with the CSP is used.

(iii) Use of a CSP of the opposite absolute configuration: this will invert the order of elution of the enantiomers, an event easily detected if the analyte is enantioenriched. This method is of no value for a racemic analyte unless used in conjuction with some other technique which is sensitive to stereochemistry (*e.g.* a chiroptic detector).

(iv) Use of a variable-wavelength detector: enantiomers have identical absorbtion spectra and must give identical detector responses. Relative peak heights of two supposed enantiomer peaks are therefore unaffected by changes in detector wavelength provided that an achiral mobile phase is used. The availability of modern full-spectrum diode array detectors makes this method especially useful.

ACKNOWLEDGEMENTS

This work was supported by a grant from the National Science Foundation, by a grant from Eli Lilly and Company, by a Department of Education Advanced Opportunities in Chemistry

Graduate Fellowhip to C.J.W. and by a generous donation of HPLC solvents from EM Scientific.

EDITORIAL NOTE

Dr. Laureano Oliveros, who is a co-author of ref. 1, has read the present paper and agrees that an experimental error was made in the study that is the subject of ref. 1. He has since been in contact with Dr. Pirkle in an effort to further clarify this situation.

REFERENCES

1 L. Oliveros, C. Minguillón, B. Desmaziéres and P.-L. Desbène, *J. Chromatogr.*, 589 (1992) 53.
2 P. Macaudiere, M. Lienne, A. Tambute and M. Caude, in A.M. Krstulovic (Editor), *Chiral Separations by HPLC*, Ellis Horwood, Chichester, 1989, p. 407.
3 T.D. Doyle, C.A. Brunner and E. Smith, presented at the *12th International Symposium on Column Liquid Chromatography, Washington, DC, June 19–24, 1988*, abstract Tu-P-212.
4 T.D. Doyle, C.A. Brunner and E. Smith, *US Pat.*, 4 919 803 (1990).
5 W.H. Pirkle and C.J. Welch, *J. Liq. Chromatogr.*, 15 (1992) 1947.
6 W.H. Pirkle, R. Däppen and D.S. Reno, *J. Chromatogr.*, 407 (1987) 211.
7 R. Matusch and C. Coors, *Angew. Chem.*, 101 (1989) 624.
8 J. Martens and R. Bhusan, *J. Liq. Chromatogr.*, 15 (1992) 1.

Journal of Chromatography, 639 (1993) 333–337
Elsevier Science Publishers B.V., Amsterdam

CHROM. 25 039

Short Communication

Determination of dissociation constants of aromatic carboxylic acids by ion chromatography

Naoki Hirayama*, Masahiro Maruo and Tooru Kuwamoto

Department of Chemistry, Faculty of Science, Kyoto University, Sakyo-ku, Kyoto 606-01 (Japan)

(First received December 29th, 1992; revised manuscript received March 4th, 1993)

ABSTRACT

The method for the numerical analysis of the substituent effect on the retention times of substituted benzoate anions in ion chromatography was applied to that of substituted naphthoate anions in order to determine the dissociation constants of several aromatic carboxylic acids. The C-5–C-8 part of naphthalene was postulated as a substituent of benzoate, and *the steric effect index* and *the positional effect correction index* of the substituent were determined. Finally, the dissociation constants of substituted naphthoic acids were determined.

INTRODUCTION

The determination of the dissociation constants of large aromatic carboxylic acids, such as substituted naphthoic acids, by using titrimetric or electrochemical methods is very difficult because these acids have a hydrophobic naphthalene structure and low solubility in water.

In high-performance liquid chromatography (HPLC), it is well known that the elution behaviours of monoprotic acidic or basic sample species can be expressed as functions of the dissociation constants (K_a) of the respective species [1–5], and this relationship is often used for the optimization of chromatographic conditions or the determination of the pK_a values of sample species [2,5–8]. In ion chromatography (IC), similar relationships and applications have been reported [9,10]. However, in these methods, the pK_a values cannot be determined without many chromatographic measurements using different eluent pH conditions.

In a previous paper [11], we investigated numerically the elution behaviours of substituted benzoate anions in IC. It was found that the analysis of the substituent effect on the retention times of these anions can be performed by dividing the effect into three terms: an "LFER-applicable effect term", a "steric effect term" and a "positional effect correction term". The first is expressed as a function of pK_a, the second as a function of the kind and number of substituents and the third as a function of the position of the substituents.

In this work, the numerical analysis method was applied to the interpretation of the elution behaviours of substituted naphthoate anions in IC by postulating $-(CH)_4-$, which is shown in

* Corresponding author.

0021-9673/93/$06.00

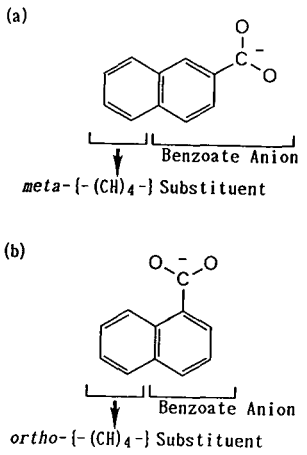

Fig. 1. Definition of $-(CH)_4-$. (a) 2-Naphthoic acid [*m*-{$-(CH)_4-$}]; (b) 1-naphthoic acid [*o*-{$-(CH)_4-$}].

Fig. 1, as *a substituent* of benzoate. Also, the dissociation constants of substituted naphthoic acids and anthracene-9-carboxylic acid were determined by the numerical analysis methods and by measurement under only a single eluent condition.

EXPERIMENTAL

Apparatus

A Tosoh HLC-601 ion chromatography system was used. For the retentions of the anions, a column (50 mm × 4.6 mm I.D.) packed with Tosoh TSKgel IC-Anion-PW (polymethacrylate gel base, particle size 10 μm, capacity 0.03 mequiv./g) or Tosoh TSKgel IC-Anion-SW (silica gel base, particle size 5 μm, capacity 0.4 mequiv./g) was used. The flow-rate was maintained at 1.0 ml/min under a pressure of 20–50 kg/cm^2. The column was placed in an oven set at 30°C. The peaks were detected with a Tosoh UV-8 Model II ultraviolet detector at a wavelength of 254 nm and recorded with a Shimadzu Chromatopack C-R1A recorder.

Eluents

A stock solution of 1 *M* hydrochloric acid was prepared by diluting the concentrated acid and a stock solution of 1 *M* tris(hydroxymethyl)-aminomethane (Tris) was prepared by dissolving

TABLE I

SUBSTITUTED BENZOIC AND NAPHTHOIC ACIDS USED IN THIS STUDY AND THEIR RETENTION TIMES

Eluent: 100 m*M* Tris–HCl (pH 7.0).

No.	Compound	pK_a (25°C) [12]	IC-Anion-PW column		IC-Anion-SW column	
			t'_R (min)	Log t'_R	t'_R (min)	Log t'_R
1	Benzoic acid	4.20	1.35	0.130	3.28	0.516
2	*o*-Chlorobenzoic acid	2.88	1.16	0.064	2.45	0.389
3	*m*-Chlorobenzoic acid	3.83	5.30	0.724	6.79	0.832
4	*p*-Chlorobenzoic acid	3.99	5.13	0.710	5.91	0.772
5	2,4-Dichlorobenzoic acid	2.68[a]	3.89	0.590	4.20	0.623
6	2,5-Dichlorobenzoic acid	2.47[a]	3.66	0.563	4.13	0.616
7	2,6-Dichlorobenzoic acid	1.59[a]	1.46	0.164	2.47	0.393
8	3,4-Dichlorobenzoic acid	3.64[b]	18.81	1.274	12.37	1.092
9	1-Naphthoic acid	3.70	5.40	0.732	9.59	0.982
10	2-Naphthoic acid	4.16	16.14	1.208	27.34	1.437
11	Anthracene-9-carboxylic acid	3.65	25.54	1.407	40.17	1.604
12	2-Hydroxy-1-naphthoic acid	3.29	96.88	1.986	72.41	1.860
13	1-Hydroxy-2-naphthoic acid	–	169.52	2.229	129.07	2.111
14	3-Hydroxy-2-naphthoic acid	2.71[c]	124.40	2.095	88.56	1.947
15	3-Amino-2-naphthoic acid	–	19.11	1.281	27.91	1.446

[a] Ref. 13.
[b] Ref. 14.
[c] Ref. 15.

the reagent in distilled water. The eluent (100 m*M* Tris–HCl, pH 7.0) was prepared by mixing these stock solutions with distilled water and deaerating the mixture.

Sample solutions

The substituted benzoates and naphthoates used in this study are shown in Table I [12–15]. Each stock solution (20 m*M*) of these sodium salts was prepared by dissolving the compound in distilled water or by neutralizing the acid with aqueous sodium hydroxide solution. Working solutions (0.2 m*M*) were prepared by diluting the stock solutions with distilled water.

Calculation of retention indices and determination of dissociation constants

In a previous paper [11], we reported that the retention times [t'_R(R)] of substituted benzoates ($RCOO^-$) can be expressed as follows:

$$\log t'_R(R) = A + (-\rho')pK_a(R) + \left(\sum_j n_{X_j} i'_{X_j} + \sum_j n_{o\text{-}X_j} i''_{o\text{-}X_j} + \sum_j n_{p\text{-}X_j} i''_{p\text{-}X_j} + \sum_j n_{X_j\text{-}X'_j} i''_{X_j\text{-}X'_j}\right)$$

$$= A + (-\rho')pK_a(R) + i'_{Cl}\left(\sum_j n_{X_j} j'_{X_j} + \sum_j n_{o\text{-}X_j} j''_{o\text{-}X_j} + \sum_j n_{p\text{-}X_j} j''_{p\text{-}X_j} + \sum_j n_{X_j\text{-}X'_j} j''_{X_j\text{-}X'_j}\right) \quad (1)$$

where

A = a constant determined by the experimental conditions;

$-\rho'$ = an "LFER-applicable effect constant";

i'_{X_j} = an "adjusted steric effect factor" of substituent X_j;

$i''_{o\text{-}X_j}$, $i''_{p\text{-}X_j}$, $i''_{X_j\text{-}X'_j}$ = "adjusted positional effect correction factors" of *ortho*-X_j, *para*-X_j and neighbouring X_j and X'_j substituent(s), respectively;

n_{X_j}, $n_{o\text{-}X_j}$, $n_{p\text{-}X_j}$, $n_{X_j\text{-}X'_j}$ = the number of respective substituent(s);

$j'_{X_j}(= i'_{X_j}/i'_{Cl})$ = a "steric effect index" of X_j;

$j''_{o\text{-}X_j}$, $j''_{p\text{-}X_j}$, $j''_{X_j\text{-}X'_j}(= i''_{o\text{-}X_j}/i'_{Cl}, i''_{p\text{-}X_j}/i'_{Cl}, i''_{X_j\text{-}X'_j}/i'_{Cl})$ = "positional effect correction indices" of the respective substituent(s).

We consider that this equation should also be applicable to the determination of the retention times of substituted naphthoates by using $i'_{-(CH)_4-}$, $i''_{o\text{-}\{-(CH)_4-\}}$, $j'_{-(CH)_4-}$ and $j''_{o\text{-}\{-(CH)_4-\}}$.

The values of A, $-\rho'$ and i'_{Cl} were regressively calculated from the retention times of Cl-substituted benzoate by using eqn. 1 and by neglecting $i''_{o\text{-}Cl}$, $i''_{p\text{-}Cl}$ and $i''_{Cl\text{-}Cl}$. The values of $i'_{-(CH)_4-}$, $i''_{o\text{-}\{-(CH)_4-\}}$, $j'_{-(CH)_4-}$ and $j''_{o\text{-}\{-(CH)_4-\}}$ were calculated from the retention times of 2- and 1-naphthoates by substituting the above-calculated values into eqn. 1. The method of calculation is detailed under Experimental in ref. 11. The pK_a values of substituted naphthoates were determined by substituting these indices into eqn. 1.

RESULTS AND DISCUSSION

Calculation of $j'_{-(CH)_4-}$ and $j''_{o\text{-}\{-(CH)_4-\}}$

Table I shows the retention times of the

TABLE II

THE CALCULATED VALUES OF THE FACTORS AND INDICES

Eluent: 100 m*M* Tris–HCl (pH 7.0).

Factor or index	IC-Anion-PW column[a]	IC-Anion-SW column[b]
i'_{Cl}	0.705	0.363
$i'_{(CH)_4-}$	1.087	0.932
$i''_{o\text{-}\{-(CH)_4-\}}$	−0.217	−0.293
j'_{Cl}	1.000[c]	1.000[c]
$j'_{-(CH)_4-}$	1.542	2.567
$j''_{o\text{-}\{-(CH)_4-\}}$	−0.308	−0.807
j'_{OH}	0.265[d]	0.446[d]
$j''_{o\text{-}OH}$	1.945[d]	2.185[d]
j'_{NH_2}	−0.700[d]	−0.723[d]
$j''_{o\text{-}NH_2}$	0.345[d]	0.257[d]

[a] $A = -2.217$, $-\rho' = 0.562$.

[b] $A = -0.959$, $-\rho' = 0.352$.

[c] Defined as unity.

[d] Ref. 11.

TABLE III

COMPARISON BETWEEN THE pK_a VALUES OF THE SUBSTITUTED NAPHTHOIC ACIDS DETERMINED BY THIS METHOD AND THOSE IN THE LITERATURE

No.	Compound	This method			Literature
		IC-Anion-PW column	IC-Anion-SW column	Mean value	
11	Anthracene-9-carboxylic acid	3.35	3.65	3.50 ± 0.15	3.65 [12]
12	2-Hydroxy-1-naphthoic acid	3.16	3.48	3.32 ± 0.16	3.29 [12]
13	1-Hydroxy-2-naphthoic acid	3.20	3.36	3.28 ± 0.08	–
14	3-Hydroxy-2-naphthoic acid	2.97	2.89	2.93 ± 0.04	2.71 [15]
15	3-Amino-2-naphthoic acid	4.74	4.67	4.71 ± 0.04	4.56 [10][a]

[a] Determined by ion chromatography with change of eluent pH [10]. Eluent: 50 m*M* Tris–HBr (pH 3.00–7.00). Column: IC-Anion-SW. Standard sample: γ-resorcylic acid (pK_a = 1.30 [12]).

substitution benzoate and naphthoate anions. By using the data for entries 1–8 in Table I, the values of A, $-\rho'$ and i'_{Cl} were regressively calculated as −2.217, 0.562 and 0.705, respectively, on IC-Anion-PW and −0.959, 0.352 and 0.363, respectively, on IC-Anion-SW. By using these values and the data for entries 9 and 10 in Table I, the values of $i'_{-(CH)_4-}$, $i''_{o\text{-}\{-(CH)_4-\}}$, $j'_{-(CH)_4-}$ and $j''_{o\text{-}\{-(CH)_4-\}}$ were calculated and are given in Table II with several previously reported indices [11].

Determination of the dissociation constants

By substituting the constants and indices shown in Table II into eqn. 1, the dissociation constants of several substituted naphthoic acids were calculated. Table III compares the dissociation constants of the acids determined by this method and those in the literature [10,12,15]. The pK_a values were similar to each other. Some discrepancies between the values obtained from the indices for IC-Anion-PW and those for IC-Anion-SW seem to be due to errors caused by the regressive calculations. From the results, it was concluded that this method is very effective for determining the pK_a values of large aromatic carboxylic acids, such as substituted naphthoic acids. The pK_a values of 1-hydroxy-2-naphthoic acid and 3-amino-2-naphthoic acid were determined as 3.28 ± 0.08 and 4.71 ± 0.04, respectively.

This method is very useful because the pK_a values can be determined by measuring the t'_R values under any eluent conditions, and it is effective for the simultaneous determination of the pK_a values of many compounds having similar structures.

ACKNOWLEDGEMENTS

This work was financially supported by the Murata Science Foundation and the Nippon Life Insurance Foundation, No. C88110012.

REFERENCES

1 Cs. Horváth, W. Melander and I. Molnar, *Anal. Chem.*, 49 (1977) 142.
2 S.N. Deming and M.L.H. Turoff, *Anal. Chem.*, 50 (1978) 546.
3 B. Rittich and M. Pirochtova, *J. Chromatogr.*, 523 (1990) 227.
4 J.W. Dolan, D.C. Lommen and L.R. Snyder, *J. Chromatogr.*, 535 (1990) 55.
5 F. Szokoli, Zs. Nemeth and J. Inczedy, *Chromatographia*, 29 (1990) 265.
6 B. Sachok, R.C. Kong and S.N. Deming, *J. Chromatogr.*, 199 (1980) 317.
7 C. Herrenknecht, D. Ivanovic, E.G. Nivaud and M. Guernet, *J. Pharm. Biomed. Anal.*, 8 (1990) 1071.
8 J.A. Lewis, D.C. Lommen, W.D. Raddatz, J.W. Dolan and L.R. Snyder, *J. Chromatogr.*, 592 (1992) 183.

9 T.B. Hoover, *Sep. Sci. Technol.*, 17 (1982) 295.
10 N. Hirayama and T. Kuwamoto, *J. Chromatogr.*, 508 (1990) 51.
11 N. Hirayama and T. Kuwamoto, *Anal. Chem.*, 65 (1993) 141.
12 J.A. Dean (Editor), *Lange's Handbook of Chemistry*, McGraw-Hill, New York, 13th ed., 1985.
13 J. Buckingham (Editor), *Dictionary of Organic Compounds*, Chapman and Hall, New York, 5th ed., 1982.
14 M.M. Davis and H.B. Hetzer, *J. Phys. Chem.*, 61 (1957) 123.
15 M. Kotake (Chief Editor), *Constants of Organic Compounds (Comprehensive Organic Chemistry Series)*, Asakura, Tokyo, 1963.

Journal of Chromatography, 639 (1993) 338–340
Elsevier Science Publishers B.V., Amsterdam

CHROM. 25 077

Short Communication

Determination of isocyanuric acid, ammelide, ammeline and melamine in crude isocyanuric acid by ion chromatography

Janusz K. Debowski* and Neil D. Wilde

AECI Limited, Research and Development Department, Modderfontein 1645 (South Africa)

(First received January 19th, 1993; revised manuscript received March 16th, 1993)

ABSTRACT

A reliable method for the determination of isocyanuric acid, ammelide, ammeline and melamine in crude isocyanuric acid is presented. The method involves using an ion chromatograph with an Omnipac PCX 500 column, 100 m*M* potassium chloride–200 m*M* hydrochloric acid–5% acetonitile solution as mobile phase and a UV detector at 215 nm.

INTRODUCTION

Isocyanuric acid is used mainly as a swimming pool stabilizer and as an intermediate in the preparation of its chloro derivatives. A reliable analytical method was required to determine the isocyanuric acid content and the impurities, ammelide, ammeline and melamine in crude isocyanuric acid. The structures of these compounds are shown opposite.

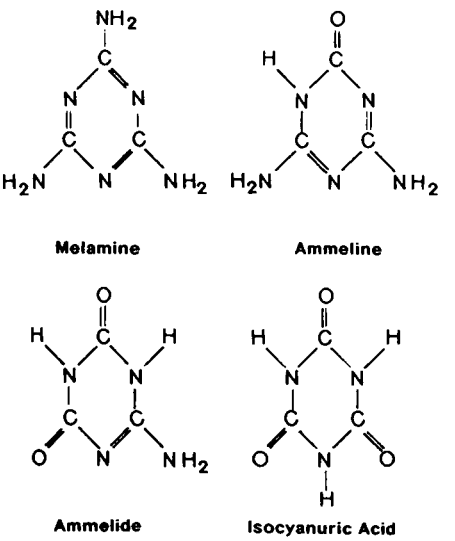

There are only a few reports relating to this problem. Although the thin-layer chromatography method [1,2] is satisfactory for qualitative analyses, the method is not entirely suitable for quantitative purposes. A gas chromatography method [3] required a preliminary derivatization procedure, which is considered a disadvantage because of the longer time required for sample preparation and the concomitant source of analytical errors.

Two HPLC methods [4,5] were also found to

* Corresponding author.

0021-9673/93/$06.00

be unsuitable for this particular application. The first one [4] (using a Lichrosorb RP-18 column, potassium phosphate buffer–methanol gradient, and a temperature of 2°C) produced broad, tailing peaks that were not completely separated. Although the second one [5] (using a Zorbax NH_2 column and acetonitrile–phosphate buffer solution) gave improved separations, the chromatograms were difficult to reproduce. This was possibly due to batch differences in Zorbax NH_2. Similar problems were also experienced with a method developed on a Diol column, which failed after replacing the column with one from a different batch. This implies that the above methods are very sensitive to small changes in stationary phase and are therefore unsuitable for routine use.

The method presented here is based on strong interaction between amines and cation-exchanger stationary phase and is considered to be an improvement upon existing procedures.

EXPERIMENTAL

Instrumentation

A Dionex 4500i ion chromatograph system equipped with a Dionex variable-wavelength detector VDM-2 at 215 nm, a Spectrophysics 4270 integrator, a manual-pneumatic injector with 10-μl sample loop, a Dionex Omnipac PCX-500 guard column (50 × 4.0 mm I.D.) and a Dionex Omnipac PCX-500 analytical column (250 × 4.0 I.D.) was used.

Chemicals and reagents

The isocyanuric acid, ammelide, ammeline and melamine were analytical-grade quality.

The mobile phase components, hydrochloric acid and potassium chloride, were analytical reagent grade, acetonitrile was HPLC grade and the water was purified through a Milli-R04/Milli-Q plus Millipore water purification system. The mobile phase was prepared to contain 100 m*M* potassium chloride, 200 m*M* hydrochloric acid and 5% acetonitrile in deionized water.

Procedure

Samples were dissolved in the mobile phase and filtered through a 0.45-μm nylon filter prior to injections. The conditions for the determination are shown in Fig. 1.

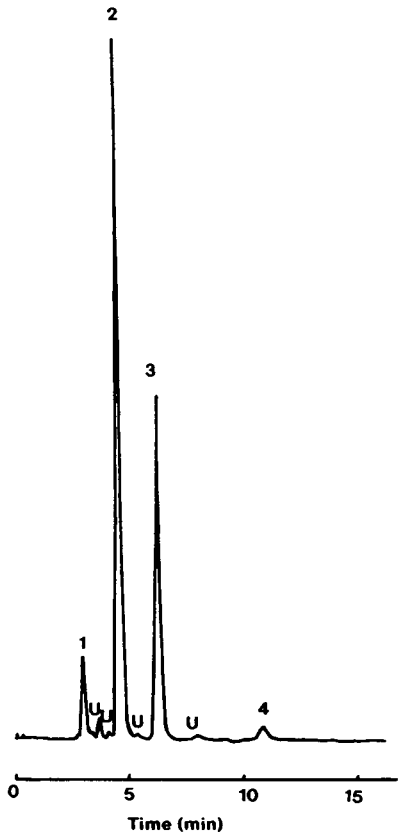

Fig. 1. Ion chromatogram of crude isocyanuric acid. Peaks: 1 = Isocyanuric acid; 2 = ammelide; 3 = ammeline, 4 = melamine; U = unknowns. Conditions: column, Omnipac PCX-500; injection, 10 μl; mobile phase, 100 m*M* potassium chloride–200 m*M* hydrochloric acid–5% acetonitrile. Flow-rate, 1.0 ml/min; UV detection at 215 nm.

The calibration graphs for isocyanuric acid, ammelide, ammeline and melamine were found to be linear within the following analytical ranges: 50–500 mg/l, 10–200 mg/l, 2–70 mg/l and 0.3–10 mg/l, respectively. The correlation coefficients were 0.99996, 0.99993, 0.99996 and 0.99998, respectively.

RESULTS AND DISCUSSIONS

The accuracy of the method was tested by adding known concentrations of isocyanuric acid, ammelide, ammeline and melamine to a typical crude isocyanuric sample dissolved in eluent and

TABLE I

RESULTS OF ISOCYANURIC ACID, AMMELIDE, AMMELINE AND MELAMINE IN A CRUDE ISOCYANURIC ACID SAMPLE

Compound	Concentration[a] (%, w/w)	R.S.D. (%)
Isocyanuric acid	70.4	2.6
Ammelide	23.9	2.1
Ammeline	4.2	1.2
Melamine	0.1	5.0
Total	98.6	

[a] Mean of five determinations.

determining the total amounts present. The recoveries varied between 100 and 102%, which indicated that the accuracy of this method was satisfactory.

The isocyanuric acid, ammelide, ammeline and melamine content of a typical crude isocyanuric acid sample is presented in Table I. A typical chromatogram of this sample is shown in Fig. 1.

As shown in Table I the total content is 98.6% (w/w). The balance of 1.4% can be related to the unidentified impurities clearly visible in Fig. 1.

It was also found that trichloroisocyanuric acid (TCICA) and dichloroisocyanuric acid sodium salt (DCICA) elute at the same time as isocyanuric acid. This can be explained by the conversion of all isocyanuric acid chloro derivatives into isocyanuric acid itself under existing chromatographic conditions (100 m*M* hydrochloric acid) [6]. The detection limits for isocyanuric acid, ammelide, ammeline and melamine were 50, 1.5, 0.6 and 0.3 ng, respectively.

REFERENCES

1 A. Cee and J. Gaspavic, *J. Chromatogr.*, 56 (1971) 342.
2 E. Knappe and I. Rodhewald, *Fresenius' Z. Anal. Chem.*, 223 (1966) 174.
3 P.G. Stoks and A.W. Schwartz, *J. Chromatogr.*, 168 (1979) 455.
4 P. Beilstein, A.M. Cook and R. Hütter, *J. Agric. Food Chem.*, 29 (1981) 1132.
5 T. Sugita, H. Ishiwata, K. Yoshihira and A. Maekawa, *Bull. Environ. Contam. Toxicol.*, 44 (1990) 567.
6 B. Solastiouk and X. Deglise, *Can. J. Chem.*, 66 (1988) 2188.

Journal of Chromatography, 639 (1993) 341–345
Elsevier Science Publishers B.V., Amsterdam

CHROM. 25 068

Short Communication

Chromatographic profiles of cyanogen bromide fragments of unreduced human serum albumin on immobilized Cibacron Blue F3G-A

Anna Compagnini, Maria Fichera, Salvatore Fisichella, Salvatore Foti* and Rosaria Saletti

Dipartimento di Scienze Chimiche, Università di Catania, V. le A. Doria 6, 95125 Catania (Italy)

(First received December 29th, 1992; revised manuscript received March 15th, 1993)

ABSTRACT

The elution profiles of cyanogen bromide fragments A (299–585), B (1–123), C (124–298) and D (1–298) of unreduced human serum albumin (HSA) on Cibacron Blue F3G-A immobilized on Sepharose CL-6B are reported. The binding properties of fragments C and D are similar to those of HSA, whereas fragment A shows a slightly lower retention time. Fragment B, in contrast, does not interact with the dye. The different chromatographic behaviour of fragments B and C allows their fast separation by combined use of gel permeation and dye–protein affinity chromatography.

INTRODUCTION

Dye–protein affinity chromatography has gained considerable importance for purification of proteins because of the advantages of using textile dyes as "pseudo-specific" ligands in place of natural biological molecules [1]. Cibacron Blue F3G-A is most commonly used in dye–protein affinity chromatography because of its ability to bind with apparent specificity to several proteins [2]. The interaction of Cibacron Blue F3G-A with proteins containing the dinucleotide fold has been explained by assuming that the dye resembles the NAD structure. However, Cibacron Blue F3G-A is also able to bind strongly to proteins that are known not to possess the dinucleotide fold [1].

Synthetic dyes commonly possess ionic groups and apolar aromatic ring systems in the same molecule, so that they can interact with the protein by ionic, hydrophobic or charge transfer forces. Presently, it is generally accepted that any protein that possesses clusters of apolar and/or ionic groups can interact with an apparent specificity with a dye molecule having appropriately spaced apolar and ionic groups [1–5]. The specificity of Cibacron Blue F3G-A for the nucleotide binding site thus appears to be a special case of the above-mentioned requirements. Human serum albumin (HSA) interacts strongly with Cibacron Blue F3G-A [6], and this property has been largely used for isolating HSA from human plasma.

We describe here the behaviour of four large

* Corresponding author.

0021-9673/93/$06.00

cyanogen bromide fragments of unreduced HSA with respect to Cibacron Blue F3G-A immobilized on Sepharose CL-6B in comparison with that of the intact HSA molecule.

EXPERIMENTAL

Materials and apparatus

Cibacron Blue F3G-A immmobilized on Sepharose CL-6B was obtained from Fluka (Buchs, Switzerland). Sephadex G-100 was provided by Pharmacia LKB (Uppsala, Sweden), HSA (Cohn Fraction V), iodoacetamide, and cyanogen bromide were purchased from Sigma (Milan, Italy). Carboxymethyl Cellulose (CM32) was obtained from Whatman (Maidstone, UK). Spectra/Por 6 dialysis membrane was obtained from Roth (Karlsruhe, Germany). All other chemicals were of the highest purity commercially available and were used without further purification. All column chromatographies were performed using Amicon glass columns. Eluates were monitored by an HP 1050 UV detector equipped with a preparative cell and coupled with an HP 3396A integrator (Hewlett-Packard). Sodium dodecyl sulphate–polyacrylamide gel electrophoresis was performed using the discontinuous method of Laemmli [7] on 12.5% (w/v) gels on a Bio-Rad instrument. Amino acid analyses were performed on a Beckman Model 119 CL amino acid analyser after acidic hydrolysis with 6 *M* hydrochloric acid for 24 h at 105°C. Circular dichroic (CD) spectra in the far-ultraviolet region of albumin solutions and isolated fragments were measured on a Jasco J-600 instrument, in the wavelength region 200–250 nm, at a protein concentration of 2.1 μM in 0.025 *M* phosphate buffer pH 7.0, using a path length of 0.5 cm.

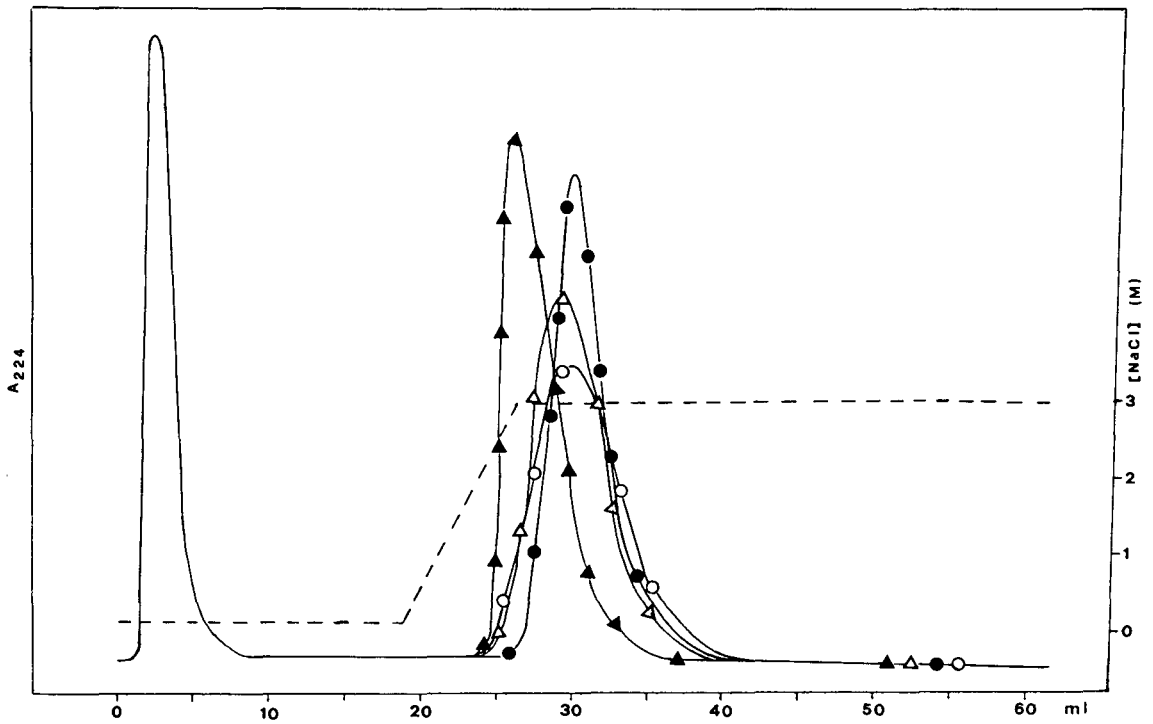

Fig. 1. Dye–protein affinity chromatography of HSA (●) and A (▲), B (—), C (△) and D (○) fragments on Cibacron Blue F3G-A–Sepharose CL-6B. The column (1.2 cm × 1 cm I.D.) was equilibrated with 0.01 *M* phosphate buffer, pH 7.5. After application of each sample the column was eluted at room temperature and at a flow-rate of 0.25 ml/min with equilibration buffer (19 ml), then with a linear gradient (----) of 0–3 *M* NaCl in phosphate buffer 0.01 *M* (8 ml) and finally with 3 *M* NaCl in phosphate buffer 0.01 *M* (35 ml).

Preparation of A, B, C and D cyanogen bromide fragments of unreduced HSA

A modification of previously described methods [8,9] was used to prepare A, B, C and D cyanogen bromide fragments of unreduced HSA. In a typical procedure the free thiol group (cysteine 34) of HSA was blocked adding 1.7 mg (six-fold molar excess) of iodoacetamide to a solution of 100 mg of HSA in 2 ml of Tris buffer 0.1 *M*, pH 8.5. The mixture was reacted for 1 h at room temperature in the dark, keeping the pH above 8 during the reaction. The solution was then dialysed against water, freeze-dried and redissolved in 1 ml of 70% formic acid. A solution of 140 mg of cyanogen bromide dissolved in 1.7 ml of 70% formic acid was added and the mixture allowed to react for 25 h at 4°C in the dark, then diluted by adding 25 ml of water, cooled in liquid nitrogen and freeze-dried. The residue, dissolved in 10 ml of 0.1 *M* NaCl in 5% propionic acid, was applied to a Sephadex G-100 column (100 cm × 3.2 cm I.D.) previously equilibrated with 0.1 *M* NaCl in 5% propionic acid. The column was eluted at room temperature using the same buffer at a flow-rate of 1 ml/min. Two fractions (peaks I and II) were collected separately and further resolved on a Whatman CM32 column. Peak I was diluted twice by water, the pH raised to 3.2, applied on a Whatman CM32 column (9 cm × 1.6 cm I.D.) and eluted at a flow-rate of 1 ml/min with a linear gradient of 0.075 *M*–0.3 *M* NaCl in phosphate buffer 0.01 *M*, pH 2.7, over 20 h. Fragments A and D were thus obtained. Peak II was fractionated in the same way, except that the starting buffer was 0.05 *M* NaCl in phosphate buffer 0.01 *M*, to give fragments B and C. Pooled peaks A, B, C and D were dialysed against water and freeze-dried. The identity of the isolated fractions was confirmed by polyacrylamide gel electrophoresis and amino acid analysis.

Column chromatography of HSA and fragments A, B, C and D on Cibacron Blue F3G-A–Sepharose CL-6B

About 3 mg of HSA and of each fragment were individually applied on the column packed with Cibacron Blue F3G-A–Sepharose CL-6B. The column was eluted according to the conditions described in Fig. 1.

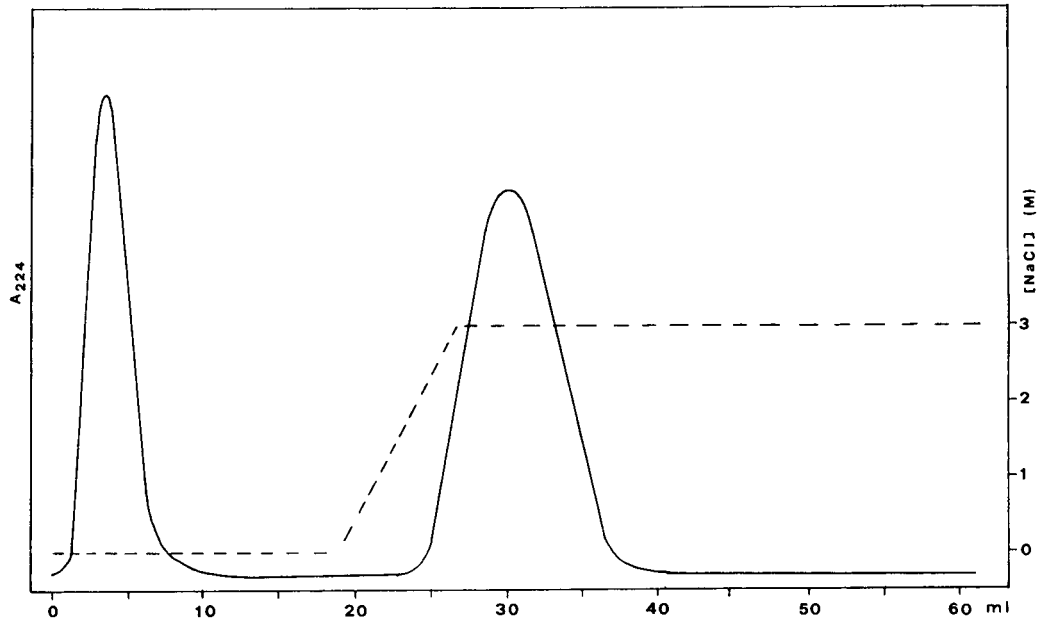

Fig. 2. Dye-protein affinity chromatography of peak II from G-100 on Cibacron Blue F3G-A–Sepharose CL-6B. Elution conditions were identical to those described in Fig. 1.

Column chromatography of peak II from Sephadex G-100 on Cibacron Blue F3G-A–Sepharose CL-6B

Peak II collected from the Sephadex G-100 column was dialysed against water and freeze-dried. About 10 mg of the sample were re-dissolved in 500 μl of 0.01 *M* phosphate buffer and applied on a column packed with Cibacron Blue F3G-A–Sepharose CL-6B. The column was eluted according to the conditions described in Fig. 2.

RESULTS AND DISCUSSION

The cleavage of unreduced HSA by cyanogen bromide gives rise to three large fragments which, according to the naming convention of McMenamy *et al.* [8], are called A, B and C (Table I).

Fragment C consists of a single polypeptide chain. Fragments A and B are composed of four and two subfragments, respectively, held together by disulphide bonds. Furthermore, incomplete cleavage at methionine 123 originates fragment D, which consists of fragments B and C linked through the uncleaved methionine [10].

To determine to what extent the secondary structure of the isolated A, B and C fragments used in this work was preserved, the CD spectra in the far-UV region were recorded. The CD

TABLE I

CYANOGEN BROMIDE FRAGMENTS OF UNREDUCED HSA

Fragment	Sequence	M_r [a]	Subfragments
A	299–585	32391	299–329 330–446 447–548 549–585
B	1–123	14040[b]	1–87 88–123
C	124–298	19990	–
D	1–298	34042	1–87 88–298

[a] Homoserine is considered to be the C-terminal amino acid.
[b] Cysteine 34 blocked with iodoacetamide.

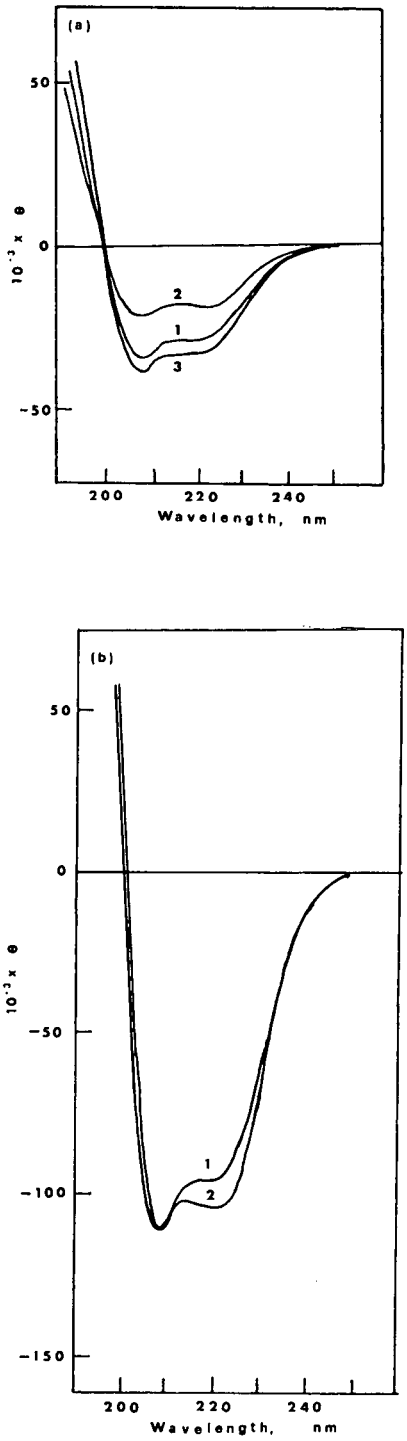

Fig. 3. Circular dichroic spectra of HSA and HSA fragments A, B and C in the far-ultraviolet region. (a) 1 = Fragment A; 2 = fragment B; 3 = fragment C; (b) 1 = equimolar mixture of A, B and C fragments; 2 = HSA.

spectra of the isolated fragments are reported in Fig. 3a. In Fig. 3b the spectra of albumin and of the equimolar mixture of the three fragments are compared. According to an earlier report [11], the spectra in Fig. 3 indicate that the secondary structure of isolated fragments is not basically impaired and that the slight decrease in the helix content observed is probably the result of disruption of bonds stabilizing the albumin tertiary structure rather than irreversible denaturation of the fragments [11].

The chromatographic pattern of HSA and A, B, C and D fragments on the Cibacron Blue F3G-A–Sepharose CL-6B column is reported in Fig. 1. Fragment B is eluted by 0.01 *M* phosphate buffer with the void column volume. The elution profile of fragments C and D is similar to that of HSA, whereas fragment A shows a slight lower retention time.

From these results it appears clearly that fragment B does not show any interaction with immobilized Cibacron Blue F3G-A, whereas fragments C and D, and to a lesser extent fragment A, interact with the dye similarly to HSA.

Since the CD spectra indicate that the secondary structure of fragments A, B and C remains essentially unchanged after cyanogen bromide cleavage, the absence of interaction for fragment B does not seem to be attributable to its denaturation. Therefore, it is very likely that the intact HSA molecule also does not present interaction sites for the immobilized dye in the sequence 1–123. The same considerations suggest, instead, that one or more interaction sites are present in each of the sequences 124–298 and 299–585 of HSA.

The different chromatographic behaviour of fragments B and C on Cibacron Blue F3G-A–Sepharose CL-6B allows their easy separation by combined use of gel permeation and dye–protein affinity chromatography.

As described in the Experimental section, peak II obtained from the Sephadex G-100 column contains unresolved fragments B and C. When peak II is applied to a Cibacron Blue F3G-A–Sepharose CL-6B column and eluted as described in Fig. 2, two peak are obtained (Fig. 2), one eluted very early by phosphate buffer and the second by 3 *M* NaCl. Gel electrophoresis and amino acid analysis identify the two peaks as highly purified fragments B and C.

As can be seen from Fig. 2, dye–protein affinity chromatography allows the separation of these two fragments in a considerably shorter time than conventional ion-exchange chromatography.

CONCLUSIONS

The three large cyanogen bromide fragments, A, C and D, interact with Cibacron Blue F3G-A immobilized on Sepharose CL-6B in a similar way to HSA, whereas fragment B does not interact with the dye. The different chromatographic behaviour of fragments B and C allows their fast separation by combined use of gel permeation and dye-protein affinity chromatography.

ACKNOWLEDGEMENT

Financial support by MURST is gratefully acknowledged.

REFERENCES

1 S.B. McLoughlin and C.R. Lowe, *Rev. Prog. Coloration*, 18 (1988) 16.
2 S. Subramanian, *Crit. Rev. Biochem.*, 16 (1984) 169.
3 G. Birkenmeier, in M.A. Vijayalakshmi and O. Bertrand (Editors), *Protein–Dye Interaction: Developments and Applications*, Elsevier, London, 1989, p. 253.
4 S. Subramanian, in M.A. Vijayalakshmi and O. Bertrand (Editors), *Protein–Dye Interaction: Developments and Applications*, Elsevier, London, 1989, p. 56.
5 G. Kopperschlager, H.J. Bohme and E. Hofmann, *Adv. Biochem. Eng.*, 25 (1982) 101.
6 J. Travis, J. Bowen, D. Tewksbury, D. Johnson and R. Pannell, *Biochem. J.*, 157 (1976) 301.
7 U.K. Laemmli, *Nature*, 227 (1970) 680.
8 R.H. McMenamy, H.M. Dintzis and F. Watson, *J. Biol. Chem.*, 246 (1971) 4744.
9 B. Meloun, M.A. Saber and J. Kusnir, *Biochim. Biophis Acta*, 393 (1975) 505.
10 C. Lapresle and N. Doyen, *Biochem. J.*, 151 (1975) 637.
11 Z. Hrkal, M. Kodíček, Z. Vodrážka, B. Meloun and L. Morávek, *J. Biochem.*, 9 (1978) 349.

Journal of Chromatography, 639 (1993) 346–351
Elsevier Science Publishers B.V., Amsterdam

CHROM. 25 022

Short Communication

Purification of two proteinases from *Aspergillus terreus* by affinity chromatography

Miglena E. Stefanova*

Institute of Biochemistry and Physiology of Microorganisms, Russian Academy of Sciences, 142292 Pushchino, Moscow Region (Russian Federation)

(First received January 4th, 1993; revised manuscript received February 26th, 1993)

ABSTRACT

A simple and effective method for purification of proteinases from *Aspergillus terreus* is described. A combination of three chromatographic techniques is proposed, starting with affinity chromatography on bacitracin–silochrome. This first stage is crucial for the enzyme separation and leads to almost full removal of contaminating proteins. It is followed by gel permeation and ion-exchange chromatography. Using this method, two extracellular proteinases (I and II) were purified from the culture filtrate of *A. terreus*. They had molecular masses of approximately 37 000 and 21 000 as determined by sodium dodecyl sulphate–polyacrylamide gel electrophoresis. The inhibitory analysis revealed that proteinase I is a serine thiol-dependent enzyme and proteinase II is a metalloproteinase. The latter was activated by the addition of magnesium and cobalt ions.

INTRODUCTION

Proteolytic enzymes have been attractive for many years because of their key role in cell metabolism as well as their practical application. Their capacity for selective protein modification (*e.g.* of enzymes and hormones) by means of limited cleavage suggests that some proteinases have regulatory functions in cellular processes [1]. Various methods of purification of proteinases from different sources have been proposed in the literature, including ammonium sulphate, ethanol and acetone precipitation, a variety of conventional chromatographic techniques (*e.g.* ion exchange, gel filtration) and preparative electrophoretic techniques [2,3]. Most of them are time and labour consuming because they include too many steps. The application of affinity sorbents, especially at earlier stages of separation, considerably simplifies the procedure and increases its effectiveness. In the present paper we report the development of a simple three-step scheme for purification of two extracellular proteinases from *Aspergillus terreus* using affinity chromatography and describe some properties of these enzymes.

EXPERIMENTAL

Chemicals

Materials were obtained from the following sources: bacitracin–silochrome was a generous

* Address for correspondence: Department of Enzyme Biosynthesis, Institute of Microbiology, Bulgarian Academy of Sciences, Acad. G. Bontchev str., Bl. 26, 1113 Sofia, Bulgaria.

0021-9673/93/$06.00

gift from Dr. G. Rudenskaya (Faculty of Chemistry, Lomonosov Moscow State University, Moscow, Russian Federation); Sephadex G-25, ribonuclease A and chymotrypsinogen A were from Pharmacia (Sweden); ovalbumin, Coomassie brilliant blue (CBB) R-250, phenylmethylsulphonyl fluoride (PMSF), 1,4-dithiothreitol (DTT), sodium dodecyl sulphate (SDS) and CM-cellulose, sodium salt, with degree of polymerization (DP) 500, were purchased from Serva (Germany); DEAE–Spheron 1000 and 4-hydroxymercuribenzoic acid, sodium salt (PHMB), were from Chemapol (Czechoslovakia). All other chemicals were of reagent grade.

Organism and culture conditions

The strain *Aspergillus terreus* VKM F-2200 D was grown in a medium with the following composition (in %, w/v): peptone (0.05), KH_2PO_4 (0.14), $CaCl_2$ (0.03), $MgSO_4 \cdot 7H_2O$ (0.03), urea (0.01), CM-cellulose, sodium-salt (1), $FeSO_4$ (0.0005), $MnSO_4$ (0.00016), $ZnSO_4$ (0.00014), $CuSO_4$ (0.00014). Fermentation was carried out at 28°C for 48 h with an agitation speed of 240 rpm.

Enzyme purification

Buffers used were as follows: (A) 0.1 *M* sodium acetate pH 5.0; (A_1) 0.05 *M* sodium acetate pH 5.0; (B) 0.025 *M* Tris–HCl pH 9.3. All purification steps were carried out at 4°C. Cells were removed by centrifugation (1800 *g*, 30 min). The pH of the cell-free medium was adjusted to 5.0, and 2600 ml were applied to a chromatographic column (10 × 1.4 cm) containing bacitracin–silochrome equilibrated with buffer A. The elution was performed with 1 *M* sodium chloride in 25% isopropanol. Fractions containing proteinase activity were pooled (total volume 95 ml). A 190-ml volume of eluate from two chromatographic runs was concentrated by ultrafiltration (Amicon UM 2 membrane). The concentrate thus obtained was dialysed on a Sephadex G-25 column (25 × 5 cm) equilibrated with buffer B, at a flow-rate of 120 ml/h. Fractions of 5.8 ml were collected. The protein fraction was collected and loaded onto a column of DEAE-Spheron equilibrated with the same buffer. The elution was performed using a linear gradient of 0–0.3 *M* sodium chloride in buffer B. The active fractions were pooled and stored at −10°C for several months without any loss of activity.

Enzyme and protein assays

Protein was determined by the method of Bradford [4] with bovine serum albumin as a standard. Protein concentrations in the column eluates were monitored by measuring the absorbance at 280 nm.

Proteinase activity was measured by the release of tyrosine from 1% casein. A 1-ml aliquot of enzyme was incubated with 1 ml of casein (prepared according to the procedure of Hammarsten [16] 1% in 0.1 *M* Tris–HCl pH 7.0) at 40°C for 20 min. The enzyme reaction was stopped with 1 ml of 10% trichloroacetic acid. Samples were filtered and the absorbance in filtrates was measured at 280 nm against an appropriate blank. One unit of enzyme activity was defined as the amount of enzyme required to catalyse the liberation of 1 μM tyrosine for 1 min at 40°C and pH 7.0.

Sodium dodecyl sulphate–polyacrylamide gel electrophoresis (SDS-PAGE)

SDS-disc PAGE was performed according to Laemmli [5] after boiling the samples with β-mercaptoethanol and SDS using 15% acrylamide (separating gel) and 6% stacking gel. A Pharmacia electrophoresis system (EPS 500/400, GE-2/4) was used. The electrophoresis was done at 150 V, 2 mA per gel rod. Gels were stained for proteins with CBB R-250. Ovalbumin (M_r 43 000), chymotrypsinogen A (25 000) and ribonuclease A (13 700) were used as molecular mass marker proteins.

RESULTS AND DISCUSSION

Separation and purification of proteinase components

The results of a typical purification procedure are presented in Table I. The crucial purification stage was the affinity chromatography on bacitracin–silochrome. The pH of the supernatant fluid had to be adjusted to 5.0 beforehand so

TABLE I

PURIFICATION OF *ASPERGILLUS TERREUS* PROTEINASES

Step	Total volume (ml)	Total activity ($U \times 10^{-3}$)	Specific activity ($U \times 10^{-3}$/mg)	Yield (%)	Purification (*n*-fold)
Culture supernatant	5200	41 340	72	100	1
Bacitracin–silochrome	190	32 656	1814	79	25
Sephadex G-25	142	20 708	5597	50	78
DEAE–Spheron					
Proteinase I	25	8138	5425	20	75
Proteinase II	45	2344	1116	6	15

that the proteinases could completely adsorb on the affinity sorbent. At the original pH (6.5–7.0) the enzymes were easily washed out of the column with acetate buffer. Except for proteinases, peptides and some endoglucanase activity (measured by the decrease in the viscosity of CM-cellulose) were retained on bacitracin–silochrome at pH 5.0 too. The latter was removed by extensive washing of the column with diluted acetate buffer (0.05 *M*) before performing the elution. Our attempts to desorb the proteinases with 1 *M* sodium chloride only failed (data not shown). This suggested that lowering the dielectric constant of the medium could perhaps increase the electrostatic interaction of the proteins with the eluent and thus facilitate the elution. Indeed proteinases were eluted with isopropanol solution of high ionic strength (Fig. 1). The enzyme preparation thus obtained was almost completely free from contaminating proteins, as indicated by the considerable increase (25-fold) in the specific proteinase activity (Table I).

Bacitracin-based affinity sorbents (Sepharose and silochrome) have been described previously as suitable matrices for purification of proteinases of different type and origin [6]. They provide both a high purification factor and a high yield of activity [7,8]. In our case bacitracin–Sepharose was unsuitable because of the presence of cellulases secreted by the fungus. First, they would adsorb on Sepharose, thus complicating the purification procedure and, second, could degrade it. But when the affinity ligand was coupled to silochrome (macroporous silica compound) it proved to be very effective in purification of *A. terreus* proteinases, providing a 79% recovery. This high effectiveness is due to the specific interaction between the peptide antibiotic bacitracin and the substrate-binding site of proteinases [9].

Further proteinases were concentrated by ultrafiltration and desalted on a Sephadex G-25 column. This was accompanied by the removal of the peptides from the enzyme preparation. The protein fraction (void volume of the column)

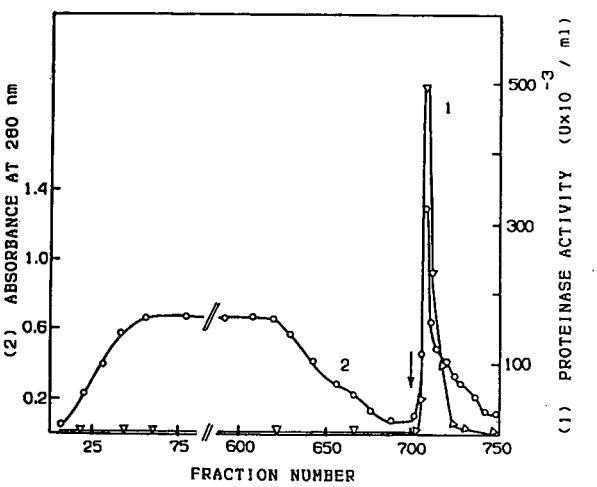

Fig. 1. Chromatography on the affinity sorbent of *A. terreus* proteinases. The column (10×1.4 cm) was prepacked with bacitracin–silochrome and equilibrated with buffer A. The supernatant fluid at pH 5.0 was applied to the column at a flow-rate of 40 ml/h. After washing the column with 200 ml of buffer A_1 the enzymes were eluted with 1 *M* sodium chloride in 25% isopropanol at the same flow-rate. Fractions of 4 ml were collected. The arrow indicates the beginning of the elution.

was fully adsorbed on an anion exchanger, DEAE–Spheron, at pH 9.3 and eluted with a linear sodium chloride gradient as two proteinase peaks (I and II) at 0.11 *M* and 0.22 *M* sodium chloride concentration, respectively (Fig. 2).

On SDS-PAGE proteinase II migrated as a homogeneous band (Fig. 3) with a molecular mass of 21 000, while proteinase I was purified to near homogeneity. It contained a major protein with molecular mass of 37 000 and a minor one with lower molecular mass.

Thus, two proteinases, I and II, were separated and purified from the culture filtrate of *A. terreus* with purification factors of 75 and 15 and recoveries of 20% and 6%, respectively. A considerable loss of activity of proteinase II after ion-exchange chromatography was observed. Most probably this is caused by chelating of the co-factor (see below) by the resin (Spheron is based on polymethacrylic acid) under the experimental conditions.

In most cases procedures for obtaining homogeneous and highly purified proteins include at least 4–5 different steps. In this paper we propose a simple and effective purification scheme of three stages which produces two purified proteinases by means of affinity ligand. Usually, starting the separation with a biospecific

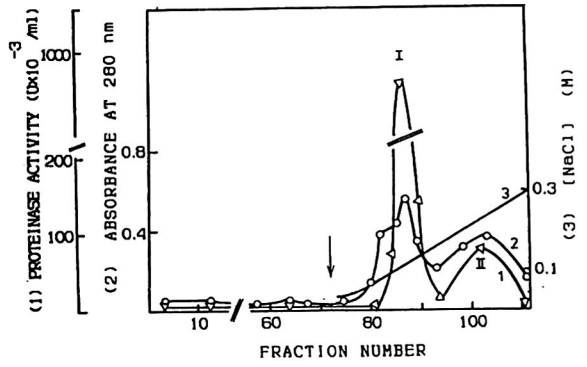

Fig. 2. Ion-exchange chromatography of proteinases from *A. terreus*. The protein fraction obtained after gel-permeation chromatography was loaded onto a column (10 × 1.4 cm) containing DEAE–Spheron previously equilibrated with buffer B. The column was washed with three bed volumes of the same buffer. Chromatography conditions were as follows: flow-rate, 25 ml/h; fraction volume, 2.5 ml; eluent, linear gradient 0–0.3 *M* sodium chloride in the equilibrating buffer.

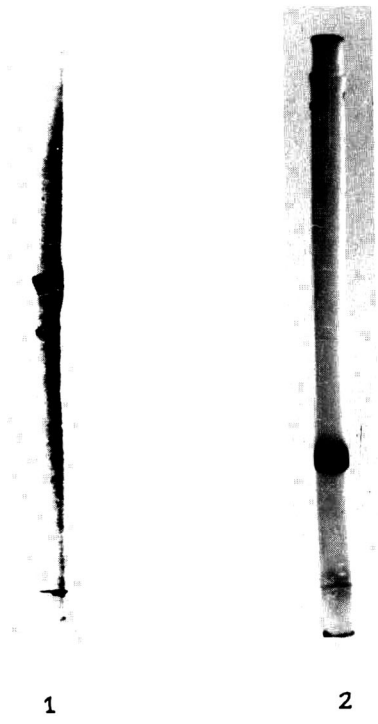

Fig. 3. SDS-PAGE pattern of the purified proteinases from *A. terreus* after chromatography on DEAE–Spheron. Experimental conditions are described in the text. 1 = Proteinase I; 2 = proteinase II.

adsorbent considerably simplifies the procedure while at the same time keeping yield high. Mosolova *et al.* [8] acquired homogeneous Glu, Asp-specific proteinase from *Actinomyces* sp. in three stages using chromatography on bacitracin–silochrome. Homogeneous carboxylic proteinase from *Aspergillus niger* was obtained in three steps by chromatography on pepstatin–Sepharose [10].

Effect of some reagents on proteinase activity

Proteinase I was fully inhibited by PMSF (Table II), which indicates the presence of serine residues in the active centre. Like most serine proteinases, it was insensitive to the chelating agents EDTA and 1,10-phenanthroline. The cysteine-binding inhibitor PHMB reduced the enzyme activity to zero, while in the presence of the reducing agent DTT a 30% increase in activity was observed. These findings indicated

TABLE II

EFFECT OF SOME REAGENTS ON PROTEINASE ACTIVITY

Aliquots of 1 ml of the enzyme were incubated with 50 μl of each reagent solution (final concentration 10 m*M*) for 1 h at room temperature. After that the enzyme reaction was carried out according to the standard assay procedure and the residual enzyme activity was determined. The activity of untreated enzyme was taken as 100%.

Reagent	Residual activity (%)	
	Proteinase I	Proteinase II
EDTA	95	6
1,10-Phenanthroline	98	66
PMSF	0	73
PHMB	0	32
DTT	130	60
Ca^{2+}	72	98
Cd^{2+}	12	16
Co^{2+}	44	140
Cu^{2+}	37	35
Mg^{2+}	81	142
Mn^{2+}	62	92
Zn^{2+}	0	27

activity and that proteinase I may be related to the subfamily of thiol-dependent serine proteinases described by Stepanov *et al.* [11]. The only enzyme of this group from *Aspergillus* fungi reported until now seems to be the intracellular proteinase from *A. niger* [12]. Cd^{2+} and Zn^{2+} almost completely inhibited enzyme activity, while the other metal ions tested were less effective —28–63% inhibition.

The inhibitory analysis of proteinase II showed more complicated results (Table II). The residual activity after EDTA treatment was 6%, suggesting that proteinase II is a metalloproteinase. At the same time 1,10-phenanthroline caused only 44% loss of activity.

Some authors have reported inhibitory effect of reducing agents (DTT, cysteine, β-mercaptoethanol) on neutral metalloproteinases because of their ability to chelate metal ions [13]. The metalloproteinase II from *A. terreus* was inhibited by DTT (Table II).

Proteinase II was activated by Mg^{2+} and Co^{2+} and strongly inhibited by Cd^{2+}, Cu^{2+} and Zn^{2+}. The enzyme activity was not influenced by Ca^{2+}. The same effect of metal ions tested was observed with the "acid" metalloproteinase from *A. oryzae* [14]. The metalloproteinase from *Penicillium roqueforti* was activated twice in the presence of 10 m*M* Co^{2+} [15]. This and some other properties of the *A. terreus* enzyme —low M_r (about 20 000) and pH optimum about 6–7 (data not shown)— are characteristic of the "acid" fungal metalloproteinases from *Aspergillus* and *Penicillium* [14,15].

Bearing in mind the effect of chelating agents and metal ions mentioned above, it is quite possible that the present (and the others described as "acid" in the literature) metalloproteinase may contain Mg^{2+} or Co^{2+} as a cofactor since both these ions increase enzyme activity to an equal extent and, in contrast to EDTA, are very weakly (if at all) chelated by 1,10-phenanthroline.

To summarize, in present communication we report on the purification of two novel proteinases, first identified in a strain of *Aspergillus terreus*. Further biochemical and enzymological characterization of these enzymes will be the subject of a subsequent paper.

ACKNOWLEDGEMENTS

This work was supported by research funds from the Bulgarian Ministry of Science and Education and the Institute of Biochemistry and Physiology of Microorganisms, Russian Academy of Sciences. Thanks are due to Dr. G. Rudenskaya (Faculty of Chemistry, Lomonosov Moscow State University) for the kind supply of bacitracin–silochrome. The author is also indebted to Professor I. Kulaev and Dr. O. Beletskaya (Institute of Biochemistry and Physiology of Microorganisms, Russian Academy of Sciences) for their constant interest in this work and Dr. J. Karadjov (Bulgarian Academy of Sciences) for the valuable discussions during the preparation of this manuscript.

REFERENCES

1 J.S. Bond and R.J. Beynon, *Molec. Aspects Med.*, 9 (1987) 173–287.

2 S. Chandrasekaran and S.C. Dhar, *Arch. Biochem. Biophys.*, 257 (1987) 402–408.
3 T.-R. Yan, N. Azuma, S. Kaminogawa and K. Yamauchi, *Appl. Environ. Microbiol.*, 53 (1987) 2296–2302.
4 M. Bradford, *Anal. Biochem.*, 72 (1976) 248–254.
5 U.K. Laemmli, *Nature*, 227 (1970) 680–685.
6 V.M. Stepanov, G.N. Rudenskaya, A.V. Gaida and A.L. Osterman, *J. Biochem. Biophys Methods*, 5 (1981) 177–186.
7 L.I. Vasil'eva, G.N. Rudenskaya, I.N. Krestyanova, O.M. Khodova, Y.E. Bartoshevich and V.M. Stepanov, *Biokhimiya*, 50 (1985) 355–362.
8 O.V. Mosolova, G.N. Rudenskaya, V.M. Stepanov, O.M. Khodova and I.A. Tsaplina, *Biokhimiya*, 52 (1987) 414–422.
9 A.V. Gaida, Yu.U. Magerovsky and V.A. Monastyrsky, *Biokhimiya*, 52 (1987) 569–576.
10 I. Kregar, I. Maljevac, V. Ruizdar, M. Derencin, A. Puc and V. Turk, in V. Turk and Lj. Vitale (Editors), *Proteinases and their Inhibitors*, Pergamon Press, Oxford, 1981, pp. 223–230.
11 V.M. Stepanov, G.G. Chestukhina, G.N. Rudenskaya, A.S. Epremyan, A.L. Osterman, O.M. Khodova and L.P. Belyanova, *Biochem. Biophys. Res. Commun.*, 100 (1981) 1680–1687.
12 H. Stevens, S.A. Hulea, D. Duncan, S. Vasu and I. Brad, *Rev. Roum. Biochim.*, 18 (1981) 63–66.
13 Y.-S. Cheng and D. Zipser, *J. Biol. Chem.*, 254 (1979) 4698–4706.
14 T.I. Vaganova, N.M. Ivanova and V.M. Stepanov, *Biokhimiya*, 53 (1988) 1344–1351.
15 J.S. Gripon, B. Auberger and J. Inoir, *Int. J. Biochem.*, 12 (1980) 451–455.
16 Hammarsten, *Catalogue No. 2242*, E. Merck, Darmstadt.

Journal of Chromatography, 639 (1993) 352–358
Elsevier Science Publishers B.V., Amsterdam

CHROM. 25 072

Short Communication

Determination of carbaryl and some organophosphorus pesticides in drinking water using on-line liquid chromatographic preconcentration techniques

M.R. Driss

Faculté de Médecine Dentaire, Rue Fattouma Bourguiba, 5019 Monastir (Tunisia)

M.-C. Hennion

Ecole Supérieure de Physique et Chimie de Paris, Laboratoire de Chimie Analytique, 10 Rue Vauquelin, 75231 Paris Cedex 05 (France)

M.L. Bouguerra*

Département de Chimie, Faculté des Sciences, Campus Universitaire, Le Belvédère, 1060 Tunis (Tunisia)

(First received September 29th, 1992; revised manuscript received March 9th, 1993)

ABSTRACT

Reversed-phase high-performance liquid chromatography (HPLC) was adapted for the determination of trace concentrations of carbaryl and seven organophosphorus pesticides in drinking water. Between 100 and 300 ml of water sample is passed through a 1.5-cm precolumn, packed with C_{18}-bonded silica or styrene–divinylbenzene copolymer (PRP-1) sorbent at a flow-rate of 3 ml/min. The HPLC system is then switched to an acetonitrile–water gradient elution programme. The analytes that have been concentrated on the precolumn are eluted and separated on a 15-cm C_{18} analytical column and are determined by measuring their UV absorption at 254 nm. This wavelength was selected as the optimum for the simultaneous determination of these pesticides. The preconcentration yields of the examined solutes obtained with the two types of precolumn are almost identical. Band broadening is avoided by a suitable choice of the C_{18} precolumn and the analytical column. With 200 ml of tap water, the recoveries for most of the examined pesticides were *ca.* 90%, except for carbaryl (54%). The detection limits are in the range 0.03–0.2 μg/l.

INTRODUCTION

Organophosphorus pesticides (OPPs) are currently used in agriculture and animal husbandry for crop protection and control of ectoparasites. However, although the OPPs are generally used alone, they may also be applied in conjunction with the carbamate insecticide carbaryl for the control of pests showing resistance to OP compounds [1,2]. Because of their widespread use, they have been found in groundwaters, surface

* Corresponding author.

0021-9673/93/$06.00

waters, lagoons and drinking water at concentrations varying from 20 ng/l up to 127 μg/l [3–7]. There is an increasing need for rapid, reliable methods to measure pesticide concentrations in waters.

Determinations of OPPs are generally carried out by gas chromatography (GC) with nitrogen–phosphorus detection (NPD) [3,8,9] or flame photometric detection (FPD) [10,11]. However, these methods are inapplicable to carbamates, which are too thermally labile. Azinphos-methyl, parathion and some polar OPPs are also difficult to determine by GC [12]. The use of liquid chromatographic (LC) methods is suitable for thermally labile and polar pesticides. Nevertheless, it should be taken into account that UV detection in LC is usually at least 2.5 orders of magnitude less sensitive than GC–FPD and GC–NPD [13]. This has led to the development of postcolumn reactions to enhance detection in LC. The great potential of postcolumn LC systems has recently been demonstrated [2,14–16]. Postcolumn reaction detection has been used for the trace determination of N-methylcarbamates in surface water samples [17]. Moreover, the monitoring of these compounds and OPPs at concentrations lower than the ppb (μg/l) level requires a trace enrichment step. Sample preconcentration based on solid-phase extraction (SPE) has been shown to be a good alternative to time-consuming liquid–liquid extraction and can be used in both off-line and on-line GC and LC methodologies. Several methods using off-line SPE have been developed for the LC–UV determination of selected carbamates and OPPs in aqueous samples [18–23]. However, disadvantages and problems still remain, such as sample/analyte dilution, possible contamination and lengthy sample preparation procedures. Many of these drawbacks can be avoided by using on-line enrichment on a precolumn packed with a suitable sorbent. In this case, the adsorbed analytes are then eluted directly from the precolumn into the analytical column. This technique has been used in the determination of many organic pollutants in aqueous samples [24,25], such as chlorophenoxy acid [26,27], chlorotriazine [28–30] and organochlorine [31], carbamate [32] and OP [33] pesticides. In the last instance, the precolumn used was packed with XAD-2 resin. However, the disadvantage of XAD resins is the generation of artifacts that are subsequently laborious to eliminate.

In this paper, we report the development of an HPLC method using on-line enrichment for the determination of carbaryl and seven OPPs in drinking water samples. The parameters investigated included analytical LC separation, the optimum wavelength for the simultaneous determination of these pesticides, the rate of sample loading on to the precolumn, the nature of the sorbent used in the precolumn and the dependence of the recovery on the sample volume. The eight pesticides chosen are of concern for the Tunisian environment [34–36].

EXPERIMENTAL

Solvents

HPLC-grade acetonitrile was purchased from Rathburn (Walkerburn, UK) and methanol from Prolabo (Paris, France). LC-quality water was prepared by purifying demineralized water with a Milli-Q filtration system (Millipore, Bedford, MA, USA).

Pesticides

The pesticide standards (Fig. 1) were purchased from several suppliers: parathion, parathion-methyl and azinphos-ethyl from Fluka (Buchs, Switzerland), azinphos-methyl and carbaryl from Serva (Heidelberg, Germany), diazinon from Supelco (Bellefonte, PA, USA) and phosmet and fenitrothion from Société Tunisienne des Engrais Chimiques (Mégrine, Tunisia). The purities of the individual standards ranged from 97.5 to 99.5%.

Standard preparation

Stock solutions of selected pesticides were prepared by weighting and dissolution in methanol. Milli-Q-purified water samples were spiked with these solutions at the ppb (μg/l) level. The final standard solutions did not contain more than 0.5% of methanol.

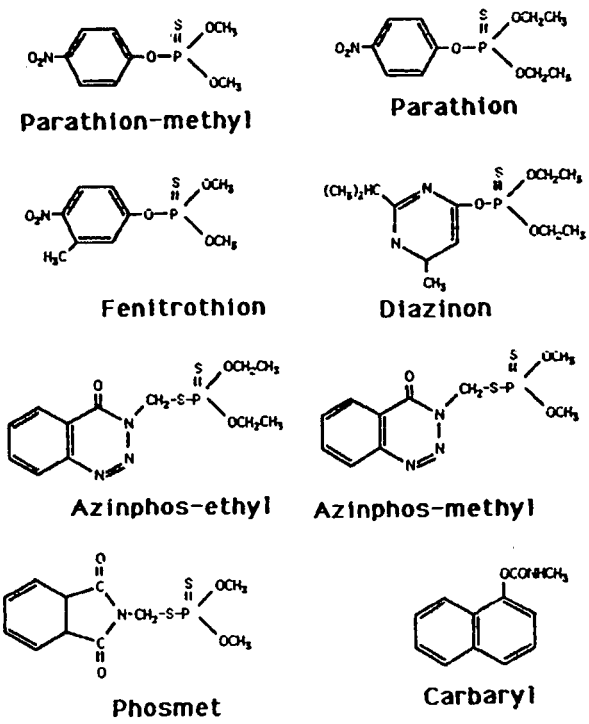

Fig. 1. Structures of the selected pesticides.

Apparatus

Precolumn elution and analysis were carried out with a Varian (Palo Alto, CA, USA) Model 5000 liquid chromatograph equipped with an Applied Biosystems (Ramsey, NJ, USA) Spectroflow 757 variable-wavelength UV detector. An auxiliary Varian Model 2010 pump was used to deliver the sample to the precolumn. Precolumn and analytical column switching was effected via a Rheodyne (Berkeley, CA, USA) Model 7010 valve. Chromatograms were recorded with a Servotrace recorder (Sefram, Paris, France).

Stationary phases and columns

The analytical column was a 150×4.6 mm I.D. stainless-steel column prepacked with 5-μm nucleosil C_{18} octadecylsilica (Macherey–Nagel, Düren, Germany). Samples were preconcentrated on a 10×2.1 mm I.D. stainless-steel precolumn prepacked with 5-μm RP-18 octadecylsilica (Merck, Darmstadt, Germany) or a 15×3.2 mm I.D. stainless-steel precolumn prepacked with 7-μm PRP polystyrene–divinylbenzene copolymer (Brownlee Columns, Applied Biosystems).

Preconcentration step

The sample loop of the injection valve (Fig. 2) was replaced with the RP-18 or PRP-1 precolumn. An auxiliary pump was used to deliver the sample solution to the precolumn via the waste vent line in the injection valve. The sample amount delivered was calculated as outlined previously. As the injector is in the "Load" position (Fig. 2), the effluent passes directly out of the valve into a waste container. Simultaneously, eluent from the reservoirs is being delivered via the other loop path to the analytical column and maintains this column in an equilibrated condition. Before each preconcentration, the precolumn was equilibrated with 10 ml of pure acetonitrile and 10 ml of LC-grade water at pH 7.

Separation step

Once the desired sample volume has been enriched, the injection valve is switched to "inject" and, simultaneously, the selected gradient is initiated, directing the eluent flow through the precolumn in a back-flush elution model. As the sample is eluted from the precolumn it enters the analytical column for completion of the separation step.

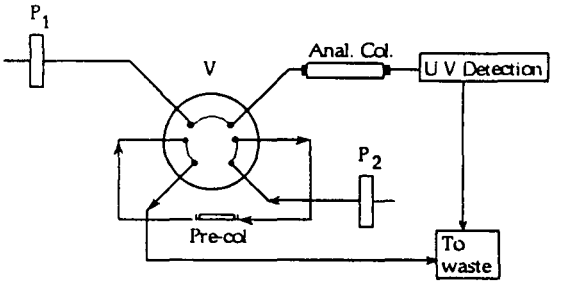

Fig. 2. Experimental set-up for the on-line preconcentration and analysis of water samples. P_1, P_2 = pumps; and V = valve; Anal. Col. = analytical column; Pre-col. = precolumn. During the preconcentration step V is in the "Load" position and P_2 delivers samples. During the analysis V is in the "Inject" position and P_1 delivers mobile phase.

RESULTS AND DISCUSSION

Analytical separation and detection

The pesticides studied (Fig. 1) included a carbamate and two OP groups, namely phosphorothionates and phosphorodithioates. The reversed-phase LC analysis of these compounds is usually performed using C_8- or C_{18}-bonded silicas [1,2,21,32,37,38]. When using a water–acetonitrile eluent, the OP pesticide separation is achieved in a reasonable time and without peak broadening if the acetonitrile concentration is greater than 50%. However, the retention of carbaryl is low.

This work started with the setting of a mobile phase gradient suitable for both the carbaryl and the OP pesticides previously sorbed on a precolumn. The gradient slope is then an important factor. In fact, when the water–acetonitrile gradient is steep, the retention time of carbaryl is short hence interference problems arise with co-extracted semi-polar compounds sorbed on the precolumn during the enrichment step; further, when the water–acetonitrile gradient is gentle, the risk of band broadening increases, especially when the precolumn sorbent is more hydrophobic than the analytical column packing.

With the gradients adopted, a fair resolution was achieved for the OP pesticides but the carbaryl retention was delayed. Table I gives the retention times of the pesticides for one of the two gradients selected.

The pesticides studied display maximum absorption bands at various wavelengths. However, these products display absorption bands between 250 and 300 nm. For our analytical conditions, 254 nm appears to be an acceptable compromise as we obtained similar responses for all the pesticides except phosmet, which exhibits a relatively small response. The instrumental detection limit (signal-to-noise ratio = 3:1) of phosmet is 3.5 ng (Table I). For the other insecticides it is in the range 0.6–1.5 ng. Hence the technique is less suitable for phosmet.

On-line preconcentration conditions

The on-line preconcentration permits the study of all the trapped compounds on the precolumn and also a reduction in the volume of the examined water samples and an improve-

TABLE I

RETENTION TIMES, LIMITS OF DETECTION (LOD) IN LC–UV AND DEPENDENCE OF RECOVERIES ON PERCOLATED SAMPLE VOLUME OF PESTICIDES STUDIED

Mobile phase, acetonitrile–water; gradient, 40% to 60% of acetonitrile in 15 min. UV detection at 254 nm. Recoveries were based on the averages of two determinations; amount of each pesticide in each percolated sample = 50 ng.

Compound		Retention time (min)	LOD[a] (ng)	Recovery (%)					
				Percolated sample volume					
				Milli-Q water			Tap water		
No.	Name			100 ml	200 ml	300 ml	100 ml	200 ml	300 ml
1	Carbaryl	8.7	1.5	98	90	80	64	54	NE[b]
2	Azinphos-methyl	12.9	1.2	100	98	90	74	78	60
3	Phosmet	13.9	3.5	97	98	95	92	91	93
4	Parathion-methyl	14.7	0.7	98	99	95	88	82	78
5	Azinphos-methyl	16.3	0.7	97	100	99	92	96	90
6	Fenitrothion	16.9	0.8	98	98	100	90	90	88
7	Parathion	18.75	0.6	100	97	98	92	88	83
8	Diazinon	19.75	0.9	100	100	98	81	87	82

[a] Signal-to-noise ratio = 3.
[b] Not evaluated.

ment in the detection limit. In order not to decrease the quality of the chromatographic separation, the on-line preconcentration technique involves precolumns with dimensions matching those of the analytical column. For a 150 × 4.3 mm I.D. column, the precolumn dimensions must be 15 × 4 mm I.D. In such cases, the most often used adsorbent size is 5 or 10 μm.

In this work, C_{18} and PRP-1 packed precolumns were tested. Preconcentration trials followed by an analytical separation for various volumes of Milli-Q-purified water spiked with various amounts of the pesticides were performed. The chromatograms obtained (Fig. 3) show the separation achieved by the two precolumn models. The peak broadening in the chromatograms resulting from enrichment on PRP-1 is significant; it is difficult to obtain quantitative results with this sorbent. For this reason, we used the C_{18} packed precolumn in subsequent work.

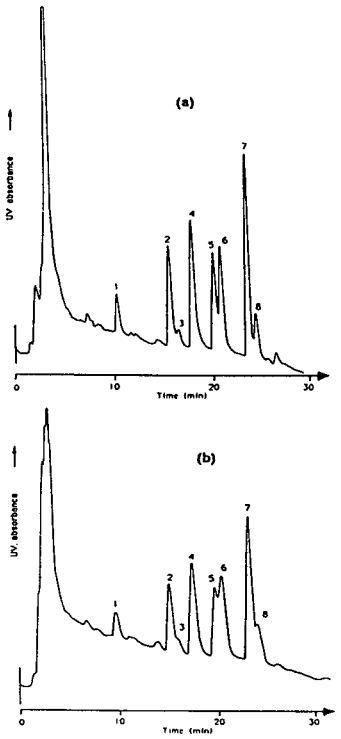

Fig. 3. RP-LC–UV traces for the on-line preconcentration of 100-ml Milli-Q-purified water samples spiked with carbaryl and seven OPPs. Preconcentration using the precolumns packed with (a) RP-18 silica and (b) PRP-1. Peak numbering corresponds to Table I. The individual concentrations of the pesticides ranged between 1 and 3 μg/l. The analytical column (15 × 0.46 cm I.D.) was packed with Nucleosil RP-18 (5 μm). Mobile phase, acetonitrile–water; gradient, 40% to 60% acetonitrile in 20 min. UV detection at 254 nm; attenuation 0.05 a.u.f.s.

The amount of solute recovered from the precolumn does not depend on the preconcentration flow-rate. These rates were changed in 1 ml/min increments from 2 to 7 ml/min. However, in order to avoid high column backpressures at flow-rates exceeding 5 ml/min, which would reduce the precolumn lifetime, a flow-rate of 3 ml/min was adopted.

Preconcentration, recovery and detection limit

Table I gives the recoveries for the preconcentrated pesticides for various volumes of Milli-Q-purified water and tap water. This recovery was calculated by means of the method described by Subra *et al.* [39]. The sample volumes were increased from 10 to 300 ml and the concentration decreased in order to have the same amount in each percolated sample. If breakthrough does not occur, the amount preconcentrated for each analyte on the precolumn is constant and the peak heights obtained after on-line elution are constant. When breakthrough occurs, the peak height decreases. Recoveries were calculated from the ratio between the peak height obtained for the sample volume studied and that obtained for a 10-ml sample. The recoveries of most of the preconcentrated pesticides from the Milli-Q-purified water reached 100% for treated volumes up to 300 ml. The decrease in the recovery of carbaryl as soon as the percolated water volume reaches 200 ml is important, however. These results show that the breakthrough on the C_{18} precolumn is greater than 300 ml for the OP pesticides on the one hand and between 100 and 200 ml for carbaryl on the other. Moreover, the observed recoveries for tap water preconcentration are, in every instance, lower than those obtained for Milli-Q-purified water. This discrepancy is not related to the amount of pesticides preconcentrated or to the breakthrough. It may arise from incomplete adsorption of trapped compounds on the precolumn owing to the formation of pesticides–humic substances complexes as suggested by

Johnson *et al.* [40]. These complexes may be poorly extracted by the octadecyl-bonded silicas.

When the proposed analytical procedure was applied to tap waters, the co-extracted compounds gave a large number of unresolved peaks at the start of the chromatogram, the intensity of which depends on the treated water volume. This part of the chromatogram affects the determination of early-eluted compounds especially when the concentrations of the latter are low. Fig. 4 illustrates the importance of this unresolved part of the chromatogram for the preconcentrates of 300 ml of tap water spiked with 0.1 ppb of each pesticide and also in the case of a blank. It is not then possible to determine carbaryl. This emphasizes the importance of the analytical gradient, as discussed earlier. Moreover, with such a drinking water sample, the solution to this problem, as has been reported [22], is to delay the carbaryl peak slightly. A very simple method without any further clean-up exists for drinking water control; it only requires optimization of the gradient.

The detection limits and the linearity of the solute peak height with concentration were assessed by adding increasing amounts to 200 ml of water, which is a compromise volume of samples of Milli-Q-purified and drinking water samples, and using the whole on-line preconcentration procedure. The detection limits were calculated for a signal-to-noise ratio of 3; in the baseline drift due to interferences, it was arbitrarily assumed that 0.5 cm was the minimum peak height that could be measured with reasonable confidence. The detection limits obtained were 0.2 μg/l for both phosmet and carbaryl. The detection limits for the other insecticides were in the range 0.03–0.06 μg/l. The calibration graphs were linear over the concentration range 0.05–1 μg/l (five data points). The regression coefficients obtained were satisfactory: azinphos-methyl, 0.9981; parathion-ethyl, 0.9994; azinphos-ethyl, 0.9976; fenitrothion, 0.9978; parathion, 0.9984; and diazinon, 0.9989.

Using the reported method, the precolumn can be re-used for analysing up to twenty 200-ml water samples without showing marked deterioration. Peak tailings are the result of possible perturbations that are often observed. Nevertheless, the precolumn can be used more times if the sample volumes are of the order of 100 ml or less. Moreover, there is no need to dry the precolumn before LC determinations, unlike the case with SPE enrichment using either on-line [9] or off-line [40] GC analysis. The described technique is amenable to automation and the whole set-up is robust.

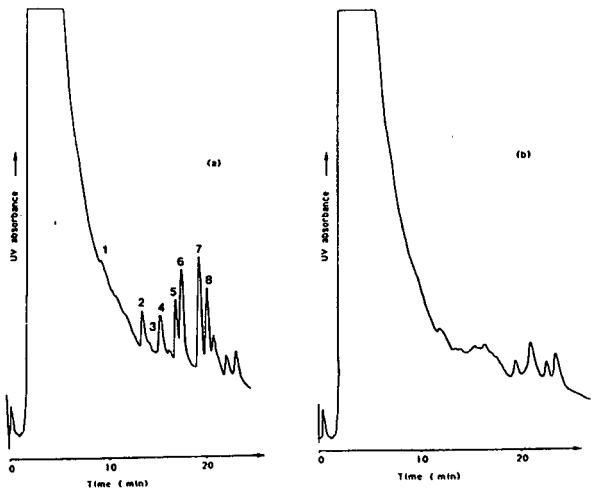

Fig. 4. RP-LC–UV traces for the on-line preconcentration of 300 ml of Paris tap water (October 1991) (a) spiked with 0.1 μg/l of each pesticide and (b) not spiked. Peak numbering corresponds to Table I. Preconcentration using the precolumn packed with RP-18 silica. Mobile phase, acetonitrile–water; gradient, 40% to 60% of acetonitrile in 15 min. UV detection at 254 nm; attenuation 0.01 a.u.f.s. Other conditions as in Fig. 3.

ACKNOWLEDGEMENTS

This work was performed in the framework of a cooperative contract between the Tunisian Fondation Nationale de la Recherche Scientifique et Technique and CNRS (France). The help of Professor R. Rosset (Paris) is gratefully acknowledged.

REFERENCES

1 J.G. Brayan, P.R. Haddad, G.J. Sharp, S. Dilli and J.M. Desmarchelier, *J. Chromatogr.*, 447 (1988) 249–255.
2 M.E. Leon-Gonzalez and A. Townshend, *J. Chromatogr.*, 539 (1991) 47–54.
3 D. Barceló, C. Porte, J. Cid and J. Albaigés, *Int. J. Environ. Anal. Chem.*, 38 (1990) 199–209.

4 H.B. Pionke and D.E. Glotfelty, *Water Res.*, 23 (1989) 1031–1037.
5 H.B. Pionke, D.E. Glotfelty and J.B. Urban, *J. Environ. Qual.*, 17 (1988) 76–84.
6 D.A. Hinckley and T.F. Bidleman, *Environ. Sci. Technol.*, 23 (1989) 995–1000.
7 R.P. Richards, J.W. Kramer, D.B. Baker and A.K. Krieger, *Nature*, 327 (1987) 129–131.
8 P.R. Loconto and A.K. Gaind, *J. Chromatogr. Sci.*, 27 (1989) 569–573.
9 P.J.M. Kwakman, J.J. Vreuls, U.A.Th. Brinkman and R.T. Ghijsen, *Chromatographia*, 34 (1992) 41–47.
10 J.F. Lawrence, *Int. J. Environ. Anal. Chem.*, 29 (1987) 289–303.
11 G.R. Verga, *J. High Resolut. Chromatogr.*, 15 (1992) 235–237.
12 C. Mallet and V.N. Mallet, *J. Chromatogr.*, 481 (1989) 27–35.
13 G. Durant, R. Forteza and D. Barceló, *Chromatographia*, 28 (1989) 597–604.
14 D. Barceló, *Chromatographia*, 25 (1988) 928–936.
15 D. Barceló, *Analyst*, 116 (1991) 681–689.
16 B.D. McGarvey, *J. Chromatogr.*, 481 (1989) 445–451.
17 H. Jansen, U.A.Th. Brinkman and R.W. Frei, *Chromatographia*, 20 (1985) 453–457.
18 A. Di Corcia and M. Marchetti, *Anal. Chem.*, 63 (1991) 580–585.
19 A. Di Corcia and M. Marchetti, *Environ. Sci. Technol.*, 26 (1992) 66–74.
20 C.H. Marvin, I.D. Brindle, C.D. Hall and M. Chiba, *Anal. Chem.*, 62 (1990) 1495–1498.
21 V.N. Mallet, M. Dugay, M. Bernier and N. Trottier, *Int. J. Environ. Anal. Chem.*, 39 (1990) 271–279.
22 R.J. Bushway, *J. Chromatogr.*, 211 (1981) 135–143.
23 D. Barceló, G. Durand, V. Bouvot and M. Nielen, *Environ. Sci. Technol.*, 27 (1993) 271–277.
24 M.W.F. Nielen, R.W. Frei and U.A.Th. Brinkman, *J. Chromatogr.*, 317 (1984) 551–567.
25 M.W.F. Nielen, U.A.Th. Brinkman and R.W. Frei, *Anal. Chem.*, 57 (1985) 806–810.
26 R. Hamman, M. Meier and A. Kettrup, *Fresenius' Z. Anal. Chem.*, 334 (1989) 231–234.
27 E.R. Brouwer, I. Liska, R.B. Geerdink, P.C.M. Frintrop, W.H. Mulder, H. Lingeman and U.A.Th. Brinkman, *Chromatographia*, 32 (1991) 445–452.
28 M.-C. Hennion, P. Subra and R. Rosset, *Int. J. Environ. Anal. Chem.*, 42 (1990) 15–33.
29 V. Coquart and M.-C. Hennion, *J. Chromatogr.*, 553 (1991) 329–343.
30 M.-C. Hennion, P. Subra, V. Coquart and R. Rosset, *Fresenius' J. Anal. Chem.*, 399 (1991) 488–493.
31 A. Braithwaite and F.I. Smith, *Chromatographia*, 30 (1990) 129–134.
32 C.H. Marvin, I.D. Brindle, C.D. Hall and M. Chiba, *J. Chromatogr.*, 503 (1990) 167–176.
33 A. Farran and J. DE Pablo, *Int. J. Environ. Anal. Chem.*, 46 (1992) 245–253.
34 M.R. Driss, S. Sabbah and M.L. Bouguerra, *J. Chromatogr.*, 552 (1991) 213–222.
35 S. Sabbah and M.L. Bouguerra, *J. Chromatogr.*, 552 (1991) 223–234.
36 M.R. Driss, L. Mahmoud, L. Bahri and M.L. Bouguerra, *Bull. Ecol.*, 19 (1988) 43–49.
37 G.J. Clark, R.R. Goodin and J.W. Smiley, *Anal. Chem.*, 57 (1985) 2223–2228.
38 A. Farran, J. De Pablo and D. Barceló, *J. Chromatogr.*, 455 (1988) 163–172.
39 P. Subra, M.-C. Hennion, R. Rosset and R.W. Frei, *J. Chromatogr.*, 456 (1988) 121–141.
40 W.E. Johnson, N.J. Fendinger and J.R. Plimmer, *Anal. Chem.*, 63 (1991) 1510–1513.

Journal of Chromatography, 639 (1993) 359–362
Elsevier Science Publishers B.V., Amsterdam

CHROM. 25 038

Short Communication

High-performance liquid chromatographic separation and determination of diastereomeric anthrone-C-glucosyls in Cape aloes

Hans W. Rauwald* and Anette Beil

Institute of Pharmaceutical Biology, Johann Wolfgang Goethe-University, Georg-Voigt-Strasse 16, W-6000 Frankfurt M. 11 (Germany)

(First received November 24th, 1992; revised manuscript received March 5th, 1993)

ABSTRACT

Isocratic high-performance liquid chromatography using reversed-phase packing (C_{18}) and the solvent system methanol–water (1:1) was successful in separating and determinating the anthrone-C-glucosyls in Cape aloes, allowing a rapid and high resolution of each diastereomer for the first time. By applying this method to fifteen commercial Cape and East African aloes of different origin, all Cape aloes samples showed the same anthrone-C-glucosyl pattern comprising 5-hydroxyaloin A, aloins A/B and aloinosides A/B. For differentiating non-official East African aloes from Cape aloes, 5-hydroxyaloin A proved to be the most specific marker of the official drugs in high-performance liquid and also thin-layer chromatography, replacing the aloinosides. Previous assumptions of chemical races of *Aloe ferox* MILL. based on the aloinosides have to be revised.

INTRODUCTION

Cape aloes (derived from *Aloe ferox* MILL. and hybrids, *Asphodelaceae*) is a remedy used worldwide. It is listed in numerous pharmacopoeias because of its purgative activity. The active principle comprises five anthrone-C-glucosyls [1] (Fig. 1): the diastereomeric aloins A/B and aloinosides A/B and the so-called "periodate-positive substance" [2], the structure of which we have recently determined to be 5-hydroxyaloin A [3].

As yet no study has simultaneously determined all five anthrone-C-glucosyls by high-performance liquid chromatography (HPLC). Although in 1979 a reversed-phase HPLC separation with 45% aqueous methanol was described for the aloins [4], all subsequent publications on the HPLC determination of anthrone-C-glucosyls from *Aloe* dealt with the analysis of aloins [5–7] or homonataloins [8].

In our study we describe a simple and rapid isocratic reversed-phase HPLC method for the baseline separation, identification and assay of aloins A/B, aloinosides A/B and 5-hydroxyaloin A in aloes. The method was applied to fifteen commercial Cape and East African aloes of different origin. It ensured an exact determination of the characteristic pattern of diastereomeric anthrone-C-glucosyls in Cape aloes.

* Corresponding author.

0021-9673/93/$06.00

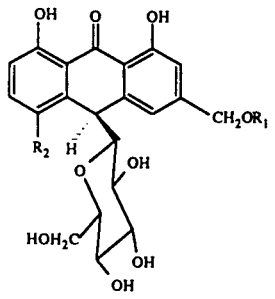

A - Type

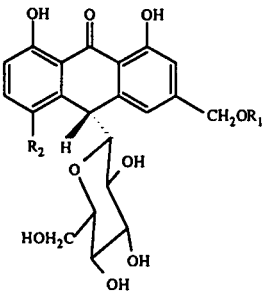

B - Type

	R_1	R_2	Configuration (10, 1'[17])
Aloin A	H	H	S, S
Aloin B	H	H	R, S
Aloinoside A	α-L-rhamnosyl	H	S, S
Aloinoside B	α-L-rhamnosyl	H	R, S
5-Hydroxyaloin A	H	OH	R, S

Fig. 1. Diastereomeric anthrone-C-glucosyls from Cape aloes.

EXPERIMENTAL

Solvents

All solvents were of technical quality and were purified by distillation.

High-performance liquid chromatography

Apparatus. The equipment consisted of a Waters 600 solvent-delivery system (Waters, Milford, MA, USA) and a U6K injector. A Waters 990 photodiode-array detector coupled with a NEC APC IV personal computer (NEC Information Systems, Boxborough, MA, USA) was used for recording UV–VIS spectra (200–500 nm) of the separated compounds and standard compounds and for controlling retention time at 360 nm.

Conditions. Separations were performed on an ET 250/8/4 Nucleosil 7 C_{18} column (Macherey, Nagel, Düren, Germany) at room temperature. The mobile phase consisted of methanol–water (1:1); the flow-rate was 1 ml/min. Each sample was chromatographed three times. The injection volume was 20 μl.

Sample preparation. A 300-mg aliquot of the powdered drug was dissolved in exactly 100 ml of methanol–water (1:1) by automatic shaking for 15 min. An aliquot of these solutions was filtered through a cellulose acetate filter (0.45 μm; Lida, Kenosha, WI, USA).

Standard samples. 5-Hydroxyaloin A was isolated according to a previously reported procedure [3]. The aloinosides A and B could be obtained from Cape aloes by preparative thin-layer chromatography (TLC) in the solvent system ethylacetate–methanol–water (100:17:13); for TLC identification of aloinosides, see refs. 9–11. Preparative separation of the aloins A and B was achieved by droplet countercurrent chromatography [12].

Precision. A solution of 100 mg of aloins A/B in 100 ml of 50% aqueous methanol was treated as described in the Sample preparation section and was chromatographed five times. The results obtained were also compared with the HPLC separation of an unfiltered solution of 100 mg of aloins A/B in 100 ml of methanol.

Thin-layer chromatography

TLC separations on silica gel F_{254} plates (Macherey, Nagel) were carried out according to the European Pharmacopoeia (Ph.Eur.).

By using chloroform–methanol–water (7:13:8; lower phase) as the solvent system, all five diastereomers can be detected separately [13]. 5-Hydroxyaloin A was detected by spraying with 5% aqueous sodium metaperiodate (Merck, Darmstadt, Germany).

RESULTS AND DISCUSSION

In order to obtain a rapid and high resolution of 5-hydroxyaloin A and aloinosides A/B the HPLC parameters described for the aloins [4] had to be modified with respect to particle size of the stationary phase, solvent system and flow-rate. This led to an isocratic baseline separation of all five diastereomers for the first time: within about 20 min each diastereomer could be determined in a single HPLC run (Fig. 2). Thus, the technique not only replaces the aloes identification and assay of Ph.Eur., but can also be applied to pharmacokinetic and toxicological studies, which have been required for aloes by the German health administration since May 1992 [14].

In contrast to the assay of Ph.Eur., the pulverized drugs were dissolved directly in methanol–water (1:1), filtered and chromatographed on reversed-phase packing (C_{18}) with methanol–water (1:1). For the aloins A/B the average recovery was 97.2% with a relative standard deviation of 0.6% ($n = 5$). In comparison to our sample preparation, the complicated but conventional Ph.Eur. solving method showed no difference. A specific peak identification was achieved by means of photodiode-array detection (comparison of spectra and control of retention time at 360 nm). In routine analysis, UV detection at 360 nm is sufficient.

In a screening of fifteen commercial drugs, this HPLC technique enabled us to monitor the characteristic pattern of anthrone-C-glucosyls in each sample. Table I shows the content of each separated anthrone-C-glucosyl. A listing of the drugs according to their origin agrees with their arrangement according to their qualitative and for the most part quantitative anthrone-C-glucosyl pattern: Cape aloes samples from the Mosselbay region (South Africa) show high contents of all five anthrone-C-glucosyls. In this case all five compounds can also be well detected by means of TLC.

5-Hydroxyaloin A is weakly detectable by means of TLC (applied amounts according to Ph.Eur.) in Cape aloes samples 8–10 from Port Elizabeth (South Africa). The Ph.Eur. TLC markers aloinoside A and B cannot be determined at all by TLC. This finding led to the commonly accepted assumption of aloinoside-free chemivars of *Aloe ferox* [9,15]. However, the qualitative and quantitative determination by HPLC shows positive proof of aloinosides A and B in Port Elizabeth samples for the first time. A differentiation of *Aloe ferox* in several chemivars could thus only be discussed with regard to the quantitative pattern of the aloinosides A and B.

East African aloes (samples 12–15) are still available commercially. It is shown for the first time that all drugs of East African origin lack 5-hydroxyaloin A (Table I) and that some of them contain more aloinosides than aloins.

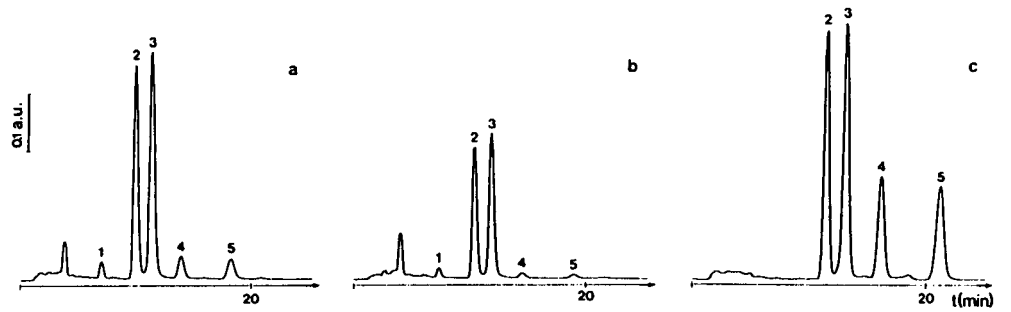

Fig. 2. Reversed-phase high-performance liquid chromatograms at 360 nm of (a) Cape aloes from Mosselbay, (b) Cape aloes from Port Elizabeth and (c) Kenyan aloes. Conditions were as described in the Experimental section. Peaks: 1 = 5-hydroxyaloin A; 2 = aloin B; 3 = aloin A; 4 = aloinoside B; 5 = aloinoside A.

TABLE I

QUANTITATIVE DETERMINATION (%) OF 5-HYDROXYALOIN A, ALOINS A/B AND ALOINOSIDES A/B IN ALOES OF DIFFERENT ORIGIN

Sample	Origin	5-Hydroxyaloin A	Aloin A	Aloin B	Aloinoside A	Aloinoside B	Sum
1–4	Mosselbay	1.7–2.9	13.0–13.9	10.9–12.0	3.1–3.9	2.8–3.6	31.7–34.9
5–7	Quality "Ph.Eur."	1.1–2.3	12.7–13.1	10.8–11.3	2.6–3.4	2.4–3.1	31.3–31.8
8–10	Port Elizabeth	0.3–0.8	6.5– 8.5	5.2– 7.1	0.3–0.9	0.4–0.8	13.3–17.8
11	Port Elizabeth	3.3	12.5	10.8	4.0	3.5	34.1
12	Kenya	–	16.3	14.0	19.6	16.9	66.8
13	East Africa	–	7.3	5.8	13.6	11.7	38.4
14	East Africa	–	14.8	11.9	2.9	2.5	32.1
15	East Africa	–	12.7	10.6	6.2	5.1	34.6

Whereas for samples 13–15 the specific origin was not declared, sample 12 was stated to be "Kenyan Cape aloes". This classification must be called in question because of the lack of 5-hydroxyaloin A, especially since *Aloe rabaiensis* RENDLE is reported to be the origin of Kenyan aloes [16]. The Ph.Eur. TLC method does not permit a differentiation between East and South African aloes, because it only monitors the aloins and aloinosides. Therefore 5-hydroxyaloin A is proposed as most specific TLC marker, replacing the aloinosides. Furthermore, our HPLC results confirm that 5-hydroxyaloin is until now the only C-glucosyl-anthrone that has not been found as a diastereomeric pair genuinely in aloes: It only occurs in the more stable A-configuration (10*R*, 1′*S* [17]).

In summary, the characteristic anthranoid pattern of Cape aloes —including Cape aloes from Port Elizabeth— comprises all five anthrone-C-glucosyls. As already pointed out, these five glucosyls cannot be detected in each case, following Ph.Eur. TLC conditions. However, the more sensitive and rapid HPLC method allows a definite determination of each anthrone-C-glucosyl in a single working step.

ACKNOWLEDGEMENTS

We are grateful to Caesar & Loretz GmbH, Hilden (Germany), Alfred Galke GmbH, Gittelde (Germany), Heinrich Klenk GmbH, Schweinfurt (Germany), Paul Müggenburg GmbH & Co., Alveslohe (Germany), and Petereit & Co. GmbH, Elmshorn (Germany) for providing the drug material.

REFERENCES

1 R.K. Mapp and T.J. McCarthy, *Planta Med.*, 18 (1970) 361.
2 H. Böhme and L. Kreutzig, *Dtsch. Apoth. Ztg.*, 103 (1963) 505.
3 H.W. Rauwald, *Pharm. Weekbl. Sci. Ed.*, 9 (1987) 215.
4 M. Grün and G. Franz, *Pharmazie*, 34 (1979) 669.
5 H. Auterhoff, E. Graf, G. Eurisch and M. Alexa, *Arch. Pharm. (Weinheim)*, 313 (1980) 113.
6 E. Graf and M. Alexa, *Arch. Pharm. (Weinheim)*, 313 (1980) 285.
7 Q.J. Groom and T. Reynolds, *Planta Med.*, 53 (1987) 345.
8 J. Beaumont, T. Reynolds and J.G. Vaughan, *Planta Med.*, 50 (1984) 505.
9 L. Hörhammer, H. Wagner and G. Bittner, *Arzneimittel-Forsch.*, 13 (1963) 537.
10 L. Hörhammer, H. Wagner and G. Bittner, *Z. Naturforschg.*, 19b (1964) 222.
11 A. Beil and H.W. Rauwald, in R. Hänsel, K. Keller, H. Rimpler and G. Schneider (Editors), *Hagers Handbuch der Pharmazeutischen Praxis*, Vol. 4, Springer, Berlin, 1992, p. 216.
12 H.W. Rauwald, K. Lohse and J.W. Bats, *Angew. Chem.*, 101 (1989) 1539.
13 H.W. Rauwald, *Arch. Pharm. (Weinheim)*, 315 (1982) 769.
14 Anonymous, *Dtsch. Apoth. Ztg.*, 132 (1992) 1164.
15 R. Hegnauer, *Chemotaxonomie der Pflanzen*, Vol. 7, Birkhäuser, Basle, 1986, p. 705.
16 J. Conner, A. Gray, T. Reynolds and P. Waterman, *Pharm. Weekbl. Sci. Ed.*, 9 (1987) 216.
17 H.W. Rauwald, *Pharm. Ztg. Wiss.*, 3/135 (1990) 169.

Journal of Chromatography, 639 (1993) 363–365
Elsevier Science Publishers B.V., Amsterdam

CHROM. 25 029

Short Communication

Potential variability problems with the alkali flame ionization detector used in gas chromatography

Kai Bester and Heinrich Hühnerfuss*

Institut für Organische Chemie, Universität Hamburg, Martin-Luther-King-Platz 6, 20146 Hamburg (Germany)

(First received November 23rd, 1992; revised manuscript received March 3rd, 1993)

ABSTRACT

Systematic gas chromatographic measurements on fourteen nitrogen- and three phosphorus-containing environmental pollutants revealed that potential variability problems may arise when using an alkali flame ionization detector. During an experimental period of 2 weeks the decrease in detector response turned out to be similar for homologous compounds, but different for compounds of diverse chemical classes. Although the absolute decrease in detector response may vary from bead to bead and, in addition, from one manufacturer to another, quantification appears to be feasable if this problem is taken into account by choosing internal standards of the same chemical class.

INTRODUCTION

Alkali flame ionization detection (AFID) is widely used in gas chromatographic analyses of environmental and pharmaceutical samples because of its unequivocal potential to detect and determine trace amounts of nitrogen- and/or phosphorus-containing organic compounds. This holds, in particular, for the trace analysis of pesticides such as triazine derivatives, *e.g.*, atrazine, and of industrially used organophosphates, *e.g.*, tri-*n*-butyl phosphate.

Although AFID is applied on a large scale and there have been many investigations on its function, the understanding of the detector is still poor [1–8]. It is assumed that pyrolysis of the analyte in the flame of the detector in the presence of alkali metal ions or excited alkali metal atoms gives rise to the formation of $CN^{-\bullet}$ and $PO_3^{-\bullet}$ species [6], which in turn lead to a sufficiently strong signal of the detector. However, these alkali metal sources, which are mostly installed as salt beads in a silicate matrix, are known to become exhausted [7]. Some beads are "consumed" more rapidly than others, which apparently is determined by how the bead is made. For example, Carlo Erba sources that were applied in this investigation are stated by the manufacturer to last for about 25 days [8]. As a consequence of this process, the signal response, *i.e.*, the peak area integral, of a given amount of analyte decreases with time. However, to the authors' knowledge, no systematic investigation has been reported that clarifies the question of whether the decrease in the signal

* Corresponding author.

0021-9673/93/$06.00

response is the same for all substances or whether it is different for each compound. This work was aimed at filling this gap.

EXPERIMENTAL

The experiments were performed with a Carlo Erba GC 6000 (Vega Series) gas chromatograph equipped with an AS 550 autosampler and an AFID system built by Carlo Erba (Milan, Italy). The gas chromatographic conditions were as follows: NB-54-column (25 m × 0.32 mm I.D., film thickness 0.25 μm) from Nordibond (Helsinki, Finland) (comparable to SE-54); on-column injection, with an injection volume of 2 μl containing 2 ng of each analyte; carrier gas, helium (98 kPa); detector temperature, 573 K (300°C); and detector gases, air (108 kPa), hydrogen (78 kPa) and make-up gas helium (70 kPa). The detector burned continuously during the experimental period of 2 weeks. The column temperature programme was initial temperature 343 K, increased at 5 K/min to 433 K (held for 20 min), then increased at 6 K/min to 523 K (held for 30 min).

4-Chloroaniline, tri-*n*-butyl phosphate, tri(2-methylpropyl) phosphate, triphenyl phosphate and ethyl acetate (analytical-reagent grade) as solvent were obtained from Merck (Darmstadt, Germany). The standard compounds propham, aldicarb, propoxur, cycloate, simazine, atrazine, propazine, terbuthylazine, pirimicarb, linuron, terbutryne, anilazine and flamprop-methyl were supplied by Promochem (Wesel, Germany).

During an experimental period of 2 weeks a standard solution containing all of the nitrogen- and phosphorus-containing compounds listed above was injected three times a day in order to test whether the decrease in the detector signal is a general or a substance-specific phenomenon. Each day, an average peak integral was calculated. At the end of the period, all integrals determined for one specific substance were normalized to the largest integral within the respective series of that specific compound.

The experiments were confined to 2 weeks instead of the complete lifetime of a salt bead (3 weeks) because we had to change the gas cylinder after that period. It is interesting that re-ignition of the gas flame caused an additional significant effect on the detector response which also has to be taken into account when planning the analytical strategy over several weeks.

RESULTS AND DISCUSSION

It would be beyond the scope of this paper to show the plots for all seventeen compounds investigated. Further, it is not our intention to claim that the data are representative of all AFID sensors available on the market on an absolute scale. The absolute values would only apply to the Carlo Erba detector used. Therefore, we refrained from running a large number of beads, and confined ourselves to two repetitions. However, it should be noted that data from many additional runs, although not performed systematically (injections three times per day, over 2 weeks, etc.) are available that clearly support the present findings.

In general, the results show that substances of different chemical classes do not necessarily exhibit the same temporal decrease in detector response. As an example, typical graphs which are characteristic of atrazine, tri-*n*-butyl phosphate and aldicarb are shown in Fig. 1. The structures of these three compounds are given in Fig. 2. Whereas the signal response of tri-*n*-butyl phosphate decreased to about 40% of its original value within 2 weeks, the responses of atrazine

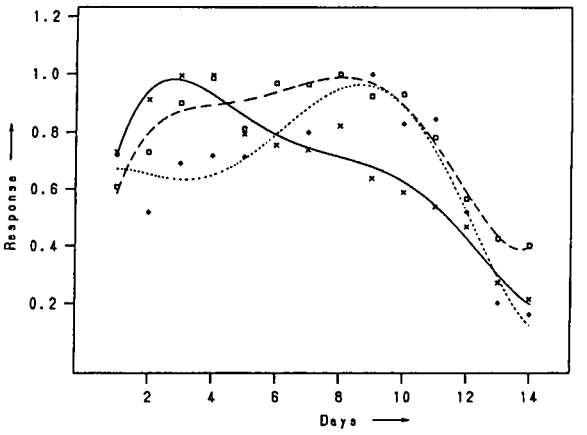

Fig. 1. Temporal decrease in AFID response to (×) atrazine, (□) tri-*n*-butylphosphate and (◆) aldicarb. The response was normalized to the maximum value for each compound.

and of aldicarb were reduced to about 25% within the same period. However, in the last two instances, the characteristics of the curves are significantly different; in particular, the position of the maxima and the slope are dissimilar. The signal responses of most compounds investigated exhibit characteristics comparable to one of the three substances displayed in Fig. 1; the curves for propazine, simazine, terbuthylazine, cycloate, pirimicarb, propham, propoxur, flamprop-methyl, linuron and terbutryne are comparable to that of atrazine, the curve for anilazine is comparable to that of aldicarb and the characteristics of the organophosphates resemble those of tri-*n*-butyl phosphate. Only the response of 4-chloroaniline shows a fourth characteristic deviating significantly from the other three curves.

At first glance, chemicals of the same class seem to cause similar responses to the detector. On the other hand, a comparison of the graphs for atrazine and anilazine shows that this observation should not be generalized. These results imply that caution must be exercised when using AFID for the determination of nitrogen- or phosphorus-containing compounds. The choice of an appropriate standard is obviously a crucial aspect. A necessary condition appears to be that the standard should belong to the same chemical class as the analyte, because it is difficult, if not impossible, to find one internal standard that shows the same detector responses as several phosphorus- and nitrogen-containing chemicals.

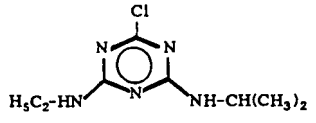

atrazine

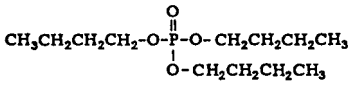

tri-n-butyl-phosphate

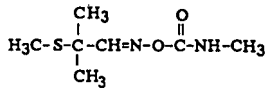

aldicarb

Fig. 2. Structures of atrazine, tri-*n*-butyl phosphate and aldicarb.

The present data can be generalized insofar as they reveal a potential problem with all AFID sensors, regardless of their specific performance characteristics such as within-day or day-to-day reproducibility. However, it will be impossible to determine a time function of the detector response for each analyte that is generally valid for more than one manufacturer. Therefore, it is recommended that recalibration with external standards should be performed every few days at least.

ACKNOWLEDGEMENT

This work was supported by the Ministry of Science and Technology of the Federal Republic of Germany (BMFT project MFU 0620, Prozesse im Schadstoffkreislauf Meer-Atmosphäre. Ökosystem Deutsche Bucht).

REFERENCES

1 C.E. Kientz, G.G. DeJong and C.A. Brinkman, *J. Chromatogr.*, 550 (1991) 461.
2 V.V. Brazhnikov, M.V. Gurev and K.I. Sakodynsky, *Chromatogr. Rev.*, 12 (1970) 1.
3 P.L. Patterson, *J. Chromatogr. Sci.*, 24 (1986) 41.
4 P.L. Patterson, *J. Chromatogr. Sci.*, 20 (1982) 97.
5 C.S. Jones, *Ph.D. Thesis*, Montana State University, Bozeman, MT, 1989.
6 D.D. Bombick and J. Allison, *J. Chromatogr. Sci.*, 27 (1989) 612.
7 P.L. Patterson and R.L. Howe, *J. Chromatogr. Sci.*, 16 (1978) 275.
8 *Vega Series 2 Gas Chromatographs Instruction Manual, Section 4.1.3, Nitrogen Phosphorus Detector NPD 40*, Carlo Erba, Milan, Italy, 1989.

Journal of Chromatography, 639 (1993) 366–370
Elsevier Science Publishers B.V., Amsterdam

CHROM. 25 049

Short Communication

Structurally informative response patterns of some monoterpenoids found in volatile oils to gas chromatography on two commercial dipentylated cyclodextrin phases

T.J. Betts

School of Pharmacy, Curtin University of Technology, GPO Box U1987, Perth, W. Australia (Australia)

(First received December 7th, 1992; revised manuscript received March 1st, 1993)

ABSTRACT

Gas chromatographic retention times relative to *n*-undecane at 100–150°C were plotted for various monoterpenoid alcohols or carbonyl compounds on two "Chiraldex" depentylated cyclodextrin phases. As the temperature was increased, the modified β-cyclodextrin ("B-DA") just showed all values decreasing. However, the α-cyclodextrin ("A-DA") exhibited distinctive solute patterns. 4- and 1-ols and aldehydes typically gave a decrease again, but 3-ols and 3-ones exhibited near constant values, whilst the relative retention times of 4-ones (especially bicyclic ones) increased. This smaller ring "Chiraldex" responded to the position of the polar group in the solute molecules, whilst the larger ring reacted to the rigid bulk of the molecules. Increases in results with change to the larger ring phase B-DA were over 70% at 125°C for bicyclics, exactly 28% at 150°C for three different dienes, and low or even negative for acyclic tepenoids like citral. Such results could indicate structural information about unidentified terpenoids.

INTRODUCTION

This author has recently used a toroid commercially available capillary gas chromatographic phase "Chiraldex-A-DA" to observe special responses by some volatile oil constituents [1], to assess its value for oil analysis [2], and in phase polarity studies [3]. It consists of modified α-cyclodextin with two-thirds of the hydroxyls on each of the ring of six α-glucose units pentylated; depicted in ref. 1. Its low polarity [3], although it still retains some polar hydroxyls, should make it appropriate for resolving various volatile oil constituents. These include a range of somewhat polar monoterpenoid alcohols and carbonyls, with their oxygen-containing function in various positions in their molecules. The molecular "fit" to the modified cyclodextrin of these various branched acyclic, monocyclic and bicyclic terpenoids as the phase temperature is changed, should be useful. It could indicate the oxygen-group position or other features in an unknown solute, and could suggest how the Chiraldex functions, if results are compared with those for unbranched alkanes, alcohols and aldehydes of similar retention times. Such deductions might be further assisted by comparing the results on the A-DA phase with those from the larger

0021-9673/93/$06.00

molecular ring B-DA consisting of the same dipentylated modification, but of β-cyclodextrin and seven α-glucose units in a ring.

Volatile oils also contain terpene hydrocarbons and their enantiomers have been resolved by Konig *et al.* [4] using fully tri-pentylated β- and γ-cyclodextrins. They were also used in 1990 by Takeoka *et al.* [5] in diluted admixture with a polysiloxane (which leaves their contribution to separations confused) to resolve the terpene hydrocarbons of ginger oil, and the esters of grapefruit juice. Recently, monopentyl, dimethyl β-cyclodextrin diluted in polysiloxane was used by Bicchi *et al.* [6] to try to resolve ten pairs of enantiomers including limonene and menthol. These, with α-pinene, fenchone, pulegone, borneol, α-terpineol and linalol were not better resolved by Schmalzing *et al.* [7] on trimethylated β-cyclodextrin when it was chemically bonded to a polysiloxane than on a mixture.

EXPERIMENTAL

Apparatus

A Hewlett-Packard 5790A gas chromatograph was used, fitted with a capillary control unit, and a splitter injection port and flame ionisation

TABLE I

RELATIVE RETENTION TIMES (*n*-UNDECANE = 1.00) ON CHIRALDEX-DA (DIPENTYL) CAPILLARIES WITH PERCENTAGE INCREASES ON CHANGING TO THE LARGER MOLECULAR RING

Average results. Percentage increase (inc) shown for solutes on changing from the smaller α- to the larger β-cyclodextrin modification. Helium holdup times on both phases 0.25–0.30 min.

Solute		Gas chromatographic phases, used at various temperatures (°C)								
		100			125			150		
		β	α	% inc	β	α	% inc	β	α	% inc
Isoborneol	I		3.46		7.78	3.45	125	6.35	3.33	91
Borneol	B		3.95		8.36	3.84	118	6.87	3.57	92
Thujone	T	3.17	1.08	193	2.69	1.24	117	2.52	1.36	85
Camphor	CM	4.55	1.67	172	4.01	1.86	116	3.84	2.04	88
α-Terpineol	α		3.65		6.96	3.47	101	5.78	3.19	81
4-Terpineol	4		2.83		5.26	2.85	85	4.54	2.88	58
Fenchone	F	2.11	0.98	115	2.02	1.16	74	2.00	1.29	55
Menthone	MN	3.16	1.59	99	2.80	1.73	62	2.65	1.85	43
Menthol	ML		3.87		5.92	3.73	59	4.71	3.33	41
Carvone	CV		3.48		5.30	3.54	50	4.53	3.54	28
Perillal	PE					6.57		7.59	5.95	28
Linalol	L	2.74	1.57	74	2.26	1.57	44	2.00	1.56	28
Pulegone	PU		2.69		3.83	2.77	38	3.56	2.84	25
Piperitone	PI		3.63		4.96	3.70	34	4.44	3.59	24
Citronellal	CA	2.60	1.82	43	2.26	1.81	25	2.15	1.79	20
Citronellol	CO				6.40	5.11	25	4.94	4.27	16
Geraniol	G				6.60	6.36	4	4.88	5.04	−3
n-Dodecane	DO	2.06	2.03	1.5	1.83	1.84	−0.5	1.70	1.73	−1.7
Citral	CT				5.27	5.93	−11	4.29	5.02	−14
n-Decanal	DA				2.96	3.78	−22	2.81	3.28	−14
n-Octanol	O	2.43	3.26	−25	2.01	2.75	−27	1.81	2.37	−24
n-Undecane retention time (min)		0.84	1.00		0.35	0.37		0.17	0.17	

detector both set at 235°C. A Hewlett-Packard 3380A recorder/integrator was attached.

The "Chiraldex-A-DA" and "B-DA" capillaries (from Advanced Separation Technologies, Whippany, NJ, USA) 10 m × 0.25 mm I.D. were heated and cooled at less than 10°C min^{-1} to preserve the phases. Helium was the mobile phase used at 1.5–2.0 ml min^{-1}, and as the "make-up" gas for the detector.

Materials and methods

Solutes used were obtained from various commercial sources including Aldrich, Allwest (Perth), BDH, Dragoco (Holzminden), Koch-Light, Sigma and T.C.I. (Tokyo). They are listed in Table I and their structures presented in Fig. 1. The formula numbering used in this figure is purely for the discussion in this paper, and is not intended to be correct in a conventional chemical sense. Thus aldehydes are considered as 1-ones, with 4-terpineol and linalol as 3-ols. Injections of traces of these solutes (strong alcoholic solutions of borneols, camphor and menthol) were made from a microsyringe which had been filled, then "emptied". Holdup times were deducted from observed retention times, and obtained by extrapolating to methane the times for *n*-heptane and *n*-hexane plotted on semi-logarithmic graph paper.

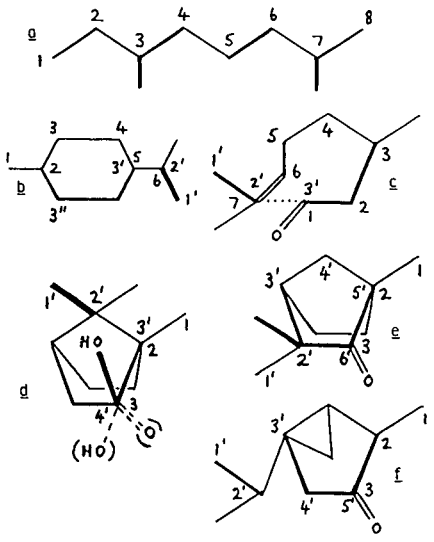

Fig. 1. Formulae of terpenoid solutes used. Their numbering does not necessarily conform to required chemical nomenclature. (a) Citral with 1-one and 2–3,6–7 diene. Citronellal with 1-one and 6–7 monoene (see also 1c). Citronellol with 1-ol and 6–7 monoene. Geraniol with 1-ol and 2–3,6–7 diene. Linalol with 3-ol and 1–2,6–7 diene. (b) Carvone with 3-one and 2–3″,1′–2′ diene. Menthol with 4-ol. Menthone with 4-one. Perillal with 1-one and 2–3,1′–2′ diene. Piperitone with 4-one and 2–3 monoene. Pulegone with 4-one and 2′–3′ monoene. α-Terpineol with 6-ol and 2–3 monoene. 4-Terpineol with 3′-ol and 2–3 monene. (c) Citronellal conformation, pseudo 3′-one. (d) Isoborneol (continuous lines). Borneol with 3-OH "down" instead of "up". Camphor with 3=O instead of OH. (e) Fenchone: 6′-one or 3-one. (f) Thujone; 5′-one or 3-one.

RESULTS AND DISCUSSION

Average results are given in Table I and mostly depicted in Fig. 2 as relative retention times to the inert *n*-undecane. A typical result for an unbranched non-polar substance can be expected from the next alkyl homologue *n*-dodecane. The plot of its retention relevant to undecane starts just above 2.0 and decreases, with temperature increase, towards 1.7 on both phases. The same typical decline (with different higher values, greatest on the α-ring phase) is shown by unbranched octanol and decanal; and also by the branched eight-carbon chains of geraniol (Fig. 2), citronellol and citral (main peak used of mixture), with geraniol giving similar values on both phases. We reported this response on conventional phases in 1970 [8]. These solutes are all 1-ols or 1-ones (Fig. 1a) and cyclic perillal is an example of the latter, with its aldehyde group at the opposite end of a rigid ring system to an isopropenyl chain. Unlike the modified α-cyclodextrin capillary the Chiraldex-B-DA showed all results (dashed lines) decreasing with increase in temperature, so there were no different patterns.

In contrast, on Chiraldex-A-DA 3-ols such as monocyclic 4-terpineol, isoborneol (at lower temperatures), and branched chain linalol, with the monocylic 3-one carvone, show virtually no change, i.e. practically a horizontal plot over a temperature range. Surprisingly, this is also exhibited by the branched chain aldehyde citronellal on this smaller ring phase. Perhaps this solute flexes its molecules to adopt a conforma-

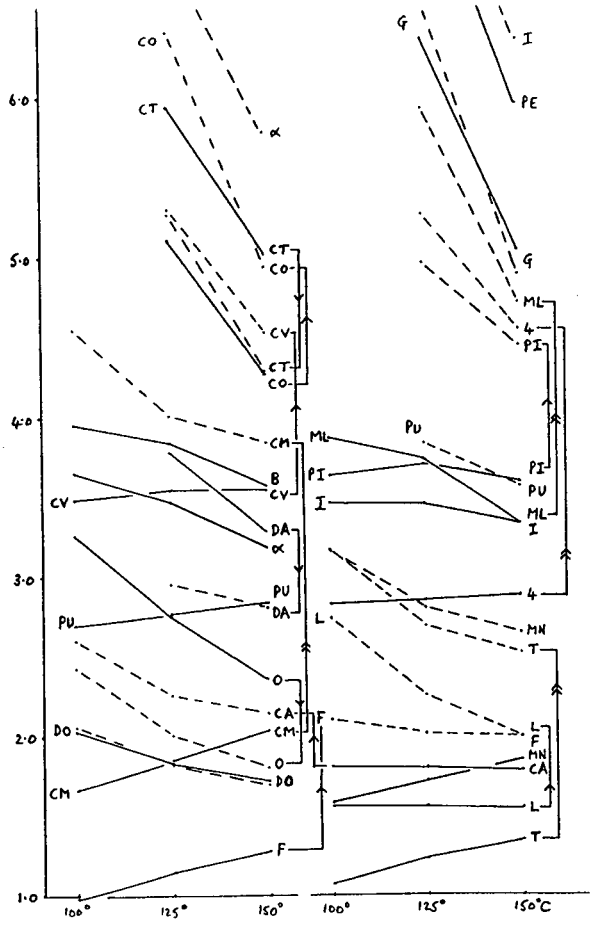

Fig. 2. Average relative retention times to *n*-undecane of monoterpenoids at three temperatures. Continuous lines, on Chiraldex-A-DA; dashed lines, on Chiraldex-B-DA. Abbreviations for solute identities in Table I.

tion making it a pseudo-3-one (Fig. 1c), unlike its comparable alcohol, citronellol? Citronellal exhibits surprisingly low retention for a C_{10} unsaturated aldehyde on other phases too [8–10] and so does not relate chromatographically to citronellol as citral does to geraniol.

Of the other alcohols studied on the smaller ring phase this leaves the monocyclic, 4-ol (from either end) menthol (Fig. 1b) behaving like the bicylic borneol which could also function as a 4-ol. They show a lesser decrease in relative retention times than the 1-ols. Isoborneol may behave like a 4-ol, and not a 3-ol, above 125°C, possibly due to the juxtaposition of its alcohol group to the paired methyls in the rigid molecule (Fig. 1d). The chiral isomers borneol and isoborneol can be resolved on normal phases, and perhaps this 3 *vs.* 4-ol behaviour is involved?

Of the ketones considered, there is the group of monocyclic, 4-ones (from either end) pulegone and menthone, which show with piperitone (at lower temperatures) an increase in relative retention times on Chiraldex-A-DA with temperature rise. Other ketones examined were the bicyclics fenchone, thujone and camphor, which although obviously 3-ones, do not behave like carvone —they may actually function as higher number ketones (Fig. 1d, e, f), giving a larger continual increase. We previously observed this relative increase [8] on normal phases with isomenthone and camphor, but not with pulegone or piperitone. These increases are not shown on Chiraldex-B-DA.

A feature of changing to the larger ring phase was the over 70% increase in relative retention times at 125°C (over 50% increase at 150°C) given by the bicyclic saturated alcohols and ketones. For most the increase was over 115% at 125°C and the lower results for fenchone could be because it is behaving as a 6-one on this phase unlike the other bicylics. It is then like α-terpineol, functioning as a 6-ol. The larger β-cycodextrin molecular rings gave virtually no change in relative relention times compared to α- for the saturated linear hydrocarbon dodecane and surprisingly for the diene geraniol also (Table I and Fig. 2). They were thus effective in retaining bulky, rigid, bicyclic molecules, but less so with flexible, elongated acyclics.

Geraniol was different to two other branched unsaturated acyclics citronellol and citronellal. These monoenes both gave a low 25% increase at 125°C in relative retention times. In this respect, citronellal is mimicking its corresponding alcohol, but with much lower retention times. The diene citral is different again in showing a small decrease in relative retention times on changing from the α- to the β-phase, like the decreases shown by saturated unbranched *n*-decanal and *n*-octanol. Chiraldex-B-DA thus only shows more retention than A-DA (for acyclics relative to undecane) with the monoenes citronellol and citronellal, and not

with saturated substances, nor the dienes geraniol and citral. This monoene affinity is supported by the α- to β-phase increase of the two terpineols, which are greater than for the other monocyclics (Table I). However, the monoenes pulegone and piperitone gave only 25% increases at 150°C, compared to the 40% for the saturated 4-one menthone, and for menthol.

Three different dienes, cyclic and acyclic, gave exactly 28% increases (α- to β-phase) in relative relention times at 150°C. These were linalol, carvone and perillal. Thus the Chiraldex-B-DA can indicate the degree of unsaturation or bicyclic nature of solutes, compared to the oxygenation position selectivity of the A-DA phase. The latter phase appears to exhibit constant relative retention of monoterpenoid 3-ols and a 3-one, despite temperature increase. Possibly their polar groups fit about midway into the α-ring molecules, unlike 1-, 4-, and other oxygenated position terpenoids? Other mechanisms like simple partition and adsorption may influence various solutes to show alterations in relative retention. Nevertheless, some distinctive features can be noted for both compared to conventional phases. On Chiraldex-DA borneol is retained more strongly than carvone, and menthol more than pulegone —a preference for saturated alcohols is exhibited rather than unsaturated ketones.

In summary, the relative retention time effects to undecane observed for a limited number (18) of monoterpenoids are as follows.

(1) Chiraldex-A-DA, with temperature increase: fall in values suggest 1- or 4-ol or aldehyde; "constant" values suggest 3-ol or 3-one; or rise in values suggest 4-, 5- or 6-one. (*Note:* Some solutes behave atypically to their obvious polar group position).

(2) Chiraldex-B-DA results compared to above at 150°C: over 80% increase suggests bicyclic; below 80% to about 25% increase suggests monocyclic, with higher values possibly monoene; 28% increase suggests diene; or below 25% increase (or fall) suggests acyclic.

REFERENCES

1 T.J. Betts, *J. Chromatogr.*, 606 (1992) 281.
2 T.J. Betts, *J. Chromatogr.*, 626 (1992) 294.
3 T.J. Betts, *J. Chromatogr.*, 628 (1993) 138.
4 W.A. Konig, R. Krebber, P. Evers and G. Bruhn, *J. High Resolut. Chromatogr.*, 13 (1990) 328.
5 G. Takeoka, R.A. Flath, T.R. Mon, R.G. Buttery, R. Teranishi, M. Guntert, R. Lautamo and J. Szejtli, *J. High Resolut. Chromatogr.*, 13 (1990) 202.
6 C. Bicchi, G. Artuffo, A. D'Amato, V. Manzin, A. Galli and M. Galli, *J. High Resolut. Chromatogr.*, 15 (1992) 710.
7 D. Schmalzing, M. Jung, S. Mayer, J. Rickert and V. Schurig, *J. High Resolut. Chromatogr.*, 15 (1992) 723.
8 P.N. Breckler and T.J. Betts, *J. Chromatogr.*, 53 (1970) 163.
9 N.W. Davies, *J. Chromatogr.*, 503 (1990) 1.
10 T.J. Betts, *J. Chromatogr.*, 600 (1992) 337.

Journal of Chromatography, 639 (1993) 371–374
Elsevier Science Publishers B.V., Amsterdam

CHROM. 25 024

Short Communication

Gas and liquid chromatographic studies of copper(II), nickel(II), palladium(II) and oxovanadium(IV) chelates of some fluorinated ketoamine Schiff bases

M.Y. Khuhawar* and Altaf I. Soomro

Institute of Chemistry, University of Sindh, Jamshoro, Sindh (Pakistan)

(First received August 24th, 1992; revised manuscript received February 26th, 1993)

ABSTRACT

The copper(II), nickel(II), palladium(II) and oxovanadium(IV) chelates of N,N′-ethylenebis(1,1,1-trifluoro-6-methyl-2-oxoheptan-4-imine) (H_2TFIVA$_2$en) and N,N′-1,2-propylenebis(1,1,1-trifluoro-6-methyl-2-oxoheptan-4-imine) (H_2TFIVA$_2$pn) were eluted from gas chromatographic columns, but their copper and nickel chelates could not be resolved. The detection limits were found to be 4–40 ng for each metal chelate. The copper, nickel, palladium and oxovanadium chelates were separated on reserved-phase HPLC columns, Nova Pak C_{18} (150 × 3.9 mm) and Microsorb C_{18} (150 × 4.6 mm). Elution was obtained with a binary mixture of methanol–water or a ternary mixture of methanol–acetonitrile–water. Detection was achieved using a UV detector. Linear calibrations were obtained over the range 10–1200 ng and detection limits were 0.4–4.0 ng for the metal chelates.

INTRODUCTION

Metal chelates appear to be convenient species for the determination of metals by gas chromatography (GC) and high-performance liquid chromatography (HPLC). A number of complexing reagents for GC and HPLC of metals as metal chelate compounds have been suggested [1,2]. The most commonly used complexing reagents are β-diketones, β-thioketones, bi- and tetradentate ketoamine Schiff bases [3,4], dialkyl dithiophosphates, dialkyl dithiocarbamates and oxines [5,6]. Tetradentate ketoamine Schiff bases are interesting because they form neutral and volatile metal chelates with copper(II), nickel(II), palladium(II), platinum(II) and oxovanadium(IV). They also have high molar absorptivities in the ultraviolet region [7,8]. The introduction of a trifluoromethyl group adjacent to carbonyl has a favourable effect on the thermal stability and volatility of metal chelates [1]. Therefore, in the present work, two new fluorinated tetradentate ligands, N,N′-ethylenebis-(1,1,1-trifluoro-6-methyl-2-oxoheptan-4-imine) [bis (trifluoroisovalerylacetone) ethylenediimine] (H_2TFIVA$_2$en) and N,N′-1,2-propylenebis(1,1,1-trifluoro-6-oxoheptan-4-imine) [bis(trifluoroisovalerylacetone)propylenediimine] (H_2TFIVA$_2$pn), have been examined for their possible use for GC and HPLC separation of copper, nickel, palladium and oxovanadium.

* Corresponding author.

0021-9673/93/$06.00

EXPERIMENTAL

The reagents H_2TFIVA_2en and H_2TFIVA_2pn were prepared by condensation of 1,1,1-trifluoro-6-methyl-heptane-2,4-dione with ethylenediamine or 1,2-propylenediamine in 2:1 molar ratio. The copper and nickel chelates were prepared by heating together equimolar solutions of reagent and copper(II) acetate or nickel(II) acetate. Palladium(II) chelates were prepared by refluxing together reagent solution and palladium–benzonitrile adduct in benzene. The oxovanadium chelates were prepared by the ligand-exchange method [9,13].

Elemental microanalyses were carried out by Elemental Micro Analysis, Devon, UK. Mass spectromet's of the reagents was performed at the HEJ Research Institute of Chemistry, University of Karachi, Pakistan. Spectrometric studies were carried out using an Hitachi 220 spectrophotometer.

Thermogravimetry (TG) and differential thermal analysis (DTA) of metal chelates were recorded on a Shimadzu TG 30 thermal analyser, with a heating rate of 15°C/min and nitrogen flow-rate of 50 cm^3/min and samples of 5–12 mg.

A Hitachi 163 gas chromatograph equipped with a flame ionization detector and a Hitachi 056 recorder was used. Stainless-steel columns (2 m × 3 mm and 3 m × 3 mm) packed with OV-101 (3%) or OV-17 (3%) on Chromosorb W HP, 80–100 mesh, and Dexil GC 400 (2%) on Uniport HP, 60–80 mesh, were used.

A Model 3700 gas chromatograph equipped with a flame ionization detector (Varian Instruments) and a DB-5 (methyl phenyl silicon) column (J. and W. Scientific) (30 m × 0.25 mm I.D., film thickness 0.25 μm) were used.

A Hitachi 655A liquid chromatograph connected to a variable-wavelength UV monitor, a Rheodyne 7125 injector and a Hitachi 561 recorder was used. Nova Pak C_{18} (150 mm × 3.9 mm I.D.) (Waters) and Microsorb (150 mm × 4.6 mm I.D.) (Hewlett Packard) columns were used.

RESULTS AND DISCUSSION

The results of elemental microanalyses corresponded to the expected values. The mass and infrared spectra agreed with the structure of ligands and metal chelates assigned (Fig. 1) [13].

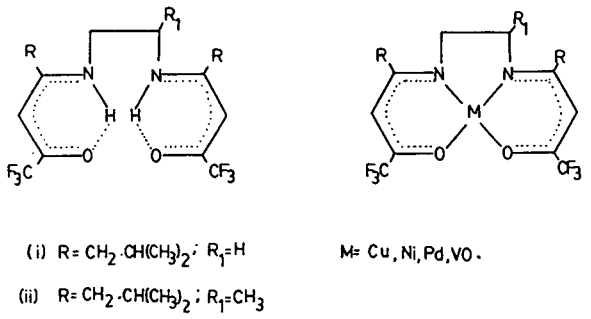

Fig. 1. Structural diagram of reagents and metal chelates.

TG and DTA of metal chelates were performed to check their volatility and thermal stability. The results of thermoanalytical studies (Fig. 2) show that rapid and single-stage weight loss of copper, nickel and palladium chelates of H_2TFIVA_2pn within 92–100% occurred in the temperature range 205–365°C. However, the oxovanadium chelate lost mass in three stages. A major loss of 59% occurred between 225 and 350°C, with a maximum rate of loss at 310°C. A secondary loss of 16% occurred by 405°C and a total loss of 84% by 500°C.

The copper, nickel, palladium and oxovanadium chelates of H_2TFIVA_2en and H_2TFIVA_2pn were investigated on different packed columns, but a better peak shape with baseline return was observed on the 3 m × 3 mm column packed with Dexil GC 400 (2%) on Uniport HP, 60–80 mesh size. When separation of copper, nickel, oxovanadium and palladium chelates of H_2TFIVA_2en was attempted, copper, nickel and oxovanadium co-eluted and only palladium could be separated. Similarly, the palladium chelate of H_2TFIVA_2pn was completely separated from the copper, nickel and oxovanadium chelates, and partial separation of oxovanadium from copper and nickel was obtained, but no separation of copper and nickel chelates was observed (Fig. 3). For the separation of copper and nickel, a DB-5 (30 mm × 0.25 mm) capillary column was also tried, but without any success.

The response of the flame ionization detector using a packed column was compared with the amount of the complex injected; calibration curves were obtained by plotting average peak

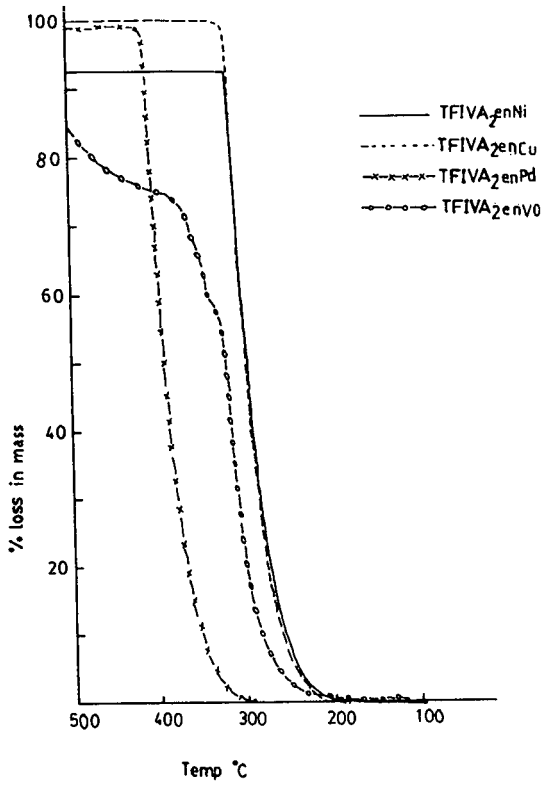

Fig. 2. TG of metal chelates at a heating rate 15°C/min and nitrogen flow-rate 50 cm^3/min.

height ($n = 3$) *versus* amount of complex injected and were found to be linear in the range 1–8 μg. The detection limit measured as three times the background noise was found to be 4–40 ng of metal chelates, corresponding to 0.5–5 ng of a metal ion, and compare favourably with related compounds [4,8,10].

The metal chelates had reasonable thermal stability and volatility on elution from GC columns, but failed to separate adequately. It was therefore decided to examine the reagents for HPLC separation of their metal chelates. HPLC was combined with variable UV detection.

The copper, nickel, palladium and oxovanadium complexes of H_2TFIVA_2en eluted easily with a binary mixture of methanol and water on a Nova-Pak C_{18} column, but optimal separation of copper, nickel, palladium and oxovanadium was obtained when complexes were isocratically eluted with a ternary mixture of methanol–acetonitrile–water (65:7:28, v/v/v) (Fig. 4). The order of elution was oxovanadium, copper, palladium and nickel, and retention volumes were 7.36, 26.21, 33.70 and 35.46 cm^3, respectively. It should be noted that resolution between palladium and nickel complexes at optimized conditions of separation was only 1.03.

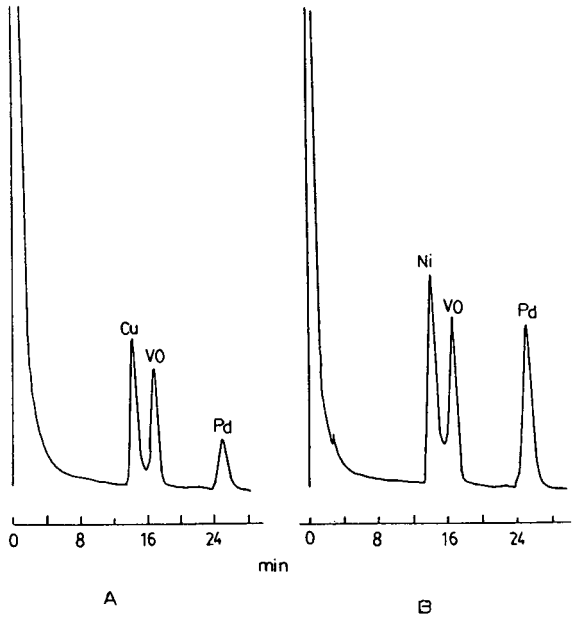

Fig. 3. GC separation of (A) copper, oxovanadium and palladium and (B) nickel, oxovanadium and palladium chelates of H_2TFIVA_2pn on a column (3 m × 3 mm) packed with Dexil GC 400 (2%) on Uniport HP, 60–80 mesh size. Column temperature, 260°C, with programmed rise in temperature of 0.5°C/min up to 280°C; injection port temperature, 290°C; nitrogen flow-rate, 30 cm^3/min.

The elution and separation of metal chelates

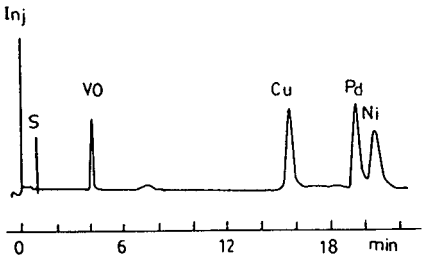

Fig. 4. HPLC separation of oxovanadium, copper, palladium and nickel chelates of H_2TFIVA_2en on a Nova Pak C_{18} (150 × 3.9 mm) column. Elution: methanol–acetonitrile–water (65:7:28, v/v/v), flow-rate 1.7 cm^3/min. Detection UV at 300 nm.

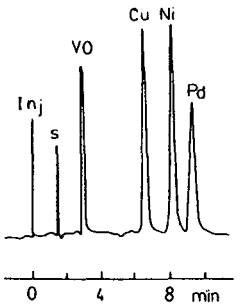

Fig. 5. HPLC separation of oxovanadium, copper, nickel and palladium chelates of H_2TFIVA_2pn on a Microsorb C_{18} (150 × 4.6 mm) column. Elution: water–methanol (15:85). Flow-rate 1 cm^3/min. Detection: UV at 260 nm.

of H_2TFIVA_2pn were investigated on a Microsorb C_{18} column. Complete separation of oxovanadium, copper, nickel and palladium was obtained when the complexes were eluted isocratically with a binary mixture of 15% water in methanol (Fig. 5). The order of elution observed was oxovanadium, copper, nickel and palladium, and retention volumes were 2.92, 6.5, 8.1 and 9.34 cm^3, respectively.

The linear calibration ranges at optimized conditions of separation were also checked and were found to be in the range 10–1200 ng of metal chelates. The detection limits were found to be 0.4–4.0 ng of metal chelates, corresponding to 44–764 pg of metal ions. Thus an improvement in detection limits has been observed as compared with related compounds [10–12].

CONCLUSIONS

The metal chelates are volatile and on elution from GC columns only complete separation of palladium from copper, nickel and oxovanadium is achieved. Calibration curves are linear at the microgram level and detection limits are 4–40 ng of metal chelate. Reversed-phase HPLC with UV detection not only provided ease of separation, but also resulted in considerable improvement in the detection limits to 0.4–4.0 ng of metal chelates. The separation of copper, nickel, palladium and oxovanadium chelates of H_2TFIVA_2pn on a Microsorb C_{18} column within 10 min may be considered as highly promising for the quantitative determination using pre-column derivatization as reported for related compounds [10–12].

REFERENCES

1 P.C. Uden, *J. Chromatogr.*, 313 (1984) 3.
2 G. Nickless, *J. Chromatogr.*, 313 (1984) 129.
3 O.W. Lau and W.I. Stephen, *Anal. Chim. Acta*, 180 (1986) 417.
4 M.Y. Khuhawar, A.G.M. Vasandani and A.I. Soomro, *J. Chem. Soc. Pak.*, 12 (1990) 119.
5 S. Dilli, P.R. Hadded and K. Htoon, *J. Chromatogr.*, 500 (1990) 313.
6 Yukio Nagaosa and Hiroki Kawabe and Alan M. Bord, *Anal. Chem.*, 63 (1991) 28.
7 S. Dilli and E. Patsalides, *Anal. Chim. Acta*, 128 (1981) 109.
8 M.Y. Khuhawar and A.G.M. Vasandani, *J. Chem. Soc. Pak.*, 10 (1988) 213.
9 D.F. Martin and K. Ramiah, *J. Inorg. Nucl. Chem.*, 27 (1965) 2027.
10 M.Y. Khuhawar and Altaf I. Soomro, *Anal. Chim. Acta*, 268 (1992) 49.
11 M.Y. Khuhawar and Altaf I. Soomro, *J. Liq. Chromatogr.*, 15 (1992) 647.
12 M.Y. Khuhawar and Altaf I. Soomro, *Talanta*, 39 (1992) 609.
13 M.Y. Khuhawar and Altaf I. Soomro, *J. Chem. Soc. Pak.*, submitted for publication.

Journal of Chromatography, 639 (1993) 375–378
Elsevier Science Publishers B.V., Amsterdam

CHROM. 25 023

Short Communication

Separation of diastereomeric derivatives of enantiomers by capillary zone electrophoresis with a polymer network: use of polyvinylpyrrolidone as buffer additive

W. Schützner[☆]

Institute for Analytical Chemistry, University of Vienna, Währingerstrasse 38, A-1090 Vienna (Austria)

S. Fanali

Istituto di Cromatografia, Consiglio Nazionale delle Ricerche, Area della Ricerca di Roma, Via Salaria km 29.300, 00016 Monterotondo Scalo, Rome (Italy)

A. Rizzi* and E. Kenndler

Institute for Analytical Chemistry, University of Vienna, Währingerstrasse 38, A-1090 Vienna (Austria)

(First received December 1st, 1992; revised manuscript received February 26th, 1993)

ABSTRACT

Diastereomeric derivatives of D- and L-tryptophan obtained by reaction with (+)-diacetyl-L-tartaric anhydride were separated using capillary zone electrophoresis with polyvinylpyrrolidone as polymeric additive to the separation buffer. This additive is able to undergo hydrophobic as well as dipolar interactions with the sample components and in this way influences the effective mobility of the analytes. As this influence is of different strength for the two diastereomers, the selectivity for these separands is enhanced. The application of such physical networks as a kind of "pseudophase" is of general significance as this method mirrors reversed-phase chromatography using aqueous mobile phases.

INTRODUCTION

The separation of enantiomeric compounds has gained widespread interest in the past decade and is still an important challenge for modern separation techniques. Gas chromatography, supercritical fluid chromatography and especially high-performance liquid chromatography (HPLC) have been the most frequently used techniques for the separation of enantiomers of compounds with a broad structural variety. Different separation strategies are applied within these chromatographic techniques. One is based on the application of chiral selectors in the chromatographic system, as a constituent of

* Corresponding author.
☆ Present address: Istituto di Cromatografia, Consiglio Nazionale delle Ricerche, Area della Ricerca di Roma, Via Salaria km 29.300, 00016 Monterotondo Scalo, Rome, Italy.

0021-9673/93/$06.00

either the stationary or the mobile phase. The alternative strategy is based on the conversion of the enantiomers into diastereomers by reacting them with an optically pure agent. These diastereomers can be separated on commonly employed non-chiral phases such as reversed-phase systems.

The concept of chiral selection has been transferred to electrophoretic methods, especially to isotachophoresis and capillary zone electrophoresis (CZE) (see, for example, refs. 1–3). In this case, it is used to try to influence the effective mobilities of the individual enantiomeric species to a different extent by utilizing interactions with chiral selectors, which are either easily soluble additives to the separation buffer or compounds that form chiral micelles. Soluble chiral selectors are successfully applied if complexes with different association constants are formed. This has been shown with chiral chelator–metal complexes [4,5] and with cyclodextrines and their derivatives [6–8], the latter forming inclusion complexes with the separated compounds. Chiral micelles [9–12], acting as a kind of "pseudophase", were introduced in analogy with chiral phases in chromatography.

This paper deals with the approach of the indirect separation of enantiomers by CZE, namely via their diastereomeric derivatives. In this case the analytes are transformed into compounds with chemically different properties. Such separations have been reported previously, *e.g.* by applying sodium dodecyl sulphate (SDS) micelles [13–15].

In the present paper a non-chiral physical network is applied instead of the charged SDS micelles as an additive to the separation buffer, namely polyvinylpyrrolidone (PVP). It is used as a polymer that is able to offer hydrophilic and hydrophobic interactions with the analytes. This paper illustrates the particular example, using diastereomeric tryptophan derivatives, of the amplification of the differences in the effective mobilities of the diastereomers. However, it is meant to be typical of the general approach of using interactions between the chains of physical networks and analytes to obtain separation.

EXPERIMENTAL

Chemicals and reagents

The chemicals used had the following specification: DL-, D- and L-tryptophan (Serva, Heidelberg, Germany), benzene-1,3-disulphonic acid (Fluka, Buchs, Switzerland) and (+)-diacetyl-L-tartaric anhydride (Aldrich, Steinheim, Germany) were all reagent grade; polyvinylpyrrolidone 15 (mean molecular mass 11 000) (Serva); $NaH_2PO_4 \cdot H_2O$, $Na_2HPO_4 \cdot 12H_2O$, NH_4OH (30%), HCl (37%) and NaOH were all "purum" quality (all from Carlo Erba, Milan, Italy). Bidistilled water was used (Menichelli, Rome, Italy). Acetonitrile was of "HiPerSolv" quality (for HPLC, BDH, Poole, UK). For the coating of the capillary 3-(trimethoxysilyl) propylmethacrylate (purum, Fluka), acrylamide, $K_2S_2O_8$ and N,N,N′,N′-tetramethylethylenediamine (TEMED) (all of electrophoresis purity; Bio-Rad Labs., Richmond, CA, USA) were used.

Apparatus

The zone electrophoretic measurements were carried out using the apparatus previously described [5], consisting of a separation capillary (kept at ambient temperature without thermostating equipment), a high-voltage power supply (Series EH; Glassmann, Whitehouse Station, NJ, USA) and a variable-wavelength UV detector (Model 2250; Varian, Palo Alto, CA, USA), connected to an integrator (Chromatopac C-R5A; Shimadzu, Kyoto, Japan).

The fused-silica separation capillary (Polymicro Technologies, Phoenix, AZ, USA) had the following dimensions: 100 μm inner diameter, 54 cm total length, 38 cm effective length to the detector. It was coated to eliminate electroosmosis [16].

The injection of the sample was carried out hydrodynamically by keeping both ends of the capillary for 5–10 s (depending on the viscosity of the buffer solution) at a height difference of about 10 cm.

Procedures

D-, L- and DL-tryptophan were reacted with (+)-diacetyl-L-tartaric anhydride to form the

corresponding tartaric acid (mono)amides using a procedure similar to that described in ref. 17: 10 m*M* tryptophan was dissolved in 25 ml of acetonitrile, and water was removed by distillation under water-jacket vacuum at 40°C for 1 min. After cooling, 20 m*M* (+)-diacetyl-L-tartaric anhydride was added and the reaction mixture was kept at 50°C for 20 h. Then acetonitrile was removed by distillation, and to the residue a 3% aqueous solution of NH_4OH was added, followed by redistillation. The final product was dried in a desiccator.

Suppression of electroosmosis was controlled by the mobility values measured from at least day-to-day injections of a reference compound (benzene-1,3-disulphonic acid) and comparison of the obtained values with the literature [18]. The constancy of this value and its agreement with the literature values allowed the conclusion that electroosmotic flow was negligible.

RESULTS AND DISCUSSION

The influence of the concentration of PVP on the migration times of the diastereomers of D- and L-tryptophan and of the reference compound benzene-1,3-disulphonate can be seen from Table I. All migration times increase with increasing concentration of PVP. The variation in the migration time of the reference component reflects, at least in part, the change in viscosity of the solution due to the addition of the polymer. The most important effect, however, is the induced difference in the migration behaviour of the diastereomers at PVP concentrations higher than 1%: the L-isomer migrates more slowly than the D-isomer. This leads to selectivity coefficients, r_{ij}, for the diastereomeric compounds i and j, larger than 1.

These selectivity coefficients (Table I) continuously increase from 1.00 at 0% PVP to 1.018 at 6% PVP. The value of 1.00 (0% PVP) is obtained within the measuring error at the pH of the separation electrolyte system; under this condition the diastereoisomers could not be separated. As the separation efficiency changes only moderately upon the addition of PVP (about a 30% decrease in the plate numbers was measured for the higher PVP concentrations), the increase in selectivity results in the separation of the analytes. It can clearly be observed from Fig. 1 that the resolution continuously increases with increasing concentration of PVP, leading finally to baseline separation of the two diastereomeric derivatives at 6% PVP.

The diastereomers, which have equal effective mobilities at 0% PVP under the given conditions, are separated by the different strength of their interaction with the polymer chains. This kind of mechanism, demonstrated here with tryptophan derivatives as analytes and PVP as a physical network, is supposed to be of wide

TABLE I

MIGRATION TIMES, t_{Ri}, AND SELECTIVITY COEFFICIENTS, r_{LD}, OF THE DIASTEREOMERIC D- AND L-TRYPTOPHAN DERIVATIVES DEPENDING ON THE CONCENTRATION OF POLYVINYLPYRROLIDONE (PVP)

Concentration of PVP (%, w/v)	t_{Ri}			r_{LD} [a]
	D-Derivative	L-Derivative	Benzene-1,3-disulphonate	
0	10.8[b]		5.61	1.00
1	10.9[b]		5.90	1.00
2	12.08	12.18	7.14	1.008
3	11.52	11.65	6.68	1.011
4	12.11	12.27	6.85	1.013
5	13.50	13.72	7.35	1.016
6	13.67	13.91	7.81	1.018

[a] The selectivity coefficients are defined as the ratios of the effective mobilities of the separands.
[b] The migration times of the diastereomers cannot be distinguished within the measuring error.

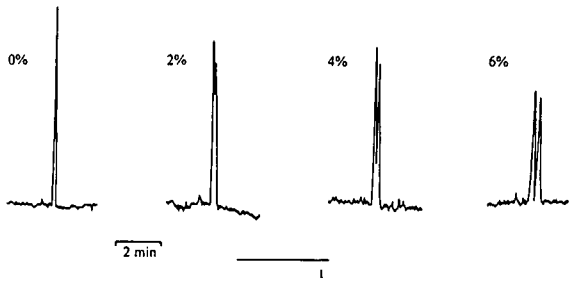

Fig. 1. Influence of the concentration of polyvinylpyrrolidone in the buffering electrolyte on the separation of the diastereoisomeric D- and L-tryptophan diacetyl-L-tartaric acid monoamides. The concentration of polyvinylpyrrolidone (mean molecular mass 11 000) is given in %(w/v), as indicated. Separation conditions: phosphate buffer pH 6.35, concentration 0.016 mol/l; coated capillary: total length 54 cm (38 cm to detector); applied voltage 10 kV; temperature 24°C; analyte concentration (in water): 10^{-4} mol/l; detection: UV absorbance at 233 nm.

applicability to other interactive additive/analyte systems, and is analogous to that operating in chromatographic reversed-phase systems.

This approach in fact seems to exhibit a general significance for the adjustment of selectivity in capillary electrophoresis far beyond the separation of diastereomeric compounds. It is an example of the important features of physical networks (polymers and gels) in CZE besides their discrimination properties according to the size of large analytes (as applied, for example, as a sieving medium for the separation of SDS complexes of proteins [19]).

ACKNOWLEDGEMENT

Financial support for this work by the "Austrian Academic Exchange Service" (project funded by the technical-scientific agreement between Austria and Italy) is acknowledged.

REFERENCES

1 J. Snopek, I. Jelinek and E. Smolkova-Keulemansova, *J. Chromatogr.*, 452 (1988) 571.
2 J. Snopek, I. Jelinek and E. Smolkova-Keulemansova, *J. Chromatogr.*, 609 (1992) 1.
3 R. Kuhn and S. Hoffstetter-Kuhn, *Chromatographia*, 34 (1992) 505.
4 A.S. Cohen, S. Terabe, J.A. Smith and B.L. Karger, *Anal. Chem.*, 59 (1987) 1021.
5 S. Fanali, L. Ossicini, F. Foret and P. Bocek, *J. Microcol. Sep.*, 1 (1989) 190.
6 J. Snopek, I. Jelinek and E. Smolkova-Keulemansova, *J. Chromatogr.*, 438 (1988) 211.
7 S. Fanali, *J. Chromatogr.*, 474 (1989) 441.
8 S. Fanali, *J. Chromatogr.*, 545 (1991) 437.
9 A.S. Cohen, A. Paulus and B.L. Karger, *Chromatographia*, 24 (1987) 15.
10 S. Terabe, M. Shibata and Y. Miyashita, *J. Chromatogr.*, 480 (1989) 403.
11 A. Dobashi, T. Ono, S. Hara and J. Yamaguchi, *J. Chromatogr.*, 480 (1989) 413.
12 K. Otsuka, J. Kawahara, K. Tatekawa and S. Terabe, *J. Chromatogr.*, 559 (1991) 209.
13 H. Nishi, T. Fukuyama and M. Matsuo, *J. Microcol. Sep.*, 2 (1990) 234.
14 I.S. Lurie, *J. Chromatogr.*, 605 (1992) 269.
15 A.D. Tran, T. Blanc and E.J. Leopold, *J. Chromatogr.*, 516 (1990) 241.
16 St. Hjerten, *J. Chromatogr.*, 347 (1985) 191.
17 W. Lindner, Ch. Leitner and G. Uray, *J. Chromatogr.*, 316 (1984) 605.
18 Ch. Schwer and E. Kenndler, *Chromatographia*, 33 (1992) 331.
19 A. Widhalm, Ch. Schwer, D. Blaas and E. Kenndler, *J. Chromatogr.*, 549 (1991) 191.

Journal of Chromatography, 639 (1993) 379–380
Elsevier Science Publishers B.V., Amsterdam

CHROM. 25 041

Book Review

Chemical analysis in complex matrices, edited by M.R. Smyth, Ellis Horwood-PTR Prentice Hall, New York, London, Toronto, 1992, 295 pp., price US$ 90.00, ISBN 0-13-127671-9.

The great interest in solving analytical problems with complex samples is clearly reflected by the number of papers published in this area. The analytical problems are to a great extent solved by sample-handling techniques in combination with selective detection principles in chromatographic separations. The present book on this subject is written by six Irish scientists. It contains 295 pages, divided into six chapters that cover five different fields. The parts are as follows: Chapter 1, an introduction to chemical analysis in complex matrices, by Malcolm R. Smyth; Chapter 2, drug analysis in biological fluids, by Mary T. Kelly; Chapter 3, analysis in the brewing industry, by Ian McMurrough; Chapter 4, the analytical laboratory in the speciality sealants/adhesives industry, by Raymond G. Leonard; Chapter 5, air pollution analysis, by Imelda Shanahan; and Chapter 6, chemical analysis of animal feed and human food, by Michael O'Keeffe.

On reading this book it is not clear until page 17 that there are several authors of the book. There are no authors' names on the cover or in the list of contents and there is no list of contributing authors. In order to find the author of each chapter, one has to go to the beginning of each part.

The first chapter contains a brief introduction to the field of "analytical science" and its definitions by the Editor. The second chapter gives numerous examples of separation techniques applied in the pharmaceutical industry. This chapter gives the largest overview of sample preparation techniques covering those most commonly used, with 271 references. Solid-phase extraction methods are addressed by both off- and on-line coupling to liquid chromatographic separation systems. When coupled column systems are discussed, the work of several leading groups in this area is not mentioned. This part could have been more extended in the chapter, especially since the sample preparation prior to analytical separation is of vital importance in all applications to biological samples. This extension would certainly have provided valuable information, as these coupled column systems have proved to be highly selective and sensitive in the determination of pharmaceutical components present in biological samples.

Two of the chapters deal with analytical applications in industry. In Chapter 3, an extensive insight is given into the analytical problems and the composition and complexity of beer. Spectroscopic methods in analyses for carbohydrates, organic acids, phenolic substances, flavanols, inorganic anions, lipid alcohols and esters, among others, are described. Separation techniques such as liquid and gas chromatography are presented. The various liquid chromatographic separation principles such as ion-exchange and reversed-phase separation methods are discussed separately and in combination with several spectroscopic detection principles. In Chapter 4, the analytical laboratory in the speciality sealant/adhesive industry is the second industrial area presented. NMR, FT-IR, MS and various separation techniques are described for the analysis of polymerizable monomers and polymers.

The last two chapters deal with air pollution analysis and the analysis of feeds and foodstuffs. In Chapter 5, air pollution systems with problems involving the ozone layer and halogen-containing, sulphur-containing and nitrogen-containing compounds are described in a clear and

logical way. Sampling procedures and methods of analysis are given for a large number of volatile airborne contaminants. In Chapter 6, the profiles of fatty acids, amino acids, starch, sugars, pesticides and toxic contaminants in animal and human feeds and foods are described. The major natural contaminants such as mycotoxins and toxic chemicals produced by microorganisms are discussed. Appropriate immunoaffinity assays for some of these compounds are also presented.

The contents of the book provide an insight into the measurement of various compounds of interest in several complex fields rather than giving a critical perspective of the problems encountered therein. It also gives a lot of information about analytical techniques commonly used for qualitative and quantitative analyses in complex matrices. What is missing is a presentation of newly developed and improved well known analytical techniques, *e.g.*, capillary electrophoresis, supercritical fluid chromatography and supercritical fluid extraction, and a broader insight into mass spectrometric techniques. The coupling of well known separation and detection techniques and the problems with interfacing these techniques is not mentioned at all. What I think is also missing is a better overview and discussion of where the problems in the analytical procedures lies, *e.g.*, the detectability of solutes in these matrices today and what detectable levels can be expected in the future.

Some of the various sample handling techniques that are of vital importance in chromatographic separation techniques today for the enhancement of both selectivity and sensitivity are mentioned in several parts in the book. Spreading this information in the various chapters makes it difficult for the reader to appreciate the usability and connection between the application fields described, especially as analyses of airborne, liquid and solid samples are dealt with.

The book can be recommended for all of those who are interested in modern analytical techniques in these types of applications, and also to academic workers involved in teaching instrumental analysis.

Lund (Sweden) György Marko-Varga

Author Index

Erratum

corrected 27 Aug. 93/AP

J. Chromatogr., 635 (1993) 307–312.

Page 307, Abstract, lines 5 and 6: "The average limit of detection was about 10 nM" should read "The average limit of detection was about 10 μM".

Page 311, first column, lines 24 and 25: "fluoroaluminum species was found to be about 10 nM ($S/N = 3$)" should read "fluoroaluminum species was found to be about 10 μM ($S/N = 3$)".

Page 311, second column, lines 1 and 2: "concentration was linear in the range of 10 to 500 nM" should read "concentration was linear in the range of 10 to 500 μM".

Wilson and Wilson's Comprehensive Analytical Chemistry Volume XXIX

Chemiluminescence Immunoassay

by **I. Weeks**, *University of Wales, College of Medicine, Cardiff, UK*

Series editor: **Prof. G. Svehla**, *Department of Chemistry, University College, Cork, Ireland*

Chemiluminescence immunoassay is now established as one of the best alternatives to conventional radioimmunoassay for the quantitation of low concentrations of analytes in complex samples. During the last two decades the technology has evolved into analytical procedures whose performance far exceeds that of immunoassays based on the use of radioactive labels. Without the constraints of radioactivity, the scope of this type of analytical procedure has widened beyond the confines of the specialist clinical chemistry laboratory to other disciplines such as microbiology, veterinary medicine, agriculture, food and environmental testing. This is the first work to present the topic as a subject in its own right.

In order to provide a complete picture of the subject, overviews are presented of the individual areas of chemiluminescence and immunoassay with particular emphasis on the requirements for interfacing chemiluminescent and immunochemical reactions. The possible ways of configuring chemiluminescence immunoassays are described. State-of-the-art chemiluminescence immunoassay systems are covered in detail together with those systems which are commercially available.

The book is aimed at researchers and routine laboratory staff in the life sciences who wish to make use of this high-performance analytical technique and also at those interested in industrial applications of the technology in the food, agricultural and environmental sciences.

1992 xvi + 294 pages
Price: US $ 151.50 / Dfl. 295.00
Subscription price:
US $ 136.00 / Dfl. 265.00
ISBN 0-444-89035-1

Elsevier Science Publishers

P.O. Box 211, 1000 AE Amsterdam, The Netherlands
P.O. Box 882, Madison Square Station, New York, NY 10159, USA

Methods for Experimental Design

Principles and Applications for Physicists and Chemists

by **J. Goupy**

Data Handling in Science and Technology Volume 12

The choice of ideal experiments is based on mathematical concepts, but the author adopts a practical approach and uses theory only when necessary. Written for experimenters by an experimenter, it is an introduction to the philosophy of scientific investigation. A method for organizing and conducting scientific experiments is described in this volume which enables experimenters to reduce the number of trials run, while retaining all the parameters that may influence the result.

Researchers with limited time and resources at their disposal will find this text a valuable guide for solving specific problems efficiently. The presentation makes extensive use of examples, and the approach and methods are graphical rather than numerical. All calculations can be performed on a personal computer; readers are assumed to have no previous knowledge of the subject. The presentation is such that the beginner may acquire a thorough understanding of the basic concepts. However, there is also sufficient material to challenge the advanced student. The book is, therefore, suitable for both first and advanced courses. The many examples can also be used in detail for self-study or as a reference.

Contents:

1993 xvi + 450 pages
Price: US $ 185.75 / Dfl. 325.00
ISBN 0-444-89529-9

ELSEVIER
SCIENCE PUBLISHERS

ORDER INFORMATION

For USA and Canada
ELSEVIER SCIENCE PUBLISHERS
Judy Weislogel
P.O. Box 945
Madison Square Station,
New York, NY 10160-0757
Tel: (212) 989 5800
Fax: (212) 633 3880

In all other countries
ELSEVIER SCIENCE PUBLISHERS
P.O. Box 211
1000 AE Amsterdam
The Netherlands
Tel: (+31-20) 5803 753
Fax: (+31-20) 5803 705

US$ prices are valid only for the USA & Canada and are subject to exchange rate fluctuations; in all other countries the Dutch guilder price (Dfl.) is definitive. Customers in the European Community should add the appropriate VAT rate applicable in their country to the price(s). Books are sent post-free if prepaid.

PUBLICATION SCHEDULE FOR THE 1993 SUBSCRIPTION

Journal of Chromatography and *Journal of Chromatography, Biomedical Applications*

MONTH	1992	J	F	M	A	M	J	J	
Journal of Chromatography	Vols. 623–627	628/1 628/2 629/1 629/2	630/1 + 2 631/1 + 2 632/1 + 2 633/1 + 2	634/1 634/2	635/1 635/2 636/1 636/2	637/1 637/2 638/1 638/2	639/1 639/2 640/1 + 2	641/1 641/2 642/1 + 2 643/1 + 2 644/1	The publication schedule for further issues will be published later.
Cumulative Indexes, Vols. 601–650									
Bibliography Section				649/1			649/2		
Biomedical Applications		612/1	612/2	613/1	613/2 614/1	614/2 615/1	615/2 616/1	616/2 617/1	

INFORMATION FOR AUTHORS

(Detailed *Instructions to Authors* were published in Vol. 609, pp. 437–443. A free reprint can be obtained by application to the publisher, Elsevier Science Publishers B.V., P.O. Box 330, 1000 AH Amsterdam, Netherlands.)

Types of Contributions. The following types of papers are published in the *Journal of Chromatography* and the section on *Biomedical Applications:* Regular research papers (Full-length papers), Review articles, Short Communications and Discussions. Short Communications are usually descriptions of short investigations, or they can report minor technical improvements of previously published procedures; they reflect the same quality of research as Full-length papers, but should preferably not exceed five printed pages. Discussions (one or two pages) should explain, amplify, correct or otherwise comment substantively upon an article recently published in the journal. For Review articles, see inside front cover under Submission of Papers.

Submission. Every paper must be accompanied by a letter from the senior author, stating that he/she is submitting the paper for publication in the *Journal of Chromatography.*

Manuscripts. Manuscripts should be typed in **double spacing** on consecutively numbered pages of uniform size. The manuscript should be preceded by a sheet of manuscript paper carrying the title of the paper and the name and full postal address of the person to whom the proofs are to be sent. As a rule, papers should be divided into sections, headed by a caption (*e.g.*, Abstract, Introduction, Experimental, Results, Discussion, etc.) All illustrations, photographs, tables, etc., should be on separate sheets.

Abstract. All articles should have an abstract of 50–100 words which clearly and briefly indicates what is new, different and significant. No references should be given.

Introduction. Every paper must have a concise introduction mentioning what has been done before on the topic described, and stating clearly what is new in the paper now submitted.

Illustrations. The figures should be submitted in a form suitable for reproduction, drawn in Indian ink on drawing or tracing paper. Each illustration should have a legend, all the *legends* being typed (with double spacing) together on a *separate sheet.* If structures are given in the text, the original drawings should be supplied. Coloured illustrations are reproduced at the author's expense, the cost being determined by the number of pages and by the number of colours needed. The written permission of the author and publisher must be obtained for the use of any figure already published. Its source must be indicated in the legend.

References. References should be numbered in the order in which they are cited in the text, and listed in numerical sequence on a separate sheet at the end of the article. Please check a recent issue for the layout of the reference list. Abbreviations for the titles of journals should follow the system used by *Chemical Abstracts.* Articles not yet published should be given as "in press" (journal should be specified), "submitted for publication" (journal should be specified), "in preparation" or "personal communication".

Dispatch. Before sending the manuscript to the Editor please check that the envelope contains four copies of the paper complete with references, legends and figures. One of the sets of figures must be the originals suitable for direct reproduction. Please also ensure that permission to publish has been obtained from your institute.

Proofs. One set of proofs will be sent to the author to be carefully checked for printer's errors. Corrections must be restricted to instances in which the proof is at variance with the manuscript. "Extra corrections" will be inserted at the author's expense.

Reprints. Fifty reprints will be supplied free of charge. Additional reprints can be ordered by the authors. An order form containing price quotations will be sent to the authors together with the proofs of their article.